DEC 18 1958
FORD MOTOR COMPANY
ENGINEERING LIBRARY
Dearborn, Michigan
SHELF

АВТОМАТИКА
и
ТЕЛЕМЕХАНИКА

Volume 18, No. 7

July 1957

SOVIET INSTRUMENTATION AND
CONTROL TRANSLATION SERIES

Automation and Remote Control

(The Soviet Journal *Avtomatika i Telemekhanika* in English Translation)

■ This translation of a Soviet Journal on automatic control is published as a service to American science and industry. It is sponsored by the Massachusetts Institute of Technology under a grant in aid from the National Science Foundation, and is distributed by the Instrument Society of America.

SOVIET INSTRUMENTATION AND CONTROL TRANSLATION SERIES

Instrument Society of America Executive Board

Robert J. Jeffries
President
Justus T. Vollbrecht
Past President
Henry C. Frost
President-Elect-Secretary
Edward C. Baran
Dept. Vice President
John Johnston, Jr.
Dept. Vice President
Philip A. Sprague
Dept. Vice President
Ralph H. Tripp
Dept. Vice President
Howard W. Hudson
Treasurer
Carl W. Gram, Jr.
Dist. I Vice President
E. Albert Adler
Dist. II Vice President
John T. Elder
Dist. III Vice President
Mifflin S. Jacobs
Dist. IV Vice President
Gordon D. Carnegie
Dist. V Vice President
Willard A. Kates
Dist. VI Vice President
John F. Draffen
Dist. VII Vice President
John V. Opie
Dist. VIII Vice President
Adelbert Carpenter
Dist. IX Vice President
John J. Hillen
Dist. X Vice President

Headquarters Office

William H. Kushnick
Executive Director
Charles W. Covey
Editor, ISA Journal
George A. Hall
Assistant Editor, ISA Journal
Herbert S. Kindler
Director Technical Programs
Ralph M. Stotsenburg
Director Section Activities
Thomas K. Hodges
Director Promotional Services

ISA Publications Committee

Nathan Cohn, *Chairman*

Jere E. Brophy	George A. Larsen	Frank S. Swaney
Floyd E. Bryan	John E. Read	Richard A. Terry
Richard W. Jones	Joshua Stern	Benjamin W. Thomas

■ This translation of the Soviet Journal *Avtomatika i Telemekhanika* is published and distributed at nominal subscription rates under a grant in aid to the Massachusetts Institute of Technology from the National Science Foundation. The translated journal will enable American scientists and engineers to be informed of work in the fields of instrumentation and automatic control reported in the Soviet Union.

The original Russian articles are translated by competent technical personnel. The translations are on a cover-to-cover basis, permitting readers to appraise for themselves the scope, status and importance of the Soviet work.

Publication of *Avtomatika i Telemekhanika* in English translation started under the present auspices in April 1958 with Russian Vol. 18, No. 1, of January 1957. The eleven remaining Russian issues of 1957 will be published in English translation prior to the end of 1958. English translations will carry the same volume and issue numbers as the Russian originals.

All views expressed in the translated material are intended to be those of the original authors, and not those of the translators, the Massachusetts Institute of Technology, nor the Instrument Society of America.

Readers are invited to submit communications on the quality of the translations and the content of the articles to ISA headquarters. Pertinent correspondence will be published in the "Letters" section of the ISA Journal. Space will also be made available in the ISA Journal for such replies as may be received from Russian authors to comments or questions by American readers.

Subscription Prices:

Per year (12 issues), starting with Vol. 18, No. 1

General: United States and Canada	$30.00
Elsewhere	33.00
Libraries of academic and other non-profit institutions:	
United States and Canada	$15.00
Elsewhere	18.00
Single issues to everyone, each	$ 3.50

Subscriptions should be addressed to the:

Instrument Society of America
313 Sixth Avenue, Pittsburgh 22, Penna.

Translated and printed by Consultants Bureau, Inc.

Copyright by Massachusetts Institute of Technology 1958

CONDITIONALLY STABLE CONTROLLED SYSTEMS (ONE CLASS OF OPTIMAL CONTROLLED SYSTEM)

A. M. Letov

(Moscow)

A linear automatic control system described by the vector $x = x(x_0, t)$ which is asymptotically stable about the trivial solution $x \equiv 0$ is considered.

The system parameters are assumed selected and fixed to correspond with some existing concept of an optimal linear system.

Let t^* be the conditional transient damping time, i.e., a number which fulfills the condition $|x(x_0; t)| \leq x_0 e^{-\pi}$ when $t \geq t^*$.

It is asserted that a t_* also exists ($0 < t_* < t^*$) for which the effector speed changes from $+\dot{\xi}$ at $t \leq t_*$ to $-\dot{\xi}$ at $t \geq t_*$ thereby changing the initial system to another, also conditionally stable system (for $t \geq t_*$), such that the transient is damped out in the first swing (i.e. on a single reversal in the controller) while the conditional transient damping time is substantially less than t^*.

A control method is proposed in which t_* is selected in relation to the initial state $x_0 = x(x_0, 0)$ and the system parameters.

t_* is determined by a special computer unit, the structure of which is analyzed.

INTRODUCTION

Maslennikov [1] proposed the idea of designing a nonlinear automatic regulator using only one sensing element which would ensure stability in the controlled object and which is described by a first-order equation without self-compensation, and which ensured that the transient was damped in the first swing. Unlike in normal controllers the effector speed was reversed not only at the instant when the controlled coordinate q passed through zero, but also at time t_* when it passed through $q = 1/\sqrt{2}q_m$, where q_m is the first extremum to the left of t_*. In this way the transient was rendered aperiodic. An advantage of such a regulator is that no controlled-coordinate derivative or feedback transducers are required, while the effect produced is similar to that obtained when such transducers are used. When assessing the value of this it should be remembered that a normal linear controller using the same sensing element and recording only errors in the controlled coordinate gives an undamped sinusoidal oscillatory transient of amplitude determined by the initial perturbation. This result is important in itself, and also encourages one to generalize. But it is extremely difficult to generalize Maslennikov's problem directly. In our opinion this difficulty is related to his computing t_* from q_m. We must devote attention to another method. The choice of a t_* to correspond with $1/\sqrt{2}q_m$ is essentially

related to the initial perturbation, and this, to use Lyapunov's terminology [2] makes it conditionally stable for $t \geq t_*$.

The condition consists in removing the partial oscillation corresponding to the positive root of the characteristic equation for $t \geq t_*$, which results in a system of any order having a transient damped in the first swing, i.e., on a single controller reversal. This approach to Maslennikov's problem is fruitful, and correct solutions can then be obtained for controlled objects of any order. The present communication considers the design of conditionally stable controlled systems and presents solutions for certain cases.

This problem differs from Maslennikov's. The main difference is in determining and considering the control law. The regulator considered is not nonlinear. Its operation is time-dependent and it includes a computer unit.

The problems dealt with here and in [1] are similar to others that have been considered [3, 4].

1. Design of Conditionally Stable Systems.

Consider a strictly linear controlled system described by

$$\dot{\eta}_k = \sum_{\alpha=1}^{n} b_{k\alpha}\eta_\alpha + n_k\xi \quad (k = 1, \ldots, n), \qquad (1.1)$$
$$\dot{\xi} = K\eta_1,$$

when the η_k are coordinates, the $b_{k\alpha}$ constant parameters of the controlled object, ξ, a coordinate, the n_k are constant parameters of the effector, K, the regulator constant, and η_1, the controlled coordinate.

We assume that (1.1) has been carefully studied by any of the normal methods for linear systems, and that K ensures stability and an optimal [5-7] transient response, specified by a known and completely applicable conditional damping time t_* [8]. We assert that if the system of (1.1) can be transferred to the conditionally stable class it will be better, in the sense that while stable its transient will be quenched in the first swing, and its conditional damping time will be less than t^*.

To prove the assertion let us add a special unit to the regulator, in future termed the computer. The computer materially improves the regulator. While its structure remains unknown, we may assume that the equation of motion of the effector may be written as

$$\dot{\xi} = Kf(t)\eta_1. \qquad (1.2)$$

f(t) is defined to be such that for the values of η_1 relating to $t \leq t_*$, $f(t) = +1$, while for values of η_1 when $t > t_*$, $f(t) = -1$. Hence when $t = t_*$ the speed of the effector changes from $\dot{\xi} = K\eta_1$ to $\dot{\xi} = -K\eta_1$. We shall show below what the computer design must be and how it must work in order to determine t_* appropriately. So we assume that $0 \leq t \leq t_*$, and that the perturbation is described by

$$\dot{\eta}_k = \sum_{\alpha=1}^{n} b_{k\alpha}\eta_\alpha + n_k\xi. \qquad (1.3)$$
$$\dot{\xi} = K\eta_1.$$

The characteristic determinant is

$$\Delta(\lambda) = \begin{vmatrix} b_{11} - \lambda, & b_{12}, \ldots, b_{1n}, & n_1 \\ \ldots\ldots\ldots\ldots & \ldots\ldots\ldots & \ldots \\ b_{n1}, & b_{n2}, \ldots, b_{nn} - \lambda, & n_n \\ K, & 0, \ldots, 0, & -\lambda \end{vmatrix}. \qquad (1.4)$$

Ex hypothesis Re $\lambda_k < 0$ ($k = 1, \ldots, n+1$). The solution to (1.3) is [9]

$$\eta_{is} = -\sum_{j=1}^{n+1}\left[\frac{\sum_{k=1}^{n}\Delta_{ks}(\lambda_j)\,\eta_k(0) + \Delta_{n+1,s}(\lambda_j)\,\xi(0)}{\Delta'(\lambda_j)}\right]e^{\lambda_j t} \qquad (s = 1, \ldots, n) \tag{1.5}$$

$$\xi = -\sum_{j=1}^{n+1}\left[\frac{\sum_{k=1}^{n}\Delta_{k,n+1}(\lambda_j)\,\eta_k(0) + \Delta_{n+1,\,n+1}(\lambda_j)\,\xi(0)}{\Delta'(\lambda_j)}\right]e^{\lambda_j t}.$$

where $\eta_k(0)$, $\xi(0)$ are initial perturbations, and the $\Delta_{ks}(\lambda_j)$ are the minors of (1.4), $\underline{k}$ being the number of rows and $\underline{s}$ the number of columns. The solution to (1.5) exists when $0 \le t \le t_*$; when $t = t_*$ we have

$$\eta_s = \eta_s(t_*),\ \xi = \xi(t_*)\ (s = 1, \ldots, n). \tag{1.6}$$

The effector is reversed at this instant, and the equations describing the subsequent control process are

$$\dot{\eta}_{ik} = \sum_{\alpha=1}^{n} b_{k\alpha}\eta_{i\alpha} + n_k\xi \qquad (k = 1, \ldots, n), \tag{1.7}$$

$$\dot{\xi} = -K\eta_{i1}.$$

The characteristic determinant is

$$\bar{\Delta}(\mu) = \begin{vmatrix} b_{11} - \mu, \ldots, b_{1n}, & n_1 \\ \cdots\cdots\cdots\cdots\cdots & \\ b_{n1} \quad \ldots\ldots b_{nn} - \mu, & n_n \\ -K, \quad \ldots\ldots 0, & -\mu \end{vmatrix}. \tag{1.8}$$

It differs from (1.4) only in the sign of K.

Let $\mu_1, \ldots, \mu_{n+1}$ be the roots of $\bar{\Delta}(\mu) = 0$; at least one of these will have a positive real part.

Then the solution for the transient when $t > t_*$ will take the form

$$\eta_{is} = -\sum_{j=1}^{n+1}\left[\frac{\sum_{k=1}^{n}\bar{\Delta}_{ks}(\mu_j)\,\eta_k(t_*) + \bar{\Delta}_{n+1,\,s}(\mu_j)\,\xi(t_*)}{\bar{\Delta}'(\mu_j)}\right]e^{\mu_j t} \qquad (s = 1, \ldots, n), \tag{1.9}$$

$$\xi = -\sum_{j=1}^{n}\left[\frac{\sum_{k=1}^{n}\bar{\Delta}_{k\,n+1}(\mu_j)\,\eta_n(t_*) + \bar{\Delta}_{n+1,\,n+1}\,\xi(t_*)}{\bar{\Delta}'(\mu_j)}\right]e^{\mu_j t}.$$

In these equalities the $\bar{\Delta}_{ks}$ are formed using the same rule as for the Δ_{ks}.

The case where there is only one real positive root in the μ_s, e.g. μ_{n+1}, is of particular interest, since the other roots then have the property

$$\operatorname{Re}\mu_k < 0\ (k = 1, \ldots, n).$$

Then if the system of (1.1) is to be conditionally stable and the transient damped in the first swing, t_* must be taken as the first real root of

$$\sum_{k=1}^{n} \bar{\Delta}_{k1}(\mu_{n+1})\,\eta_k(t_*) + \bar{\Delta}_{n+1,1}(\mu_{n+1})\,\xi(t_*) = 0. \tag{1.10}$$

Then the partial oscillation relating to μ_{n+1} will vanish and the system will be conditionally stable. In fact the minors of (1.8) are related as follows:

$$\bar{\Delta}_{ks}\bar{\Delta}_{lm} = \bar{\Delta}_{km}\bar{\Delta}_{ls}, \tag{1.11}$$

where l and m are any chosen numbers which can take the values 1, . . ., n + 1. Then

$$\bar{\Delta}_{k1} = \frac{\bar{\Delta}_{km}\bar{\Delta}_{l1}}{\bar{\Delta}_{lm}}, \tag{1.12}$$

and (1.10) can be given a new form

$$\frac{\bar{\Delta}_{l1}}{\bar{\Delta}_{lm}}\left[\sum_{k=1}^{n} \bar{\Delta}_{km}(\mu_{n+1})\,\eta_k(t_*) + \bar{\Delta}_{n+1,m}(\mu_{n+1})\,\xi(t_*)\right] = 0. \tag{1.13}$$

Comparison of (1.9), (1.10) and (1.13) shows that if $\dfrac{\bar{\Delta}_{l1}}{\bar{\Delta}_{lm}} \neq \infty$ for any m = 1, . . ., n + 1, the system of (1.1) will be conditionally stable.

This is essentially based on the assumption that $\bar{\Delta}(\mu) = 0$ has only one real positive root.

To demonstrate that this assumption is not sterile it is sufficient to consider one example where it is complied with.

Example . Assume

$$\begin{gathered}\dot{\zeta}_1 = 0{,}5\,\zeta_2, \quad \dot{\zeta}_2 = -0{,}38\,\zeta_2 - 9\,\zeta_3 - 4\,\xi, \\ \dot{\zeta}_3 = \zeta_2 - 0{,}235\,\zeta_3, \ \dot{\xi} = K\zeta_1.\end{gathered} \tag{1.14}$$

Let K = 0.75. The roots of (1.4) are

$$\lambda_1; \lambda_2 = -0.0825 \pm 0.1785\,i, \quad \lambda_3; \lambda_4 = -0.2250 \pm 2.9875\,i. \tag{1.15}$$

The transient is oscillatory (full lines in Figure 1) when $\zeta_1(0) = 2.5$, $\zeta_2(0) = \zeta_3(0) = \xi(0) = 0$.

The damping time τ_1^*, determined from the condition that the amplitude of oscillation in ζ_1 be reduced by a factor 20, is $\tau_1^* = 35.2$.

When k = −0.75 the roots of $\bar{\Delta}(\mu) = 0$ are

$$\mu_1; \mu_2 = -0.385 \pm 3.015\, i, \quad \mu_3 = -0.1315, \quad \mu_4 = -0.2905. \tag{1.16}$$

The transcendental equation (1.10) has to be solved to determine the instant when the motion reverses. The closest real root is $\tau_* = 3.86$. When $\tau_* > 3.86$, the transient is shown by the dashed curves. The conditional damping time: τ_1, determined from the above requirements, is $\tau_2^* = 18.16$. Comparison of the full and dashed curves shows that the transient in a conditionally stable system a) is aperiodic, showing no overshoot; b) has a damping time 1.93 times less than in a normal design.

Several important additional problems arise in studying conditionally stable systems. We shall attempt to cast light on them by considering an example.

First of all we shall show that there can be only one positive real root to $\bar{\Delta}(\mu) = 0$ no matter how many real roots there are.

We have

$$\mu^4 + 0.615\,\mu^3 + 9.089\,\mu^2 - 2K\mu - 0.47\,K = 0.$$

The roots of this are related as follows by Vieta's equations:

$$\mu_1 + \mu_2 + \mu_3 + \mu_4 = -0.615 \tag{A}$$

$$\mu_1(\mu_2 + \mu_3 + \mu_4) + \mu_2(\mu_3 + \mu_4) + \mu_3\mu_4 = 9.089. \tag{B}$$

$$\mu_1(\mu_2\mu_3 + \mu_2\mu_4 + \mu_3\mu_4) + \mu_2\mu_3\mu_4 = 2K, \tag{C}$$

$$\mu_1\mu_2\mu_3\mu_4 = -0.47\,K. \tag{D}$$

We assume all the μ_k real. In view of (A) we cannot have $\mu_k > 0$, $k = 1, 2, 3, 4$. (D) shows that either $\mu_1 < 0$, $\mu_2 < 0$, $\mu_3 < 0$, $\mu_4 > 0$, or $\mu_1 < 0$, $\mu_2 > 0$, $\mu_3 > 0$, $\mu_4 > 0$. We shall show that the latter is impossible. To this end we multiply (A) by $(\mu_2 + \mu_3 + \mu_4)$, and after subtracting (B) from the result we get the contradictory relation

$$\mu_2^2 + \mu_3^2 + \mu_4^2 + \mu_2(\mu_3 + \mu_4) + \mu_3\mu_4 = -0.615(\mu_2 + \mu_3 + \mu_4) - 9.089.$$

μ_1 and μ_2 may be real, while $\mu_3 = \alpha + i\beta$, $\mu_4 = \alpha - i\beta$ are complex conjugate roots.

Vieta's formulas take the form

$$\mu_1 + \mu_2 + 2\alpha = -0.615, \tag{A}$$

$$\mu_1(\mu_2 + 2\alpha) + 2\alpha\mu_2 + \alpha^2 + \beta^2 = 9.089. \tag{B}$$

$$\mu_1(2\alpha\mu_2 + \alpha^2 + \beta^2) + \mu_2(\alpha^2 + \beta^2) = 2K, \tag{C}$$

$$\mu_1\mu_2(\alpha^2 + \beta^2) = -0.47\,K. \tag{D}$$

The following sign combinations are in principle possible:

1) $\mu_1 > 0$, $\mu_2 > 0$, $\alpha > 0$,

2) $\mu_1 > 0$, $\mu_2 > 0$, $\alpha < 0$,

3) $\mu_1 > 0$, $\mu_2 < 0$, $\alpha > 0$,

4) $\mu_1 < 0$, $\mu_2 > 0$, $\alpha > 0$,

5) $\mu_1 > 0$, $\mu_2 < 0$, $\alpha < 0$,

6) $\mu_1 < 0$, $\mu_2 > 0$, $\alpha < 0$,

7) $\mu_1 < 0$, $\mu_2 < 0$, $\alpha > 0$.

1) is made impossible by (A), 2) and 7) by (D).

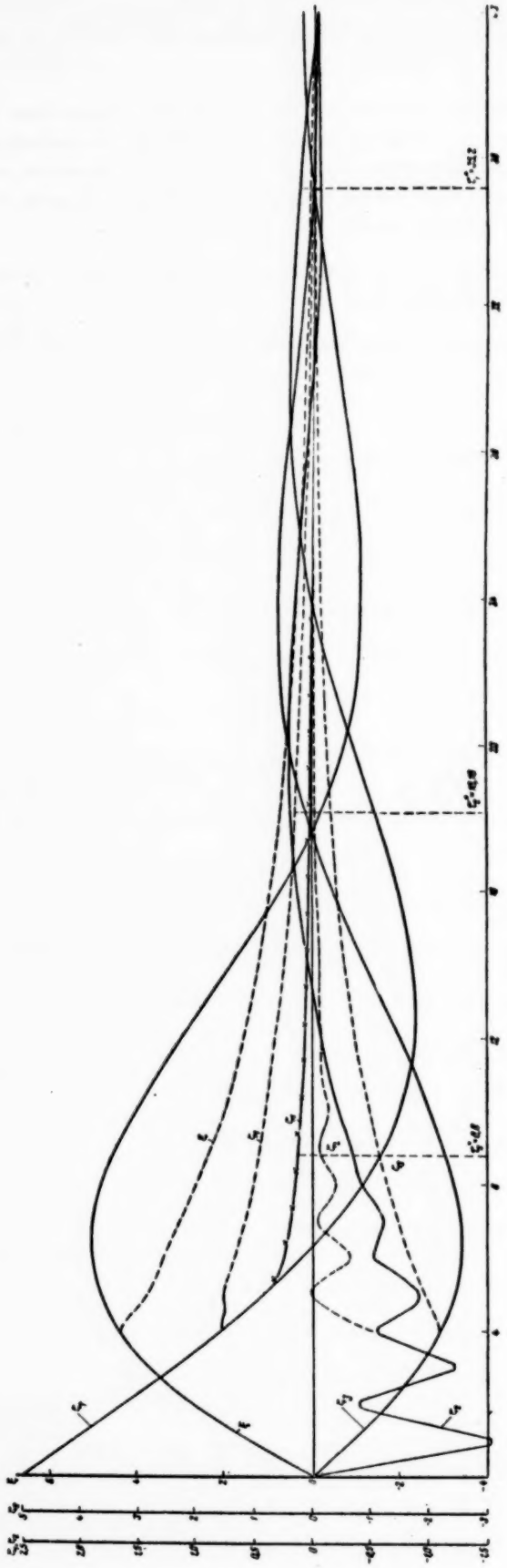

Fig. 1.

Further, multiplying (A) by $2\alpha\mu_2 + \alpha^2 + \beta^2$, and subtracting the result from (C) we get $-2\alpha\mu_2^2 - 2\alpha[2\alpha\mu_2 + \alpha^2 + \beta^2] = 2K + 0.615\,[2\alpha\mu_2 + \alpha^2 + \beta^2]$, which contradicts 4). In an analogous fashion we form $-2\alpha\mu_1^2 - 2\alpha[2\alpha\mu_1 + \alpha^2 + \beta^2] = 2K + 0.615\,[2\alpha\mu_1 + \alpha^2 + \beta^2]$, which is contrary to 3). Only 5) and 6) remain, which can be realized with differing values of K.

So the system of (1.14) can always be made conditionally stable.

Let us elucidate the shape of the transient at $\tau = \tau_*$ as a function of the K chosen. Firstly attention must be paid to the relation between the μ_k and K; see Table.

K	μ_1, μ_2	μ_3	μ_4
0.75	-0.385 ± 3.015	-0.1315	0.2905
1.5	-0.463 ± 3.035	-0.159	0.4695
3	-0.6007 ± 3.0935	-0.1845	0.771
4.5	-0.722 ± 3.1575	-0.197	1.026
7.5	-0.9025 ± 3.292	-0.2095	1.445
12.5	-1.29 ± 3.602	-0.221	2.185

The table shows that $|\mu_1|$, $|\mu_2|$, $|\mu_3|$, increase favorably with K, so by changing K stepwise the transient convergence can be substantially improved.

Figure 1 shows ζ_1 for K = 4.5. Although the step in K makes τ_* later, τ_3^* (see full line for ζ_1 denoted by crosses) drops by more than a factor 2 as compared with τ_2^*, and by a factor 4 compared with τ_1^*.

A still more surprising example is that of an armature position control system for a motor with independent field excitation, which has been considered [6]. The initial equations of perturbed motion are

$$L\frac{di}{dt} + Ri + \lambda\Omega = U_2, \qquad U_2 = k_2(x - y),$$
$$J\frac{d\Omega}{dt} = \sigma i, \qquad \frac{dx}{dt} = -k_1\Omega, \qquad y = \varkappa i. \tag{1.17}$$

Here k_2 is the gain in the armature supply circuit, R and L, the resistance and inductance of the armature circuit, J, the moment of inertia of the moving parts, referred to the motor shaft, Ω, the shaft speed, $\underline{y}$, the voltage, $\varkappa$, the feedback coefficient, $\underline{x}$, the error signal at the measuring head, k_1, λ, σ being positive constants.

We use the symbols

$$T = \frac{JR}{\lambda\sigma}, \quad K = \frac{Tk_1k_2}{\lambda}, \quad \beta = \frac{\sigma\lambda L}{JR^2}, \quad \gamma = \frac{\varkappa k_2}{R} \tag{1.18}$$

and transform linearly to the new variables $t = T\tau$, $(JR/L\sigma)\,\Omega = \eta_1$, $i = \eta_2$, $(k_2T/L)\,x = \xi$.

In these variables the equations take the form

$$\dot\eta_1 = \frac{1}{\beta}\eta_2, \quad \dot\eta_2 = -\eta_1 - \frac{1+\gamma}{\beta}\eta_2 + \xi, \quad \dot\xi = -K\eta_1. \tag{1.19}$$

The choice of variables is influenced by the need to obtain a characteristic determinant $\Delta(\lambda)$ containing only β, γ, and K for which the system is optimal. Their optimum values [6] when $\beta = 1$ are $K = 0.192$, $\gamma = 0.73$.

The roots of (1.4) are $\lambda_1, \lambda_2 = -0.625 \pm 0.09682\,i$, $\lambda_3 = -0.48$.

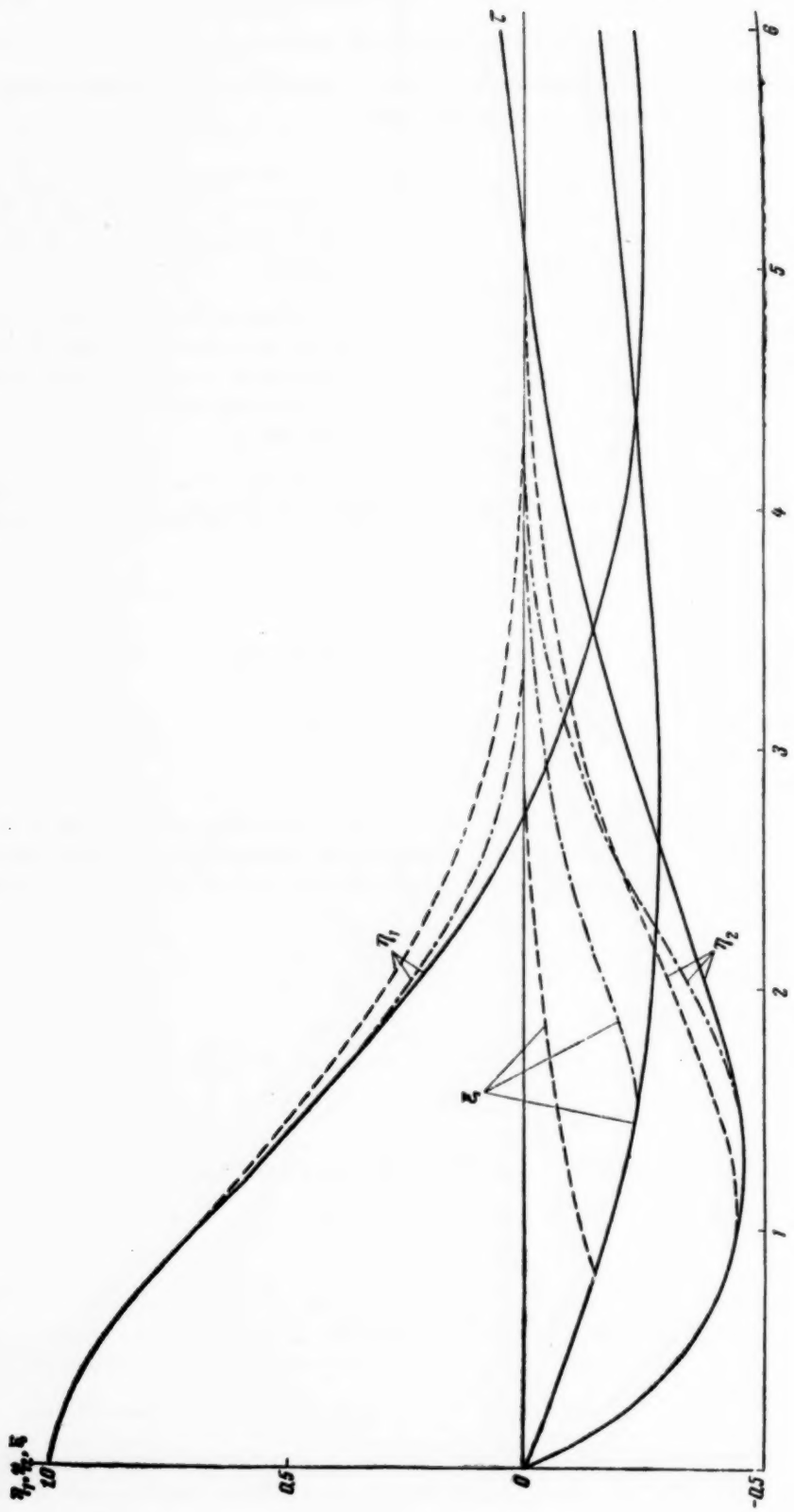

Fig. 2.

Figure 2 (full lines) shows the transient when $\eta_1(0) = 1$, $\eta_2(0) = \xi(0)$.

The damping time, defined as the time for the amplitude of oscillation in η_1 to fall by 20 times, is $\tau_1 = 11$. When $K = -0.192$ the roots of (1.8) are μ_1, $\mu_2 = -0.94 \pm 0.630\,i$, $\mu_3 = 0.15$.

τ^* is the first real root of the transcendental equation (1.10). It is $\tau_* = 0.83$.

The transients for $\tau > \tau_*$ in a conditionally stable system are shown by dashed lines.

The transients are completely over at $\tau_1^* = 4.4$. If we apply a stepwise change in K (to $K = -1$) at $\tau = \tau_*$, then $\tau_* = 1.55$, and the total damping time is reduced to $\tau_2^* = 3.4$.

2. Structureof the Computer Unit.

To make the system conditionally stable τ_* must be determined as the first real root of (1.10). A computer unit must be added for this purpose; its structure is determined by (1.10). From (1.5) we write this as

$$\sum_{j=1}^{n+1}\left[\sum_{l=1}^{n}\left\{\sum_{k=1}^{n}\bar{\Delta}_{kl}(\mu_{n+1})\,\Delta_{lk}(\lambda_j) + \bar{\Delta}_{n+1,1}(\mu_{n+1})\,\Delta_{ln+1}(\Delta_j)\right\}\eta_l(0) + \right. \tag{2.1}$$

$$\left. + \left\{\sum_{k=1}^{n}\bar{\Delta}_{k1}(\mu_{n+1})\,\Delta_{n+1,k}(\lambda_j) + \bar{\Delta}_{n+1,1}(\mu_{n+1})\,\Delta_{n+1,n+1}(\lambda_j)\right\}\xi(0)\right] e^{\lambda_j t} = 0.$$

Suppose the regulator to have a complete assembly of sensitive elements to measure the η_k, ξ ($k = 1, \ldots, n$) when $t \geq 0$.

There are two ways of calculating t_*.

In (2.1) each pair of braces $\{\{\ \}\}$ contains a definite number N_{lj} ($l = 1, \ldots, n$) or N_j. Suppose the initial perturbations $\eta_l(0)$, $\xi(0)$ to appear at the computer input. The computer must have scalar elements of the form $N_{lj}\eta_l(0)$, $N_j\xi(0)$ and a summing unit, to which the outputs of the scalar units are supplied. The summing unit must have $n + 1$ channels; from each output must appear one of the quantities

$$\bar{M}_j = \sum N_{lj}\eta_l(0), \quad M_j = N_j\xi(0).$$

The $\bar{M}_j$, M_j are fed to a computer unit which solves

$$\sum_{j=1}^{n+1}\left[\bar{M}_j + M_j\right]e^{\lambda_j t} = 0. \tag{2.2}$$

This method is to be preferred when t_* has to be determined accurately. The computer unit, if digital, can determine t_* with the required accuracy and rapidity. Figure 3 shows a scheme for such a unit.

In the second case it is more convenient to use (1.10). Suppose that the sensitive elements give out $\eta_k(t)$, $\xi(t)$ for $t \geq 0$ as electrical signals. The signals are passed to the scalar units and thence to a summing unit. t_* corresponds to zero output from the latter. Figure 4 shows the scheme of a unit working in this fashion.

If the computer unit is a rough one and gives t_* with an appreciable error each solution to (1.9) will contain a partial residual component of type $A_s e^{\mu_{n+1} t}$.

The constant A_s depends on the t'_* actually given by the computer, and tends to zero as $t_* - t'_* \to 0$. Under these circumstances the controlled coordinate will increase in modulus without bound, the modulus passing through zero or a minimum. Thus to ensure correct operation in both cases the computer must cause the effector to switch over from a speed $\dot{\xi} = -K\eta_1$ to $\dot{\xi} = K\eta_1$. Suppose t'_* ($t'_* > t_*$) is the instant of switch-over, and

$$\eta_{1k} = \eta_k(t'_*) \quad (k = 1, \ldots, n), \quad \xi = \xi(t'_*) \tag{2.3}$$

and the coordinates determined from (1.9). We shall term the time $0 \leq t \leq t'_*$ the "cycle" of the conditionally stable system.

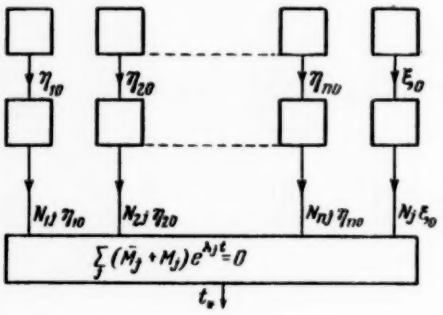

Fig. 3

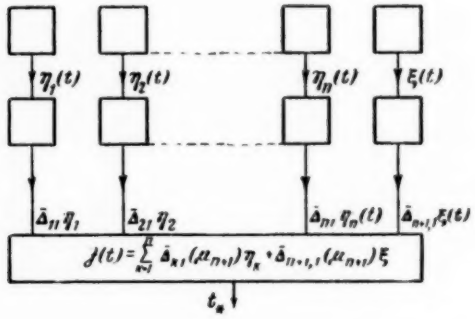

Fig. 4

Since ex hypothesi the system of (1.1) is stable and optimal the above control cycle is repeated with the initial perturbations of (2.3).

When a sufficient number of cycles have been run through the transient dies away. But the damping will take longer the greater the error in computing t_*.

3. Critical remarks.

It may be shown that when we need to use a complete assembly of sensing elements we can produce a normal stable control system of the form

$$\dot{\eta}_{1k} = \sum_{\alpha=1}^{n} b_{k\alpha}\eta_{1\alpha} + n_k\xi \quad (k = 1, \ldots, n), \qquad \dot{\xi} = \sum_{\alpha=1}^{n} p_\alpha\eta_{1\alpha} - r\xi \tag{3.1}$$

(where p_α and r are controller parameters) without a computer, such a system differing in a favorable sense (transient damping time) from a conditionally stable one, as of (1.1). One critic (V. A. Kotelnikov) has remarked on this.* In answer to this we at once convert (3.1)to a conditionally stable scheme:

$$\dot{\eta}_{1k} = \sum_{\alpha=1}^{n} b_{k\alpha}\eta_{1\alpha} + n_k\xi, \qquad \dot{\xi} = f(\sigma, \rho, t),$$
$$\sigma = \sum_{\alpha=1}^{n} p_\alpha\eta_{1\alpha} - r\xi, \qquad \rho = \sum_{\alpha=1}^{n} k_\alpha\eta_{1\alpha} - s\xi. \tag{3.2}$$

* The criticisms relate to the first draft of the article, submitted January 23, 1956.

Here k_α and $\underline{s}$ are regulator parameters, given, in particular, by

$$k_1 = -Np_1, \quad k_\alpha = p_\alpha \quad (\alpha = 2, \ldots, n), \quad s = r,$$

where N is now an arbitrary positive number. The same applies to f (σ, ρ, t), this being selected as previously. That is, for the values of $\eta_1, \ldots, \eta_n, \xi$, which these coordinates have when $t \leq t_*$, we put

$$f(\sigma, \rho, t) = K\sigma, \tag{3.3}$$

and for the values of $\eta_1, \ldots, \eta_n, \xi$ for $t > t_*$ we put

$$f(\sigma, \rho, t) = K\rho. \tag{3.4}$$

Then we assert that the system will be conditionally stable, and its transient response will last a shorter time than in an optimal system designed round any other chosen criterion. This will be demonstrated by an example.

For this we consider a controlled system [7] of the type

$$\begin{gathered} \varphi + \dot{\varphi} + k^*\varphi - \mu = 0, \\ \dot{\mu} = \frac{1}{W}\sigma, \quad \sigma = -n\mu - \varphi - M\dot{\varphi} - L^2\ddot{\varphi}. \end{gathered} \tag{3.5}$$

Here all constants are positive and are regulator parameters except k^*.

It has been shown [7] that the best values of these parameters, which give the highest possible stability δ, are defined by

$$1 + \frac{L^2 + n^2}{W} = 3\delta, \quad k^* + \frac{M + n}{W} = 3\delta^2, \quad 1 + nk^* = W\delta^3. \tag{3.6}$$

From now on we will use these equations and, putting $\varphi = \eta_1$, $\dot{\varphi} = \eta_2$, $\mu = \xi$, transform the system to the normal form

$$\begin{gathered} \dot{\eta}_1 = \eta_2, \quad \dot{\eta}_2 = -k^*\eta_1 - \eta_2 + \xi, \quad \dot{\xi} = f(\sigma, \rho, t), \\ \sigma = (k^*L^2 - 1)\eta_1 + (L^2 - M)\eta_2 - (n + L^2)\xi, \\ \rho = (k^*L^2 + N)\eta_1 + (L^2 - M)\eta_2 - (n + L^2)\xi. \end{gathered} \tag{3.7}$$

When $t \leq t_*$, (3.3), is written as $f(\sigma, \rho, t) = \frac{\sigma}{W}$, and when $t > t_*$, (3.4) is written as $f(\sigma, \rho, t) = \frac{\rho}{W}$ $(K = \frac{1}{W})$.

When $t \leq t_*$ the solution to (3.7) is determined by the roots of the characteristic equation

$$\lambda^3 + 3\delta\lambda^2 + 3\delta^2\lambda + \delta^3 = (\lambda + \delta)^3 = 0$$

and takes the form

$$\eta_1 = \left[\eta_{10} + (\sigma\eta_{10} + \eta_{20})\, t + \frac{1}{2}\{\xi_0 + (\delta^2 - k^*)\,\eta_{10} + (2\delta - 1)\,\eta_{20}\}\, t^2\right] e^{-\delta t},$$

$$\eta_2 = \left[\eta_{20} + \{\xi_0 - k^*\eta_{10} + (\delta - 1)\,\eta_{20}\}\, t - \right.$$

$$\left. - \frac{\delta}{2}\{\xi_0 + (\delta^2 - k^*)\,\eta_{10} + (2\delta - 1)\,\eta_{20}\}\, t^2\right] e^{-\delta t}, \tag{3.8}$$

$$\xi = \left[\xi_0 + \{(5\delta^2 + 3\delta + k^* - 1)\,\eta_{20} + (3\delta k^* - k^* - \delta^3)\,\eta_{10} - (2\delta - 1)\,\xi_0\}\, t + \right.$$

$$\left. + \frac{\delta^2 + k^* - \delta}{2}\{\xi_0 + (\delta^2 - k^*)\,\eta_{10} + (2\delta - 1)\,\eta_{20}\}\, t^2\right] e^{-\delta t}.$$

When $t > t_*$, the solution to (3.7) is determined by the roots of

$$\bar{\Delta}(\mu) = \begin{vmatrix} -\mu, & 1, & 0 \\ -k^*, & -1-\mu, & 1 \\ \frac{k^* L^2 + N}{W}, & \frac{L^2 - M}{W}, & -\frac{L^2+n}{W} - \mu \end{vmatrix} = (\mu + \delta)^3 - \delta^3 (N+1) = 0. \tag{3.9}$$

Let us consider these roots. One, μ_3, which is positive, is clearly

$$\mu_3 = \delta\left(\sqrt[3]{1+N} - 1\right). \tag{3.10}$$

The two other roots are given by

$$\mu_1, \mu_2 = -\frac{\sqrt[3]{1+N}+2}{2}\,\delta \pm i\,\frac{\sqrt{3\sqrt[3]{(1+N)^2}}}{2}\,\delta. \tag{3.11}$$

Before writing out the solution to (3.7) here we find t_*. From the above we should consider (1.10). It takes the form

$$\bar{\Delta}_{11}(\mu_3)\,\eta_1(t) + \bar{\Delta}_{21}(\mu_3)\,\eta_2(t) + \bar{\Delta}_{31}(\mu_3)\,\xi(t) = 0. \tag{3.12}$$

(3.9) gives

$$\bar{\Delta}_{11}(\mu_3) = \frac{tN}{W\mu_3} - k^*,\ \bar{\Delta}_{21}(\mu_3) = \mu + 3\delta - 1,\ \bar{\Delta}_{31}(\mu_3) = 1.$$

The sought equation, corresponding with this and with (3.6) and (3.8), is

$$At^2 + Bt + C = 0, \tag{3.13}$$

where

$$A = \left[\frac{N}{W\mu_3} - \delta(\mu_3 + 3\delta) + \delta^2\right][(\delta^2 - k^*)\eta_{10} + (2\delta - 1)\eta_{20} + \xi_0],$$
$$B = \frac{N}{W\mu_3}(\delta\eta_{10} + \eta_{20}) + (\mu_3 + 3\delta)\{\xi_0 - k^*\eta_1 + (\delta - 1)\eta_{20}\} -$$
$$- \delta\{2\xi_0 + (\delta^2 - 2k^*)\eta_{10} + (3\delta - 2)\eta_{20}\}, \qquad (3.14)$$
$$C = \xi_0 + \left(\frac{N}{W\mu_3} - k^*\right)\eta_{10} + (\mu_3 + 3\delta - 1)\eta_{20}.$$

We shall transform the coefficients in (3.14) to a new form. For this we introduce a fresh parameter z, given by

$$\sqrt[3]{1+N} - 1 = z. \qquad (3.15)$$

Then we have

$$\frac{N}{W\mu_3} - \delta(\mu_3 + 3\delta) + \delta^2 = \delta^2(1+z)^2.$$

Returning to (3.14) we finally get the coefficients in (3.13) as

$$A = \frac{\delta^2(1+z)^2}{2}[(\delta^2 - k^*)\eta_{10} + (2\delta - 1)\eta_{20} + \xi_0],$$
$$B = [\delta^3(z^2 + 3z + 2) - k^*\delta(1+z)]\eta_{10} + \qquad (3.16)$$
$$+ [\delta^2(z^2 + 4z + 2) - \delta]\eta_{20} + \delta(1+z)\xi_0,$$
$$C = [\delta^2(z^2 + 3z + 3) - k^*]\eta_{10} + [\delta(z+3) - 1]\eta_{20} + \xi_0.$$

Let us consider a particular case corresponding to (3.6), e.g. the following figures

$$\delta = 0{,}4,\ n = 0,\ W = 15{,}6,\ M = 2{,}5,\ L^2 = 3{,}12,\ k^* = 0{,}32,\ N = 1. \qquad (3.17)$$

Then from (3.15) z = 0.26. Suppose $\eta_{10} = \eta_{20} = 10$, $\xi_0 = 5$. Then from (3.16) we have A = −1.09, B = = −1.34, C = 0.95.

The root of (3.13) of interest to us is t = 0.505. Further, from (3.10) and (3.11) we get

$$\mu_3 = 0{,}104,\quad \mu_1, \mu_2 = -p \pm qi,\quad p = 0{,}652,\ q = 0{,}436. \qquad (3.19)$$

The regulator reversal at $t = t_*$ causes the subsequent transient to be defined by

$$\eta_1 = -\frac{\overline{\Delta}_{11}(\mu_1)\eta_1(t_*) + \Delta_{21}\eta_2(t_*) + \Delta_{31}\xi(t_*)}{\overline{\Delta}'(\mu_1)} e^{\mu_1 t} -$$
$$- \frac{\overline{\Delta}_{11}(\mu_2)\eta_1(t_*) + \overline{\Delta}_{21}(\mu_2)\eta_2(t_*) + \overline{\Delta}_{31}(\mu_2)\xi(t_*)}{\overline{\Delta}'(\mu_2)} e^{\mu_2 t},$$

$$\eta_2 = -\frac{\bar{\Delta}_{12}(\mu_1)\eta_1(t_*) + \bar{\Delta}_{22}(\mu_1)\eta_2(t_*) + \bar{\Delta}_{32}(\mu_1)\xi(t_*)}{\bar{\Delta}'(\mu_1)} e^{\mu_1 t} -$$
$$-\frac{\bar{\Delta}_{12}(\mu_2)\eta_1(t_*) + \bar{\Delta}_{22}(\mu_2)\eta_2(t_*) + \bar{\Delta}_{32}(\mu_2)\xi(t_*)}{\bar{\Delta}'(\mu_2)} e^{\mu_2 t},$$
$$\xi = -\frac{\bar{\Delta}_{13}(\mu_1)\eta_1(t_*) + \bar{\Delta}_{23}(\mu_1)\eta_2(t_*) + \bar{\Delta}_{33}(\mu_1)\xi(t_*)}{\bar{\Delta}'(\mu_1)} e^{\mu_1 t} -$$
$$-\frac{\bar{\Delta}_{13}(\mu_2)\eta_1(t_*) + \bar{\Delta}_{23}(\mu_2)\eta_2(t_*) + \bar{\Delta}_{33}(\mu_2)\xi(t_*)}{\bar{\Delta}'(\mu_2)} e^{\mu_2 t}.$$

These formulae can be simplified, bearing in mind (3.12). In particular, to draw up the transient response we need write only the expression for η_1:

$$\eta_1 = -\frac{[\bar{\Delta}_{11}(\mu_1) - \bar{\Delta}_{11}(\mu_3)]\eta_1(t_*) + [\bar{\Delta}_{21}(\mu_1) - \bar{\Delta}_{21}(\mu_3)]\eta_2(t_*)}{\bar{\Delta}'(\mu_1)} e^{\mu_1 t} -$$
$$-\frac{[\bar{\Delta}_{11}(\mu_2) - \bar{\Delta}_{11}(\mu_3)]\eta_1(t_*) + [\bar{\Delta}_{21}(\mu_1) - \bar{\Delta}_{21}(\mu_3)]\eta_2(t_*)}{\bar{\Delta}'(\mu_2)} e^{\mu_2 t}.$$

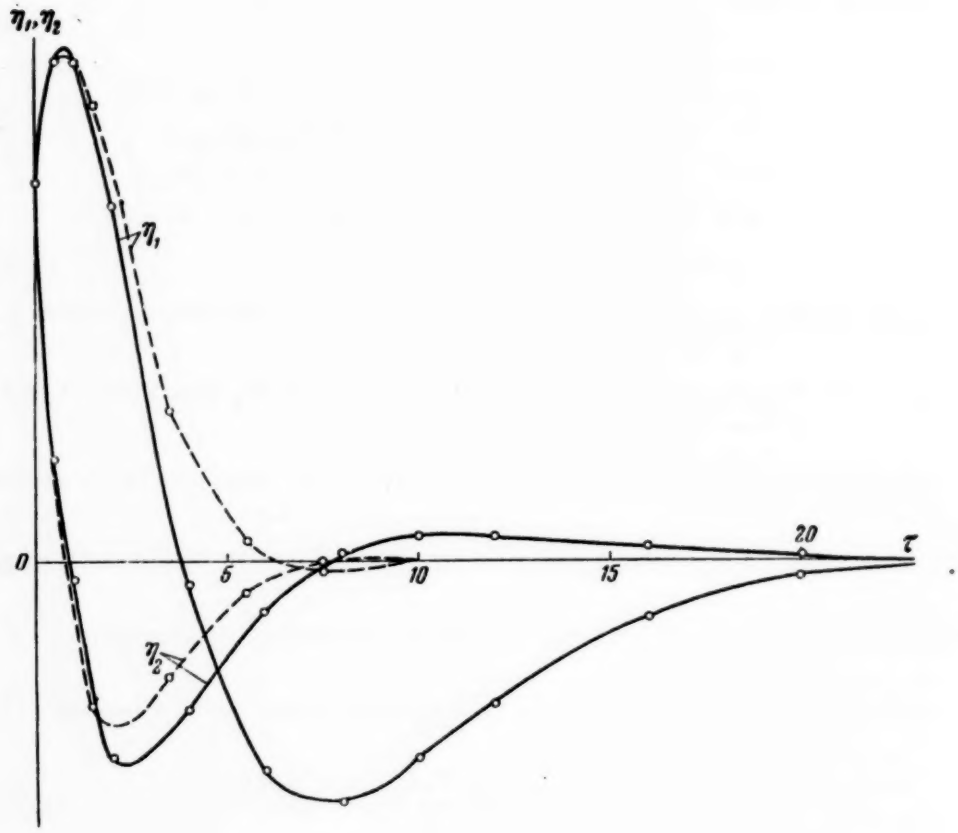

Fig. 5

Further, we have

$$\tilde{\Delta}_{11}(\mu_s) - \bar{\Delta}_{11}(\mu_3) = \frac{\mu_3 - \mu_s}{W\mu_3\mu_s} \quad (s = 1, 2).$$

Finally, we get

$$\eta_{11} = \frac{1}{\mu_2 - \mu_1}\left[\{\mu_2\eta_{11}(t_*) - \eta_{12}(t_*)\}\, e^{\mu_1 t} + \{-\mu_1\eta_{11}(t_*) + \eta_{12}(t_*)\}\, e^{\mu_2 t}\right].$$

Taking (3.18) into account we can now put the expressions for ξ, η_1, η_2, into forms suitable for graphical construction.

Figure 5 shows the graphs. The full lines represent the transients in a system optimal by Bulgakov's criterion, while the dashed curves are for that in a conditionally stable system.

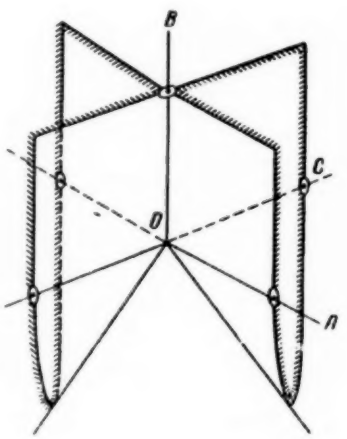

Fig. 6.

It is clear that in the conditional system the transient is virtually finished at $t^* \leq 10$, while in a Bulgakov optimal system it persists to $t > 20$.

The Figure also shows that the system of (3.1) can, as we supposed, be converted successfully to a conditionally stable one. We have three comments to make on this example.

Firstly, the conversion is only possible if (3.13) has at least one real positive root. It is necessary and sufficient for this for any one of the coefficients in (3.13) to be negative and the condition $B^2 \geq 4$ AC to be fulfilled.

Let δ, $\underline{z}$, and k^* be chosen numbers. Then (3.16) may be considered as formulae for transforming the space of η_{10}, η_{20}, ξ_0 into that of A, B, C and vice versa. Evidently, for any A, B, C falling within the cone $B^2 = 4$ AC (Figure 6) and for the space enclosed by the planes A = 0, C = 0 (denoted by cross-hatching) will remain within the frame-work of this optimality criterion; at all other values of A, B and C the system may be made conditionally stable.

Secondly, as previously, N can be chosen arbitrarily, and an endeavor to obtain still shorter transient damping times made. (3.11) shows that this can be done by increasing N.

But N cannot be increased without limit. The choice must be made to correspond with the conditions for an optimal system when the initial perturbations η_{10}, η_{20}, ξ_0 are selected arbitrarily. If the computer could analyze the solution to (3.13) and produce an N corresponding to optimal transient response then a strictly linear system would be self-adjusting. Finally, the latter remarks are applicable to extending the present arguments to nonlinear systems. This topic will form the subject of a separate paper.

SUMMARY

It has been shown that a strictly linear system designed to accord with any preconceived criterion of optimum quality can be altered to provide damping within the first swing by converting it to one which is conditionally stable. The conditional damping in such a system will be substantially less than in the initial one.

This result is obtained without any essential alteration in existing systems by adding a computer of simple design.

The author is indebted to V. A. Kotelnikov and B. V. Shirokorad for valuable comments and advice.

Received February 26, 1957

LITERATURE CITED

[1] V. A. Maslennikov, Qualitative control of a neutral object using an astatic regulator. Automation and Remote Control 17, No. 2 (1956).*

[2] A. M. Lyapunov, The general problem of motional stability. (State Tech. Press, 1950).**

[3] H. J. Behnke, Über ein Verfahren zur unstetigen Regelung von Schwingungen. Fachtagung Regelungstechnik, Heidelberg (1956).

[4] L. M. Silva, Anticipatory control provides optimal automatic controller operation. Machine Design, No. 8 (1956).

[5] N. G. Chetaev, Motional stability. (State Tech. Press, 1956).**

[6] A. A. Feldbaum, Electrical automatic control systems. (State Defense Press, 1954).**

[7] B. V. Bulgakov, Oscillations. (State Tech. Press, 1954).**

[8] A. M. Letov, Stability in nonlinear controlled systems. (State Tech. Press, 1955).**

[9] A. I. Lurye, Operational calculus. (State Tech. Press, 1950).**

* [See C. B. Translation.]

** [In Russian.]

DEFINITION OF AN OPTIMAL LINEAR DYNAMIC SYSTEM FROM AN EXTREMUM CRITERION APPLIED TO A PARTICULAR FORM OF FUNCTIONAL

N. I. Andreev

(Kharkov)

A method is proposed for determining the dynamic system which corresponds to an extremum of a functional which can be represented as a differentiable function of several square functionals of the unit pulse transient function of the system. The necessary condition for the functional to have an extremum is deduced.

The criteria to be used for comparing dynamic systems depend on the problems the systems are designed to solve. In many practical problems (e.g., self-regulation) convenient criteria are the spread in the system error or the initial second-order moment of this error (mean-square error). Methods of selecting dynamic systems from the first criterion have been dealt with in several papers [1-4, etc.]. The second, more general criterion has been dealt with similarly [5-7, etc.]. The necessary and sufficient conditions for these parameters (criteria) to be minimal have been given, and methods of determining the corresponding optimal operators have been developed.

The present communication presents a more general criterion, which includes the two above as particular cases, for the same purpose.

The method of selection depends on the problem the system deals with, on the operating conditions, on the criterion used and on the class of permissible systems. We shall first take this class to be linear systems given a unit pulse transient function $k(t, \tau)$ to this perturbation. In general $k(t, \tau)$ depends on time t as on a parameter. Therefore t will in future be omitted.* The dispersion $D = \sigma^2$ [1-5, 8] is a square functional I_1 of $k(\tau)$. This means that $I_1 = I_1[k(\tau)]$ has the following property [8]:

$$I_1[k_0(\tau) + \Delta\kappa(\tau)] = A_0 + A_1\Delta + A_2\Delta^2,$$

where A_0, A_1 and A_2 are certain numbers dependent on $k_0(\tau)$ and $\kappa(\tau)$ $k_0(\tau)$, $\kappa(\tau)$ being arbitrary functions from the class of permissible functions.

The square of the mathematically expected error for a linear system, a^2, is also a square functional $I_2 = I_2[k(\tau)]$ of $k(\tau)$. The initial second-order moment of the system error is $I_1 + I_2$, i.e., is also a square functional.

* τ is here the time-interval between the given time and the time when the unit pulse perturbation acts.

In certain cases a more accessible selection criterion may be the functional I, which can be represented as a given function of n + 1 square functionals $I_1 = I_1[k(\tau)], \ldots, I_{n+1} = I_{n+1}[k(\tau)]$. For example, if we take the selection criterion to be the probability that the error distribution will not exceed a given value $\underline{c}$ in modulus, and assume the error distribution normal, the mathematical expression for the criteria is

$$I = \frac{1}{\sqrt{2\pi}\,\sigma}\int_{-c}^{c} e^{-\frac{(a-x)^2}{2\sigma^2}}\,dx = I(a^2, \sigma^2), \tag{1}$$

where $a = a[k(\tau)]$ is the mathematically expected error, $\sigma = \sigma[k(\tau)]$ is the mean-square deviation of the system error. Then I is a function of the two square functionals a^2 and σ^2, i.e., n = 1.

Let us suppose that in general I is a differentiable function of n + 1 functionals

$$I_i = I_i[k(\tau)] \quad (i = 1, 2, \ldots, n+1).$$

The necessary condition which the $k_0(\tau)$ which corresponds to an optimal system (i.e., a system which has an extremum in I) must satisfy is that the first variation of I must be zero. We write this as

$$\left.\frac{dI[k^0(\tau) + \Delta\varkappa(\tau)]}{d\Delta}\right|_{\Delta=0} = 0, \tag{2}$$

where $\varkappa(\tau)$ is an arbitrary function of this class.

Since $I_i = I_i[k(\tau)]$, (2) may be written in developed form as

$$\left.\frac{\partial I}{\partial I_1}\frac{dI_1}{\Delta}\right|_{\Delta=0} + \cdots + \left.\frac{\partial I}{\partial I_{n+1}}\frac{dI_{n+1}}{d\Delta}\right|_{\Delta=0} = 0. \tag{3}$$

Let $\frac{\partial I}{\partial I_{n+1}} \neq 0$ when I_{n+1} changes in some region $I_{n+1} = I^0_{n+1} = I_{n+1}[k^0(\tau)]$. (The particular case where for some $k(\tau)$ all the $\frac{\partial I}{\partial I_i}$ $(i = 1, 2, \ldots, n+1)$ are zero also satisfies (3) and can be studied as a special case). Then (3) can be written as

$$\frac{\partial I}{\partial I_1}\Big/\frac{\partial I}{\partial I_{n+1}}\left(\frac{dI_1}{d\Delta}\right)_{\Delta=0} + \cdots + \frac{\partial I}{\partial I_n}\Big/\frac{\partial I}{\partial I_{n+1}}\left(\frac{dI_n}{d\Delta}\right)_{\Delta=0} + \left(\frac{dI_{n+1}}{d\Delta}\right)_{\Delta=0} = 0. \tag{4}$$

If I has an extremum for some $k^0(\tau)$ then (4) may be written as

$$a_1\left(\frac{dI_1}{d\Delta}\right)_{\Delta=0} + \cdots + a_n\left(\frac{dI_n}{d\Delta}\right)_{\Delta=0} + \left(\frac{dI_{n+1}}{d\Delta}\right)_{\Delta=0} = 0, \tag{5}$$

where the a_i are numbers given by

$$a_i = \frac{\partial I}{\partial I_i} \Big/ \frac{\partial I}{\partial I_{n+1}}. \tag{6}$$

Here I, the I_i and their derivatives are computed for $k(\tau) = k^0(\tau)$.

Equation (5) can also be put as

$$\frac{dI_{II}[k^0(\tau) + \Delta x(\tau)]}{d\Delta}\Big|_{\Delta=0} = 0, \tag{7}$$

where $I_{II} = a_1 I_1 + \ldots + a_n I_n + I_{n+1}$ is a square functional of $k(\tau)$. (7) is the condition that I_{II} turns at an extremum. Thus the problem of finding the extremum of I reduces to doing the same for I_{II}, which depends on the n undetermined parameters a_i.

In general the extremum of a square functional is found by approximation, e.g., by the canonical expansion method of Pugachev [5-7], or Kantorovich's steepest descent method [8].

When finite solutions exist for the extremum of I_{II} and for the $k^0_{II}(\tau)$ corresponding to this [1, 3, 4],

$$k^0_{II}(\tau) = k^0_{II}(a_1, \ldots, a_n, \tau), \tag{8}$$

the search for the extremum of I and the $k^0(\tau)$ which provides this extremum leads to the problem of solving a system of equations deriving from (6):

$$a_i = \left(\frac{\partial I}{\partial I_i} \Big/ \frac{\partial I}{\partial I_{n+1}}\right)_{k(\tau)=k^0_{II}(\tau)} = f_i(a_1, \ldots, a_n) \quad (i = 1, 2, \ldots, n). \tag{6a}$$

Equation (6a) is either algebraic or transcendental, and may not have a unique solution. When (6a) has several solutions all must be studied at the extremum in I.

When the extremum of I_{II} has no solution of finite form, (8), for the relation of k^0_{II} to the a_i, is found by one of the above approximate methods, the solution to (6a) then being derived, i.e., the a_i are evaluated to correspond to the extremum in I.

When n is large the above operations with I and $k^0(\tau)$ involve laborious and involved calculations. Another method of evaluating the coefficients at the extremum in I may then be more convenient. This method will now be presented.

Let a solution for the extremum in I_{II} be known. This solution depends on n unknown parameters

$$k^0_{II}(\tau) = k^0_{II}(a_1, \ldots, a_n, \tau).$$

The extremum in I is found in a class of the k^0_{II} having a certain combination of the a_i. Thus to determine the extremum in I we have to find that of a function of n variables, $a_1, \ldots, a_n$:

$$F(a_1, \ldots, a_n) = I[k^0_{II}(a_1, \ldots, a_n, \tau)]. \tag{9}$$

The extremum in F is found by a known method, by equating the partial derivatives of F with respect to the a_i to zero and solving the system of n equations in n variables thus obtained. But when the a_i are numerous and their relation to F complicated it is extremely difficult to do this. The approximate methods of solving a system of n equations do not always converge well. Thus the following approximate method of finding the extremum in $F = F(a_1, \ldots, a_n)$ is based on the method of steepest descent.

We are given the zero approximation, i.e., the assembly

$$a_i = a_{i0} \quad (i = 1, 2, \ldots, n).$$

Then we seek the normalized combination of numbers b_{i0} such that the derivative

$$\left.\frac{dF(a_{10} + \Delta b_{10}, \ldots, a_{n0} + \Delta b_{n0})}{d\Delta}\right|_{\Delta=0} \tag{10}$$

is maximal. As norm of the combinations of the b_{i0} we take the sum of their squares: $b_{10}^2 + \ldots + b_{n0}^2$. The sought combination of the b_{i0} determines the direction of the gradient of F at $(a_{10}, \ldots, a_{n0})$ in an n-dimensional space. On the condition $b_{10}^2 + \ldots + b_{n0}^2 = \text{const}$ the extremum of (10) is determined as the unconditional extremum of

$$\left(\frac{dF(a_{10} + \Delta b_{10}, \ldots, a_{n0} + \Delta b_{n0})}{d\Delta}\right)_{\Delta=0} + \lambda(b_{10}^2 + \cdots + b_{n0}^2). \tag{11}$$

A necessary condition that the b_{i0} must satisfy if (11) is to have an extremum is that the following are complied with

$$\left(\frac{\partial F(a_j)}{\partial a_i}\right)_{a_j = a_{j0}} + 2\lambda b_{i0} = 0 \quad \begin{pmatrix} i = 1, 2, \ldots, n \\ j = 1, 2, \ldots, n \end{pmatrix}. \tag{12}$$

Consequently, accurate to a constant factor, the sought b_{i0} are

$$b_{i0} = -\left(\frac{\partial F(a_j)}{\partial a_i}\right)_{a_j = a_{j0}} \quad \begin{pmatrix} i = 1, 2, \ldots, n \\ j = 1, 2, \ldots, n \end{pmatrix}. \tag{13}$$

So for our first approximation for the a_i we should take

$$a_{i1} = a_{i0} + \Delta_1 b_{i0} \quad (i = 1, 2, \ldots, n), \tag{14}$$

where the multiplier Δ_1 is determined from the condition of turning at an extremum in

$$\varphi(\Delta) = F(a_{10} + \Delta b_{10}, \ldots, a_{n0} + \Delta b_{n0}). \tag{15}$$

If $\varphi(\Delta)$ has several extrema all the corresponding Δ are investigated. These Δ can be determined analytically or graphically, depending on the form of $\varphi(\Delta)$.

The second and subsequent approximations for the a_i at the extremum in $F(a_1, \ldots, a_n)$ are found by analogy.

Calculations for particular cases with n from 3 to 5 have shown good convergence (the fourth approximation usually gave satisfactory results).

The case considered above was one where the class of system from which selection is permissible was taken as one of given unit pulse transient functions. But it is sometimes convenient to take the class as one with given finite numbers of parameters, e.g., a system described by ordinary differential equations. Here to find the optimum assembly of system parameters we can use the above successive approximations method. To do this we must put down an explicit expression for the criterion selected in terms of the system parameters and determine the assembly of parameters ensuring an extremum in the criterion, which is here a known function of many variables (the system parameters) by the above method.

The existence and uniqueness of extrema in functionals are not considered here. These problems may comprise the subject of future studies.

Solutions can often be obtained from physical considerations essential to the case in practical problems.

We will trace out the method of passing from I to I_{II} using a very simple example. Suppose I takes the form $I = 1/(\sigma \exp[-a^2/2\sigma^2])$, where a and σ are the mathematical expectation and mean-square deviation in the system error respectively. Then $n = 1$, so the accessory functional I_{II} (see(7)) may be put as

$$I_{II} = a_1 a^2 + \sigma^2, \tag{7a}$$

where, from (6a),

$$a_1 = \frac{\partial I}{\partial a^2} \Big/ \frac{\partial I}{\partial \sigma^2} = \left(1 - \frac{a^2}{\sigma^2}\right)^{-1}.$$

If the function $k_{II}^0(\tau)$ providing an extremum in (7a) can be expressed in finite form as $k_{II}^0(\tau) = k_{II}^0(a_1, \tau)$ then (6a) will here be

$$a_1 = \left(1 - \frac{a^2(a_1)}{\sigma^2(a_1)}\right)^{-1},$$

where $a^2(a_1) = a^2[k_{II}^0(a_1, \tau)]$, $\sigma^2(a_1) = \sigma^2[k_{II}^0(a_1, \tau)]$ are known functions of a_1. F[see (9)] here takes the form

$$F(a_1) = \frac{1}{\sigma(a_1)} e^{-\frac{a^2(a_1)}{2\sigma^2(a_1)}}.$$

The value if a_1 corresponding to the maximum in I is here readily determined.

SUMMARY

The search for an optimal linear dynamic system corresponding to an extremum in the type of functional considered can lead to the problem of finding a linear dynamic system which ensures an extremum in a certain square functional which includes several undetermined (artificially introduced) coefficients.

Received September 20, 1956

LITERATURE CITED

[1] V. V. Solodnikov, Introduction to the statistical dynamics of automatic control systems. (State Tech. Press, 1952).*

[2] N. Wiener, Extrapolation, interpolation and smoothing of stationary time series (1949).

[3] V. M. Semenov, Theory of extrapolation of random processes. Collection of scientific papers from the Zhukovsky Air Force Academy (1934).

[4] L. Zadeh and J. Ragazzini, An extension of Wiener's theory of Prediction. Journ. Appl. Physics, vol. 21, No. 27 (1950).

[5] V. S. Pugachaev, General synthesis theory for dynamic systems allowing for random perturbations. Collection of scientific papers from the Zhukovsky Air Force Academy (1934).

[6] V. S. Pugachaev, A general condition for minimum mean square error in a dynamic system. Automation and Remote Control 17, No. 4 (1956).**

[7] V. S. Pugachaev, Application of canonical expansions of random functions to the determination of optimal linear systems. Automation and Remote Control 17, No. 6 (1956).**

[8] L. V. Kantorovich, Functional analysis and applied mathematics. Prog. Math. Sci 3, No. 6 (28) (1948).

* [In Russian.]

** [See C. B. Translation.]

THE EQUATION FOR DETERMINING THE DISTRIBUTION LAW FOR THE INTEGRAL OF A SYSTEM OF ORDINARY DIFFERENTIAL EQUATIONS CONTAINING RANDOM PARAMETERS

B. G. Dostupov and V. S. Pugachev

(Moscow)

A general equation is deduced which defines the probability density for the integral of a system of ordinary differential equations containing random parameters, and one possible way of integrating this equation convenient for use with computers is indicated. When the distribution law has been found all the necessary moments of the integral can be found from the usual probability theory formulae, in particular the mathematical expectation and the correlation matrix. The method presented can also be applied to differential equations containing random functions if all such random functions appearing are approximated by finite sections of their canonical expansions. The method is applicable to any system of ordinary differential equations provided all the functions appearing are continuous relatively unknown functions having piecewise-continuous derivatives with respect to all the unknown functions. This method, being complex and laborious in calculation, is mostly at present of theoretical importance as a possible starting-point for developing new methods of statistical analysis for nonlinear systems.

INTRODUCTION

Differential equations containing random parameters or functions are frequently encountered in practical problems, particularly in the theory of automatic control. With equations linear in the unknowns and in the random parameters and functions the problem of determining the moments of the integrals has been finally solved in a general form [1-3]. But the differential equations found in practical problems are often nonlinear. Various current automatic systems present us with many examples of this. If all the functions in the equations are continuous and have partial derivatives with respect to the unknowns and to the random parameters and functions which are continuous, we can frequently assume that for any given value of the independent variable all the functions differ but little from linear within the practically possible ranges of the arguments. Linearization [1, 2] can then be used successfully to determine the probability characteristics of the integrals approximately. Latterly the linearization method has been generalized to the case where the functions need not be differentiable but only need be continuous [4]. The normal linearization method is completely inapplicable if the equation contains essentially nonlinear functions, e.g., discontinuous ones. Such equations are particularly common in automatic control theory, since the systems contain elements with discontinuous characteristics. The same applies when the functions, although differentiable and continuous are highly nonlinear in all practical possible ranges of the random arguments. Hence the problem of determining the probability characteristics of integrals of differential equations containing essentially nonlinear functions is very important in the theory of random functions. This problem has latterly been considered by Kazakov [6-8] who has developed a fairly general approximate method of determining the probability characteristics for integrals of differential equations containing essentially nonlinear functions, including discontinuous ones. Kazakov's statistical

linearization method is at present the simplest and most general method for probability studies on nonlinear systems. It is in particular incomparably simpler as regards computation than the method of moments proposed [2].

The linearization methods (normal and statistical) are evidently sufficient for practical problems of probability analysis for dynamic systems of known structure and parameters, where the probability characteristics have to be determined. As regards system synthesis, in which both structure and parameters have to be determined to obtain what are in some sense optimal probability characteristics, the linearization methods may be too rough. So the probability analysis of ordinary differential equations containing essentially nonlinear functions cannot at present be considered adequately developed for practical purposes. A particularly important problem is that of determining distribution laws for the integrals of differential equations containing random functions.

Canonical expansion theory applied to random functions is extremely fruitful in developing a linearization method. This is because any such expansion for a random function (including a vector one) of the form

$$X(t) = m_x(t) + \sum_r V_r u_r(t) \tag{1}$$

expresses the random function via normal random quantities $V_1, V_2, \ldots$. When the expansion of (1) replaces $X(t)$ in the differential equations, $V_1, V_2, \ldots$ enter the equations as parameters, so all methods in the theory of differential equations applicable to those containing parameters apply. Thus by using canonical expansions the problem of determining integral distribution laws for equations with random functions reduces to that for equations with random parameters. So for practical purposes we only need a method of determining distribution laws for differential equations with random parameters.

1. The Equation Determining the Distribution Law for the Integral of a System of Ordinary Differential Equations

Let us consider a system of ordinary differential equations reduced to normal form:

$$\frac{dY_\lambda}{dt} = f_\lambda(t, Y_1, \ldots, Y_n, V_1, \ldots, V_m) \quad (\lambda = 1, \ldots, n), \tag{2}$$

which can be written in the short form

$$\frac{dY_\lambda}{dt} = f_\lambda(t, Y_\mu, V_\nu) \quad (\lambda = 1, \ldots, n), \tag{3}$$

where $V_1, \ldots, V_m$ are random parameters.

We assume given the probability density $p_0(y_\lambda, v_\nu)$ for the system for the initial values Y_λ^0 of the Y_λ at $t = t_0$, and of the V_ν. We are required to determine $p(y_\lambda, v_\nu, t)$ for the integral of (3). For this we suppose that all the f_ν have piecewise-continuous bounded first-order partial derivatives with respect to the y_μ.

Let Y_λ^1 denote the value of Y_λ at $t + \Delta t$. Then (3) gives

$$Y_\lambda^1 = Y_\lambda + f_\lambda(t, Y_\mu, V_\nu)\,\Delta t + o(\Delta t) \quad (\lambda = 1, \ldots, n). \tag{4}$$

The Y^1_λ are functions of the random quantities Y_μ and V_ν. Thus using certain formulae from probability theory [9] which define the distribution laws for functions of random argument, we may write

$$p(y_\lambda, v_\nu, t) = p[y_\lambda + f_\lambda(t, y_\mu, v_\nu)\Delta t + o(\Delta t), v_\nu, t + \Delta t] \left| \frac{\partial(y_1^1, \ldots, y_n^1)}{\partial(y_1, \ldots, y_n)} \right|, \tag{5}$$

where the Jacobian $\left| \frac{\partial(y_1^1, \ldots, y_n^1)}{\partial(y_1, \ldots, y_n)} \right|$ is from (4) defined by

$$\frac{\partial(y_1^1, \ldots, y_n^1)}{\partial(y_1, \ldots, y_n)} = \begin{vmatrix} 1 + \frac{\partial f_1}{\partial y_1}\Delta t + o(\Delta t); & \frac{\partial f_1}{\partial y_2}\Delta t + o(\Delta t); \ldots & \frac{\partial f_1}{\partial y_n}\Delta t + o(\Delta t) \\ \frac{\partial f_2}{\partial y_1}\Delta t + o(\Delta t); & 1 + \frac{\partial f_2}{\partial y_2}\Delta t + o(\Delta t); \ldots & \frac{\partial f_2}{\partial y_n}\Delta t + o(\Delta t) \\ \ldots\ldots\ldots\

Passing to the limit $\Delta t \to 0$ we get a linear equation in partial derivatives for the sought p:

$$\frac{\partial p}{\partial t} + \sum_{\mu=1}^{n} \frac{\partial (f_\mu p)}{\partial y_\mu} = 0 \tag{9}$$

or in explicit form

$$\frac{\partial p(y_\lambda, v_\nu, t)}{\partial t} + \sum_{\mu=1}^{n} \frac{\partial}{\partial y_\mu} [f_\mu(t, y_\lambda, v_\nu)\, p(y_\lambda, v_\nu, t)] = 0. \tag{10}$$

At $t = t_0$ $p(y_\lambda, v_\nu, t)$ must be the same as $p_0(y_\lambda, v_\nu)$ for the system of Y_λ^0 values of the Y_λ and V_ν. So the problem of determining the distribution law for the system of (2) leads to Cauchy's • problem for (9).

By using the theory of integral invariants, (9), or what is the same, (10), can be derived in another way. To this end we consider the motion of a dynamic system corresponding to (2) in phase space for given fixed values v_ν of the V_ν. Let us consider all possible motions for which the image point lies in the region Σ_1 at $t = t_1$. If Σ_1 contains no singular points of (2) then one and only one integral curve of (2) will pass through each point in this region. The assembly of image points for $t = t_2$ on these curves will form some region Σ_2. If none of these integral curves passes through a singular point of (2) during $t_1 \leq t \leq t_2$ there will be a unique relation between the points in Σ_1 and Σ_2. If at $t = t_1$ the image point is in Σ_1 then at $t = t_2$ it is obliged to be in Σ_2. And conversely, if it is in Σ_2 at $t = t_2$ it must have been in Σ_1 at $t = t_1$. So the conditional probability of finding the point in Σ_1 at $t = t_1$ for fixed values v_ν of the V_ν is equal to that of finding it in Σ_2 at $t = t_2$ with the same values v_ν for the V_ν. So using $\psi(y_\lambda; t \mid v_\nu)$ to denote the conditional probability density of the integral Y_λ for (2) at time t, we can put

$$\int\cdots\int_{\Sigma_1} \psi(y_\lambda; t_1 \mid v_\nu)\, dy_1 \cdots dy_n = \int\cdots\int_{\Sigma_2} \psi(y_\lambda; t_2 \mid v_\nu)\, dy_1 \cdots dy_n. \tag{11}$$

This implies that the probability is here an integral invariant of order n for (2), with fixed v_ν values for the V_ν. So from a theorem on integral invariants [12] $\psi(y_\lambda; t_1 \mid v_\nu)$ is a post multiplier•• of the system

$$\frac{dy_1}{f_1} = \cdots = \frac{dy_n}{f_n} = \frac{dt}{1} \tag{12}$$

• I. e., the search for some partial solution of (9).

•• Let $\varphi_1, \ldots, \varphi_{n-1}$ be a system of $n-1$ independent first integrals of (2). Then any other integral $\varphi(y_1, \ldots, y_n)$ must satisfy the necessary condition

$$J_a = \frac{\partial(\varphi_1, \ldots, \varphi_{n-1}, \varphi)}{\partial(y_1, \ldots, y_n)} = 0.$$

Let the A_j be the minors of Ja corresponding to the element $\frac{\partial \varphi}{\partial y_j}$. Then the post multiplier of (1) is

$\frac{A_1}{f_1} = \ldots = \frac{A_n}{f_n} = M$. (Editor's note).

and so must satisfy the equation in partial derivatives

$$\frac{\partial \psi}{\partial t} + \sum_{\lambda=1}^{n} \frac{\partial (f_\lambda \psi)}{\partial y_\lambda} = 0. \tag{13}$$

By multiplying (12) by the probability density $\varphi(v_\nu)$ for the random parameters V_ν, and remembering that

$$\varphi(v_\nu)\, \psi(y_\lambda; t \mid v_\nu) = p(y_\lambda; v_\nu, t), \tag{14}$$

we arrive at (9).

We note that (9) and (13) differ only in the unknown function symbol. So $p(y_\lambda, v_\nu, t)$ and $\psi(y_\lambda, t \mid v_\nu)$ are integrals of the same equation in partial derivatives.

2. Integration of (9).

If a general integral of (2) is known the desired distribution law can be found directly from formulae in the theory of probability. In fact, suppose

$$y_\mu = \varphi_\mu(t, v_\nu, t_0, y_\lambda^0) \quad (\mu = 1, 2, \ldots, n) \tag{15}$$

is the integral of

$$\dot{y}_\mu = f_\mu(t, y_\mu, v_\nu) \quad (\mu = 1, 2, \ldots, n). \tag{16}$$

satisfying the initial condition

$$t = t_0, \quad y_\mu = y_\mu^0 \quad (\mu = 1, 2, \ldots, n), \tag{17}$$

Then the solution of (15) for y_λ^0 will be expressed in terms of the same φ_μ in the form*

$$y_\mu^0 = \varphi_\mu(t_0, v_\nu, t, y_\lambda) \quad (\mu = 1, 2, \ldots, n), \tag{18}$$

So

$$p(y_\lambda, v_\nu, t) = p_0[\varphi_\mu(t_0, v_\nu, t, y_\lambda), v_\nu] \left| \frac{\partial (y_1^0, \ldots, y_n^0)}{\partial (y_1, \ldots, y_n)} \right|; \tag{19}$$

while the variables y_μ^0 in the Jacobian must be replaced by their expressions from (18). The same result is obtained of course if we integrate (9) by general methods from the theory first-order differential equations in

* See, for instance, [13].

partial derivatives. This theory also shows that to integrate (9) we should find n + 1 first integrals of a system of ordinary differential equations [10]:

$$\frac{dt}{1} = \frac{dy_1}{f_1} = \frac{dy_2}{f_2} = \cdots = \frac{dy_n}{f_n} = \frac{dp}{-p\sum\limits_{\lambda=1}^{n}\frac{\partial f_\lambda}{\partial y_\lambda}}. \tag{20}$$

This system differs from the initial one of (16) only in the extra equation

$$\frac{dp}{dt} = -p\sum_{\lambda=1}^{n}\frac{\partial f_\lambda}{\partial y_\lambda}. \tag{21}$$

As the n first integrals of (16), and hence of (20), we may take (18). Substituting (15) into (21) and integrating, we get

$$p = C\exp\left\{-\int_{t_0}^{t}\sum_{\lambda=1}^{n}\frac{\partial f_\lambda[\tau, \varphi_\mu(\tau, v_\nu, t_0, y_\varkappa^0), v_\nu]}{\partial\varphi_\lambda}d\tau\right\}. \tag{22}$$

Solving this equation for the arbitrary constant C and substituting for the $y_\varkappa^0$ for (18) we get the (n + 1)th first integral of (20):

$$C = p\exp\left\{\int_{t_0}^{t}\sum_{\lambda=1}^{n}\frac{\partial f_\lambda[\tau, \varphi_\mu(\tau, v_\nu, t_0, \varphi_\varkappa(t_0, v_\nu, t, y_\sigma)), v_\nu]}{\partial\varphi_\lambda}d\tau\right\}. \tag{23}$$

The general integral of (9) may now be given as

$$p\exp\left\{\int_{t_0}^{t}\sum_{\lambda=1}^{n}\frac{\partial f_\lambda}{\partial\varphi_\lambda}d\tau\right\} = F(\varphi_\mu(t_0, v_\nu, t, y_\lambda)), \tag{24}$$

where $F(y_\mu)$ is an arbitrary function of the n first integrals of (20) – i.e., (18). To determine F we use the initial condition

$$p(y_\lambda, v_\nu, t_0) = p_0(y_\lambda, v_\nu), \tag{25}$$

where p_0 is a given function. Putting $t = t_0$ in (24) and remembering that

$$\varphi_\mu (t_0, v_\nu, t_0, y_\lambda) = y_\mu \quad (\mu = 1, 2, \ldots, n), \tag{26}$$

we get

$$F (y_\mu) = p_0 (y_\mu, v_\nu). \tag{27}$$

Substituting this expression into (24) and solving for p, we finally get

$$p (y_\lambda, v_\nu, t) = p_0 [\varphi_\mu (t_0, v_\nu, t, y_\lambda), v_\nu] \exp \left\{ - \int_{t_0}^{t} \sum_{\lambda=1}^{n} \frac{\partial f_\lambda (\tau, \eta_\mu, v_\nu)}{\partial \eta_\mu} d\tau \right\}, \tag{28}$$

where for brevity we use the symbol

$$\eta_\mu = \varphi_\mu [\tau, v_\nu, t_0, \varphi_\varkappa (t_0, v_\nu, t, y_\sigma)] \quad (\mu = 1, 2, \ldots, n). \tag{29}$$

To establish that (19) and (28) are exact it is sufficient to set up a system of equations which determine the derivatives of the integrals of (16) with respect to the initial values. Differentiating (16) with respect to the y_μ^0 we get

$$\frac{d}{dt} \left(\frac{\partial y_\lambda}{\partial y_\mu^0} \right) = \sum_{\varkappa=1}^{n} \frac{\partial f_\lambda}{\partial y_\varkappa} \frac{\partial y_\varkappa}{\partial y_\mu^0} \qquad (\mu, \lambda = 1, 2, \ldots, n). \tag{30}$$

Thus the $\frac{\partial y_\lambda}{\partial y_\mu^0}$ form a fundamental system of solutions to the system of linear differential equations

$$\frac{dz_\lambda}{dt} = \sum_{\varkappa=1}^{n} \frac{\partial f_\lambda}{\partial y_\varkappa} z_\varkappa \quad (\lambda = 1, 2, \ldots, n). \tag{31}$$

According to a formula due to Jacobi (see, for instance [10], vol. III, ch. 2, p. 438)

$$\frac{\partial (y_1, \ldots, y_n)}{\partial (y_1^0, \ldots, y_n^0)} = \exp \left\{ \int_{t_0}^{t} \sum_{\lambda=1}^{n} \frac{\partial f_\lambda [\tau, \varphi_\varkappa (\tau, v_\nu, t_0, y_\mu^0), v_\nu]}{d\varphi_\lambda} d\tau \right\}. \tag{32}$$

So

$$\frac{\partial(y_1^0, \ldots, y_n^0)}{\partial(y_1, \ldots, y_n)} = \frac{1}{\dfrac{\partial(y_1, \ldots, y_n)}{\partial(y_1^0, \ldots, y_n^0)}} = \exp\left\{-\int_{t_0}^{t} \sum_{\lambda=1}^{n} \frac{\partial f_\lambda [\tau, \varphi_\varkappa(\tau, v_\nu, t_0, y_\mu^0), v_\nu]}{\partial \varphi_\lambda} d\tau\right\}. \tag{33}$$

Substituting this expression into (19) and replacing the y_μ^0 by their expressions in terms of y_λ from (18) we get (28) – Q.E.D.

When (2) can be integrated in a general form the probability density of the integral can be found directly from (19),and (9) deduced, and its integration is of no practical value. But in most cases with arbitrary values of the V_ν (2) will be so complex that a general integral cannot be found. Then p for (2) can be found by approximate integration of (9) or (10). One of the possible approximate methods of integrating (10) numerically is by replacing $\frac{\partial p}{\partial t}$ by a ratio of finite differences. Doing this, we get from (10)

$$p(y_\lambda, v_\nu, t + \Delta t) \approx p(y_\lambda, v_\nu, t) - \sum_{\mu=1}^{n} \frac{\partial}{\partial y_\mu} [f_\mu(t, y_\lambda, v_\nu)\, p(y_\lambda, v_\nu, t)]\, \Delta t. \tag{34}$$

This can be used to determine p at $t + \Delta t$ approximately if it is known at some $\underline{t}$. By dividing the range of $\underline{t}$ of interest to us into sufficiently small intervals, and iterating (34) we can find p at any $\underline{t}$ if it is known at t_0. This method may be suitable for use with high-speed computers. Of course for each $\underline{t}$ the integration must be performed for several y_μ and v_ν, so the y_μ must be taken sufficiently close together to ensure that the $\partial p/\partial y_\mu$ can be determined approximately.

(34) can be used to derive a formal exact expression for the integral of (10). For this we put (34) in the form

$$p(y_\lambda, v_\nu, t_{n+1}) \approx \left\{1 - \sum_{\mu=1}^{n} \left[\frac{\partial f_\mu}{\partial y_\mu} + f_\mu(t_n, y_\lambda, v_\nu) \frac{\partial}{\partial y_\mu}\right] \Delta t_n\right\} p(y_\lambda, v_\nu, t_n). \tag{35}$$

Putting n = 1, 2, . . . , N successively, we have

$$p(y_\lambda, v_\nu, t_{N+1}) \approx \prod_{n=0}^{N} \left\{1 - \sum_{\mu=1}^{n} \left[\frac{\partial f_\mu}{\partial y_\mu} + f_\mu \frac{\partial}{\partial y_\mu}\right] \Delta t_n\right\} p_0(y_\lambda, v_\nu). \tag{36}$$

Passing to the limit where $\max\{\Delta t_n\} \longrightarrow 0$ we get the exact formula

$$p(y_\lambda, v_\nu, t) = \prod_{0}^{t} \left\{1 - \sum_{\mu=1}^{n} \left[\frac{\partial f_\mu(\tau, y_\lambda, v_\nu)}{\partial y_\mu} + f_\mu(\tau, y_\lambda, v_\nu) \frac{\partial}{\partial y_\mu}\right] d\tau\right\} p_0(y_\lambda, v_\nu). \tag{37}$$

Thus the required probability density for the integral of (2) and for the V_ν is expressed via a given p_0 for the initial values Y_λ^0 and the V_ν by using a linear differential operator, operated on by the product-integral, which contains the known function f_μ.

Example. The random function Y(t) is connected with the normally distributed real stationary random function X (t), which latter has a mathematical expectation of zero and a correlation function $k_X(\tau)$, by the differential equation

$$\frac{dY}{dt} = Y^s X(t). \tag{38}$$

We are required to determine the one-dimensional probability density for Y(t) in the finite interval $t_0 \leq t < t_0 + T$, supposing that $Y_0 = Y(t_0)$ is normally distributed, independently of X(t), and has its mathematical expectation and dispersion Δ both zero.

Expanding X(t) in canonical form in the range $t_0 < t < t_0 + T$ [2, 3, 15] in the real form

$$X(t) = V_0 + \sum_{\nu=1}^{\infty} (V_{2\nu-1} \cos \omega_\nu t + V_{2\nu} \sin \omega_\nu t), \tag{39}$$

we replace X in (38) by an infinite assembly of independent normally distributed random quantities $V_0, V_1, \ldots$, having zero mathematical expectations and dispersions, given by

$$\begin{aligned} D_0 &= D[V_0] = \frac{1}{T} \int_0^T k_x(\tau)\, d\tau, \\ D_\nu &= D[V_{2\nu-1}] = D[V_{2\nu}] = \frac{2}{T} \int_0^T k_x(\tau) \cos \omega_\nu \tau d\tau, \quad \omega_\nu = \frac{\pi\nu}{T} \quad (\nu = 1, 2, \ldots). \end{aligned} \tag{40}$$

By restricting (39) to a finite section of the expansion, corresponding to ν varying from 1 to n, we get the probability densities of $Y_0, V_0, V_1, \ldots, V_{2n}$ as

$$p_0(y_0, v_\nu) = \frac{1}{(2\pi)^{n+1} D_1 \ldots D_n \sqrt{D_0 \Delta}} \exp\left\{ -\frac{y_0^2}{2\Delta} - \frac{v_0^2}{2D_0} - \sum_{\nu=1}^{n} \frac{v_{2\nu-1}^2 + v_{2\nu}^2}{2D_\nu} \right\}. \tag{41}$$

(9), which simultaneously defines the densities for Y(t) and $V_0, V_1, \ldots, V_{2n}$, here takes the form

$$\frac{\partial p}{\partial t} + y^s \varphi(v_\nu, t) \frac{\partial p}{\partial y} + s y^{s-1} \varphi(v_\nu, t)\, p = 0, \tag{42}$$

where for brevity we put

$$\varphi(v_\nu, t) = v_0 + \sum_{\nu=1}^{n} (v_{2\nu-1} \cos \omega_\nu t + v_{2\nu} \sin \omega_\nu t). \tag{43}$$

The system of ordinary differential equations corresponding to (2) takes the form

$$\frac{dt}{1} = \frac{dy}{y^s \varphi(v_\nu, t)} = \frac{dp}{-sy^{s-1}\varphi(v_\nu, t)\, p}. \tag{44}$$

This system has two first integrals given by

$$[y^{1-s} - \psi(v_\nu, t)]^{\frac{1}{1-s}} = y_0,$$
$$p/[1 - y^{s-1}\psi(v_\nu, t)]^{\frac{s}{1-s}} = p_0, \tag{45}$$

where

$$\psi(v_\nu, t) = \int_{t_0}^{t} (1-s)\,\varphi(v_\nu, t)\, dt. \tag{46}$$

The general theory of equations in first-order partial derivatives shows the complete integral of (42) to be determined by [10]

$$p = [1 - y^{s-1}\psi(v_\nu, t)]^{\frac{s}{1-s}} F([y^{1-s} - \psi(v_\nu, t)]^{\frac{1}{1-s}}), \tag{47}$$

where F is an arbitrary function. To determine it we use the condition that $\underline{p}$ at $t = t_0$ is the same as p_0 given by (41). This gives

$$F(y_0) = \frac{1}{(2\pi)^{n+1} D_1 \cdots D_n \sqrt{D_0 \Delta}} \exp\left\{-\frac{y_0^2}{2\Delta} - \frac{v_0^2}{2D_0} - \sum_{\nu=1}^{n} \frac{v_{2\nu-1}^2 + v_{2\nu}^2}{2D_\nu}\right\} \tag{48}$$

and (47) becomes

$$p(y, v_\nu; t) = \frac{[1 - y^{s-1}\psi(v_\nu, t)]^{\frac{s}{1-s}}}{(2\pi)^{n+1} D_1 \cdots D_n \sqrt{D_0 \Delta}} \times$$
$$\times \exp\left\{-\frac{[y^{1-s} - \psi(v_\nu, t)]^{\frac{2}{1-s}}}{2\Delta} - \frac{v_0^2}{2D_0} - \sum_{\nu=1}^{n} \frac{v_{2\nu-1}^2 + v_{2\nu}^2}{2D_\nu}\right\}. \tag{49}$$

The required one-dimensional probability density for Y(t) is now determined by integrating (49) over all the variables $v_0, v_1, \ldots, v_{2n}$ [9, 15]: The formula

$$f_1(y;\ t) = \int_{-\infty}^{\infty} \cdots \int_{-\infty}^{\infty} \frac{[1 - y^{s-1}\psi(v_\nu,\ t)]^{\frac{s}{1-s}}}{(2\pi)^{n+1} D_1 \cdots D_n \sqrt{D_0 \Delta}} \times$$

$$\times \exp\left\{ - \frac{[y^{1-s} - \psi(v_\nu,\ t)]^{\frac{2}{1-s}}}{2\Delta} - \frac{v_0^2}{2D_0} - \sum_{\nu=1}^{n} \frac{v_{2\nu+1}^2 + v_{2\nu}^2}{2D_\nu} \right\} dv_0\, dv_1 \ldots dv_{2n}. \qquad (50)$$

shows that (49) can be found without having to integrate (42) (in partial derivatives), since here (38) is integrable in quadratures..

This example is purely illustrative, since in practice the most interesting case is when we cannot find sufficient first integrals to the system of ordinary differential equations corresponding to the system in partials of (9).

SUMMARY

The equation in partial derivatives which defines the probability density for a system of ordinary differential equations containing random parameters is given above: an approximate method of integrating this equation is stated. This method is suitable for use with current fast computers. But it can only be sufficiently simple (certainly for fast computers) when the number of the V_ν appearing is not large. When the V_ν are numerous the calculations must be made for many combinations of the V_ν values, so the volume of work may be enormous. If the method is to be of practical use even with fast computers, we must have recourse to representing the random functions appearing in the equation in canonical expansion form, using few terms. It is clear that the problem of representing an arbitrary random function or system of such functions by canonical or other such expansions containing the fewest possible terms is one of the most important in contemporary general theory of random functions.

As it is complex and laborious to integrate numerically an equation in partial derivatives which defines both the probability density for the integral of the differential equation system and for the random parameters, the practical use of the method developed here may be difficult. Methods much simpler for computational use when deriving the probability characteristics of ordinary nonlinear differential equations approximately are available [5-8]. In particular these characteristics can be determined approximately by first finding the moments of the integral by a published method [5], after which approximate expressions for the probability densities of random quantities in terms of their moments are used [14, 15]. So the results given here are mainly of theoretical interest as being a possible starting-point for developing new methods of studying the accuracies of nonlinear systems. To develop a practical method of studying the accuracies of nonlinear systems from the basis given here we must find sufficiently simple approximate methods of integrating equations in partial derivatives which define both the probability density for the integral of the differential equation system and for the random parameters. This problem might be solved by using Chebyshev-Hermite multidimensional polynomial expansions, or more general expansions of this type, for the probability densities.

Received September 20, 1956

LITERATURE CITED

[1] V. S. Pugachev, Fundamentals of the general theory of random functions. (Trans. Acad. Artillery Science, 1952).

[2] V. S. Pugachev, General correlation theory for random functions. Bull. Acad. Sci. USSR, mathematics series 17, No. 5 (1953).

[3] V. S. Pugachev, Elements of the theory of random functions. Bull. Zhukovsky Air-Force Academy, 1954).

[4] B. G. Dostupov, Determination of the probability characteristics of linearized integrals to systems of ordinary differential equations. Coll. Sci. Papers from Zhukovsky Air Force Academy, vol. 1 (1954).

[5] B. G. Dostupov, Approximate determination of the probability characteristics of solutions. Trans. Zhukovsky Air Force Academy, No. 592 (1956).

[6] I. E. Kazakov, An approximate method of statistical study for nonlinear systems. Trans. Zhukov Air Force Academy, No. 394 (1954).

[7] I. E. Kazakov, The study of dispersion in nonlinear automatic systems. Coll. Sci. Papers from Zhukovsky Air Force Academy, vol. 1 (1954).

[8] I. E. Kazakov, Approximate probability analysis of the operational accuracies of essentially nonlinear systems. Automation and Remote Control 17, No. 5 (1956).*

[9] E. S. Venttsel, Theory of probability. (Zhukovsky Air Force Academy Press, 1952).**

[10] V. I. Smirnov, Course in higher mathematics, vols. II and III. (State Tech. Press, 1949).**

[11] Sh. E. Mikeladze, Numerical methods of integrating differential equations in partial derivatives. (Acad. Sci. of USSR Press, 1936).**

[12] V. V. Golubev, Lectures on the integration of the equations of motion of a heavy solid body about a fixed point. (State Tech. Press, 1953).**

[13] E. Gursa, Course in mathematical analysis, vol. II, ch. 2, (State Tech. Press, 1934).**

[14] G. Kramer, Mathematical methods in statistics. IL (1948).

[15] V. S. Pugachev, The theory of random functions and its application to problems in automatic control. (State Tech. Press, 1957).**

* [See C. B. Translation.]

** [In Russian.]

AN APPROXIMATE DETERMINATION OF THE SELF-OSCILLATION STARTUP PROCESS IN CERTAIN NONLINEAR AUTOMATIC CONTROL SYSTEMS

A. A. Voronov

(Leningrad)

An approximate method for determining the changes in amplitude and phase of the fundamental in self-oscillations in certain nonlinear systems is given for the case where the changes are sufficiently slow. It is shown that a high-order equation can be approximated by two nonlinear equations of first order comparable with those given in [1] for a second-order system. It is demonstrated how a piecewise-linear approximation to certain functions $\xi(a)$ encountered in solving the problem enables one to get an approximate solution simply. The method is often of adequate accuracy even when the oscillations practically die away in 1-3 periods.

Consider the system of the structure shown in Figure 1.

The linear part L and the nonlinear element N are here separated. We have to determine how self-oscillations, if any, are set up at the nonlinear link input.

Let the equation for the linear part be

$$D(p)\,x = -K(p)\,(y), \tag{1}$$

where $p \equiv \frac{d}{dt}$, D (p) and K (p) being polynomials with constant coefficients.

Suppose we are also given the equation for the nonlinear link

$$y = f(x). \tag{2}$$

Let us seek a solution to (1) in the form

$$x = x_n + a \sin(\Omega t + \psi), \tag{3}$$

where x_n, a and ψ are the desired time-functions, Ω being a certain constant.

To simplify the explanation we assume y dependent only on x. But this restriction is not essential, and the method can be extended to systems with inertial nonlinear links.

Substituting (2) and (3) into (1) we get

$$D(p)[x_n + (a\sin\psi)\cos\Omega t + (a\cos\psi)\sin\Omega t] + \\ + K(p) f[x_n + (a\sin\psi)\cos\Omega t + (a\cos\psi)\sin\Omega t] = 0. \tag{4}$$

Further we suppose the mean value of the steady-state oscillation to be zero: $x_n = 0$.

Then the equation reduces to

$$D(p)[(a\sin\psi)\cos\Omega t + (a\cos\psi)\sin\Omega t] + K(p) f[(a\sin\psi)\cos\Omega t + \\ + (a\cos\psi)\sin\Omega t] = 0. \tag{5}$$

Applying to (5) the theorem on the replacement of the differential operator, as in [2]:

$$D(p)[u(t)\sin\Omega t] = \sin\Omega t D_1(p)u(t) + \cos\Omega t D_2(p)u(t), \\ D(p)[u(t)\cos\Omega t] = \cos\Omega t D_1(p)u(t) - \sin\Omega t D_2(p)u(t), \tag{6}$$

where

$$D_1(p) = \frac{1}{2}[D(p + j\Omega) + D(p - j\Omega)] = \mathrm{Re}\, D(p + j\Omega), \\ D_2(p) = \frac{1}{2j}[D(p + j\Omega) - D(p - j\Omega)] = \mathrm{Im}\, D(p + j\Omega). \tag{7}$$

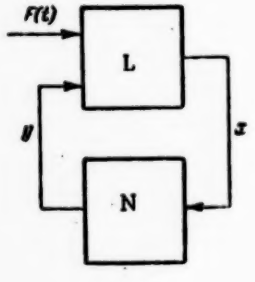

Fig. 1.

Strictly speaking this theorem can only be used on the linear part of (5), i.e., to the first component. But we will also apply it to the nonlinear part (second component) supposing that $\underline{a}$ and ψ change so slowly compared with Ωt that they can be considered constant in any one period at their mean values for the period, while being variable over the whole time of the process. Then using the harmonic balance formula we have

$$f(x) = g(a)\, a\sin(\Omega t + \psi) + b(a)\, a\cos(\Omega t + \psi), \tag{8}$$

where

$$g(a) = \frac{1}{\pi a}\int_0^{2\pi} f(a\sin\varphi)\sin\varphi d\varphi, \qquad b(a) = \frac{1}{\pi a}\int_0^{2\pi} f(a\sin\varphi)\cos\varphi d\varphi. \tag{9}$$

We have now to find $\underline{a}$, g(a), b(a) and ψ as functions of time.

Substituting (7) into (5) and applying the theorem we get

$$\cos \Omega t D_2(p)(a\cos\psi) + \sin \Omega t D_1(p)(a\cos\psi) + \cos \Omega t D_1(p)(a\sin\psi) -$$
$$- \sin \Omega t D_2(p)(a\sin\psi) + \cos \Omega t \{K_2(p)[g(a)a\cos\psi - b(a)a\sin\psi] +$$
$$+ K_1(p)[g(a)a\sin\psi + b(a)a\cos\psi]\} + \sin \Omega t \{K_1(p)[g(a)a\cos\psi -$$
$$- b(a)a\sin\psi] - K_2(p)[g(a)a\sin\psi + b(a)a\cos\psi]\} = 0. \qquad (10)$$

This equation becomes fairly complex when D and K are high-order polynomials. Performing all the differentiations (10) becomes

$$M\sin(\Omega t + \psi) + N\cos(\Omega t + \psi) = 0, \qquad (11)$$

where M and N are complex functions of $\underline{p}$, $\underline{a}$ and ψ.

If we assume M and N not to be periodic time-functions with frequencies of multiples of Ω (from the assumption that $\underline{a}$ and ψ change slowly) then the requirement that (11) be correct for all $\underline{t}$ gives two equations:

$$M = 0, \quad N = 0. \qquad (12)$$

This method, which considers only one fundamental in the self-oscillation, is identical with the harmonic balance method, which is in principle inexact. Thus, there is no point in making the solution complicated by attempting to derive it from (12), which is in general form extremely complex. By assuming $\underline{a}$ and ψ slowly varying we can simplify further.

If

$$D(p) = a_0 + \sum_{\nu=1}^{n} a_\nu p^\nu,$$

then

$$D(p + j\Omega) = a_0 + \sum_{\nu=1}^{n} a_\nu (p + j\Omega)^\nu = a_0 + \sum_{\nu=1}^{n} a_\nu \Omega^\nu \left(\frac{p}{\Omega} + j\right)^\nu.$$

"Slow" changes in $\underline{a}$ and ψ, which have the symbol p^ν before them, means that we take their rates of changes at any instant to be small relative to Ω. So assuming p^ν/Ω^ν small compared to p/Ω we reject all the small higher orders, $(p/\Omega)^\nu$, $\nu > 1$*, in (11) and replace the polynomial in $D(p + j\Omega)$ by one of first order:

---

* The assumption that the higher derivatives are small,

$$\frac{d^\nu a}{\Omega^\nu dt^\nu} \ll \frac{da}{\Omega dt}, \quad \frac{d^\nu \psi}{\Omega^\nu dt^\nu} \ll \frac{d\psi}{\Omega dt} \quad (\nu = 2, 3, \ldots)$$

is less strong than that $\underline{a}$ and ψ vary slowly, where we must have

$$\frac{da}{\Omega dt} \ll 1, \qquad \frac{d\psi}{\Omega dt} \ll 1,$$

which is not so. Thus we can only assume the self-oscillation set up slowly when using (9). But here the assumption is extremely strong, as has been shown [6]. This possibly explains why the method is applicable to certain problems where $\underline{a}$ and ψ vary comparatively rapidly.

$$D(p+j\Omega) \approx a_0 + \sum_{\nu=1}^{n} a_\nu \Omega^\nu \left(j^\nu + \nu j^{\nu-1} \cdot \frac{p}{\Omega} \right).$$

This means that the "replaced" polynomials D_1, D_2, K_1 and K_2 may be represented approximately as first-order ones:

$$\begin{aligned} D_1(p) &= m_1 p + n_1, \quad K_1(p) = l_1 p + r_1, \\ D_2(p) &= m_2 p + n_2, \quad K_2(p) = l_2 p + r_2, \end{aligned} \tag{13}$$

where $\underline{m}$, $\underline{n}$, l and $\underline{r}$ are constants.

Some simple manipulations after substituting (14) into (11) give two equations of the form of (12):

$$\begin{aligned} &\left\{ m_1 + l_1 \left[g(a) + a \frac{\partial g}{\partial a} \right] - l_2 \left[b(a) + a \frac{\partial b}{\partial a} \right] \right\} pa - \{ m_2 + l_2 g(a) + \\ &\quad + l_1 b(a) \} ap\psi = -a [n_1 + r_1 g(a) - r_2 b(a)], \\ &\left\{ m_2 + l_2 \left[g(a) + a \frac{\partial g}{\partial a} \right] + l_1 \left[b(a) + a \frac{\partial b}{\partial a} \right] \right\} pa + \{ m_1 + l_1 g(a) - \\ &\quad - l_2 b(a) \} ap\psi = -a [n_2 + r_2 g(a) + r_1 b(a)]. \end{aligned} \tag{14}$$

These equations relate three unknowns, Ω, $\underline{a}$ and ψ. The excess of unknowns is because we have so far taken Ω to be an unknown constant. We select Ω to be the angular frequency of the steady-state self-oscillation. Then (14) (in which we put p = 0) gives two further equations needed to determine the parameters of the steady-state self-oscillation.

$$n_1 + r_1 g(a_y) - r_2 b(a_y) = 0, \quad n_2 + r_2 g(a_y) + r_1 b(a_y) = 0. \tag{15}$$

Here a_{ss} is the steady-state self-oscillation amplitude.

(15), being a special case of (12) is none other than the harmonic balance equation. Goldfarb [3], Kochenburger [4], Popova [5] and others have proposed graphical methods of solving these equations.

Assuming Ω and a_{ss} found from (15), we turn now to (14).

We eliminate ψ from (14) and obtain an equation in $pa = \frac{da}{dt}$.

It is

$$\frac{da}{dt} = \frac{\Delta_a}{\Delta} = \xi(a), \tag{16}$$

where Δ is the main determinant of (14), Δ_a being the conjoint determinant and $\xi(a)$ a known function of a.

(16) gives the quadrature

$$t = \int \frac{da}{\xi(a)} + \ln C. \tag{17}$$

*[Here, and in subsequent equations, "a_y" = "a_{ss}" where subscript ss stands for steady state. – Editor's note.]

It may be fairly difficult to compute this quadrature, since $\xi(a)$ is sometimes a complicated function of $\underline{a}$. Then we use a piecewise-linear approximation to $\xi(a)$ (Figure 2) and solve (17) at intervals.

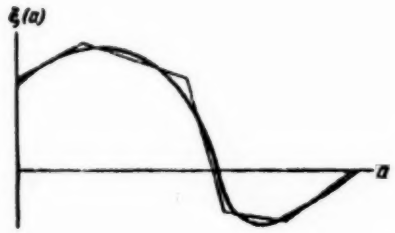

Fig. 2.

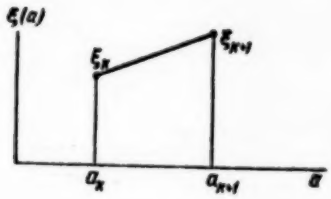

Fig. 3.

Suppose that $\xi(a)$ has the values ξ_k and ξ_{k+1} at the ends of some range a_k, a_{k+1} $(a_{k+1} > a_k)$, and is linear inside the range (Figure 3). Then in this range

$$\xi(a) = \xi_k + \frac{\xi_{k+1} - \xi_k}{a_{k+1} - a_k}(a - a_k) = k_0 + k_1(a - a_k),$$

$$t = \int \frac{da}{k_0 + k_1(a - a_k)} + \ln C = \frac{1}{k_1} \ln C\left(\frac{k_0}{k_1} - a_k + a\right),$$

So

$$a = a_k - \frac{k_0}{k_1} + \frac{1}{C} e^{k_1 t}.$$

C is determined from the initial conditions and from the condition that $\xi(a)$ is continuous at the junctions. For example, if $\underline{a}$ increases then at $t = 0$ we have $a = a_k$, so

$$\frac{1}{C} = \frac{k_0}{k_1},$$

and finally

$$a = a_k = \frac{k_0}{k_1}(1 - e^{k_1 t}) \tag{18}$$

in the range $a_k < a < a_{k+1}$.

If $\underline{a}$ falls then, putting $a = a_{k+1}$ at $t = 0$, we get

$$a = a_k - \frac{k_0}{k_1} + e^{k_1 t}\left[a_{k+1} - a_k + \frac{k_0}{k_1}\right].$$

$a(t)$ is approximately a series of joined exponential sections. This is a damped oscillation.

To determine $\underline{a}$ at the beginning of the first range we proceed as follows.

We assume the initial amplitude a_0 as being the distance of the mean position about which the steady

oscillations occur from the initial value of x. Thus, when a perturbation $x_0 = -a_0$ is applied, the choice of a_0 is shown by Figure 4.

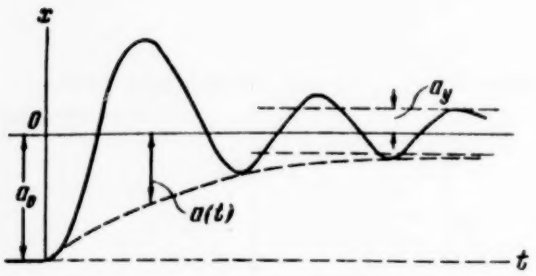

Fig. 4.

The phase changes can by analogy be found from

$$\frac{d\psi}{dt} = \frac{\Delta_\psi}{\Delta} = \eta(a) = \zeta(t).$$

If a and ψ are known for any t we can also find $x = a\sin(\Omega t + \psi)$, for which, as Figure 4 shows, we take ψ_0 as being $-\frac{\pi}{2}$ (for the case of Figure 4).

This will be illustrated by an example.

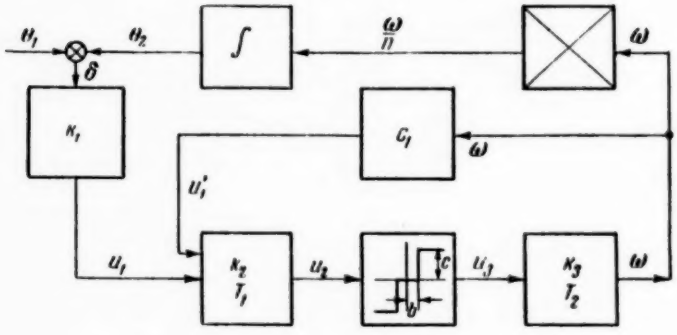

Fig. 5.

Example•. A servo with a relay. Figure 5 shows the block diagram.

Motor equation

$$(T_2 p + 1)\,\omega = k_3 u_3;$$

Output equation

$$\theta_2 = \frac{1}{p}\,\frac{1}{n}\,\omega = \frac{k_3 u_3}{np(1 + T_2 p)};$$

Error equation

$$\delta = \theta_1 - \theta_2 = \theta_1 - \frac{k_3 u_3}{np(1 + T_2 p)};$$

Error signal equation

$$u_1 = k_1 \delta;$$

• For simplicity this example is taken from [6].

Inertial amplifier equation

$$u_2 = \frac{k_2 u_1}{1 + T_1 p} - \frac{k_2 u_1'}{1 + T_1 p};$$

Feedback equation

$$u_1' = c_1 \omega;$$

The equation relating the input and output from the nonlinear link

$$u_2 = \frac{k_1 k_2 0_1}{1 + T_1 p} - \frac{k_1 k_2 k_3 u_3}{np(1 + T_1 p)(1 + T_2 p)} - \frac{c_1 k_2 k_3 u_3}{(1 + T_1 p)(1 + T_2 p)}.$$

Consider the case $\theta_1 = \text{const}$, $p\theta_1 = 0$. By transforming the last equation we get

$$(T_1 p + 1)(T_2 p + 1)\, p u_2 + K(\tau p + 1)\, u_3 = 0, \tag{19}$$

where

$$K = \frac{k_1 k_2 k_3}{n}, \quad \tau = \frac{n c_1}{k_1}.$$

Put u_2 as $u_2 = a \sin(\Omega t + \psi)$. Then $u_3 = g(a)\, a \sin(\Omega t + \psi)$, since $b(a) = 0$ as the nonlinear element here has a symmetric characteristic.

We have

$$\begin{aligned}
D(p) &= (T_1 p + 1)(T_2 p + 1)\, p, \\
D_1(p) &= T_1 T_2 p^3 + (T_1 + T_2)\, p^2 + (1 - 3 T_1 T_2 \Omega^2)\, p - \Omega^2 (T_1 + T_2), \\
D_2(p) &= \Omega [3 T_1 T_2 p^2 + 2(T_1 + T_2)\, p + 1 - \Omega^2 T_1 T_2], \\
K(p) &= K(\tau p + 1), \\
K_1(p) &= K(\tau p + 1), \\
K_2(p) &= K \Omega \tau.
\end{aligned}$$

Putting these into (11) we get

$$\begin{aligned}
&\Big\{ T_1 T_2 [p^3 a - 3\, pa\, (p\psi)^2 - 3\, ap\psi\, (p^2\psi)] + (T_1 + T_2)[p^2 a - a\, (p\psi)^2] + \\
&\quad + (1 - 3\, T_1 T_2 \Omega^2)\, pa - \Omega^2 (T_1 + T_2)\, a - \Omega [3\, T_1 T_2 (2\, pap\psi + ap^2\psi) + \\
&+ 2(T_1 + T_2)\, ap\psi] + K \left[\tau g(a)\, pa + \tau a \frac{\partial g}{\partial a}\, pa + g(a)\, a \right] \Big\} \sin(\Omega t + \psi) + \\
&+ \{ T_1 T_2 [3\, p\psi p^2 a + 3\, pap^2\psi + ap^3\psi - a\, (p\psi)^3] + (T_1 + T_2)[2\, pap\psi + ap^2\psi] + \\
&\quad + (1 - 3\, T_1 T_2 \Omega^2)\, ap\psi + \Omega [3\, T_1 T_2 (p^2 a - a\, (p\psi)^2) + 2(T_1 + T_2)\, pa + \\
&\quad + (1 - \Omega^2 T_1 T_2)\, a] + K\tau [\Omega g(a)\, a + g(a)\, ap\psi] \} \cos(\Omega t + \psi) = 0.
\end{aligned} \tag{20}$$

(12) is found by the method above, and the equations linearized:

$$T_1T_2p^3a + (T_1+T_2)\,p^2a + (1-3\,T_1T_2\Omega^2)\,pa - \Omega^2(T_1+T_2)\,\Delta a - \\ - \Omega\,[3\,T_1T_2a_y p^2\psi + 2\,(T_1+T_2)\,a_y p\psi] + \\ + K\left[\tau g(a_y)\,pa + \tau a_y\left(\frac{\partial g}{\partial a}\right)_{a_y} pa + g(a_y)\,\Delta a + a_y\left(\frac{\partial g}{\partial a}\right)_{a_y}\Delta a\right] = 0,$$

$$T_1T_2a_y p^3\psi + (T_1+T_2)\,ap^2\psi + (1-3\,T_1T_2\Omega^2)\,a_y p\psi + \\ + \Omega\,[3\,T_1T_2p^2a + 2\,(T_1+T_2)\,pa + (1-\Omega^2T_1T_2)\,\Delta a] + \\ + K\left[\Omega\tau g(a_y)\,\Delta a + \Omega\tau a_y\left(\frac{\partial g}{\partial a}\right)_{a_y}\Delta a + \tau g(a_y)\,a_y p\psi\right] = 0. \qquad (21)$$

Rejecting higher derivatives and products of derivatives in (20) we get in a first approximation an abbreviated equation for the rise in the self-oscillation

$$\left\{(1-3\,T_1T_2\Omega^2) + K\tau\left[g(a) + a\,\frac{\partial g}{\partial a}\right]\right\} pa + [Kg(a) - \Omega^2(T_1+T_2)]\,a - \\ - 2\,\Omega\,(T_1+T_2)\,ap\psi = 0,$$

$$\Omega\,\{2\,(T_1+T_2)\,pa + [1-\Omega^2T_1T_2 + K\tau g(a)]\,a\} + [(1-3\,T_1T_2\Omega^2) + K\tau g(a)]\,ap\psi = 0. \qquad (22)$$

The steady-state equation is

$$[Kg(a_y) - \Omega^2(T_1+T_2)]\,a_y = 0, \quad \Omega\,[1-\Omega^2T_1T_2 + K\tau g(a_y)]\,a_y = 0, \qquad (23)$$

whence

$$\tau = \frac{\Omega^2T_1T_2 - 1}{\Omega^2(T_1+T_2)}, \qquad \Omega^2 = \frac{1}{T_1T_2 - \tau(T_1+T_2)}. \qquad (24)$$

Self-oscillation is clearly impossible if $T_1T_2 < \tau\,(T_1+T_2)$. The first equation in (23) gives

$$g(a_y) = \frac{\Omega^2(T_1+T_2)}{K}. \qquad (25)$$

Consider a numerical example. Suppose $T_1 = 0.05$ sec, K = 20, b = 6v, $T_2 = 0.05$ sec, $\tau = 0.01$ sec, c = 120v. (24) gives $\Omega = 25.8$ radians/sec (4.1 cycles/sec). (25) gives $g(a_{ss}) = 3^{1/3}$. Since

$$g(a_y) = \frac{4c}{\pi a_y}\sqrt{1 - \frac{b^2}{a_y^2}},$$

then

$$a_y = \frac{2c}{\pi g(a_y)}\sqrt{2 \pm \sqrt{4 - \frac{\pi^2g^2b^2}{c^2}}}.$$

This gives two values: $a_{ss_1} = 45.4v$ and $a_{ss_2} = 6.08v$.

To reject the clearly unstable solution it is simplest first to use a necessary but not sufficient criterion of stability for (22). Linearizing it, we get its principal determinant as

$$\Delta = a_y p \left\{ \left[1 - 3T_1T_2\Omega^2 + K\tau \left(g(a_y) + a_y \left(\frac{\partial g}{\partial a} \right)_{a_y} \right) \right] p + \right.$$

$$\left. + K \left[g(a_y) + a_y \left(\frac{\partial g}{\partial a} \right)_{a_y} \right] - \Omega^2 (T_1 + T_2) \right\} [1 - 3T_1T_2\Omega^2 + K\tau g(a_y)] +$$

$$+ a_y p 2\Omega^2 (T_1 + T_2) \left\{ 2(T_1 + T_2) p + 1 - \Omega^2 T_1 T_2 + K\tau \left[g(a_y) + a_y \left(\frac{\partial g}{\partial a} \right)_{a_y} \right] \right\}$$

It has a zero root, which corresponds to the system being neutral against phase changes.

The necessary but not sufficient conditions for stability (since the oldest coefficient in (21) is positive) lead to the coefficients of p and the free term in the polynomial $\Delta / a_{ss} p$ being positive. It is not difficult to see that the necessary conditions are complied with when $a_{ss} = 45.4$ and not when $a_{ss} = 6.08$.

A test of the stability using (21) with $a_{ss} = 45.4$ also shows the periodic solution stable.

We pass now to the transient response. We shall determine this for two initial amplitudes $a_0 = 500$ v and $a_0 = 15$ v.

We rewrite (22) substituting the figures and for brevity putting $\left(\frac{\partial g}{\partial a} \right) = g'$:

$$[0.2(g + ag') - 4] \frac{da}{dt} + [20g - 66.7] a - 0.2\Omega a \frac{d\psi}{dt} = 0.$$

$$0.2\Omega \frac{da}{dt} + \Omega (0.2g - 0.667) a + (0.2g - 4) a \frac{d\psi}{dt} = 0.$$

Be eliminating $\frac{d\psi}{dt}$ from these we get

$$\frac{da}{dt} = \frac{a(3.3 - g)(g - 13.3)}{0.01(g + g'a - 20)(g - 20) + 6.7} = \xi(a).$$

Figure 6, which gives ξ (a), shows that when $45.4 < a < 500$, ξ (a) can sufficiently accurately be replaced by a line ξ (a) $= -6.15 \times (a - 45.4)$.

Then (18) gives

$$a = 45.4 + 454.6 e^{-6.15t}. \qquad (26)$$

The full line in Figure 7 shows x computed from an exact solution•, the dashed lines showing the exponential of (26). It coincided very closely with the oscillation, and so the approximate solution is of satisfactory accuracy.

• E. I. Perovsky has determined the exact solution.

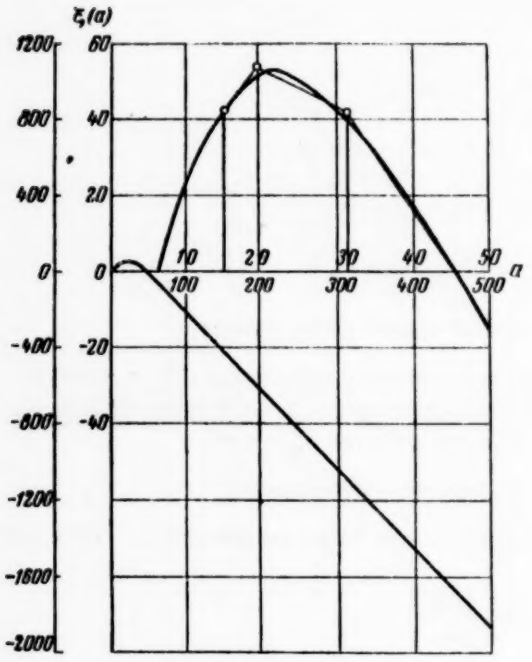

Fig. 6.

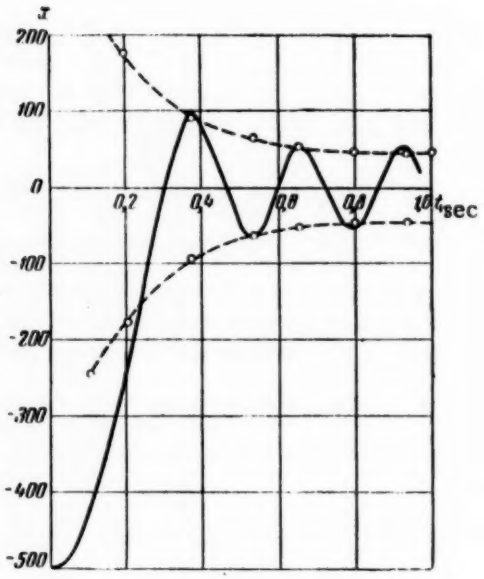

Fig. 7.

In the range $15 < a < 45.4$, Figure 6 shows that $\xi(a)$ may be approximated by three abutting linear sections:

$$\xi(a) = 42.5 + 2.52(a - 6.08) \quad \text{when } 15 < a < 19.4,$$

$$\xi(a) = 54 - 0.975(a - 19{,}4) \quad \text{when } 19.4 < a < 31.2,$$

$$\xi(a) = 42.5 - 2.99(a - 31.2) \quad \text{when } 31.2 < a < 45.4.$$

So the amplitude curves computed from (18) are approximately sections of three exponentials:

$$a = 15 - 16.85(1 - e^{-2.52t}) \quad \text{when } 15 < a < 19.4,$$

$$a = 19.4 + 55.4\ (1 - e^{-0.975t}) \quad \text{when } 19.4 < a < 31.2,$$

$$a = 31{,}2 + 14.2\ (1 - e^{-2.99t}) \quad \text{when } 31.2 < a$$

(in each case the origin of time is taken at the beginning of the section).

The full line in Figure 8 shows $\underline{x}$ computed from the exact equation, the dashes showing the exponential sections found. Here again the curves come very close together.

Calculations on other examples show that the accuracy of this method is approximately the same as for the parameters found by the harmonic balance method in many practical cases.

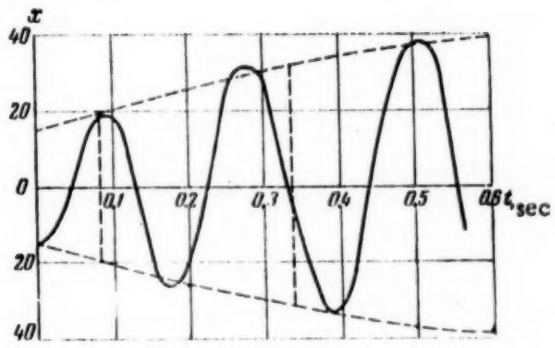

Fig. 8.

There is no difficulty in determining the changes in ψ during the transient. The law followed by ψ is of no real interest and we shall not pause over it.

APPENDIX

An Explanation of the Differential Operator Rule

We are given a function

$$u(t)\,e^{\alpha t} \qquad (\alpha = \text{const}). \tag{A}$$

Suppose

$$p^k\,[u(t)\,e^{\alpha t}] = e^{\alpha t}\,(p+\alpha)^k\,u(t) \qquad \left(p \equiv \frac{d}{dt}\right). \tag{B}$$

Differentiating (B) we have

$$p^{k+1}\,[u(t)\,e^{\alpha t}] = e^{\alpha t}\,p\,(p+\alpha)^k\,u(t) + \alpha e^{\alpha t}\,(p+\alpha)^k\,u(t) = e^{\alpha t}\,(p+\alpha)^{k+1}\,u(t).$$

Thus if (B) is correct for some k, integral and positive, it is correct for all such k.

We shall show (B) correct for some k, e.g., k = 1:

$$p\,[u(t)\,e^{\alpha t}] = e^{\alpha t}\,pu(t) + \alpha e^{\alpha t}\,u(t) = e^{\alpha t}\,(p+\alpha)\,u(t).$$

Then

$$p^k\,[u(t)\,e^{j\Omega t}] = e^{j\Omega t}\,(p+j\Omega)^k u(t), \quad p^k\,[u(t)\,e^{-j\Omega t}] = e^{-j\Omega t}\,(p-j\Omega)^k\,u(t).$$

So

$$p^k\,[u(t)\sin\Omega t] = \frac{1}{2j}\,p^k\,[u(t)\,e^{j\Omega t} - u(t)\,e^{-j\Omega t}] =$$

$$= \frac{1}{2j}\,\{\cos\Omega t\,[(p+j\Omega)^k - (p-j\Omega)^k] + j\sin\Omega t\,[(p+j\Omega)^k + (p-j\Omega)^k]\}\,u(t) =$$

$$= [\sin\Omega t\,\mathrm{Re}\,(p+j\Omega)^k + \cos\Omega t\,\mathrm{Im}\,(p+j\Omega)^k]\,u(t).$$

The theorem of linearity and superposition implies

$$D(p)[u(t)\sin\Omega t] = [\sin\Omega t \operatorname{Re} D(p+j\Omega) + \cos\Omega t \operatorname{Im} D(p+j\Omega)]\,u(t).$$

The first is found from (7). The second is found analogously.

Received September 21, 1956

LITERATURE CITED

[1] N. N. Bogolyubov, Single-frequency oscillations in nonlinear systems with many degrees of freedom. Collected papers from the Institute of Structural Mechanics, Academy of Sciences of the Ukrainian SSR, No. 10 (1949).

[2] M. A. Aizerman and I. M. Smirnova, The use of the small parameter method for studying hunting modes in automatic control systems not containing a small parameter. Symposium in honor of A. A. Andronov, pp. 77-92, (Acad. Sci. USSR Press, 1955).

[3] L. S. Goldfarb, Certain nonlinearities in control systems. (Automation and Remote Control, No. 4 1947).

[4] R. J. Kochenburger, A frequency response method for analyzing and synthesizing contactor servomechanisms. Trans. AIEE, vol. 69, part I (1950).

[5] E. P. Popov, Allowing for nonlinearities when designing servos. (Automation and Remote Control, No. 6 1953).

[6] E. P. Popov, Approximate study of transients in nonlinear automatic control systems by harmonic linearization. Bull. Acad. Sci. USSR, Tech. Sci. Section, Nos. 9 and 12 (1956).

A PHASE METHOD USING ULTRASHORT WAVES FOR MEASURING THE LEVEL OF A LIQUID AUTOMATICALLY

V. B. Brodsky

(Moscow)

The theory of the method is presented. It is shown that by using coupling transformers and dielectric loading in the measuring line one can measure liquid levels over ranges which can be considerably greater (or less) than the displacement of the standing-wave minimum.

The errors and field of application of the method are considered.

INTRODUCTION

The need to check liquid levels automatically in inaccessible regions arises in many branches of industry. The liquid is frequently aggressive and mechanical transducers with moving parts in contact with the liquid are difficult to use. Then the reflection of radio waves from the surface, using phase methods, can be used efficiently. The method consists in measuring the distance to the reflecting surface by detecting the standing-wave minimum produced by the reflected and incident waves in a transmission line. The end of the line enters the liquid container.

This method is well known in measurement technology [1]. But it cannot be used directly for automatic liquid level measurement. The reason is as follows. If the measurement is to be unique any level in the line must give only one minimum. On the other hand the range to be covered is often several meters while the line-length in the measuring head is only some tens of centimeters. So the range over which the minimum is displaced must be restricted relative to the level changes. The relation between the two must be nearly linear. A servo must be used to find the minimum.

The phase method can give high accuracy and reliability in liquid level measurement. A great advantage is that the transducer involves no contact with the liquid and is simple. The method has bounds both to its accuracy and range. Here we consider methods of reducing standing-wave minimum displacement in the line, and the errors and field of application of the method.

Theoretical Design of the Phase Method for Automatic Liquid Level Measurement.

The theoretical design of the phase method for automatic liquid level measurement is given in Figure 1.

The radio wave from the generator (1) passes through a matching stub (2) and a quarter-wave transformer (3) to the measuring line (4) of impedance Z_{01} and propagation constant β_1. Then the wave passes through the coupling transformer (5), with parameters D, φ_1, φ_2 [2], to the transmission line (6) inserted into the liquid container (transducer line). The transducer line impedance and propagation constant are Z_{02} and β_2 respectively.

If the liquid is a poor conductor a wave absorber (7) is placed in the liquid at the end of the line. Interference between the incident and reflected waves in the measuring line gives a current or voltage minimum of position dependent on the liquid level in the transducer. The differential signal detector (8) seeks the minimum automatically. This detector contains two detector units with line probes.

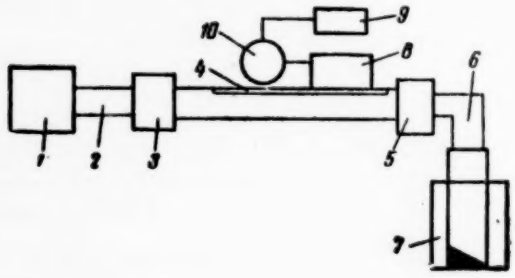

Fig. 1.

The detector units are connected in opposition and a difference signal is produced at the output, of amplitude and phase dependent on the relative positions of detector and minimum. The h.f. generator is amplitude-modulated at line frequency. The difference signal is fed to an amplifier (9), with phase-sensitive output, and actuates the servomotor (10), which drives the differential head along the measuring line. The minimum position corresponds to zero difference signal. The differential head is stationary at this position. The phase of the difference signal changes by 180° on passing through the minimum and the servomotor always drives the differential head towards the minimum. It is readily seen that a standing-wave maximum represents a point of unstable equilibrium in this servo, so the system follows only minima. A similar device has been described [3, 4]. The demand for single-valued readings implies that the wavelength must exceed twice the range in the measured level.

A Method of Altering the Range of Change in the Standing-Wave Minimum.

We now consider how to reduce or increase the movement of the minimum in the line. The range is reduced by filling the line with a dielectric and inserting a coupling transformer between measuring and transducer lines. Consider an ideal conducting liquid. The liquid surface is then a local short-circuit. Denote the distance from a current minimum in the measuring line to the coupling transformer by l_1 (Figure 2) and from the coupling transformer to the liquid surface by l_2. Neglecting line losses we get the relations between these as an S-curve equation [2].

$$\operatorname{ctg}\alpha = k \operatorname{tg}\theta, \tag{1}$$

where

$$k = \frac{1+D}{1-D} \quad (0 \leqslant D \leqslant 1), \quad \alpha = \beta_1 l_1 - \frac{\varphi_1}{2}, \quad \theta = \beta_2 l_2 + \frac{\varphi_2}{2}. \tag{2}$$

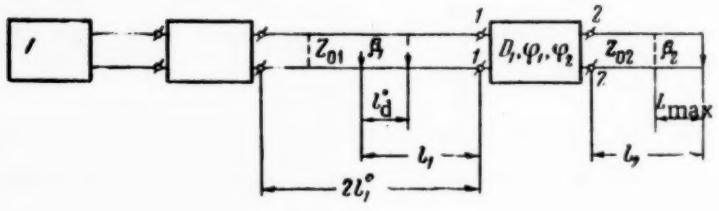

Fig. 2.

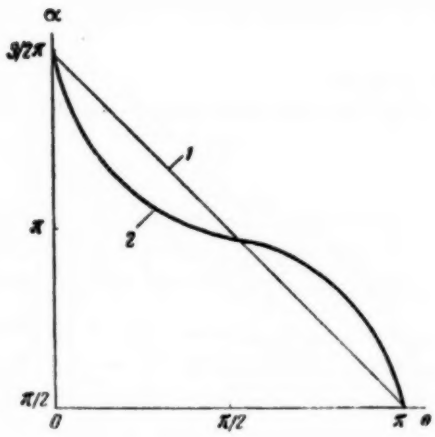

Fig. 3

Figure 3 shows the sections we will subsequently need. We select an S-curve such that positive values of θ from 0 to π correspond to α positive. When $k = 1$ the S-curve degenerates to the straight line 1. This corresponds to a matching coupling transformer. When $\theta = N\pi$ and $\theta = N\pi + \frac{\pi}{2}$, where N is an integer (including zero), the S-curve has an inflection. When $\theta = N\pi + \frac{\pi}{2}$ the S-curve is nearly linear for a wide range in θ, so we can use this region for level measurement. Expanding $\beta_1 l_1$ as a series in θ at a point $\theta = N\pi + \frac{\pi}{2}$ at the center of the compressed region of minimum motion accurate to quantities of the third order inclusive we have

$$\beta_1 l_1 - M\pi - \frac{\varphi_1}{2} = -\frac{\Delta\theta}{k} - \frac{1}{3}\frac{k^2-1}{k^3}(\Delta\theta)^3, \tag{3}$$

where

$$M = 0, \pm 1, \pm 2, \ldots,$$
$$\Delta\theta = \theta - N\pi - \frac{\pi}{2}. \tag{4}$$

The relative deviation from S-curve linearity in the range of expansion may be estimated as the ratio between the nonlinear and linear terms:

$$\eta = \frac{k^2-1}{3k^2}(\Delta\theta)^2. \tag{5}$$

Denote by L_{max} the level deviation from the mean position, corresponding to η reaching a set value. Then, putting $\beta_2 l_2 = (2\pi/\lambda) l_2$, we get

$$L_{max} = \frac{\lambda}{2\pi}\frac{k}{\sqrt{k^2-1}}\sqrt{3\eta}, \tag{6}$$

where L_{max} is half the range of the measured level.* When $\underline{k}$ is large this expression is independent of the coupling transformer parameters.

* $\underline{k}$ in (6) can approach unity as long as L_{max} is less than $1/3$ wave. (6) becomes meaningless on reducing $\underline{k}$ further. With $\underline{k}$ close to 1 we should use (5) to estimate η, substituting $\Delta\theta = \frac{2\pi L_{max}}{\lambda}$. This remark applies to all expressions containing $\frac{k^2-1}{k^2}$.

When β_1 is constant we get

$$\beta_1 = \frac{2\pi}{\lambda}\sqrt{\varepsilon}, \tag{7}$$

where ε is the dielectric constant of the line loading. (3) and (7) imply that the ratio between the minimum and level changes (reduction factor) is

$$K = k\sqrt{\varepsilon}. \tag{8}$$

Given the deviation from linearity η, at the ends of the working range, the displacement of the differential head $2l_d^0$, the distance from the coupling transformer to the center of the measuring line l_1^0, the line loading constant ε, the working range in the level and the distance from the coupling transformer to the center of the working range in the level measured along the transducer line l_2^0, we can find the coupling transformer parameters. The reduction factor is found from

$$K = \frac{L_{max}}{l_d^0}. \tag{9}$$

The generator wavelength and $\underline{k}$ are found from (6) and (8). The condition that the centers of the line and of the liquid level correspond, which follows from the demand that the S-curve deviates least from the rectilinear (see Fig. 2) implies that

$$\frac{\varphi_1}{2} = \frac{2\pi\sqrt{\varepsilon}}{\lambda} l_1^0 + M\pi, \quad \frac{\varphi_2}{2} = N\pi + \frac{\pi}{2} - \frac{2\pi l_2^0}{\lambda}. \tag{10}$$

The case k = 1 is excepted, as corresponding to a matching coupling transformer. The reduction in minimum shift then only occurs because of the changed phase velocity in the loaded line. The wavelength restriction implied by the linearity deviations at the ends of the range drops out, and shorter wavelengths can be used. In certain cases considered below this is the best choice of method for reducing the minimum shift range.

On using the method k, φ_1, φ_2 enter as impedance parameters of the coupling transformer. It is not difficult to derive the parameters if the impedances are given. But here we have the converse problem—transformer design. We now solve this. A normal coupling transformer is a symmetric four-terminal T-network inserted between measuring and transducer lines. The transformer losses may be neglected and the transformer impedances assumed reactive. The series impedances as usual are denoted by Z_s and the parallel impedance by Z_p, so we get the network parameters in the usual form

$$Z_{aa} = Z_s + Z_p, \quad Z_{ab} = -Z_p. \tag{11}$$

Inserting the reflection coefficient of section 1 (Fig. 2) as

$$r_1 = |r_1| e^{j\psi}, \tag{12}$$

we can put down

$$\beta_1 l_1 = M\pi + \frac{\psi}{2}. \tag{13}$$

From the parameters Z_{aa} and Z_{ab} for the network loaded by the short-circuited transducer line we can find an expression for the phase of the reflection coefficient of section 1, and using (13) determine cot $\beta_1 l_1$:

$$\operatorname{ctg}\beta_1 l_1 = \frac{\frac{Z_{aa}^2 - Z_{ab}^2}{Z_{01}Z_{02}} + j\frac{Z_{aa}}{Z_{01}}\operatorname{tg}\beta_2 l_2}{j\frac{Z_{aa}}{Z_{01}} - \operatorname{tg}\beta_2 l_2}. \tag{14}$$

This is a bilinear transform of $\tan \beta_2 l_2$. The expression for cot $\beta_1 l_1$ can also be found directly from S-curve equation, (1), and is also a bilinear transform of $\tan\beta_2 l_2$. Using the uniqueness of the bilinear transform and equating coefficients in the two transforms we get the network parameters in terms of those of the coupling transformer:

$$\frac{Z_{aa}^2 - Z_{ab}^2}{Z_{01}Z_{02}} = \frac{k\operatorname{ctg}\varphi_1/2\operatorname{tg}\varphi_2/2 - 1}{\operatorname{tg}\varphi_2/2\operatorname{ctg}\varphi_1/2 - k}, \tag{15}$$

$$j\frac{Z_{aa}}{Z_{01}} = \frac{k\operatorname{ctg}\varphi_1/2 + \operatorname{tg}\varphi_2/2}{\operatorname{tg}\varphi_2/2\operatorname{ctg}\varphi_1/2 - k}, \qquad j\frac{Z_{aa}}{Z_{02}} = \frac{k\operatorname{tg}\varphi_2/2 + \operatorname{ctg}\varphi_1/2}{\operatorname{tg}\varphi_2/2\operatorname{ctg}\varphi_1/2 - k}.$$

It may be shown that not all values for the transformer parameters can be realized in a passive four-terminal network transformer. The condition that they be physically possible is that one of the following inequalities applies:

$$\operatorname{tg}\varphi_1/2\operatorname{tg}\varphi_2/2 < -k, \quad \operatorname{tg}\varphi_1/2\operatorname{tg}\varphi_2/2 > -\frac{1}{k}. \tag{16}$$

In practice the given quantities are usually Z_{01}, Z_{02}, $\varphi_1/2$, and k. $\varphi_2/2$ and hence the transducer line length, to an integral number of halfwaves, are found from these and the second expression in (10). Then the following relations for $\tan\varphi_2/2$, Z_{aa} and Z_{ab} are correct:

$$\operatorname{tg}\varphi_2/2 = \frac{pk-1}{k-p}\operatorname{ctg}\varphi_1/2, \qquad j\frac{Z_{aa}}{Z_{01}} = \frac{(k^2-1)\operatorname{ctg}\varphi_1/2}{(pk-1)\operatorname{ctg}^2\varphi_1/2 - k(k-p)},$$

$$-\frac{Z_{ab}^2}{Z_{01}Z_{02}} = \frac{p(k^2-1)^2\operatorname{ctg}^2\varphi_1/2}{[(pk-1)\operatorname{ctg}^2\varphi_1/2 - k(k-p)]^2} + \frac{k(pk-1)\operatorname{ctg}^2\varphi_1/2 - (k-p)}{(pk-1)\operatorname{ctg}^2\varphi_1/2 - k(k-p)}, \tag{17}$$

где $p = Z_{01}/Z_{02}$.

where $p = Z_{01}/Z_{02}$.

Since Z_{ab} can be selected with either sign from (15) or (17) a transformer of given parameters can be realized via two networks, in one of which the parallel impedance is capacitative and in the other inductive.

So far we have considered reducing the minimum shift on the measuring line. We now briefly consider a use for increased shift. The maximum slope of the S-curve occurs at $\theta = N\pi$. The series expansion is

$$\beta_1 l_1 - M\pi - \frac{\pi}{2} - \frac{\varphi_1}{2} = -k\Delta\theta - \frac{1}{3}k(1-k^2)(\Delta\theta)^3, \tag{18}$$

where $\Delta\theta = \beta_2 l_2 + \varphi_2/2 - N_\pi$.

The relative deviation from linearity is

$$\eta = -\frac{k^2-1}{3}(\Delta\theta)^2. \tag{19}$$

This shows that the linear range falls as k increases.

Relation of the Standing-Wave Minimum Position in the Measuring Line to the Level of an Arbitrary Liquid

We now consider the relation of the standing-wave minimum in the measuring line to the level of an arbitrary liquid of given dielectric constant and loss angle. The relation can be shown to remain linear over a large liquid level range only if the reflection coefficient remains constant along the section of the transducer line in the liquid. This is so if the wave propagating within the liquid is absorbed and so there is no reflection at the end of the transducer. If the liquid conducts a short column of it is an adequate absorber. With a low-loss liquid a matching absorber must be placed at the end of the transducer. With no absorber the relation between minimum position and level can be found from the general expression for the reflection coefficient in Section 1 (Figure 2) in terms of that in Section 2 and the coupling transformer parameters [2]:

$$r_1 = e^{j\varphi_1} \frac{D + r_2 e^{-j\varphi_1}}{1 + D r_2 e^{-j\varphi_1}}. \tag{20}$$

The reflection coefficient of Section 2 is

$$r_2 = b e^{-2j\beta_2 l_2 + j\psi'}, \tag{21}$$

where ψ' is the phase of the reflection coefficient in the line section coinciding with the surface, b the modulus of the reflection coefficient. (20) gives a relation between $\beta_1 l_1$ and $\beta_2 l_2$:

$$\operatorname{tg}(2\beta_1 l_1 - \varphi_1) = \frac{-A \sin(2\beta_2 l_2 + \varphi_2 - \psi')}{1 + B\cos(2\beta_2 l_2 + \varphi_2 - \psi')}, \tag{22}$$

$$A = \frac{b(1 - D^2)}{D(1 + b^2)}, \quad B = \frac{b(1 + D^2)}{D(1 + b^2)}. \tag{23}$$

When the transducer is matched ψ' and b are level-independent and enter (23) as parameters. The inflexion in the contracted region occurs at $\beta_2 l_2$, given by

$$\beta_2 l_2 = -\frac{\varphi_2}{2} + N\pi + \frac{\psi'}{2}. \tag{24}$$

When the ideal conducting liquid is replaced by one of given dielectric constant and loss angle the phase of the reflection from the liquid becomes other than π and b becomes other than unity. So the inflexion is displaced and the contraction coefficient of the working range alters. It is of importance that $b/(b^2 + 1)$ is a maximum at b = 1. So when b deviates slightly from one the correction to the reflection coefficient, as may be shown from (23) will vary as the square of Δ, given by

$$\Delta = 1 - b. \tag{25}$$

The coupling transformer contraction coefficient we get as

$$k \approx k_0 \left(1 - \frac{k_0^2 - 1}{4k_0^2}\ \Delta^2\right), \tag{26}$$

where k_0 is the minimum shift contraction coefficient for an ideal conducting liquid. With a liquid of high dielectric constant and low loss we get

$$k \approx k_0 \left(1 - \frac{k_0^2 - 1}{\varepsilon_0 k_0^2}\right). \tag{27}$$

Thus if the modulus of the reflection coefficient is close to one the minimum shift contraction coefficient is not sensitive to the modulus of the reflection coefficient, the more so the higher the dielectric constant.

The expression for the modulus of the reflection coefficient with a matched transducer is

$$b = \sqrt{\frac{\varepsilon_0 + \cos\delta - 2\sqrt{\varepsilon_0}\cos\ \delta/2\ \sqrt{\cos\delta}}{\varepsilon_0 + \cos\delta + 2\sqrt{\varepsilon_0}\cos\ \delta/2\ \sqrt{\cos\delta}}}, \tag{28}$$

where δ is the loss angle and ε_0, the real part of the dielectric constant. When k = 1 the minimum position is independent of the modulus of the reflection coefficient.

We now consider the effect of the phase of the reflection coefficient on the level measurement. Here we replace ψ' by ψ'' given by

$$\psi' = \psi'' + \pi. \tag{29}$$

$\psi'' = 0$ corresponds to an ideal conducting liquid. (22) implies that a ψ'' different from zero causes a shift of minimum in the measuring line equivalent to that caused by a level change of

$$\Delta l_2 = \frac{\lambda}{4\pi}\psi''. \tag{30}$$

Thus the level measurement can be in error because of unknown changes in the electrical properties of the liquid. We now estimate these errors. Putting the complex dielectric constant in the form

$$\varepsilon = \varepsilon_0(1 - j\,\mathrm{tg}\,\delta) \qquad \left(0 \leqslant \delta \leqslant \frac{\pi}{2}\right) \tag{31}$$

and using the expression for the reflection coefficient for a liquid in a matched transducer

$$r = -\frac{\sqrt{\varepsilon}-1}{\sqrt{\varepsilon}+1}, \tag{32}$$

we get ψ'' as

$$\operatorname{tg} \psi'' = \frac{-2\sqrt{\varepsilon_0}\sqrt{\cos\delta}\sin\delta/2}{\varepsilon_0 - \cos\delta}. \tag{33}$$

An ideal insulating liquid ($\delta = 0$), $\psi'' = 0$ is just like an ideal conducting one ($\delta = \pi/2$). Thus there is a loss angle at which ψ'' show an extremum. It is readily shown from (33) that the loss angle δ_m corresponding to the extremal phase is given by

$$\cos\delta_m = \frac{\varepsilon_0}{2\varepsilon_0 - 1}. \tag{34}$$

In particular, when the dielectric constant is high (30) and (33) give on substitution into (34) the following expression for the maximum level shift.

$$(\Delta l_2)_{\max} \approx \frac{\lambda}{4\pi\sqrt{2\varepsilon_0}}. \tag{35}$$

On choosing the wavelength from (6) with given range-end nonlinearities we get an expression for the relative maximum displacement of the level readings:

$$\frac{(\Delta l_2)_{\max}}{2L_{\max}} \approx \frac{1}{4\sqrt{6\eta\varepsilon_0}} \frac{|\sqrt{k^2-1}}{k}. \tag{36}$$

Even at high dielectric constants unknown changes in the loss within arbitrary limits can cause real errors in level measurement when the permitted deviations from linearity at the ends of the range are small. For example, with water ($\varepsilon_0 = 80$) $k = 3$ and $\eta = 2\%$ we get $(\Delta l_2)_{\max}/2L_{\max} \approx 7.2\%$ (or $\pm 3.6\%$ with appropriate scale displacement). When the conductivity changes in an unknown fashion between arbitrary limits we should therefore use a matching coupler ($k = 1$). Then, selecting the wavelength so as to leave some reserve to cover the demand for unique readings,

$$\lambda = 6L_{\max} \tag{37}$$

we get the relative maximum error in level measurements as

$$\frac{(\Delta l_2)_{\max}}{2L_{\max}} = \frac{3}{4\pi\sqrt{2\varepsilon_0}}. \tag{38}$$

The error is reduced by the shorter wavelength. The above example then gives $(\Delta l_2)_{\max}/L_{\max} \approx 1.9\%$ (or $\pm 0.95\%$). An aqueous solution of acid or alkali of arbitrary concentration is an example of a liquid of high dielectric constant and variable loss. As above, changes in the reflection coefficient due to conductivity changes cause no shift in the standing-wave minimum if a matching coupler is used.

Temperature variations in the dielectric constant can also cause errors. But at high dielectric constants and with normal temperature coefficients it can be shown that the errors are slight.

At low dielectric constants this method can, for a given error, only be used with liquids with restricted loss changes. The limiting permissible loss changes can be determined from (30), (35) and (37).

Errors and Field of Use of the Method.

We now consider the errors not dependent on the electrical properties of the liquid. The main sources are 1) variation in the electrical length of the measuring line, 2) ditto for transducer line, 3) frequency instability, 4) development of a conducting layer on the liquid seal in the transducer line, 5) inexact setting on the standing-wave minimum in the measuring line, 6) inexact absorber matching.

The errors due to these effects will now be considered.

Changes in the electrical length of the measuring line are due to changes in the filler dielectric constant with temperature and humidity. The shift in the minimum is

$$\Delta l_1 = \left\{ -\frac{l_1}{2} + \frac{\lambda}{4\pi\sqrt{\varepsilon}} \frac{\operatorname{ctg} \beta_1 l_1}{1 + \operatorname{ctg}^2 \beta_1 l_1} \right\} \frac{\Delta\varepsilon}{\varepsilon}. \tag{39}$$

When k is large (in particular when $k > 3$) the relative error in the level readings is

$$\frac{\Delta l_2}{2L_{max}} = -\frac{6\eta}{k^2} \frac{\Delta\varepsilon}{\varepsilon}. \tag{40}$$

When k is close to one, by selecting L_{max} from (37) and $\beta_1 l_1$ so that we get the maximum Δl_1 from (39) we get the maximum relative error as

$$\frac{\Delta l_2}{2L_{max}} = -0{,}61 \frac{\Delta\varepsilon}{\varepsilon}. \tag{41}$$

The error is independent of the range contraction. When moisture-stable ceramics with low temperature coefficients are used to load the line the error is negligibly small.

The transducer changes cause a relative error in the level reading given by

$$\frac{\Delta l_2}{2L_{max}} \approx \frac{l_2}{2L_{max}} \left(\alpha + \frac{\Delta\varepsilon_2}{2\varepsilon_2} \right), \tag{42}$$

where l_2 is the transducer length ($l_2 >> L_{max}$), α the thermal expansion coefficient for the cable joining the measuring and transducer lines, $\Delta\varepsilon_2/\varepsilon_2$ the temperature coefficient of the cable insulation dielectric constant.

When the ambient temperature changes are large a unit which automatically balances the changes in the electric length of the cable has to be added. Then the error due to changes in the transducer length can be made unimportant.

Frequency changes are conditioned by the changes in the electric lengths of measuring and transducer lines and in the coupling transformer parameters, which displace the S-curve and alter its slope. The general analytic expression for the error is very complicated. But with the practical line lengths used the main frequency-dependent error is due to equivalent cable length changes, given approximately by

$$\frac{\Delta l_2}{2L_{max}} = -\frac{l_2}{2L_{max}} \frac{\Delta\omega}{\omega}. \tag{43}$$

The simplest exact expression for the frequency error is obtained with a matching coupler:

$$\Delta l_2 = -(l_1\sqrt{\varepsilon} + l_2)\,\frac{\Delta\omega}{\omega} - \frac{\Delta\lambda}{2\pi}\,\frac{\operatorname{ctg}(\beta_1 l_1 - \psi_1)}{1+\operatorname{ctg}^2(\beta_1 l_1 - \psi_1)}\,\frac{\Delta\omega}{\omega}, \tag{44}$$

where

(45)

$$\operatorname{ctg}\psi_1 = -\frac{\sqrt{p^2-p+1}-\sqrt{p}}{p-1},\quad p = \frac{Z_{01}}{Z_{02}},$$

$$\Delta = \sqrt{p}\,\frac{\sqrt{p^2-p+1}-\sqrt{p}}{(\sqrt{p^2-p+1}-\sqrt{p})^2+(p-1)^2}. \tag{46}$$

The maximum value of the second term in (44) can be shown to be $0.25\,\lambda\Delta\omega/2\pi\omega$. $l_1\sqrt{\varepsilon}$ is usually much less than l_2 and can be neglected. So when the transducer line is long enough the frequency error is given by (43). This error is unimportant if the generator is frequency stabilized.

The hermetic seal in the transducer is often made from an insulator. A conducting film of condensed vapor may form on this with conducting liquids, and this will distort the results.

To analyze this error we introduce the dimensionless quantity

$$\sigma' = Z_{02}\sigma, \tag{47}$$

where σ is the film conductivity. Consider the error in the level when σ' is small. As before the transformer liquid distance is l_2, while the liquid-film distance is l_4; solving for the minimum shift in the measuring line when the shunting film is produced we get the level error as

$$\Delta l_2 = \frac{-(1-D^2)\,2P\sin\theta' + Q\,[(1-D^2)\cos\theta' + (1-D^2)(1+D^2)]}{2\beta_2(1-D^2)(1+D^2)}\,\sigma'^2, \tag{48}$$

where

$$P = \frac{\operatorname{tg}^4\beta_2 l_4}{(1+\operatorname{tg}^2\beta_2 l_4)^2},\qquad Q = \frac{2\operatorname{tg}^2\beta_2 l_4}{(1+\operatorname{tg}^2\beta_2 l_4)^2},\qquad \theta' = -2\beta_2 l_2 - \varphi_2. \tag{49}$$

As the error is proportional to the square of σ' the error falls rapidly as the film resistance increases.

When D = 0 we get for Δl_2

$$\Delta l_2 = \frac{\lambda}{2\pi}\,\frac{\operatorname{tg}^3\beta_2 l_4}{(1+\operatorname{tg}^2 l_4)^2\beta_2}\,\sigma'^2. \tag{50}$$

The maximum Δl_2 is

$$(\Delta l_2)_{\max} = 0.35\,\frac{\lambda}{2\pi}\,\sigma'^2. \tag{51}$$

So using (37) we get the maximum relative error:

$$\frac{\Delta l_2}{2L_{\max}} = 0.165\,\sigma'^2. \tag{52}$$

For example, when $\sigma' = 0.245$ this is 1%, so when $Z_{02} = 70$ ohms this implies a film resistance of about 290 ohms. To derive an expression for the error when the line is loaded we restrict ourselves to the most favorable case, where the film falls at a voltage node when the liquid level is at the mean position. The maximum error then falls at the ends of the range. Restricting discussion to normal k($k > 3$) we get the relative error at the range-ends as

$$\frac{\Delta l_2}{2L_{\max}} = \frac{2P(\sqrt{3\eta})\sin\sqrt{3\eta} + Q(\sqrt{3\eta})(1-\cos\sqrt{3\eta})}{4\sqrt{3\eta}}\,\sigma'^2 \approx \frac{3}{2}\,\eta\sigma'^2, \tag{53}$$

where

$$P(\sqrt{3\eta}) = \frac{\operatorname{tg}^4\sqrt{3\eta}}{[1+\operatorname{tg}^2(\sqrt{3\eta})]^2}, \quad Q(\sqrt{3\eta}) = \frac{2\operatorname{tg}^2\sqrt{3\eta}}{[1+\operatorname{tg}^2(\sqrt{3\eta})]^2}. \tag{54}$$

For example, when $\eta = 2.5\%$ this error is 1% when $\sigma' = 0.5$, corresponding to a film resistance of about 140 ohms when $Z_{02} = 70$ ohms.

Now consider the error due to inexact setting on the standing-wave minimum. This is determined by the ratio of the width of the minimum to the range of change in the signal from the differential head, and depends on differences in the temperature changes in the germanium diodes and probe components. If we take the distance between the probes to be much less than one wavelength in the line we get the following expression for the relative error due to inexact setting on the minimum:

$$\frac{\Delta l}{2L_{\max}} = \frac{\Delta g_1 - \Delta g_2}{g}\,\frac{\sqrt{k^2-1}}{8b_1\sqrt{3\eta}}. \tag{55}$$

g is a coefficient of proportionality between the high-frequency amplitude and the low-frequency output from one probe,* Δg_1 and Δg_2 being the deviations in g for the two probes respectively, b_1 being the modulus of the reflection coefficient in the measuring line. The expression is correct for k large.

With a matching coupler we get, remembering (37), that the relative error in the level measurement, instead of (55), is

$$\frac{\Delta l}{2L_{\max}} = \frac{\Delta g_1 - \Delta g_2}{g}\,\frac{3}{8\pi b_1}. \tag{56}$$

Experiment shows that $(\Delta g_1 - \Delta g_2)/g$ is about 1% at 10°C when $b_1 = 1$ in experimental rigs, the separation of the probes being about 0.1 wavelength. Correspondingly, $\Delta l/2L_{\max} \approx 0.1\%$ at 10°C.

* The differential head consists of two probes with their outputs connected in opposition. Each probe has a probe-wire inserted in the measuring line to pick up the high-frequency signal, and a detector. (For further details see [4]).

Consider now the error due to inexact absorber matching in the transducer with a low-loss liquid. This mismatch leads to the phase of the reflection being level-dependent. This in turn causes the relation between minimum setting and level to be nonlinear.

Putting the absorber reflection coefficient as $r = |r|\exp(j\chi)$, we get the phase at the surface in the case of slight mismatching as

$$\psi' \approx \frac{4|r|\sin(2\beta' l - \chi)}{\sqrt{\epsilon_0}}, \tag{57}$$

where $\beta' = 2\pi\sqrt{\epsilon_0}/\lambda$ is the propagation constant in the liquid, l, the distance from the surface to the absorber. From (23) we get the shift in the measured level relative to a linear scale corresponding to exact absorber matching as

$$\Delta l_2 \approx \frac{|r|}{\pi\sqrt{\epsilon_0}}\lambda\sin(2\beta' l - \chi). \tag{58}$$

This error is a deviation from the linear scale and can be removed by using a nonlinear scale. The maximum deviation from linearity is given by

$$\frac{(\Delta l_2)_{\max}}{2l_{\max}} = \frac{|r|\sqrt{k^2-1}}{\sqrt{\epsilon_0}\,k\sqrt{3\eta}} \tag{59}$$

and for a matching transformer

$$\frac{(\Delta l_2)_{\max}}{2l_{\max}} = \frac{3|r|}{\pi\sqrt{\epsilon_0}}. \tag{60}$$

For instance when the standing-wave ratio is about 1.1 (readily obtained) the modulus of the absorber reflection coefficient is 0.05. Then with distilled water, assuming $\eta = 2.5\%$ and $k > 3$, we get $(\Delta l_2)_{\max}/2L_{\max} \approx$ $\approx 2\%$. When $k = 1$ we get $(\Delta l_2)_{\max}/2L_{\max} \approx 0.5\%$. The modulus of the absorber reflection coefficient must be reduced by a factor $\sqrt{\epsilon_0}$ as ϵ_0 falls if we are to retain a constant relative deviation from linearity. E. g. when $\epsilon_0 = 4$ the reflection coefficient must be 0.01 and the standing-wave ratio 1.02, which requires very careful absorber matching.

This study of the main errors shows that when cable changes are compensated, no conducting layer appears on the seal and the electrical parameters of the liquid are unchanged; the error is determined by that in setting on the minimum. The theoretical error is $\approx 0.5\%$ when the temperature changes by 40-50°C.

In conclusion we consider the bounds to the measured level using phase methods. The lower bound is determined by the concept of a level which has so far been considered as a stepwise change in dielectric constant at an interface between two media. The upper bound is determined by the dielectric constants of current insulators which can be used to load the measuring line. In fact the error in detecting the minimum, as (56) shows, does not depend on the working range in the level if the working range in the measuring line is contracted by using a matching transformer. Then the ratio of differential head displacement to measuring line wavelength is independent of the contraction factor. But the working level range using a matching transformer can only be increased by increasing the dielectric constant of the line loading material to the maximum possible. Further

increase in working level range requires the use of large $\underline{k}$ values and this, as (55) shows, increases the error in setting on the minimum in proportion to $\underline{k}$.

The current upper limit is a working level range of about 10 m, assuming the above accuracy to be maintained.

SUMMARY

1) An advantage of the radio wave reflection method for measuring levels automatically is that it can be used with aggressive media in inaccessible sites (where γ-ray level meters cannot be used) while having no moving parts in the transducer. This determines its place among ways of measuring levels.

2) The working range of the standing-wave minimum in the measuring line can be reduced relative to the range in the level by loading the line with dielectric and using a coupling transformer between the measuring line and the cable. The wavelength is determined by the need for the readings to be unique and by the relative deviation from linearity at the ends of the working range.

3) When the dielectric constant and loss in the liquid are constant the error is due to that in setting on the minimum: in experimental rigs this was $\sim 0.5\%$.

4) Additional errors can arise with conducting liquids due to conducting films forming on the transducer seal. This error is proportional to the square of the ratio of the transducer characteristic impedance to the film resistance, and is negligibly small when this ratio is less than 0.1.

5) Unknown changes in the liquid's conductivity alsocause an error. This error is proportional to the wavelength and is least when using a matching transformer. The error is slight at high dielectric constants. For example, it may be about 1% with aqueous solutions.

6) The upper bound to the measurable level at a given error of measurement is determined by the dielectric constants of loading materials usable with the measuring line. The error can be kept constant up to a range of 10 m with current materials. Further range increase involves increased error (at constant measuring line length).

Received September 12, 1956

LITERATURE CITED

[1] R. A. Valitov and V. N. Sretensky, Radio measurements at super-high frequencies. (Military Press, 1951).

[2] J. Slater, The electronics of superhigh frequencies. (Soviet Radio,1948).

[3] V. B. Brodsky, Measurement of liquid levels using superhigh frequencies. Sci.-Tech. Information Bull., Lab. Equip. Res. Inst. (1953).

[4] V. B. Brodsky, Automatic measurement of a liquid level using radio-wave reflection. Equipment design, No. 11 (1957).

THE LAYOUT OF TELEMECHANICS LINES WITH DISTRIBUTED OBJECTS

V. A. Ilyin

(Moscow)

The structural reliabilities and relative lengths of transmission lines are considered. A recommended choice of lines for use with distributed objects is given.

As telemechanics develops there arises a need for systems with fairly numerous small stations distributed over an area or along a line (oil industry, irrigation systems, factories, mines, oil and gas pipes). The number of points controlled from one control point is usually some tens or hundreds, while the total number of control, telemetering and signalling operations at each point is small, often not exceeding 3 — 6. The remote control of such objects is very important but it has received little attention in the literature.

When producing such systems for distributed objects we have to select the layout of the connecting lines.

This paper is concerned with this. In general the terminal equipment has to be considered as well, as this depends on the line layout. This involves the general design of remote control systems, including the line links. This problem is still unsolved. Here we consider a particular case, where the line layout is not particularly dependent on the terminal equipment. This is so when the line links cost much more than the terminal equipment.

The structural reliability and line-length is analyzed on the assumption that the objects are uniformly distributed over an area, as in oil-fields and other such systems.

1. Layout and Line Length

Figure 1 shows the basic layouts of line links. Figure 1a is the simplest for distributed objects. All the others are applicable to objects distributed along a line (1,b) or over an area (1,c-g).

In the radial layout (1,c) all points are joined to the control by separate feeders. The single-feeder line (1,e) passes through all points in a definite sequence. The branched layout (1,c) differs in having intermediate distribution points at which several lines are combined into one "trunk." Special equipment to separate the signals is then required at the branch points.

In the group schemes (1, f and g) the controlled points are grouped and each joined to the control by a separate feeder. Within a group the line passes through the points in a definite sequence. Figure 1,f and g show schemes with m = 4 and m = 6 branches.

A very important criterion determining the cost of the system is the total line length. This criterion becomes more important as the line cost increases, the latter frequently exceeding that of the terminal equipment.

The single-feeder line gives the lowest length per point. The total length L_0 for uniformly distributed points joined rationally to a control point near the center at one of the points may be found from

$$L_0 = l_0 (N - 1), \tag{1}$$

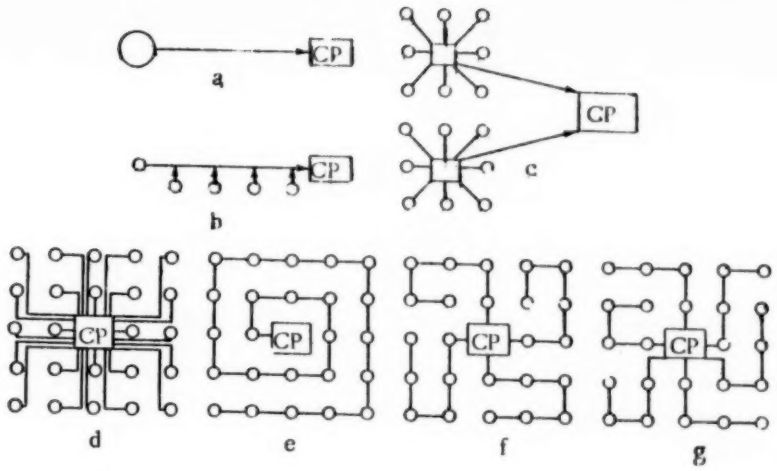
CP
a
CP
b
CP
c
CP
CP
CP
CP
d
e
f
g

Fig. 1.

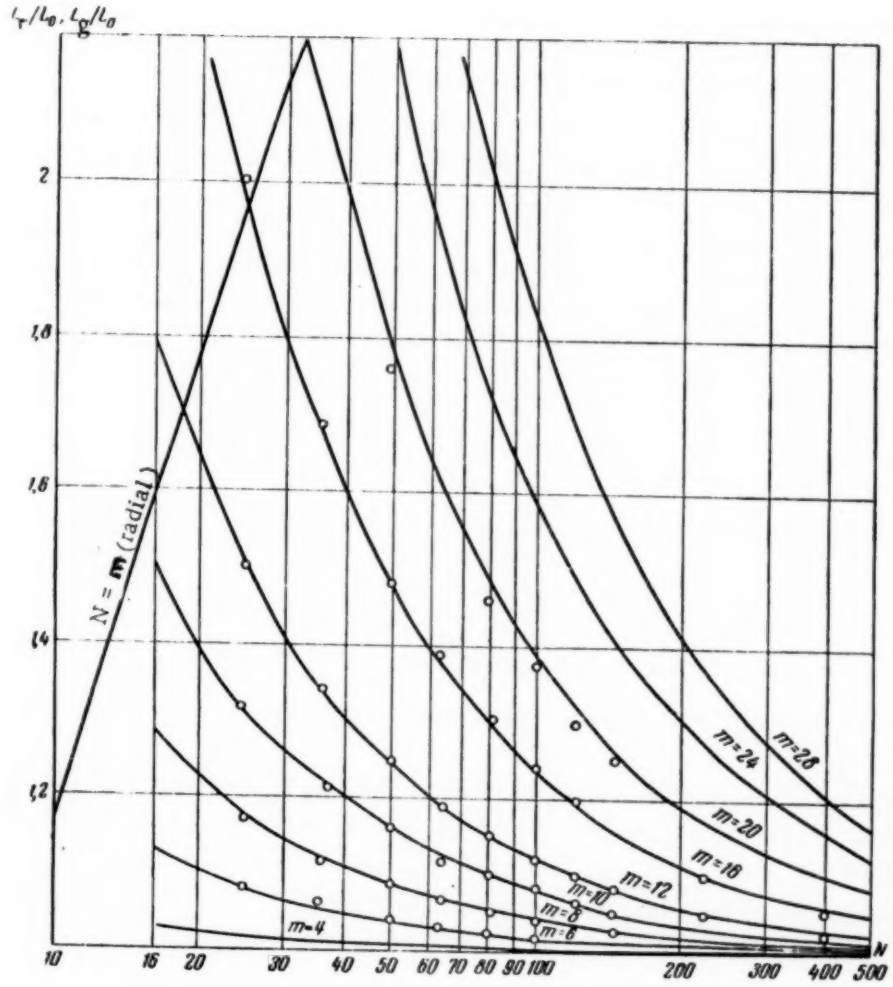
l_r/l_0, l_g/l_0
2
1,8
1,6
1,4
1,2
N = m (radial)
m=4
m=6
m=8
m=10
m=12
m=16
m=20
m=24
m=28
10
15
20
30
40
50
60
70
80
90
100
200
300
400
500
N

Fig. 2.

where l_0 is the distance between adjacent points, N being the total number.

It is convenient to take the relative length of a single-feeder line as unit, the lengths of other lines with the same points being referred to this. Then in the radial and grouped schemes the relative lengths are given by the empirical formulae

$$\frac{L_I}{L_0} \approx \frac{\sqrt{N}-1}{2}, \tag{2}$$

$$\frac{L_g}{L_0} \approx \frac{N-1+0.12\,(m-2)^2}{N-1}. \tag{3}$$

Figure 2 shows these relations. The dots in Figure 2 denote the exact lengths when the lines are laid out in a rectangular grid. The Figure shows that (3) is of low error when $4 < m < 24$ and $m < N$, i.e., in the cases of greatest practical interest.

Figure 2 also implies that the lengths of single-feeder and grouped lines differ but slightly if the appropriate grouping is used. A radial line is much longer when $N > 10$.

2. Reliability of Line Links

Reliable operation of a remote control system depends on the system being immune to noise and on lines and terminal equipment working properly. The lines are often very unreliable in industrial conditions, so an analysis of reliability in order to choose the most efficient line is of considerable interest.

Consider the single-feeder, radial and grouped schemes. The branched layout is not considered because the equipment in the intermediate points affects the reliability, and we are not considering the choice of equipment.

It is convenient to use as criterion the mean time for which an object in the system is inoperative due to line faults. In systems in continuous use this is most important, it being usually known from operational experience. If we assume only two states possible – operative and nonoperative, while line damage is random, then this is found as the probability P that one point is inoperative due to line damage, i.e.,

$$P = \lim_{n\to\infty} \frac{\sum_{i=1}^{n} t_{n_i}}{\sum_{i=1}^{n} (t_{n_i} + t_{o_i})},$$

where t_{n_i} and t_{o_i} are the nonoperative and operative times during the i'th line fault.

P is related to the mean fault frequency $\overline{f}_n$ by the simple expression $\overline{f}_n = P/\overline{T}_n$, where $\overline{T}_n$ is the mean nonoperative time.

We now consider P_1 – the probability of finding a section of length l_0 nonoperative (l_0 being the distance between adjacent points). P_1 is assumed constant and independent of the states of other parts of the line for an arbitrarily chosen length l_0.

Then the probability of finding a length l nonoperative is

$$P_l = 1 - (1 - P_1)^{l/l_0}. \tag{4}$$

We assume initially that damage at any point interrupts the operation of all objects connected to that section. This corresponds to a short-circuit.

A single-feeder system of total length $L_0 = l_0(N-1)$ when damaged at any point ceases to work at all N points. Then from (4) the probability that a point is nonoperative is

$$P_0 = 1 - (1 - P_1)^{N-1}. \tag{5}$$

When $NP_1 \ll 1, P_0 \approx P_1(N-1)$.

With the grouped layout a line length is l_g; damage to such a line causes all objects on it to become inoperative; from (3)

$$l_g = \frac{L_g}{m} = \frac{N - 1 + 0{,}12(m-2)^2}{m} l_0, \tag{6}$$

and from (4) and (6) the probability of one point being inoperative is

$$P_g = 1 - (1 - P_1)^n, \tag{7}$$

where

$$n = \frac{N - 1 + 0.12(m-2)^2}{m}.$$

When $nP_1 \ll 1$

$$P_g \approx P_1 \frac{N - 1 + 0.12(m-2)^2}{m}.$$

In the radial layout the points are connected to the control by separate wires of length l_r where

$$l_0 < l_r < l_0(\sqrt{N} - 1). \tag{8}$$

The mean probability of one point being nonoperative is

$$P_r = \frac{\sum_{i=1}^{N} \left[1 - (1 - P_1)^{\frac{l_{ri}}{l_0}}\right]}{N}. \tag{9}$$

From (2), (8) and (9), when $P_1 \sqrt{N} \ll 1$

$$P_r \approx P_1 \frac{\sqrt{N} - 1}{2}. \tag{10}$$

Figure 3 shows $P_g / P_0 = \varphi(N)$ and $P_r / P_0 = \varphi(N)$ computed from (5), (7) and (10) for $P_g \ll 1$, $P_r \ll 1$. The curves show that the reliability of a grouped line with an appropriate grouping differs from that of the radial system and much exceeds that of a single-feeder line.

The reliability was considered above assuming damage to cause all points connected to that line section to fail. This corresponds to a short-circuit.

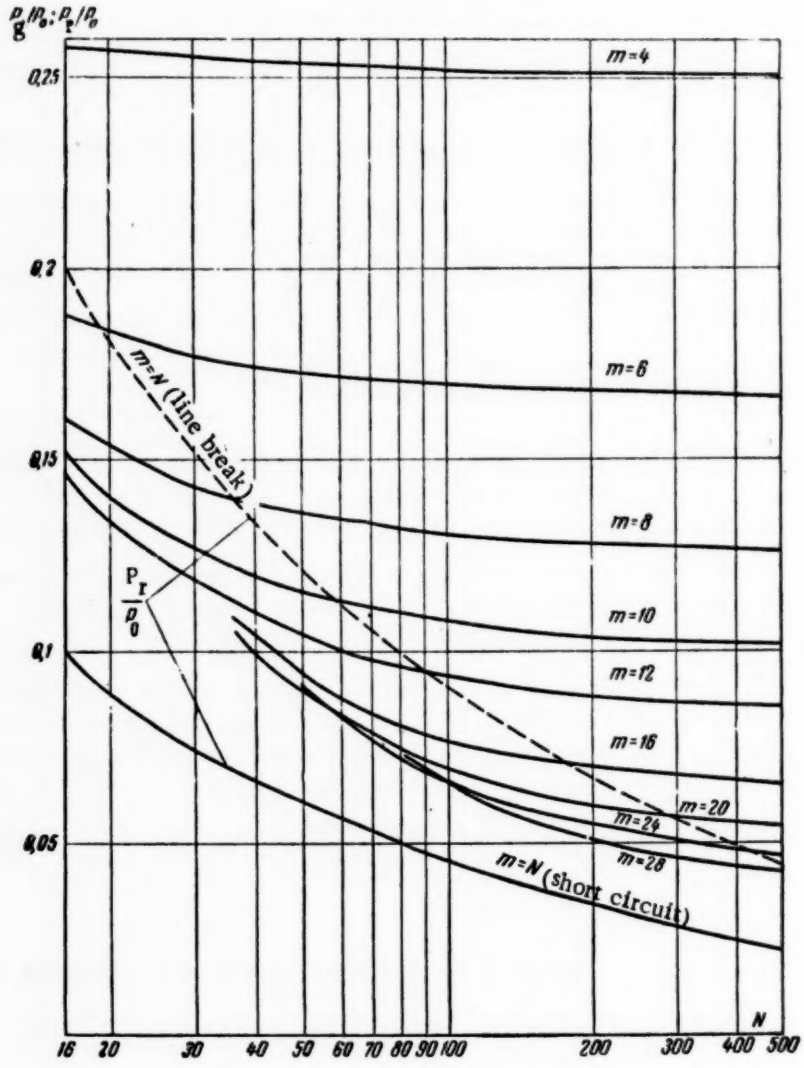

Fig. 3.

When a line breaks in the radial scheme the corresponding point becomes inoperative. But in the grouped and single-feeder systems line breaks on average only cut out half the points on the line. So on the average the relative unreliability against line breaks in the radial scheme increases by a factor two. This corresponds to the dashed curve of Figure 3.

Both types of damage occur under real conditions, so the curve of Figure 3 will pass between the curves for radial lines. Its position will depend on the relative probabilities of the two faults, which are determined by experiment.

Figure 3 implies that a group scheme may be more reliable than a radial one.

The structural reliability requirement to a certain extent is contrary to that of short line lengths. Thus the radial system is the most reliable while the single-feeder is the shortest.

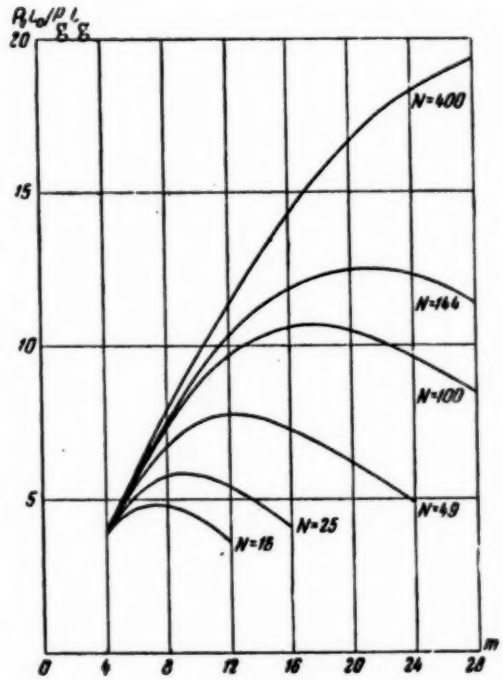

Fig. 4.

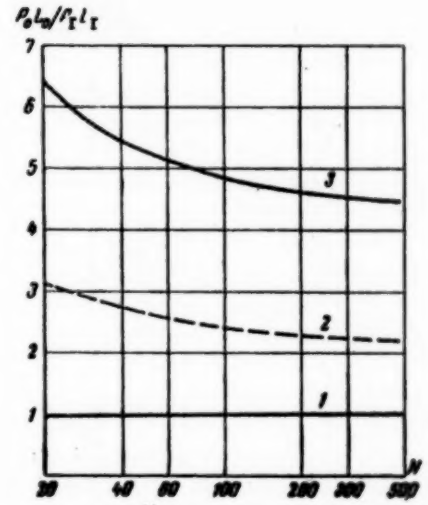

Fig. 5. 1) Single-feeder (m = 1); 2) radial (line breaks); 3) radial (short-circuit).

The choice of line layout should thus combine high safety with relative shortness. So the line quality should be estimated from

$$\gamma = \frac{P_0 L_0}{PL}, \tag{11}$$

where P is the probability of damage to the line, and L the total line length.

γ_0 for a single-feeder line is taken as unity. γ_g and γ_r for grouped and radial lines with $NP_1 \ll 1$ are, from (2), (3), (5), (7) and (10) found as

$$\gamma_g = \frac{P_0 L_0}{P_g L_g} = \frac{m(N-1)^2}{[N-1+0.12(m-2)^2]^2}, \tag{12}$$

$$\gamma_r = \frac{P_0 L_0}{P_r L_r} = \frac{4(\sqrt{N}+1)}{\sqrt{N}-1}. \tag{13}$$

Figure 4 shows $\gamma_g = \varphi(m)$, and Figure 5 shows $\gamma_r = \varphi(N)$. The dashed curve of Figure 5 corresponds to the dashed one of Figure 3 (line breaks).

Figure 4 and 5 imply that a group line is much better, the extent depending on N and m. For a given number of points there is always an optimum, m_{opt}, for which γ_g is maximal.

m_{opt} is determined from (12) by differentiation with respect to m. This amounts to solving

$$N = 0.36m_{opt}^2 - 0.48m_{opt} + 0.52. \tag{14}$$

Figure 6 shows $m_{opt} = f(N)$.

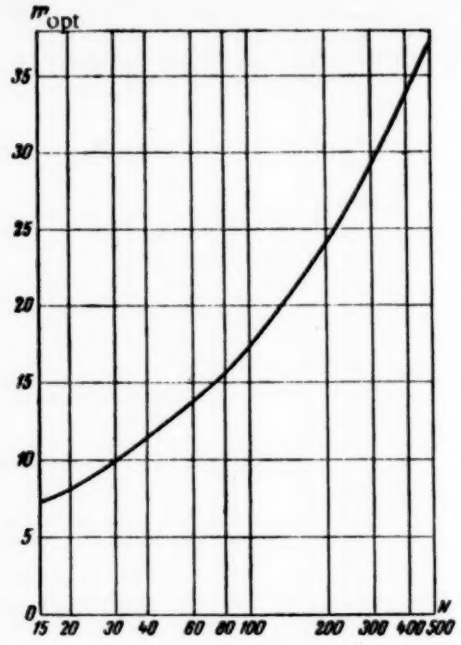

Fig. 6.

The analysis leads to the following conclusions.

1) The grouped system is best. So this system is recommended for objects distributed over an area when $N \gg 1$.

2) The $\gamma_g = P_0 L_0 / P_g L_g = \varphi(m)$ curves have broad maxima (Figure 4). Thus when m is increased or decreased by a factor 1.5 relative to m_{opt}, γ_g falls by only about 10%. So m can be chosen 1.5-2 times greater or less than m_{opt} without making the lines less reliable.

3) If it is more important to reduce line length than to increase reliability we must have $m < m_{opt}$, and in the converse case $m > m_{opt}$.

4) These results involve the mean permissible probability of nonoperation of a line, while sometimes a grouped structure may be one with feeders of different lengths. If we assume a maximum permissible probability of nonoperation the m_{opt} will be close to $\sqrt{N}$.

Received November 21, 1956

DESIGN ASPECTS OF MULTISTAGE MAGNETIC AMPLIFIERS

N. P. Vasilyeva and M. A. Boyarchenkov

(Moscow)

Certain aspects of low-power magnetic amplifier design are discussed. The choice of circuit and number of stages are considered,* and the design parameters of multistage amplifiers are derived from the need for a given rise time.

Multistage magnetic amplifiers are very often used in automatic electric drive controls as they provide very high gains with comparatively short rise times.

The design of such amplifiers has a number of aspects scarcely covered in the literature.

The data for designing them are usually the first-stage input parameters and the final-stage output ones. If the number of stages and intermediate stage parameters are chosen from the data given here, design mainly amounts to designing the separate stages, either full or half-wave, depending on the overall design selected. But the design of low-power amplifiers has certain special features to be dealt with here.

Special Features of Low-Power Amplifier Design

An important property of magnetic amplifiers is that there is no linear relation between the steel volume and output power at a given gain and with the same restricted range of load current k.

It has been shown [1] that the output power and steel volume are proportional when B_0 is the induction with zero magnetizing field, B_k, the induction at maximum magnetizing field, and H_k, the a.c. field strength at maximum magnetizing field are unchanged. It has also been shown that when $H_k/H_{con} = n_{opt}$, where H_{con} is the maximum magnetizing field, has a definite value the steel required per unit power is minimal. So from this we may say that the minimum steel volume is proportioned to the output power only when B_0, B_k and H_k are unchanged if $n_{opt}H_{con} = H_k$.

The amplifier gain, defined as the ratio of load power P_L to control power P_{con} is alone characteristic of the magnetic conditions in the core, being directly related to H_{con}.

$$k_p = \frac{P_L}{P_{con}} = \frac{P_L k_f S_{a\,con}}{\pi f_y^2 \rho l_{st}^2 l w_y (1 - k_{fb})^2}. \qquad (1)$$

Here k_{fb} is the positive feedback coefficient, k_f, the copper infilling factor, $S_{a\,con}$, the cross-section of

* The special circuits with single half-wave transients are not considered.

the control winding, l_{st}, the mean length of a line of force in the steel, $l\,W_{con}$, the mean length of a control turn, and ρ, the copper specific resistance.

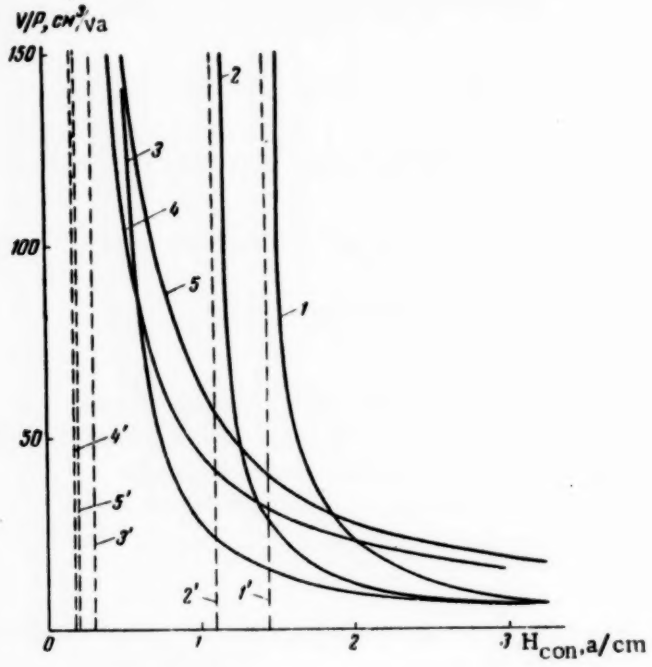

Fig. 1. Relation of the specific volumes to the maximum magnetizing field strength for different materials at f = 50 cycles, k = 10 and cos φ = 1; 1) KhT-18; 2) 0-NP, 3) 65-NP, 4) 79-NM5, 5) 80 NKhS; 1)-5) are asymptotes to their respective curves.

So, if we keep H_{con}, B_0, B_k and H_k unchanged while reducing the steel volume the usable power decreases in proportion, i.e., in proportion to the cube of the linear dimensions, while the control power is reduced only as the first power. So the gain falls with the steel volume.

To prevent gain reduction in low-power amplifiers H_{con} is chosen to be smaller. When k_{fb} cannot be increased this is the sole way of raising the gain. But reducing H_{con}, as has been shown [1] involves increasing the steel volume. This is illustrated by the specific volume curves given in Fig. 1 for various materials.

For each material at a given load current factor reducing H_{con} means increasing the steel volume. At a definite minimal value, $H_{con\,cr}$, termed critical, the steel volume increases without limit.

The physical significance of this is as follows. At a given $\underline{k}$ the coil inductance changes at zero and maximal excitation, x_0 and x_k, must always satisfy.

$$\frac{x_0}{x_k} > k. \qquad (2)$$

x_0/x_k is proportional to the permeability ratio μ_0/μ_k. When H_{con} is reduced μ_k increases, and at some $H_{con\,cr}$, μ_0/μ_k becomes as large as k. If the load current gain is to remain $\underline{k}$ it is in theory necessary to have zero-resistance coils, or that the inductance be infinitely greater than the resistance. The latter occurs if the steel volume becomes infinite, as reflected in Fig. 1.

When drawing up the specific steel volumes $H_{con\,cr}$ is easily found, since when $H_{con} = H_{con\,cr}$, B_k equals B_0.

The following conclusions may thus be drawn.

1) When reducing the power while maintaining the current gain and feedback coefficient the same, the steel required per unit power at first rises slowly and then more sharply, tending ultimately to infinity.

2) Each core material has its own $H_{con\,cr}$ at which it is no longer possible to construct an amplifier of a given current gain.

$H_{con\,cr}$ is less the lower the current gain needed.

The $H_{con\,cr}$ values for various materials differ. The table below gives approximate $H_{con\,cr}$ values for various alloys at k = 10, 5 and 2.

TABLE
Critical Maximal Exciting Field Strengths

Material	$H_{con\,cr}$, a/cm at gains of		
	k = 10	k = 5	k = 2
80-NKhS	0.2	0.1	0.025
79-NM5	0.18	0.0875	0.0219
KhT-18.5	1.4	0.7	0.175
50-NP	1.1(1.15)	0.5	0.13
65-NP	0.3	0.135	0.066
Frequency	f = 50 cycles		

3) When an amplifier of given low power and current gain cannot be built from existing materials, two-stage amplifiers should be used as these work at very low coil current gains (k = = 1.1 — 1.5) and give theoretically infinite gains, which are in practice restricted by the sensitivity threshold and zero drift.

The table was drawn up from the properties of materials given in [7].

Choice of Circuit and Number of Stages

Two-channel circuits are most often used for two-phase magnetic amplifiers. The first stages in such circuits work into a magnetically-coupled d.c. load (Fig. 2). This circuit has a much higher efficiency than a multistage amplifier with each stage a two-phase one with a rectified current load (Figs. 3-5). The lower efficiencies in such circuits are due to the need for ballast resistances. The circuit of Fig. 3 has a theoretical efficiency [2] of 17%, those for Figs. 4 and 5 [3,4] being 50%, while the efficiencies of single-phase amplifiers with d.c. outputs can in theory be close to unity. In practice the efficiency falls with the output power, since the rectifier resistance relative to the load becomes much larger.

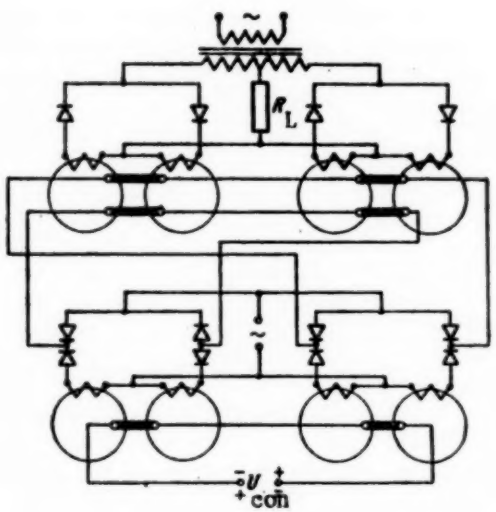

Fig. 2.

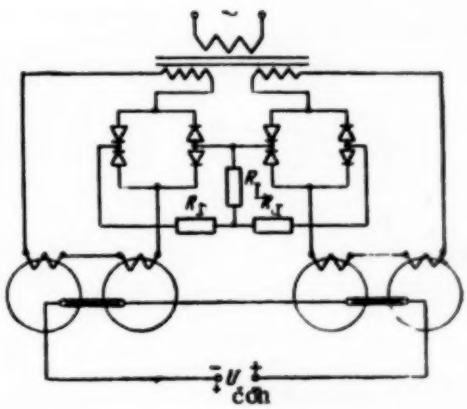

Fig. 3.

The first stages in a two-channel circuit also differ favorably from the above circuits (Figs. 3 and 5) in being simple. But the presence of two magnetically coupled loads makes a two-channel circuit somewhat less convenient to build.

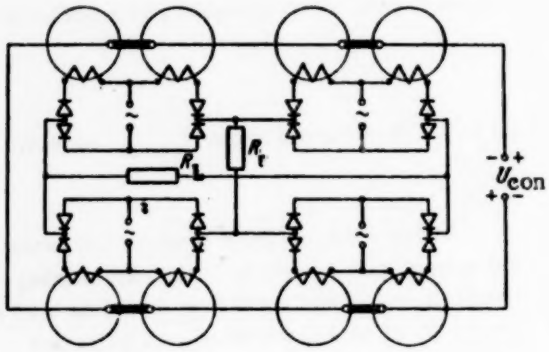

Fig. 4.

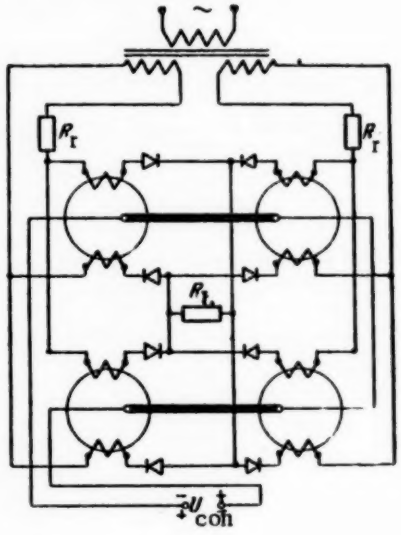

Fig. 5

The circuits of Figs. 4 and 5 can be used as the output stages of two-channel circuits when there is only one d.c. load. The design of a multistage amplifier must start with the choice of number of stages, and with a decision whether to employ an open system or one with negative feedback [5].

The choice of number of stages is usually determined by the required rise time and gain.

The number of stages for an open system can be found from

$$k_{p_{over}} = k_{p1}k_{p2}k_{p3} \dots k_{pn} = k_p^n, \tag{3}$$

$$T_n = \frac{n\sqrt{k_{r\,over}}(1 - k_{fb})}{4f\eta}. \tag{4}$$

With a closed-loop system the number of stages is found from

$$k_{p_{des}} = mk_{p_{over}}, \tag{5}$$

$$m = 1 + \beta k_u^n, \tag{6}$$

$$T_n = \frac{n\sqrt{mk_{p_{over}}}(1 - k_{fb})}{4fm\eta}. \tag{7}$$

In (3) - (7) it is assumed that all n stages are identical, with identical gains k_{p_1}, k_{p_2},...,k_{pn}, feedback factors k_{fb} and efficiencies η, and the symbols used are $k_{p\,overall}$, given overall useful power gain, β, negative feedback coefficient, k_u^n, voltage gain, in the ratio of open and closed-loop voltage gains, T_n the overall time-constant.

When the number of stages and stage gain have been selected the load current and resistance of the first stage can be selected. When the first-stage output power is very small rectification involves large losses in the rectifiers. So the current and resistance must be selected to give the maximum possible efficiency in stage one. The efficiency is

$$\eta = \frac{I_L^2 R_L}{I_L^2 (R_L + R_o + R_r)} = \frac{P_L}{P_L + I_L^2 (R_o + R_r)},$$

where R_L is the load resistance, R_o, the winding resistance, R_r, the rectifier resistance and I_L, the load current.

The area of the working windings is usually selected from the permissible current density, and we may assume the winding resistance inversely proportional to the load current:

$$R_o = \rho \frac{l_{av} \Delta}{I_L} = \frac{C_1}{I_L},$$

where l_{av} is the mean length of a turn, Δ is the current density.

The rectifier resistance rises as the current falls, approximately as $R_r = C_2 + C_3 / I_L$, where C_2 and C_3 are constants readily found from the rectifier characteristic.

Thus

$$\eta = \frac{P_n}{P_L + (C_1 + C_3) I_L + C_2 I_L^2}.$$

This shows that the efficiency rises as the load current falls. So to increase the efficiency we must make the first-stage load resistance R_{L_1} as large as possible. But R_{L_1} cannot be increased without limit due to winding limitations (as it is the control coil of stage two) and the rectification efficiency falls with the current. The second factor is particularly important with selenium rectifiers. The amplifier supply voltage has to increase along with R_L (at a given load power) and so the rectifier reverse current increases, or else the number of plates has to be increased. All these factors, together with a possible drop in feedback coefficient with reduced rectification efficiency, must be carefully allowed for when selecting the load resistance of the first stage. And even so, if the output power of the first stage is in the hundred microwatt range the rectifier resistance will vastly exceed any practicable load resistance. The efficiency and k_{fb} will then be so low that the useful output power of the stage may be comparable with the input power. It is then impossible to have equal gains in all stages [5] and the first stage has to be made of higher gain to increase its efficiency.

When the first stage gain has been settled the gains of the other stages are found from

$$k_{p_{over}} = k_{p_1 p} k_{p_2 p} \ldots k_{p_n p}, \tag{8}$$

where $k_{p_1 p}$ $k_{p_2 p}$,..., k_{pnp} are the gains of the 1, 2,..., $\underline{n}$ stages, defined as the ratio of the useful power to the input power in each stage.

The design gain of each stage is

$$k_p = \frac{I_L^2 R_L + P_r + P_o}{I_{con}^2 R_{con}}. \tag{9}$$

Here P_r is the power loss in the rectifier, P_o being that in the working winding, I_{con} the control current and R_{con} the control winding resistance. A preliminary value for the working winding resistance $R_{o\sim}$ can be found from $R_{o\sim} = a R_L$, where a = 0.05 — 0.25. As the power increases, $\underline{a}$ falls.

When the design gains of all stages have been fixed we consider the time-constant of the whole system via

$$T_{over} = \sum_{i=1}^{i=n} T_i, \tag{10}$$

$$T_i = \frac{k_{p_i}(1 - k_{fb})}{4f\eta_i} \tag{11}$$

When the design gain of stage one is much higher than those of the other stages because of rectifier resistance the time-constant of stage one largely determines the time-constant for the whole system. So all measures necessary to increase feedback at constant gain in the first stage should be taken. This can be done via additional external feedback while simultaneously reducing the control winding turns.

A fault in this solution is that the input resistance drops sharply.

The overall time-constant can be reduced and input resistance increased simultaneously by using overall negative electrical feedback while increasing the stage gains as much as possible.

If the above approximate derivation of the time-constant gives a satisfactory value we can proceed to design each stage normally [1, 6].

It must be remembered that in practice it is easy by using a few extra turns on the external feedback winding to increase the feedback coefficient to 0.95 or more.

But for reasons of stability k_{fb} should not be very high.

Since in fact the intermediate stages present inductive loads to the rectified current the amplifier may have a strongly nonlinear characteristic [3]. This readily causes a "relay" mode of operation over a short section. The more the core material differs from an ideal one with a rectangular magnetization curve the less linear the amplifier characteristic will be. This is true even with purely resistive loads. So if high feedback coefficients are required without the danger of "relay" operation the following conditions must be observed.

1) Materials with rectangular magnetization loops must be used.

2) The load inductance must be reduced, i.e., the control winding must occupy only a small part of the winding space.

3) The main feedback circuit must be fed from separate rectifiers drawing working, and not load, current [3].

If these conditions are observed the multistage amplifier will operate more stably.

Design Example

We are required to design an amplifier (circuit as of Fig. 2) with the following parameters: P_L = 10 watts, $k_{p\,overall} = 10^5$, T = 0.5 sec, R_{con} = 1000 ohms, R_L = 400 ohms. We estimate the time-constant of a single-stage amplifier with these parameters, taking k_{fb} = 0.96, roughly, and η = 0.8:

$$T = \frac{k_p(1 - k_{fb})}{4f\eta} = \frac{10^5(1 - 0.96)}{4 \times 50 \times 0.8} = 25 \text{ sec}$$

So a single-stage amplifier with the required rise time is impossible.

With a two-stage one with equal stage gains we have:

Stage gain

$$k_{p1} = k_{p2} = \sqrt{k_{p_{over}}} = \sqrt{10^5} = 316;$$

Time-constant

$$T = \frac{n\sqrt{k_{p_{over}}}(1 - k_{fb})}{4f\eta} = \frac{2 \times 316(1 - 0{,}96)}{4 \times 50 \times 0{,}8} \approx 0{,}163 \text{ sec.}$$

A two-channel circuit is used for the first stage.

The subsequent calculation is as follows:

$$P_{in} = \frac{P_L}{k_{p_{over}}} = \frac{10}{10^5} = 10^{-4} \text{ w}, \quad P_L = k_{p1}P_{in} = 316 \times 10^{-4} = 3{,}16 \times 10^{-2} \text{ watt.}$$

If the no-load power is negligible relative to the maximum P_{L_1} in each arm we can assume the power input to stage two to be about P_{L_1}.

To select the load current and resistance for stage one, some rough calculations are made.

1) Putting the load current $I_{L_1} = 60$ ma we get the load resistance

$$R_{L_1} = \frac{P_{L_1}}{I_{L_1}^2} = \frac{0{,}0316}{0{,}06^2} = 8.8 \text{ ohm}$$

We assume high inverse voltage germanium rectifiers used, one per arm.

From the rectifier bridge a.c. voltage-current curve (Fig. 6) we get $R_T = 11.7$ ohms. The a.c. winding is taken as having a resistance 15% of R_{L_1} : $R_{O\sim} = 1.32$ ohms. Then we get the design k_{p1} as

$$k_{p1des} = \frac{I_{L_1}^2 \Sigma R}{P_{in}} = \frac{0.06^2(8.8 + 11.7 + 1.32)}{10^{-4}} = 785.$$

Then

$$\eta = \frac{R_L}{\Sigma R} = \frac{8.8}{21.8} \approx 0.4.$$

Assuming that approximately $R_{ap} = R_L + R_T + R_{O\sim} \approx X_C$, where X_C is the inductive impedance of the coil at maximum signal, we find the supply voltage $U_\sim$ roughly (it must be found exactly when carrying out the complete design) as

$$U_\sim = I\sqrt{R_{ap}^2 + X_c^2} = IR_{ap}\sqrt{2} = 0.06 \times 21.8\ \sqrt{2} = 1.86 \text{ v.}$$

2) Let us use the value of the load current $I_{L_1} = 10$ ma; then $R_{L_1} = P_{L_1}/I_{L_1}^2 = 0.0316 \times 10^4 = 316$ ohm, the resistance of the bridge at this current $R_T = 50$ ohm, $R_O = 45$ ohm.

The design power gain and efficiency are

$$k_{p1des} = \frac{0\,01^2(316 + 50 + 45)}{10^{-4}} \approx 410. \quad \eta \approx \frac{316}{410} = 0.77.$$

Thus this second design gives more than double the efficiency and reduces the stage power gain, which determines the size and time-constant by a factor 2.5. The supply voltage will now be

$$U_\sim \approx 10 \times 10^{-3} \times 410\sqrt{2} = 5.8 \text{ v.}$$

3) When I_{L1} = 2 ma we get R_L = 8000 ohms, R_r = 180 ohms, $R_{O\sim}$ = 1200 ohms, k_{p1des} = 375, η = 0.85 and $U_\sim \approx$ 26.5 volts. This latter design gives an efficiency 7% higher but the load resistance rises from 316 to 8000 ohms, i.e., the production of the second stage is made more difficult.

Therefore we select the second design.•

The time-constant of stage one is

$$I_1 = \frac{k_p(1-k_{fb})}{4f\eta} = \frac{410(1-0.96)}{4\times 50\times 0.77} \approx 0{,}1 \text{ sec.}$$

The output current and load are

$$I_{L2} = \sqrt{\frac{P_{L2}}{R_{L2}}} = \sqrt{\frac{10}{400}} = 0.158 \text{ a.}$$

The equivalent rectifier resistance is half the bridge resistance at this current: R_r = 2 ohms. The load winding resistance is taken as 5% of R_L: R_O = 20 ohms.

$$k_{p2\,des} = \frac{I_{L2}^2 \Sigma R}{P_{L1}} = \frac{0.158^2(400+20+2)}{0{,}0316} = 334, \quad \eta_2 = \frac{400}{422} = 0{,}95,$$

$$T_2 = \frac{334(1-0{,}96)}{4\times 50\times 0{,}95} = 0{,}07 \text{ sec.}$$

The total time-constant is $T_1 + T_2$ = 0.17 sec. The subsequent design steps are as usual.

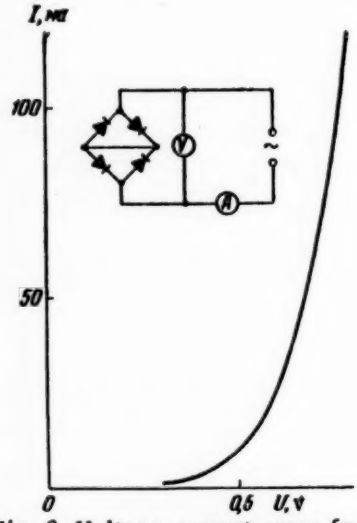

Fig. 6. Voltage-current curve for a bridge made from DG-Ts26 rectifiers.

Received April 28, 1956

• When designing round selenium rectifiers we should have to increase the number of plates, which would reduce the efficiency and increase the design gain.

LITERATURE CITED

[1] N. P. Vasilyeva and O. A. Sedyk, Design of coil magnetic amplifiers with complex loads. Automation and Remote Control 16, No. 1 (1955).

[2] M. Rozenblat, Magnetic amplifiers. State Power Press (1949).*

[3] H. F. Storm, Magnetic Amplifiers. J. Wiley and Sons,(N. Y. 1955).

[4] R. Kh. Balyan, Two-phase magnetic amplifiers with d.c. outputs. Automation and Remote Control 17, No. 2 (1956).**

[5] N. P. Vasilyeva and M. A. Boyarchenkov, Effect of overall feedback in a multistage magnetic amplifier. Automation and Remote Control 17, No. 10 (1956).**

[6] N. P. Vasilyeva, Design of two-phase power magnetic amplifiers. Automation and Remote Control 17, No. 1 (1956).**

[7] O. I. Aven, Magnetic alloys for magnetic amplifier cores and their single-cycle magnetization curves. Automation and Remote Control 17, No. 4 (1956).**

* [In Russian.]

** [See C. B. Translation.]

AN ELECTRONIC ANALOG TO A WIRE POTENTIOMETER

M. A. Schnaidman

(Moscow)

An analog to a wire potentiometer used as the transducer of an automatic regulator is described and analyzed. The model allows for wiper backlash and the stepwise nature of the winding.

1. The Problem

The sensitive element plus potentiometer acts as a transducer and is used in regulators for transducing the controlled quantity to a voltage. When automatic control systems are analyzed such units are sometimes considered as having two links: a linear one with a time-constant, and a nonlinear one with a static characteristic determined by hysteresis in the sensitive element, by the finite potentiometer subdivision and the bounds to the senser or potentiometer. Figure 1 shows such a characteristic where

$$|U_{in_1}| = |U_{in_2}| - |U_{in_1}| = \ldots = |U_{out_1}| = |U_{out_2}| - |U_{out_1}| = \ldots$$

In most cases the potentiometer steps or senser hysteresis are neglected, but cases occur where this is impermissible. Many control systems belong to this class, as the control range covers few turns of the potentiometer.

It is very difficult to analyze systems with such nonlinearities, particularly when the order is comparatively high and the system has yet other nonlinearities.

So an analog to the transducer with a characteristic as of Fig. 1 is required. The analog must be very accurate, have high input and low output resistances and large input and output voltage ranges. The design must also envisage large step-height and output voltage variations.

This indicates that standard operational amplifiers used in analog equipment should be used.

2. Operating Principle of the Wire Potentiometer Analog

Figure 2 shows the block diagram, the system being closed-loop with negative feedback, containing a summing unit Σ, the nonlinear unit NE and a memory unit MU. Figure 3 shows the characteristic of NE. The memory unit was an integrator.

Let the input and output voltages be zero at time zero. If the input increases the input U_1 to NE will increase. While this is less than the setting voltage U_s the circuit is open, no signal passes to the integrator and the output remains zero. When U_1 equals U_s the nonlinear element operates and a step-signal is applied to the integrator. The loop is closed and the high integrator gain causes the output voltage to rise rapidly. The negative voltage returned to the summing unit increases simultaneously, and so U_1, being the difference between the

input and feedback voltages, falls rapidly, which opens the loop. Then the output (from the integrator) will remember a voltage step of height ΔU_{out}.

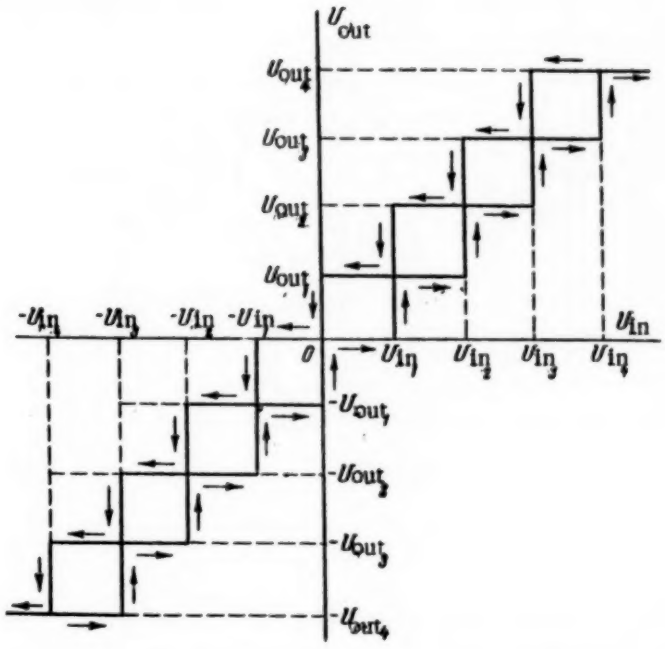

Fig. 1.

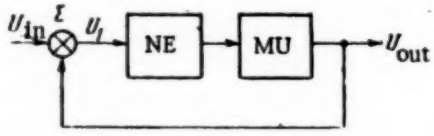

Fig. 2.

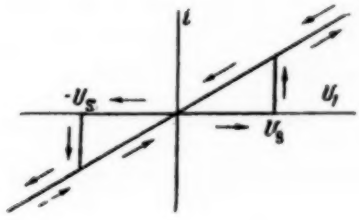

Fig. 3.

When U_{in} increases further and we once again have $U_1 = U_s$ the nonlinear element again operates and produces an output voltage step. The output becomes 2 ΔU_{out}, etc. The output will be constant during any given step until the input voltage has changed sufficiently to cause the next stepping operation. Thus the rising branch of Fig. 1 is followed.

When the sign of the rate of input change alters the output will remain constant until U_1 equals $-U_s$. The nonlinear element then operates in the reverse sense and a signal of opposite sign passes to the integrator. The output will change stepwise by ΔU_{out} with sense reversed. The falling branch of Fig. 1 will be followed. When the sign of the rate of input change alters the output will remain constant until U_1 equals $+U_s$, the rising branch will again be followed, giving a closed loop.

The desired step height is produced by changing the summing unit gain, the insensitive zone being adjusted via U_s.

So far as the author is aware, Meneley [1] was the first to propose a potentiometer analog. In his circuit (Fig. 4) two thyratrons were used as the nonlinear element. Thyratrons reproduce the desired characteristic of Fig. 3 very inaccurately since the extinction voltage can never be zero. Symmetric operation is difficult due to

scatter in the thyratron characteristics. A major fault is that their operation depends on the ambient temperature.

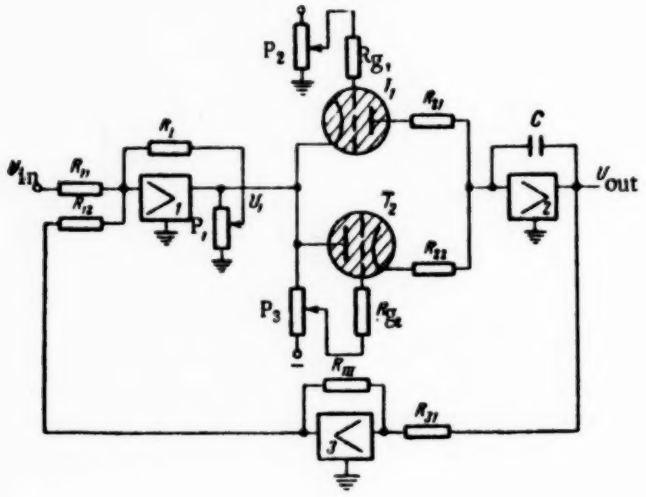

Fig. 4.

So two ways of developing an analog circuit were chosen: a) improving the above thyratron circuit, as this is relatively simple, and b) developing a fresh circuit without thyratrons, of higher accuracy and stability.

3. The Nonlinear Element in the Potentiometer Analog

a) Thyratron nonlinear devices. The thyratron characteristic i = f(U) is defined by the striking and extinction voltages and by the slope in the conducting mode. The striking voltage depends on the negative bias on the grid while the slope depends on the sum of thyratron and load resistances. The extinction voltage depends both on grid bias and plate load.

Two thyratrons are used to reproduce the nonlinear characteristic of Fig. 3; these are inserted in the integrator input circuit, one having its plate joined to the input, and the other, its cathode. The thyratrons show a scatter in their characteristics. This can be removed by using adjusters.

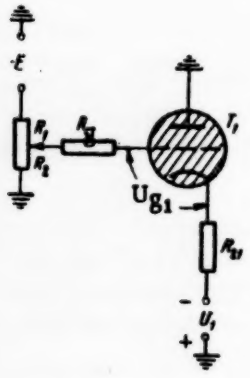

Fig. 5.

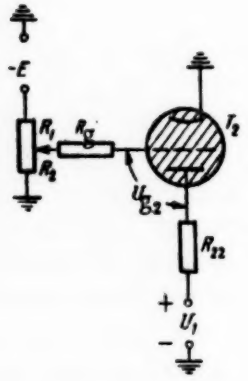

Fig. 6.

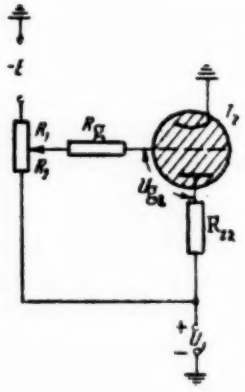

Fig. 7.

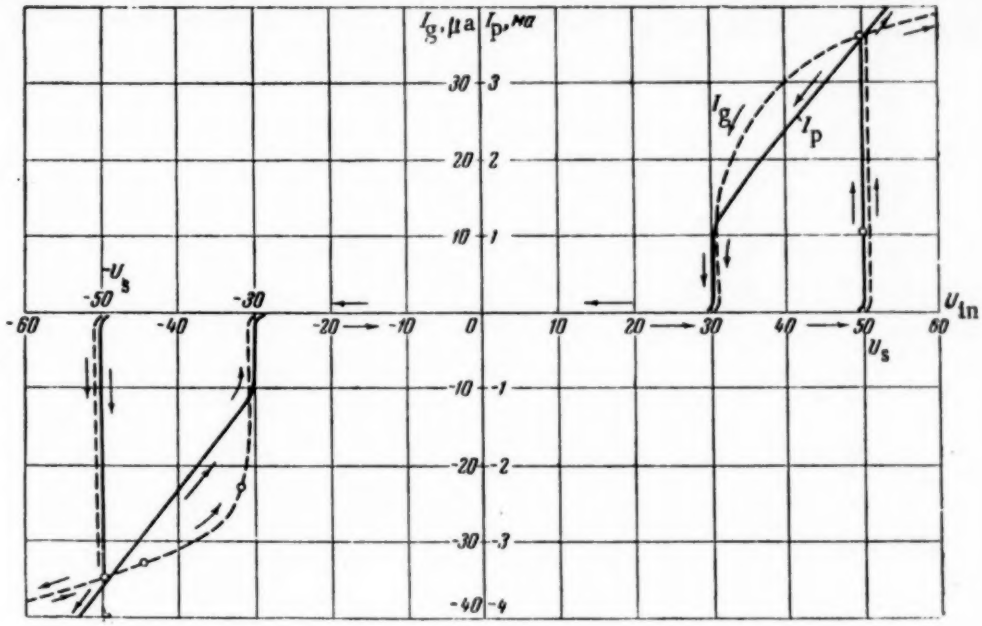

Fig. 8.

The grid currents must also be zero at all input signals prior to striking if the two thyratrons are to operate identically. This is so if their grid voltages are always negative and sufficiently large.

For the negative branch (Fig. 5) the following relation applies:

$$U_{g_2} = -E\frac{R_1}{R_1 + R_2} + U_1. \tag{1}$$

The grid voltage depends on U_1, but even at maximum U_1 its is negative so no grid current flows.

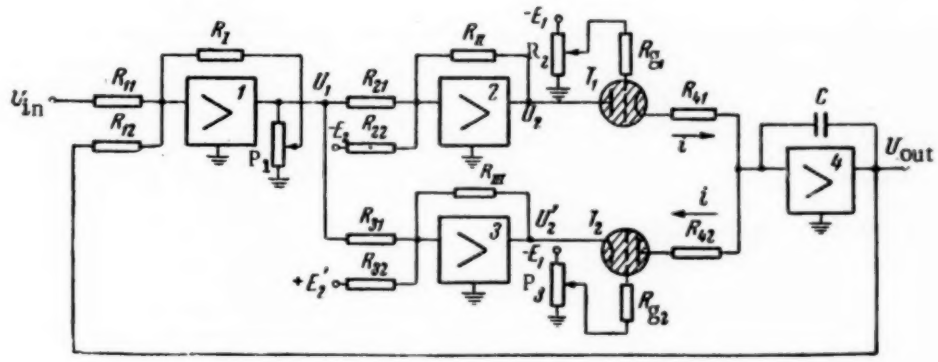

Fig. 9.

The second branch, if as of Fig. 6, shows the following relation:

$$U_{g_2} = -E\frac{R_1'}{R_1' + R_2'}. \tag{2}$$

U_{g_2} is then small in absolute value (almost zero) which is why grid current flows and distorts the characteristic. To prevent grid current in the positive branch the thyratron is connected to a bridge circuit, the bias voltage being applied to a diagonal (Fig. 7). Then we have

$$U_{g_2} = U_1 - \frac{U_1 + E}{R_1 + R_2} R_2 = U_1\left(1 - \frac{R_2}{R_1 + R_2}\right) - E\,\frac{R_1}{R_1 + R_2}. \tag{3}$$

U_{g_2} then changes roughly as in the negative branch. Figure 8 shows experimental voltage-current curves for both branches of the thyratron circuit.

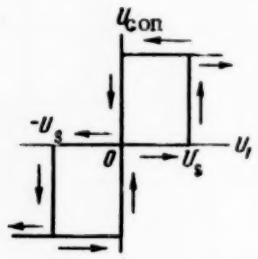

Fig. 10.

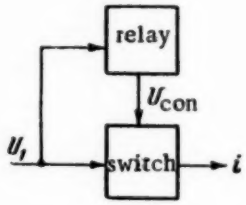

Fig. 11.

If an amplifier is inserted before the thyratrons (Fig. 9) and balancing voltages $-E_2$ and $+E_2'$ are used, the extinction voltages of both thyratrons can be made zero, thus making the branches symmetric and of the form of Figure 3.

b) Nonlinear element as a relay controlled by a diode switch. The desired nonlinear characteristic can be produced by applying U_1 to a diode switch and a relay element with the characteristic of Fig. 10, the relay output voltage acting as a control voltage for the switch. The block diagram of such a system is shown in Fig. 11. When $U_1 < U_s$ the switch is open and no signal reaches the integrator. When U_1 equals U_s in absolute value a voltage appears at the relay output which balances the switch bias and the switch closes, passing a step signal to the integrator. When the signal subsequently becomes smaller the relay output will stay constant as U_{con} which will keep the switch closed and let it open only when the signal falls to zero.

The operating principles of the relay and switch circuits have been studied [3].

The condition for the nonlinear element to work properly in the complete analog circuit will here be $|U_s| = E_1$, $U_{con} = E_b$, $E_b > E$. Figure 12 shows the complete circuit using this nonlinear element.

4. Circuit Analysis and Parameter Calculations

We will put down the equations for the various potentiometer analog circuits.

The summing unit equation is

$$U_1 = -k_1(U_{in} - U_{out}), \tag{4}$$

where k_1 is the transfer coefficient.

The nonlinear element is described by:

positive branch

$$i = \begin{cases} 0 & \text{when } U_1 < U_s \text{ and } \dot{U}_1 > 0, \\ \dfrac{U_1}{R} & \text{when } U_1 > U_s \text{ and } \dot{U}_1 > 0, \\ \dfrac{U_1}{R} & \text{when } U_1 > 0 \text{ and } \dot{U}_1 < 0; \end{cases} \tag{5}$$

negative branch

$$i = \begin{cases} 0 \text{ when } U_1 > -U_s \text{ and } \dot{U}_1 < 0, \\ \frac{U_1}{R} \text{ when } U_1 \leqslant -U_s \text{ and } \dot{U}_1 < 0, \\ \frac{U_1}{R} \text{ when } U_1 < 0 \quad \text{and } \dot{U}_1 > 0. \end{cases} \tag{6}$$

In (5) and (6) $R = R'_t + R_{21} = R''_t + R_{22}$, where $R'_t + R''_t$ are the thyratron resistances in the first design and those of the diodes in the second. Since when $|U_1| < U_s$ the integrator input current is zero the integrating capacitor retains its initial charge and the output remains as initially

$$i = 0, \quad U_{out} = U_{out_0} \tag{7}$$

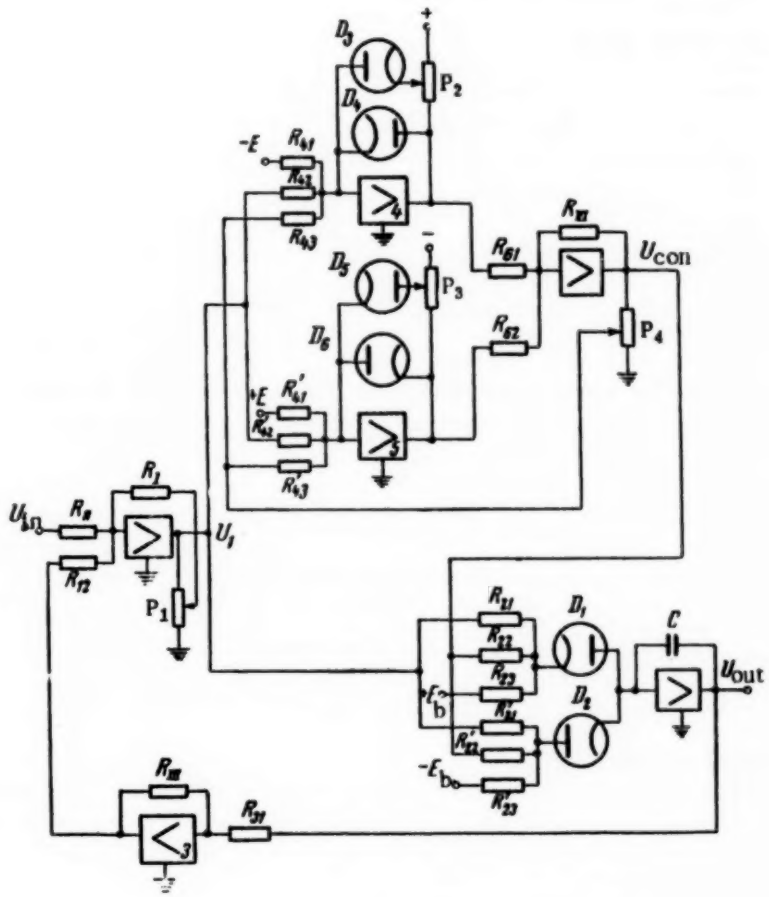

Fig. 12

This corresponds to the output voltage falling on some definite step.

When $|U_1| \geq U_s$ the switch closes and a current flows in one branch:

$$i = -CpU_{out} \tag{8}$$

The transient corresponding to the voltage rise from one step to the next is given for the closed-loop state by

$$[RCp + k_1]\, U_{out} = k_1 (U_{in} - U_{out})_{max} \tag{9}$$

which is derived from (4) - (8).

Solution of this gives

$$U_{out} = (U_{in} - U_{out})_{max}\left[1 - e^{-\frac{k_1}{RC}t}\right] + U_{out_0} \tag{10}$$

In the steady state (t = ∞)

$$U_{out_{ss}} = (U_{in} - U_{out})_{max} + U_{out_0} = U_{out_0} + \Delta U_{out} \tag{11}$$

where $\Delta U_{out} = (U_{in} - U_{out})_{max}$ defines the step height.

The rate of output voltage rise is

$$\dot{U}_{out} = \frac{k_1}{RC} \Delta U_{out}\, e^{-\frac{k_1}{RC}t}. \tag{12}$$

when t = 0

$$\dot{U}_{out} = \dot{U}_{out_{max}} = \frac{k_1}{RC} \Delta U_{out} \tag{13}$$

The rise rate determines the leading-edge distortion: the rate rising with the open-loop gain

$$k_{open} = \frac{k_1}{RC}. \tag{14}$$

ΔU_{out} is determined by the maximum difference of input and output voltages:

$$\Delta U_{out} = (U_{in} - U_{out})_{max} = \frac{U_s}{k_1}. \tag{15}$$

The number of output voltage steps is

$$n = \frac{U_{in_{max}}}{\Delta U_{out}} = \frac{U_{in_{max}}}{U_s} k_1. \tag{16}$$

Keeping U_s constant at, say, 50 volts when n = 2 — 20 and $U_{in_{max}}$ = 100 volts, we get k_1 = 1 — 10.

The analog must be studied for stability. The inherent time-constants of d.c. amplifiers prevent one increasing the open-loop gains without limit since they eventually become unstable.

Experiment shows that operational amplifiers from standard analog equipment have maximum k_{open}

values at which stability is guaranteed of 5000. Hence the integrator gain is

$$k_2 = \frac{k_{open}}{k_{1max}} = \frac{1}{R_{21}C} = \frac{5000}{10} = 500.$$

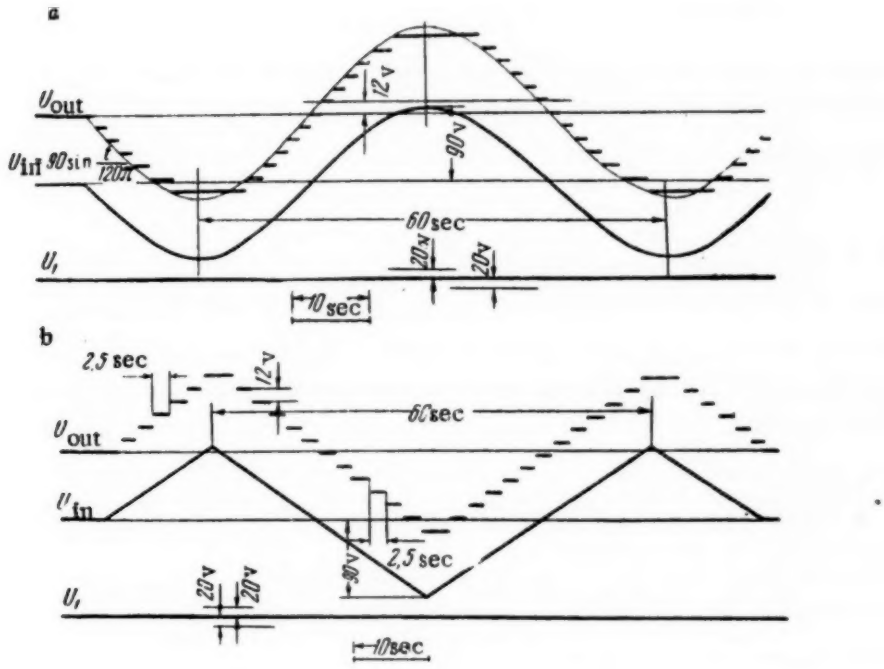

Fig. 13

5. Estimation of Output Voltage Distortions From Step-Form, and Experimental Results

The steps are distorted because the leading edge rises at a finite rate, and also the integrator voltage does not remain constant on any one step.

The rate of rise increases with the open-loop gain

$$\dot{U}_{out_{max}} = \frac{k_1}{RC} U_{in}$$

The greatest distortions occur when the open-loop gain is least, i.e,, when fewest steps are used. Then the rate of rise of the leading edge is specified by the angle

$$\alpha = \operatorname{arc\,tg} k_{open} = \operatorname{arc\,tg} \frac{k_1}{RC} = \operatorname{arc\,tg} 500 \approx 89°55'.$$

In pulse work it is assumed that the leading edge rise is practically complete at $U_{out} = 0.95\ U_{out_{max}}$.

Hence the duration of the leading edge is $\Delta t = RC \ln 0.05$. When RC = 0,002 sec, Δt = 0,008 sec.

On switching off the integrator the voltage should remain constant until the passage to a fresh step. There

are two main causes of distortion here: leakage resistance in the integrating capacitor and zero drift in the d.c. amplifier.

Particular attention must be paid to capacitor quality and amplifier input grid insulation to reduce the leak. Drift-free amplifiers should be used to eliminate zero drift, and the duration of the operation should be restricted.

Figure 13 shows curves obtained for triangular and sinusoidal inputs.

SUMMARY

This circuit is a basic one for use in analogs to the nonlinear static characteristics of wire potentiometers, allowing for wiper backlash and finite winding subdivision.

The author is indebted to V. G. Spichkina for assistance with the experimental work.

Received July 6, 1956

LITERATURE CITED

[1] C. A. Meneley, Applications of Electronic Differential Analyzers to Engineering Problems. Proc. IRE, vol. 41, No. 10 (1953).

[2] A. M. Bonch-Bruevich, Use of electronic tubes in experimental physics. State Tech. Press (1956).*

[3] Ya. O. Kogan, Analogs to automatic control systems with typical nonlinear characteristics. Automation and Remote Control 16, No. 2 (1955).

* [In Russian.]

OPERATIONAL DESIGN OF RELIABILITY IN SYSTEMS CONTAINING MANY ELEMENTS

G. V. Druzhinin

(Moscow)

The wide use of systems with many elements demands the development of designing for reliability.

Quantitative relations between the probability of a fault in the whole system and the probabilities of faults in the parts have been given [1]. The data used to compute reliability by Siferov's method are the mean working life of an element and the mean square deviation from this mean. These data are derived in tests and can be used in design.

But in some devices used industrially, in aircraft, or at sea, the true reliability may differ materially from that so computed. The reasons are as follows.

a) The operating conditions may affect the working life greatly. It has been stated [2] that electronic equipment exposed to climatic changes develops faults 13 times more frequently than in laboratory conditions.

b) The elements may have been manufactured several years previously and since stored under unfavorable conditions; correct usage may not have been observed.

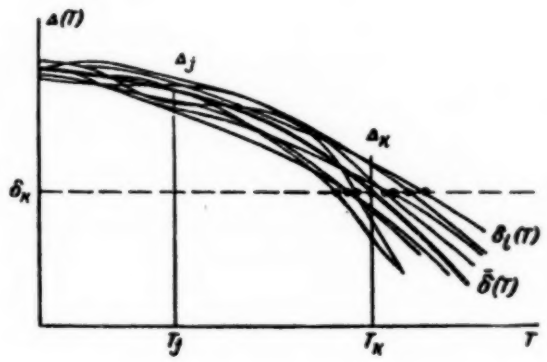

Fig. 1

Statistical tests of reliability on equipment destined to work under defined conditions are costly and do not provide the data until the equipment is obsolescent. During this time the equipment is often used under conditions very different from those originally intended. So we need a way of estimating reliability for a particular specimen under specific conditions.

Elements can fail in two ways: suddenly breaking down, or gradually deteriorating. Sudden failures are usually mechanical (cracks, breaks, etc.) and depend on design and manufacture. Sudden failure is difficult to preduct other than from tests on the equipment.

Consider gradual deterioration. Each element has a parameter δ which specifies its quality (e.g., curvature of characteristic in a tube). If δ changes the system may fail. Denote the critical fail value of δ by δ_k. In a system containing n identical elements δ is a random function of working time, $\Delta(T)$. From the points where the random function of $\Delta(T)$ for each element $\delta_i(T)$ cuts the straight line $\delta = \delta_k = \text{const}$ we can determine the distribution law in correct operating time about the mean value T_k (Fig. 1).

If the law is known we can compute the reliability. Since the law is usually assumed normal we need only T_k and the mean-square deviation from this, σ_T. Consider the approximate determination of T_k and σ_T for two different δ's.

Suppose that at time T_j and T_{j+1}, which are read off from the beginning of the operation, the calculation was carried out for the values of the parameter δ for all elements of the system. To derive the random quantities Δ_j and Δ_{j+1} the numerical statistical characteristics are found, i.e., the mean value (mathematical expectation) and the mean square deviation, from

$$\bar{\delta}_j = \frac{\sum_{i=1}^{n} \delta_{ji}}{n}, \quad \sigma_j = \sqrt{\frac{\sum_{i=1}^{n} (\delta_{ji} - \bar{\delta}_j)^2}{n-1}}, \tag{1}$$

where i is the element number, n is the number of elements, j is the measurement number.

Supposing δ and σ to change linearly during operation (Fig. 2) we get approximate relations for T_k and σ_T. Figure 2 shows that

$$\bar{\delta}(T) = \bar{\delta}'_0 + aT,$$

where

$$a = \frac{\bar{\delta}_{j+1} - \bar{\delta}_j}{T_{j+1} - T_j}, \quad \bar{\delta}'_0 = \frac{T_{j+1}\bar{\delta}_j - T_j\bar{\delta}_{j+1}}{T_{j+1} - T_j}. \tag{2}$$

When $\bar{\delta} = \delta_k$

$$T_k = \frac{\delta_k - \delta'_0}{a} \quad \text{or} \quad T_k = \frac{\delta_k - T_{j+1}\bar{\delta}_j + T_j\bar{\delta}_{j+1}}{\bar{\delta}_{j+1} - \bar{\delta}_j}. \tag{3}$$

The mean-square deviation of δ from δ_k at T_k will be

$$\sigma_k = \frac{\sigma_{j+1} - \sigma_j}{T_{j+1} - T_j} T_k + \frac{T_{j+1}\sigma_j - T_j\sigma_{j+1}}{T_{j+1} - T_j}. \tag{4}$$

As $\delta(T)$ is linear we have

$$\sigma_T = \frac{1}{|a|}\sigma_k$$

$$\sigma_T = \frac{(\sigma_{j+1} - \sigma_j)T_k + T_{j+1}\sigma_j - T_j\sigma_{j+1}}{|\bar{\delta}_{j+1} - \bar{\delta}_j|}. \tag{5}$$

Knowing T_k, σ_T and n we can [1] calculate the probability y that the whole system will be inoperative during time T from

$$\frac{y}{n} = \frac{1}{2} - \Phi(x), \tag{6}$$

where

$$x = \frac{T_k - T}{\sigma_T}, \tag{7}$$

and $\Phi(x)$ is the tabulated Laplace function.

Given the permissible y we can find the time during which operation is correct from

$$T = T_k - \sigma_T x, \tag{8}$$

deriving from (7).

Figure 3 illustrates the course of the calculation, the equation numbers being shown in brackets.

The above approximate method for elaborate systems, when applied by extrapolating linearly the numerical characteristics of $\Delta(T)$, may by successive approximation be used to predict operational reliability from operational experience.

Suppose $T = 0$ on commissioning, and we know the mathematical expectation of δ, i.e., δ_0, and σ_0.

At time T_1, we measure δ for all elements. Δ_1 is found from (1) as is its statistical mathematical expectation δ_1 and statistical mean-square deviation σ_1. From $\bar{\delta}_0$ and $\bar{\delta}_1$, σ_0 and σ_1 we get the reliability or time of correct operation for the whole system from (3)-(8). The values obtained are approximate. But at the beginning, as the probabilities are small the exact accuracy with which the reliability is predicted when the distribution laws are normal is not very important.

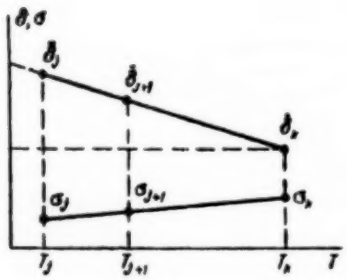

Fig. 2.

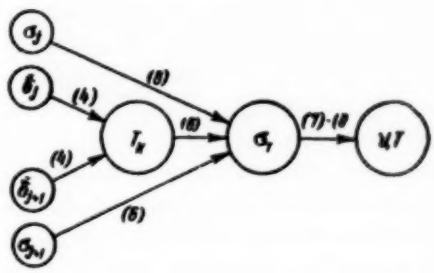

Fig. 3.

Measurements of δ at time T_2 for all elements gives $\bar{\delta}_2$ and σ_2. Using (3)-(8) we again estimate the reliability or residual correct operating time from $\bar{\delta}_1$ and $\bar{\delta}_2$, σ_1 and σ_2 in a second approximation. On subsequent occasions we get $\bar{\delta}_{j+1}$ and using σ_{j+1} and $\bar{\sigma}_j$ found previously we again find the reliability in the $(j+1)$th approximation.

Since the curve $\bar{\delta}(T)$ is a monotonically decreasing one, i.e., the parameter deteriorates during use on the average (failure occurring when $\delta = \delta_k$) the reliability computed after each fresh measurement becomes closer to the true value. This is very important since the probability of break-down increases with the operating time.

When the mean δ varies linearly with operating time (which is common in practice) the reliability can be fairly exactly estimated from the first measurement.

Thus, by the above method we can predict the subsequent reliability after each regular test. Sudden breakages are not susceptible of such prediction.

Received November 3, 1956

LITERATURE CITED

[1] V. I. Siforov, Methods of computing reliabilities for systems containing many elements. Bull. Acad. Sci. USSR, Tech. Sci. Section, No. 6 (1954).

[2] G. W. A. Dummer, Maintainability of services equipment. Part I. J. Brit. Inst. Radio Engrs. vol. 15, No. 6 (1955).

A THREE-PHASE MAGNETIC AMPLIFIER

V. V. Gorsky

(Moscow)

The three-phase magnetic amplifier design proposed is described as regards operating principles, construction and experimental test.

Magnetic amplifiers are now being used for controlling high-power loads. The control of three-phase asynchronous motor speeds is an example. Special three-phase magnetic amplifiers fed from a three-phase line [1] are used, as well as three single-phase amplifiers. A disadvantage of the three-phase amplifier is the difficulty in making it. Therefore three single-phase units are currently preferred to one three-phase one.

The present writer [2] has proposed a three-phase magnetic amplifier (TMA) which has, in his opinion, advantages over existing models.

1. Construction and Operating Principle of the TMA

A notable feature of the TMA (Fig. 1) is that all three phase coils are accomodated on one two-loop core.

The magnetic circuit has two arms of equal cross-section made from standard figure-8 stampings of transformer or special steel. The phase windings (2) are split into two separate equal-turn coils. The six coils are arranged on the six arms of the magnetic circuit as shown in Fig. 1,a.

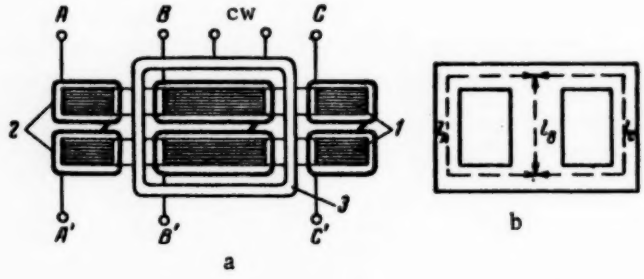

Fig. 1. Three-phase magnetic amplifier: a) layout; b) shape of magnetic circuit.

The coils of any phase are joined in series (Fig. 2,a) or parallel (Fig. 2,b) in such a way that their fields act in opposition.

The magnetizing winding (3) (Fig. 1) and all other control coils are placed above those of phase B on the center arms of the circuit. Thus a single control coil acts on all three phases, so its size is roughly the same as that in a normal single-phase amplifier. Since the central leg is twice as wide as the outer ones the induction

produced by the magnetizing winding will be the same everywhere. But the a.c. induction produced by the a.c. coils in each phase will differ if the phase coils have equal turns.

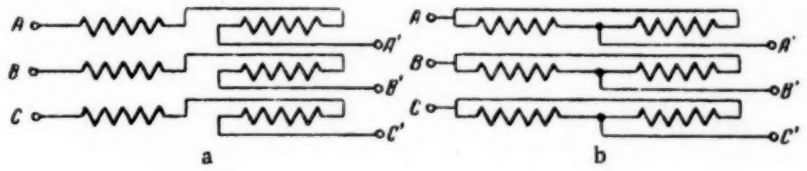

Fig. 2.

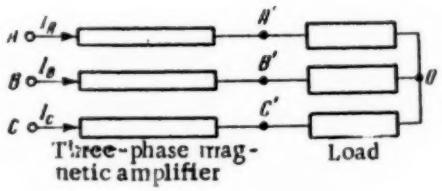

Fig. 3.

Calculations and experiments show that if W_B on the center legs (of phase B) has 1.8-2.3 times less turns than W_A on phase A there will be a point where the currents in all three phases increase almost identically on raising the magnetization. The turns relation between phases A and B depends mainly on the lengths l of their lines of force (Fig. 1,b) and on the operating conditions. If $l_A/l_B > 2$ then we should have $W_A/W_B > 2$ and vice versa.

But the voltage drops in the A and B windings will differ. That in phase B will be about 1.5-2 times less than in A and C. Figure 3 shows the circuit of TMA plus load. The load windings can be star or delta connected.

2. Experimental Results

An experimental amplifier was built. Figure 4 is a photograph of it. The magnetic circuit contains two assemblies made from Sh-40 standard transformer steel stampings. The width of one assembly was 26 mm. The turns on phases A and C on the outside legs were $W_A = W_C = 280 + 280$. For phase B (center legs) $W_B = 140 + 140$, tapped at turns nos. 120. The control coil had 2000 turns. The a.c. windings used d = 0.55 mm wire and the control coil had d = 0.21 mm.

The voltage-current curve for the TMA (current flowing to applied voltage) in star connection is shown in Fig. 5. The abscissa is line voltage. The curve was taken with $W_B = 140 + 140$.

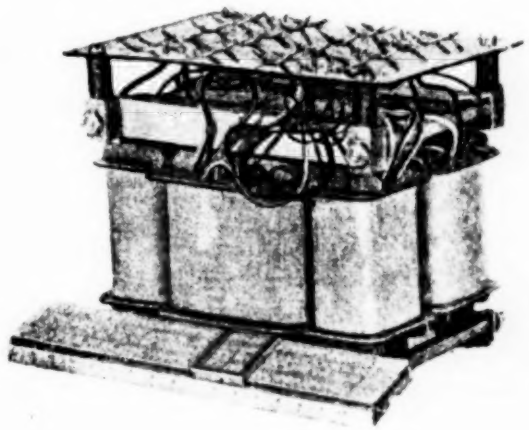

Fig. 4.

Figure 5 shows that the relations of voltage to $I_A = I_C$ and I_B differ slightly. The same applies to the phase-line voltage relations. The voltage on phase B is a factor 1.5-1.6 less than that on B. The relations of I_A, I_B and I_C to the mmf AW_0 at constant line voltage $U_l = 1/3\,(102 + 97 + 101) = 100$ v are shown in Fig. 6. The solid lines relate to $W_B = 140 + 140$, the dashed ones to $W_B = 120 + 120$. The horizontal straight lines are the phase voltages. The graphs show that when $W_A / W_B = 2$ the curves for I_A, $I_C(AW_0)$ and $I_B(AW_0)$ practically coincide, but when $W_A / W_B = 2.33$, $I_B(AW_0)$ runs somewhat higher (dashed line). The phase voltages also alter.

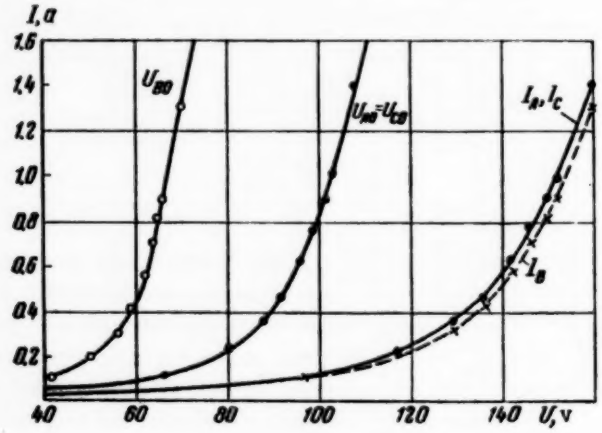

Fig. 5.

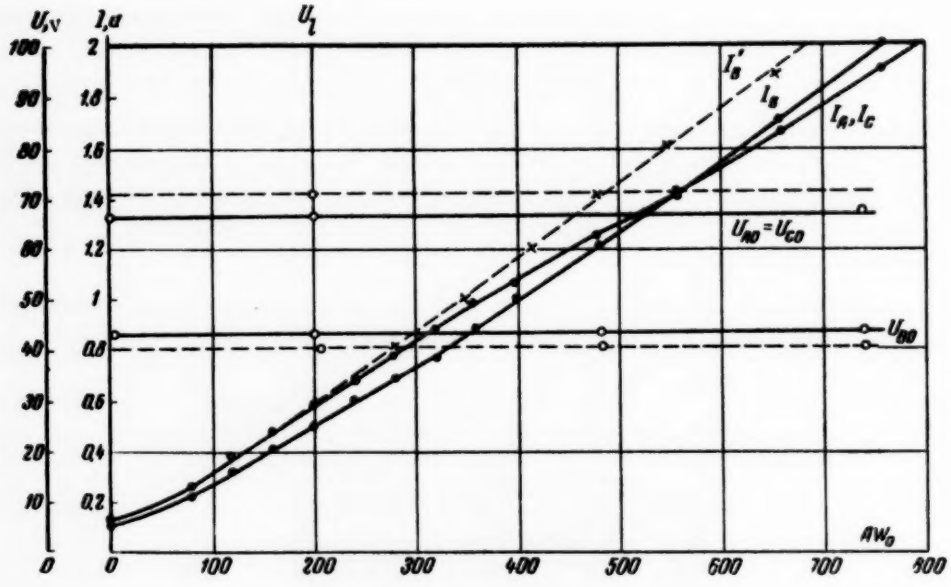

Fig. 6. Control curve for the TMA.

But tests show that the loaded TMA (Fig. 3) shows relations of I_A, I_B and I_C to AW_0 which practically coincide at $W_A / W_B = 2.33$.

Figure 7 shows I_A, I_B and I_C, the terminal voltages $U_{A'B'} = U_{B'C'} = U_{C'A'}$, the phase voltages in the amplifier $U_{BB'}$ and $U_{AA'} = U_{CC'}$ as functions of the magnetizing mmf when a stationary asynchronous motor with short-circuited rotor is used as load. Since the load is symmetric and the current changes identical the motor terminal voltages are symmetric.

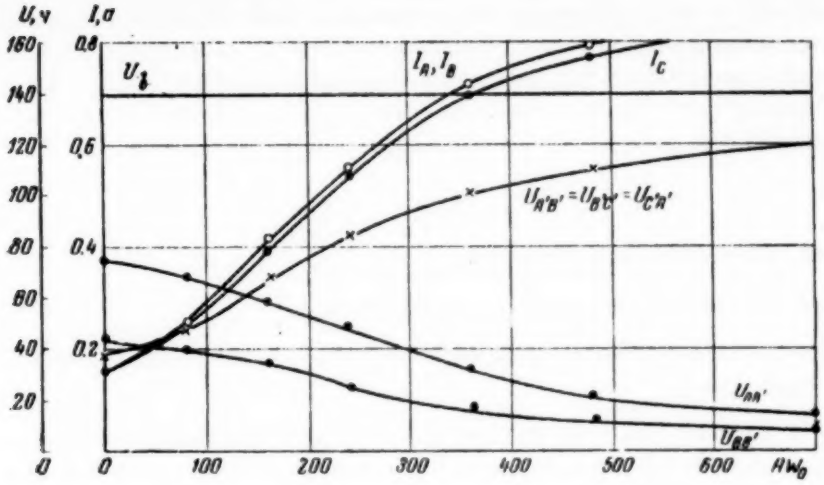

Fig. 7. Control curve for the TMA with a compound load (braked asynchronous motor).

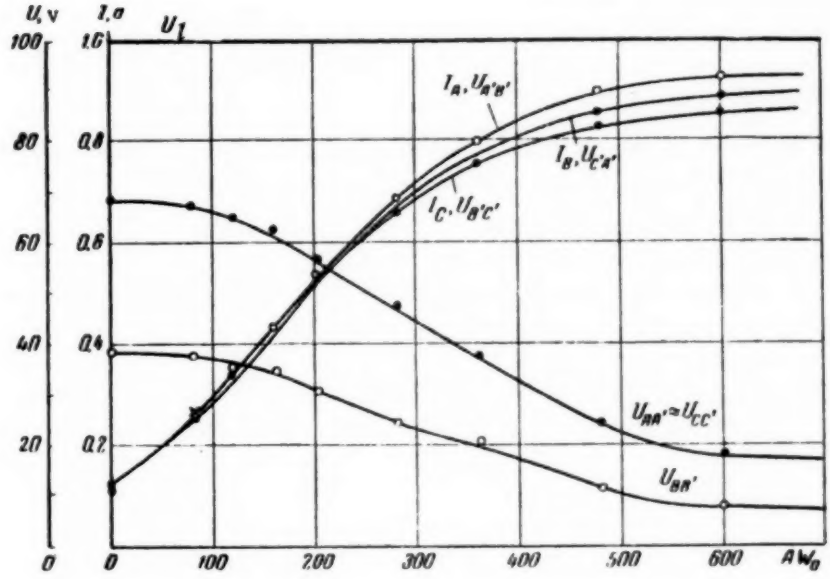

Fig. 8. Control curve for the TMA on a resistive load.

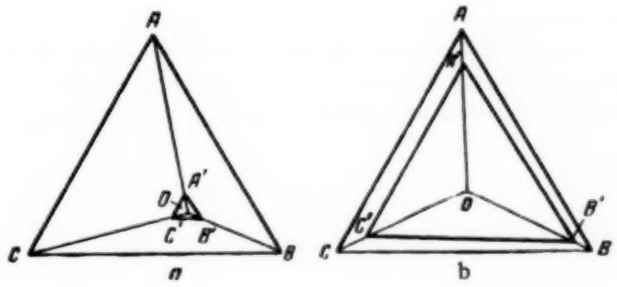

Fig. 9.

Figure 8 shows the same curves when three pure resistances R = 60 ohms are used as load (star-connected). The unbalance between the A and C currents for AW_0 = constant in both cases is due to asymmetry line voltage. The voltage drop across phase B winding is one-half that across A or C. This means that with a symmetric load the neutral is displaced. Figure 9 shows two topographic diagrams for the TMA plus 3 × 60 ohms load (star-connected) at zero magnetizing mmf (Fig. 9,a) and at complete magnetization (9, b). The load terminal voltages are evidently symmetric in both cases but the neutral displacement is considerable.

SUMMARY

Two conclusions can be drawn from the above.

a) The TMA is distinguished by compactness and smaller size.

b) The power gain in a TMA is much higher since one control coil of the size normal for a single-phase amplifier acts on all three phases.

c) The volume of magnetic core is 20-30% less than in systems with three separate phase amplifiers. This is implied by the known relation between the weights of one three-phase and three one-phase transformers.

A disadvantage is the difference in voltage drop between B and A or C. But when the load is symmetric this has no effect on the line and phase voltages on the load terminal. A somewhat serious disadvantage is the unequal voltage drop in the TMA coils which deserve further attention.

Received October 6, 1956

LITERATURE CITED

[1] H. F. Storm, Magnetic Amplifiers, Wiley and Sons, New York (1955).

[2] V. V. Gorsky, Author's affidavit No. 97548.

MODULATION OF RADIOACTIVE EMISSIONS IN AUTOMATIC MEASURING DEVICES

D. I. Ageikin, L. V. Melttser and N. N. Shumilovsky

(Moscow)

Various methods of modulating the radiations used in automatic measuring devices are considered.

New possibilities have been found in using modulated radiations for automatic measurements in industrial processes, giving more reliable and exact equipment without using d.c. amplifiers and special transducers. In some cases [1,2] it is in principle possible to use only modulated radiations for measurements. Methods using modulated emissions are undoubtedly very promising and they can solve many automation problems.

In principle all radiation modulation methods fall into two groups: mechanical and field modulation

Mechanical Modulation

In the simplest case the modulator is simply a chopper placed in the radiation flux. Its window size and rate of rotation are determined by the necessary frequency and pulse duration.

The thickness of the chopper depends on the nature and energy of the radiation.

With α-rays only mechanical strength is involved since a few hundredths of a mm suffice for complete absorption. With β-rays the thickness must be not less than the maximum range of the particles in the material (to give maximum modulation depth):

$$d_m \geqslant \frac{0.546\,E_{max} - 0.16}{\rho_m}. \qquad (1)$$

d_m is the modulator (chopper) thickness, ρ_m the density of the chopper material, E_{max} the maximum β-ray energy.

The chopper thickness when modulating γ-rays has to be so great that it is more convenient to alter the system and attach the isotope to a rotating disc, placing a screen with a hole in front. The radiation will pass through the screen only when the active area on the disc is opposite the hole. Since γ-rays are attenuated exponentially on passing through matter some residual radiation in practice leaks through during the "off" period. The maximum screen thickness d_s is usually taken to give 8-10 fold intensity reduction, so

$$d_s = \frac{2{,}1}{\mu}, \qquad (2)$$

where μ is the linear absorption coefficient.

Sometimes it is more convenient to use a small electromagnetic vibrator of the type used to modulate infrared radiation in place of the chopper [3]. The isotope is then placed behind a chopper fixed to the vibrator (α and β - emitters) or else it is fixed to the moving element behind a fixed screen with a hole in it (γ -rays). The chopper or screen thickness is selected as before (formulae (1) and (2)).

A disadvantage of mechanical modulation is the use of moving parts.

Field Modulation

In principle only α-and β-emissions can be field-modulated as they are charged particles. γ-rays, being of wave nature, are not deviated in electric or magnetic fields and so cannot be field-modulated.

The figure shows the basic arrangement used in field modulation (1 is the screening stop, 2 the collimator, 3 the isotope).

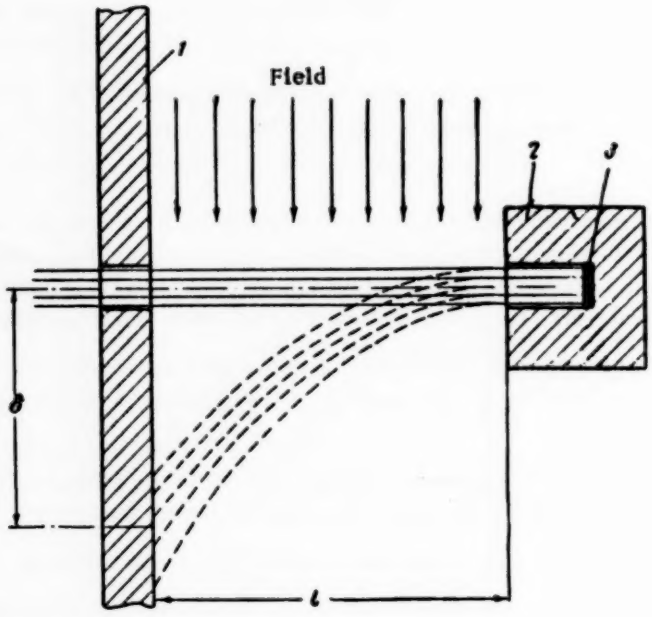

At zero field a beam of particles passes through the slot in the screen, producing a radiation pulse beyond the screen. The beam propagates nonrectilinearly when a field is present, falling on and being absorbed by the screen; no radiation passes through the screen. If the field oscillates at some frequency the radiation behind the screen will pulsate at the same frequency. By adjusting the field strength and law of field charge, pulses of the desired duration and shape can be produced.

The deviation δ produced by a uniform electric or magnetic field over a length l is given [4] by

a) electric field

$$\delta_e = \frac{l^2}{2}\frac{qE}{mV^2}; \tag{3}$$

b) magnetic field (when $l \gg \delta$)

$$\delta_m = \frac{l^2}{2}\frac{qH}{mV}. \tag{4}$$

Here m is the particle mass, V the particle speed, q its charge, E the electric field strength, H the magnetic field strength.

m depends on velocity with fast particles:

$$m = \frac{m_0}{\sqrt{1-\beta^2}}, \qquad (5)$$

where m_0 is the rest-mass, $\beta = V/c$ = ratio of particle velocity to that of light.

Elementary calculations using (3) and (4) show that when the deviation is 1 cm (when l = 4 cm) an electric field of 660 kv/cm or a magnetic field of 40,000 oersted are required with Po-210 α-particles (E = 5.3 Mev). For Tl -204 β-particles (E = 0.8 Mev) fields of 139 kv/cm and 470 oersted are required.

The above figures show that in practice only β-particles and magnetic modulation are readily usable. The minimum screen thickness is then taken from (1).

We made a magnetic β-modulator with a working gap induction of 0 - 2000 oersted.

The 30 mC Tl -204 source was placed between the poles of the small magnet.

The screen was placed close to the pole-tips, with its slot opposite the radiator: it was a sheet of plexiglass 4 mm thick.

An ionization chamber was placed behind the screen: it was connected to an electrometer amplifier. The amplifier output pulses were viewed on an oscillograph for various direct and alternating voltages applied to the magnet. The test data showed that this modulator was unsuitable for producing short pulses because the magnet current changed slowly and the β-rays were not monochromatic, so particles of differing energy were differently deviated, spreading out like a fan. But it is quite useful when the radiation output must change smoothly. To obtain short or sharp fronted pulses mechanical modulation should be used.

Received September 4, 1956

LITERATURE CITED

[1] N. N. Shumilovsky and L. V. Melttser, Use of radioisotopes for measuring gas speeds and for measuring gas flows automatically by the "labeled molecule" method. Proc. Acad. Sci. USSR 106, No. 4 (1956).

[2] N. N. Shumilovsky and L. V. Melttser, Measuring gas flows automatically by the "labeled molecule" method. Equipment design No. 3 (1956).

[3] I. C. S. Richards, Portable radiation detectors employing photoconductive cells. Journ. scientific instruments, vol. 32, No. 9 (1955).

[4] M. Curie, Radioactivity. State.Tech. Press (1947).

AUTOMATION AND REMOTE CONTROL IN ENGLISH TRANSLATION

August, 1957

TABLE OF CONTENTS

	Page	Russ. Page
1. Improvement of the Static Characteristic of a Pneumatic Relay by Means of Flow Restrictors of Constant Pressure Drop. V. N. Dmitriev	744	689
2. Some Methods of Stabilization and Control of Low Flow Rates of Operating Liquid in Hydraulic Automatic Systems. I. N. Kichin	757	702
3. Certain Problems in the Theory of Magnetic Amplifiers and Magneto-Modulation Probes of the "Second Harmonic" Type. V. N. Mikhailovskii and Iu. I. Spektor	771	716
4. Choice of Mode and Calculation of Electronic Voltage Stabilizer. L. I. Baida and V. K. Zakharov	778	724
5. Certain Properties of Circuits Containing Thermoresistances. G. K. Nechaev	793	740
6. Exponential Pulse-Time Converters. A. I. Novikov	802	749
7. Code Rings and Their Uses in Remote Control Equipment. A. N. Radchenko	809	756
8. Calculations on Electromagnetic Systems Using Electrical Analogs. S. A. Aleskerov	815	764

IMPROVEMENT OF THE STATIC CHARACTERISTIC OF A PNEUMATIC RELAY BY MEANS OF FLOW RESTRICTORS OF CONSTANT PRESSURE DROP

V. N. Dmitriev

(Moscow)

The possibilities for improvement of the static characteristic of a pneumatic relay by installation of flow restrictors of constant pressure drop are examined. The equations for static characteristics of such relays are derived, and the results of experimental investigations are given.

INTRODUCTION

Almost all modern industrial regulators utilize amplifiers that contain a pneumatic relay of the nozzle-baffle type. The static characteristics of relays [1-3] have the approximate form of Curve 1 in Fig. 1. To increase sensitivity of regulators and improve their accuracy it is necessary to increase the slope of the working portion of the static characteristic, its linearity, and to displace the working portion of the characteristic curve as far as possible to the right from the origin of coordinates, and to raise the preceding portion into the region of high inter-restriction chamber pressures, P_1. Such a transformation of the characteristic curve allows the increase of the range of total pressure changes in the inter-restrictor chamber, and to effect this change with sufficiently large distances between baffle plate and nozzle, which in turn allows the requirements for hermetic tightness between nozzle and baffle, when they are touching, to be lowered.

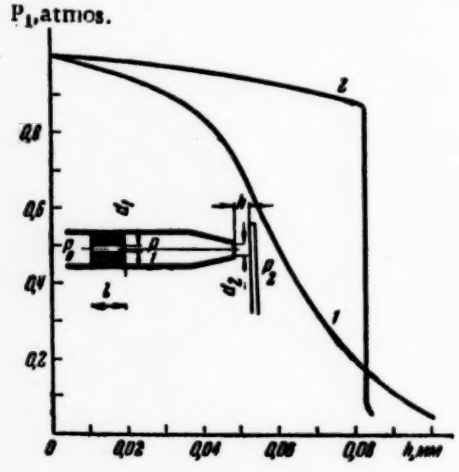

Fig. 1.

The aim of the indicated transformation is the movement of characteristic Curve 1 toward Curve 2 (Fig. 1).

To achieve this, during the past years, special devices are included in the relay, which solves this problem by maintaining constant pressure drop at one of the restrictors (fixed or variable) or at both. An example of a pneumatic relay with such devices [4, 5] is shown in Fig. 2. A constant pressure drop at the fixed restrictor 1 $\Delta P_f = P_0^* - P_1$ is maintained by means of deflection of the metal bellows 2, which moves the ball valve 3 depending on pressure P_1 and in this way changing the supply pressure P_0^*. Since the deflections of the metal bellows are insignificant, the ΔP_f remains practically constant during the operation of the relay.

The constant pressure drop at the variable restrictor 4 is effected by creation of a back pressure on the nozzle. Since the deflections of the membrane 5, controlling the ball valve 6 of the amplifying relay, are small, the force of the spring 7 may be considered constant, which in turn guarantees the constancy of the pressure drop $\Delta P_v = P_1 - P_2^*$.

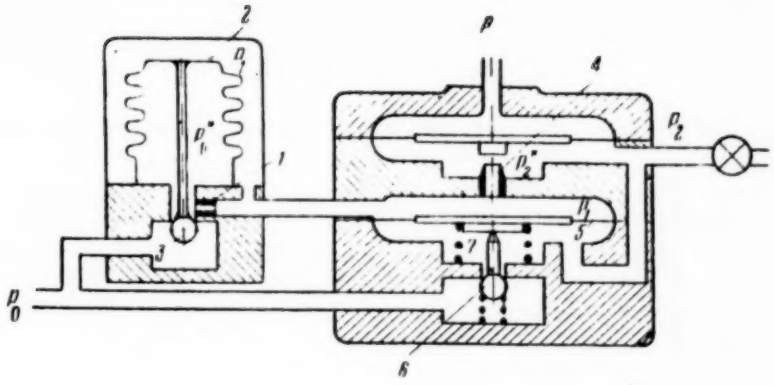

Fig. 2.

In this paper we examine the theory of a relay with constant pressure drop at the fixed restrictor, constant pressure drop at the variable restrictor and with constant pressure drop at both fixed and variable restrictors, and conclusions are reached regarding the effect of design and operational parameters on the static characteristic. Data of experimental investigations are given, indicating confirmation of theoretical conclusions.

1. Basic Equations

The formulation of equations of static characteristics of pneumatic relays is based on equating air flows with the assumption $\gamma = \text{const}$ (γ is the specific weight of air). In this case these equations are approximate, since the assumed specific weight of the air is the specific weight downstream of the restrictor.*

For the subcritical regime, the equation of flow is

$$G = f_1 \sqrt{\frac{2g}{RT_1} P_1 (P_0 - P_1)} \quad \left(\frac{P_1}{P_0} \geqslant 0.5\right) \tag{1}$$

and for the supercritical regime, the equation of flow is

$$G = f_1 P_0 \sqrt{\frac{g}{2RT_1}} \quad \left(\frac{P_1}{P_0} \leqslant 0.5\right) \tag{1a}$$

where G is the weight flow of air, g is the acceleration of gravity, P_1 is the air pressure beyond the orifice, P_0 is the air pressure before the orifice, T_1 the absolute air temperature beyond the orifice, R is the gas constant, f_1 is the effective area: $f_1 = \mu_1 F_1$, where μ_1 is the coefficient of contraction, F_1 is the passage cross section area.

Let us now obtain the equation of the static characteristic of a common relay.** It will be found from the equality of flows, under static conditions, through the fixed and variable restrictors. We shall consider that the process of transition from the region before the restrictor to the region beyond the restrictor is isothermal, i.e., $T_0 = T_1 = T_2 = T$.*** With the purpose of revealing primarily the qualitative effect of the relay parameters

---

* The studies described in (6) showed that the use of these equations in place of the exact equations of St. Venant for an adiabatic process (air, in these studies), results in a maximum error of 3.4% over the entire range of pressure drops (both subcritical and supercritical ranges).

** "Common relay" ≡ a relay without a constant pressure drop at the fixed and variable restrictors; i.e., a relay that operates with $P_0 = \text{const}$, $P_2 = \text{const}$.

*** See basis for this in [7].

on the static characteristic, let us assume that $\mu_1/\mu_2 = 1$. Then for the combination of regimes $\partial - \partial^*$ we have

$$h = \frac{d_1^2}{4d_2}\sqrt{\frac{(P_0 - P_1)P_1}{(P_1 - P_2)P_2}}. \qquad (2)$$

Here h is the distance between nozzle and baffle, d_1 and d_2 are, respectively, the diameters of the fixed and the variable restrictors.

The equations of the static characteristics of a common relay for other combinations of flow regimes are given in Table 2 (see Supplement 1). The analysis of effect of relay parameters on its static characteristic will from here on, be conducted by means of equations derived for the case ∂-∂, since in industrial pneumatic automation practice it is the most widely used case. Equations for other combinations of flow regimes will be placed in corresponding tables (see Supplement 1).

2. Relay with Constant Pressure Drop at Fixed Restrictor.

A constant pressure drop is maintained at the fixed restrictor $P_0^* - P_1 = \Delta P_f = \text{const}$. In this case the static characteristic curve of the relay will have two regions (Fig. 3,a). The first region ($h_0 \geq h \geq 0$) coincides with the static characteristic curve of an ordinary relay (Curve 1), the second region ($h \geq h_0$) is the region of operation (Curve 2).

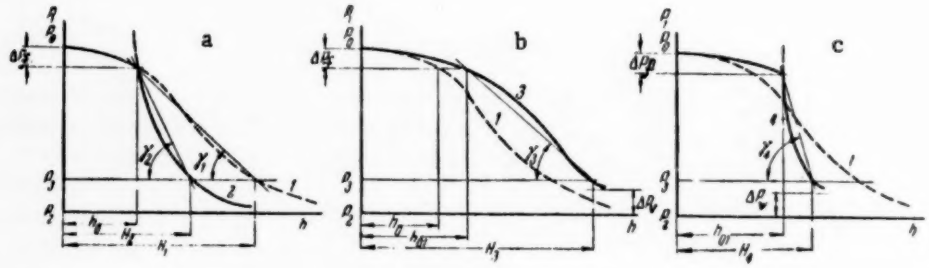

Fig. 3.

The division of the static characteristic curve into two regions is facilitated by the fact that at $h = 0$, the pressure in the inter restrictor chamber is equal to the initial supply pressure P_0. To obtain the required pressure drop at the fixed restrictor, ΔP_f, which can be subsequently maintained constant, it is necessary that the pressure in the inter restrictor chamber fall to a level at which the difference $P_0 - P_1$ will be equal to the required value of ΔP_f. For this, the baffle must travel the distance h_0. Since in this case $P_0 = \text{const}$ and $P_2 = \text{const}$, the relay is operating as an ordinary relay. The distance h_0 will then be determined by the formula

$$h_0 = \frac{d_1^2}{4d_2}\sqrt{\frac{\Delta P_f\ (P_0 - \Delta P_f)}{(P_0 - \Delta P_f - P_2)P_2}}. \qquad (3)$$

Further increase of the distance h beyond h_0 takes place with a constant pressure drop at the fixed restrictor, that is, with a decreasing supply pressure P_0^*. Thus, the pressure in the inter restrictor chamber, in the operating region, decreases not only because of the increase in h, but because of the drop in P_0^* as well. As a result, the operating region of the curve takes on a high slope. The first region of the static characteristic curve ($h_0 \geq h \geq 0$)

* The following designations will be used for the possible combinations of flow regimes: $\partial - \partial$, $n - \partial$, $\partial - n$ and $n - n$, which means respectively – subcritical flow through fixed and variable restrictors, supercritical flow through fixed restrictor and subcritical through the variable, and so on.
The conditions for existence of the various combinations of regimes of flow are given in Table 1, of Supplement 1.

is described by Equation (2), the operating, second region ($h \geq h_0$) by the equation

$$h = \frac{d_1^2}{4d_2}\sqrt{\frac{P_1\Delta P_f}{(P_1 - P_2)P_2}}. \tag{4}$$

Assuming that the operating region of Curve 1 originates at $h = h_0$, let us show that the average slope of the operating region of Curve 2 is always greater than the corresponding slope of Curve 1. Let us define the average slope of the operating region as the tangent of the angle of inclination of a straight line that runs from a point with the abscissa $h = h_0$ to a point that defines the end of the operating stroke,* in the given case, the point with abscissas $h = H_1$ and $h = H_2$. Designating the pressure at the end of the working stroke as P_3, and using Equations (2) - (4), we obtain

$$\tan\gamma_1 = \frac{P_0 - \Delta P_f - P_3}{H_1 - h_0} = \frac{P_0 - \Delta P_f - P_3}{\frac{d_1^2}{4d_2}\left[\sqrt{\frac{P_3(P_0 - P_3)}{(P_3 - P_2)P_2}} - \sqrt{\frac{(P_0 - \Delta P_f)\Delta P_f}{(P_0 - \Delta P_f - P_2)P_2}}\right]}, \tag{5}$$

$$\tan\gamma_2 = \frac{P_0 - \Delta P_f - P_3}{H_2 - h_0} = \frac{P_0 - \Delta P - P_3}{\frac{d_1^2}{4d_2}\left[\sqrt{\frac{P_3\Delta P_f}{(P_3 - P_2)P_2}} - \sqrt{\frac{(P_0 - \Delta P_f)\Delta P_f}{(P_0 - \Delta P_f - P_2)P_2}}\right]}. \tag{6}$$

Equating the expressions for $\tan\gamma_2$ and $\tan\gamma_1$ it is apparent that they differ only in the denominators and in the first of the two square root terms.

Since the difference $P_0 - P_3$ is always greater than ΔP_f**, we get the inequality $\tan\gamma_2 > \tan\gamma_1$. For example, in the case $P_0 = 2$ atmos. a, $P_3 = 1.2$ atmos. a, $P_2 = 1$ atmos. a, $\Delta P_f = 0.05$ atmos. g, $\tan\gamma_2/\tan\gamma_1 = 8.25$.

The curve of the operating region of the static characteristic of the relay with constant pressure drop at the fixed restrictor, is a uniformly decreasing function, having a positive second derivative $d^2P_1/dh^2 > 0$. Therefore, the maximum slope of the operating region of the static characteristic will occur at the point with abscissa $h = h_0$. This point can be found by finding the limit

$$\lim_{P_1 \to P_0 - \Delta P_f} \tan\gamma_2 = \left|\frac{dP_1}{dh}\right|_{\max},$$

which yields

$$\left|\frac{dP_1}{dh}\right|_{\max} = \frac{8d_2(P_0 - \Delta P_f - P_2)^{3/2}}{d_1^2}\sqrt{\frac{P_0 - \Delta P_f}{\Delta P_f P_2}}.$$

Analyzing expressions (3) and (6), conclusions may be reached regarding the effect of parameters of relays with constant pressure drop at the fixed restrictor on the distance h_0 and on the average slope of the operating region of the static characteristic curve. Thus, an increase in d_1 increases h_0, and an increase in d_2 decreases h_0. The average slope decreases with an increase in d_1, and increases with an increase in d_2. An increase in P_0 decreases h_0 and increases the average slope. Increasing ΔP_f acts in the opposite direction: h_0 increases, while the average slope decreases. Proof of this is given in Supplement 2.

3. Relay with Constant Pressure Drop at the Variable Restrictor

The static characteristic of a relay with constant pressure drop at the variable restrictor (Fig. 3, b, Curve 3) is described by the equation

$$h = \frac{d_1^2}{4d_2}\sqrt{\frac{(P_0 - P_1)P_1}{\Delta P_V (P_1 - \Delta P_V)}}. \tag{7}$$

* The end of the operating stroke corresponds to the maximum possible displacement of the baffle, limited by the restricting effect on the nozzle $0 \leq h \leq d_2/4$.

** When $P_0 - P_3 = \Delta P_f$ the relay reverts to the ordinary type.

Because of the back pressure beyond the variable restrictor, the pressure P_1 in the inter restrictor chamber increases, and therefore the static characteristic of such a relay will fall above the static characteristic of an ordinary relay (Fig. 3,b, Curve 1). This can be shown by comparing the distance of the baffle from the nozzle, $\underline{h}$, in a relay with constant pressure drop at the variable restrictor with that in an ordinary relay, when P_1 is identical in both (see Equations (2) and (7)):

$$\sqrt{\frac{(P_1-P_2)P_2}{\Delta P_v\,(P_1-\Delta P_v)}}=\sqrt{\frac{(P_1-P_2)P_2}{(P_1-P_2^*)P_2^*}}>1. \tag{8}$$

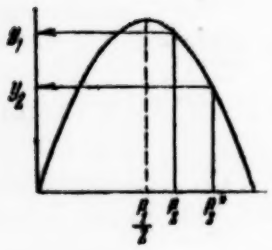

Fig. 4. $y_1=(P_1-P_2)P_2$, $y_2=(P_1-P_2^*)P_2^*$

It follows from such a comparison that $\underline{h}$ for a relay with constant pressure drop at the variable restrictor, is always greater than $\underline{h}$ for an ordinary relay, since $P_2^*\geq P_2$, $P_2^*/P_1>0.5$ and $P_2/P_1>0.5$ (see Fig. 4).

Let us determine the average slope of the operating region of the static characteristic curve. Since the static characteristic of a relay with constant pressure drop at the variable restrictor is described by one equation, and therefore there is no clearly defined boundary between operating and nonoperating regions, let us for convenience consider that the operating region begins in the same way as in the preceding case, at the value $P_1=P_0-\Delta P_f$.*

Then the distance h_{01} will be (Fig. 3,b)

$$h_{01}=\frac{d_1^2}{4d_2}\sqrt{\frac{\Delta P_f\,(P_0-\Delta P_f)}{\Delta P_v\,(P_0-\Delta P_f-\Delta P_v)}} \tag{9}$$

and the average slope of the operating region

$$\tan\gamma_3=\frac{P_0-\Delta P_f-P_3}{H_3-h_{01}}=$$

$$=\frac{P_0-\Delta P_f-P_3}{\frac{d_1^2}{4d_2}\left[\sqrt{\frac{P_3(P_0-P_3)}{\Delta P_v\,(P_3-\Delta P_v)}}-\sqrt{\frac{(P_0-\Delta P_f)\Delta P_f}{\Delta P_v\,(P_0-\Delta P_f-\Delta P_v)}}\right]} \tag{10}$$

The average slope of the operating region of the static characteristic of a relay with constant pressure drop at the variable restrictor may be greater as well as lower than the corresponding slope $\tan\gamma_1$ of the static characteristic of an ordinary relay. This depends on the choice of the magnitude of ΔP_f and P_3, or in other words, depends on the region of the static characteristic at which the comparison is made.

Thus, for example, if we calculate the relationship $\tan\gamma_3/\tan\gamma_1$, using Expressions (10) and (5) for an ordinary relay (P_0= 2 atmos. a, P_3 = 1.2 atmos. a, P_2 = 1 atmos. a) and for a relay with constant pressure drop at the variable restrictor (with the same parameters and ΔP_v = 0.1 atmos. g) then for ΔP_f = 0.05 atmos. g and ΔP_f = 0.3 atmos. g we obtain the corresponding values of $\tan\gamma_3/\tan\gamma_1$ = 0.8 and $\tan\gamma_3/\tan\gamma_1$ = 1.14 .

4. Relay with Constant Pressure Drop at the Fixed and Variable Restrictors

When constant pressure drops are established simultaneously at the fixed and variable restrictors, the static characteristic of the relay divides into two regions. The first region ($h_{01}\geq h\geq 0$) precedes the operating region (Fig. 3,c, Curve 3) which is the second region ($h\geq h_{01}$), (Fig. 4).

The first region coincides with the static characteristic of the relay with constant pressure drop at the variable restrictor. This is explained by the fact that the constant pressure drop at the variable restrictor can be created

* Recall that ΔP_f does not here mean a constant difference between supply pressure and the pressure in the inter-restrictor chamber, but only the pressure differential corresponding to the distance h_{01} (Fig. 3,b).

while h = 0, while the required constant pressure drop at the fixed restrictor appears only when $h = h_{01}$. In this way, the relay operates over the first region only under constant pressure drop at the variable restrictor, while over the second operating region it operates with constant pressure drop at both fixed and variable restrictors.

The distance h_{01} is determined by formula (9). The equation of the first region of the static characteristic ($h_{01} \geq h \geq 0$) is given by (7) and that of the second region ($h \geq h_{01}$) by the expression

$$h = \frac{d_1^2}{4d_1^2} \sqrt{\frac{\Delta P_f \, P_1}{\Delta P_v \, (P_1 - \Delta P_v)}}. \qquad (11)$$

The operating region of the static characteristic has a high slope and is near a straight line, which is apparent from an analysis of formula (11).

It follows from (11) that h varies but little with P_1. Let us find the average slope of the operating region of the static characteristic curve of a relay with constant pressure drop at both fixed and variable restrictors. Let us consider that the end of the operating region corresponds to the pressure in the inter-restrictor chamber $P_1 = P_3$. Then, from (11) and (9) and Fig. 3,c, we get

$$\tan \gamma_4 = \frac{P_0 - \Delta P_f - P_3}{h_4 - h_{01}} =$$

$$= \frac{P_0 - \Delta P_f - P_3}{\frac{d_1^2}{4d_2}\left[\sqrt{\frac{\Delta P_f \, P_3}{\Delta P_v \, (P_3 - \Delta P_v)}} - \sqrt{\frac{\Delta P_f \, (P_0 - \Delta P_f)}{\Delta P_v \, (P_0 - \Delta P_f - \Delta P_v)}}\right]}. \qquad (12)$$

The maximum slope of the operating region of the static characteristic of the relay will occur at the point having abscissa $h = h_{01}$. The maximum slope can be found by finding the limit

$$\lim_{P_3 \to P_0 - \Delta P_f} \tan \gamma_4 = \left|\frac{dP_1}{dh}\right|_{max},$$

which yields

$$\left|\frac{dP_1}{dh}\right|_{max} = \frac{16 d_2}{d_1^2} \frac{(P_0 - \Delta P_f - \Delta P_v)^{1/2} \Delta P_v}{P_0 - 2(P_0 - \Delta P_f - \Delta P_v)\sqrt{\Delta P_v}}.$$

Comparing (6) and (12), it is apparent that the average slope of the static characteristic curve of the relay with constant pressure drop at both fixed and variable restrictors, $\tan \gamma_4$, is greater than the corresponding slope of the static characteristic of the relay with constant pressure drop at fixed restrictor only, $\tan \gamma_2$. The proof of this is given in Supplement 3.

To illustrate the degree by which $\tan \gamma_4$ can exceed $\tan \gamma_2$, let us calculate the ratio $\tan \gamma_4 / \tan \gamma_2$ for a relay having the following parameters: P_0 = 2 atmos. a, P_3 = 1.2 atmos. a, P_2 = 1 atmos. a, ΔP_f = 0.05 atmos. g and ΔP_v = 0.1 atmos. g. This ratio is equal to 10.3.

Analyzing the expression for $\tan \gamma_4$ (12) it can be shown that increasing P_0 increases $\tan \gamma_4$, while increasing ΔP_f and ΔP_v decreases $\tan \gamma_4$ (see Supplement 3).

The effect of relay parameters when pressure drop is constant at both fixed and variable restrictors, on the distance h_{01}, can be traced by analyzing expression (9). Thus, an increase in P_0 and ΔP_v produces a decrease in h_{01}, while an increase in ΔP_f increases h_{01} (see Supplement 4).

The distance of the point of maximum slope from the origin of coordinates h_{01} for the relay with constant

pressure drop at both fixed and variable restrictors, exceeds the corresponding distance h_0 for the relay with constant pressure drop only at the fixed restrictor, which in a general sense is shown by (8). As an illustration let us find the ratio h_{01}/h_0, using formulas (3) and (9), for a relay with the parameters $P_0 = 2$ atmos. a, $P_2 = 1$ atmos. a, $\Delta P_f = 0.05$ atmos. g and $\Delta P_v = 0.1$ atmos. g. This ratio is equal to 2.26.

5. Experimental Investigation of Relays with Constant Pressure Drop Restrictors

To check the theoretical conclusions, a series of experiments was performed on the apparatus arrangement shown in Fig. 5. The constant pressure drop at the fixed restrictor was established at each point in the following manner. By means of pressure reducer 1, the required supply pressure, P_0^*, was established at the fixed reducer. Then by moving the baffle toward or away from the nozzle the required pressure P_1 was established. The baffle

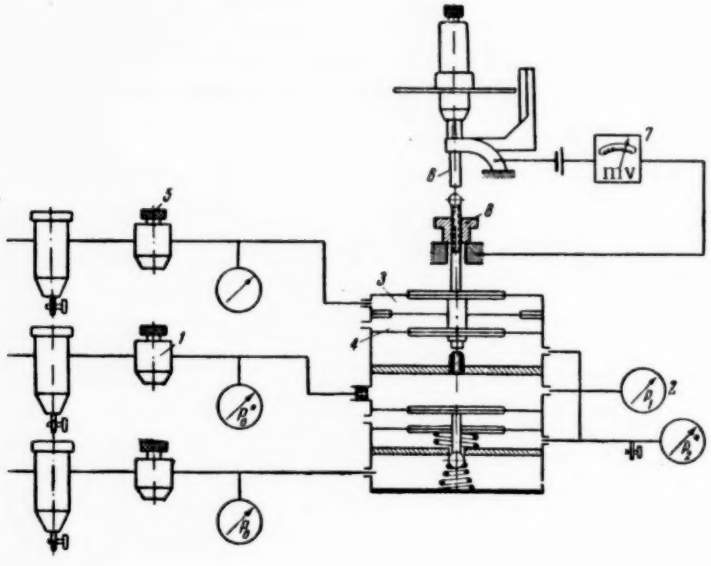

Fig. 5.

was moved by admitting pressure to chamber 3 or chamber 4, through the pressure reducer 5, where the pressure was regulated. At the variable restrictor the constant pressure drop was maintained automatically. The gap between nozzle and baffle was measured by a micrometer, 6, having an auxiliary thimble whose graduations were equal to 1μ. The initial reading (at moment of contact) was established by millivoltmeter 7. The pressure P_0 was maintained constant during the entire experiment. When working with the relay with constant pressure drop at the fixed restrictor and with the ordinary relay, the chamber over the nozzle was opened to the atmospheric pressure and the baffle was moved by means of the nut 8, since feedback was absent in this condition.

Figure 6 shows a family of static characteristics of a relay with constant pressure drop at fixed restrictor. The relay has the following parameters: $d_2 = 0.50$ mm, $d_1 = 0.18$ mm, $l = 18$ mm (capillary). The curves are drawn for various values of ΔP_f with $P_0 = 1$ atmos. g. The static characteristic curve of an ordinary relay is shown in the same figure. Figure 6 shows that a constant pressure drop at the fixed restrictor considerably increases the slope of the operating region of the static characteristic curve, bringing it closer to pure relay action. Increasing ΔP_f displaces the characteristic curve to the right, thus increasing h_0. The slope of the operating region decreases when ΔP_f is decreased. The total drop in pressure over the operating region decreases.

The static characteristic characteristic curves of a relay with constant pressure drop at the fixed restrictor, having $d_2 = 3.08$ mm, are shown in Fig. 7. The characteristic curves were obtained for various diameters d_1 of the fixed restrictor. As is evident from the figure, in the region $0 \leq h \leq h_0$ the static characteristics of an ordinary relay coincide with the characteristic curves of a relay with constant pressure drop at the fixed restrictor. An increase in d_1 produces an increase in h_0 and somewhat decreases the slope of the operating region of the static characteristic curve.

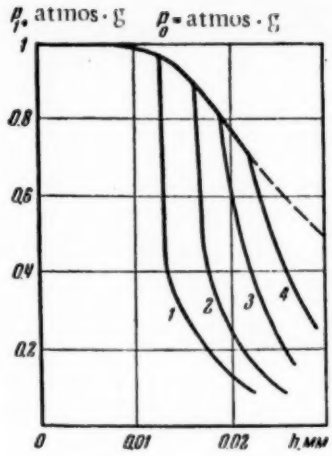

Fig. 6. 1) ΔP_f = 0.033 atmos.g, 2) ΔP_f = 0.1 atmos.g, 3) ΔP_f = = 0.2 atmos.g, 4) ΔP_f = 0.3 atmos.g.

The static characteristic curves of a relay with constant pressure drop at the variable restrictor when d_1 = 0.18 mm, d_2 = = 0.5 mm, l = 18 mm are shown in Fig. 8. During the experiment the pressure P_0 was maintained constant and equal to 1 atmos.g. The curves were obtained for various values of ΔP_v.

As is evident from Fig. 8, the static characteristics of a relay with constant pressure drop at the variable restrictor fall above the static characteristic of an ordinary relay. When ΔP_v is lowered the curves approach each other in the region of higher pressures P_1.

The family of static characteristics of a relay (d_1 = 0.18 mm, d_2 = 0.50 mm, l = 18 mm) taken at various values of ΔP_v and at a single value of ΔP_f, is shown in Fig. 9. The curves shown indicate that a reduction in ΔP_v displaces the operating region of the static characteristic to the right. The slope simultaneously increases.

Figure 10 shows the static characteristics of the same relay, obtained for various values of ΔP_f and a single value of ΔP_v. On the same figure are shown the static characteristic of an ordinary relay and the static characteristics of a relay with constant pressure drop at the variable restrictor. Comparing these curves with the curves of Fig. 6, obtained under various values of ΔP_f, but without a constant pressure drop at the variable restrictor, it is seen that a constant pressure drop at the variable restrictor displaces the part of the static characteristic preceding the operating region, into the zone of higher pressures in the inter-restrictor chamber and displaces the operating region to the right.

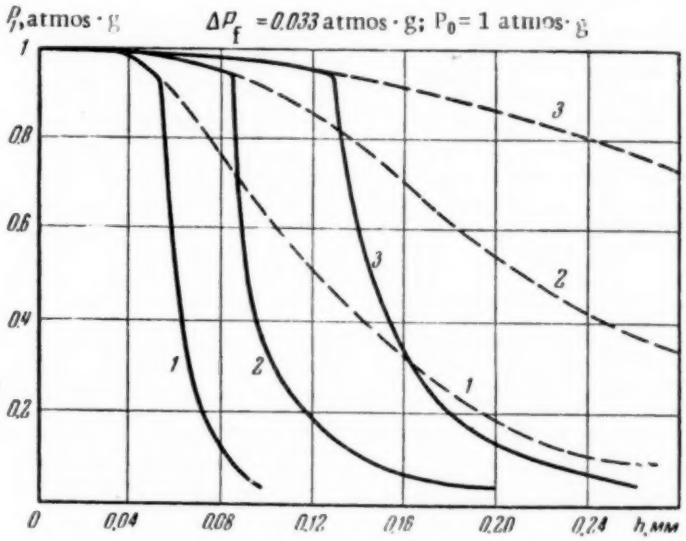

Fig. 7. 1) d_1 = 1.04 mm, 2) d_1 = 1.63 mm, 3) d_1 = 2.00 mm.

Increasing ΔP_f in a relay with constant pressure drop at the constant and variable restrictors, as is evident in Fig. 10, increases the distance h_{01}. From Figs. 9 and 10, it is also evident that when constant pressure drop at the variable restrictor is adopted in a relay the total pressure drop at the operating region increases appreciably.

SUMMARY

1) Maintaining a constant pressure drop at the fixed restrictor, appreciably increases the slope of the operating region of the static characteristic curve of a relay. Increasing the constant pressure drop at the fixed restrictor

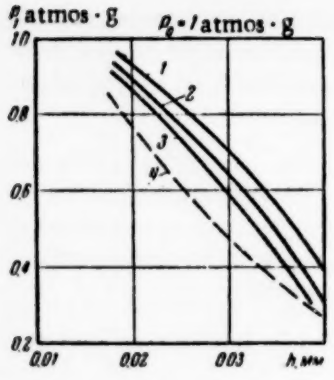

Fig. 8. 1) $\Delta P_v \approx 0.11$ atmos. g, 2) $\Delta P_v \approx 0.17$ atmos. g, 3) $\Delta P_v \approx 0.2$ atmos. g, 4) ΔP_v = var, $P_2 = 0$ atmos. g.

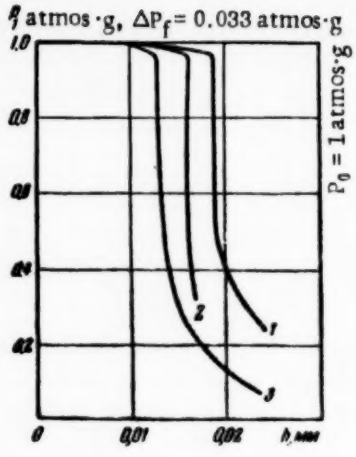

Fig. 9. 1) $\Delta P_v \approx 0.14$ atmos. g, 2) $\Delta P_v \approx 0.35$ atmos. g, 3) ΔP_v = = var, $P_2 = 0$ atmos. g.

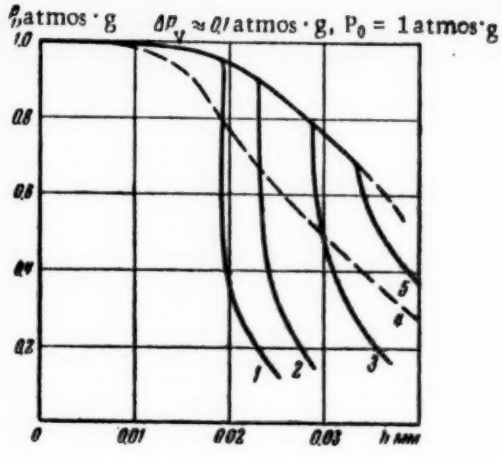

Fig. 10. 1) $\Delta P_f = 0.03$ atmos. g, 2) ΔP_f = = 0.1 atmos. g, 3) $\Delta P_f = 0.2$ atmos. g, 4) $P_2 = 0$ atmos. g, 5) $\Delta P_f = 0.3$ atmos. g.

displaces the operating region of the static characteristic curve to the right. The slope then decreases.

2) Maintaining a constant pressure drop at the variable restrictor displaces the static characteristic curve of the relay into the zone of higher pressures in the inter-restrictor chamber. A constant pressure drop at the variable restrictor only, does not significantly improve the static characteristic.

3) The simultaneous creation of constant pressure drops at the fixed and variable restrictors, significantly increases the slope of the operating region of the static characteristic curve, its linearity, and also displaces the section preceding the operating region into the zone of higher inter-restrictor chamber pressures. Increasing the constant pressure drop at the fixed restrictor has the same effect on the static characteristic as in the case of the relay that has a constant pressure drop only at the fixed restrictor. The reduction of the constant pressure drop at the variable restrictor increases the slope of the operating region and displaces it to the right.

Thus in building a relay with constant pressure drop at the fixed restrictor and with constant pressure drop at the fixed and variable restrictors, the additional possibility of controlling the static characteristic by changing the values of ΔP_f and ΔP_v is created.

SUPPLEMENT 1

TABLE 1
Conditions Defining the Various Regimes

Regime	Condition
д–д	$P_1 > \Delta P_f$, $P_1 > 2\Delta P_v$
п–д	$\Delta P_f > P_1 > 2\Delta P_v$
д–п	$2\Delta P_v > P_1 > \Delta P_f$
п–п	$P_1 < \Delta P_f$, $P_1 < 2\Delta P_v$

TABLE 2

Equations of the Static Characteristic Curves of Ordinary Relays

Regime	Formula
∂—∂	$h=\frac{d_1^2}{4d_2}\sqrt{\frac{(P_0-P_1)P_1}{(P_1-P_2)P_2}}$
к—∂	$h=\frac{d_1^2}{8d_2}\frac{P_0}{\sqrt{P_2(P_1-P_2)}}$
∂—к	$h=\frac{d_1^2}{2d_2}\sqrt{\frac{P_0}{P_1}-1}$
к—к	$h=\frac{d_1^2}{4d_2}\frac{P_0}{P_1}$

TABLE 3

Relay with Constant Pressure Drop at the Fixed Restrictor. Equations for h_0

Regime	Formula
∂—∂	$h_0=\frac{d_1^2}{4d_2}\sqrt{\frac{\Delta P_f\ (P_0-\Delta P_f)}{(P_0-\Delta P_f-P_2)P_2}}$
к—∂	$h_0=\frac{d_1^2}{8d_2}\frac{P_0}{\sqrt{P_2(P_0-\Delta P_f-P_2)}}$
∂—к	$h_0=\frac{d_1^2}{2d_2}\sqrt{\frac{\Delta P_f}{P_0-\Delta P_f}}$
к—к	$h_0=\frac{d_1^2}{4d_2}\frac{P_0}{P_0-\Delta P_f}$

TABLE 4

Equations for the Operating Regions of the Static Characteristic Curves of Relays with Constant Pressure Drop at the Fixed Restrictor

Regime	Formula	Regime	Formula
∂—∂	$h=\frac{d_1^2}{4d_2}\sqrt{\frac{\Delta P_f\ P_1}{(P_1-P_2)P_2}}$	∂—к	$h=\frac{d_1^2}{2d_2}\sqrt{\frac{\Delta P_f}{P_1}}$
к—∂	$h=\frac{d_1^2}{8d_2}\frac{\Delta P_f+P_1}{\sqrt{(P_1-P_2)P_2}}$	к—к	$h=\frac{d_1^2}{4d_2}\left(\frac{\Delta P_f}{P_1}+1\right)$

TABLE 5

Maximum Slope of the Operating Region of the Static Characteristic Curve of Relays with Constant Pressure Drop at the Fixed Restrictor

Regime	Equation
∂—∂	$\left\lvert\frac{dP_1}{dh}\right\rvert_{max}=\frac{8d_2}{d_1^2}(P_0-\Delta P_f-P_2)^{3/2}\sqrt{\frac{P_0-\Delta P_f}{\Delta P_f\ P_2}}$
к—∂	$\left\lvert\frac{dP_1}{dh}\right\rvert_{max}=\frac{16d_2}{d_1^2}\frac{(P_0-\Delta P_f-P_2)^{3/2}\sqrt{P_2}}{(2P_2+2\Delta P_f-P_0)}$
∂—к	$\left\lvert\frac{dP_1}{dh}\right\rvert_{max}=\frac{4d_2}{d_1^2}\frac{(P_0-\Delta P_f)^{3/2}}{\sqrt{\Delta P_f}}$
к—к	$\left\lvert\frac{dP_1}{dh}\right\rvert_{max}=\frac{4d_2}{d_1^2}\frac{(P_0-\Delta P_f)^2}{\Delta P_f}$

TABLE 6

Relay with Constant Pressure Drop at the Variable Restrictor and with Constant Pressure Drop at the Fixed and Variable Restrictors. Equations for h_{01}

Regime	Equation
$\partial-\partial$	$h_{01}=\frac{d_1^2}{4d_2}\sqrt{\frac{\Delta P_f\ (P_0-\Delta P_f)}{\Delta P_v\ (P_0-\Delta P_f-\Delta P_v)}}$
$\kappa-\partial$	$h_{01}=\frac{d_1^2}{8d_2}\frac{P_0}{\sqrt{\Delta P_v\ (P_0-\Delta P_f-\Delta P_v)}}$
$\partial-\kappa$	Same, as for h_0 (Table 3)
$\kappa-\kappa$	Same, as for h_0 (Table 3)

TABLE 7

Equations of the Static Characteristics of Pneumatic Relays with Constant Pressure Drop at the Variable Restrictor

Regime	Equation
$\partial-\partial$	$h=\frac{d_1^2}{4d_2}\sqrt{\frac{(P_0-P_1)\,P_1}{\Delta P_v\ (P_1-\Delta P_v)}}$
$\kappa-\partial$	$h=\frac{d_1^2}{8d_2}\frac{P_0}{\sqrt{\Delta P_v\ (P_1-\Delta P_v)}}$
$\partial-\kappa$	Same, as for h for an ordinary relay (Table 2)
$\kappa-\kappa$	Same

TABLE 8

Equations for Static Characteristics of Pneumatic Relays with Constant Pressure Drop at Fixed and Variable Restrictors.

Regime	Equation
$\partial-\partial$	$h=\frac{d_1^2}{4d_2}\sqrt{\frac{\Delta P_f}{\Delta P_v}\frac{P_1}{(P_1-\Delta P_v)}}$
$\kappa-\partial$	$h=\frac{d_1^2}{8d_2}\frac{\Delta P+P_1}{\sqrt{\Delta P_v\ (P_1-\Delta P_v)}}$
$\partial-\kappa$	Same as for h of a relay with constant pressure drop at the fixed restrictor (Table 4)
$\kappa-\kappa$	Same

TABLE 9

Maximum Slope of the Operating Region of the Static Characteristic Curve of a Relay with Constant Pressure Drop at the Fixed and Variable Restrictors

Regime	Formula
$\partial-\partial$	$\left\lvert\frac{dP_1}{dh}\right\rvert_{max}=\frac{16d_2}{d_1^2}\frac{(P_0-\Delta P_f-\Delta P_{v_*})^{3/4}\Delta P_v}{P_0-2(P_0-\Delta P_v-\Delta P_{ne})\sqrt{\Delta P_v}}$
$\kappa-\partial$	$\left\lvert\frac{dP_1}{dh}\right\rvert_{max}=\frac{8d_2}{d_1^2}\frac{(P_0-\Delta P_f-\Delta P_v)^{3/4}\sqrt{P_0-\Delta P_f}}{\Delta P_f}$
$\partial-\kappa$	Same as for $\left\lvert\frac{dP_1}{dh}\right\rvert_{max}$ for relay with constant pressure drop at the fixed restrictor (Table 5)
$\kappa-\kappa$	Same

SUPPLEMENT 2

The effect of changes in parameters P_0 and ΔP_f on the distance h_0 can be shown by an analysis of the derivatives $\partial h_0 / \partial P_0$ and $\partial h_0 / \partial \Delta P_f$. The first of these derivatives is negative. The second derivative is positive. In considering the derivative $\partial h_0 / \partial \Delta P_f$ note the inequality $P_0 > 2\Delta P_f$, which is the condition for the subcritical flow through the fixed restrictor.

To clarify the effect of changes in parameters ΔP_f and P_0 on the quantity $\tan\gamma_2$ let us write expression (6) in the form

$$\operatorname{tg}\gamma_2 = \frac{4d_2}{d_1^2\sqrt{P_2\Delta P_f}}\left[(P_0 - \Delta P_f - P_2)\sqrt{P_3(P_3 - P_3)} + \right.$$
$$\left. + \sqrt{(P_0 - \Delta P_f)(P_0 - \Delta P_f - P_2)}(P_3 - P_2)\right],$$

from which it follows that an increase in P_0 leads to an increase in $\tan\gamma_2$, while an increase in ΔP_f leads to a decrease.

SUPPLEMENT 3

Expression (12) differs from expression (6) by the inclusion of ΔP_v in (12) in place of P_2, as in (6). Replacing P_2 by ΔP_v in the equation for $\tan\gamma_2$ (see Supplement 2) we obtain the expression for $\tan\gamma_4$.

From the equation obtained in this manner it is evident that $\tan\gamma_4$ decreases with increases in ΔP_v. $\operatorname{Tan}\gamma_2$ decreases with increases in P_2 in an analogous manner. Since $P_2 > \Delta P_v$, then $\tan\gamma_4 > \tan\gamma_2$.

SUPPLEMENT 4

The positive sign of the derivative $\partial h_{01} / \partial \Delta P_f$ in conjunction with the negative sign of the derivative, indicates the growth of h_{01} with increases in ΔP_f and the diminution of h_{01} with increases in P_0. To demonstrate that h_{01} does decrease with increases in ΔP_v, let us write the derivative with respect to ΔP_v of the expression that enters into equation (9):

$$\frac{\partial}{\partial \Delta P_v}\left[\frac{1}{\Delta P_v (P_0 - \Delta P_f - \Delta P_v)}\right] = \frac{-P_0 + \Delta P_f + 2\Delta P_v}{\Delta P_v^2 (P_0 - \Delta P_f - \Delta P_v)^2}.$$

To show that this derivative is negative let us prove the inequality $P_0 > \Delta P_f + 2\Delta P_v$. Since $\Delta P_f = P_0 - P_1$, then $P_0 > P_0 - (P_1 - 2\Delta P_v)$. It is, in addition, a known fact that under subcritical regimes of flow it is always true that $P_1 > 2\Delta P_v$ and therefore it follows that the inequality is proven.

Received January 8, 1957

LITERATURE CITED

[1] V. N. Dmitriev, Calculation of the static characteristic of a pneumatic relay. Automation and Remote Control, Vol. XVII, No. 9, 1956.*

[2] A. G. Shashkov, The theory of a control system of the type "nozzle-baffle," operating on oil. Automation and Remote Control, Vol. XVII, No. 11, 1956.*

[3] E. Samal, Pneumatische Messwertumformer für Regelzwecke. Regelungstechnik, Heft 3, 1954.

[4] G. T. Berezovets, New developments in pneumatic automatic control. Automation and Remote Control, Vol. XVII, No. 1, 1956.*

[5] S. A. Bergen, Pneumatic Force Balance Instrumentation. Instrument Practice, No. 4, 1954. (see this article in Regelungstechnik, Heft 1, 1954).

*[See C. B. Translation.]

[6] G. T. Berezovets, V. N. Dmitriev and E. M. Nadzhafov, On the allowed simplifications in calculations for pneumatic regulators. Instrumentation, No. 4, 1957.

[7] L. A. Zalmanzon, Graphs for determination of parameters of steady state air flow through a system of calibrated orifices in pneumatic regulators. Automation and Remote Control, Vol. XIII, No. 2, 1952.

SOME METHODS OF STABILIZATION AND CONTROL OF LOW FLOW RATES OF OPERATING LIQUID IN HYDRAULIC AUTOMATIC SYSTEMS

I. N. Kichin

(Moscow)

The phenomenon of obliteration (fouling) of small cross section passages in hydraulic automatic systems is discussed, and mechanical, hydraulic methods for its elimination are proposed. The effectiveness of the indicated methods is determined; these methods facilitate the establishment of controllable, stable flows through restricting devices in hydraulic automatic systems.

INTRODUCTION

There is a whole series of devices in modern hydraulic automatic systems that require stable flows, both controllable and fixed, of small quantities of the working fluid. Such regimes are characteristic of metal working tools under low feed rates, and of hydraulic regulators with large static periods, etc. Under steady state operation, the regulation of flows in such systems is usually effected by changing passage cross sections of restricting devices. However the flow of viscous liquids through small cross section passages posesses unique characteristics and is dependent on poorly understood phenomena. According to the data of a series of authors [1-6], small flows of working liquids such as mineral oils, kerosene, and some others, that are established with the aid of common restricting devices having gaps 0.007-0.022 mm in width and even up to 0.06 mm, or having orifices of less than 0.2 mm diameter, are unstable with time, and such flows may decrease significantly in the first few minutes after initiation of operation. This phenomenon occurs even with thorough filtration of the liquid that excludes the possibility of mechanical fouling of the flow channel. The explanation that the observed effect is occasioned by the fouling (obliteration) of small cross section passages by polarized molecules of the liquids [1, 2], has been advanced. There are other opinions regarding the nature of obliteration, however we are not aware of any systematic investigations in this area, investigations that might yield recommendations for establishment of stable small flows.* Conversely the opinion is widely held that conditions under which obliteration may arise should be avoided, that is, it is proposed that restricting devices with large cross section passages only be used, which significantly raises the lower limit of small flow rates. Concurrently it is recommended that small flow rates be obtained by lowering the pressure drop [7], which is not always possible.

In this paper, on the basis of experimental investigations, several methods for obtaining stable low flow rates of the working liquid are discussed; the method of elimination of basic obliteration, and also the use of restricting devices that exclude the possibility of initiation of obliteration. At the same time the approaches for solution of the problem of getting controllable low flow rates, stable with time, are indicated.

1. The Phenomenon of Instability of Low Flow Rates

For establishment of low flow rates of working liquid, runs were conducted with common restricting devices that include small cross section passages – fixed (restrictor bushings of diameter d = 0.2, 0.3, 0.4 and

* Papers [2,3] point out that mechanical displacement of the surfaces that form the restricting cross section, eliminates incipient obliteration.

0.5 mm) and variable (restricting devices of the nozzle-baffle type,* with nozzle diameter d = 0.5, 1 and 2 mm and gaps h = 0.02, 0.04 and 0.06 mm).

Transformer oil GOST982-58, at a temperature of 25°C, was used as the working fluid (density of γ = = 0.876 g/cm^3 and kinematic viscosity of ν = 0.27 st). The oil pressure P at entrance to the flow restricting device was taken equal to 0.5, 1, 1.5 and 2 kg/cm^2, and discharge was to the atmosphere. Thorough filtration was performed by a system of filters (mesh, silk, ceramic).

On the basis of the flow characteristics obtained in the tests it was established that basic obliteration incipience was observed in bushings of orifice diameter less than 0.4 mm and in the case of the nozzle-baffle combination, it was observed when the gap distance was below 0.06 mm, regardless of the nozzle diameter.

With certain dimensions of passage cross sections (for instance when bushing orifice diameter was 0.2 mm and when the gap between nozzle and baffle was 0.02 mm) complete shut off of flow was observed in most cases, that is, total obliteration. Minimum flow in the absence of obliteration was no less than 30-90 cm^3/min under pressure drops of ΔP = 1 kg/cm^3.

Obliteration developed more rapidly as pressure drops for a given passage cross section were increased (and consequently, the flow of the working fluid) across the restricting device being tested. Obliteration was also speeded with increases in nozzle diameter. At the same time increasing the gap, h, or the bushing orifice diameter, d, for given pressure drops, somewhat prolonged the time for initiation of obliteration. This may be explained by the fact that in addition to increases in the flow through the restricting channel, the dimensions of the passage cross section increased, which gave dominance to factors unfavorable to the initiation of obliteration.

During the onset of obliteration small, rapid changes in pressure drop, and also shocks on the walls of the channels, reestablished the initial maximum flow rates. Stabilized (constant with time) partial obliteration in most cases was eliminated in the same manner, but in this case greater changes in pressure drop were required and sharper shocks to the channel walls. In this case the time for obliteration to be established, initial (after first initiating operation) as well as subsequent (after reestablishment of pressure drop or ending of wall shocks), in the above-indicated restricting devices, in most cases fell within the limits of 5 sec to 10 min, sometimes reaching 2 hrs and more. A noticeable reduction in flow rates, that is, real, observable obliteration, occurred basically during the last 10-30% of the total time of establishment of obliteration.

Established total (and occasionally partial) obliteration could be eliminated only by motion of one of the working surfaces of the flow restricting channel, or by running a thin wire through the channel. After elimination of obliteration in this manner, drop of flow rate and in most cases the full reestablishment of obliteration was observed after a time whose length depended on the type of operation and on the geometry of the passage cross sections. The time for full reestablishment of obliteration in these cases occasionally exceeded the times indicated above.

It was noted that long times for establishment of obliteration usually were reduced considerably (occasionally up to 5 sec-10 min) if the experiment with a given restricting device was conducted after a 12 to 48 hour interruption in operation. Explanation of this effect requires additional investigations.

2. Mechanical Means for Elimination of Obliteration

Let us examine some methods for obtaining controllable, stable low flow rates of the working fluid by mechanical elimination of possible obliteration. The method of displacement (rotation, vibration) of one of the working surfaces (baffle) of the channel of the restricting device of the nozzle-baffle type, as well as the impulse feeding of the working fluid through the constant orifice restricting bushing (pulsating pressure in the flow channel) were adopted as methods of this type.

a) Rotating Baffle

Figure 1 shows the scheme of the flow restricting device of the nozzle-baffle type with rotating baffle.

* At the present time this restricting device is finding ever increasing application in hydraulic automation, particularly in connection with the tendency toward block regulators, working on the force compensation principle.

The nozzle, 3, was fixed to the movable carriage, 2, which moves inside the body block, 1, by means of the micrometer screw, 5. The little baffle shaft, 4, was located in the bushing, 6, with a radial clearance of 0.015 mm, and was fixed in the axial direction by the spring, 7. Amplitude of dynamic pulsations at the shoulder of the baffle shaft were not greater than 0.002 mm. The gap h = 0.02, 0.04 and 0.06 mm was established by means of gauged spacer plates, and was checked before and after each experiment. Pressure drops ΔP = 0.5, 1, 1.5 and 2 kg/cm^2 were established for each gap with nozzle diameters of d = 0.5, 1 and 2 mm. The baffle was rotated at speeds n = 1.5, 10, 50, 100 and 150 rpm through speed reducers.

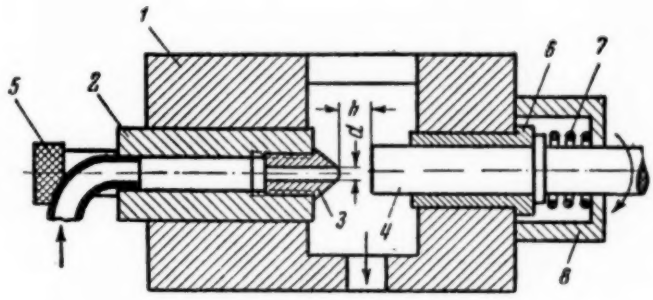

Fig. 1.

On the basis of the conducted experiments, flow characteristics were plotted as Q = f(H) (Fig. 2) for various pressure drops ΔP and for various values of diameter d, both in the absence of obliteration (solid curves) and with obliteration (dashed curves). The minimum flow obtained was equal to 3 cm^3/min with a gap of 0.02 mm, nozzle diameter of 0.5 mm, and pressure drop of 1 kg/cm^2. The maximum relative error in the measurement of δQ in this experiment was 5.1%.

It was determined that when n $\geq$ 1 rpm, the obliteration that had been established for a gap h, was eliminated practically immediately. Increasing the revolutions did not produce any noticeable change in the flow rates at constant geometries of the flow restricting device and at constant pressure drops through the device; only the form of the emerging stream of fluid changed. If under n = 1 to 5 rpm, the emergent stream of fluid "smeared out" over the face of the baffle, then under further increases in rpm, especially at n = 100 to 150 rpm, the stream "wound itself around" the shaft and splashed out to the sides. Control of small flow rates during operation was done by changing the gap h.

Within the limits of the experiment it was also established that rotation of the baffle shaft through an angle equal to or greater than 5 to 10°, also eliminated previously established obliteration. Following such rotation, obliteration could reinstate itself, essentially after a time lapse indicated in Appendix 1.

b) Vibrating Baffle

In Figure 3 is shown a diagram for a flow restricting device of the nozzle-baffle type, incorporating a vibrating baffle. The nozzle, 3, is installed in a fixed base, 1; the baffle, 4, is installed on shaft, 2, which is movable in the axial direction. The shaft, together with the actuating armature, 9, is fixed by means of flexible membranes, 10, within the channel in the magnetic pole, 6, and is locked in place by selected bushings, 8, and nuts, 11. The magnet pole together with the electromagnetic winding, 7, is securely fixed in the body of the electromechanical transducer, 5, which is installed on the base, 1. The electromechanical transducer is a dynamic relay, in which the electromagnetic winding is fed direct current of 0.15 amps at 24 v potential. By feeding direct current signals of I = 0 to 30 m amps to the winding, it is possible to vary the gap, h, within the limits 0 to 0.3 mm, corresponding to the linear characteristic h = f(I). The superposition of a supplementary signal of alternating current i = 0 to 1.5 m amps at a frequency of 50 cps produces an axial vibration of the baffle shaft at an amplitude of 0 to 15 μ.

A fixed gap, h equal to 0.01, 0.02, 0.03, 0.04 and 0.06 mm was established by a fixed displacement of the baffle relative to the fixed nozzle, and was checked during the entire experiment against a vernier by means

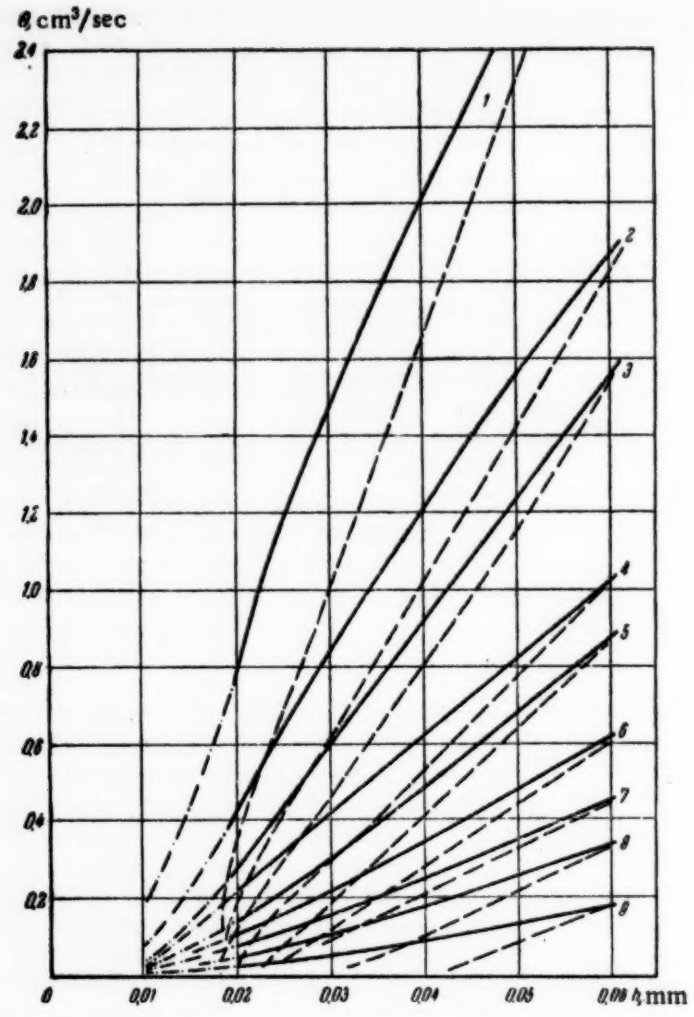

Fig. 2. Flow characteristics with a rotating baffle.

Curve No.	1	2	3	4	5	6	7	8	9
ΔP, kg/cm^2	2.0	1.0	2.0	0.5	1.0	2.0	0.5	1.0	0.5
d, mm	2.0	2.0	1.0	2.0	1.0	0.5	1.0	0.5	0.5

of a microscope MIR-1 (magnification to 180) with optical adapter AM-9-2. The amplitude of vibration of the baffle was also checked through the microscope by the width of the blur of the baffle face.

For each gap, pressure drops were established equaling $\Delta P = 0.5$, 1, 1.5 and 2 kg/cm^2 with nozzle diameters d = 0.5, 1 and 2 mm.

Flow characteristics Q = f (h) without obliteration and in the presence of obliteration, for the given case are analogous to those shown in Fig. 2 in the region h = 0.02 to 0.06 mm. Minimum flow rate was 1.2 cm^3/min with h = 0.01 mm, d = 0.5 mm and $\Delta P = 1$ kg/cm^2. Maximum relative error of measurement of δQ in this experiment was equal to 10%.

It was established that under vibration of the baffle at amplitudes equal to certain optimum values, A, the obliteration existing in gap h before the vibration was eliminated practically instantly; for elimination of

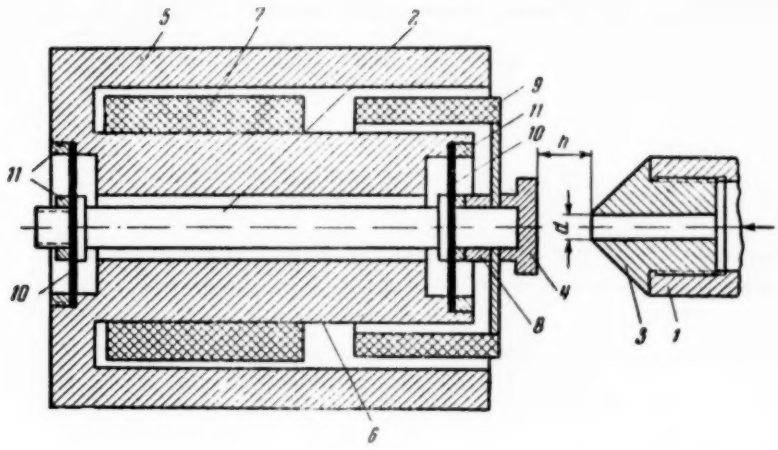

Fig. 3.

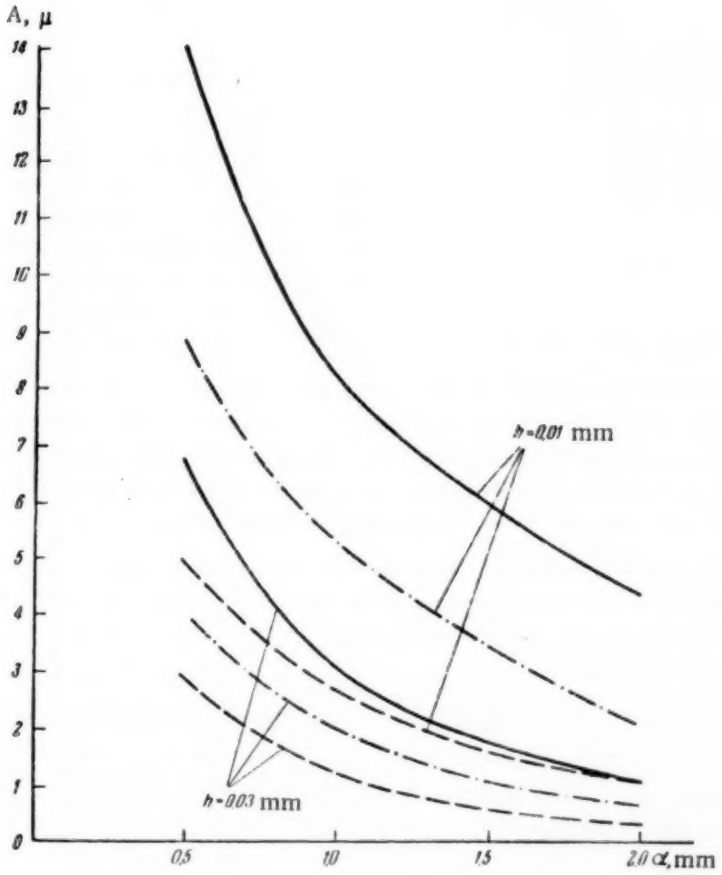

Fig. 4. Optimum amplitude of vibration A as a function of nozzle diameter, d. Dashed lines) ΔP = kg/cm^2, dash-dotted lines) ΔP = 1 kg/cm^2, and solid lines) ΔP = 2 kg/cm^2.

established or more extensive obliteration, a large value of A was required. An amplitude of vibration lower than the optimum also decreased obliteration, which usually returned to its original value when amplitudes were less than 0.5 A.

Figure 4 shows the relationship A = f(d) under various values of the gap, h and various pressure drops ΔP.

Control of small flow rates during operation was effected by varying the gap h ($h \geq A$).

c) Impulse Flow

In Figure 5 is shown the diagram of a flow restricting device for creating impulses of flow of the working fluid. The fluid is fed into the interior cavity of the cylinder 4, of diameter D. The small cylinder is installed in a fixed liner, 3, with a clearance of 0.02 mm. When the cylinder rotates the oil flows through the replaceable restricting bushing, 5, when it coincides with the passage in the liner. The liner is held by the clamp, 2, to the mounting base, 1, in a position such that the passage in the liner leads to the sump in the base. The diameters of the flow restricting bushing were, d = 0.5, 1 and 2 mm; the length of the liner opening was l_1 = 6.12 and 20 mm, while the width was l_2 = 2 and 4 mm. At each combination of dimensions of the restricting device the pressure drops ΔP = 0.5, 1, 1.5 and 2 kg/cm^2 • were established, and speeds of rotation of the cylinder of n = 50, 150 and 600 rpm were used.

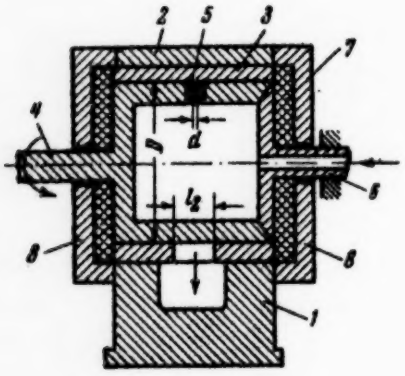

Fig. 5.

As a result of the conducted experiments, flow characteristics were drawn for Q = f(u) (Fig. 6) where the value U is equal to $Fl_1/\pi D$, and characterizes the passage cross section that is open in the process of impulse flow, regardless of the speed of revolutions (F is the area of the passage cross section of the restricting bushing). Minimum flow rate that was obtained with d = 0.3 mm, l_1 = 6 mm, n = 50 rpm and ΔP = 1 kg/cm^2, was 2.2 cm^3/min. Maximum relative error of measurement in this experiment was δQ = 5.3%.

In the process of impulse flow, the flow rate of the working fluid is equal to $m l_1 F/\pi D\,[(2g/\gamma k)\Delta P]^{1/2}$, where k is the total hydraulic loss coefficient in the restrictor when n = 0, the coefficient m accounts for the increase in pressure in the cavity of the cylinder during stoppage of the flow (when the passage cross section of the restrictor bushing is not coincident with the cut out in the liner) and also accounts for the rise in this pressure due to inertia forces and changes in the coefficient of hydraulic losses as the speed of revolution increases.

In accordance with the experimentally obtained relationship m = f(n) as the speed of revolution changed from 50 to 600 per minute, the flow rate increased on the average by 25%. The coefficient m, concurrently rose from 1.65 to 2.06 for the case d = 0.5 mm, ΔP = 2 kg/cm^2, k = 2 and from 2.03 to 2.5 for the case d = 2 mm, ΔP = 0.5 kg/cm^2, k = 3.8 and so on.••

Changing the width of the slot, l_2, larger than the diameter of the restricting bushing, did not result in any substantial changes of flow rate.

Control of small flow rates during operation was accomplished by changing the speed of revolution of the small cylinder. The same result can be obtained by axially displacing the liner having a wedge shaped slot, that is, a variable length of slot $l_1 > d$.

3. Hydraulic Means for Eliminating Obliteration

Let us examine some methods for obtaining small, stable, controllable flow rates of the working fluid, with

• These values of pressure drop were established before beginning of the experiment, for the condition when oil was flowing through the restrictor.

•• The values of the total hydraulic loss coefficients of the restrictor bushings, for n = 0 are taken from [8].

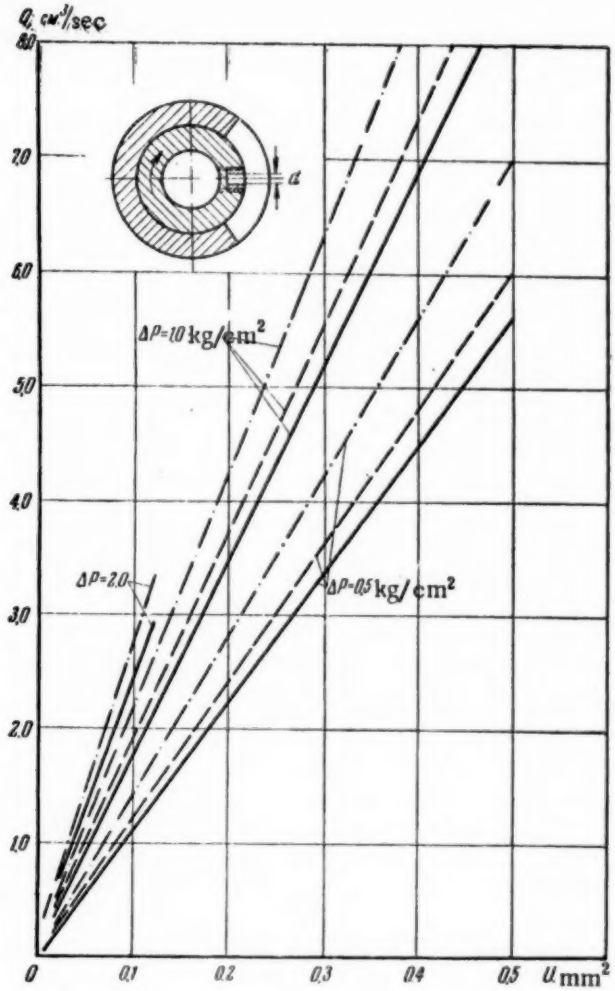

Fig. 6. Flow characteristics for the case of impulse flow. Solid lines are for n = 50 rpm, dashed lines for n = 150 rpm, dot-dashed lines for n = 600 rpm.

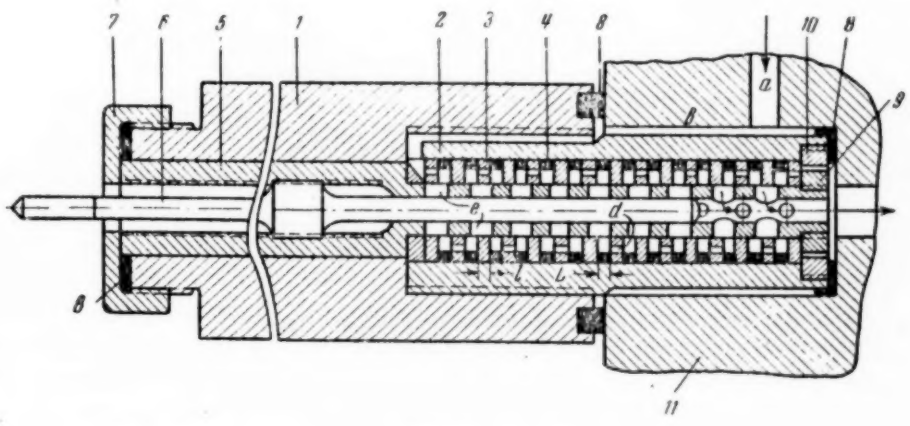

Fig. 7.

hydraulic elimination of obliteration. For realization of this method, special multi-step flow restricting devices were used, having passage cross sections that are not susceptible to noticeable obliteration.

The required low flow rates were assured through changes in pressure drops in the restricting channels, produced by changes in the number of consecutive local restrictions included in the flow circuit of the working fluid.

a) Controllable Flow Restricting Assembly

Figure 7 shows the diagram of a restricting device in the form of a controllable assembly. The working fluid enters a collection of individual restricting bushings through channels a, b and c, the restrictors being in the form of spacers, 3, with restricting apertures, d, of length 1. The degree of flow restriction is controlled by axial displacement of the shaft, 6, in the tube 5, and this motion, closes or opens passage openings, e. The maximum flow corresponds to a fully withdrawn shaft, at which time all openings e are open and the oil from the channel, c, passes directly through the extreme left side passage, e, and out to the exit port. For minimum flow the shaft is fully inserted and all the passages, e, except the extreme right side, are closed; this is the condition when a maximum number of restrictions are in the flow path. To achieve good sealing, the spacers, 3, are assembled on a polished mating surface of the tube, 5, with clearance less than 0.02 mm and are then drawn together with spacer rings, 4, by the nut, 9. Mating surfaces of the shaft and the tube are lapped so that the clearance between them does not exceed 0.03 mm. The complete assembly is installed into the holder, 2, with clearance of 0.1 mm, and is fastened by nuts, 7, and 10. The holder, 2, is screwed into the block 1 to bottom, and block 1 is fastened to base 11. Sealing at the block faces is done by rubber "o" rings, 8. The openings e, 1 mm in diameter, are run in two directions at 90° in alternate order, so that for a spacer thickness of 0.3 mm, they are never completely covered by the spacers. The exposed part of the shaft, 6, carries markings indicating the number of restricting passages that are in the flow path.

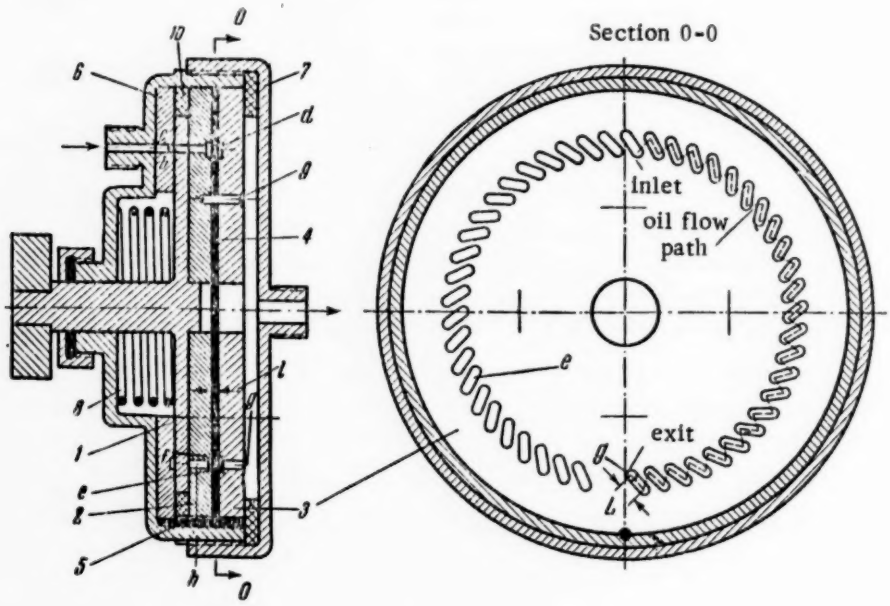

Fig. 8.

The following parameters were used in the experiments: maximum number of spacers, n = 60; diameter of flow restricting openings, d = 0.6 and 0.8 mm; length of flow channel, l = 0.3 mm; distance between spacers, L = 0.3 and 0.6 mm. The arrangement of the restricting openings was labyrinthic. Both sides of the restricting openings were chamfered 45° × 0.05 mm. The flow characteristics Q = f (n) under pressure drops of ΔP = = 1.1 and 2.2 kg/cm^2 are shown on Fig. 10.

The results obtained, demonstrated that in a restricting device of this design, a fundamental role is played

by the distance between spacers, L. Thus, for example, when L = 0.5, d = 0.3 mm, the flow rates by comparison to those obtained for L = d = 0.6 mm were one seventh for $\Delta P = 2.2$ kg/cm^2 and one tenth for $\Delta P = 1.1$ kg/cm^2 (curves 1m-2p and 1n-2o in Fig. 10).

b) Controllable Change of Direction Resistances

Figure 8 shows a diagram of a flow restricting device with a "face" arrangement. The working fluid enters a circular channel, b, and from there is directed through the only opening c, in the selector baffle 1, and through one of the openings, h, in the forward disc, 2, that coincides with opening c, to the grooves f and e of the forward and rear discs, 2 and 3, that are separated by the spacer, 4, containing the restricting opening, d. The grooves f and e, are milled out in the form of short channels, 2 mm wide and deep, and 2.5 mm + 2d long. These channels are so arranged that their rounded ends coincide, and they form a zig zag labyrinthic flow path. The oil flowing along this layrinth, passes from one groove to the next through the flow restricting openings, d, of length l, and exits through the only opening g to the groove e, of disc 3, at the end of the labyrinth channel. The degree of flow restriction may be varied by moving the baffle, 1, relative to the openings h, that are contained in each groove f, of disc 2. Maximum flow corresponds to the coincidence of openings c and h, opposite the opening, g, of the rear disc. Only one restricting opening d, is included in the flow path, and the baffle, 1, is up against the stop, 5. By turning the baffle in the opposite direction through an angle less than 360°, to the stop, minimum flow is obtained, in which the working fluid, passing into the corresponding opening h, follows the entire labyrinth through all the resistances d, to the outlet opening, g. Under intermediate positions of the baffle 1, the opening with a diameter of 4 mm is always connected with one or two of the openings h, whose diameter is equal to 2 mm. To seal the surfaces, the rear and forward discs and the spacers 4, are lapped and pressed together by screws, 9. Mating surfaces of ring 6, ring 10 and the forward disc 2, are also lapped and solidly pressed together by the nut 7, and the spring 8. The baffle 1, rotates because of an axial clearance of 0.004 mm, that is held by ring 10. The discs 2 and 3 are kept from rotating by the pin, 5. In order to obtain very small flows between discs 2 and 3 it is possible to install not one, but several spacers, 4, that have flow restricting openings d, and between which are installed intermediate discs of thickness L with openings of diameter 2 mm, coaxial with openings d and h. In this case, the oil in flowing from groove f to groove e, passes consecutively through a corresponding number of flow restricting openings. A scale is fixed to the base, indicating the number of restricting openings that are included in the flow path.

The following parameters were used in the experiments: maximum number of flow openings, n = 100 (1 spacer); diameter of restricting openings d = 0.6 mm; length of flow channel l = 1.5 and 0.3 mm; axial distance between restricting openings L = 2.5 mm. The restricting openings were chamfered on both sides, 45° × 0.05 mm. The flow characteristics Q = f (n) are shown in Fig. 10 for pressure drops, ΔP, equal to 1.1 and 2.2 kg/cm^2.

In addition the effect of temperature of working fluid on the flow characteristic, with maximum number of flow openings and pressure drop of 2.2 kg/cm^2, is shown in this same figure. The characteristic given shows that in the case where length of channel l = 1.5 mm (l = 2.5 d), the total flow is essentially dependent on the oil temperature. Thus, in changing temperature from 16 to 40°C the flow changed by a factor of more than two (the points c' and c'' with n = 100, Fig. 1). However in the case l = 0.3 mm (l = 0.5 d) under the same temperature change, the change in flow did not constitute more than 8-10% (points q' and q'' with n = 100, Fig. 10).

Figure 9 shows the diagram of a flow restricting device that is analogous to the preceding device, but with a different – "ring type" – distribution of the working fluid. The oil flows through the channel a, into the toroidal channel b that is cut in body 1; then into c, the only channel in the ring 5; and further through the corresponding channel h, into the labyrinth formed by the grooves f and e, that are cut in the body 1 and the cover 2, in the same manner as in the device shown in Fig. 8. The channels h are 2 mm in diameter and are distributed around the outer periphery of the body 1, and are connected with each groove f on the face of the body. After passing through the proper number of resistances, the working fluid enters the channel g, which is 2 mm deep and wide, and then flows to the exit through the channel i, 2 mm in diameter. The maximum and minimum flows are obtained through the same principle as in the previous device. In intermediate positions of the ring, the channel, c, is always connected with one or two of the h channels, through the cut out k. For sealing, the mating surfaces of the body face, spacers, and cover are lapped and drawn together by the screws 7.

The inside surface of the ring, and the external surface on the body that mates with it, are also lapped (the clearance here is not over 0.05 mm). In addition, to prevent leakage of the fluid from the toroidal channel b into the channels h and then out, rubber "o" rings, 6, were used with compression of 0.3 mm. By installing not one, but several spacers, 3, of thickness L, having flow restricting openings d, between the body and the cover (and corresponding spacing discs 4, with openings 2 mm in diameter, situated on the axis of the d openings), it is possible to obtain, as in the previous case, extremely small flows by an increase in the number of local resistances included in the flow path. A scale is fixed to the face of the ring, indicating the number of flow restricting openings that are in the flow path.

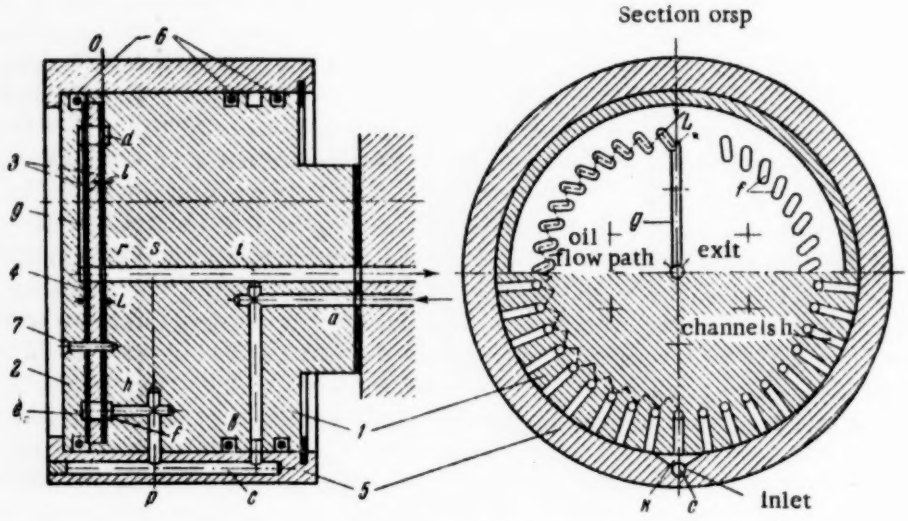

Fig. 9.

The following parameters were used in the experiments: maximum number of flow openings n = 75 (1 spacer), n = 150 (2 spacers), n = 225 (3 spacers); diameter of flow restricting openings d = 0.6 and 0.8 mm; length of flow channel l = 0.3 mm; axial distance between restricting openings L = 2.5 mm.

The flow characteristics Q = f(n) for ΔP = 1.1 and 2.2 kg/cm^2 are shown in Fig. 10. These curves show that the data taken with various numbers of spacers, coincide over regions that correspond to identical numbers of flow openings. The minimum flow of oil, which was obtained with three spacers (n = 225, d = 0.6 mm, and ΔP = 1.1 kg/cm^2), was 4cm^3/min. The maximum relative error of measurement of δQ, under these conditions, was 2.6%. Changing the temperature from 16 to 40°C resulted in changes of less than 5% in the flow (points r' and r" with n = 150, l = 0.38d, Fig. 10).

c) Results of the Experiments

In the course of the experiments no obliteration was observed and the flow rates were stable for 4 to 8 hours of uninterrupted operation of each device.

A comparison of flow characteristics obtained under identical operating conditions from different designs of controllable flow restricting devices, shows that in some degree they differ from each other. Such a divergence of characteristics occurred following additional hydraulic resistances in the controllable restricting devices, resistances that differed in form and length of the supply and exit channels of 2 mm diameter, located in the base bodies of the devices. These channels were determined by the installation conditions of the restricting devices in hydraulic test assemblies for testing in a common hydraulic system.

In connection with this, it is essential to consider the following factors when constructing the devices described here and subsequently arranging the resistances:

a) to limit the flow of working fluid by means of local resistances only, the distance L between resistances must be chosen to be no less than the diameter of restricting opening;

b) to decrease the effect of temperature on the flow characteristic the length of flow channels must be minimum ($l \leq 0.5$ d);

c) the supply and exit channels in the body of the device must be made as short as possible, and over 2 mm diameter;

d) since the effective diminution of flow with n> 50 to 80 is low, in order to obtain sufficiently low flows with a minimum number of local resistances, the diameters of the flow passages of the restricting openings, d, should be chosen less than 0.6 mm but no less than 0.4 mm (to preclude the possibility of obliteration arising, see paragraph 1);

e) when using devices of this type, thorough filtration of the working fluid is required. Note, that in case of fouling of the restricting devices, the latter two types are considerably easier to disassemble and clean than the first type of device.

d) Calculations for Multistep Flow Restrictors

For the case of similar geometry of all restricting channels, the flow of fluid through a multistep restricting device is determined by the relationship

$$Q = F\sqrt{\frac{2g\Delta P}{\gamma k n}}, \tag{1}$$

from which it is evident that under constant pressure drops, the variation of flow with number of resistances included in the flow path, has the form of an exponential hyperbola. A sharp change in flow rate occurs when the first resistances are included in the flow path, and relatively insignificant changes occur with further increases in the number of local resistances (Fig. 10). Thus, according to the data of the experiments, with inclusion in the flow path of the first ten resistances, the flow decreases by $^1/_3$ to $^1/_{12}$ of its original value, while the inclusion of the following twenty decreases the flow by only $^1/_2$ to $^1/_3$.• Such nonuniform change of the flow rates considerably complicates control of the flow in the region of the first 20 to 30 local resistances.

For convenience of control the relationship Q = f(n) can be linearized or, through the essential conditions for low flow rates, the relationship Q = f(n) can be given any form. To do this it is only necessary to vary the diameters of succeeding flow resistances in accordance with some definite rule.

On the basis of Bernoulli's equation the sum of pressure drops through a restricting device having n resistances included in the flow path, which have varying flow passage diameters, is equal to••

$$\Delta P = \sum_{i=1}^{n} \Delta P_i = \sum_{i=1}^{n} \frac{k_i^n}{d_i^4}\left(\frac{8Q_n^2\gamma}{\pi^2 g}\right), \tag{2}$$

where ΔP_i is the pressure drop at the i'th resistance, which has the passage diameter d_i; k_i^n is the coefficient of over-all hydraulic losses of this resistance (the superscript designates the number of resistances included in the flow path).

The diameter of each of the n restricting openings, from [2], is found by the expression

$$d_i = \sqrt[4]{\frac{8Q_i^2\gamma k_i^i}{\pi^2 g\Delta P_i}} = \sqrt[4]{\frac{8Q_i^2\gamma}{\pi^2 g}\left(\frac{k_i^i}{\Delta P - \sum_{i=1}^{i-1}\Delta P_i}\right)}. \tag{3}$$

• According to the data of [6] and [8] the corresponding decrease in flow rate was 3.2 to 4 and 1.5 to 1.8 times.

•• We neglect the flow velocities in the supply and exit channels, while the flow velocity in the restricting channel is $V_i = 4Q_n/\pi d_i^2$.

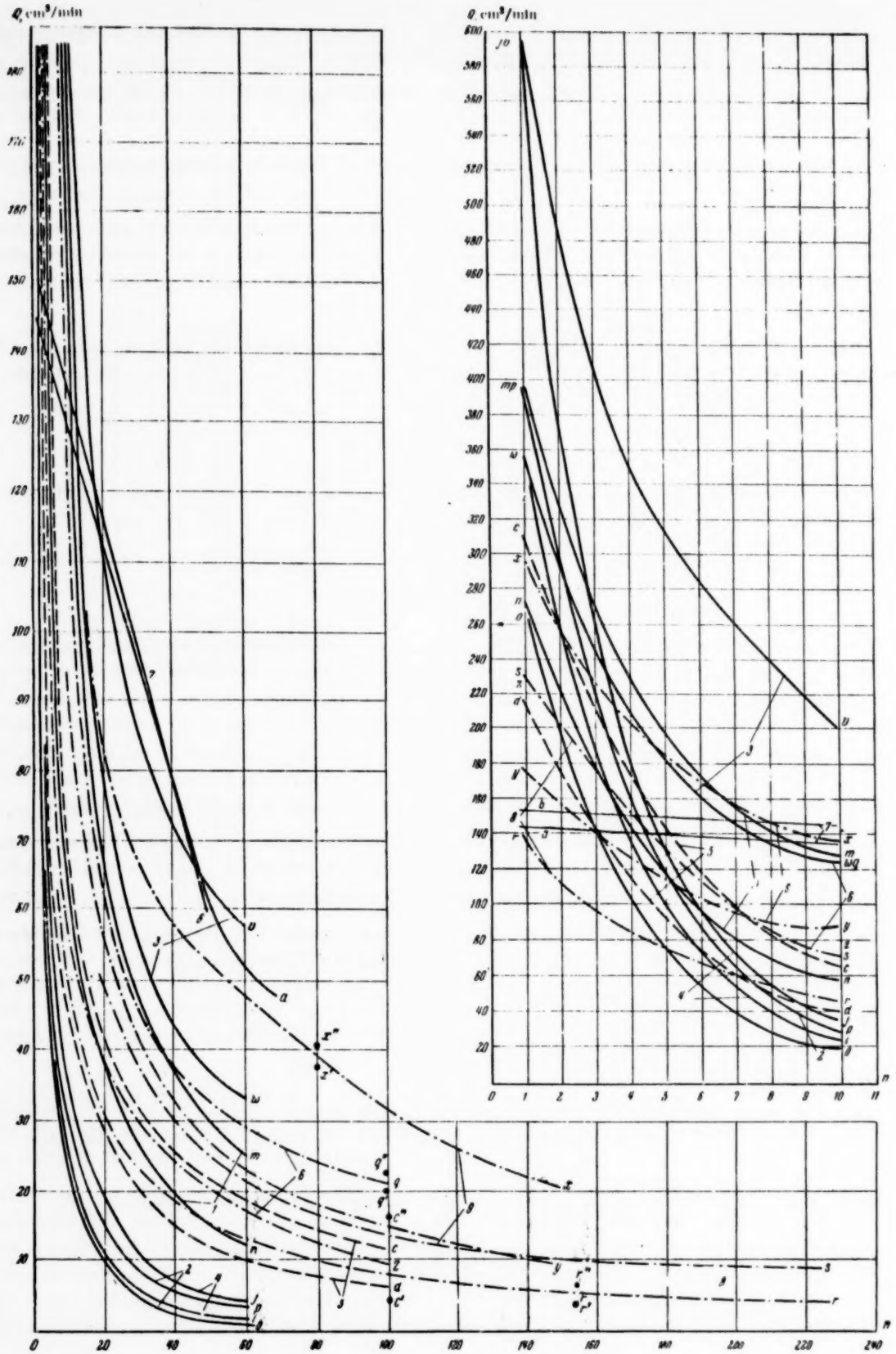

Fig. 10. Flow characteristics Q = f(n) for multistep flow restricting devices. Points x', c', q', r' correspond to a temperature of 16°C, points x", c", q", r" to a temperature of 40°C.

Type of restrictor	d, mm	l, mm	L, mm	Curve conditions $\Delta P = 1.1$ kg cm^2	Curve conditions $\Delta P = 2.2$ kg cm^2	Notes
Controllable Assembly	0.6	0.3	0.6	1 n	1 m	$n_{min} = 1$
	0.6	0.3	0.3	2 o	2 p	"
	0.8	0.3	0.6	3 w	3 v	"
	0.8	0.3	0.3	3 i	4 j	"
Controllable Face	0.6	1.5	2.5	5 d	5 c	1 spacer; $n_{min} = 1$
	0.6	0.5	2.5	6 z	6 q	"
	–	1.5	2.5	7 b	7 a	"
				calc.	exper.	
Controllable Ring	0.6	0.3	2.5	8 r	8 s	1-3 spacers; $n_{min} = 1$-3
	0.8	0.3	2.5	9 y	9 x	1 and 2 spacers; $n_{min} = 1$-2

Fig. 10 (continued)

Using Equation (2), we obtain

$$d_i = \frac{1}{\sqrt[4]{\frac{\Delta P \pi^2 g}{8Q_i^2 \gamma k_i^4} - \frac{1}{k_i^4}\left(\frac{k_i^4}{d_1^4} + \frac{k_2^4}{d_2^4} + \cdots + \frac{k_{i-1}^4}{d_{i-1}^4}\right)}}. \quad (4)$$

As a result of analysis of the data given by the flow characteristics of the controllable devices it was established that the coefficients of overall hydraulic losses for these devices, analogous to the coefficients for non-controllable assemblies and restrictor bushings [8], are first order functions of the quantity $l/0.05d\,\mathrm{Re}$,* where l is the length of flow restricting channel; $\mathrm{Re} = 4Q/\pi d\nu$, the Reynolds number. Taking into account the last two relations, we get for the system of n resistances with equal lengths of flow channels

$$\mathrm{Re}_1 d_1 = \mathrm{Re}_2 d_2 = \ldots = \mathrm{Re}_i d_i = \ldots = \mathrm{Re}_n d_n,$$

from which

$$k_1^n = k_2^n = \ldots = k_i^n = \ldots = k_n^n.$$

Using the last equation, we get from (3) and (4) the formula for calculation of the varying diameter

$$d_i = \frac{1}{\sqrt[4]{\frac{\Delta P \pi^2 g}{8Q_i^2 \gamma k_i^4}\left(\frac{1}{d_1^4} + \frac{1}{d_2^4} + \cdots + \frac{1}{d_{i-1}^4}\right)}} =$$

$$= \frac{1}{\sqrt[4]{\frac{\Delta P \pi^2 g}{8\gamma}\left[\frac{1}{Q_i^2 k_i^4} - \frac{1}{Q_{i-1}^2 k_{i-1}^{i-1}}\right]}}. \quad (5)$$

The dependence $Q = f(n)$ in the particular case will be made linear according to the rule

$$Q_i = Q_1 - \tan\psi n, \quad (6)$$

where Q_i is the flow rate present through the assembly with i resistances in the path; Q_1 is the desired maximum flow rate when only one resistance is included in the path; ψ is the desired angle of slope of the linear characteristic $Q = f(n)$.

Let us examine for example the calculation for the restricting device having the linear characteristic $Q = f(n)$, when flow rates change from $Q_1 = 2.5$ cm^3/sec to $Q_n = 1$ cm^3/sec. Taking $\tan\psi = 0.03$, we get on the basis of equation (6), $n = 50$. Let us select $d_1 = 0.06$ cm, $l = 0.15$ cm.

The required pressure drop $\Delta P_1 = 950$ g/cm^2 is determined by formula (2) with $n = 1$, where $k_1^I = 2.69$ (from graph $k = f(l\nu\pi/0.2Q)$ [8]). When restricting resistances are included in the path,

*Thus, in the case $L > d$ (Curves 6, 8, 9 in Fig. 10) the relationship $k = f(l/0.05\,d\,\mathrm{Re})$, can be represented by Curve 10 (Fig. 5 in [8]) and in the case $L < d$ (Curves 2, 4 in Fig. 10), by Curves 7, 8 (Fig. 5 in [8]).

$Q_2 = 2.47$ cm^3/sec, $k_2^{II} = 2.71$, $d_2 = 0.182$ cm [by Formula (5)].

When three restricting resistances are included in the path, $Q_3 = 2.44$ cm^3/sec, $k_3^{III} = 2.73$, $d_3 = 0.165$ cm and so on. When 50 resistances were included in the path, $Q_{50} = 1$ cm^3/sec, $k_{50}^{L} = 3.72$, $d_{50} = 0.058$ cm.

Restricting openings were selected by the indicated calculation, for a device with controllable face (Fig. 8) and a flow characteristic was obtained (Fig. 10, Curve 7a). Its departure from the theoretical characteristic (Curve 7b) did not exceed 12%.

SUMMARY

1) Low flow rates of working fluid through narrow gaps ($h < 0.06$ mm), capillary openings ($d < 0.4$ mm) usually are accompanied by the occurrence of obliteration, leading to a reduction of the flow rate.

2) The intensity of obliteration grows with increasing flow rates of the working fluid (transformer oil) under increasing pressure drops, and also grows with reduction of the characteristic dimension of the passage cross section. The persistence of obliteration decreases with reduction of its degree and stage of development.

3) Mechanical elimination of basic obliteration occurs with rotation (at a speed $n \geq 1$ rpm), turning (through an angle greater than 5°) and vibration (with amplitude equal to or greater than A), of the baffle of the flow restricting device of the nozzle-baffle type. The stable, low flow rates of working fluid that are obtained can be regulated by changing the gap, h, between nozzle and baffle.

4) To obtain controllable, stable low flow rates, flow restricting devices that work on the principle of impulse delivery of working fluid with control of the flow rates by changes in the number of turns or in the length of flow passage (time – cross section).

5) Flow restricting devices with consecutively placed local resistances not subject to obliteration, ensure stable low flow rates of the working fluid from 6 to 4 cm^3/min and less. Control of the flow rates is effected by changing the number of local resistances included in the flow path.

6) Formulation of a definite rule for changing the diameters of consecutively placed restricting openings, allows the linearization of the relationship of flow rate on the number of individual local resistances.

Received November 28, 1956

LITERATURE CITED

[1] A. S. Akhmatov, On the critical thickness of the boundary lubricating layer, determining the appearance of elementary slipping action, Bull. of the Acad. of Sci. USSR, Vol. XXX, No. 2, 1941.

[2] T. M. Bashta, Aircraft hydraulic components and assemblies. Defense State Pub. House, 1951.

[3] G. P. Vovk, Experimental investigation of narrow passage blocking. Dissertation. Machine & Instrument Institute, M. 1946.

[4] L. C. Bron, Hydraulic copying device. Collection "Automation of technical processes." Mashgiz, 1951.

[5] L. A. Zalmanzon and B. A. Cherkasov, Control of gas turbine and ram jet air breathing power plants. Defense State Pub. House, 1956.

[6] A. G. Shashkov, Experimental and theoretical investigation of flow restricting agents and hydraulic relays of the nozzle-baffle type, operating with oil. Dissertation. IAT Acad. of Sci. USSR, 1955.

[7] T. M. Bashta, Flow restrictor control of liquid flow rates. Machine Building News, No. 5, 1956.

[8] I. N. Kichin, Determination of coefficients of hydraulic loss for flow restricting resistances in hydroautomatic systems. Automation and Remote Control, Vol. XVIII, No. I, 1957.•

• See C. B. Translation.

CERTAIN PROBLEMS IN THE THEORY OF MAGNETIC AMPLIFIERS AND MAGNETO-MODULATION PROBES OF THE "SECOND HARMONIC" TYPE

V. N. Mikhailovskii and Iu. I. Spektor

(L'vov)

The operation of magnetic amplifiers and magneto-modulation probes of the second-harmonic type is considered at no load when excited by sinusoidal current, with allowance for the magnetizing losses and eddy current.

It is shown that the presence of losses causes the phase of the output voltage to depend on the phase of measured magnetic field.

At the present time, very weak dc currents and dc magnetic fields are extensively measured with the aid of "second-harmonic" magnetic amplifiers.

The Russian and foreign literatures contain a great number of articles devoted to the investigation of these devices [1-5]. However, in all the References known to us, the processes that take place in the magnetic amplifiers and in second-harmonic probes have been analyzed under the assumption of a magnetization curve without hysteresis. This assumption was used to derive the independence of the phase of the individual harmonic components of the output voltage on the intensity of the measured magnetic field.

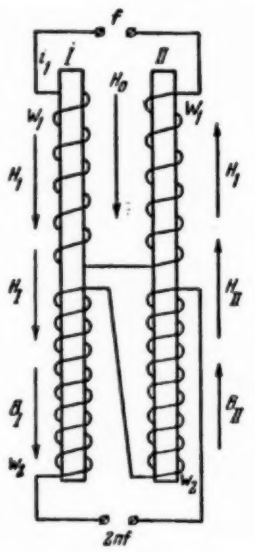

Fig. 1.

Actually, the presence of losses due to magnetization and eddy currents causes the individual harmonic components of the output voltage to have a phase dependence on the intensity of the measured field. This dependence assumes a substantial significance in many cases.

This article is an attempt to investigate analytically the transformation properties of the magnetic amplifiers and probes of the second harmonic type with allowance for the magnetization and eddy current losses.

Let us consider the widely used two-element magnetic amplifier (probe) with the excitation winding connected in series adding and the measuring winding connected in series bucking (Fig. 1).

We shall start with the following assumption;

1) The electromagnetic processes in the amplifier (probe) cores follow the limiting hysteresis-cycle loop.

2) The cores are excited by purely-sinusoidal current. The exciting coil produces an excitation field that is homogeneous over the length of the cores.

If the limiting hysteresis loop is piecewise-linearly approximated (Fig. 2), the voltage induced in the measuring winding can be represented at various instants of time by the following equation:

$$e = \begin{cases} -2\omega W_2 S \dfrac{dB_I(H_1)}{dt} 10^{-8} = -2\omega W_2 S H_{1m} \mu_0 10^{-8} \sin \omega t & \\ & \text{if} \quad \alpha_2 \geqslant \omega t \geqslant \alpha_1, \\ 0 & \text{if} \quad \alpha_3 \geqslant \omega t \geqslant \alpha_2, \\ -2\omega W_2 S \dfrac{dB_{II}(H_1)}{dt} 10^{-8} = -2\omega W_2 S H_{1m} \mu_0 10^{-8} \sin \omega t & \\ 0 & \text{if} \quad \alpha_4 \geqslant \omega t \geqslant \alpha_3, \\ & \text{if} \quad \alpha_1 + 2\pi \geqslant \omega t \geqslant \alpha_4, \end{cases} \tag{1}$$

where

$$\alpha_1 = \arccos \frac{H_s - H_c - H_0}{H_{1m}}, \qquad \alpha_2 = \arccos \frac{H_s + H_c - H_0}{H_{1m}},$$
$$\alpha_3 = \arccos \frac{H_s - H_c + H_0}{H_{1m}}, \qquad \alpha_4 = \arccos \frac{H_s + H_c + H_0}{H_{1m}}, \tag{2}$$

W_2 is the number of turns of the measuring winding, S is the area of the transverse cross-section of the core, H_1 and H_{1m} are the respective instantaneous and maximum values of the magnetic field intensity produced by the excitation current, and H_0 is the intensity of the measured external field or the intensity produced by the dc in the control winding of the magnetic amplifier.

In order to determine the spectral composition of the voltage in the measuring winding let us expand the functions (1) into a Fourier series

$$e_I = \sum_{n=1}^{\infty} (E_{na} \cos n\omega t + E_{nb} \sin n\omega t),$$

where

$$E_{na} = \frac{2}{\pi} \omega W_2 H_{1m} S \mu_0 10^{-8} \left[\int_{\alpha_1}^{\alpha_2} \sin \omega t \cos n\omega t \, d\omega t + \int_{\alpha_3}^{\alpha_4} \sin \omega t \cos n\omega t \, d\omega t \right],$$

$$E_{nb} = \frac{2}{\pi} \omega W_2 H_{1m} S \mu_0 10^{-8} \left[\int_{\alpha_1}^{\alpha_2} \sin \omega t \sin n\omega t \, d\omega t + \int_{\alpha_3}^{\alpha_4} \sin \omega t \sin n\omega t \, d\omega t \right].$$

Upon integration [6], the last expressions can be represented as

$$E_{na} = -\frac{2}{\pi} \omega W_2 H_{1m} S \mu_0 10^{-8} \left[\frac{\cos(1-n)\omega t}{2(1-n)} \Big|_{\alpha_1}^{\alpha_2} + \frac{\cos(1+n)\omega t}{2(1+n)} \Big|_{\alpha_1}^{\alpha_2} + \right.$$
$$\left. + \frac{\cos(1-n)\omega t}{2(1-n)} \Big|_{\alpha_3}^{\alpha_4} + \frac{\cos(1+n)\omega t}{2(1+n)} \Big|_{\alpha_3}^{\alpha_4} \right],$$

$$E_{nb} = \frac{2}{\pi}\omega W_2 H_{1m} S \mu_0 10^{-8}\left[\frac{\sin(1-n)\omega t}{2(1-n)}\Bigg|_{\alpha_1}^{\alpha_2} - \frac{\sin(1+n)}{2(1+n)}\Bigg|_{\alpha_1}^{\alpha_2} + \right.$$

$$\left. + \frac{\sin(1-n)\omega t}{2(1-n)}\Bigg|_{\alpha_3}^{\alpha_4} - \frac{\sin(1-n)\omega t}{2(1+n)}\Bigg|_{\alpha_3}^{\alpha_4}\right].$$

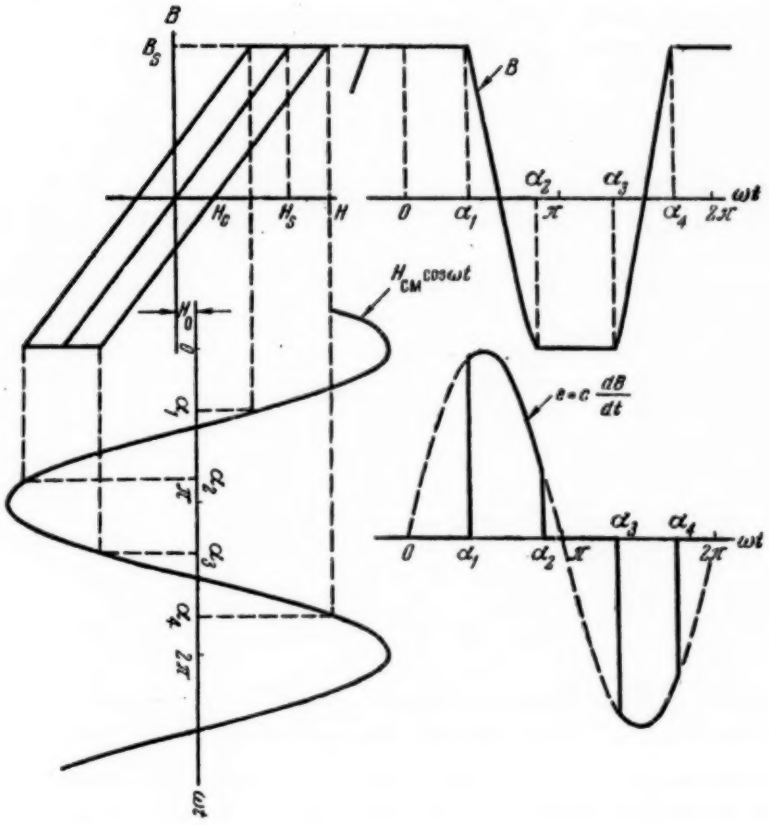

Fig. 2.

Inserting the integration limits and taking expression (2) into account, we get

$$E_{na} = \frac{2}{\pi}\omega W_2 H_{1m} S \mu_0 10^{-8}\left\{\frac{1}{2(1-n)}\left[\cos(1-n)\arccos\frac{H_s - H_c - H_0}{H_{1m}} - \right.\right.$$

$$- \cos(1-n)\arccos\frac{H_s + H_c + H_0}{H_{1m}} + \cos(1-n)\arccos\frac{H_s - H_c + H_0}{H_{1m}} -$$

$$\left. - \cos(1-n)\arccos\frac{H_s + H_c - H_0}{H_{1m}}\right] + \frac{1}{2(n+1)}\left[\cos(1+n)\arccos\frac{H_s - H_c - H_0}{H_{1m}} - \right.$$

$$- \cos(1+n)\arccos\frac{H_s + H_c + H_0}{H_{1m}} + \cos(1+n)\arccos\frac{H_s - H_c + H_0}{H_{1m}} -$$

$$\left.\left. - \cos(1+n)\arccos\frac{H_s + H_c - H_0}{H_{1m}}\right]\right\}, \qquad (3)$$

$$E_{nb} = -\frac{2}{\pi}\omega W_2 H_{1m} S\mu_0 10^{-8}\left\{\frac{1}{2(1-n)}\left[\sin(1-n)\arccos\frac{H_s - H_c - H_0}{H_{1m}} - \right.\right.$$

$$-\sin(1-n)\arccos\frac{H_s + H_c + H_0}{H_{1m}} + \sin(1-n)\arccos\frac{H_s - H_c + H_0}{H_{1m}} -$$

$$\left.-\sin(1-n)\arccos\frac{H_s + H_c - H_0}{H_{1m}}\right] - \frac{1}{2(1+n)}\left[\sin(1+n)\arccos\frac{H_s - H_c - H_0}{H_{1m}} - \right.$$

$$-\sin(1-n)(1+n)\arccos\frac{H_s + H_c + H_0}{H_{1m}} + \sin(1+n)\arccos\frac{H_s - H_c + H_0}{H_{1m}} -$$

$$\left.\left.-\sin(1+n)\arccos\frac{H_s + H_c - H_0}{H_{1m}}\right]\right\}. \qquad (4)$$

It follows from expressions (3) and (4) that the modulus and phase of the individual components of the measuring-winding voltage depend on the intensities of both the excitation field H_{1m} and of the measured field H_0. Most frequently one assumes the second harmonic of the voltage of the secondary winding to be the output quantity in devices of this type. For the second harmonic of the voltage (n = 2) expressions (3) and (4) become, after the obvious transformations

$$E_{2a} = \frac{32}{\pi}\omega W_2 H_{1m} S\mu_0 10^{-8}\frac{H_s H_c H_0}{H_{1m}^3}, \qquad (5)$$

$$E_{2b} = \frac{4}{3\pi}\omega W_2 H_{1m} S\mu_0 10^{-8}\left\{\left[1-\left(\frac{H_s + H_c + H_0}{H_{1m}}\right)^2\right]^{3/2} - \left[1-\left(\frac{H_s - H_c - H_0}{H_{1m}}\right)^2\right]^{3/2} + \right.$$

$$\left. + \left[1-\left(\frac{H_s - H_c + H_0}{H_{1m}}\right)^2\right]^{3/2} - \left[1-\left(\frac{H_s + H_c - H_0}{H_{1m}}\right)^2\right]^{3/2}\right\}. \qquad (6)$$

It should be noted that for a selected approximation of the hysteresis-cycle curve, the product $\mu_0 H_s H_c$ is proportional to the area of the loop, i.e., to the losses due to magnetization reversal and eddy currents.

Figures 3 and 4 show the dependence of the modulus and of the phase of the second harmonic of the voltage as a function of the ratio of the intensity of the measured field to the ratio of the excitation field, calculated from the following equations

$$E_2 = \sqrt{E_{2a}^2 + E_{2b}^2}, \qquad (7)$$

$$\tan\varphi = \frac{E_{2a}}{E_{2b}}, \qquad (8)$$

where E_{2a} and E_{2b} are respectively the amplitude of the cosine and sine components of the vector of the second harmonic voltage, calculated from Equations (5) and (6).

Let us establish the limits to which E_2/H_0 and $\tan\varphi$ tend as H_0 approaches zero.

Expanding (6) into a Taylor series in powers of H_0/H_{1m}, neglecting H_c compared with H_s, and putting $H_0 \to 0$, we obtain

$$\lim_{H_0\to 0} E_2/H_0 = \frac{8}{\pi} W_2\omega S\mu_0 10^{-8}\frac{H_s}{H_{1m}}\sqrt{1-\left(\frac{H_s}{H_{1m}}\right)^2}, \qquad (9)$$

$$\lim_{H_0\to 0} \operatorname{tg}\varphi = 4\frac{H_c}{H_{1m}}\cdot\frac{1}{\sqrt{1-\left(\frac{H_s}{H_{1m}}\right)^2}} = \operatorname{tg}\varphi_0. \qquad (10)$$

Figure 5 shows the dependence of $e_{20} = \frac{E_2}{\frac{8}{\pi} W_2 \omega S \mu_0 H_0 10^{-8}}$ and $\tan \varphi_0$ on the amplitude of the exciting-field intensity for various values of H_c/H_{1m}.

Experimental Verification

To verify the above analytical results experimentally, we assembled a special experimental set-up, the block diagram of which is shown in Fig. 6. The symbols on Fig. 6 are: AG – type ZG-10 audio generator for the exciting current; T_{p1} – symmetrical output transformer for the generator; PS – phase shifting network insuring a smooth variation of the phase of the generator voltage; PA – power amplifier, employing 6P6 tubes in push pull; T_{p_2} and T_{p_3} – matching transformers; R_4 = 10,000 ohms – active resistance, maintaining the specified current in the exciting circuit of the probe; V_1 – type LV-9, vacuum tube voltmeter serving to monitor the excitation current; SA – selective amplifier for 1,000 cycles with calibrated gain, with an attenuation on the order of 60 db at 500 and 1500 cycles; BA – broadband voltage amplifier; PD – phase-sensitive detector, employing type DG-Ts6 Germanium diodes; R_5 – zero-setting potentiometer for the phase-sensitive detector; R_7 – regulator of sensitivity in the rectified-current circuit of the phase-sensitive detector; R_8 and R_9 – regulating rheostat; R_{10} = 10,000 ohms – active resistance in the magnetizing-current circuit.

The material of the probe cores, with which the experiments were carried out, was molybdenum permalloy type 79 NM4, subjected to optimum heat treatment in a hydrogen medium. The core dimensions of the probe $l \times d \times \delta$ = 75 × 1.5 × 0.1 mm. The probe excitation winding (w_1 = 2 × 3300 turns PEL wire with d = = 0.13 mm) were uniformly distributed over the entire length of the cores; the measuring winding (w_2 = 2500 turns PEL, d = 0.10 mm) was concentrated at the center of the cores over a length of 10 mm.

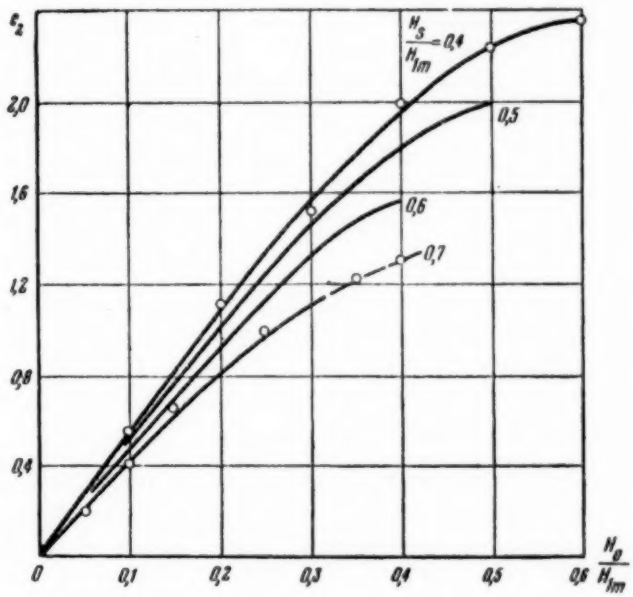

Fig. 3.

As can be seen from the diagram in Fig. 6, the magneto-modulation probe was connected to the exciting-current generator through a power amplifier, whose grid circuit contained two phase-shifting networks. The first of these networks, comprising the symmetrical output transformer of the generator, resistance R_1, and capacitance C_1, made it possible to change smoothly the phase of the output voltage of the generator over a wide range; the second made it possible to change the phase of the exciting voltage in steps of ± 22.5°, corresponding to a ± 45° change in phase of the second harmonic at the output of the probe produced by a constant field.

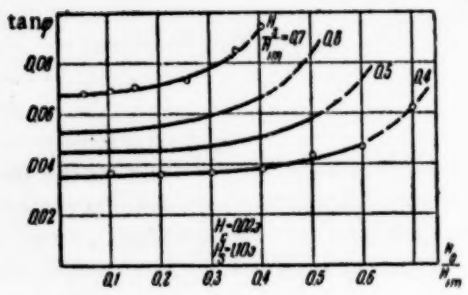

Fig. 4.

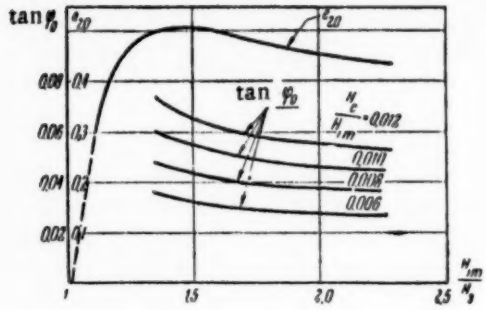

Fig. 5.

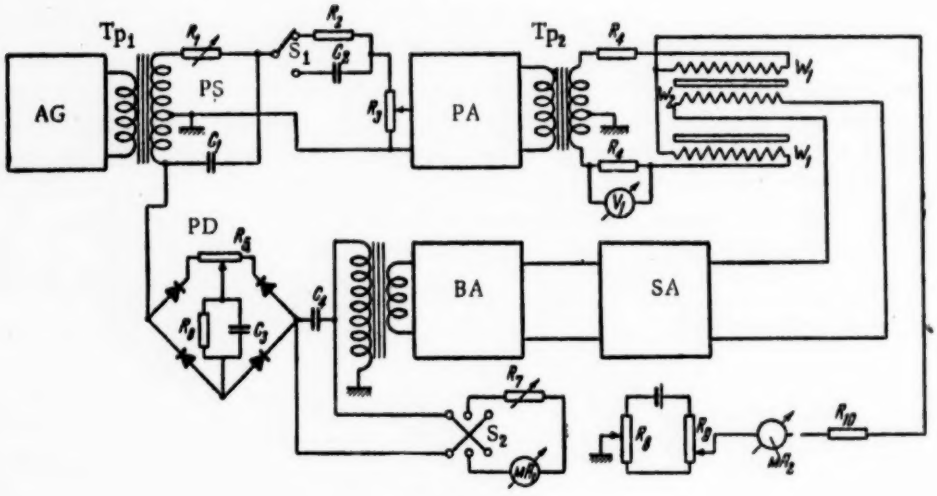

Fig. 6.

The second harmonic at the output voltage of the probe, filtered and amplified by the selective and the broadband voltage amplifiers, was applied through matching transformer T_{p3} to the input of the phase-sensitive detector. The control voltage was applied to the phase-sensitive detector directly from the output transformer of the generator. As can be seen from the connection diagram of the diodes, the phase-sensitive detector employed rectified only the even harmonics.

By virtue of the fact that during the measurement process the control voltage of the phase-sensitive detector remained constant in modulus and in phase, the readings of the output instrument of the phase-sensitive detector were proportional to the product of the modulus of the output voltage of the second harmonic of the probe by the cosine of the angle between the control and measured voltages. Shifting the measured voltage by ± 45°, one could measure the projection of its vector in a certain Cartesian coordinate system, the orientation of which relative to the control-voltage vector was determined by the parameters of the phase-shifting network. The projections of the vector were used to calculate its modulus and phase.

The experimentally-obtained values of the modulus and phase of the output voltage of the second harmonic as a function of the ratio of the magnetizing current to the amplitude of the excitation current for values $H_s/H_{1m} = 0.4$ and 0.7 are indicated by circles on the corresponding curves of Figs. 3 and 4. The agreement between the calculated and experimental data is better.

The above analytically-derived experimentally-confirmed results throw light on certain phenomena observed in the operation of magnetometric devices, in which magneto-modulation probes operating on the second harmonic are used. Thus, for example, it is known that in the measurement of the increments of the intensity

of a homogeneous magnetic field and in the compensation of its initial (basic) value by an inhomogeneous field (usually produced by a permanent magnet), the second-harmonic voltage, changing its phase by 180°, does not pass through zero. Felch and Potter, who investigated the influence of several factors on the value of this residual voltage (quadrature component) of second harmonic, indicate in Ref. [5] that the character of the causes leading to the appearance of the quadrature components under the action of fields of various waveforms on the probe is still unknown. However, starting with the argument given above, the observed phenomena can be explained. If the distance from the center of the magnet to the center of the probe is small, the intensity of the magnetic field produced by the magnet is sharply inhomogeneous over the length of the probe: in the parts of the probe close to the magnet, the field produced by the magnet may exceed by several times the compensating field, and to the contrary, in those parts of the probe that are remote from the magnet, the field compensated will exceed the field of the magnet. Let us represent such a probe in the form of n elementary probes each with a length $l' = l/q$, where l is the length of the real probe, and q is the number of elementary probes, with q being so large that the field can be assumed homogeneous over the length of each elementary probe. In this case the above conclusions concerning the operation of the probe are applicable to each of the elementary probes, with allowance for the losses due to magnetization reversal and eddy currents.

With this, the voltage induced in the measuring winding of each of the elementary probes will consist of two components

$$e_{ia} = f_1(H_i - H_0) \text{ and } e_{ib} = f_2(H_i - H_0),$$

where H_0 is the compensated homogeneous magnetic field, and H_i is the intensity produced by the compensating magnet in the i'th elementary probe.

The voltage averaged over the length of the actual probe is

$$E_a = \frac{1}{l}\int_0^l f_1(H_i - H_0)\,dl, \quad E_b = \frac{1}{l}\int_0^l f_2(H_i - H_0)\,dl.$$

Complete compensation takes place only if E_a and E_b are simultaneously zero.

In view of the different character of the functions f_1 and f_2, it is impossible to satisfy these two conditions simultaneously by changing only a single parameter, for example, the distance between the magnet and the probe, or by changing only the magnetic moment. In view of the above argument, to obtain complete compensation for the homogeneous magnetic field by means of an inhomogeneous one, the magnet-probe system must have two degrees of freedom.

Received October 24, 1956

LITERATURE CITED

[1] G. R. Gertsenberg and L. S. Gol'dfarb, "Determination of the Voltage and Current Harmonics in Electric Circuits Containing Iron." Elektrichestvo, 1939.

[2] J. A. Krumhause and R. T. Beger, Berkhausen Noise and Magnetic Amplifier. J. Appl. Phys., Vol. 20, May, 1949.

[3] F. C. Williams, The Fundamental Limitation of the secondharmonic Type of Magnetic Modulator. Proc. Inst. El. Engs., part II, Vol. 97, Aug. 1950.

[4] Rudolf Kühne, Magnetfeldmessung mit Eisenkern – Magnetometer nach dem Obverfahnen. ATM, Bd. 392–1, Aug. 1952.

[5] E. P. Felch and J. L. Potter, Preliminary Development of a Magnettor Current Standard. Trans. AIEE, part I, Vol. 72, 1953.

[6] I. M. Rizhik and I. S. Gradshtein, Tables of Integrals, Sums, and Products. Gostekhizdat, 1951.

CHOICE OF MODE AND CALCULATION OF ELECTRONIC VOLTAGE STABILIZER

L. I. Baida and V. K. Zakharov

(Leningrad)

Electronic voltage stabilizers of the compensation type are considered.

An engineering procedure is proposed for the design of the above stabilizers and for the selection of their principal components.

By way of illustration, the circuits and parameters of two types of developed and built voltage stabilizers are described.

To maintain constant a voltage across a certain load as the power supply voltage fluctuates about its nominal value, or as the load resistance varies, is a problem frequently encountered in the use of apparatus for automatic control, regulation, and electric measurements.

The supply voltage usually fluctuates over a range of ± (10-15)%, and the load resistance may vary from 0 to its maximum value. The load voltage must frequently stay constant with an accuracy to hundredths or thousandths of a percent.

To realize such a high degree of stabilization one employs at the present time, almost exclusively, electronic voltage stabilizers.

The stabilizers most frequently employed in practice are those of the compensation type, incorporating a dc amplifier with deep negative feedback.

The block diagram of such a stabilizer is shown in Fig. 1, where 1 is the power element, with which the output voltage is regulated, 2 is the auxiliary dc amplifier in the feedback loop, 3 is the detecting or sensitive element, containing a standard-voltage source.

The coefficients K_{t_1}, K_{t_1}, K_{t_2}, K_{t_3} denote respectively the dc transfer coefficients of the stabilizer elements. Here K_{t1} represents the transfer coefficient of the power element in response to a change in the voltage applied to it through the feedback loop, and K'_{t1} is a transfer coefficient of the same power element in response to changes in the input voltage.

The operating quality of the stabilizer is usually judged from the accuracy at which the output voltage V_{out} is maintained constant about a specified nominal value. This accuracy is determined by the maximum value of the relative instability of the output voltage [1].

$$\sum_{out} = \frac{1}{M_{ir}} \frac{\Delta V_{in}}{V_{in}} + r \frac{\Delta I_{out}}{V_{out}} + \frac{\delta_0}{V_{out}}. \qquad (1)$$

Here $M_{ir} = (V_{out}/V_{in})(\Delta V_{in}/\Delta V_{out})$ is the relative stabilization coefficient, $r = \Delta V_{out}/\Delta I_{out}$ is the internal or dynamic resistance of the stabilizer, δ_0 is the slip or "drift" of the null during a specified time interval.

The coefficient δ_0 determines the deviation of the output voltage from the nominal value owing to changes in the parameters of the components of the circuit (tubes, resistances, etc.) while the input voltage and load resistance remain constant.

If the stabilizer is intended to supply automatized devices, operating for a prolonged time without human supervision, the relative instability of the output voltage depends very strongly on the null drift, and to reduce the influence of the latter it becomes necessary to employ special stabilization circuits, which will not be considered in this article.

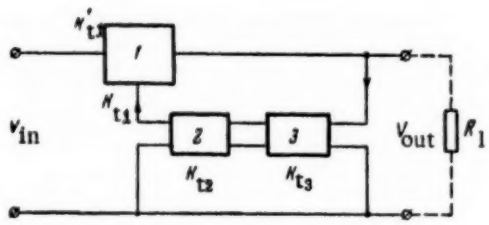

Fig. 1.

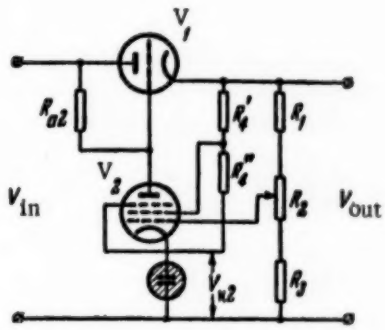

Fig. 2.

In many cases, when the stabilizer is used for measurements or investigations with participation of service personnel, the null drift can be compensated for by periodic adjustment of the output voltage. Here the quality of the stabilizer will be determined principally by the stabilization coefficient and by the internal resistance. The basis of these parameters is the stabilization coefficient, since the internal resistance depends on the stabilization coefficient and diminishes as the latter increases.

The stabilization coefficient is determined in turn by the dc transfer coefficients of the individual stabilizer elements

$$M_{ir} = \frac{V_{out}}{V_{in}} \frac{1 + K_{t1} K_{t2} K_{t3}}{K'_{t1}} . \qquad (2)$$

The internal resistance is

$$r = \frac{V_{out}}{V_{in}} \frac{R_{i_1}}{M_{ir}} , \qquad (3)$$

where R_{i_1} is the internal (dynamic) resistance of the power element.

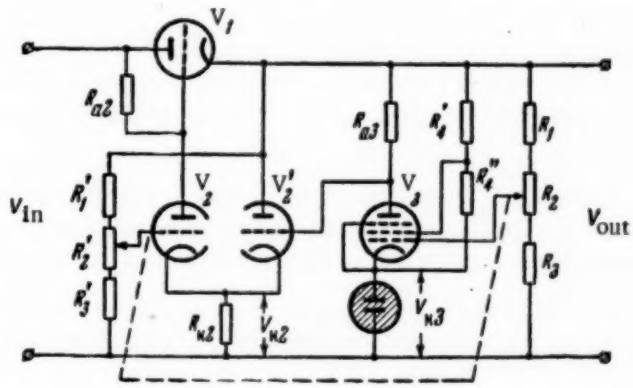

Fig. 3.

Depending on the required stabilization coefficient, one can employ one of the principal circuits (Figs. 2, 3, and 4).

The fundamental difference between these circuits lies in the realization of the auxiliary dc amplifier in the negative feedback circuit.

In the circuit of Fig. 2 a single-stage pentode amplifier is used. Here the attainable stabilization coefficient M_{ir} can range from 100 to 500 and the internal resistance $\underline{r}$ is on the order of several ohms.

A two stage amplifier is employed in the circuit of Fig. 3. The first stage employs a pentode (tube V_3) and the second a triode (tube V_2). The cathode follower (tube V'_2) insures the right relationships between the signs of the input and output voltages of the amplifier without reducing the load resistance of the first stage. In addition, the rise in the cathode-follower current compensates the feedback from the resistance R_{k_2} in the circuit of the second stage and increases correspondingly the gain of the latter by a considerable amount.

Circuits of this type produce a stabilization coefficient on the order of 500-5,000 with an internal resistance on the order of tenths or hundredths of an ohm.

The principal causes of the deviations of the input voltage from the nominal value in these circuits are the fluctuations of the filament voltage of the pentodes and the fact that the voltage across the stabilizing tube is not constant, owing to the instability of its parameters.

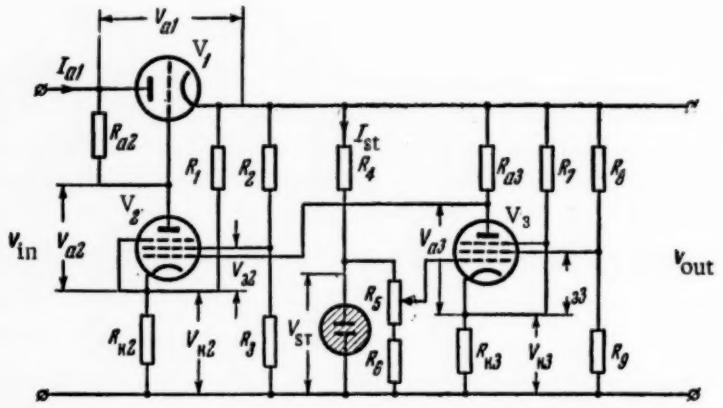

Fig. 4.

The circuit of Fig. 4 contains a two-stage pentode amplifier with cathode coupling. In spite of the fact that the gain of each stage is reduced considerably by the current feedback through the cathode resistances, it is possible to obtain with this circuit quite considerable stabilization coefficients, ranging from 2,000 to 10,000 and above, and very small internal resistances on the order of hundredths of an ohm and less.

Such results can be obtained only provided the filament supply of the amplifier tubes is well stabilized (usually, by employing for this purpose the output voltage of the stabilizer) and provided one hand picks a stabilizing tube with small drift or one replaces the stabilizer tube with a dry battery. In the latter case the accuracy with which the voltage is maintained at the output of the stabilizer will be almost the same as that of a battery operating practically under self-discharge conditions.

One must bear in mind that in the circuits shown in Figs. 3 and 4 it is necessary to shield thoroughly the input circuits against the influence of external interference, and that the resistors of the voltage divider in the sensitive element must be chosen to have high stability (it is desirable to employ wire-wound resistors).

When practical electronic stabilizers are built in accordance with the above or similar circuits, the operating conditions for the fundamental elements of the stabilizer are usually chosen by methods that give rather approximate results.

The final selection of the operating mode and the determination of the working parameters is carried out through an experimental investigation of a finished model or breadboard; this frequently leads to an insufficient utilization of the capabilities of the individual units and correspondingly of the entire circuit as a whole. We give below a design procedure, which permits the choice of sufficiently rational operating conditions for the principal elements of the device and permits computation of the stabilizer parameters corresponding to these conditions. This simplifies substantially the experimental tests and the alignment of the finished instruments.

The circuit elements are designed in the following sequence: a) power elements, b) auxiliary amplifier, and c) sensitive element.

The operating conditions of the power tubes in a stabilizer circuit differ from the operating conditions of analogous tubes in an ordinary power amplifier, where plate-current changes due to changes in the grid voltage are always accompanied by corresponding changes in the plate voltage. The load resistance and the supply voltage remain constant, and the position of the operating point for specified value of grid voltage are determined uniquely by the dynamic characteristic $I_a = (V_0 - V_a)/R_a$ and by the family of the static anode tube characteristics.

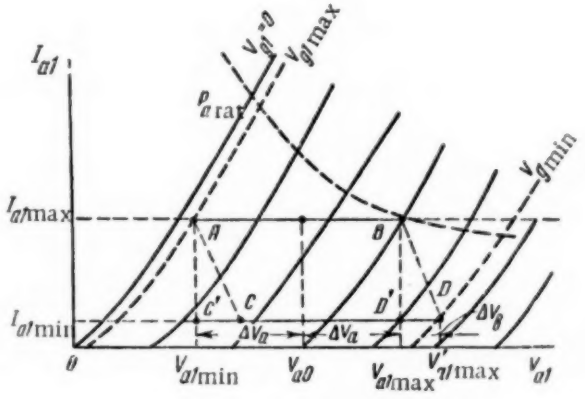

Fig. 5.

In a stabilizer circuit, the grid voltage of the power-element tube is not an independent variable, but depends on changes in the supply (input) voltage and the load resistance. If only the input voltage changes in this case, the plate voltage of the power tubes also changes while the plate current remains constant. On the other hand, if only the load resistance varies, the plate current varies, and the tube plate voltage remains constant.

Thus, the geometric locus of the points whose coordinates determine the operating conditions of the tube during the stabilization process, i.e., the dynamic characteristic of the power element of the stabilizer, is a certain region ABDC (Fig. 5), which should contain the operating point for arbitrary changes in the input voltage and load resistance, not exceeding certain limits.

The initial data for the design of the power element are:

1) nominal value of the output voltage $V_{out\,nom}$;

2) the limits of the necessary regulation of the output voltage $\pm \Delta V_{out\,nom}$;

3) maximum and minimum values of the load current $I_{l\max}$ and $I_{l\min}$;

4) relative changes in the supply voltage (usually the ac line) $\pm \Delta V_{sup}/V_{sup} = \pm \Delta V_{in}/V_{in}$, where V_{in} is the dc voltage at the input of the stabilizer (output voltage of the rectifier in the stabilizer circuit).

The power tubes usually employed in electronic stabilizers are either power triodes of the 6S4 or 6N5 type, or else the triode-connected pentodes and beam-power tetrodes GU-50, 6P3, 6P6, 6P1P.

To determine the suitability of any one tube it is obviously necessary to determine their most difficult operating conditions.

Difficult conditions for a voltage stabilizer are the following:

I. When the input voltage V_{in} is a minimum and load current I_l is a maximum. In this case the tube grid voltage must not exceed the zero value ($V_{g1\max} \leq 0$);

II. When the input voltage is a maximum, and the load current is a maximum.

•English equivalents of Russian tubes: 6S4 ≡ 6B4; 6S45 ≡ 6B4-G; 6P1P ≡ 6AQ5.

Here the power dissipated by the tube plate must be exceed the permissible (rated) value ($P_{a1\ max} \leq P_{a\ rat}$).

In the graph of Fig. 5 the line parallel to the abscissa corresponds to the maximum current through the tube

$$I_{a1\ max} = I_{l\ max} + I_{st} \tag{4}$$

Here I_{st} is the total current consumed by the circuit elements, usually 15-20 ma.

The point A of the dynamic characteristic, corresponding to mode I, is chosen so as to avoid the flow of grid current when the grid voltage is $V_{g1\ max} = -(2\text{-}4)$ volts.

The projection of point A on the horizontal axis gives the minimum tube voltage $V_{a1\ min}$.

The maximum permissible tube voltage at a current $I_{a1\ max}$ is determined from

$$V_{a1\ max} = \frac{P_{a1\ rat}}{I_{a1\ max}}. \tag{5}$$

Point B of the dynamic characteristic corresponds to this voltage, and consequently also to mode II.

The value of the stabilizer input voltage, i.e., the voltage for which the rectifier should be calculated, is

$$V_{in} = \frac{V_{a1\ max} + V_{a1\ min}}{2} + V_{out\ nom} \tag{6}$$

The increment of the input voltage is

$$\Delta V_{in} = V_{in} \frac{\Delta V_{sup}}{V_{sup}}. \tag{7}$$

The increment of the tube voltage above nominal is

$$\Delta V_{a1} = \frac{V_{a1\ max} - V_{a1\ min}}{2}. \tag{8}$$

To insure normal operation of the stabilizer, one must satisfy the condition

$$\Delta V_{a1} \geqslant \Delta V_{in} + \Delta V_{out\ min}. \tag{9}$$

If this condition is not satisfied, one must either choose another type of tube, or else connect several tubes in parallel. In the latter case the calculations are carried out with the same method, taking into account the fact that

$$I_{a1\ max} = \frac{I_{l\ max} + I_{st}}{n}, \tag{10}$$

where n is the number of tubes connected in parallel.

In view of the fact that the requirement indicated above can be satisfied for various types of tubes, the final choice must be carried out on the basis of the minimum number of envelopes and minimum losses in the tubes of the power element.

The minimum voltage on the tube grids, $V_{g\ min}$, corresponds to the point D of the dynamic characteristic with the following coordinates

$$I_{a1\,min} = I_{1\cdot min} + I_{st} \tag{11}$$

$$V'_{a1\,max} = V_{a1\,max} + \Delta V_r \tag{12}$$

where $\Delta U_r = (I_{a1\,max} - I_{a1\,min})\, r_r$ is the increment in rectifier voltage corresponding to the total variation of the load current.

The internal resistance r_r of the rectifier can be assumed to be approximately 500—150 ohms for Kenotron rectifiers rated 50-300 watts.

Let us consider the design of the amplifier in the feedback loop. Since the stabilization coefficient increases with the gain of the amplifier, it is necessary to employ pentodes and high-μ triodes in the amplifier. The problem in the design is to determine the maximum and minimum voltages on the amplifier-tube plates, the voltages on the screen grids, the compensating voltages V_c and the resistances in all the circuit elements.

For tube V_2 (Figs. 2-4) the following relationships hold

$$V_{a2\,max} \geqslant V_{out\,nom} + \Delta V_{out\,nom} - V_{a2} - |V_{g1\,max}|, \tag{13}$$

$$V_{a2\,min} \leqslant V_{out\,nom} - \Delta V_{out\,nom} - V_{a2} - |V_{g1\,min}|. \tag{14}$$

If pentodes are used, the value of $V_{a2\,min}$ is determined by the start of the linear portions of the plate characteristics for rated value of screen-grid voltage (Fig. 6).

In the case of triodes, owing to the absence of a sharply pronounced boundary between the linear and nonlinear portions of the characteristics, the recommended voltage $V_{a2\,min}$ is 10-30 volts.

Knowing the value of $V_{a2\,min}$ we obtain from Equation (14) the maximum permissible value of V_{k2}

$$V_{k2} \leqslant V_{out\,nom} - \Delta V_{out\,nom} - |V_{g1\,min}| - V_{a2\,min} \tag{15}$$

Substituting the values of V_{k2} in Expression (13) we obtain $V_{a2\,max}$.

The nominal value of the tube plate voltage is obtained from

$$V_{a02} = \frac{V_{a2\,max} + V_{a2\,min}}{2}. \tag{16}$$

To obtain a high gain in the amplifier stage it is necessary to employ the so-called "starved mode" [2]. In this mode the tube operates at very small currents (on the order of microamperes) and very high resistances in the plate circuit. The gain of the stage can approach in this case the static amplification factor of the tube.

It should be noted that operation in the starved mode is of practical interest only if pentodes are used. For triode amplifier stages, the use of this mode does not insure a considerable increase in gain, and consequently is not very effective.

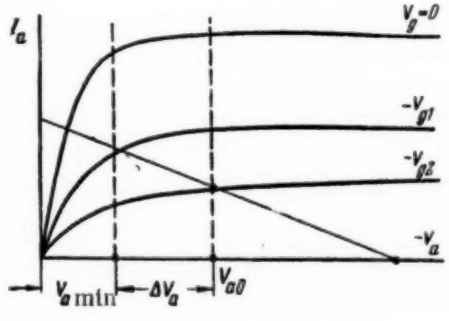

Fig. 6. Graph for determining $V_{a.\,min}$ of a pentode.

As is known, in pentode amplifier stages one frequently has $R_a \ll R_1$. This condition holds also in the starved mode, for at low plate currents the internal resistance of the tube is many times the rated value. The gain of the stage containing tube V_2 then becomes

$$K_2 \approx S_2 R_{a2}, \tag{17}$$

where S_2 is the static transconductance of the tube at the operating point.

The load resistance R_{a2} can be determined from

$$R_{a2} = \frac{V_{in} - V_{a02}}{I_{a02}}. \tag{18}$$

Substituting the right half of (18) into (17) we get

$$K_2 \approx \frac{S_2}{I_{ao2}} (V_{in} - V_{ao2}). \tag{19}$$

For the chosen voltages V_{in} and V_{ao2}, the maximum of K_2 is determined by the maximum value of the ratio S_2/I_{ao2}.

Curves showing the dependence $S/I_{ao} = f(I_{ao})$ for various screen grid voltages V_{sg}, plotted experimentally for tubes 6Zh3*, 6Zh4, 6Zh8, and 12Zh1L at V_a = 100 v are given in Fig. 7.

Curves 1, 2, and 3 were obtained for screen grid voltages V_{sg} of 12, 20, and 50 volts respectively.

As can be seen from the graph, it is possible to increase the gain further by reducing the screen grid voltage below the rated value.

However, the screen grid voltage can be reduced only to a certain limit. Since reducing the screen grid voltage involves the need for increasing the control-grid voltage, the effect obtained depends on the maximum voltage that can be applied to the latter and still produce no grid current. For most receiving and amplifying tubes this voltage is $-(0.5\text{-}1)$ v.

The limits of the variation of control grid voltage V_g for the extreme values of the plate current I_{ao} are shown on the graph for each of the characteristics.

One must bear in mind that the quantities I_{ao} and $V_{sg\,min}$ are practically independent of the plate voltage of the tube.

After the current I_{ao} is determined from the graph of Fig. 7 for the maximum ratio S/I_{ao}, we obtain from Expressions (17) and (18) the load resistance and the gain of the stage with tube V_2.

The resistances R_1 and R_{k2} are chosen on the basis of the following considerations. The presence of resistance in the tube cathode circuit produces negative current feedback and a considerable reduction in the gain of the stage. In the dynamic mode, the equivalent resistance of R_1 and R_{k2} in parallel is connected in the cathode circuit of the tube. The gain of the stage, with allowance for the feedback, will now be

$$K_2' = \frac{K_2}{1 + K_2 \frac{R'_{k2}}{R_{a2}}}, \tag{20}$$

where

$$R'_{k2} = \frac{R_{k2} R_1}{R_{k2} + R_1}.$$

Since $K_2 \gg 1$, it is obvious that the ratio R'_{k2}/R_a and correspondingly the resistance R'_{k2} for a previously obtained value of R_{a2} should be chosen as small as possible. However, if R'_{k2} is low, the current flowing in the divider circuit will be quite large, $I_{k2} \approx V_{k2}/R_{k2}$. It is usually desirable to keep the value of this current below 2-5% of the load current. Choosing the resistance R_{k2} to satisfy this condition, we obtain

$$R_1 = \frac{V_{out\,nom} - \Delta V_{out\,nom} - V_{k2}}{V_{k2}} R_{k2}. \tag{21}$$

With such a choice of resistances R_{k2} and R_1, the gain is nevertheless reduced by several times.

The effect of feedback can be reduced considerably by connecting a voltage-regulator tube instead of R_{k2}, since the dynamic resistance of the voltage-regulator is small compared with its static resistance. The reduction in the gain may turn out to be only a few percent in this case.

*[English equivalents of Russian tubes: 6Zh3 ≡ 6SH7; 6Zh4 ≡ 6AC7; 12Zh1L – not identifiable – Ed.]

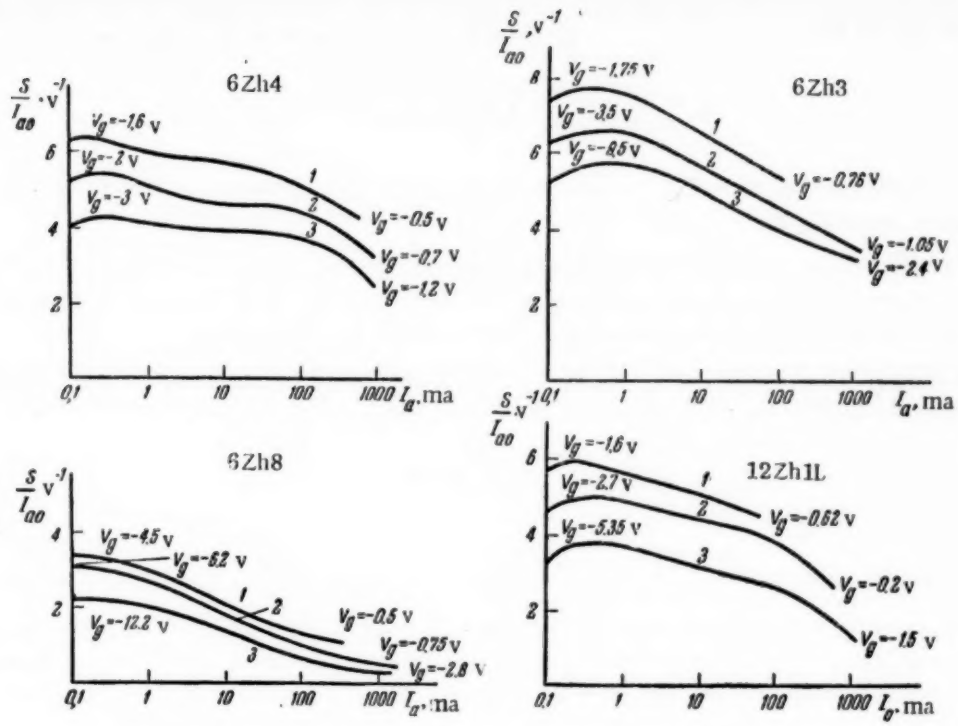

Fig. 7.

Resistances R_2 and R_3 are determined from the relationship

$$\frac{R_2}{R_2 + R_3} \approx \frac{V_{\text{out nom}}}{V_{sg2} + V_{n2}} . \tag{22}$$

Now the summary value of these resistances is chosen to make the current through the voltage divider considerably greater than the screen grid current, in order to reduce the effect of current fluctuations in the screen grid circuit on the operation of the tube. For the modes considered above, this current may be assumed to be 2-3 ma.

The minimum plate voltage of tube V_3 is determined by

$$V_{a3\min} \approx V_{n2} - V_{n3}, \tag{23}$$

hence

$$V_{n3} \approx V_{n2} - V_{a3\min} \tag{24}$$

The value of $V_{a3\ min}$ should be as low as possible, so as to increase the load resistances R_{a3} and correspondingly the gain of the stage. The value of this voltage can be obtained from the family of plate characteristics in the same manner as was done for tube V_2.

On the other hand, the voltage V_{k3} can be given by the following relation

$$V_{n3} \approx V_{st} - 2\Delta V_{\text{out nom}} \frac{V_{st}}{V_{\text{out nom}}} . \tag{25}$$

Equating the right halves of Expressions (24) and (25) and solving the resultant equation for the voltage stabilizer voltage V_{st}, we get

$$V_{st} = \frac{V_{out\,nom}(V_{k2} - V_{a3min})}{V_{out\,nom} - 2\Delta V_{out\,nom}}. \tag{26}$$

The voltage stabilizer is so chosen as to make the rated value of its operating voltage equal or less than the voltage obtained with Eq. (26).

If there is a difference between the computed and rated voltage-stabilizer tube voltages, it is necessary to reduce V_{k2} or to increase $V_{a3\,min}$ by an amount equal to this difference. From the point of view of obtaining a higher gain in the auxiliary amplifier, it is better to reduce the voltage V_{k2}.

The calculation of resistances R_{a3}, R'_{k3}, R_7, R_8, R_9 and the gain coefficients K_3 and K'_3 are calculated in analogy by the methods used for the preceding stage, from the following equations

$$R_{a3} \approx \frac{V_{out} - \Delta V_{out} - V_{k3\,min}}{I_{a03}} \tag{27}$$

$$K'_3 = \frac{K_3}{1 + K_3 \frac{R'_{k3}}{R_{a3}}}, \tag{28}$$

$$R'_{k3} = \frac{R_{k3} R_7}{R_{k3} + R_7}, \tag{29}$$

$$K_3 \approx \frac{S_3}{I_{a03}} (V_{out\,nom} - \Delta V_{out\,nom} - V_{a3min}). \tag{30}$$

$$R_7 \approx \frac{V_{out\,nom} + \Delta V_{out\,nom} - V_{st}}{V_{st}} R_{k3}, \tag{31}$$

$$\frac{R_8}{R_8 + R_9} \approx \frac{V_{out\,nom}}{V_{sg3} + V_{k3}}. \tag{32}$$

Resistance R_4 is determined from the expression

$$R_4 = \frac{V_{out\,nom} - \Delta V_{out\,nom} - V_{st}}{I_{st\,min}}. \tag{33}$$

The current $I_{st.\,min}$ should be assumed 5-10 ma for standard Russian voltage regulator tubes.

Resistances R_5 and R_6 comprise a high-resistance divider for regulation of the nominal value of the output voltage of the stabilizer. The total value of these resistances $R_5 + R_6$ is chosen to be on the order of hundreds of kilohms.

Since the nominal value of the output voltage corresponds to the center position of the slider on resistance R_5, the following equation will obviously hold

$$\frac{\frac{R_5}{2}}{\frac{R_5}{2} + R_6} = \frac{\Delta V_{out\,nom}}{V_{out\,nom}}, \tag{34}$$

hence

$$\frac{R_5}{R_5 + R_6} = \frac{2\Delta V_{out\,nom}}{V_{out\,nom} + \Delta V_{out\,nom}}. \tag{35}$$

The relative stabilization coefficient is determined on the basis of Expression (2) by substituting the corresponding values of the transfer coefficient. In this case one can neglect unity compared with second term of the numerator in the right half of Expression (2), and put

$$M_{ir} \approx \frac{V_{out}}{V_{in}} \frac{K_{t1}K_{t2}K_{t3}}{K'_{t1}}. \tag{36}$$

For the circuits of Figs. 2-4, the ratio K_{t1}/K'_{t1} is

$$\frac{K_{t1}}{K'_{t1}} = \frac{\mu_1}{1 + m\mu_1}. \tag{37}$$

The coefficient m takes into account the oscillations of the plate voltage of tube V_2 and of the corresponding oscillations of the grid voltage of tube V_1, due to the direct effect of the change in the input voltage:

$$m = \frac{R_{i2} + \mu_2 R'_{k2}}{R_{a2} + R_{i2} + \mu_2 R'_{k2}}. \tag{38}$$

If tube V_2 is a pentode (Figs. 2 and 4) we have $R_{i2} + \mu_2 R'_{k2} \gg R_{a2}$, and consequently $m \approx 1$.

In some circuits the plate circuit of the amplifying stage with tube V_2 is fed from the output voltage of the stabilizer (Fig. 8). In this case the supply voltage to V_2 remains practically constant, the coefficient m becomes equal to zero, and the ratio K_{t1}/K'_{t1} rises to a value μ_1. In this case, however, the resistance R_{a2} must be reduced considerably, which in turn leads to a considerable reduction in the gain of the amplifier and to a corresponding reduction in the stabilization coefficient. The result of connecting the plate circuit of tube V_2 in accordance with Fig. 8 is that the stabilization coefficient is usually lower than when the circuits of Figs. 2-4 are used.

The expression for the transfer coefficient K_{t2} for the circuit of Fig. 2 is of the form

$$K_{t2} = K_2, \tag{39}$$

and that for the circuit of Fig. 3

$$K_{t2} = K_2 K_{2cf} K_3, \tag{40}$$

where K_{2cf} is the gain of the cathode follower.

$$K_{2cf} = \frac{\mu_2 R_{k2}}{R_{i2} + (1 + \mu_2) R_{k2}}.$$

For the circuit of Fig. 4, the transfer coefficient will be

$$K_{t2} = K'_2 K'_3. \tag{41}$$

The transfer coefficient K_{t3} for all three circuits is given by the expression

$$K_{t3} \approx \frac{V_{k3}}{V_{out\,nom} + \Delta V_{out\,nom}}. \tag{42}$$

Equation (42) corresponds to the mode of maximum voltage at the stabilizer output and gives the minimum value of transfer coefficient, and consequently, of the stabilization coefficient. If the voltage at the output is nominal and lower, the values of the transfer coefficient K_{t2} and of the stabilization coefficient will be higher.

Were the input voltage of the stabilizer to remain constant upon change in the load current, its internal resistance could be determined from Equation (3), in which M_{ir} should be calculated by putting m = 0.

In practice, however, it is necessary to take into account the internal resistance of the rectifier, the presence of which leads to a change in the input voltage of the stabilizer whenever the load current changes. The expression for the internal resistance of the stabilizer now becomes

$$r = \frac{R_{i1} + r_r(1 + m\mu_1)}{\mu_1 K_{t1} K_{t2}}. \tag{43}$$

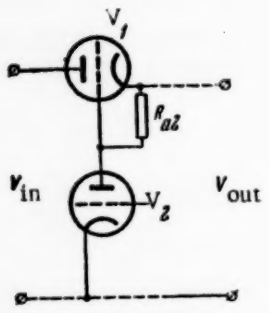

Fig. 8. Principal connection diagram for a second amplifier stage fed from an unstabilized voltage.

A procedure for the calculation of the stabilizer parameter was considered by us as applied to the circuit of Fig. 4. The calculations for the circuits shown in Figs. 2 and 3 are fundamentally the same, since all the circuits contain elements of the same type.

The choice of the type and operating conditions for tube V_2 in the last two circuits remains unchanged. For this purpose, one determines the value of V_{k2} from Equation (15) for the circuit of Fig. 2, after which the type of regulator tube is so chosen that $V_{st} \leq V_{k2}$ and is as close as possible to the rated value. Assuming henceforth the new value $V_{k2} = V_{st}$, we determine the values of V_{a0}, $V_{a2\ min}$, and $V_{a2\ max}$ from Eqs. (16), (13), and (14).

Using the above arguments about the choice of the operating conditions of the stage, we assume the voltage V_e and determine the values R_{a2} and K_2 from Eqs. (18) and (19).

Taking into account that $R'_4 + R''_4 = R_4$ is determined by Eq. (33), we find

$$R_4 = \frac{V_e}{I_{st\ min}}. \tag{44}$$

The resistances R_1, R_2, and R_3 in the divider circuit can be determined from the following considerations:

$$V_{st} \approx \frac{R_2 + R_3}{R_1 + R_2 + R_3}(V_{out\ nom} - \Delta V_{out\ nom}) \approx \frac{R_3}{R_1 + R_2 + R_3}(V_{out\ nom} + \Delta V_{out\ nom}). \tag{45}$$

Specifying the value R_2, we find

$$R_3 = \frac{V_{out\ nom} - \Delta V_{out\ nom}}{2\Delta V_{out\ nom}} R_2, \tag{46}$$

$$R_1 = \frac{(V_{out\ nom} - \Delta V_{out\ nom} - V_{k2})(V_{out\ nom} + \Delta V_{out\ nom})}{2\Delta V_{out\ nom} V_{st}} R_2. \tag{47}$$

It is desirable that the current in the divider circuit not exceed 1-2 ma.

For the circuit of Fig. 3, we first find the value of V_{k2} using Eq. (15), and then determine the load resistance R_{a2} from the relationship

$$R_{a2} \approx \frac{V_{in\ min} - V_{k2} - V_{a2\ min}}{I_{a2\ max}}, \tag{48}$$

where $I_{a2\ max} = V_{a2\ min}/R_{i2}$, and the resistance R_{i2} is determined at the point corresponding to $V_{a2\ min}$ and $V_{g2} = 0$.

The resistance in cathode circuit of tubes T_2 and T_2' is chosen on the basis of the condition

$$R_{k2} = \frac{V_{k2}}{I_{a2\,max} + I'_{a2\ min}}. \tag{49}$$

The minimum current of the cathode follower $I'_{a2\ min}$ must be taken to equal (0.1-0.2) $I_{a2\ max}$.

The values of resistances R_1', R_2', and R_3' can be calculated from Equations (45), (46), and (47), by substituting the voltage V_{k2} in lieu of V_{st}. The amplifier stage with tube V_3 is designed analogously with the same stage of Fig. 4, with the exception of the voltage-regulator circuit and the divider R_1, R_2, and R_3, which are computed in accordance with the procedure given for the circuit of Fig. 2.

It should be noted that for normal operation of the circuit it is essential that the sliders of potentiometers R_2 and R_2' be mounted on a single shaft. This requirement is dictated by the fact that when the output voltage of the stabilizer is regulated by moving the slider of R_2, the voltage V_{k2} must remain constant (with an accuracy $\pm \Delta V_{g2}$).

As a rule, after the electronic stabilizer is assembled, the negative feedback in it changes to positive feedback as a result of the presence of parasitic phase shifts and self oscillations occur with a frequency having a range on the order of tens of kilocycles.

The simplest measure recommended for the elimination of these oscillations, in the case of the circuit with a single amplification stage (Fig. 2), is to connect a capacitance of 10 to 40 microfarads across the load at the output of the stabilizer.

In circuits with two stages of amplification (Figs. 3 and 4) it is necessary to connect the capacitances of 0.1 to 0.01 microfarad between the plates of T_3 and the negative terminal of the supply.

If the stabilizer must meet particular requirements with respect to the quality of the transients (for example, in case of pulsed load), it is necessary to introduce special correcting networks into the circuit [1].

The null drift of the stabilizer [the value of the coefficient δ_0 in Expression (1)] cannot be determined by calculation. The final estimate of the instability of the output voltage in time can be made only by testing out the circuit.

In the Laboratory of Automation and Remote Control of the V. I. Ul'ianov (Lenin) Leningrad Electrotechnical Institute several types of electronic voltage stabilizers were developed and produced in small batches (in lots of 5-10). By way of example we shall consider two of these types.

Figure 9 shows the electric circuit of the EST-2 stabilizer, designed for an input power up to 200 watts at a nominal output of 350 v (with regulation within ± 10%) and a load current varying from 0 to 500 ma.

The stabilizer is based on the block diagram of Fig. 4 with a two-stage amplifier employing 12Zh1L pentodes in the feedback circuit. The filaments of the pentodes are fed with stabilized voltage, picked off the output of the stabilizer.

The power tubes employed are four triode-connected GU-50 pentodes in parallel. The losses in the power-element tubes amount to 175 watts at the maximum load current.

The stabilizer has a relative stabilization coefficient of approximately 4,000 and an internal resistance of approximately 0,06 ohms. The null drift is approximately 50 millivolts in one hour of continuous operation.

It should be noted that the discrepancy between the computed data and the parameters of the constructed models does not exceed 10-12%.

Analogous results could be obtained by using 6P3S and 6N5 tubes in the power element of the stabilizer. However, in the former case it is necessary to connect in parallel eight tubes and the tube losses amount to 200 watts. In the second case it is necessary to use six triodes (three envelopes) with losses of approximately

100 watts. The filaments of the 6N5 tubes should be heated before the plate voltage is applied. This calls for an additional device in the stabilizer to connect the supply circuit automatically in the above sequence.

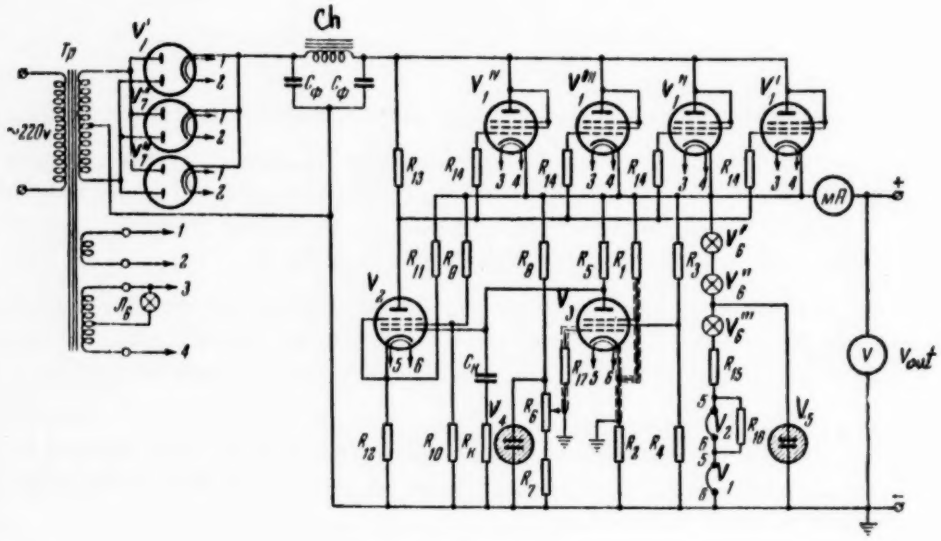

Fig. 9.

The use of 6N5 tubes insures minimum losses, but leads to a certain complication of the circuit. For the conditions specified above the 6N5 tubes are approximately equivalent to the GU-50 tubes.

Figure 10 shows an over-all view of the EST stabilizer with the cover removed. A detailed description of the circuit and the electrical data on its elements were published in Ref. [3].

As already noted, electronic stabilizers are designed most frequently for input voltage fluctuations not exceeding ± 10%, corresponding to the possible fluctuations of the ac power line. In certain cases, however, particularly when operating under nonstationary conditions, the supply voltages may change over a considerably wider range. In addition, comparatively large frequency deviations from the nominal value are possible. In this case a stabilization of the output voltage with an accuracy of ± (0.05-0.1)% is usually quite satisfactory, but the dimensions and weight of the apparatus become important.

To meet the above conditions, the EST-3 stabilizer was developed, intended for ± 25% supply-voltage and ± 10% frequency fluctuations. The output power of this stabilizer is up to 90 watts at a voltage of 250 v (with regulation over a range of ± 20%). The load current may vary from 30 to 300 ma.

Figure 11 shows the electric circuit of EST-3 stabilizer. It is based on the principal diagram shown in Fig. 3. To reduce the nominal value of the input voltage, and consequently the power losses, and to reduce the dimensions and weight of the stabilizer, the power element employs 6N5 double triode tubes (tubes T_1). The nominal value of the input voltage is in this case 375 v and the loss in the power tubes is approximately 80 watts. The amplifier in the feedback loop employs 6Zh8* (T_3) and 6N8 (T_2) tubes. The reference voltage is supplied from a voltage regulator tube type SG2S (T_8).

Since it is necessary, in order to produce stabilization under the specified variations of the input voltage, to have large voltage swings on the grids of the power tubes (+ 60 v and −120 v) relative to the nominal value (−60 v), and since tube T_2 cannot provide such swings at an output voltage of the stabilizer of 250 v, then to increase the dynamic range of voltages between the grids of the power tubes and the plate of tube T_2, additional unstabilized dc voltages are added to the grid circuit of T_1 and to plate circuit of T_2 additional unstabilized dc voltages.

The sources of these voltages are two small-power half-wave rectifiers employing a double diode 6Kh6 (tube T_6 with capacitive filters).

*[English equivalents: 6Zh8 ≡ 6SJ7; SG2S ≡ VR75-30; 6N8 — not identified — Ed.]

Since it is not permissible to operate a vacuum tube with filament voltage fluctuations of ± 25%, the circuit provides for a rough stabilization of the filament circuits of all the tubes with the aid of barreters (not shown in the diagram), the use of which reduces the filament voltage fluctuations to ± 10%.

To regulate the nominal value of the output voltage, the grid circuits of tubes T_3 and T_4 contain a ganged potentiometer R_8, R_{14} with which the output voltage can be varied ± 25% from the nominal value.

The influence of fluctuations in the filament current of the amplifier tubes on the operation of the stabilizer is reduced by connecting in series with the voltage divider in the grid circuit of tube T_3 a double diode 6Kh6 (T_4). When the filament voltage changes, the current through the diode varies and consequently also the voltage on the grid of T_3. Since the effect of the grid-voltage swing on the plate current opposes the effect of the swing of the filament voltage, the latter is canceled out to a considerable extent.

To turn on the plate circuits of the power tubes after the filaments are brought up to temperature, the circuit employs a time delay relay, consisting of a voltage regulator tube type SG3S* (T_3), a neon bulb type MN-3 (T_{10}), a capacitor C_7, resistances R_{20}, R_{21}, and R_{22}, and a type RPN electromagnetic relay (R). The time delay is approximately 60 seconds.

The power rectifier of the stabilizer is of the full-wave type with capacitive filter. Kenotrons 5Ts3S (T_7) are used as rectifier tubes.

The EST-3 stabilizer has a stabilization coefficient of approximately 500 and an internal resistance less than 0.1 ohms with supply voltage fluctuations of ± 25%.

When the variation of the supply voltage is reduced to ± 10%, the stabilization coefficient increases to approximately 1200, and the null drift after the stabilizer heats up for 30-40 minutes does not exceed 150 mv for one hour of continuous operation.

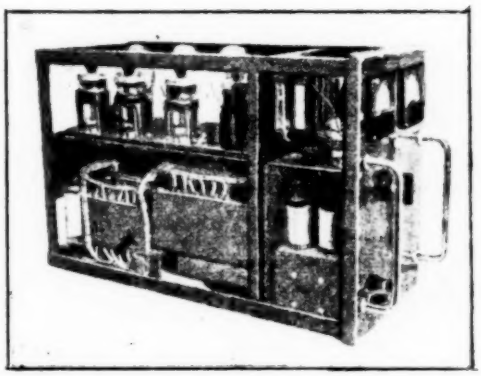

Fig. 10

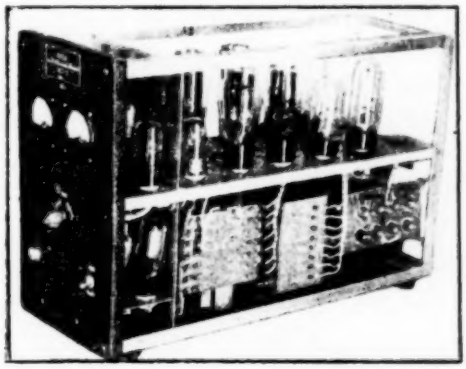

Fig. 12.

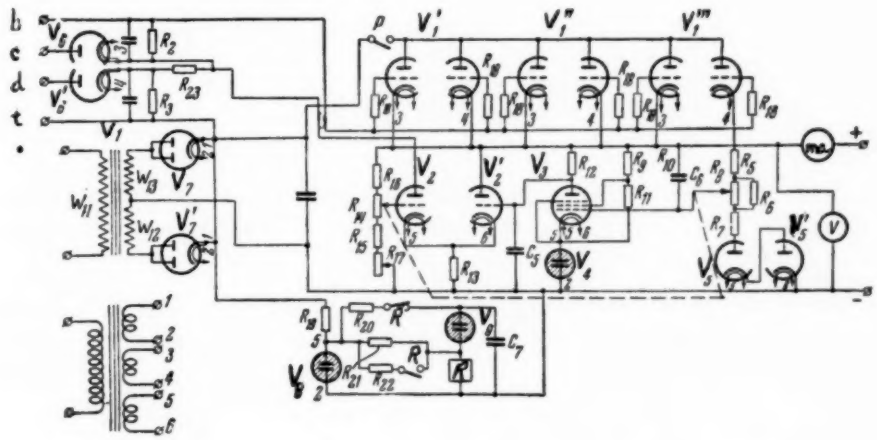

Fig. 11.

*[English equivalent: SG35 ≡ V5105-30 — Ed.]

An over-all view of the EST-3 stabilizer with the cover removed is shown in Fig. 12.

Stabilizers of the EST-3 type, like the EST-2 stabilizers, can be fed from either a 127 or 220 v ac line.

Received May 10, 1956

LITERATURE CITED

[1] L. I. Baida and V. K. Zakharov, "Static and Dynamic Modes of Electronic Voltage Stabilizers." Izvestia (News) of the V. I. Ul'ianov (Lenin) Leningrad Electrotechnical Institute, No. XXIX (1957).

[2] G. E. Gaufer, Starved Amplifiers. Electronic Engineering, Nov. (1954).

[3] L. I. Baida, "Type EST-2 Electronic Voltage Stabilizer." Academy of Sciences, USSR, Institute of Technical-Economic Information. Instruments and Test Stands (1955).

CERTAIN PROPERTIES OF CIRCUITS CONTAINING THERMORESISTANCES

G. K. Nechaev

(Kiev)

Discussion of the temperature dependence of the conductance and resistance of a two-terminal network containing thermoresistors. The conditions are derived under which the above relationships are close to linear. A method is given for the design of a temperature compensator for linear resistances.

Two-terminal networks containing thermoresistances are used in systems for the measurement and regulation of temperature, in temperature-compensation devices, etc.

The temperature dependence of the conductance and resistance of such two-terminal networks and of the parameters of other elements of the circuits were determined by Beakley [1] and Bleuze [2] for certain particular cases. Let us consider the most general case of the two-terminal network containing one thermoresistance and three linear resistances that do not depend on temperature. Corresponding to this case will be the two circuits shown in Figs. 1, a and 1, b, to which one can reduce by transfiguration all more complicated two-terminal networks that contain a single thermoresistance. The conductance of the circuit shown in Fig. 1, a is given by the expression

$$Y_a = \frac{r_1 + r_2 + R_t}{R_t (r_2 + r_3) + r_3 (r_1 + r_2) + r_1 r_2} . \tag{1}$$

The conductance of the circuit shown in Fig. 1,b will be

$$Y_b = \frac{R_t (r_1 + r_2 + r_3) + r_1 (r_2 + r_3)}{r_3 [R_t (r_1 + r_2) + r_1 r_2]} . \tag{2}$$

Expressions (1) and (2) can be represented in the form of a general formula

$$Y = \frac{aR_t + b}{cR_t + d} . \tag{3}$$

The values of the coefficient in Formula (3) for the circuit of Fig. 1,a will be: $a = 1$, $b = r_1 + r_2$, $c = r_2 + r_3$, $d = r_3 (r_1 + r_2) + r_1 r_2$, and for the circuit of Fig. 1, b: $a = r_1 + r_2 + r_3$, $b = r_1 (r_2 + r_3)$, $c = r_3 (r_1 + r_2)$, $d = r_1 r_2 r_3$.

Let us introduce the concept of the temperature sensitivity of the circuit with respect to the conductance, $S_T^Y = dY/dT$ and with respect to resistance $S_T^R = dR/dT$. The differential conductance sensitivity for these circuits will be

$$S_T^Y = \frac{dY}{dT} = R_t' \frac{ad - cb}{(cR_t + d)^2} . \tag{4}$$

The maximum of S_T^Y is determined by letting the derivative dS_T^Y/dT vanish. After transformations we arrive at

$$\frac{d}{c} = 2\frac{(R_t')^2}{R_t''} - R_t. \tag{5}$$

The temperature dependence of the thermoresistance is determined by the known expression

$$R_t = Ae^{\frac{B}{T}}, \tag{6}$$

where A and B are constant coefficients, characterizing the electrical properties of the thermoresistance.

The derivatives of R_t will be

$$\begin{aligned}
R_t' &= -\frac{B}{T^2}R_t \\
R_t'' &= \frac{B}{T^3}\left(\frac{B}{T}+2\right)R_t \\
R_t''' &= -\frac{B}{T^4}\left(\frac{B^2}{T^2}+6\frac{B}{T}+6\right)R_t \\
R_t^{IV} &= \frac{B}{T^5}\left(\frac{B^3}{T^3}+12\frac{B^2}{T^2}+36\frac{B}{T}+24\right)R_t \\
R_t^{V} &= -\frac{B}{T^6}\left(\frac{B^4}{T^4}+20\frac{B^3}{T^3}+120\frac{B^2}{T^2}+240\frac{B}{T}+120\right)R_t
\end{aligned} \tag{7}$$

Solving (5) and (7) simultaneously we obtain

$$\frac{d}{c} = R_{ti}\frac{B-2T_i}{B+2T_i} = R_{ti}\psi. \tag{8}$$

This expression represents the condition of the maximum conductance differential sensitivity for the circuits 1, a and 1, b at a certain point in the temperature range, corresponding to a selected value of T_i. It is obvious that the temperature T_i depends on the ratios of the resistances r_1, r_2, and r_0, contained in the coefficients a, b, c, and d, and on the parameter B. One must also note that the vanishing of d^2Y/dT^2 denotes the presence of a point of inflection in the curve Y (T) in a certain region. Here the curve Y (T) has a shape similar to that shown in Fig. 2. Analysis of Expression (8) leads also to the conclusion that this vanishing of the second derivative can be retained upon variation of the values of r_1, r_2 and r_3. Consequently, by thus varying the resistances, it is possible to change the sensitivity of the circuit, leaving the temperature corresponding to the point of inflection of the curve Y (T) unchanged. The value of the conductivity at the point of inflection is obtained on the basis of (3) and (8):

$$Y_n = \frac{ad+bc\psi}{cd(1+\psi)}. \tag{9}$$

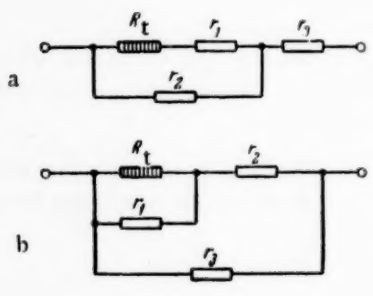

Fig. 1.

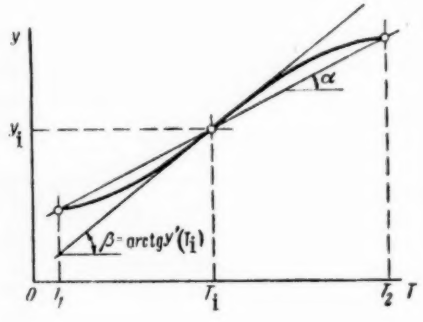

Fig. 2.

The existence of an inflection of the Curve Y(T) is one of the conditions under which it can be approximated by a linear relationship (4).

Let us investigate the accuracy with which the function Y(T) can be approximated by a straight line. The dependence Y(T) can be represented in the form of a Taylor series in powers of $\theta = T - T_i$

$$Y(T) = Y(T_i) + Y'(T_i)\frac{\theta}{1!} + Y''(T_i)\frac{\theta^2}{2!} + Y'''(T_i)\frac{\theta^3}{3!} + \cdots \tag{10}$$

The higher-order derivatives can be represented as

$$Y^{III}(T_i) = -Y'(T_i)\frac{B^3}{2T_i^4},$$

$$Y^{IV}(T_i) = Y'(T_i)\frac{2B^2}{T_i^5},$$

$$Y^{V}(T_i) = Y'(T_i)\frac{B^2}{T_i^6}\left(\frac{3}{4}\frac{B^2}{T_i^2} - 10\right). \tag{11}$$

Assuming that $Y''(T_i) = 0$, we get

$$Y(T) = Y(T_i) + Y'(T_i)\theta\left[1 - \frac{B^2\theta^2}{2T_i^4\,3!} + \frac{2B^2\theta^3}{T_i^5\,4!} + \frac{B^2}{T_i^6}\left(\frac{3}{4}\frac{B^2}{T_i^2} - 10\right)\frac{\theta^4}{5!}\right]. \tag{12}$$

The equation of the straight line approximating the Curve Y(T) will be

$$Y_c = Y(T_i) + k\theta, \tag{13}$$

where $k = \tan\alpha$ (Fig. 2).

The error in the approximation, of interest to us, is determined by the expression

The error in the approximation, of interest to us, is determined by the expression

$$\Delta Y = Y(T) - Y_c = I'(T_i)\left[\theta - \frac{B^2\theta^3}{2T_i^4\,3!} + \frac{2B^2\theta^4}{T_i^5\,4!} + \frac{B^2}{T_i^6}\left(\frac{3}{4}\frac{B^2}{T_i^2} - 10\right)\frac{\theta^5}{5!}\right] - k\theta. \tag{14}$$

The condition under which ΔY has a maximum can be determined from the expression $d(\Delta Y)/dT = 0$, which leads to a fourth-degree equation. To simplify the solution of the problem, let us check whether it is possible in certain cases to neglect several terms in the square brackets. For this purpose let us specify actual values of B, T_i and θ. Let us take B = 2100°K, T_i = 300°K, and θ = 25°C. Then the ratio of the second term in the square brackets of Expression (14) to the first term will be

$$\frac{B^2\theta^2}{2T_i^4\,3!} = \frac{2100^2 \times 25^2}{2 \times 300^4 \times 6} = 0.028, \tag{15}$$

and the ratio of the third to the first will be

$$\frac{2B^2\theta^3}{T_i^5\,4!} = \frac{2 \times 2100^2 \times 25^3}{300^5 \times 24} = 0.00233 \tag{16}$$

and the ratio of the fourth to the first will be

$$\frac{B^2}{T_i^6}\left(\frac{3}{4}\frac{B^2}{T_i^2} - 10\right)\frac{\theta^4}{5!} = \frac{2100^2}{300^6}\left(\frac{3}{4}\frac{2100^2}{300^2} - 10\right)\frac{25^4}{5!} = 0.00053. \tag{17}$$

This example shows that terms higher than the second can be neglected in certain cases, without introducing

a substantial error into the result. Now Expression (14) reduces to

$$\Delta Y = Y'(T_i)\,\theta\left(1 - \frac{B^2\theta^2}{2T_i^4\,3!}\right) - k\theta, \tag{18}$$

hence

$$\frac{d(\Delta Y)}{d\theta} = Y'(T_i) - \frac{3}{2}\,\frac{B^2\theta^2}{T_i^4\,3!}\,Y'(T_i) - k = 0 \tag{19}$$

and

$$\theta_m = \frac{2T_i^2}{B}\sqrt{\frac{Y'(T_i) - k}{Y'(T_i)}}\,. \tag{20}$$

On the basis of (18) and (20) we get

$$\Delta Y_{max} = \frac{4}{3}\,\frac{T_i^2}{B}\sqrt{\frac{Y'(T_i) - k}{Y'(T_i)}}\,[Y'(T_i) - k]. \tag{21}$$

The value of k can be determined from the condition that the moduli of ΔY must equal at the points corresponding to $T_i - \theta_m$ and T_i. We then obtain from (18) and (21)

$$Y'(T_i)\,\theta_1\left(1 - \frac{B^2\theta_1^2}{2T_i^4\,3!}\right) - k\theta_1 = \frac{4}{3}\,\frac{T_i^2}{B}\sqrt{\frac{Y'(T_i) - k}{Y'(T_i)}}\,[k - Y'(T_i)], \tag{22}$$

from which we can get the value of k. Let us next investigate the temperature dependence of the resistance of the circuits under consideration. For the circuit of Fig. 1, a we get

$$R_a = \frac{R_t(r_2 + r_3) + r_1r_2 + r_3(r_1 + r_2)}{R_t + r_1 + r_2}\,, \tag{23}$$

and for the circuit of Fig. 1, b

$$R_b = \frac{R_t(r_1 + r_2)r_3 + r_1r_2r_3}{R_t(r_1 + r_2 + r_3) + r_1(r_2 + r_3)}\,. \tag{24}$$

If we use the symbols employed in (3), the general equation for the resistance will be

$$R = \frac{cR_t + d}{aR_t + b}\,. \tag{25}$$

Obviously, the curve for R(T), in analogy with the above, can have a point of inflection for certain conditions. To determine these conditions let us find R' and R"

$$R' = R_t'\,\frac{cb - ad}{(aR + b)^2}\,, \tag{26}$$

$$R'' = (cb - ad)\,\frac{R_t''(aR_t + b) - 2a(R_t')^2}{(aR_t + b)^3}\,, \tag{27}$$

Taking R" = 0, we obtain the condition for the point of inflection

$$\frac{b}{a} = 2\frac{(R'_{\mathrm{ti}})^2}{R''_{\mathrm{ti}}} - R_{\mathrm{ti}} \tag{28}$$

or after substituting R'$_{ti}$ and R"$_{ti}$

$$\frac{b}{a} = R_{\mathrm{ti}}\ \frac{B-2T}{B+2T} = R_{\mathrm{ti}}\,\psi. \tag{29}$$

The resistance of the circuit at the point of inflection will be

$$R_{\mathrm{i}} = \frac{bc + ad\,\psi}{ab\,(1+\psi)}\,. \tag{30}$$

Representing R(T) in a Taylor series in powers of $\theta = T - T_i$, we get

$$R(T) = R(T_{\mathrm{i}}) + R'(T_{\mathrm{i}})\frac{\theta}{1!} + R''(T_{\mathrm{i}})\frac{\theta^2}{2!} + R'''(T_{\mathrm{i}})\frac{\theta^3}{3!} + \cdots \tag{31}$$

The higher-order derivatives of R(T) can be represented as

$$\begin{aligned} R'''(T_{\mathrm{i}}) &= -R'(T_{\mathrm{i}})\frac{B^2}{2T_{\mathrm{i}}^4}\,,\\ R^{\mathrm{IV}}(T_{\mathrm{i}}) &= R'(T_{\mathrm{i}})\frac{2B^2}{T_{\mathrm{i}}^5}\,,\\ R^{\mathrm{V}}(T_{\mathrm{i}}) &= R'(T_{\mathrm{i}})\frac{B^2}{T_{\mathrm{i}}^6}\left(\frac{3}{4}\frac{B^2}{T_{\mathrm{i}}^2} - 10\right). \end{aligned} \tag{32}$$

Expression (31) is transformed into

$$R(T) = R(T_{\mathrm{i}}) + R'(T_{\mathrm{i}})\frac{\theta}{1!} - R'(T_{\mathrm{i}})\frac{B^2}{2T_{\mathrm{i}}^4}\frac{\theta^3}{3!} + R'(T_{\mathrm{i}})\frac{2B^2}{T_{\mathrm{i}}^5}\frac{\theta^4}{4!} + \cdots \tag{33}$$

As shown above, in certain cases it is possible to neglect the terms of higher orders, thus simplifying considerably the solution of the problem. The curve may have a shape similar to that shown in Fig. 3.

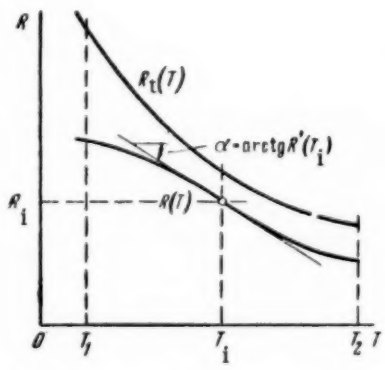

Fig. 3.

Particular cases of the circuits considered above will be circuits consisting of a thermoresistance and two supplementary resistances (Fig. 4), as well as circuits having a single thermoresistance and a single supplementary resistance (Fig. 5). The expressions for the conductances and resistances of these circuits can be obtained from the equations derived above. The equations for all the circuits are listed in Table 1.

The following conclusions can be drawn from the table.

1) For all circuits, except for the circuit shown in Fig. 5,b the curves Y(T) can have an inflection point under certain conditions, i.e., there is a condition for obtaining a relationship for Y(T) that is nearly linear.

2) For all circuits, with the exception of that represented by Fig. 5, a, the R(T) curves have a point of inflection under

certain conditions, i.e., there is a condition for obtaining a nearly linear relationship for R(T).

3) The expressions corresponding to the inflection points of Y(T) and R(T)(second and fourth columns of Table 1) contain only resistances that are included in the external parallel branch. Thus, the same expressions hold for circuits containing two and three supplementary resistances.

4) The temperatures corresponding to the point of inflection of curve Y(T) and R(T) are not the same for one and the same circuit.

5) It is possible to use for temperature compensation all the circuits, with the exception of the circuit in Fig. 5, a, for in the latter the relationship for R(T) cannot be made nearly linear.

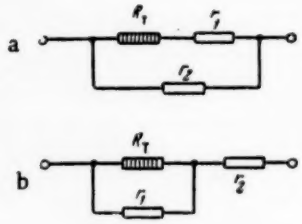

Fig. 4.

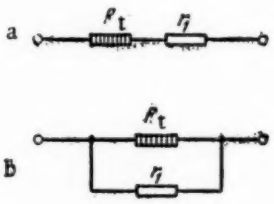

Fig. 5.

Let us consider in greater detail the circuit for temperature compensation. At the present time the proposed compensator is based on the circuit shown in Fig. 5, b [3, 4]. But this circuit cannot always ensure the best conditions for compensation, since the resistance r_1, designed for the compensation conditions, may yield for the curve R(T) an inflection point that is not in the middle of the temperature range, and this is undesirable because of the reduced accuracy. Better results are therefore obtained with the circuit of Fig. 4,a, which has two supplementary resistances.

Let us carry out the calculations for a compensator having two supplementary resistances r_1 and r_2. Most metallic resistances have a linear temperature dependence of resistance

$$r = r_0 (1 + \alpha\theta), \tag{34}$$

where α is the temperature coefficient of resistivity.

We assume that the point of inflection of curve R(T) should be at the center of the working range; the resistance of the compensator at temperatures T_1 and T_2 (at the end of the working range) will then be

$$R_1 = R(T_i) - R'(T_i)\theta - R'''(T_i)\frac{\theta^3}{3!},$$
$$R_2 = R(T_i) + R'(T_i)\theta + R'''(T_i)\frac{\theta^3}{3!}. \tag{35}$$

Obviously, to obtain compensation in the given range of temperatures the change in the compensator resistance should be equal and opposite to the change in the resistance r, i.e.,

$$\Delta r = 2r_0\alpha\theta = R_1 - R_2 = -2\left[R'(T_i)\theta + R'''(T_i)\frac{\theta^3}{3!}\right] \tag{36}$$

or

$$r_0\alpha = -R'(T_i)\left(1 - \frac{B^2}{2T_i^4}\frac{\theta^2}{3!}\right). \tag{37}$$

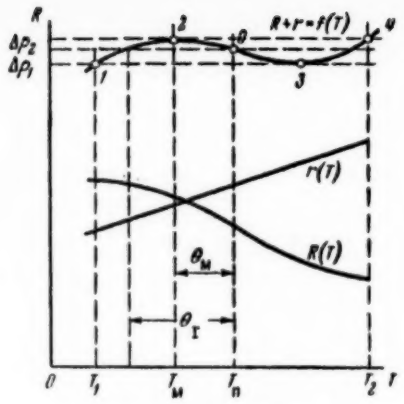

Fig. 6.

For the circuit of Fig. 4, a, we obtain on the basis of (26) and (29) the value of $R'(T_1)$ satisfying the conditions under which one obtains a curve R(T) with an inflection point in the middle of the temperature range

$$R'(T_1) = -\frac{r_2^2}{4R_1}\frac{(B+2T_1)^2}{BT_1^2}. \tag{38}$$

Inserting (38) into (37) we get

$$r_0\alpha = \frac{r_2^2(B+2T_1)^2}{4R_{t1}BT_1^2}\left(1-\frac{B^2}{2T_1^4}\frac{\theta^2}{3!}\right), \tag{39}$$

from which we obtain the value of r_2

$$r_2 = \frac{2T_1}{B+2T_1}\sqrt{\frac{BR_{t1}r_0\alpha}{1-\frac{B^2}{2T_1^4}\frac{\theta^2}{3!}}}. \tag{40}$$

It is now easy to obtain

$$r_1 = R_{t1}\frac{B-2T_1}{B+2T_1} - r_2. \tag{41}$$

The thermoresistance for the thermal compensator is chosen to satisfy the condition that the change in the value of the thermoresistance in the given temperature range is greater than the change in the compensated resistance, i.e., $\Delta R_t > \Delta r$. As a result of a certain linearity in the compensator, it is impossible to obtain an absolutely constant resistance for the entire circuit with changing temperature. The change in the circuit resistance (the error in compensation) can be determined from (34) and (35):

$$\Delta\rho = \Delta R - \Delta r = R'(T_1)\theta + \\ + R'''(T_1)\frac{\theta^3}{3!} - r_0\alpha\theta. \tag{42}$$

The condition for the maximum $\Delta\rho$ is obtained from

$$\frac{d(\Delta\rho)}{d\theta} = R'(T_1) - r_0\alpha + R_1'''(T_1)\frac{\theta^2}{2} = 0, \tag{43}$$

hence

$$\theta_m = \sqrt{2\frac{r_0\alpha - R'(T_1)}{R'''(T_1)}}. \tag{44}$$

On the basis of (42) and (44) it is possible to obtain the maximum of $\Delta\rho$.

As noted correctly in [4], on the basis of the Chebyshev approximation theory, to obtain the minimum value of $\Delta\rho_m$ it is necessary that this quantity change its sign four times in the compensation range T_2-T_1. In view of this, it is necessary to choose the rated values of θ_r somewhat smaller than $\theta = T_1-T$, so that the moduli of $\Delta\rho$ at the points 1, 2, 3 and 4 (Fig. 6) become approximately equal. This can be obtained by taking $\theta_r = (0.75 \text{ to } 0.8)\theta$.

Example. Design a temperature compensator using the circuit of Fig. 4, a for a copper resistance having $\theta = 0°C$ at $r_0 = 300$ ohms and operating in the range from -50 to $+50°C$ ($\theta = 50°C$). The temperature coefficient of resistivity of copper is $\alpha = 0.425\%$ per °C. The thermoresistance used for the compensator will have A = 1.57 ohms and B = 1890 °K.

TABLE 1

Formulae for Circuits with Thermoresistances

Circuit of Fig. No.	Equation for the inflection point of the Y(T) curve	Value of conductance at the inflection point of the Y(T) curve	Equation for the inflection point of the R(T) curve	Value of the conductance at the inflection point of the R(T) curve
1. *a*	$\frac{(r_1+r_2)r_3+r_1r_2}{r_2+r_3}=\frac{B-2T}{B+2T}R_t$	$\frac{2(r_1+r_2)r_3B+r_1r_2(B+2T)}{2B(r_2+r_3)[(r_1+r_2)r_3+r_1r_2]}+$ $+\frac{(r_1+r_2)r_2(B-2T)}{2B(r_2+r_3)[(r_1+r_2)r_3+r_1r_2]}$	$r_1+r_2=\frac{B-2T}{B+2T}R_t$	$\frac{[2Br_1+(B+2T)r_2]r_2}{2B(r_1+r_2)}+r_3$
1. b.	$\frac{r_1r_2}{r_1+r_2}=\frac{B-2T}{B+2T}R_t$	$\frac{2B(r_1+r_2+r_3)r_2+(B-2T)r_1r_3}{2B(r_1+r_2)r_2r_3}$	$\frac{r_1(r_2+r_3)}{r_1+r_2+r_3}=\frac{B-2T}{B+2T}R_t$	$\frac{[2B(r_1+r_2+r_3)r_2+(B+2T)r_1r_2]r_3}{2B(r_2+r_3)(r_1+r_2+r_3)}$
4. *a*	$r_1=\frac{B-2T}{B+2T}R_t$	$\frac{1}{r_2}+\frac{1}{r_1}\left(\frac{1}{2}-\frac{T}{B}\right)$	$r_1+r_2=\frac{B-2T}{B+2T}R_t$	$\frac{[2Br_1+(B+2T)r_2]r_2}{2B(r_1+r_2)}$
4. b	$\frac{r_1r_2}{r_1+r_2}=\frac{B-2T}{B+2T}R_t$	$\frac{r_2+r_1\left(\frac{1}{2}-\frac{T}{B}\right)}{r_2(r_1+r_2)}$	$r_1=\frac{B-2T}{B+2T}R_t$	$\frac{2Br_2+(B+2T)r_1}{2B}$
5. *a*	$r_1=\frac{B-2T}{B+2T}R_t$	$\frac{1}{r_1}\left(\frac{1}{2}-\frac{T}{B}\right)$	The curve of R(T) has no inflection point	
5. b	The curve of Y(T) has no inflection point		$r_1=\frac{B-2T}{B+2T}R_t$	$\left(\frac{1}{2}+\frac{T}{B}\right)r_1$

TABLE 2

θ, °C	T, °K	R_t, ohms	r, ohms	R, ohms	$R_i = r + R$, ohms	$\Delta R_i = R_i - R_{i0}$, ohms	ΔR_i %
−50	223	7540	236.5	428.0	664.5	−2.5	−0.375
−40	233	5200	249.5	417.5	667.0	0.0	0.0
−20	253	2700	274.5	394.0	668.5	+1.5	+0.23
0	273	1570	300.0	367.0	667.0	0.0	0.0
+20	293	970	325.5	340.0	665.5	−1.5	−0.23
+40	313	650	350.5	316.5	667.0	0.0	0.0
+50	323	545	363.5	306.0	669.5	+2.5	+0.375

We assume $\theta_r = 0.80$, or $\theta_r = 40°C$. From the formula $R_t = Ae^{B/T}$ we determine the values of the thermo resistance corresponding to $T_1 = 273 - 40 = 233°K$, $T_i = 273°K$, and $T_2 = 273 + 40 = 313°K$, viz: $R_{t1} = 5200$ ohms, $R_{ti} = 1570$ ohms, and $R_{t2} = 650$ ohms respectively.

On the basis of (29), considering that for this circuit $a = 1$ and $b = r_1 + r_2$, we get

$$r_1 + r_2 = \frac{B - 2T_i}{B + 2T_i} R_{ti} = \frac{1890 - 2\times 273}{1890 + 2\times 273} 1570 = 870 \text{ ohms.}$$

According to (40), we obtain for r_2

$$r_2 = \frac{2T_i}{B + 2T_i} \sqrt{\frac{BR_{ti}r_0\alpha_0}{1 - \frac{B^2}{2T_i^4}\frac{\theta^2}{3!}}} = \frac{2\times 273}{1890 + 2\times 273} \sqrt{\frac{1890\times 1570\times 300\times 0{,}00425}{1 - \frac{1890^2}{2\times 273^4}\frac{40^2}{6}}} = 450 \text{ ohms.}$$

Then $r_1 = 870 - 450 = 420$ ohms.

As a check, let us calculate the resistances of the entire circuit for several points within the range. The results are listed in Table 2.

The calculation results show that the errors in the compensation, effected in the proposed manner, are small.

Received November 26, 1956

LITERATURE CITED

[1] W. R. Beakley, Design of Thermistor Thermometers with Linear Characteristics, J. Sci. Instr. 28, No. 6 (1951).

[2] J. Bleuze, Properties and Applications of Thermistors, L'Onde Electrique, No. 317-318 (1953).

[3] G. K. Nechaev, Temperature Compensation of Elements of Electric Circuits, Elektrichestvo, No. 10 (1951).

[4] I. T. Sheftel', Temperature Compensation of Linear Resistances with Positive Temperature Coefficients with the Aid of Semiconducting Thermocompensators, Avtomatika i Telemekhanika, Vol. XIV, No. 2 (1953). [Automation and Remote Control.]

EXPONENTIAL PULSE-TIME CONVERTERS

A. I. Novikov

(Moscow)

The main functions of pulse-time converters are considered. Circuits are given for the converters and for a simple multichannel pulse telemetering system using exponential converters without commutators.

INTRODUCTION

Multichannel systems with pulse-time modulation are much used in radiotelemetering [3-5, 7]. Such systems are comparatively insensitive to interference, occupy narrow channel widths and have simple circuits. The Kipp relay or "compounding modulator" circuits are commonly used in the converters. There are important shortcomings in such converters. The Kipp relay system is of poor stability and is sensitive to ambient temperature and line voltage fluctuations, and also to tube age.

The compounding modulator compares a constant standard voltage with the sum of a linearly increasing and the modulating voltage. The converter is of high accuracy only if the saw-tooth voltage is stable. The saw-tooth generator circuit becomes more complex if increased linearity and accuracy are demanded, and in some cases if the repetition period is increased.

To eliminate metering errors due to converter instability in radiotelemetering systems, standard signals are transmitted periodically to correspond to zero and maximum levels.

In industrial telemetering pulse-time modulation (PTM) has not been much used because simple and stable converters have not been available. Industrial PTM telemetering equipment is mainly of single-channel type with mechanical or electromechanical converters [1, 2, 6].

Converters of the two types above cannot give adequate accuracy without using corrector channels. So if PTM is to be introduced into industrial systems simple and stable converters are required. Exponential converters* fall in this class as they are very reliable and have highly linear amplitude responses. The whole circuit, except for the comparator unit diode, can be built round cold-cathode tubes and transistors. The stability varies little with line voltage. Simple multichannel commutatorless systems can also be used.

The primary transducer in an exponential converter can be an R, L or C element.

Systems designed to transmit slowly varying signals can use mechanically controlled resistors. For high resistance values these should be sectional with the section leads connected to a rotary switch. In RL converters the controlling element can be an inductor with a magnetized ferrite or permalloy core.

*V. A. Il'in proposed the exponential converter.

Least work has been devoted to transducing the primary quantity to its RL or C equivalent in exponential or frequency converters. This creates certain difficulties and is a disadvantage.

The Main Functions of the Converter

The operative principle is to compare an exponentially varying voltage (varying as $e^{-t/\tau}$) with a set voltage U_{R_2} (Fig. 1). At time $1 - e^{-t/\tau}$ they are equal and the device produces a pulse, the time when the pulse is produced being determined by the time-constant $\tau = RC$. Thus by varying either R or C we get time modulation.

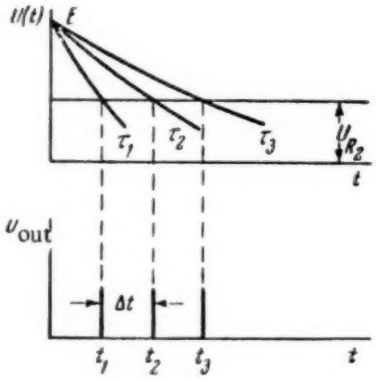

Fig. 1.

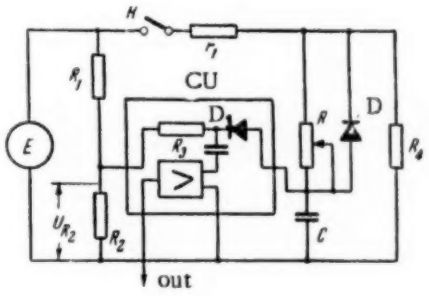

Fig. 2.

Figure 2 shows the principles of the circuit. The commutator is represented as the key K and resistance r_1. When K is closed C charges via the internal resistance and the transducer resistance R to the comparison voltage U_{R_2}.

The comparator unit CU can be a diode plus amplifier. Other systems can be used, e.g., triggers.

When charging is complete the contact opens, E being disconnected from the RC circuit. C discharges to zero voltage with a short time-constant $\tau \approx R_4C$ via diode D and resistor R_4, after which the process is repeated.

Taking the internal resistance of the comparator as infinite up to the instant of equality and assuming that CU then operates instantly,* we can write the equations describing the charge on the condenser in the equivalent circuit (Fig. 3), as subjected to Laplace transforms, in the form

$$\frac{E}{p} = i_1(r_1 + R_4) - i_2R_4, \quad 0 = i_2\left(R_4 + R + \frac{1}{Cp}\right) - i_1R_4. \tag{1}$$

Solving (1) for i_2 and remembering that $U_C(p) = i_2/Cp$, we get the voltage on the capacitor as

$$U_C(t) = \frac{E}{k}\left(1 - e^{-\frac{k}{CR'}t}\right) \quad \left(R' = r_1 + Rk;\ k = \frac{R_4 + r_1}{R_4}\right).$$

The moment of equality is given by

$$U_C(t) = U_{R_2} \text{ or } \frac{E}{n} = \frac{E}{k}\left(1 - e^{-\frac{k}{CR'}t}\right) \text{ where } n = \frac{R_1 + R_2}{R_2}.$$

Solving for t we have

$$t = \left(R + \frac{r_1}{k}\right) C \ln \frac{n}{n - k}. \tag{2}$$

* These assumptions are correct if the comparator resistance is large and does not shunt the capacitor appreciably and the delay in CU operating is much less than the time deviation. Both conditions are realizable.

Assuming $R = R_{max} - \Delta R$ we get the time deviation Δt:

$$\Delta t = t_{max} - t = \Delta RC \ln \frac{n}{n-k} = \Delta\tau \ln \frac{n}{n-k}, \quad (3)$$

where

$$t_{max} = (R_{max} + \frac{r_i}{k}) C \ln \frac{n}{n-k}.$$

When C is modulated

$$\Delta t = \Delta C (R + \frac{r_i}{k}) \ln \frac{n}{n-k} = \Delta\tau \ln \frac{n}{n-k}. \quad (4)$$

Equations (3) and (4) imply that the time deviation is linear and does not depend on whether R or C is modulated. It is also independent of E.

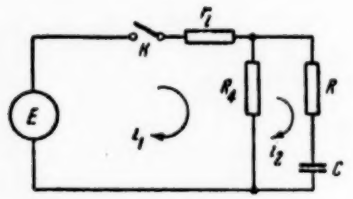

Fig. 3.

There are two main causes of error in exponential converters:

1) jitter in the voltage on the capacitor at the start of the cycle; this can arise if r_i varies, for instance;

2) jitter in the operate threshold of the comparator, Δe.

To determine the absolute error arising from the first cause the change in capacitor voltage, ΔE, must be incorporated into (1). Equation (1) then takes the form:

$$\frac{E}{p} = i_1(r_i + R_4) - i_2R_4, \quad 0 = i_2 (R_4 + R + \frac{1}{Cp}) - i_1R_4 + \frac{\Delta E}{p}. \quad (5)$$

The instant of equality is then given by

$$t' = \tau \ln \frac{n}{n - \frac{Ek}{E - \Delta Ek}} \qquad [\tau = C (R + \frac{r_i}{k})],$$

and the absolute error due to ΔE is found as

$$\alpha_{\Delta E} = t' - t = \tau \ln m_1 \quad (m_1 = \frac{n-k}{n - \frac{Ek}{E - \Delta Ek}}).$$

The relative error will then be

$$\delta_{\Delta E} = \frac{\alpha_{\Delta E}}{\Delta t_{max}} = \frac{\tau \ln m_1}{\Delta\tau_{max} \ln \frac{n}{n-k}},$$

where Δt_{max} is the maximum time deviation.

The error due to threshold shift in the comparator can be determined from

$$E \frac{1}{n} \pm \Delta e = \frac{E}{k} (1 - e^{-\frac{t''}{\tau}}),$$

where $\pm \Delta e$ is the threshold shift caused by various instabilities. This expression gives the instant of equality t". The absolute error is then

$$\alpha_{\Delta E} = t'' - t = \tau \ln m_2 \quad (m_2 = \frac{n-k}{n - k \mp \frac{\Delta ekn}{E}}),$$

and the relative error

$$\delta_{\Delta e} = \frac{\tau \ln m_2}{\Delta\tau_{max} \ln \frac{n}{n-k}} .$$

The modulation index Φ in the case of pulse-time modulation is

$$\Phi = 2\pi \frac{\Delta t_{max}}{T} ,$$

where T is the unmodulated pulse repetition time.

In this case the ratio of Δt_{max} to T will be given by

$$\frac{\Delta t_{max}}{T} = \frac{\Delta\tau_{max}}{\tau} .$$

The relative error can be represented in general form as

$$\delta = \frac{2\pi}{\Phi} f\left(\frac{\Delta\lambda}{\lambda}\right) \quad \left(f\left(\frac{\Delta\lambda}{\lambda}\right) = \frac{\ln m_1}{\ln \frac{n}{n-k}}\right). \tag{6}$$

In (6) this error is shown to be inversely proportional to the modulation index.

Converter Circuits

In the converter to be considered r_i must be constant and independent of E ($r_i \ll R$). If this condition is not fulfilled, e.g., if the commutator is a cold-cathode tube, τ and Δt will be functions of r_i. This circuit can be used at both high and low currents in the RC circuit. In some cases a voltage stabilizer circuit is desirable (No. 2 in Table 1).

Inserting the key before the R_1R_2 and R_3C subcircuits enables one to keep E constant during the working cycle using the voltage stabilizer T_1. The converter operation is then independent of internal resistance changes. The formulas for the time deviations given in the table show these to be independent of r_i in this circuit.

It is readily shown that when the stabilizer is omitted the time deviation will only be linear (when C is modulated) if r_i is constant. It is in principle impossible to obtain a linear relation if R changes, as is evident from the formulas for No. 3 in Table 1.

Estimating the degree of nonlinearity β in the modulation characteristic from the nonlinearity coefficient on the section between the beginning and end of the characteristic,

$$\beta = \frac{\left|\frac{d(\Delta t)}{d(\Delta R)}\right|_{beg} \left|\frac{d(\Delta t)}{d(\Delta R)}\right|_{end}}{\left|\frac{d(\Delta t)}{d(\Delta R)}\right|_{beg}},$$

we get

$$\beta = 1 - \frac{\frac{\Delta_{end}}{n-\Delta_{end}} + \ln\frac{n-\Delta_{end}}{n-k}}{\frac{\Delta_{beg}}{n-\Delta_{beg}} + \ln\frac{n-\Delta_{beg}}{n-k}},$$

where

$$\Delta_{beg} = \frac{\frac{r_i}{k}}{1+\frac{r_i}{Rk}}, \qquad \Delta_{end} = \frac{\frac{r_i}{k}}{\left(1-\frac{\Delta R}{R}\right)+\frac{r_i}{Rk}} .$$

β falls with r_l. If $r_l \ll R$ we may put $r_l \approx 0$ and the expressions given for circuit No. 2 are then correct for No. 3. A converter circuit using a RC chain and the capacitor working in discharge is shown in Table 1 (No. 4). The current in the RC circuit can vary widely. The effect of r_{l_1} can here be balanced out by inserting a unit of internal resistance r_{l_2} which varies according to the same law as r_{l_1} in series with R_1R_2. If $r_{l_1} = r_{l_2}$ and $R_4 = R_1 + R_2$ the time deviation is given by

$$\Delta t = \Delta RC \ln \frac{R_4}{R_2}, \quad \Delta t = \Delta C (R + R_4) \ln \frac{R_4}{R_2}.$$

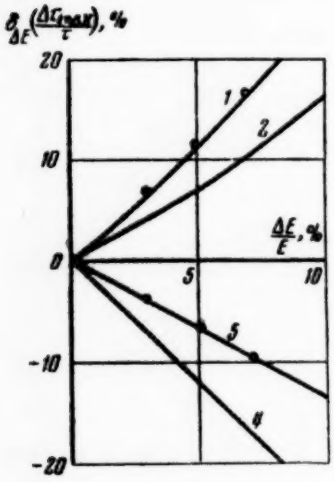

Fig. 4.

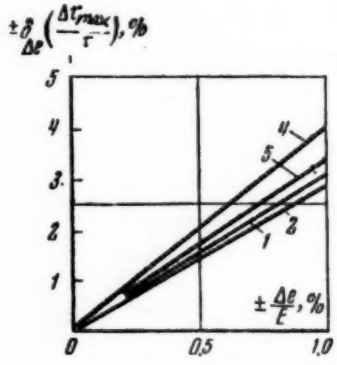

Fig. 5.

Then Δt and the linearity do not depend on r_l. Data on an exponential converter using a RL circuit are given in Table 1 (No. 5). This circuit is advantageous when very fast response is required.

Figures 4 and 5 illustrate the relative errors of circuits Nos. 1, 2, 4 and 5 (curves numbered as circuits) computed for identical conditions with n = 2, k = 1, 2, and γ = 0, 2, where $\gamma = r/R_{tot}$ is the ratio of the coil resistance to the total circuit impedance in the RL transducer (see No. 5, Table 1).

Multichannel System

Exponential converters can be used to devise commutatorless multichannel telemetering systems with time-division channels. This simplifies the transmitter circuit and makes it more reliable. Consider for instance the three-channel telemetering system shown in Figure 6.

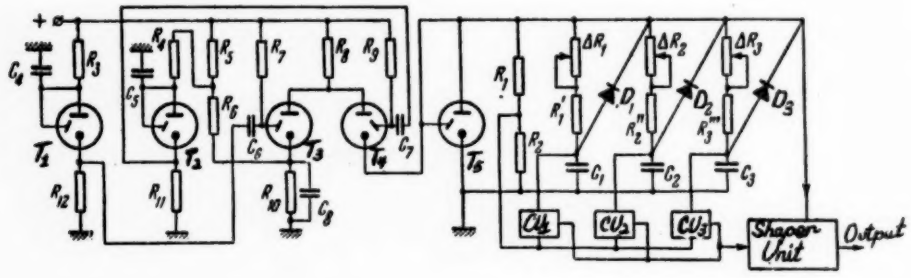

Fig. 6.

This system has two parts: the control unit using the cold-cathode tubes T_1, T_2 and T_3 and three RC transducers connected as in circuit No. 2 of Table 1.

TABLE 1

No.	Circuit	Converter in circuit	Character of operation	Modulated parameter	Time deviation	Error due to instability in ΔE: absolute : $^{a}_{\Delta E}$, relative $-\delta_{\Delta E}$	Error due to threshold shift in CU $\pm \Delta e$: absolute $^{a}_{\Delta e}$, relative $-\delta_{\Delta e}$	Notation
1	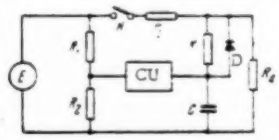	RC	Charge	C	$\Delta t = \Delta C\left(R + \frac{r_i}{k}\right)\ln\frac{n}{n-k}$	$^{a}_{\Delta E} = \tau \ln \frac{n-k}{n-\frac{Ek}{E-\Delta Ek}}$	$^{a}_{\Delta e} = \tau \ln \frac{n-k}{n-k \mp \Delta enk/E}$	$k = \frac{R_4 + r_i}{R_4}$, $n = \frac{R_1 + R_2}{R_4}$
				R	$\Delta t = \Delta RC \ln \frac{n}{n-k}$	$\delta_{\Delta E} = \frac{\tau \ln \frac{n-k}{n-Ek/(E-\Delta Ek)}}{\Delta\tau \ln n/(n-k)}$	$\delta_{\Delta e} = \frac{\tau \ln \frac{n-k}{n-k \mp \Delta enk/E}}{\Delta\tau_{max} \ln \frac{n}{n-k}}$	
2	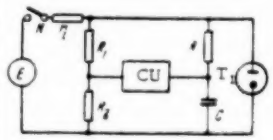	RC	Charge	C	$\Delta t = \Delta CR \ln \frac{n}{n-1}$	$^{a}_{\Delta E} = \tau \ln \frac{n-1}{n-\frac{E}{E-\Delta E}}$	$^{a}_{\Delta e} = \tau \ln \frac{n-1}{n-1 \mp \Delta en/E}$	$n = \frac{R_1 + R_2}{R_4}$
				R	$\Delta t = \Delta RC \ln \frac{n}{n-1}$	$\delta_{\Delta E} = \frac{\tau \ln \frac{n-1}{n-E/(E-\Delta E)}}{\Delta\tau_{max} \ln \frac{n}{n-1}}$	$\delta_{\Delta e} = \frac{\tau \ln \frac{n-1}{n-1 \mp \Delta en/E}}{\Delta\tau_{max} \ln \frac{n}{n-1}}$	
3	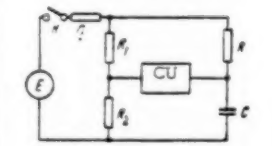	RC	Charge	C	$\Delta t = \Delta C\left(R + \frac{r_i}{k}\right)\ln\frac{n - \frac{kr_i}{Rk + r_i}}{n-k}$			$k = \frac{r_i + R_1 + R_2}{R_1 + R_2}$, $n = \frac{r_i + R_1 + R_2}{R_2}$
				R	$\Delta t = \Delta RC \ln \frac{n - \frac{kr_i}{(R-\Delta R)k + r_i}}{n-k} + \left(R + \frac{r_i}{k}\right)C \ln \frac{n - \frac{kr_i}{Rk + r_i}}{n - \frac{kr_i}{(R-\Delta R)k + r_i}}$			
4	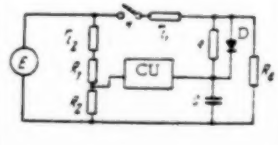	RC	Discharge	C	$\Delta t = \Delta C (R + R_4) \ln \frac{n}{k}$	$^{a}_{\Delta E} = \tau \ln \frac{E - \Delta Ek}{E}$	$^{a}_{\Delta e} = \tau \ln \frac{E}{E \mp \Delta en}$	$k = \frac{R_4 + r_{it}}{R_4}$, $n = \frac{R_1 + R_2 + r_{ct}}{R_4}$
				R	$\Delta t = \Delta RC \ln \frac{n}{k}$	$\delta_{\Delta E} = \frac{\tau \ln \frac{E - \Delta Ek}{E}}{\Delta\tau_{max} \ln \frac{n}{k}}$	$\delta_{\Delta e} = \frac{\tau \ln \frac{E}{E \mp \Delta en}}{\Delta\tau_{max} \ln \frac{n}{k}}$	
5	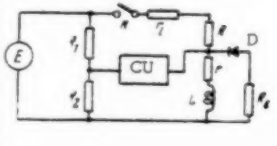	RL	Discharge	L	$\Delta t = \frac{\Delta L}{R_{tot}} \ln \frac{(1-\gamma)n}{1-\gamma n}$	$^{a}_{\Delta E} = \tau \ln \frac{1 - \gamma - \frac{\Delta E}{E}}{1-\gamma}$	$^{a}_{\Delta e} = \tau \ln \frac{1-\gamma n}{1-\gamma n \mp \Delta en/E}$	$n = \frac{R_1 + R_2}{R_2}$, $\Delta E = \Delta i (R + r_i)$,
						$\delta_{\Delta E} = \frac{\tau \ln \frac{1 - \gamma - \frac{\Delta E}{E}}{1-\gamma}}{\Delta\tau \ln \frac{(1-\gamma)n}{1-\gamma n}}$	$\delta_{\Delta e} = \frac{\tau \ln \frac{1-\gamma n}{1-\gamma n \mp \Delta en/E}}{\Delta\tau_{max} \ln \frac{(1-\gamma)n}{1-\gamma n}}$	$\gamma = \frac{r}{R_{tot}}$, $R_{tot} = R + r + r$

A pulse from the relaxation oscillator constructed round T_1 fires the left tube in the trigger T_3. T_4 then goes out. T_5, which acts as voltage stabilizer and is connected in the cathode circuit of T_4, also goes out. The transducer capacitors C_1, C_2 and C_3 discharge via the diodes D_1, D_2 and D_3 and the resistors R_1 and R_2 (grounded). The voltage appearing at the cathode of T_3 then causes C_5 to charge up to the striking voltage of T_2. T_2 operates and the pulse from its cathode fires T_4, and hence T_5. When T_5 fires a fresh cycle begins.

The voltage on T_5 operates the shaper unit, which produces a synchropulse. The transducer capacitor voltages simultaneously begin to rise according to a $1 - e^{-t/\tau}$ law. Since the transducer time-constants differ and the condition $\tau_{1\,max} < \tau_{2\,min} < \tau_{2\,max} < \tau_{3\,min}$ is fulfilled the voltage on the capacitor in each channel rises with a delay relative to that in the previous channel. This provides the time separation between channels. When the voltage $U_C(t)$ on the capacitor in a given channel reaches the value U_{R_2} the appropriate CU produces an output pulse.

The maximum time deviations Δt_{max} for the channels can be the same, so the maximum change in time constant must be $\Delta\tau_{n_{max}} = C\Delta R_{n_{max}}$.

So the C's, like the $\Delta R_{n_{max}}$ should, preferably be made identical.

The different τ_n can be produced by inserting extra resistors $R_{n_{min}}$, i.e., $\tau_{n_{max}} = CR_{n_{min}} + C\Delta R_{max}$, where $R_{n_{min}}$ is the additional resistor in the nth channel. At the end of the working cycle T_1 produces a fresh pulse and the process repeats. Since the referred errors δ are proportional to τ the channel accuracies are not equal. They fall from channel one onwards. This is a dasadvantage of this circuit, so it is not applicable if many channels are required. To increase the accuracy a reference pulse, constant in position relative to the synchronizing pulse, can be produced in each channel. The interval between the reference and working pulses in the signals received simplify the receiver design considerably since pulse regeneration is not required. The reference pulses can be produced by including additional fixed RC circuits. The RC values must be chosen so the reference pulses fall at the beginnings or ends of the channel intervals.

SUMMARY

1) The time deviation in the pulse-time converters does not, in principle depend on the supply voltage, which is an important advantage. The circuits are comparatively simple.

2) The converters have a very wide speed range. They can be used for telemetering fast or slow processes.

3) Multichannel commutatorless telemetering systems using exponential converters have simpler transmitters and are more reliable.

This is undoubtedly a very considerable advantage of exponential converters.

Received January 2, 1957

LITERATURE CITED

[1] A. L. Abrukin, A pulse-time converter for telemetering. "Remote Control in the National Economy," (in Russian), Izd. AN SSSR (1956).

[2] R. V. Bilik, Pulse-time system telemetering apparatus. "Remote Control in the National Economy," (in Russian), Izd. AN SSSR (1956).

[3] Generation of special waveforms (in Russian). Translation of "Waveforms," compiled from MIT (USA) reports. Sovetskoe Radio (1951).

[4] V. A. Il'in, Time-division multichannel telemetering equipment. "Remote Control of Power Systems," (in Russian), Izd. AN SSSR (1954).

[5] V. A. Il'in and A. I. Novikov, Review of multichannel pulsed telemetering systems, (in Russian), Automatika i Telemekhanika 26, No. 4 (1955).

[6] V. S. Malov, "Remote Control in Power Systems (in Russian), Gosenergoizdat (1951).

[7] Radiotelemetering technique (in Russian). Collection of translations edited by P. I. Evdokimov, B. Kh. Krivitskii and Iu. A. Voenizdat (1955).

CODE RINGS AND THEIR USES IN REMOTE CONTROL EQUIPMENT

A. N. Radchenko

(Leningrad)

A new way of representing a complete set of codes which presents the same information in a more compact form is presented. Ring coding principles are derived from which existing pulse-code telemetering and remote control equipment may be considerably simplified.

The considerable interest attached at present to code (digital) methods of transmitting and transforming information arises from the fact that such methods enable one to solve many problems while ensuring the highest performance as to requirements such as accuracy, remoteness of operation, flexibility and automatic control, and rapid response. Current electronic computers are a good illustration of pulse-code developments as they are now used for handling nonmathematical information. Coding methods are also important in telemechanics work as they are insensitive to interference (particularly in remote control) and accurate (in telemetering). In this field all other methods of transmitting information are in many cases being replaced by code ones.

But code methods are often difficult to use in practice because of coding and decoding equipment complexity. This has restricted the use of code methods in spite of their positive advantages.

The present work was concerned with radical simplifications to the structures of coding devices, and in process of solving this problem a new way of representing a complete set of codes (code rings) was proposed. Principles and methods of ring coding were subsequently developed.

In most coding devices the codes are generated by special memory devices in which all the codes used are recorded. These units may be selector plates on coding tubes, magnetic-matrix and diode-matrix networks, optical masks, contact coders, etc. The number of elements (contacts, tubes, etc.) in such a unit is the product of the number of codes and the number of terms in each code. In essence the number of elements equals the number of signs required to record the code tables. Thus to represent 32 five-term binary codes we need 160 elements, for 48 five-term substitution type codes (3 symbols) we need 240 elements etc. In some cases (e.g., when tubes are used) the number can be reduced somewhat by combining functions performed by separate elements. But the total number of elements remains very large and is a serious obstacle to simplifying the apparatus. The number of elements can be reduced by using abbreviated code representations. A way of thus combining a complete assembly of n-term codes is to use code rings.

A code ring is one inscribed specially with a sequence of symbols designed to represent the code assembly in a more compact form. The sequence law is such that within a single cycle there are no sections with repeating n-term combinations of pulses, while the sum of all the possible n-term sections (including mutually overlapping ones) which can be selected gives the total number of possible code combinations. The ring thus contains all possible codes, each code being present once only.

Figure 1 shows a code ring representing a family of binary five-member codes. By comparing the numbers

$k=2$,		$n=5$,	$m=k^n=32$
1	*aaaaa*	17	*baaaa*
2	*aaaab*	18	*baaab*
3	*aaaba*	19	*baaba*
4	*aaabb*	20	*baabb*
5	*aabaa*	21	*babaa*
6	*aabab*	22	*babab*
7	*aabba*	23	*babba*
8	*aabbb*	24	*babbb*
9	*abaaa*	25	*bbaaa*
10	*abaab*	26	*bbaab*
11	*ababa*	27	*bbaba*
12	*ababb*	28	*bbabb*
13	*abbaa*	29	*bbbaa*
14	*abbab*	30	*bbbab*
15	*abbba*	31	*bbbba*
16	*abbbb*	32	*bbbbb*

a

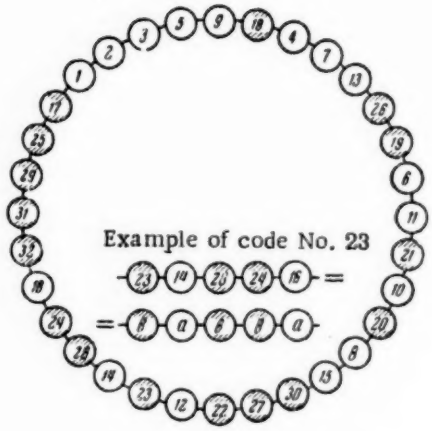

b

Fig. 1. A code ring containing binary five-term codes; a) table of codes, b) code ring $k = 2$, $n = 5$, $m = k^n = 32$. The open circles represent state a, the cross-hatched state b.

given in the code table (Fig. 1,a) and those on the code ring (Fig. 1, b) it can be seen that the codes denoted by the same numbers are the same when the ring is read clockwise. This example shows that the code-ring form enables us to reduce the number of elements required from 160 to 32, i.e., by a factor 5. The reduction factor obtained by this form of representation is equal to the number of terms in the code, n. When 6-term codes are used the reduction factor is 6, with ten-term codes 10, etc. This implies that the number of elements in the ring always equals the number of codes, i.e., one code requires one element no matter what code is used. Hence the larger the number of terms in the code the greater the advantages from the ring representation.

To demonstrate the power of this method we show in Fig. 2 the selector plates for a 128-code tube of normal form (a) and for 256 codes in the ring form (b). Although the set is twice as large in the latter case the selector plate is much simpler. To reproduce the codes with a type two plate television-type scanning is used, and the code has to be formed by gating one of the n-element sections of the selector plate. The code can then be shifted on one or on two adjacent columns.

Any complete code assembly known at present can be represented in ring form no matter how many terms or symbols are used. The existence of code rings can be demonstrated in general for various laws linking the members of an assembly if the following conditions are fulfilled.

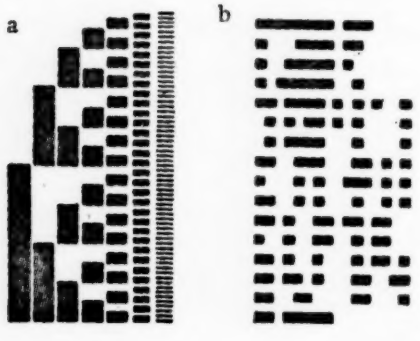

Fig. 2. Configurations of coding tube selector plates. a) normal code representation (128 codes) b) ring representation (256 codes).

First condition. Identical left and right $(n-1)$ term combinations entering into the codes of the assembly must be encountered equal numbers of times.

If the left $n-1$ elements of one code form a combination identical with the right combination of another then such codes are termed overlapping.

Second condition: this must be that it is impossible to divide the code assembly into two parts such that the first contains not even one code overlapping with one in the second part.

Both conditions are fulfilled for position-number codes. These conditions can also be shown to be correct for code assembly constructed according to other laws. In particular it can be shown

that code rings exist for replaceable-symbol codes and for codes formed by limiting permutations (A_k^{k-1}). Other code construction laws using sequential pulse alternation which would be of practical use are unknown to us. So at this stage we can consider code rings as a general way of representing code assemblies. Figures 3-5 show code rings for the code assemblies most frequently used. The rings can be changed by using one of their properties which, owing to limitations of space, will be stated here without proof. This property is that the ring elements can be read in reverse order of the symbols transposed or cyclically permuted. The main property of the code ring – that it contains each code in the assembly once only – is not thereby destroyed, only the sequence of the codes being affected.

Fig. 3. Code ring for binary number-position codes:
$k = 2$, $n = 6$, $m = k^n = 64$.

To transmit a code some section of the ring must be read off. Magnetic tape attached to the ring or a magnetic drum with a closed sequence of recorded signals may be used. The signal sequences must correspond to the symbol permutation in the code ring. The same result can be produced by using ring pulse-counting circuits with the rings coupled to generators. Finally, the code ring can be read off using a circular time-base with pulse regeneration or by means of any other of the devices commonly used in circulating memory equipment. Here the recording and erasing units are not required.

Fig. 4. Code ring for replaceable-symbol codes: $k = 3$, $n = 4$, $m = k(k-1)^{n-1} = 24$.

Fig. 5. Limiting permutations code ring: $A_k^{k-1} = k!$, $k = 4$, $m = k! = 24$.

The coding unit must provide exact selection of the ring section containing the required code. There are three distinct methods of performing this operation. In the first the read-off operation is linked to a ring-switching circuit. Then the introduction of each ring element will correspond either to closing a definite circuit or to the transmission of a pulse to one of m possible circuits. A pulse in any of these circuits can be used to gate a switching unit which remains operative during n cycles and ensures that the code ring pulses are transmitted to the communication channel. The circuit selected by the ring-switching circuit governs the code transmitted.

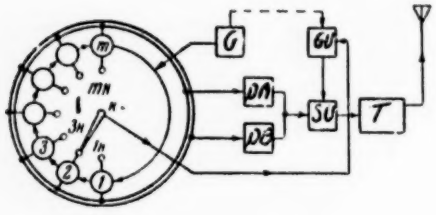

Fig. 6. Block-diagram of the telemeter coding device (distribution principle).

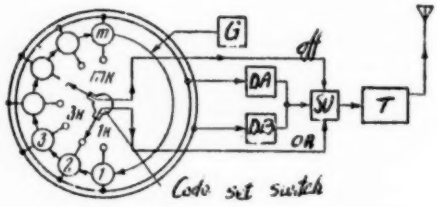

Fig. 7. A modification to the block-circuit using distribution principle coding.

Figure 6 shows the block-diagram of such a coding unit. The circles 1, 2,..., m denote the separate ring counting units. The input is continuously supplied with pulses from the generator G which produce sequential switching in the 1k, 2k, ..., mk circuits. The output circuits of the counting rings are joined to two busbars (in general the number of such busbars equals the number of symbols) which are connected to the generators Da, Db. The mode of connection is such that the signals generated correspond to the arrangement of the symbols on the code ring. The output circuits of these generators are coupled to the switching unit SU and then to the transmitter T. The instant when the switching unit opens the gate is set by the code selection switch K. This instant is determined parametrically, by the time (a flip-flop trigger may be used for the gating unit, for instance). To define the gate-opening instant more accurately a synchronizing signal can be taken from the pulse generator. The synchronizing circuit is shown dashed.

Double-pulse methods of defining the code in the ring are better used with some types of apparatus. The concepts on which this method is based are illustrated by Figure 7. Here the parametric method of reading the code elements is replaced by a circuital one. Two pulses are taken from the ring counter, the first being used to cut in the switching unit and the second to cut it off. The pulse spacing is set by the angular separation of the brushes on the code set switch and corresponds to the number of elements in the code.

Double pulses can also be produced in a single circuit if the output circuits of the counting system are combined via tubes. The steps in the coupler tubes must correspond to the number of terms in the code. A double switch is then unnecessary. In this case a bistable trigger can be used. The number of circuits required to be switched on setting a fresh code is reduced by a factor two. This is valuable in electronic switching units.

In telemetering equipment the measured quantity itself effects the code circuit switching, e.g., via a quantizator.

So the most notable feature of this coding principle consists in using ring switching circuits to distribute pulses to gating circuits. Hence the method may be termed the distribution method of ring coding.

In the second instance the selection of the various codes from the ring can be effected with only one gating unit using a variable delay on the gating pulse. Figure 8 shows the block-diagram of such a device. The most important difference between this circuit and the preceding ones is that no mechanical switching circuits are required. This advantage is of particular value in electronic systems. A pulse from one of the rings (RP-reference pulse) in the counting system is transmitted to the delay generator DG. The delayed pulse from DG cuts in the gating unit GU at some point on the code ring dependent on the voltage applied to DG. The control signal is quantized by synchronizing DG from the pulse generator G. DG is assumed to be a slave sweep unit, flip-flop, phantastron, etc. G simultaneously synchronizes GU, thus providing a distinctly marked end to the code.

This method will be termed the pulse-time ring coding method.

The main difference between the first and second methods is that in the first case the signals are presented individually for each ring element, whereas in the second only one ring element is presented individually, all the others being selected by using parametric time relationships. The advantage of the second – absence of switching circuits – is somewhat negated by the need for exact time correspondence between the operations in the separate units. This is easily effected when tube circuits are used but may be impossible in others (relay contact units) or inconvenient (magnetic or gas-filled devices). It is therefore logical to provide locking signals between the gating circuits and the code ring reading ones so that each of the code ring elements will be presented individually in the locking signal. Hence it is desirable that this signal should not demand many circuits but should be available from one point, as in the second case.

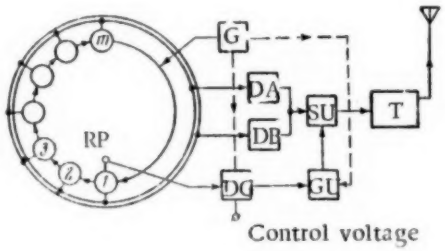

Fig. 8. Block diagram of a telemetering coding device (pulse-time principle).

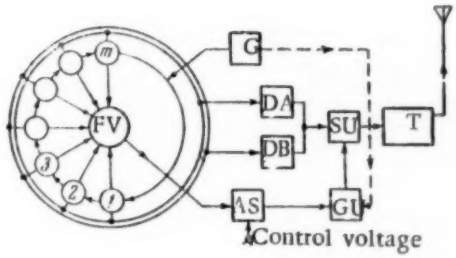

Fig. 9. Block diagram of a telemetering coding device using the functional voltage principle.

In this sense the most convenient form in which to express the functional relation is a stepped voltage or current. When these are used the correspondence is established by assigning each code ring element a definite amplitude. Thus the number of amplitude steps must equal the number of elements in the code ring. In some cases this result can be produced using a saw-tooth of period equal to the ring cycling time. But a stepped voltage is more convenient since the signal being coded is thereby automatically quantized.

Figure 9 shows a block-diagram of a coding device using this functional voltage principle. A distinguishing feature of this circuit is the functional voltage node FV connected to all the counting system units. Another distinguishing feature is that the gating unit is controlled via the amplitude selector, in which the functional voltage and voltage to be coded are compared. The stepped functional voltage can be built up from pulses taken from the counting rings via resistors of differing magnitudes. In passing we note that in all cases it is preferable to use binary scaling-circuit counters for reproducing the code ring and functional voltage. When the functional voltage and voltage to be coded are equal the amplitude selector produces a pulse which gates the units, which latter then select the required sector of the code ring.

These are the basic principles of code-ring use in telemetering devices. Only the first method codes the measured quantity in such a way as to give the larger quantities corresponding to the larger codes, if the latter are reckoned as numbers in an appropriate (e.g., binary) system. This proportionality system is at present commonly adopted although it is arbitrary. The other methods do not give proportional correspondence, but their considerable advantages (signal quantization and absence of switched circuits) outweigh this. It should also be remembered that the use of code rings built round pulse-counting systems for telemetering purposes is not always logical and it is better to use other methods. The production of reference pulses or functional voltages then present no problems.

In remote control devices, unlike in telemetering ones, the first method is to be preferred because the individual gating circuits for the various instructions make the system very reliable. There is also no point in economizing on switching circuits since each trigger unit cannot be represented by less than one contact (circuit). In this case only one circuit is required to select the code.

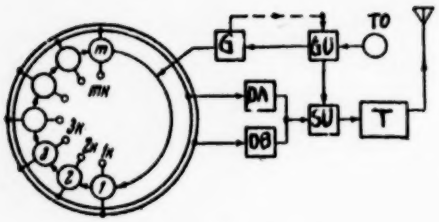

Fig. 10. Block-diagram of a ring-coding device for remote control.

The continuous code sampling required for telemetering is not necessary in remote control and can therefore be replaced by periodic scanning. In this connection it is desirable to use a somewhat different method of coding. This consists in one of the counting rings (or some other device) being activated before the code is scanned. A series of pulses is then applied to the counting circuit of number corresponding to the number of terms in the code. As the counting circuit operates adjacent rings are successively excited by determining the pulse train of one of the codes on the ring. The choice of code is defined by the number of the counting ring first excited.

Figure 10 shows the block-diagram of such a coding device. The prior excitation is effected by the switches 1k, 2k, ..., mk. Pulse generator G activates the gating unit GU when the trigger device TD operates. The required number of pulses from G is determined by calibration of the gating pulse. The exactitude of this operation can be increased by synchronizing GU to G (synchronizing circuit shown dashed). At the same time as gating G the gating unit cuts in the switching unit SU, which passes the selected sectors of the code ring to the transmitter. The transmitter switching is required because otherwise the first and last pulses in the code would be of unlimited length.

This ring coding method for remote control signals enables one to code using simpler (and hence more reliable) apparatus. In essence the method eliminates differences in the technical devices and coding and distribution methods in remote control systems. Correspondingly, devices using ring coding should be coupled with simplicity in the distributor devices and freedom from interference in the codes. Existing remote control systems can be simplified by adopting ring coding principles. The coder circuits are then much simplified and the coding devices can readily be made electronic.

Received March 12, 1956

CALCULATIONS ON ELECTROMAGNETIC SYSTEMS USING ELECTRICAL ANALOGS

S. A. Aleskerov

(Baku)

A method of producing electrical analogs when solving magnetic field distribution problems for electromagnetic systems is proposed for cases where the problems amount to the solution of Dirichlet's exterior problem. The method enables one to solve the problem when the magnetic circuit is arbitrary and with any potential distribution over the bounding surfaces of the field. It is demonstrated that when the magmetic potential has been determined at various field points the space permeability can be calculated for the field of the mechanism.

When electromagnetic systems are being designed and their working in various automatic devices analyzed it is sometimes necessary to compute the specific magnetic permeability in regions exterior to the currents (permeabilities of leakage paths and working air gaps, etc.). These calculations amount to solving Dirichlet's interior and exterior problems for Laplace equations.

The computational work involved in determining the specific magnetic permeability as a function of system dimensions is however laborious even for two-dimensional fields. Some have proposed empirical formulas and graphical methods for use in practical calculations which involve field-mapping and which sometimes give results deviating widely from those of exact solutions.

These graphical methods are not general ones and the computational errors can vary widely, no prior estimate of the errors being possible [1].

The empirical formulae are usually only applicable when the dimensions of the system have certain particular relationships [2].

Attempts to apply analytic methods, including potential networks, are limited by the complexity of the numerical calculations [3]. The more stringent demands being made on apparatus (electromechanical in particular) force us to improve our methods of computing magnetic permeabilities, particularly specific magnetic permeabilities.

It is of some practical value to develop methods employing computing equipment, electrical analogs especially.

Calculations have been reported on several physical problems carried out on electrical analogs, as have numerical solutions obtained by finite-difference methods to problems which are in essence only interior problems stemming from the Laplace equation [3-5], and so have graphical methods of solving magnetic field distribution equations [6].

Here we present methods of solving magnetic field distribution equations using electrical network analogs

for cases amounting to the solution of Dirichlet's interior and exterior boundary problems.

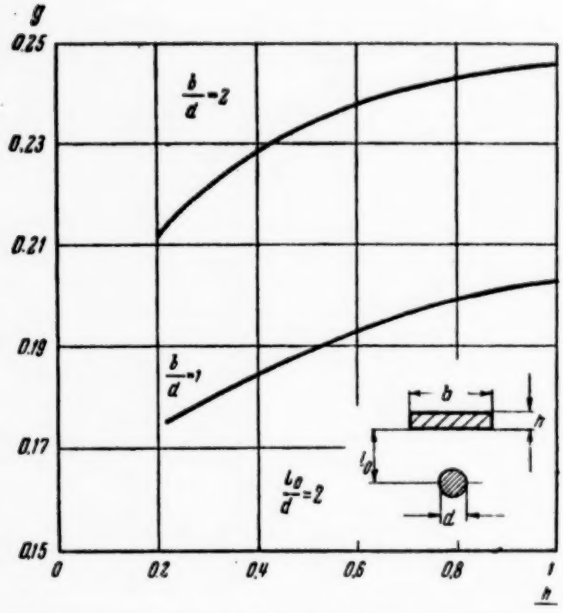

Fig. 1. Relation of leakage specific magnetic permeability to ratio dimensions in the electromagnetic system.

It will be shown that the analogs in general give a more exact solution for the magnetic field potentials as well as speeding-up the calculations considerably.

Possible and desirable methods of setting up the system are given (depending on the number of lattice points in the analogs).

It is shown that when the magnetic potential distribution has been determined by experiment the air-space permeability can be calculated. Using these methods on the EM-8 electrical analog developed and produced at the Institute of Precision Mechanics and Computing Technique, Academy of Sciences of the USSR, the author has studied the field distributions and computed the specific magnetic permeabilities for certain types of electromechanical mechanisms.

These results are to be published separately. Figure 1 illustrates the methods by showing the relation of leakage specific magnetic permeability as between core and armature in a relay to ratio of dimensions in the electromagnetic system.

The accuracy of the field calculations made on the EM-8 was checked by using results obtained analytically by Govorkov's potential network method [3].

The calculations and measurements* were made in relative units.

In the plane-parallel magnetic fields considered here we can use the scalar magnetic potential $\varphi_m(x, y)$ in regions outside the currents, this potential satisfying Laplace's equation [7].

$$\Delta\varphi_m = 0. \tag{1}$$

The determination of $\varphi_m(x, y)$ for the air about the mechanisms with a given potential distribution over the bounding surfaces of the field leads to Dirichlet's interior and exterior problems for (1).

Analog Studies Of the Interior Problems Described by (1)

As an example the field of a horseshoe magnet with a keeper separated from it by a certain distance was studied. The potential field distribution was approximated on the analog network. As in Govorkov's analytic calculations the keeper was assumed unsaturated; the potential was also assumed to vary linearly along its surface. These assumptions were only made in order to compare the experimental data with Govorkov's calculations, made by finite-difference methods. To the same end the boundary values in the analog studies were taken the same as in the analytic calculations. These values were applied to the boundary nodes from the boundary conditions divider, this latter being an inductive voltage divider with 200 steps. The potentials were measured by null methods using an electronic detector and ac potentiometer. Figure 2 shows the distribution of potential φ_m in the field (figures above the lines) as measured. Govorkov's results are given below the lines. The largest discrepancy is 1.6%. Allowing for the advantages of using electrical analogs, we may conclude that this result demonstrates the power of analog studies on electromagnetic mechanisms which give rise to the interior problem described by (1).

*Engineer K. M. Chal'ian participated in the experimental work on the analogs and in calculating the permeabilities for various electromagnetic systems.

Analog Studies of the Exterior Problem Described by (1)

The leakage field between core and armature of a telephone relay was studied (Figure 3).

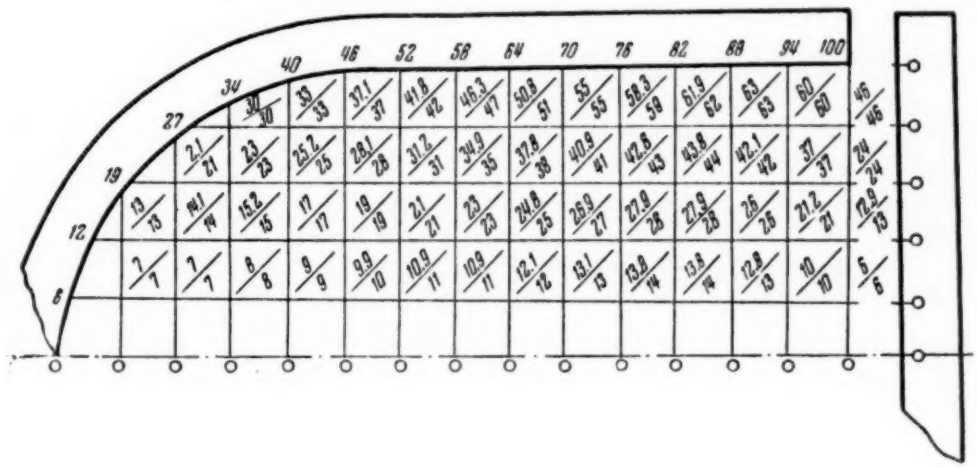

Fig. 2. Distribution of potential φ_m in the field of a horseshoe magnet.

Three banks of EM-8 units were used, comprising 3515 nodes. The transverse section of the armature C_1 was approximated by a rectangle, and that of the core C_2 by a polygon (Fig. 3)

Without restricting the generality of the method the boundary values of φ_m at the edges of C_1 and C_2 were taken as $\varphi_m/C_1 = 100$ and $\varphi_m/C_2 = 0$ all round. Since the edges of C_1 coincide with those of the adjacent grid region the boundary values need not be given more accurately. The boundary values at the nodes of the polygon approximating to C_2 were determined by successive approximation in such a fashion that when the solution had been found the φ_m found at the edge of C_2 agreed with the set values. The boundary values for the approximating polygon were corrected using Collatt's formulas [8].

$$\varphi_m = \frac{h\varphi_0 \mp \delta\varphi_2}{h \mp \delta} \qquad (2)$$

where φ_0 is the set boundary value at points on the edge, φ_2 is the value at the adjacent node, h is the grid pitch, δ the distance from the boundary point to the boundary node. In (2) the signs are taken as "+" if the boundary node falls within the edge, and "−" if outside.

The errors in these corrections are of h^2 order. When h is large it is better to correct the boundary values using Mikeladze's formulas [8]. The error is then of h^3 order. When all three banks of the EM-8 are used, as here, the pitch was reduced by a factor eight, so the first formulas give sufficiently correct values for practical calculations.

Initially the boundary nodes of the approximating polygon were assigned the values existing at the closest point where the grid intersected the circle. The appropriate potentials were supplied from the boundary conditions divider and readings taken at adjacent nodes. Calculations using (2) gave corrected boundary values which were then set up to give stage two corrections. In this example the boundary values were set after the third correction. These values are given in Table 1 (as the polygon is symmetrical only half are given).

TABLE 1

Boundary Values at Points on the Curve Approximating to C_2

$\varphi_1^{(1)}$	$\varphi_1^{(2)}$	$\varphi_1^{(3)}$	$\varphi_1^{(4)}$	$\varphi_1^{(5)}$	$\varphi_1^{(6)}$	$\varphi_1^{(7)}$	$\varphi_1^{(8)}$	$\varphi_1^{(9)}$	$\varphi_1^{(10)}$
1.6	5.86	2.42	3.69	0.88	0.72	2.65	1.74	2.00	0.52

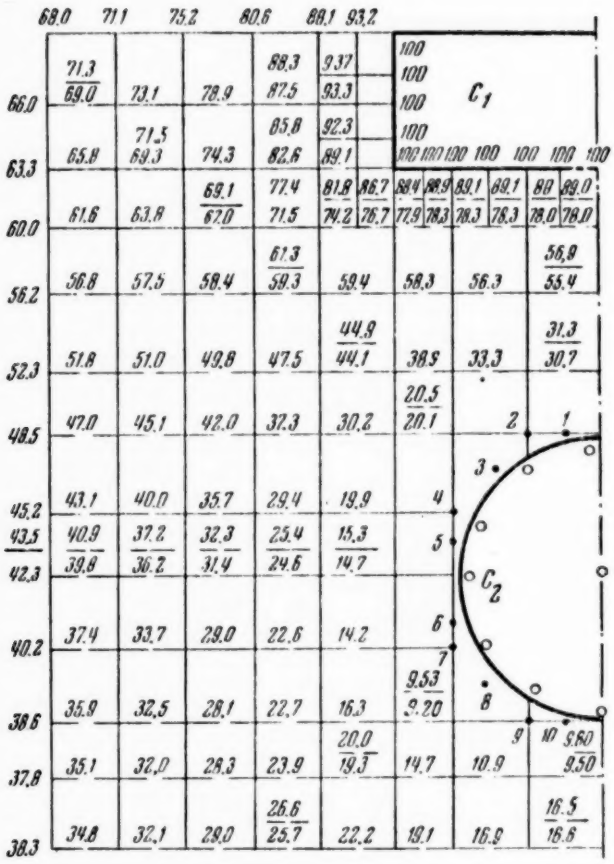

Fig. 3. Distribution of φ_m in the leakage field between the core and armature of a telephone relay (direct experimental investigations of higher models).

The potential distribution over the nodes was determined with the above boundary values over the whole region, which enabled one to check the measured values. Figure 3 shows only the measured values for half the region (which is symmetrical).

The theoretical reasoning supporting the method of handling the exterior problem for (1) on a model about 3500 nodes (which we have put forward) is not given here, but it has been shown on several examples that the accuracy of the results is within the limits to be expected from the analog. The experimental and theoretical studies show that this method (using many nodes) is applicable to practical calculations. It may be used in experimental solutions to Dirichlet's planar exterior problem obtained by finite-difference methods.

It would be of interest to develop a method in which the above problem for (1) could be solved on an analog with few nodes (small model). This is all the more desirable because many research and teaching institutions use small Soviet network analogs with about 400 nodes. A network analog comprised of 444 nodes was used for this. To determine φ_m [solution to an exterior problem for (1)] conformal mapping of the $\underline{z}$ plane on the $\underline{w}$ plane was performed using the function

$$w = \frac{c}{z - z_0}, \qquad (3)$$

where $\underline{c}$ is an arbitrary constant (here we took $c = 24$), and z_0 is a complex number specifying the position of the origin in the plane.

To simplify the problem the origin was taken as being at the center of the circle, i.e., $z_0 = 0$.

The relation between the w- and z-plane coordinates if found from

$$w = \xi + i\eta = \frac{k}{z} = \frac{k}{x + iy} . \tag{4}$$

Hence

$$\xi = \frac{kx}{x^2 + y^2} , \quad \eta = \frac{-ky}{x^2 + y^2} . \tag{5}$$

Thus the exterior problem in the $\underline{z}$ region goes over to the interior one for the $\underline{w}$ region, and the finite-difference method and the one presented above can be applied directly to solve internal problems using electrical analogs with fewer nodes. When the infinite region bounded by C_1 and C_2 is conformally mapped it goes over to the region bounded by the curves C_3 and C_4 (Fig. 4) in the $\underline{w}$ plane, $z = \infty$ going over to $w = 0$. C_3 and C_4 in $\underline{w}$ are appropriately approximated on the network. The boundary nodes are assigned the values at the closest points where the grid intersects the curve (Fig. 4).

In this case the boundary conditions for the curves approximating to C_3 and C_4 are corrected simultaneously as above, using (2). Three corrections suffice for C_3, with C_4 requiring six.

Figure 4 gives the potentials measured at the nodes for this field region.

The potentials given in Fig. 3 are enclosed between C_4 and the dashed line in Fig. 4. When a point in the z-plane did not lie at a node in the w-plane a linear interpolator (ten-step resistance voltage divider) was used to determine the potential. The potential distribution in the z-plane can be determined using (4) and (5). Figure 3 shows the results obtained with large and small models for this instance. The figures above the line were determined by the second method, which is exact, and below by the first. Figure 3 clearly shows that the discrepancies do not exceed 4%, which is within the limits to be expected from electrical network analogs.

The discrepancy between the measured potentials at point A in the $\underline{w}$ plane which is equivalent to $z = \infty$ lies within these limits as do the potentials found by the first method at the edge nodal points in the grid approximating the $\underline{z}$ region. Solution of exterior problems on (1) on small models by the first method* gives larger discrepancies, particularly at large distances from the areas about the bounding edges of C_3 and C_4, where the potentials are given.

Thus the method may be selected to suit the type of equipment when performing practical calculations on magnetic field distributions which amount to solution of exterior problems for Equation (1). With large equipments (more than 3500 nodes) it is advisable to use the first method, with small ones (some hundreds of nodal points) the second.

The experimental results so obtained for the magnetic potentials can be used to find the induction distribution over the bounding surface of the field and also for computing space permeabilities in the field by a published [3] method.

For the leakage field between core and armature of a telephone relay considered above, graphical integration of the normal component of the magnetic induction over the lower half and side surfaces of the armature gave a flux (relative units) of 101.75. As the region is symmetrical this value should be doubled, so the leakage flux per unit length of core will be

$$\frac{2 \times 101.75}{100} = 2.035.$$

The relative permeability per unit length of the air-gap between core and armature in a direction perpendicular to the section (Fig. 3) was 2.035.

These results were compared with Govorkov's, obtained by finite difference methods, and with Sotskov's, obtained by graphical field-mapping [6].

The magnetic permeabilities obtained for this case by these methods in [6] are respectively, finite-difference

* Without prior conformal mapping of the $\underline{z}$ plane on the $\underline{w}$ plane.

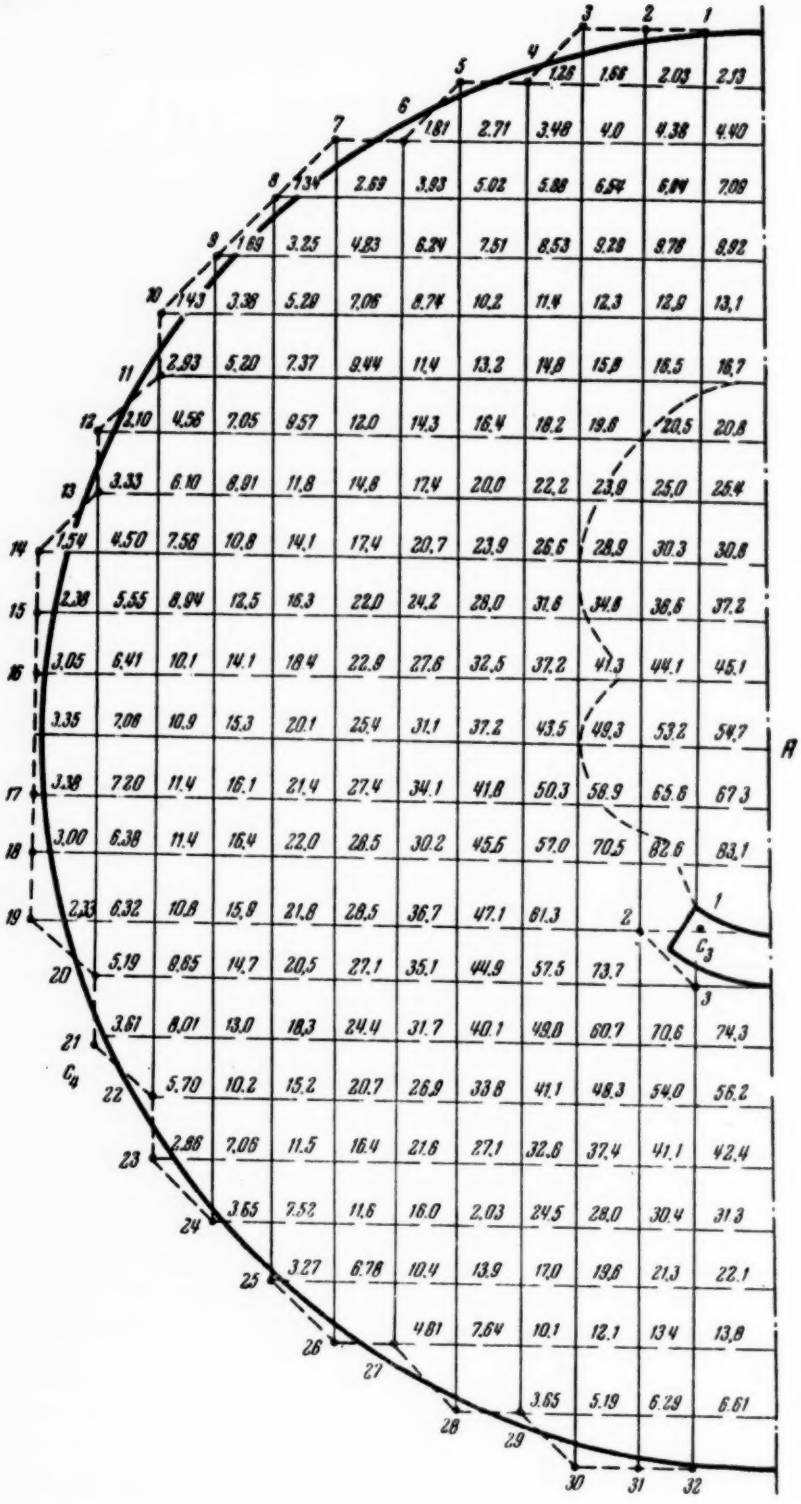

Fig. 4. Distribution of φ_m in the leakage field (the experiments were done on small equipments after conformal mapping).

2.025, graphical mapping 1.75-1.9. The lower results in the latter case are due to the difficulties of the graphical construction. The external region was restricted in Govorkov's calculations and the potentials were assumed. This also explains the discrepancies in the potential values within the region we found by two different methods, and Govorkov's, on the one hand, and our own on setting up the problem as an interior one of (5) on the other. The data of Figure 3 show that the potential is not constant on a straight line projecting downwards from the center of the core. An erroneous assumption is made in [3]: this line is taken as a line of constant (zero) potential. This assumption affects the potentials found at other points.

The fairly good agreement between the permeability values obtained by finding the potential distribution on analogs by these two method suggested and those found by the finite-differences [3] can only be explained by the leakage flux being determined using potentials near the edge of C_1, where the boundary values were given. There are considerable divergences in the field mapping over the whole region.

In graphical mapping calculations the practicable construction encompassed a smaller region of field than did ours, as Govorkov correctly remarks, and errors were expected, but no prior estimate of these could be made.

The experimental method of studying magnetic fields on electrical analogs is a powerful tool in designing and computing the optimum parameters of the electromagnetic mechanisms which are used in automatic electrical devices.

Received October 29, 1956

LITERATURE CITED

[1] K. Shmiedel, Wirkungsweise und Entwurf der Motor-Elektrizitätszähler (1916).

[2] W. Cramp and W. Colderwood, The Calculation of Air-Space Flux, Journ. In. El. Engrs. Vol. 61, No. 323 (October, 1923).

[3] V. A. Govorkov, Calculation of electrical and magnetic fields by potential network methods. Elektrichestvo No. 3 (1949).

[4] L. I. Gutenmakher, L. G. Kogan and I. N. Popov, Electromagnetic calculations on an integrator. Elektrichestvo No. 11 (1945).

[5] S. A. Aleskerov and K. M. Chal'ian, Calculation of the magnetic fields of electromagnetic mechanisms on an EM-8 electrical analog. Doklady Akad. Nauk Azerb. SSR 10, No. 8 (1954).

[6] B. S. Sotskov, Components of remote control and automatic apparatus. Oborongiz (1938).

[7] G. A. Grinberg, Selected topics in the mathematical theory of electrical and magnetic phenomena. Izd. Akad. Nauk (1948).

[8] D. Iu. Panov, Sourcebook on the numerical solution of differential equations in partial derivatives. (1951).

THE MOTION OF A LOADED HYDRAULIC ACTUATOR WITH A FEEDBACK LOOP

V. A. Khokhlov

(Moscow)

The motion of a loaded hydraulic actuator mechanism with a feedback loop is analyzed assuming constant positional and inertial loadings on the piston. It is demonstrated that the equation of continuity for the liquid flow, which determines the piston motion, is only correct if the inertial mass of the load does not exceed a critical value. An equation for calculating the critical mass is given.

1. Introduction

When control systems containing hydraulic actuators regulated by restrictors (or throttles) are analyzed and synthesized, the actuators are usually considered as ideal integrating links. The load acting on the piston is neglected, as are such factors as liquid leakage, oil compressibility and pipeline deformation. But in some cases these factors must be allowed for in the analysis. External loads – inertial and positional (spring) – are usually of particular interest. The piston motion when these forces act and the restrictor is suddenly displaced by a fixed amount has been adequately dealt with [1, 2]. But this case is not typical of control systems. When a feedback link is present in the actuator, the control valves do not remain in a fixed position.

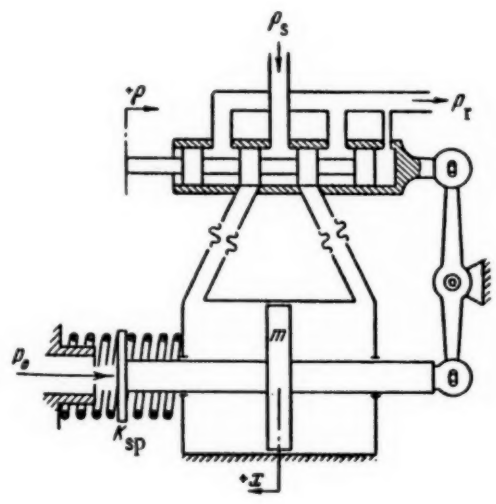

Fig. 1.

The feedback has been allowed for in several papers (e. g., [3, 4]). The restrictor losses are not evaluated vigorously in [3] and the transient response is not analyzed. This latter topic is dealt with for the case of a load plus feedback in [4], but the fact that the supply and return lines connected to the cylinders change places when the restrictor passes through the center position is neglected.

A typical hydraulic actuator is shown in Figure 1. The following assumption are made: the leakages in the restrictor and pump are zero, the restrictor shows no overlap, the liquid is incompressible, and the discharge factor for the flow through the restrictor opening is constant.

2. Equation of Motion of the Hydraulic Actuator

First let us consider the equation for zero load and zero feedback. In this case the piston velocity is (see, e. g., [5]) given by

$$v = \mu \sqrt{\frac{g}{\gamma}} \sqrt{p_s - p_{cr}} \frac{f}{F},$$

where p_s is the pressure in the supply line, p_r that in the return line, μ the discharge factor, $\underline{t}$ the actual area of the restrictor opening, and F the effective piston area.

When the restrictor opening is rectangular in shape, the above equation takes the form

$$v = \mu \sqrt{\frac{g}{\gamma}} \frac{l}{F} \sqrt{p_s - p_{cr}}\, \rho,$$

where l is the length of the working aperture in the restrictor and ρ the restrictor displacement.

This equation shows that the direction of piston motion is determined by the sign of the restrictor displacement from the center position. This means that the supply and takeoff cylinders change places when the throttle moves to opposite sides of the center position (v = 0). Hence the second equation should be more strictly written as

$$v = \mu \sqrt{\frac{g}{\gamma}} \frac{l}{F} \sqrt{|(p_s - p_{cr}) \operatorname{sign} \rho|}\, \rho. \tag{1}$$

Let us consider the actuator motion when the piston has a finite mass and is subject to external loading. Then the pressure difference between the cylinders will not be zero, being

$$\Delta p = \frac{m\frac{d^2x}{dt^2} + h\frac{dx}{dt} + k_{sp}x + P_0}{F}, \tag{2}$$

where $\underline{x}$ is the piston coordinate, $\underline{m}$ the mass, $\underline{h}$ the coefficient of viscous friction, k_{sp} the rigidity factor of the spring load and P_0 the constant load.

When external forces act, the pressure drop in the throttle openings, and hence the piston speed, is altered. From (1) and [5] we get the speed as

$$\frac{dx}{dt} = \mu \sqrt{\frac{g}{\gamma}} \frac{l}{F} \sqrt{|(p_s - p_{cr}) \operatorname{sign} \rho - \Delta p|}\, \rho.$$

For subsequent use it is more convenient to have the equation in another form, namely

$$\frac{dx}{dt} = \mu \sqrt{\frac{g}{\gamma}} \frac{l}{F} \sqrt{|(p_s - p_{cr}) - \Delta p \operatorname{sign} \rho|}\, \rho. \tag{3}$$

When the actuator operates solely as a motor we have

$$p_s - p_{cr} > \Delta p \operatorname{sign} \rho. \tag{4}$$

Equation (3) for the motion of an open-loop loaded hydraulic actuator can be put in the form

$$\frac{dx}{dt} = \mu \sqrt{\frac{g}{\gamma}} \frac{l}{F} \sqrt{p_0 - \Delta p \operatorname{sign} \rho}\, \rho, \tag{5}$$

where $p_0 = p_s - p_r$.

3. Stability and Transient Responses in a Loaded Hydraulic Actuator with Error Feedback

A. Piston loaded by a constant force P_0. In this case the motion is determined by the open-loop equation

$$\frac{dx}{dt} = \mu \sqrt{\frac{g}{\gamma}} \frac{l}{F} \sqrt{p_0 - \frac{P_0}{F} \operatorname{sign} \varepsilon}\, \varepsilon$$

and by the feedback equation

$$\epsilon = \rho - k_{fb} x,$$

where ϵ is the tracking error and k_{fb} the feedback coefficient. Combining these equations we get

$$\frac{dx}{dt} + \mu \sqrt{\frac{g}{\gamma}} \frac{l}{F} k_{fb} \sqrt{p_0 - \frac{P_0}{F} \operatorname{sign} \varepsilon}\, x = \mu \sqrt{\frac{g}{\gamma}} \frac{l}{F} \sqrt{p_0 - \frac{P_0}{F} \operatorname{sign} \varepsilon}\, \rho.$$

The motion produced by an initial deviation in x with $\rho(t) \equiv 0$, is defined by

$$\frac{dx}{dt} + \mu \sqrt{\frac{g}{\gamma}} \frac{l}{F} k_{fb} \sqrt{p_0 - \frac{P_0}{F} \operatorname{sign} \varepsilon}\, x = 0.$$

If the throttle overlaps are zero

$$\operatorname{sign} \varepsilon = \operatorname{sign} \frac{dx}{dt}. \tag{6}$$

Then

$$\frac{dx}{dt} + \mu \sqrt{\frac{g}{\gamma}} \frac{l}{F} k_{fb} \sqrt{p_0 - \frac{P_0}{F} \operatorname{sign} \frac{dx}{dt}}\, x = 0. \tag{7}$$

The motion of the image point in the phase plane (x, $v = \frac{dx}{dt}$), as defined by the nonlinear differential Equation (7), is shown in Figure 2; it is clear that the hydraulic actuator plus feedback, loaded with a fixed load, is stable.

Here the external forces only affect the slope of the velocity characteristic, i. e., alter the gain. The transient response to a step-function is exponential with a time constant dependent on the external force.

B. Piston loaded by a position-dependent spring load. In this case the equation of motion for actuator plus feedback becomes

$$\begin{aligned} \frac{dx}{dt} + \mu \sqrt{\frac{g}{\gamma}} \frac{l}{F} k_{fb} \sqrt{p_0 - \frac{k_{sp} x}{F} \operatorname{sign} \frac{dx}{dt}}\, x = \\ = \mu \sqrt{\frac{g}{\gamma}} \frac{l}{F} \sqrt{p_0 - \frac{k_{sp} x}{F} \operatorname{sign} \frac{dx}{dt}}\, \rho. \end{aligned} \tag{8}$$

When $\rho = 0$, we have

$$\frac{dx}{dt} + \mu \sqrt{\frac{g}{\gamma}} \frac{l}{F} k_{fb} \sqrt{p_0 - \frac{k_{sp} x}{F} \operatorname{sign} \frac{dx}{dt}}\, x = 0. \tag{8a}$$

Figure 3 shows the phase diagram for the motion of the system defined by the nonlinear Equation (8a); it is clear that the system remains stable no matter what the restoring-force constant. A load of this type only serves to reduce the gain when the piston is displaced.

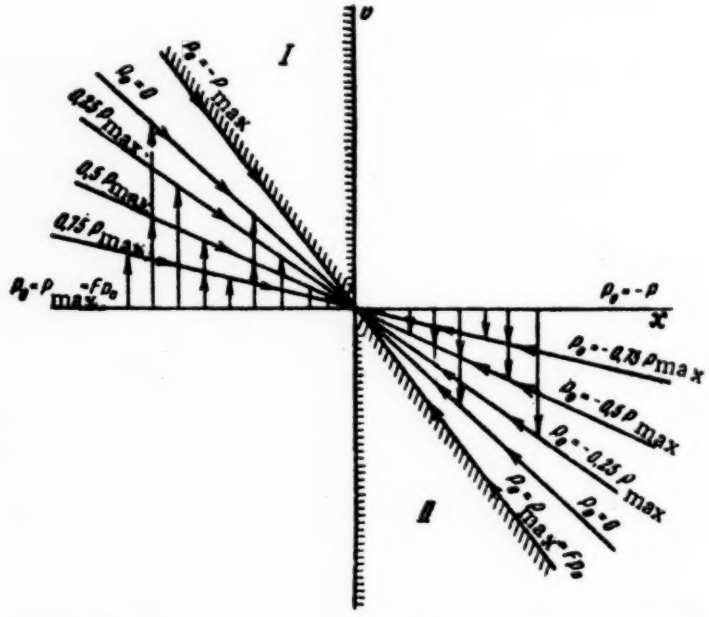

Fig. 2. Phase diagram for a system with a fixed load. I) Region of cavitation in the right-hand half-cylinder; II) ditto for left-hand half-cylinder.

To determine the transient response we integrate (8). Putting $\mu \sqrt{\frac{g}{\gamma}} \frac{l}{F} = k$ and assuming $\frac{dx}{dt} > 0$, we get

$$\frac{dx}{k \sqrt{\frac{k_{sp}}{F}} \sqrt{p_0 \frac{F}{k_{sp}} - x}\, k_{fb} \left(\frac{\rho}{k_{fb}} - x \right)} = dt.$$

The integration will be performed for the case where the throttle is instantaneously displaced from $\rho = 0$ to $\rho = \rho^* = p_0 \frac{F}{k_{sp}} \cdot k_{fb}$ $(\epsilon > 0)$:

$$\int \frac{dx}{k k_{fb} \sqrt{\frac{k_{sp}}{F}} \sqrt{p_0 \frac{F}{k_{sp}} - x} \left(p_0 \frac{F}{k_{sp}} - x \right)} = t + c,$$

or

$$\frac{2}{kk_{fb}\sqrt{\frac{k_{sp}}{F}}\sqrt{p_0\frac{F}{k_{sp}}-x}}=t+c.$$

Let us determine the constant of integration. Let x = 0 at t = 0. Then $c=\frac{2}{kk_{fb}\sqrt{p_0}}$, and the solution takes the form

$$x=p_0\frac{F}{k_{sp}}\left[1-\frac{4}{(2+\sqrt{p_0}\,kk_{fb}\,t)^2}\right]. \tag{9}$$

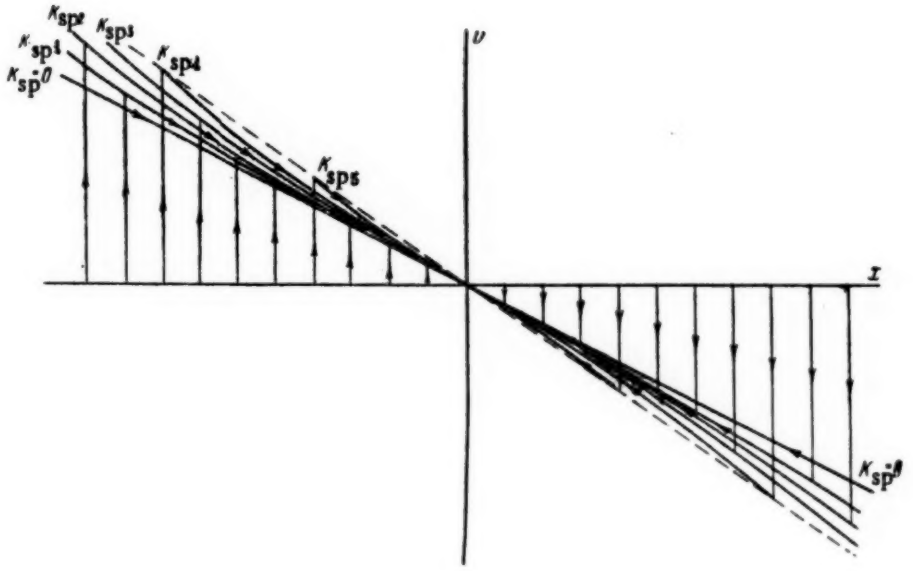

Fig. 3. Phase diagram for a system with a position-dependent load: $k_{sp5} > k_{sp4} > k_{sp3} > k_{sp2} > k_{sp1} > 0$.

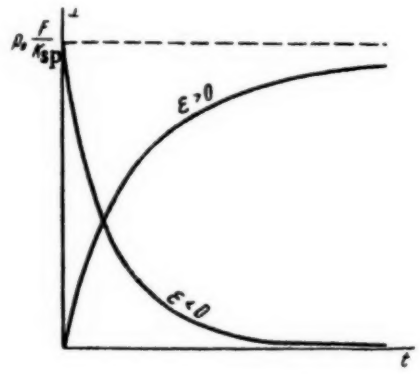

Fig. 4.

Figure 4 shows the transient response defined by (9). Now suppose the throttle is instantaneously displaced from $\rho = \rho^* = p_0\frac{F}{k_{sp}}k_{fb}$ to $\rho = 0$. Here $\epsilon < 0$, so the equation of motion of the actuator plus feedback becomes

$$\frac{dx}{dt}=k\sqrt{p_0+\frac{k_{sp}x}{F}}(-k_{fb}x).$$

Integration then gives

$$\frac{1}{kk_{fb}\sqrt{p_0}}\ln\frac{\sqrt{p_0+\frac{k_{sp}}{F}x}-\sqrt{p_0}}{\sqrt{p_0+\frac{k_{sp}}{F}x}+\sqrt{p_0}}=-t+c.$$

With the above initial condition we have $c=\frac{\ln 0{,}17}{kk_{fb}\sqrt{p_0}}$, but the solution takes the form

$$x=\frac{p_0F}{k_{sp}}\left[\left(\frac{1+0{,}17\,e^{-kk_{fb}\sqrt{p_0}\,t}}{1-0{,}17\,e^{-kk_{fb}\sqrt{p_0}\,t}}\right)^2-1\right]. \tag{10}$$

Figure 4 shows the transient response defined by (10).

C. Piston subject to an inertial load. In this case the equation of motion for actuator plus feedback becomes

$$\frac{dx}{dt}+\mu\sqrt{\frac{g}{\gamma}}\frac{l}{F}k_{fb}\sqrt{p_0-\frac{m}{F}\frac{d^2x}{dt^2}\operatorname{sign}\frac{dx}{dt}}\,x=$$
$$=\mu\sqrt{\frac{g}{\gamma}}\frac{l}{F}\sqrt{p_0-\frac{m}{F}\frac{d^2x}{dt^2}\operatorname{sign}\frac{dx}{dt}}\,p. \tag{11}$$

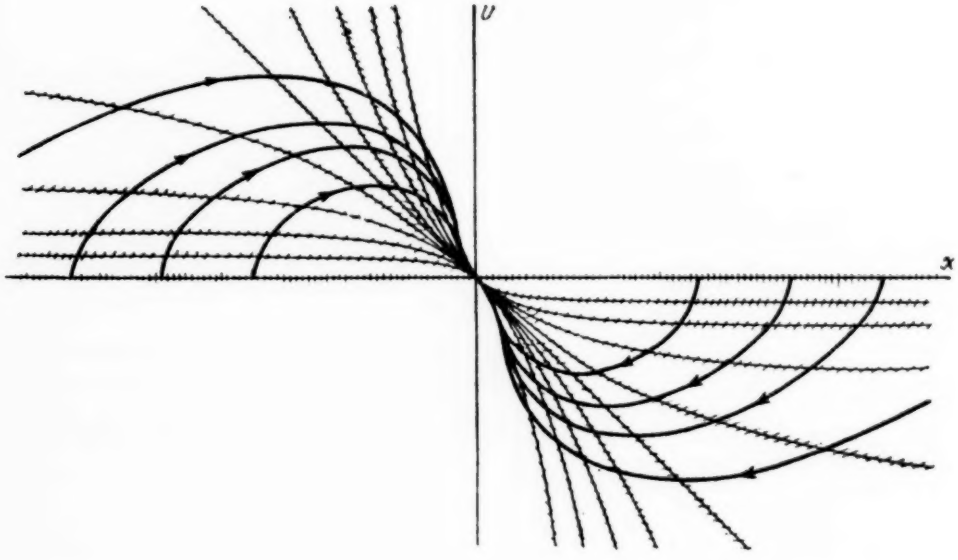

Fig. 5. Phase diagram for the system subject to an inertial load.

Let us consider only free motion. Phase-plane analysis will be used.

Using the same notation as before we get

$$v + kk_{fb}\sqrt{p_0}\sqrt{1 - \frac{m}{Fp_0}\frac{dv}{dx}v}\,\text{sign}\,v\,x = 0. \tag{12}$$

The phase diagram defined by (12) will be drawn up by isocline methods. For this we put $\frac{dv}{dx} = c$. Then the isocline equation takes the form

$$v = kk_{fb}\sqrt{p_0}\sqrt{1 + \frac{m}{Fp_0}cv}\,\text{sign}\,v\,x = 0.$$

By taking different values for c we get a family of isoclines. This family is shown in Fig. 5, as well as the phase trajectories of the system.

The nature of the phase trajectories shows that the system is stable for all inertial loads. But this is not found to be so by experiment. In practice it is found that increasing the inertial loading on a hydraulic servo causes it to perform continuous oscillations. We may suppose this to be due to neglect of oil compressibility, pipe extensibility, transfer mechanism distortion, give in the fixings, etc., in the theoretical analysis. It is usually rather difficult to incorporate these factors into the theoretical analysis. Even when special measures are taken by which design defects such as lack of rigidity, etc., are eliminated and the system made to operate with small pressure changes so that compressibility is negligible, the theoretical and experimental results are still discrepant.

Let us consider one cause of such discrepancies which can be allowed for precisely. It has been shown [5] that the pressures in the working cylinders of the actuator are redistributed when the piston propels an external load (including an inertial one). It is clear that the pressure in the cylinders during acceleration cannot exceed that in the supply line or fall below zero. But in deceleration the high load inertia may cause the pressure in the chamber to fall below atmospheric. The piston then breaks away from the liquid and cavitation bubbles form. No discontinuity will occur if

$$-\frac{m}{F}\frac{d^2x}{dt^2}\,\text{sign}\,\frac{dx}{dt} \leqslant p_0.$$

The limiting mass with respect to the piston at which no cavitation occurs will be termed critical. Since mineral oils show cavitation at pressures below atmospheric, the critical mass is given by

$$m_{cr} = \frac{p_0F}{\left|\left(\frac{d^2x}{dt^2}\right)_{max}\right|} \quad \text{or} \quad m_{cr} = \frac{p_0F}{\left|\left(\frac{dv}{d\varepsilon}\frac{d\varepsilon}{dt}\right)_{max}\right|}.$$

To compute the critical mass we must determine the largest rate of piston-speed reduction or the maximum of $\left(\frac{dv}{d\varepsilon}\frac{d\varepsilon}{dt}\right)$. The solution of this problem presents a certain amount of difficulty: it cannot be expressed in terms of system parameters. Thus to compute the critical mass we assume

$$\left|\left(\frac{dv}{d\varepsilon}\frac{d\varepsilon}{dt}\right)_{max}\right| = \left|\left(\frac{dv}{d\varepsilon}\right)_{max}\right|\left|\left(\frac{d\varepsilon}{dt}\right)_{max}\right|.$$

Since the product of the maxima of two functions is greater than the maximum of the product, the value found for the critical mass on the above assumptions is bound to ensure absence of cavitation.

When ρ const

$$\left|\frac{d\epsilon}{dt}\right| = k_{fb}\left|\frac{dx}{dt}\right|.$$

Then

$$\left|\left(\frac{d^2x}{dt^2}\right)_{max}\right| = \left|\left(\frac{dv}{d\epsilon}\right)_{max} v_{max}\right| k_{fb}$$

where $\left(\frac{dv}{d\epsilon}\right)_{max}$ is the maximum slope of the speed characteristic for the actuator and v_{max} is the maximum piston speed.

The maximum slope of the speed characteristic for the actuator in deceleration is defined by

$$\left|\left(\frac{dv}{d\epsilon}\right)_{max}\right| = \sqrt{2}\left|\left(\frac{dv}{d\epsilon}\right)\right|,$$

where $\left(\frac{dv}{d\epsilon}\right)_{nl}$ is the no-load speed characteristic slope.

The increase in the speed characteristic slope by a factor $\sqrt{2}$ relative to no-load on deceleration is due to a pressure drop in the throttle being doubled.

Hence the critical mass (referred to the piston) for flow discontinuity to be absent in this system is given by

$$m_{cr} = \frac{p_0 F}{\sqrt{2} k_{fb}\left|\left(\frac{dv}{d\epsilon}\right)_{nl} v_{max}\right|}. \qquad (13)$$

If the actuator is a rotary one (with direct feedback) the critical moment of inertia is given by an analogous expression

$$J_{cr} = \frac{p_0 q}{\sqrt{2} k_{fbl}\left|\left(\frac{d\omega}{d\epsilon}\right)_{nl} \omega_{max}\right|}, \qquad (14)$$

where q is the specific volume of the hydraulic motor, k_{fbl} is the feedback factor, $\left(\frac{d\omega}{d\epsilon}\right)_{nl}$ is the slope of the actuator speed characteristic at no-load on the motor and ω_{max} is the (low) angular velocity of the motor.

The above analysis shows why the theoretical and experimental results diverge for automatic control systems using hydraulic actuators with inertial loads in excess of the critical.

SUMMARY

1. A spring load acting on the piston of a hydraulic actuator with error feedback reduces the gain of the system.

2. The responses of an automatic control system with a throttle-controlled hydraulic actuator should not be analyzed till the mass (referred to the piston) has been compared with the critical value.

If the mass is above the critical value, the analytical results will be incorrect because cavitation can occur in the working fluid.

LITERATURE CITED

[1] M. A. Aizerman, Transmitter switching automatics. Mashgiz, 1948.

[2] Iu. P. Portnov-Sokolov, The motion of a hydraulic piston actuator subject to typical loads. Collected papers on automation and remote control, Izd. Akad. Nauk, SSSR 1953.

[3] Z. Sh. Blokh, The Theory of Servomotors in Hydraulic Drives. Izv. Akad. Nauk SSSR, Otdel. Tekho Nauk, No. 2, 1947.

[4] B. L. Korobochkii, Study of the Hydraulic Servos in Copying Machines. Dissertation submitted for the science degree of candidate in technical sciences. Stankin, 1954.

[5] V. A. Khokhlov, "Speed characteristics of throttle-controlled hydraulic actuator mechanisms." Automatika i telemkhanika 16, No. 5, 1955.

Received February 6, 1957

A RELAY AUTOMATIC POSITION CONTROL SYSTEM USING A COMPOUND-WOUND MOTOR

V. V. Gorskii

(Moscow)

A relay automatic position control system using a compound-wound motor as the actuator is considered.

The formulas for determining the output shaft speed and rotation angle during follow-up are deduced. Motor transients are analyzed with allowance for magnetic saturation.

The nonlinear velocity feedback law giving the minimum insensitive zone and zero overshoot is determined.

The velocity feedback voltage converter unit is described, together with the method of connection.

This relay system is considered to be close to optimal.

INTRODUCTION

Relay automatic control systems have several well-known advantages over those using continuous control. One of these is that the follow-up time can be minimized.

Many highly developed relay systems are known [1-5]. Of these, the so-called "optimal systems" are of great interest: in these, the transient response is given a preset optimal form by introducing nonlinear velocity feedbacks [2]. But when optimal systems are being designed not only should internal nonlinear feedbacks be used, leaving the system unchanged, but the properties of all elements should be correctly chosen and maximally utilized.

One of the ways of improving response time of systems is by using compound-wound dc motors. The series winding increases the starting torque considerably and hence reduces the follow-up time.

We consider here such a relay system, the motor run-up being analyzed with allowance for magnetic saturation.

To ensure very close follow-up and zero overshoot, nonlinear velocity feedback is used.

1. Description of System

Figure 1 shows the theoretical circuit. The error voltage taken from the measuring bridge diagonal and the nonlinear feedback voltage are fed to an RP-5 polarized relay which controls the reversing contactor RK. The motor armature rotates the controlled object and feedback potentiometer wiper via the reducing gear K_r. The insensitive zone in the three-position RP-5 relay (Fig. 2) enables one to eliminate the small-amplitude hunting that occurs with two-position relays. Hunting is undesirable here because the motor starting currents are large.

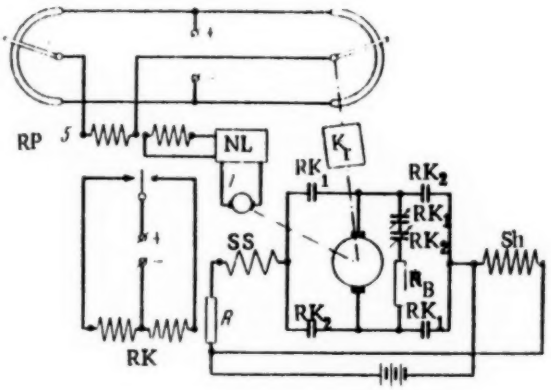

Fig. 1. Theoretical circuit of the compound-wound motor servo: Sh is the shunt winding, Ss the series winding, T the tachometer, NE a nonlinear element, RK_1 and RK_2 the reversing contacts of RK, R the armature impedance, R_B the braking resistance.

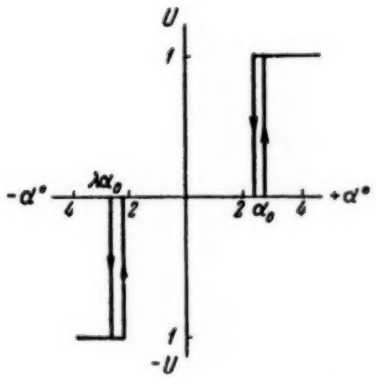

Fig. 2. Characteristic of RP-5 relays.

When the contacts of RP-5 and RK open, the motor is dynamically braked. We have considered dynamic braking with the series winding cut out solely because RK did not have an extra contact to connect the series winding to the shunt during dynamic braking. The braking time is reduced by making the braking resistance as small as the maximum permissible commutation current allows. Thus the motor circuit varies while the angle is being followed up, hence two different motor operating conditions must be distinguished. The first is when the motor accelerates and runs at a constant speed, the second when the motor is dynamically braked via the shunt winding.

Since the systems of equations describing these two modes are different, each will be considered separately.

2. First mode

The runup process in a dc motor is usually divided into three stages [6]; the first corresponds to the current rising to some value at which the motor starts while the armature is still; the second to the time interval between the motor starting and the current reaching its maximum value; the third to the current falling from the maximum and the motor speed rising to a steady value.

Solely for simplicity we neglect the first two stages, since they occupy only a minute fraction of the total run-up time (see Fig. 5, which illustrates the start-up) and only stage three is considered.

Since the rate of current fall is comparatively low in stage three we can neglect the emf due to armature and series winding inductances [6] relative to the voltage drop in the resistance and the back emf.

If we also neglect the eddy currents, hysteresis, armature reaction and relay and reversing contactor operating times, the equations for an automatic control system using a motor working in the first mode are as follows:

error equation

$$\theta = \theta_s - \theta_{fb}; \tag{1}$$

the equation for the element which converts the error angle into the error voltage:

$$\Delta U_0 = k_0 \theta = \frac{k_0}{\alpha_M} \alpha; \tag{2}$$

the equation for the relay element which switches in RP-5 and RK (assuming for simplicity $\lambda = 1$):

$$u = f[\Delta U_0 - \Delta U(\varphi)] = \begin{cases} 1 \text{ when } \Delta U_0 - \Delta U(\varphi) > \Delta U_{0*}, \\ 0 \text{ when } |\Delta U_0 - \Delta U(\varphi)| < \Delta U_{0*}, \\ -1 \text{ when } \Delta U_0 - \Delta U(\varphi) < -\Delta U_{0*}; \end{cases} \tag{3}$$

the equation for the electrical circuit of the motor

$$u = i\rho + k\varphi\psi, \tag{4}$$

where k is a coefficient of proportionality:

the equation for the magnetic flux in the motor

$$\psi = \psi_0 + \psi(i); \tag{5}$$

the equation of motion for the rotation masses

$$\frac{d\varphi}{d\tau} = i\psi - \mu_r; \tag{6}$$

the equation for the angle of rotation

$$\delta \frac{d\theta}{d\tau} = \varphi. \tag{7}$$

In (1) - (7), $\theta_s = \alpha_s / \alpha_M$ is the relative set angle, $\theta_{fb} = \alpha_{fb} / \alpha_M$ is the relative follow-up angle, $\theta = \alpha / \alpha_M$ is the relative angle of rotation, α and α_M are the actual and maximum angles of rotation of the output shaft, k_θ is the converter element coefficient, $u = U/U_n$ is the relative value of the voltage U, $i = I/I_n$ is the relative value of the current I, $\rho = R/R_n = RI_n/U_n$ is the relative value of the resistance R of the entire armature circuit, $\varphi = \omega/\omega_n$ is the relative value of the angular velocity ω, $\psi = \Phi/\Phi_n$ is the relative value of the magnetic flux Φ, $\mu_r = M_r/M_n$ is the relative value of the resistance torque, $\theta_\theta = \alpha_\theta / \alpha_M$ is the relative value of the relay insensitive zone, α_θ, $\tau = t/T$ is the relative time, $T = J\omega_n / M_n$ is the time-constant, J the reference moment of inertia of all rotating parts, $\delta = \alpha_M k_r / T\omega_n$, k_r being the reducing gear reduction factor, $\Delta U(\varphi)$ is the voltage from the nonlinear velocity feedback, and λ is the relay return coefficient.

The subscript n denotes nominal values.

The first mode occurs with the relay contacts closed, i. e.,

$$u = f[\Delta U_0 - \Delta U(\varphi)] = 1.$$

The magnetic flux is produced by both series and shunt windings. Let us approximate the magnetization curve by a rational-fraction function

$$\psi = \psi_0 + \frac{bi}{1 + ci}, \tag{5'}$$

where ψ_θ is the magnetic flux produced by the magnetomotive force from the shunt winding $(mmf)_0$, $bi/1 + ci = \psi_s$ is the magnetic flux produced by the magnetomotive force from the series winding $(mmf)_s$.

The coefficients b and c are determined from the magnetization curve. Figure 3 shows the curve and the flux distribution between windings when their mmfs are equal with nominal conditions applying. To determine

the run-up curve we must therefore solve (4), (5') and (6) simultaneously.

To solve this system of nonlinear equations we will simplify (4).

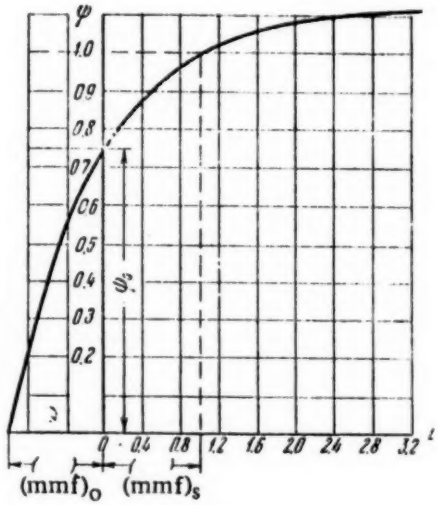

Fig. 3. Magnetization curve of the compound motor.

$$\psi = \psi_0 + \frac{bi}{1 + ci} = 0.75 + \frac{0.51i}{1+1.1i}$$

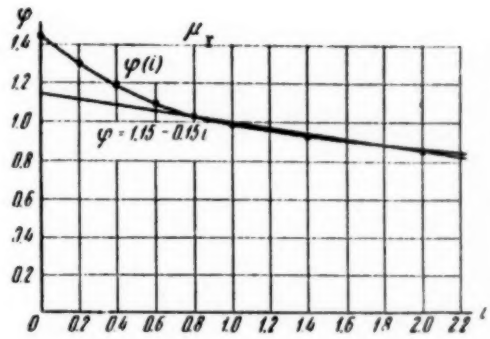

Fig. 4. φ(i) for the compound motor and the approximating straight line

$$\varphi = \varphi_0 - k_\varphi i = 1.15 - 0.15i$$

Figure 4 shows the actual mechanical characteristics for a compound motor with equal shunt and series mmfs and $\varphi = 1$. This curve is approximately a hyperbola. But in the high-current region the hyperbola can be approximated by the straight line $\varphi = \varphi_0 - k_\varphi i$ (Fig. 4) with quite sufficient accuracy in practice. When the motor starts under load ($\mu_r = 1$) the working range will be a rectilinear section of the mechanical characteristic.

Multiplying both parts of $\varphi = \varphi_0 - k_\varphi i$ by k_ω, the coefficient of proportionality between voltage and rotation speed, we get

$$u = k_\omega \varphi_0 = k_\varphi k_\omega i + k_\omega \varphi = \rho^* i + k_\omega \varphi, \tag{4'}$$

where $\rho^* = k_\varphi k_\omega$ is some equivalent resistance. Figure 4 shows that the error in this linearization increases as μ_r falls, or, what is the same, as the steady-state current falls.

Eliminating the intermediate variables from (4'), (5') and (6), we get the following differential equation for φ:

$$\frac{d\varphi}{d\tau} - k_1^2 (\psi_0 c + b) \frac{\varphi^2 - A\varphi + B}{d - ck_1\varphi} = 0, \tag{8}$$

or

$$\frac{(d - ck_1\varphi)\, d\varphi}{k_1^2 (\psi_0 c + b)(\varphi^2 - A\varphi + B)} = d\tau, \tag{8'}$$

where

$$k_1 = \frac{k_\omega}{\rho^*}, \quad d = 1 + ci_k, \quad i_k = \frac{u}{\rho^*},$$

$$A = \frac{\psi_0 (d + ci_k) + 2bi_k - \mu_r c}{k_1 (\psi_0 c + b)}, \quad B = \frac{bi_k^2 + d (\psi_0 i_k - \mu_r)}{k_1^2 (\psi_0 c + b)}.$$

The differential equation of (8) is easily integrated.

The final form of the solution depends on the character of the roots of the denominator in the LHS of (8') [7]. For simple real roots the final solution is

$$\tau = \frac{D}{\varphi_2 - \varphi_3} \left[(\varphi_2 - \varphi_1) \ln \frac{\varphi - \varphi_2}{\varphi_{in} - \varphi_2} - (\varphi_3 - \varphi_1) \ln \frac{\varphi - \varphi_3}{\varphi_{in} - \varphi_3} \right], \tag{9}$$

where $\varphi_1 = d/ck_1$, φ_2 and φ_3 are the roots of $\varphi^2 - A\varphi + B = 0$, $D = -\frac{c}{k_1 (\psi_0 c + b)}$, φ_{in} being the initial rotation rate.

Equation (9) is not soluble for φ, and the way θ varies with time is determined by integrating $\varphi(\tau)$ graphically.

Another method of determining $\theta(\tau)$ is to use the phase trajectory equation $\theta(\varphi)$ for the first mode (see Section 5).

3. Second Mode

As we remarked above, dynamic braking occurs when the contacts of RP-5 open. The motor armature is short-circuited via R_B. The system of equations is then

error equation

$$\theta = \theta_s - \theta_{fb}; \tag{1'}$$

converter equation

$$\Delta U_0 = k_0 \theta; \tag{2'}$$

relay element equation

$$u = f[\Delta U_0 - \Delta U(\varphi)] = 0; \tag{3'}$$

electric circuit of motor

$$0 \approx -\rho_B i + k_\omega^* \varphi; \tag{4''}$$

magnetic flux equation

$$\psi = \psi_0; \tag{5''}$$

equation of motion for the rotating mass

$$\frac{d\varphi}{d\tau} = -i\psi - \mu_r; \tag{6''}$$

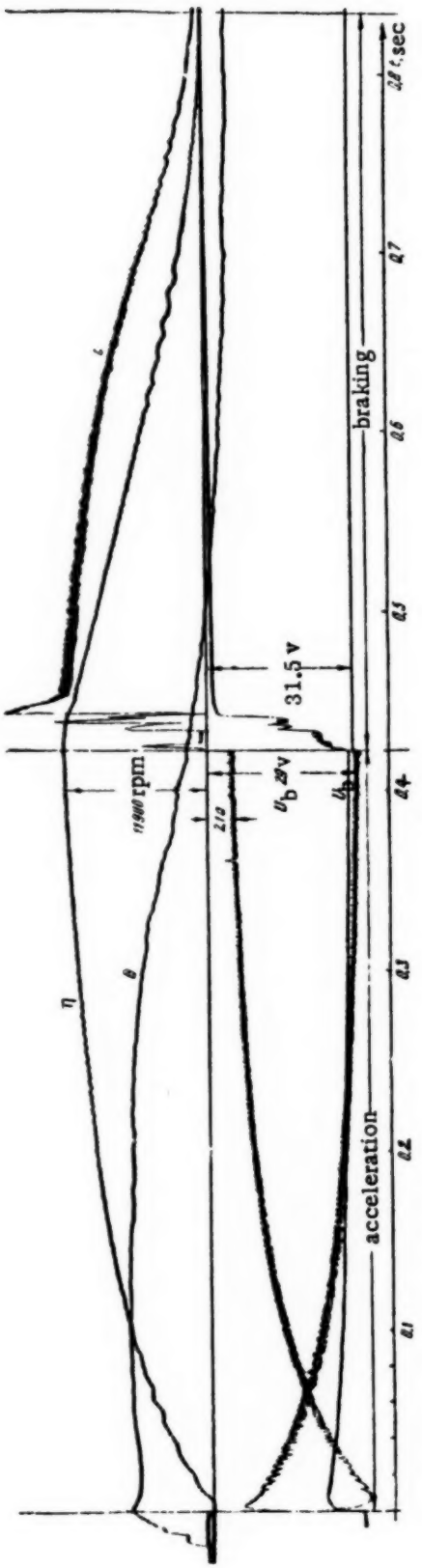

Fig. 5.

equation for the angle of rotation

$$\delta \frac{d\theta}{d\tau} = \varphi. \qquad (7')$$

Here ρ_B is the relative armature resistance during braking, k^*_ω that part of coefficient k_ω in (4') determined by the magnetic flux $\psi = \psi_0$.

Solving (4"), (5") and (6') for φ we get

$$\varphi = \varphi_{in} e^{-\beta\tau} - \varphi_\mu (1 - e^{-\beta\tau}), \quad (10)$$

where φ_{in} is the initial rotation speed on braking, $\beta = \psi_0 k_I^*$, $\varphi_\mu = \mu_r / \beta$, and $k_I^* = k^*_\omega / \rho_B$.

The way θ varies with time is found by integrating (7) and (10) together between limits θ_{in} ($\tau = 0$) to θ:

$$\theta - \theta_{in} =$$

$$= \frac{1}{\delta\beta} (\varphi_{in} + \varphi_\mu)(1 - e^{-\beta\tau}) - \frac{\varphi_\mu}{\delta} \tau. \quad (11)$$

These are the equations for $\varphi(\tau)$ and $\theta(\tau)$ during dynamic braking.

4. An Example of a Calculation, and Experimental Data

As an example we will consider the follow-up of an angle θ_s by the relay system of which the theoretical circuit is shown in Figure 1, for the case where velocity feedback is used.

Motor data: Nominal power P_n = 50 watts, nominal voltage U_n = 30 v, nominal current I_n = = 2.1 amps, nominal torque $M_n = 3.9 \times 10^{-3}$ kg·m, motor speed when loaded with $M_r = M_n$ being n = = 12,500 rpm, moment of inertia referred to the motor shaft $J = 3 \times 10^{-6}$ kg·m², armature resistance R_a = 0.8 ohm. Figure 3 shows the magnetization curve. Circuit parameters: accumulator emf U = 31.5 v, total armature circuit resistance $R = R_a + R_r$ = 2.0 ohms, braking resistance R_B = 1.3 ohms, reduction factor k_r = 3500. The characteristics of the RP-5 relay are given in Figure 2, recalculated to degrees rotation.

Figure 5 shows an oscillogram illustrating follow-up of an angle $\alpha_s = 7°15'$. The speed η, current I, source voltage U, brush voltage U_b and error angle θ, are shown. The acceleration and braking processes are seen. Relay delay time is 0.02 sec. Overshoot is not greater than 1° 10'.

Figure 6 shows computed acceleration, braking and angle α of the potentiometer slider when $\alpha_s = \theta_s \alpha_M \approx 7°$. The above formulas were used in the calculations. Curves derived from Figure 5 are also shown (by small circles). It is clear that when saturation is allowed for, the two are in good agreement.

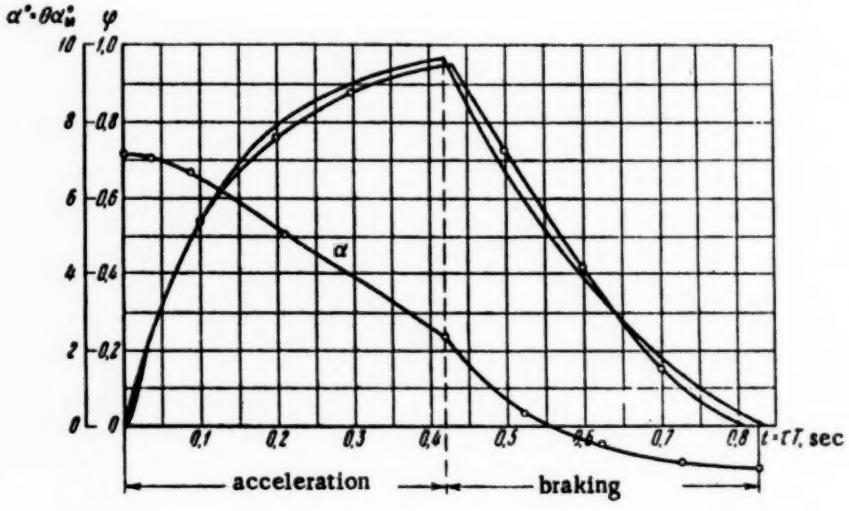

Fig. 6.

5. Phase Diagram of the System and Choice of Nonlinear Velocity Feedback Type

It is convenient to study stabilities and choose parameters for relay control systems by phase-plane methods.

Let us determine the phase trajectory equations for both modes.

First mode. The phase trajectory equations are found from (7) and (8) by elminating τ:

$$\frac{d\varphi}{d\theta} = \frac{\delta}{\varphi}\left[k_1^2(\psi_0 c + b)\ \frac{\varphi^2 - A\varphi + B}{d - ck_1\varphi}\right]. \tag{12}$$

Integrating (12) we get

$$\theta - \theta_{in} = \frac{D}{\delta}(\varphi - \varphi_{in}) + \frac{D}{\delta}\ \frac{1}{\varphi_2 - \varphi_3} \times$$
$$\times \left[\varphi_2(\varphi_2 - \varphi_1)\ln\frac{\varphi - \varphi_2}{\varphi_{in} - \varphi_2} - \varphi_3(\varphi_3 - \varphi_1)\ln\frac{\varphi - \varphi_3}{\varphi_{in} - \varphi_3}\right], \tag{13}$$

where θ_{in} and φ_{in} are the initial values.

This equation, taken with (9), can be used to determine $\theta(\tau)$.

Second mode. The phase trajectory equations are found from (4"), (5"), (6') and (7):

$$\frac{d\varphi}{d\tau} = -(\psi_0 k_1^* \varphi + \mu_\tau) \text{and } \delta\frac{d\theta}{d\tau} = \varphi. \tag{14}$$

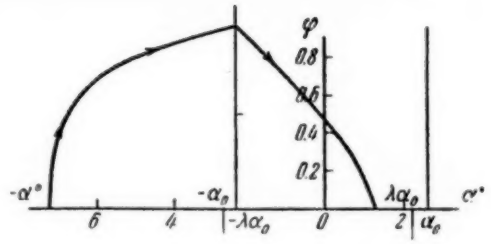

Fig. 7. Phase diagram for the system without velocity feedback.

Eliminating τ and integrating we have

$$0 - 0_{in} = \frac{1}{\delta\psi_0 k_1^*}\left[(\varphi_{in} - \varphi) + \varphi_\mu \ln\frac{\varphi + \varphi_\mu}{\varphi_{in} + \varphi_\mu}\right]. \quad (15)$$

Since the phase trajectory equations are known, it is not difficult to study the stability and choose the parameters: it can be done as in [3].

Here we consider the choice of nonlinear feedback type from the conditions that the insensitive zone be minimal and overshooting absent.

Figure 7 shows the phase diagram for the example above.

Without velocity feedback the insensitive zone cannot be made narrower than $\pm 2°$ (Fig. 7). Velocity feedback enables one to make the insensitive zone much narrower (Fig. 8a) provided, of course, that k_θ is increased.

Nonlinear velocity feedback gives even better results. The type of nonlinear feedback is on the whole determined by the phase trajectory. The insensitive zone becomes minimal if the switch-over and phase trajectory lines are described by one equation.

In our case this coincidence must apply to the phase trajectory equation for the second mode, i. e. (15).

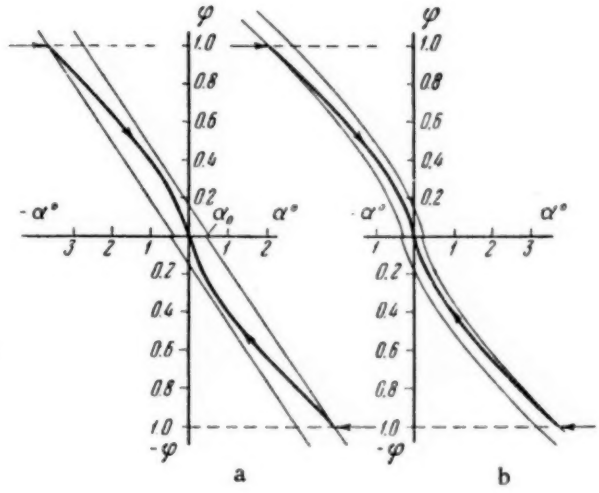

Fig. 8. Phase diagrams: a) Linear velocity feedback, b) nonlinear velocity feedback of the form

$$\Delta U(\varphi) = k_2\varphi^{1.5}\ \text{sign}\ \varphi.$$

It is difficult to realize such a type of feedback [5]. But if we introduce a nonlinear feedback of the form

$$0 = k_2\varphi^{1.5}\,\text{sign}\,\varphi, \quad (16)$$

we get a good approximation to the phase trajectory.

Figure 8b shows the insensitive zone of a system bounded by switch-over lines when the nonlinear velocity feedback is of (16) type, and the phase trajectory of (15) type. The insensitive zone is only ± 0.25° wide.

A voltage proportional to the rate of rotation may be transformed into one proportional to a fractional power of the speed using the functional converter described below.

6. Functional Velocity Feedback Converter

The tachometer in the functional converter is a normal synchronous generator with permanent magnets of single-phase or three-phase style [8, 9].

A capacitor C, a rectifier, and a resistor R_1 are connected to the tachometer generator as shown in Fig. 9.

For the current I we have the equation

$$I = \frac{E}{\sqrt{R^2 + \left(\frac{1}{\omega C}\right)^2}} = \frac{k_0\omega}{\sqrt{R^2 + \left(\frac{1}{\omega C}\right)^2}}, \quad \text{or} \quad I = \frac{k_0\omega_n}{R}\frac{\varphi^2}{\sqrt{\varphi^2 + k_c^2}},$$

where $E = k_0\omega$ is the tachometer emf, ω_n the nominal angular velocity, $k_c = \frac{1}{RC\omega_n}$, and R is the net resistance of the whole circuit.

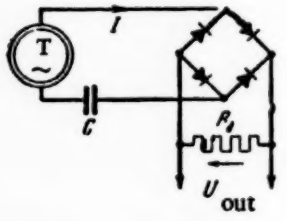

Fig. 9. Functional velocity feedback converter using a single-phase tachometer generator.

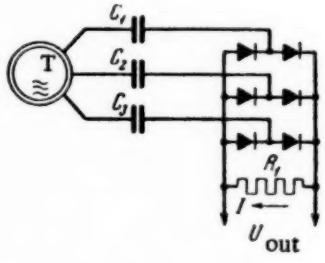

Fig. 10. Functional velocity feedback converter using a three-phase tachometer generator.

Any $I(\varphi)$ relation of the form $I = \varphi^s$ (s = 1 to 2) can be obtained by choice of the relation between R and C.

In our case when $k_c = 1$, the rectified current flowing in R_1 or the relay coil is proportional to $\varphi^{1.5}$. To obtain a good rectified current wave-shape a three-phase generator connected to a bridge circuit (Fig. 10) should be used.

A shortcoming in this converter is that it does not sense the sign of the angular velocity. Hence suitable switching on change of direction of rotation has to be used with this circuit.

7. Relay System With Functional Velocity Feedback Converter

Figure 11 shows the theoretical circuit of a relay system in which the above functional velocity feedback converter is used.

The RP-5 polarized relay is triple-wound. One coil is connected in the diagonal of the measurement bridge and the other identical two are connected in the differential circuit of Figure 11. The rectified voltage is switched over from one winding of the RP-5 to the other by the relay R, which has one normally closed

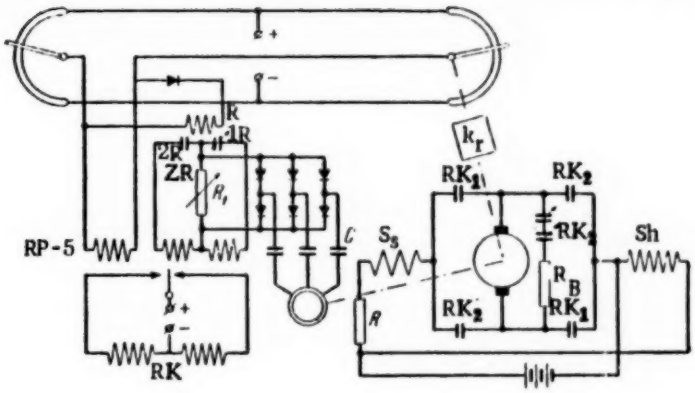

Fig. 11.

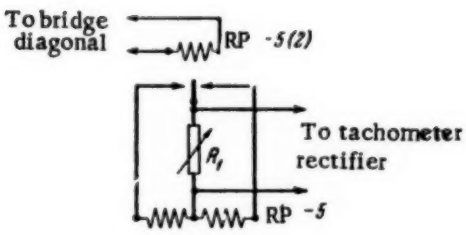

Fig. 12.

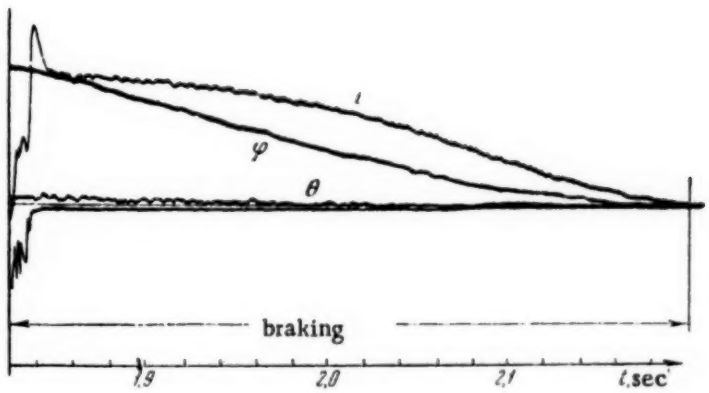

Fig. 13.

contact 1R and one normally open, 2R. The winding of relay R is connected in the diagonal in the measuring bridge, in parallel with the main winding of the RP-5, via a rectifier.

The relay only operates when the voltage in the bridge diagonal is of appropriate polarity, thereby ensuring that the velocity feedback windings are correctly switched. R_1 is used for setting-up. The switching circuit for the windings of the RP-5 can be as of Figure 12, using the additional polarized relay RP-5(2).

Figure 13 shows part of an oscillogram illustrating the follow-up of an input angle (only braking shown) when nonlinear velocity feedback of the type of (16) is used. The system tends exactly to the balance point.

SUMMARY

1. The use of compound-wound dc motors in relay automatic position control systems reduces the acceleration time considerably, i. e., makes the system quicker-acting.

2. The functional converter presented provides very simple methods of nonlinear conversion in the case of velocity feedback.

3. To reduce the insensitive zones in relay systems using dynamic braking on shunt-wound dc motors loaded at $\mu_r = 1$, nonlinear feedback must be used with the feedback signals proportional to a fractional power of the rotation speed. In particular a feedback signal proportional to $\omega^{1.5}$ may be used.

LITERATURE CITED

[1] A. Attley and P. Hammond, Relay Servo Systems Stabilization. Automatic control, IL, 1954.

[2] A. Ia. Lerner, Improvement in the Dynamic Properties of Automatic Compensators by Using Nonlinear Circuits. Automation and Remote Control 13, Nos. 2 and 4, 1952.

[3] A. A. Fel'dbaum, Electrical Systems of Automatic Control. Oborongiz, 1954.

[4] A. A. Fel'dbaum, The Synthesis of Optimal Control Systems. Trans. 2nd All-Union Conference on Automatic Control. Vol. II, Izd. AN SSSR, 1955.

[5] Ia. Z. Tsypkin, Theory of Relay Automatic Control Systems. Gostekhizdat, 1955.

[6] V. S. Kulebakin, and V. D. Nagorskii, Aircraft electrification, Vol. II, Izd. N. E. Zhukov Airforce Engineering Academy, 1952.

[7] I. M. Rykhik and I. S. Gradshtein, Tables of Integrals, Sums, series and Products. Gostekhizdat, 1951.

[8] V. V. Gorskii, A Simple Circuit for Producing a Voltage Proportional to the Square of a Rotation Speed. Automation and Remote Control, 17, Vol. 10, 1956.

[9] V. V. Gorskii, A Simple Circuit for Producing a Voltage Proportional to the Square of a Rotation Speed. Author's Certificate No. 104559.

Received March 13, 1956

CIRCUIT DESIGN FOR AC MAGNETIC AMPLIFIERS

N. A. Kaluzhnikov

(Kharkov)

A method of circuit design for ac magnetic amplifiers with iron-nickel alloy cores is proposed which is based on the theory of ideal magnetic amplifiers.

The operation of an ac magnetic amplifier into a complex (inductive-resistive) load is considered and the working of push-pull amplifiers into inductive loads is analyzed.

1. General Aspects

The main difficulty in designing a magnetic amplifier is in designing the ac circuit because the nonlinearities are very marked.

Most existing design methods start from the assumption that the ac side can be represented as having a linearly varying inductance. This assumption distorts the true picture considerably since these amplifiers are by their nature nonlinear inductive units, and hence the currents and voltages cannot in principle be sinusoidal.

This common assumption is supported by the fact that it enables one to use the highly developed computational methods available for sinusoidal current circuits. The errors in the computed u_c, although large (20-30%), may not be serious. This is because an amplifier operating in set circumstances gives approximately the required output current at a fixed number of control ampere-turns over a large range of ac voltage. But the computed u_c is higher than the real value, which can sometimes have serious consequences because the control current demanded is then much higher than the calculation would indicate.

Attempts have been made to approximate the magnetization curve for a magnetic amplifier with various functions, and in this way to derive computational methods. But these methods have not yet come into common use because the computational formulas are cumbersome.

Here we attempt to derive a computational method from the theory of ideal magnetic amplifiers. This latter enables us to obtain fairly simple computational relations which, as experiment shows, are quite applicable to the design of amplifiers with iron-nickel alloy cores.

The Problem

The most characteristic properties of a magnetic amplifier can be derived by assuming the core to consist of ideal material (Fig. 1). Then it can readily be demonstrated that $I_{\sim av} W_{\sim} = I_{=} W_{=}$. This relation is correct no matter what the magnitude, wave-shape and frequency of the applied voltage provided that we observe the condition that the voltage applied is not high enough to produce magnetic saturation in the absence of a control current.

A real magnetic amplifier can be represented by the equivalent circuit of Figure 2. Here D is a magnetic amplifier using an ideal material, L_1 an inductance representing the initial slope of the magnetization curve,

Fig. 1. Magnetization curve for an ideal material

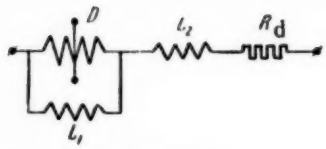

Fig. 2. Equivalent circuit of a magnetic amplifier.

L_2 an inductance representing the leakage and the slope of the saturation section of the curve, R_d the resistance of the ac winding. For an ideal system $R_d = L_2 = 0$, $L_1 = \infty$. Even-harmonic distortion is very important when analyzing amplifier processes. Under real conditions this distortion appears in the fluxes and emfs from the separate units (if the amplifier is built round two cores with the ac windings in series, as usual) and in the control and bias currents.

Two operating modes can be differentiated:

a) natural magnetization, the resistance for even-harmonic currents being zero and even-harmonic distortion appearing solely in the currents;

b) forced magnetization, the resistance then being infinite and even-harmonic distortion appearing solely in the fluxes.

Real operating conditions approach closely to case a. Hence in what follows we consider this case. Case b, which is typical of dc transformers, has been considered in detail in [1].

Lamm [2] concludes from the fact that in case a the current waveform is peaked, and in case b flattened, that the third harmonic changes sign and is therefore zero in some intermediate mode. We may thus conclude that case a is one of the limiting ones as regards nonsinusoidal (odd-harmonic) distortion.

The most typical operating conditions for a magnetic amplifier are when the load is either purely resistive or else inductive (cos φ small) and may be connected either directly to the output (ac output) or via a bridge rectifier (dc output).

Except for the last all these cases will be considered below. For generality we shall also consider a complex load, although in most practical instances such a load can be replaced either by a resistive or an inductive one without much effect on the accuracy.

3. Operation of a Magnetic Amplifier with a Resistive Load

This case has been considered in detail before [3].

Figures 3 and 4 illustrate the operation of a magnetic amplifier with a resistive load. The ac circuit operation splits up into two sections. In the first, one core becomes saturated. The difference between the magnetic states of the cores causes even-harmonic balancing currents to flow in the control circuit. In case a this current causes the voltages on both to be equal. Since the voltage on the saturated unit is zero, as the material is taken as ideal the unsaturated one will be zero also, and all the line voltage will be applied to the load.

Thus the mean line voltage taken over the half-period will equal the sum of the corresponding voltages on coil and load. This conclusion is correct for any load because it follows from the magnetization curve being ideal. The coil current follows the voltage curve if the load is purely resistive.

The alternating flux linkage $\Psi_\sim$ varies sinusoidally between Ψ_{max} and Ψ_{min} and has a saturation region which occurs when the flux linkage of one unit reaches the value corresponding to the kink in the magnetization curve at Ψ_k. There is also a constant flux-linkage component Ψ_0 of magnitude such that the condition $i_{\sim\,av} = i_{\sim} w_{\sim}/w_{\sim}$ is fulfilled. In Figure 4, I denotes the current equivalent to the total mmf of all windings on the core.

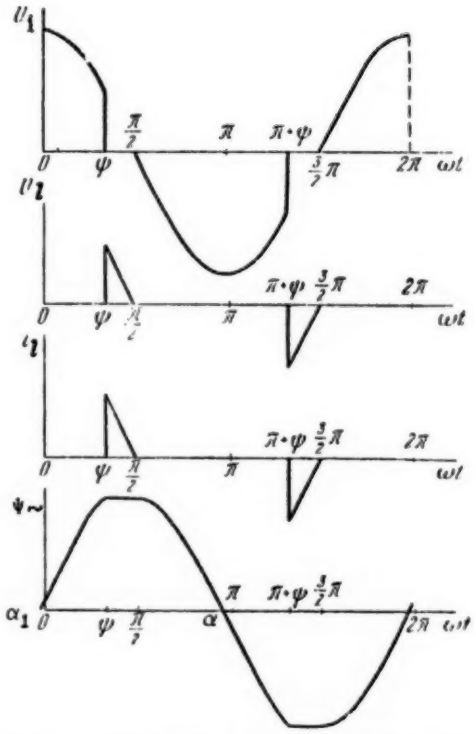

Fig. 3. Load characteristics of a magnetic amplifier with a resistive load.

Let us now calculate the quantities U_c, U_l and I_l (Figure 3):

$$U_c = \frac{1}{\pi}\int_0^{\psi} u_m \cos\omega t\, d\omega t - \frac{1}{\pi}\int_{\pi/2}^{\pi} u_m \cos\omega t\, d\omega t =$$

$$= \frac{2}{\pi} u_m \frac{1+\sin\psi}{2} = U_s \frac{1+\sin\psi}{2},$$

$$U_l = \frac{1}{\pi}\int_{\psi}^{\pi/2} u_m \cos\omega t\, d\omega t = U_s \frac{1-\sin\psi}{2},$$

$$I_l = \frac{1}{\pi}\int_{\psi}^{\pi/2} I_m \cos\omega t\, d\omega t = \frac{2}{\pi} I_m \frac{1-\sin\psi}{2} =$$

$$= I_{l\max}\frac{1-\sin\psi}{2}.$$

Here U_s is the half-wave supply voltage; $I_{max} = U_s/R_l$.

Figure 5 shows the load characteristics of the coil computed using effective values (linear inductances) in relative units (Curve 1) and from mean values (ideal magnetic amplifier – Curve 2). In the first case the calculations give an exaggerated value for $\overline{U}_c$, in the second

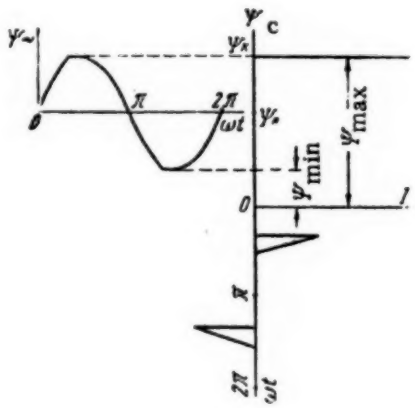

Fig. 4.

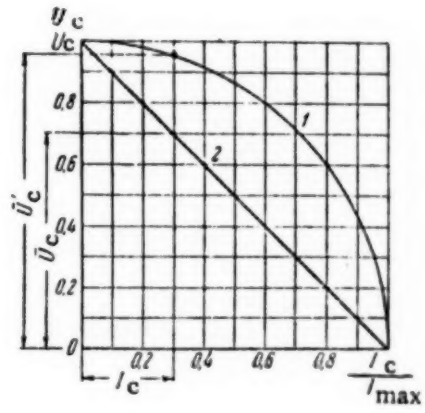

Fig. 5.

an underestimate of $\overline{U}_c$. The true curve lies between 1 and 2, approaching 2 when the material quality is improved and 1 (arc of a circle) as it gets worse.

The mean value calculation gives a unit of somewhat too large size, and the effective one a unit somewhat too small. But the one deriving from the effective values may require more control power than the calculation indicates.

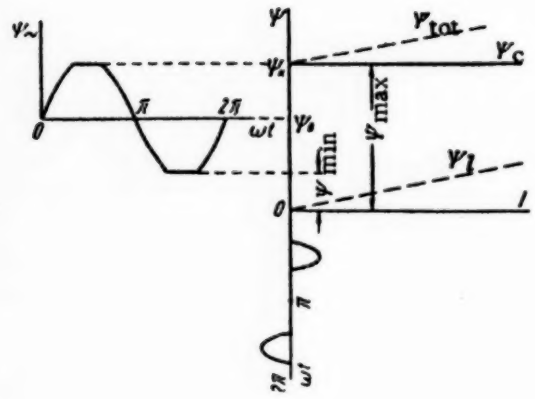

Fig. 6.

4. Operation of a Magnetic Amplifier with an Inductive Load

When an inductive load is used the process differs somewhat from that of the previous case. Figures 6 and 7 explain what happens.

Some difference between the curves of Figures 3 and 7 is evident. In the second case the current shows a phase-shift of 90° relative to the voltage and is in phase with the choke current. The load voltage is symmetric about the points $\frac{\pi}{2}$ and $\frac{3\pi}{2}$. This is a natural consequence of the inductance storing energy and then returning it completely to the source. In Figures 6 and 7, Ψ_c denotes the flux linkage of the amplifier core, Ψ_l that of the (inductive) load, and $\Psi_{tot} = \Psi_c + \Psi_l$.

Let us determine U_c, U_l and I_l for this case.

$$U_l = \frac{2}{\pi}\int_{\psi}^{\pi/2} u_m \cos\omega t\, d\omega t = \frac{2}{\pi}\, u_m (1 - \sin\psi) = U_s\ (1 - \sin\psi),$$

$$I_l = \frac{2}{\pi}\int_{\psi}^{\pi/2} I_m (\sin\omega t - \sin\psi)\, d\omega t = \frac{2}{\pi} I_m \left[\cos\psi - \left(\frac{\pi}{2} - \psi\right)\sin\psi\right] =$$

$$= I_{max}\left[\cos\psi - \left(\frac{\pi}{2} - \psi\right)\sin\psi\right],$$

where $I_{max} = \frac{u_s}{\omega L_l}$.

When analyzing these expressions attention should be given to the fact that $U_l / I_l = X_{eq}$ depends on ψ. This is because the inductive impedance varies with the applied voltage wave-shape. The ratio increases as the magnetization falls, the current wave becoming more distorted.

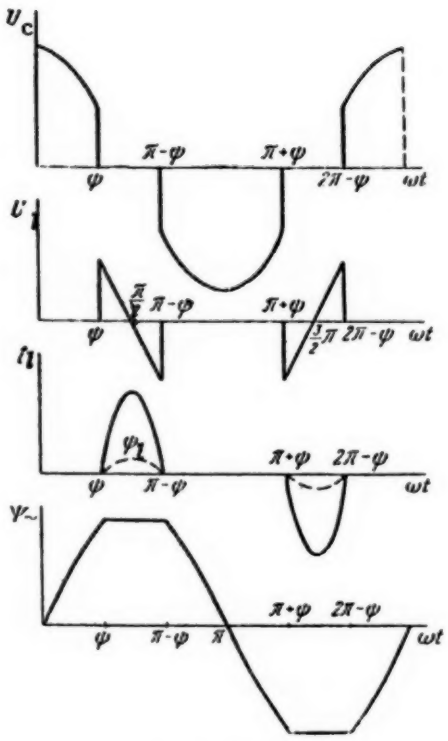

Fig. 7.

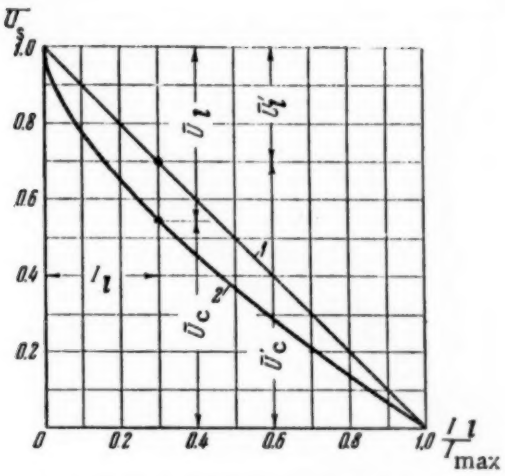

Fig. 8. Load characteristics of a magnetic amplifier with an inductive load.

Figure 8 shows the load characteristics of the coil with an inductive load. Curve 2 was drawn using $U_c/U_s = \sin\psi$ and $I_l/I_{max} = \cos\psi - (\pi/2 - \psi)\sin\psi$. By assigning values from $\pi/2$ to $-\pi/2$ to ψ the whole characteristic is easily computed. For comparison the same curve computed from effective values is shown on the same graph (Curve 1). As previously the effective-values calculation gives U_c too high. The real curve lies between 1 and 2, since in a real choke the nonsinusoidal distortions are less than in an ideal one. It is convenient to use the curve $\lambda_X = f(k_B)$, where $\lambda_X = X_{equiv}/\omega L_l$ and $k_B = U_{c\,max}/U_c$, for calculations. Here $k_B = U_s/U_c$.

Figure 9 shows this relationship. For the real case it will deviate from that given particularly strongly at small k_B, since the current in the real case will become less nonsinusoidal as the signal decreases below some particular point.

In practice magnetic amplifiers seldom operate at small k_B because the material is then poorly utilized, so such modes are of no real importance.

Instead of $X_l = \omega L_l$, one should use $X_{equiv} = \lambda_X \omega L_l$ in the calculations, selecting λ_X from Figure 9. λ_X can also be determined directly from Figure 8. We will illustrate this with a numerical example. For the point shown in Figure 8, $\bar{U}_c = 0.54$, $\bar{U}_l = 0.46$ and $\bar{I}_l = 0.3$. Then $k_B = 1/\bar{U}_c = 1/0.54 = 1.85$ and $\lambda_X = \bar{U}_l/\bar{I}_l = 0.46/0.3 = 1.53$.

5. Operation of a Magnetic Amplifier with a Complex Load

Operation of a magnetic amplifier with a complex load is the general case, the above cases being limiting instances of this. Figure 10 illustrates the process under these conditions. Here U_l changes sign near $\frac{\pi}{2}$ and $\frac{3\pi}{2}$ but U_l at $\frac{\pi}{2} - \psi_1$ is greater than at $\psi_2 - \frac{\pi}{2}$ (the values being equal for an inductive load). This is because some of the energy is dissipated in the resistance and only part is returned to the line. The Ψ_p curve takes about the same form as with a resistive load but the saturation region does not extend up to $\frac{\pi}{2}$ but to ψ_2 and α falls closer to π.

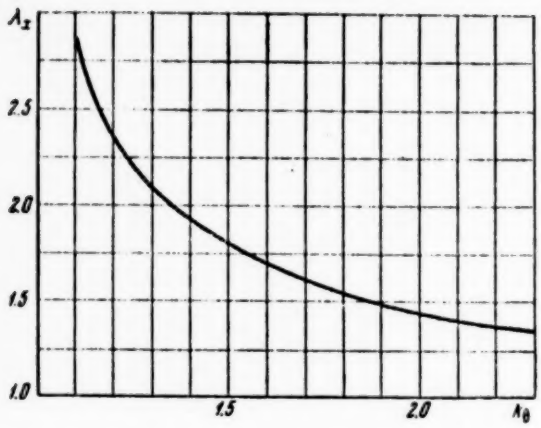

Fig. 9. Computed $\lambda_X = f(k_B)$ for a magnetic amplifier working into an inductive load.

The current curve is the most complicated one. Its shape is distorted, the maximum falling at an angle less than $\pi/2$. The current curve equation is as follows:

$$I_l = I_m [\cos(\omega t - \varphi) - \cos(\psi_1 - \varphi) e^{-\frac{\omega t - \psi_1}{\tau}}],$$

where $\tau = \omega L_l / R_l$ and $\varphi = \tan^{-1} \tau$. Figure 10 shows the sinusoidal and exponential components of the current (dashed) for $\tau = 1$.

φ_2 is found from the condition that the current is zero, which gives the following transcendental equation:

$$\cos(\psi_2 - \varphi) = \cos(\psi_1 - \varphi) e^{-\frac{\psi_2 - \psi_1}{\tau}}.$$

Let us find the expressions for U_c, U_l and I_c for a complex load:

$$U_l = \frac{1}{\pi}\int_0^{\psi_1} u_m \cos\omega t \, d\omega t - \frac{1}{\pi}\int_{\psi_2}^{\pi} u_m \cos\omega t \, d\omega t = U_s \frac{\sin\psi_1 + \sin\psi_2}{2},$$

$$U_l = \frac{1}{\pi}\int_{\psi_1}^{\pi/2} U_m \cos\omega t \, d\omega t - \frac{1}{\pi}\int_{\pi/2}^{\psi_2} u_m \cos\omega t \, d\omega t = U_s\left[1 - \frac{\sin\psi_1 + \sin\psi_2}{2}\right],$$

$$I_l = \frac{1}{\pi}\int_{\psi_1}^{\psi_2} i_{(l)} d\omega t = I_{max}\left[\frac{\sin(\psi_2 - \varphi) - \sin(\psi_1 - \varphi)}{2} - \right.$$

$$\left. - \frac{\tau}{2}\cos(\psi_1 - \varphi)(1 - e^{-\frac{\psi_2 - \psi_1}{\tau}})\right] = I_{max}\frac{\sin\psi_2 - \sin\psi_1}{2\cos\varphi},$$

where

$$I_{max} = \frac{U_s}{\sqrt{R_l^2 + \omega^2 L_l^2}}.$$

$Z_{equiv} = \dfrac{U_l}{I_c}$ here also differs from $Z_l = \sqrt{R_l^2 + \omega^2 L_l^2}$

In future we will assume the approximation $\lambda = \dfrac{\sqrt{1 + \lambda_x^2 \tau^2}}{\sqrt{1 + \tau^2}}$, where λ_X is taken from Figure 9.

Figure 11 shows $\lambda = f(k_B)$ computed by the exact and approximate methods for $\tau = 1$ (Curves 1 and 2 respectively). The agreement is quite satisfactory and is in any case within the accuracy to be expected from the calculations.

For τ large (5 or more) we may simply take $\lambda = \lambda_X$.

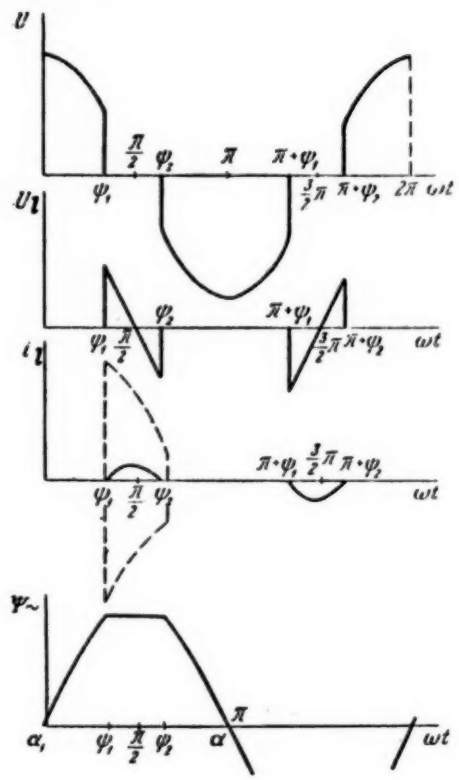

Fig. 10.

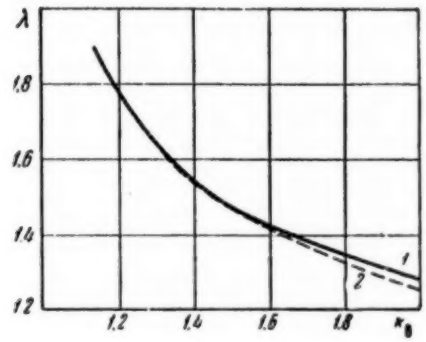

Fig. 11.

6. Special Features of the Push-Pull Circuits

We will consider the operation of a bridge magnetic amplifier into an inductive load (Fig. 12) when one pair of cores is maximally saturated while the other is subject to no magnetizing field at all. This mode is of most interest for calculation. Figure 13 illustrates the operation processes in these conditions. The complete process consists of two cycles. In the first all cores are unsaturated, half the line voltage being applied to each,and U_l is zero. In the second only two remain unsaturated (e. g., 1 and 4 in Fig. 12), the other pair being completely saturated. In these conditions the unsaturated components and the load are effectively connected in parallel to the line voltage (as in the choke circuit). But the U_{c1} (voltage on the nonmagnetized choke) and U_{c2} (magnetized) curves alter their shapes somewhat.

U_{c1}, U_{c2}, U_l and I_l are given by

$$U_{c1} = U_s\left(1 - \frac{\sin\psi}{2}\right), \quad U_{cp2} = U_s\,\frac{\sin\psi}{2}, \quad U_l = U_s\,(1 - \sin\psi),$$

$$I_l = I_{max}\left[\cos\psi - \left(\frac{\pi}{2} - \psi\right)\sin\psi\right].$$

If we introduce the computed quantity $k'_B = 2U_{c2}/U_s = \sin\psi$ we can use Figure 9 for push-pull circuits by replacing k_B by k'_B. k'_B and $k_B = U_{c1}/U_{c2}$ are related by $k'_B = \frac{1}{2}(k_B + 1)$.

These results can also be related to the general case of a complex load and are in addition correct for other push-pull circuits (differential and transformer).

7. Effect of Equivalent Circuit Parameters

Returning to the circuit of Fig. 2,we shall determine how its parameters distort the operation of an ideal magnetic amplifier.

Effect of R_d. In most magnetic amplifiers R_d does not exceed 5-10% of Z_l. Hence this parameter has little effect. If the load is inductive this parameter does not have to be reckoned with in practice. With a resistive one R_d can be allowed for by increasing the load resistance by 5-10%.

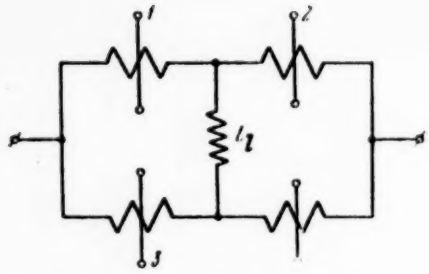

Fig. 12. Circuit of a bridge magnetic amplifier.

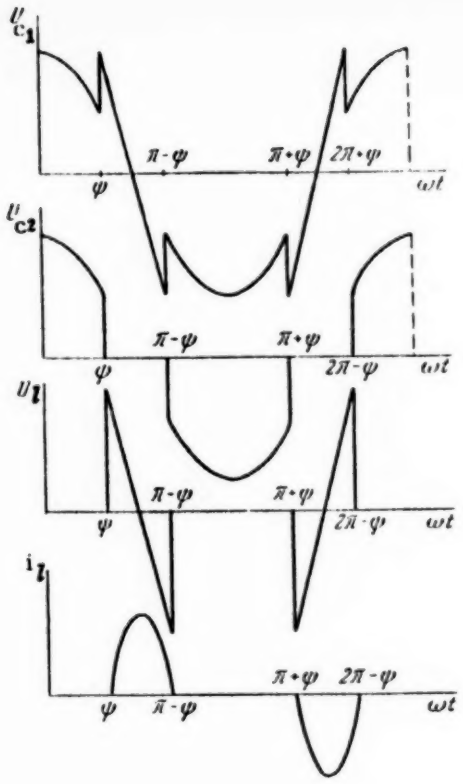

Fig. 13.

Effect of L_2. L_2 is defined by the slope of the upper section of the magnetization curve and by the leakage and by gaps and joints. The worse the material and the less perfect the design, the greater L_2.

If the load is inductive, L_2 adds arithmetically to L_1. Then at a given I_l the voltage on the nonlinear element D is reduced (k_B rises) and this reduces the nonsinusoidal distortions and λ_x. L_2 is readily allowed for by adding to L_l.

If the load is resistive L_2 distorts the processes still more. Then the process is as for a complex load with τ small. $U_s = U_c + U_l$ no longer applies because the voltage on L_2 is included in U_c. In fact U_c will be greater than $U_s - U_l$. L_2 can be allowed for by incorporating it in Z_l and treating the latter as a complex load.

k_B	$\lambda_{x\tau}$	$\lambda_{x\,exp}$	δ_{eff} %	δ_{av}, %
1,21	2,33	1,16	+1,4	— 9,6
1,32	2,04	1,25	+3,5	—11,1
1,67	1,67	1,20	+6,7	—15,8
2,03	1,41	1,16	+9,9	—15,4
2,50	1,25	1,10	+10,4	—15,0

Effect of L_1. Allowance for distortion due to L_1 is the most difficult. This inductance passes current through D. If the load is inductive this reduces the nonsinusoidal distortions and λ_x; with a resistive one $U_c = U_s - U_l$ does not apply because at the instant when the core is unsaturated a current of approximately sinusoidal form passes through the load. The nonsinusoidal distortions in both cases become smaller the more rapidly L_l / L_1 increases.

Experimental Test Data

The applicability of ideal magnetic amplifier theory in its most simplified form to computing real amplifiers (without allowing for the upper and lower slopes of the magnetization curve) was tested by experiment.

Amplifiers with iron-nickel alloys in the cores were used for this. Normal selenium rectifiers were used with them. No special measures were taken to ensure natural magnetization in the amplifier.

The accuracy of $U_c = U_s - U_l$ was checked with a resistive load and compared with the accuracy with which $U_c = \sqrt{U_s^2 - U_l^2}$ was fulfilled.

For k_B from 1.15-1.5 the first relation was fulfilled with a mean error of -25% and the second with a mean error of $+20.5\%$. In other words the true U_c was about the average of the calculated values obtained by using effective and mean values.

With an inductive load λ_x was checked, together with the accuracy of the magnetic amplifier calculations using mean values (using λ_x) and effective ones (neglecting λ_x).

The test data are given in the table.

The data lead to the following conclusions.

The theoretical (λ_{xT}) and experimental ($\lambda_{x\,exp}$) values of λ_x diverge considerably, particularly at low k_B. The effective-values calculation gives less error (but still a positive one) which tends to rise with k_B (mean error 6.5%). The mean one gives a somewhat larger (but negative) error which varies little when k_B ranges from 1.25 to 2.5 (mean error 14.3%). Thus the appreciable deviation of the real λ_x from the calculated does not lead to substantial errors.

These tests are of course not exhaustive but they completely confirm all the results deriving from the theory.

SUMMARY

The proposed method of using mean values in the calculations corresponds with the physical processes in a magnetic amplifier. The complexity is not greater than that of the usual effective values one.

The main advantage of this method is its high reliability, its main disadvantage the somewhat overestimated size obtained for the magnetic amplifier.

The ac circuit design method for magnetic amplifiers corresponds best to materials with rectangular hysteresis loops.

When high-power magnetic amplifiers are being designed it is desirable to introduce corrections into the equivalent circuits.

LITERATURE CITED

[1] Iu. G. Tolstov, Instrument dc transformers (in Russian) Gosenergoizdat, 1951.

[2] U. Lamm, "The transductor and its applications." ASEA Journal, Nos. 5-6, 1939.

[3] M. A. Rozenblat, Magnetic amplifiers (in Russian) Radiotekhnika, No. 2, 1953.

Received November 26, 1956

AN INDUCTION TRANSDUCER OF INCREASED SENSITIVITY FOR RECORDING LINEAR AND ANGULAR MOVEMENTS

A. S. Sadovskii

(Odessa)

A grooved induction transducer of sensitivity higher than for one with a continuous armature is considered. The transducer enables one to measure displacements and to record equal or unequal intervals over the whole length of the armature, which latter can be of any length. The armature can be a cylinder and the grooves rings or screw threads.

This measuring head is used on the precision coordinate-boring machine produced by the machine-tool industry for setting the coordinate and measuring the displacements, replacing the optical method of reading the coordinates and displacements; in this way the machine table can be driven automatically to a preset coordinate, which is not possible with the optical system.

Figure 1 shows a transducer with a continuous armature which is sensitive to armature displacements. The faces of the armature are so cut that the cores face the armature, the lines of force from the cores intersecting. This device, if connected in the circuit of Figure 2, gives zero reading on the meter M when the armature is at the central (equilibrium) position, and when the armature passes through this equilibrium position the sign of I_n reverses. The relationships defining the air-gap permeability in such a transducer have been given [1].

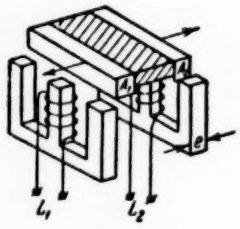

Fig. 1.

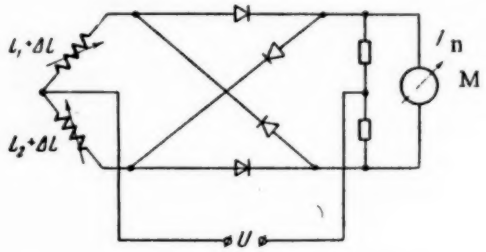

Fig. 2. Bridge measuring circuit.

1. The Grooved Transducer

To obtain higher sensitivity and to get repeated balance points at small intervals a grooved transducer can be used [2], the design of this being shown in Figure 3. This design provides distances, i. e., zero readings on meter M (Figure 2), at equal intervals much shorter than the length of the armature. The transducer is also made sensitive by the teeth, and so can be made smaller in size. Pole projections are used which increase the active air-gap length and enable one to use small-size coils. The core elements can be of III and II shapes (Figure 3).

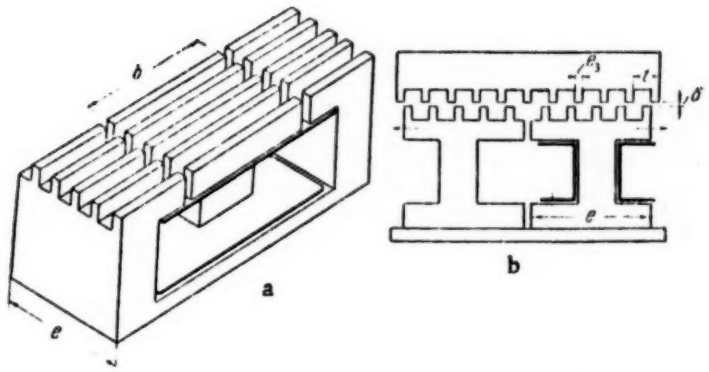

Fig. 3. Grooved transducer design. The arrows denote shifts of the cores relative to the fixed armature.

Let us consider the air-gap permeability of this transducer at the position of maximum sensitivity to armature displacement (Figure 3) [1].

Let e be the width of the iron core and n the number of teeth. The width of one tooth is

$$e_t = k\frac{e}{n} = kt, \tag{1}$$

where $t = \frac{e}{n}$ is the tooth pitch, k = 0.25–0.5. Hence e_t must be such that

$$0.5t > e_t > 0.25t. \tag{2}$$

The air-gap permeability G_t for one tooth, and the change ΔG_t when the cores and armature are displaced will be determined for the case where the length of the overlapping part $\lambda = 0$, which gives greatest sensitivity. We assume that e_t is the same on cores and armature and that the tooth height is greater than δ. Then (see [1]) the magnetic permeability is

$$G_t = \frac{4\mu_0 b}{\pi} \ln 1.76\frac{e_t}{\delta},$$

where b is the active length of one gap, δ is the air-gap between the end faces of the teeth (Figure 3), and μ_0 is the permeability of air.

The permeability change when the teeth cover one another is given by

$$\Delta G_{tc} = \mu_0 b\left(\frac{1}{\delta} - \frac{4}{\pi e_3}\right)\Delta\lambda,$$

and when they are separated by

$$\Delta G_{ts} = \frac{4\mu_0 b}{\pi e_t}\Delta\lambda,$$

$\Delta\lambda$ being the armature displacement relative to the cores, reckoned from a balance position.

The total permeability of the n gaps is

$$G_n = nG_t = n\frac{4\mu_0 b}{\pi}\left(\ln 1.76\,\frac{e}{\delta} - \ln\frac{n}{k}\right). \tag{3}$$

The permeability change due to a shift of $\Delta\lambda$ (teeth covering one another) is

$$\Delta G_{nc} = n\Delta G_{tc} = n\mu_0 b\left(\frac{1}{\delta} - \frac{4}{\pi e}\frac{n}{k}\right)\Delta\lambda, \tag{4}$$

and when they are separated

$$\Delta G_{ns} = n\Delta G_{ts} = n^2\frac{4\mu_0 b}{\pi e k}\,\Delta\lambda. \tag{5}$$

The sensitivity to armature shift is given by $\frac{\Delta G_n}{G_n}$.

In the first case this is

$$\frac{\Delta G_{nc}}{G_n} = \frac{\left(\frac{1}{\delta} - \frac{4}{\pi e}\frac{n}{k}\right)\Delta\lambda}{\frac{4}{\pi}\left(\ln 1.76\,\frac{e}{\delta} - \ln\frac{n}{k}\right)}, \tag{6}$$

in the second

$$\frac{\Delta G_{ns}}{G_n} = \frac{n}{k}\,\frac{\Delta\lambda}{e\left(\ln 1.76\,\frac{e}{\delta} - \ln\frac{n}{k}\right)}. \tag{7}$$

Let us compare the sensitivities of the flat and grooved units.

It is clear that if we put n = 1 and k = 1 in (6) and (7) we get the flat unit case with an armature of the same size with $e_t = e$.

The sensitivity is evaluated from $\Delta G/G$.

The table gives computed results for the flat and grooved units.

The transducer dimensions given are indicated in Figure 3.

Type	Dimensions, mm	G	Teeth covered		Teeth separated	
			ΔG_c	$\frac{\Delta G_c}{G}$	ΔG_s	$\frac{\Delta G_s}{G}$
Flat	$e = e_t = 40.$ $\delta = 0.05$	$9.35\mu_0 b$	$19.7\mu_0 b\Delta\lambda$	$2.13\Delta\lambda$	$0.032\mu_0 b\Delta\lambda$	$3.5\times10^{-3}\Delta\lambda$
Toothed	$e = 40.$ $\delta = 0.05$	$15.9\mu_0 b$	$187.00\mu_0 b\Delta\lambda$	$8.4\Delta\lambda$	$12.8\mu_0 b\Delta\lambda$	$77.5\times10^{-3}\Delta\lambda$

These data give rise to the following conclusions.

1. The toothed style is of considerably higher $\Delta G_n/G$ in both cases. It is therefore most logical to use this in differential systems.

2. The relative sensitivity increases with $\underline{n}$ at any given size.

3. The smaller $\underline{e}$ is, and hence e_t, the greater ΔG_{ns}. As regards ΔG_{nc}, the value varies little with $\underline{e}$, since the first term in (4) begins to predominate.

Figure 4 shows the experimental curves for two units of identical external dimensions, one flat (Curve 1) and the other grooved (Curve 2). The flat one had the following dimensions: e = 22 mm, δ = 0.15 mm. The other (Figure 5) had e = 22.5 mm, δ = 0.15 mm, e_t = 1.5 mm (n = 5, k = 0.33).

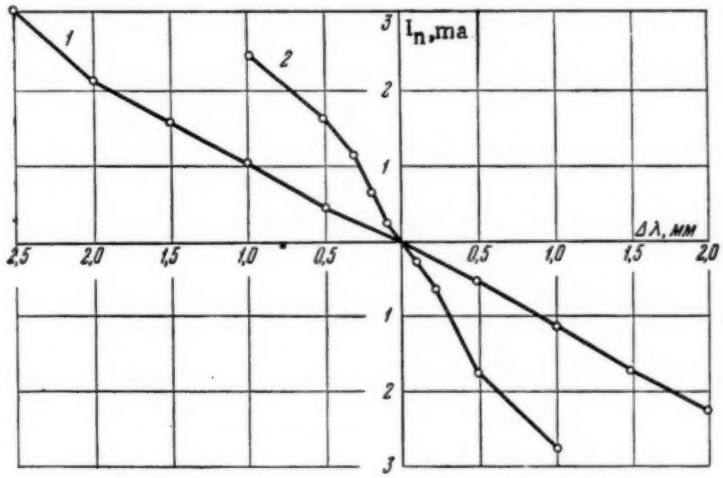

Fig. 4.

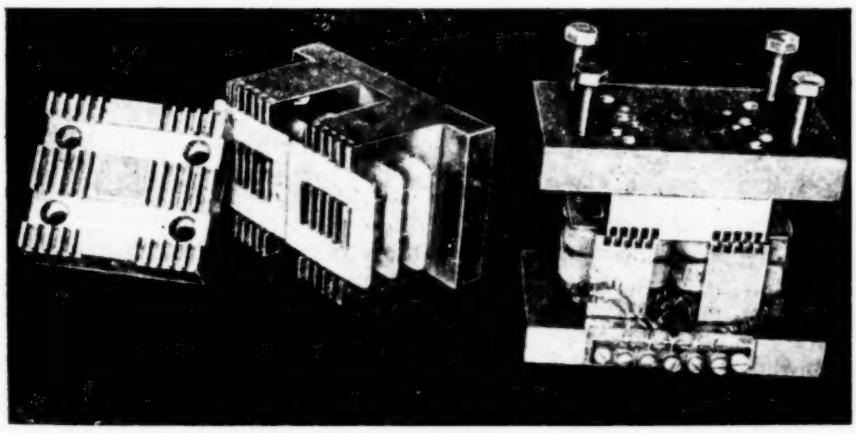

Fig. 5. Views of the grooved unit.

Figure 5 shows I_n, the rectified current in M (Figure 2), plotted against displacement. It is clear that with n = 5 the grooved unit is 2.5 times more sensitive than the other. The production of the grooves was not very precise, so the sensitivity obtained was somewhat below the maximum possible.

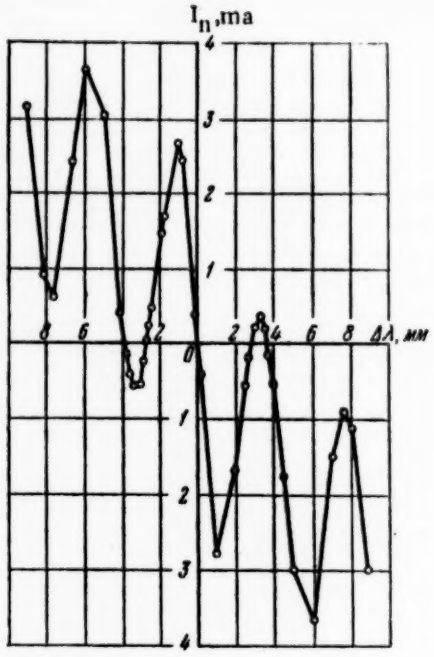

Fig. 6.

Figure 6 shows the experimental $I_n = f(\Delta\lambda)$ taken over several teeth for the unit of Figure 5.

Figure 6 indicates that an equilibrium position, i. e., that corresponding to zero reading on M, is obtained in several positions of the armature other than the symmetrical one. For instance $I_n = 0$ when $\Delta\lambda$ is somewhat less than 3 mm, i. e., $q < 2$. Again $I_n = 0$ at about 3.5 mm, i. e., when $q \approx 2.3$, etc. We cannot therefore use this unit at displacements greater than $2e_t$ because a false zero may be obtained. This is particularly inconvenient if this type of unit is to be used for automatic control. Below we consider a grooved unit in which false zeros are avoided by using a special tooth distribution. The repeated zeros appearing at equal spacings can be used for registering points lying at equal, but small, separations. We describe below a unit of this type for registering any small interval.

2. Tooth Profile Eliminating False Zeros

As we said above the false zeros are a flaw when registering a single point at large displacements. A tooth distribution which ensures that such false zeros are absent can be found graphically. This does not enable us to decide the absolute magnitude I_n will attain when connected in the measuring circuit. The problem is to determine the points on the displacement curve at which I_n changes sign, other than the equilibrium (symmetrical) position.

If the overlaps on the right and left legs are equal a balance position at which I_n changes sign is possible.

If the number of exactly opposed teeth on the right leg (right coil) is greater than on the left there will be no balance point. We assume I_n positive in this instance. If the situation is reversed I_n is also, and its direction is therefore taken as negative.

The absolute current will obviously increase with the difference between the numbers of exactly opposed teeth on the right and left legs, the current direction being positive if more teeth are opposed on the right, and conversely.

Example 1. Consider the unit shown in Figure 7a, in which the tooth width is half the gap between teeth. Suppose the armature is displaced from the zero position, as in Figure 7a, to the right (or the core to the left). Assume $e_t = 1$ and the displacement to be by one tooth ($q = 1$). Then the number of exactly opposed teeth on the right will be five. Lay off along the horizontal axis in Figure 7b the distance corresponding to one tooth (armature shift) and on the vertical the number of opposed teeth m_1 (here $m_1 = 5$). Join the origin to this point. The number of opposed teeth on the left, m_2, is then zero, as shown in the lower section of Figure 7b.

Now displace the armature by one more tooth ($q = 2$). Then we have $m_1 = 0$ and the corresponding line drops down to $m_1 = 0$. At this point four teeth are opposed on the left ($m_2 = 4$). The straight line in the lower part of Figure 7b is now drawn. By thus displacing the armature each time by one tooth stepwise we will get discontinuous lines representing m_1 and m_2 for each successive position.

Summing m_1 and m_2 at the end of each displacement we get an approximate graph of ordinate proportional to I_n (right section of Figure 7c). The graph for displacements leftwards is derived analogously (left section of Figure 7c). This construction is not of course presented as being accurate since many factors are neglected. But the points where I_n changes sign are given approximately. Figure 7c shows that the first change in sign in I_n (false pulse) occurs at about 3/2 of a tooth width to right or left of the center balance point, which agrees with Figure 6, which was obtained by experiment on a unit with $e_t = 1.5$ mm. When e_t is the same on legs and armature the range over which the unit can be used without producing false pulses is restricted to three tooth widths (3-4 mm).

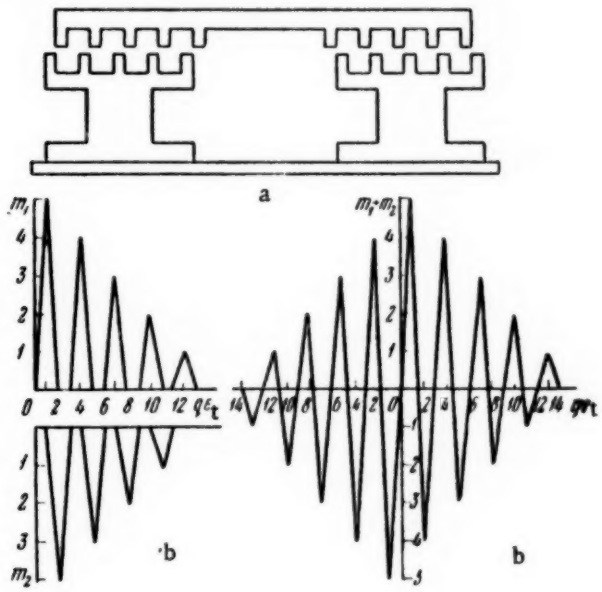

Fig. 7. Determination of the false zeros from a grooved transducer with identical teeth.

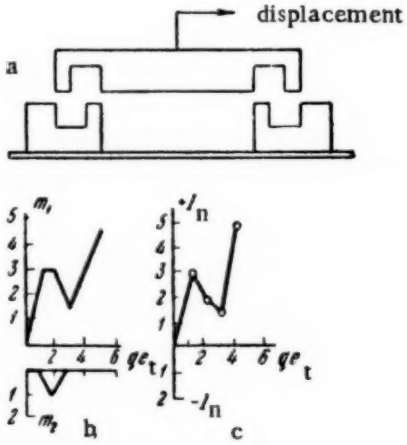

Fig. 8. Functioning of a unit giving no false zero pulses using a two-tooth armature with nonidentical teeth.

To increase the range free from false pulses we can make the teeth nonidentical. By selecting combinations of narrow and wide teeth the range can be increased as desired while retaining the increased sensitivity [3].

Example 2. Consider the tooth profile shown in Figure 8a. Here the section of the armature common to both halves is, as it were, a widened tooth. The right tooth on the right leg is twice the ordinary width. When a wider tooth faces an ordinary one the permeability will of course be higher than when two ordinary ones face one another. Allowing for this we will assume that if such a broad tooth completely overlaps an ordinary one that it is equivalent to two teeth of 3/2 width completely opposed.

We will take double-width teeth not overlapping completely as equivalent to 3/2 of a tooth. We take double and triple-width teeth overlapping completely as equivalent to two and three teeth respectively.

Figure 8, b and c, was drawn up on this basis. The left section is not shown on the graph since it can easily be constructed by analogy.

Figure 9b was drawn up similarly from Figure 9a.

The following conclusions can be drawn from Figures 8c and 9b, which have ordinates proportional to the current in M of Figure 2. By using nonidentical teeth and nonidentical gaps we can produce a tooth distribution which will always give more teeth opposed on one leg than on the other on moving to right or left. Thus one coil can be made to predominate over the other at any displacement.

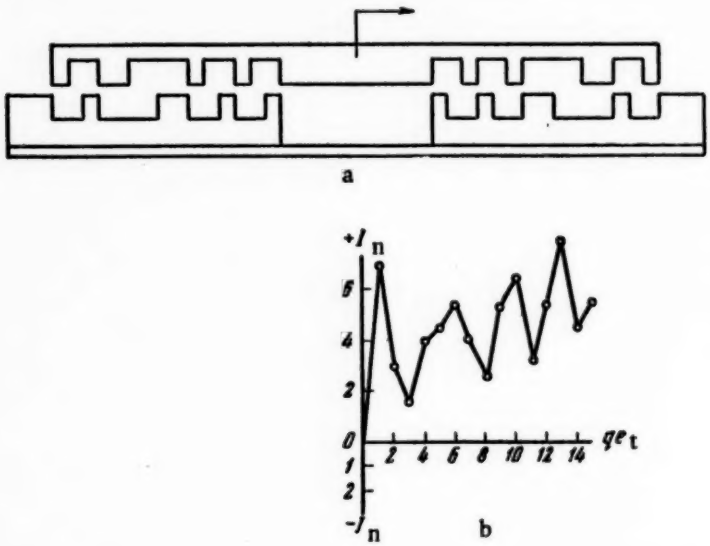

Fig. 9. Functioning of a unit giving no false zero pulses using a multi-tooth armature and nonidentical teeth.

As it is undesirable to make the profile complex the teeth should be of single, double and occasionally (tooth edge) triple width. The gaps must also be multiples of the tooth widths.

3. Unit with a Screw Armature for Repeat Recording of Small Identical Displacements

A grooved unit (Figure 3) with identical teeth of width e_t and tooth pitch t can be used for repeat recording of small identical displacements. For this the armature must be of a length such that the cores which are to be displaced can have as many positions symmetrical in relation to the armature teeth as there are intervals to be recorded. These equal intervals will correspond to zero readings on M.

The design is improved and the sensitivity further raised if the armature is made as a cylinder cut with a rectangular screw thread (Figure 10a). The cores, which can be of III or II type, are fitted with pole fittings shaped like nuts which enclose the armature* (Figure 10b).

The thread acts as the teeth, the tooth pitch being the thread pitch t.

The screw armature A is rigidly fixed. The core-nuts move freely over the armature leaving a small gap, δ = 0.05-0.1 mm.

Figures 11 and 12 show experimental curves for I_n obtained on moving the cores relative to the fixed armature. The cores were nut-ended (Figure 10b). Also t = 5 mm. The troughs were 3.75 mm wide. This implies a tooth (thread) width e_t = 1.25 mm. I_n in Figure 11 passes through zero at 2.5 mm intervals. Intervals equal to integral and half-integral multiples of t are thus recorded.

*In a subsequent modification the shape of the magnetic circuit was altered and was made symmetrical about the screw. The principle of operation is the same. Each of the two coils, being split into two parts, was disposed symmetrically about the screw. The field symmetry reduces the leakage flux and also reduces interference from external ferromagnetic masses while increasing the sensitivity. When the symmetrical form is used the accuracy of the formulas given later on for calculating the magnetic impedance of the gap is improved.

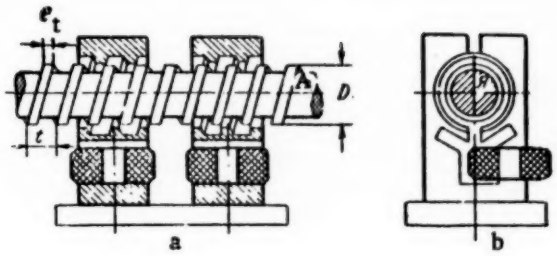

Fig. 10.

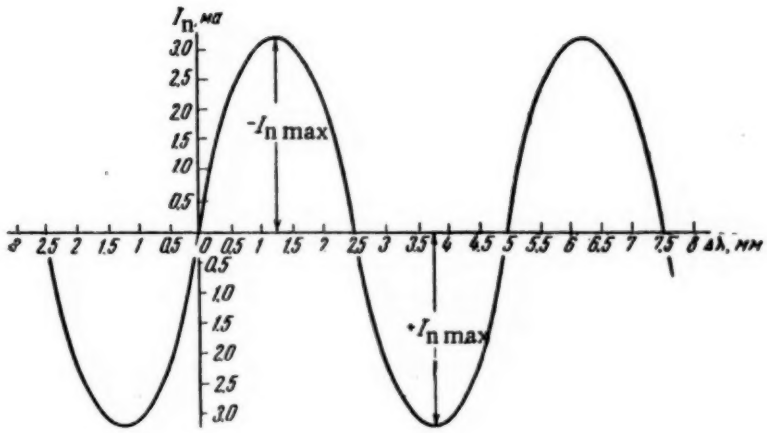

Fig. 11.

Figure 12 shows that a 1μ displacement gives a current of 2 μa , equivalent to one division on a M-495 with a 25-0-25 μa scale. Displacements in the 70-100 μ range can be measured in both directions from the zero directly on the meter if this is graduated suitably in linear units.

If the use is such that zero readings are recorded at integral multiplesof the pitch it is not essential to have the tooth (thread) width 0.25 t. Here it can be chosen such that $0.5\,t > e_t > 0.25\,t$.

This latitude in the choice of thread width makes it easier to produce the thread, as the thread crests can be worked without trouble due to excessive reduction in area on repeated polishing: the accuracy of the thread of course determines that of the displacement measurement.

The tolerance on the pole-nuts can be much larger than on the thread because the error in measuring a displacement is determined by that with which the symmetrical (balance) position is reproduced. * The error is thus mainly determined by that in producing the thread. Hence the pole-nuts can be made of soft iron which, though difficult to work, is of high permeability.

Figure 10a shows that the fluxes of several turns are operative simultaneously over the whole surfaces of threads and nuts. This is an advantage as mechanical errors in the thread pitch are averaged.

Many other uses can be found for the unit if the thread 2 (Figures 13 and 14) is fixed in bearings which permit rotation but not axial movement [4].

* This has been confirmed on a large number of pole-nuts; in making these, errors in thread width of up to 0.1 mm were permitted.

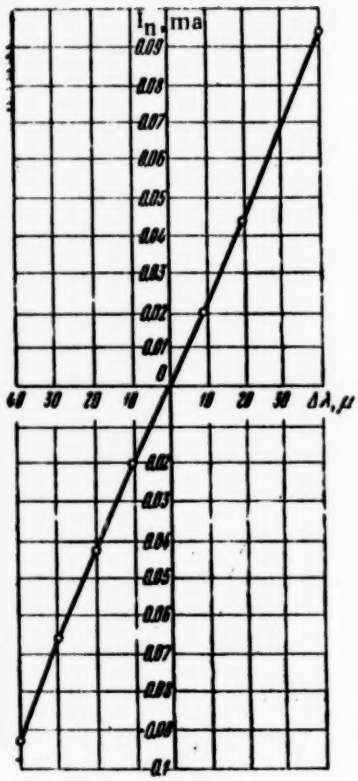

Fig. 12.

The cores 1 can be moved, together with the working carriage, relative to the fixed screw 2.

If the screw is turned through part of a full turn with the handle 3 bearing the drum 4 (Figure 13) all the zero readings on M (Figure 2) will be displaced by the same fraction of t when the cores are moved relative to the fixed thread. In this way displacements falling within the range of the screw which are not integral or half-integral multiples of the pitch can be measured. Drum 4 is graduated in linear displacement units.

A unit of this type is used for measuring displacements (coordinates) in the coordinate milling machine type 2430 (Figure 14) produced by the Kirov milling machine factory, Odessa. This unit replaces the optical system used on similar machines produced by other factories and foreign firms. The unit is fed from a 50 cycles per second line. In this machine,screw 2 was 500 mm long with t = = 5 mm, only integral pitch steps being used to take readings. Drum 4 was made of such a size that 500 divisions of spacing about 0.8 mm were accomodated. The linear displacement corresponding to one scale division is 0.01 mm. Readings can readily be taken to 2 μ with the vernier 5.

Smaller displacements can be read if the drum and vernier are made of larger diameter.

Displacement measurements are made on this machine by first selecting an appropriate coordinate.

The following example illustrates how the reading unit works.

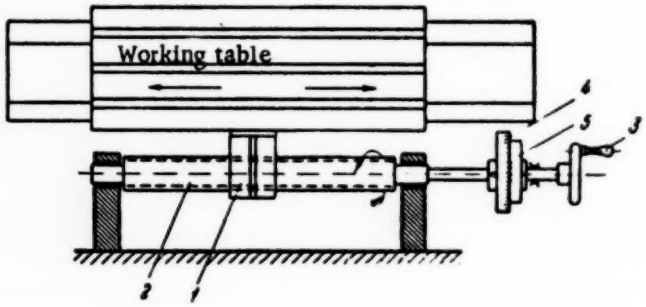

Fig. 13.

Suppose we have to measure a displacement of 52.158 mm. The displacement coordinate is first selected. A number of divisions corresponding to ten whole pitch steps, i. e., 50 mm, is selected by moving the contact which cuts in the measuring circuit to a position corresponding to the start of the eleventh step.

Having disconnected 4 and 5 from 2 (Figure 13) the former is set in the zero (starting) position.

Then, coupling 4 rigidly to 2, the handle 3 is rotated and the drum plus vernier set to read 2.158 mm and the working table plus the nuts displaced. When the nuts have been moved by about 10 pitch steps (50 mm) they cut in the measuring circuit and M shows a reading other than zero.

By moving the table further the needle is brought to zero, which corresponds to setting the table at the desired coordinate, or at a displacement of 52.158 mm.

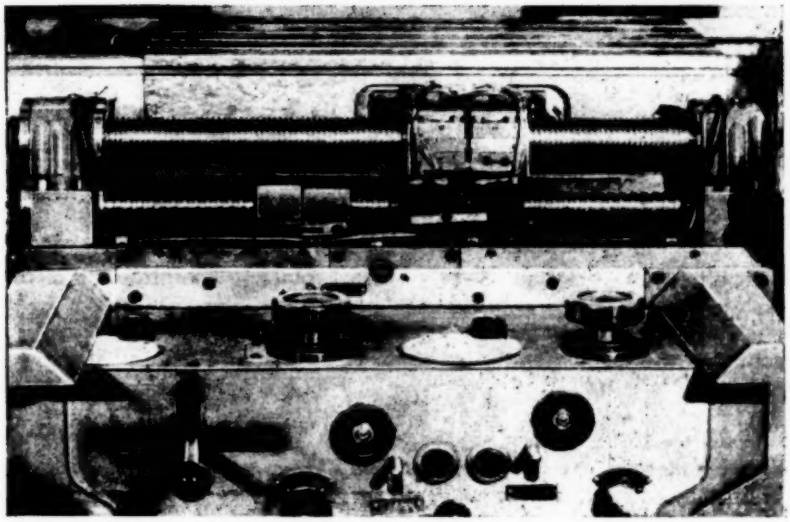

Fig. 14. The unit fitted to a coordinate milling machine from the Kirov factory, Odessa.

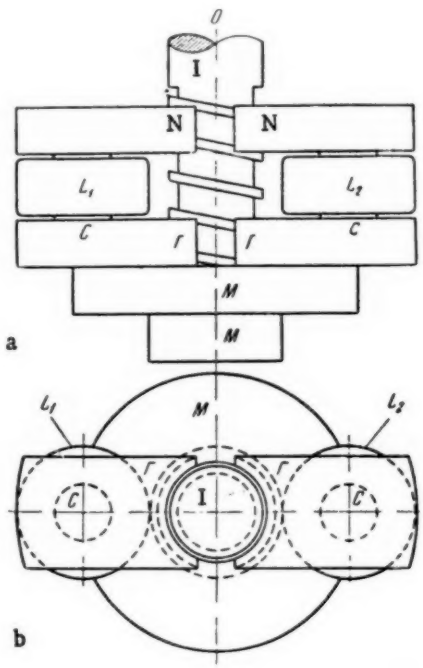

Fig. 15. Transducer for measuring angular displacements.

An electric drive propels the table in the 2430. The zero pulse produced by the unit serves to cut off the motor automatically and to set the table near the set coordinate (within 10-15 μ). Subsequent adjustment to zero is done manually. The total error in measuring any displacement up to 400 mm does not exceed 3 μ. This can be appreciably reduced by more careful manufacture of the machine and transducer, mainly the table slides and the screw.

Let us determine the permeability of the air-gaps in the unit using core nuts (Figure 10, a and b).

The effective length of each gap is about one-half the screw circumference, b = 0.5πD, D being the screw diameter.

Substituting b into (3), (4) and (5), and incorporating (1), we get for the n gaps of one half-unit.

$$G_n = nG_t = 2n\mu_0 D \ln \frac{e_t}{\delta}.$$

The change ΔG produced by an armature displacement $\Delta\lambda$ can be found as follows.

When the teeth are opposed

$$\Delta G_{nc} = n\Delta G_{tc} = n\mu_0 D\left(\frac{\pi}{2\delta} - \frac{2}{e_t}\right)\Delta\lambda,$$

and when they are separated

$$\Delta G_{n\,s} = n\Delta G_{ts} = 2n\frac{\mu_0 D}{\rho_t}\Delta\lambda.$$

4. A Screw Armature Transducer for Measuring Angular Displacements

The transducer described above (rotating screw armature) can also be used for measuring angular displacements. To this end I (Figure 15) is enclosed by two half-nuts N-N which are really extensions of the cores C-C and act as pole tips. The half-nuts are fixed rigidly while I rotates. The pitches t of the armature and nuts are identical; the thread is taken as 0.25 t thick.

The magnetic resistance of the cores assumes the same value twice in one full turn, at angles of $\varphi = 180°$ and $\varphi = 360°$.

Coils L_1 and L_2 are connected in the circuit of Figure 2. When I rotates, M records the rectified current In, which changes from 0 (at balance) at $\varphi = 0°$, 180°, 360°, to $\pm I_{n\,max}$ at $\varphi = 90°$ and 270° (Figure 11). M may be graduated directly in degrees.

A screw angle transducer using a 40 mm diameter thread and t = 10 mm was tested; I_n had a range of ± 3 ma. The unit was fed from a 50 cps line.

The test results were satisfactory.

LITERATURE CITED

[1] A. S. Sadovskii, "A linear inductive transducer." Automation and Remote Control 15, No. 6 (1954).

[2] A. S. Sadovskii, I. I. Kniazhitskii, Z. E. Vainer and M. P. Rashkovich, Authors' certificate on an inductive transducer, No. 83473, 4, 3 (1950).

[3] A. S. Sadovskii, Author's certificate on an inductive transducer, No. 89995, 11/3/1950.

[4] A. S. Sadovskii, D. M. Sukhorubov, M. Kh. Moldavskii, and Iu. A. Koroshkin, Authors' certificate on an inductive transducer, No. 95261, 3/14/1953.

Received June 29, 1954

USE OF RADIOACTIVE EMISSION IN AUTOMATIC CONTROL DEVICES

Iu. V. Gushchin, L. V. Mel'ttser, M. I. Tolokonnikov and
N. N. Shumilovskii

(Moscow)

The main methods and trends in the use of radioactive emissions in automatic control devices are considered. The characteristics of the radiation sources and detectors are briefly described. Examples of their practical application are given.

I. INTRODUCTION

Before we review and analyze the various most typical uses of radioactive emissions in automatic devices we briefly survey the properties of the radiation sources and detectors used.

1. The Main Characteristics of α-, β- and γ-Rays

α-Rays. These are He^4 nuclei. They usually consist of a single definite group of high-energy particles and several lower-energy α-particle groups. For instance polonium is considered as a monochromatic α-particle source in practice though twelve α-particle groups are actually present. The main polonium α-particle group (5.3 Mev) is some $5 \cdot 10^3$ times more common than any of the others.

The range of an α-particle in air $R_{0\,air}$ (cm) is proportional to E (Mev) to the three-halves power and is given fairly accurately by the empirical formula

$$R_{0\,air} = 0.318 E^{3/2}\ \text{cm}. \tag{1}$$

The range of an α-particle in an absorber other than air can be found from

$$R = 3.2 \times 10^{-4}\left(\frac{R_{0\,air} A^{1/3}}{\rho}\right), \tag{2}$$

where A is the mean atomic weight of the absorber and ρ its density.

When an α-particle passes through a gas its electric field interacts with the outer electron shells of the molecules and accelerates or ejects some. The gas is therefore ionized. The formation of one ion pair (free electron + ionized molecule) requires 32.5 ev. The α-particle loses energy in this interaction and slows down. The ionization probability rises as the α-particle slows down.

β-Rays. These are electrons or positrons emitted by nuclei; they show a continuous energy spectrum. This continuous β-spectrum is now explained in terms of particles which are electrically neutral and of very small mass (neutrinos). The Pauli principle indicates that this particle is emitted simultaneously with the β-ray and carries off energy ΔE, reducing the β-particle energy below E_{max} (the maximum β-ray energy in Mev):

$$\Delta E = E_{max} - E_1. \tag{3}$$

where E_1 is the energy remaining to the β-ray.

The absorption of beta rays is adequately described by the exponential law

$$J = J_0 e^{-\mu x}, \tag{4}$$

where μ is the linear absorption coefficient (in cm^{-1}), x is the path length of the β-rays in the medium (in cm), J_0 is the initial intensity (number of β-particles emitted per unit time (usually 1 sec) from the source) and J is the intensity emerging from the layer of thickness x. μ/ρ, where ρ is the density of the absorber in g/cm^3, is termed the mass absorption coefficient. It is also used for determining β-ray absorption. μ/ρ is practically independent of the atomic number, Z. The β-particle range in any substance can be found from

$$\rho d = R_{max} = 0.546\, E_{max} - 0.16, \tag{5}$$

where d is the absorbing layer thickness in cm and R_{max} is the range in g/cm^2.

A more accurate relation which applies over a wide energy range is

$$R_{max} = 0.412\, E_{max}^{1.205 - 0.0954 \ln E_{max}}. \tag{6}$$

The β-particle absorption law then takes the form

$$J = J_0 e^{-\mu d} = J_0 e^{-\frac{\mu}{\rho}(\rho d)} = J_0 e^{-\frac{\mu}{\rho} R_{max}}. \tag{7}$$

γ-Rays. These are electromagnetic wave packets emitted by nuclei and have definite wavelengths. Wavelengths of γ-rays are measured in x-units (one x-unit is 10^{-11} cm). The wavelength and γ-ray energy are related by

$$\lambda = \frac{12.38}{E_\gamma}, \tag{8}$$

where λ is the wavelength in x-units and E_γ the γ-ray energy in Mev.

When γ-rays pass through matter they are scattered and absorbed by the atoms. The attenuation is again exponential:

$$J = J_0 e^{-\mu x}, \tag{9}$$

where μ is the linear absorption coefficient, having the dimensions cm^{-1}.

The absorber thickness Δ required to halve the initial intensity J_0 is termed the half value thickness

$$\Delta = \frac{0.693}{\mu} \text{ cm}. \tag{10}$$

It is readily perceived that a thickness of 2Δ produces an attenuation of 2^2 times, one of 3Δ of 2^3 times, etc. The exponential γ-ray attenuation law is true for a narrow parallel monochromatic beam of radiation in a uniform absorber.

If the γ-ray spectrum contains several lines the attenuation law becomes

$$J = J_1 + J_2 + \ldots = J_{01}e^{-\mu_1 x} + J_{02}e^{-\mu_2 x} + \ldots, \tag{11}$$

where $\mu_1, \mu_2 \ldots$ are the linear absorption coefficients for the corresponding spectral lines.

If the chemical composition of the absorber is complex the expression for the linear absorption coefficient becomes

$$\mu = p_1 \frac{\mu_1}{\rho_1} + p_2 \frac{\mu_2}{\rho_2}, \tag{12}$$

where p_1 and p_2 are the relative weight contents of the components and ρ_1 and ρ_2 their densities.

In addition to the linear absorption coefficient and μ / ρ, the atomic and electron absorption coefficients μ_a and μ_ϵ are often used. The latter three are related by:

$$\mu_a = \frac{\mu}{Np}, \quad \mu_\epsilon = \frac{\mu}{\rho NZ}, \quad \mu_a = \mu_\epsilon Z, \tag{13}$$

where $N = 6.02 \cdot 10^{23}$ is Avogadro's number and Z the atomic number of the element.

These latter coefficients have the dimensions cm^2. Therefore, μ_a and μ_e are frequently termed effective cross sections.

The attenuation of electromagnetic radiation is complicated. Twelve elementary processes are known by which γ-rays interact with matter, of which we list the main ones.

Photoelectric: photoelectric or true absorption of the γ-quantum by an atomic electron which is accompanied by the electron being ejected from its orbit. The ionized atom is left in an excited state. The empty level is filled by an outer electron. Some of the γ-ray energy thus goes over to kinetic energy of the photoelectron or of an Auger electron, the rest being emitted as fluorescence. The absorption coefficient due to photoelectric capture is denoted by τ.

Compton effect: this occurs when a γ-quantum interacts with an electron. The photon is deflected by the collision and loses some of its energy to the electron. The change in γ-ray energy is given by

$$\lambda_s - \lambda_{inc} = \frac{h}{mc}(1 - \cos\theta), \tag{14}$$

where $h/mc = 0.024 \cdot 10^{-8}$ cm = 24 x units is the Compton wavelength, θ the angle between incident and scattered γ-ray directions and λ_s and λ_{inc} the wavelengths of the scattered and incident photons. The Compton absorption coefficient is denoted by σ.

Pair production: this occurs when the photon energy $h\nu$ exceeds that for pair production, $2m_0c^2 = 1.022$ Mev. The probability of the process rises with the γ-ray energy and is approximately proportional to the square of the atomic number. The pair production absorption coefficient is denoted by κ. Hence the linear absorption coefficient is given by the following relation when the above three processes occur:

$$\mu = \tau + \sigma + \kappa. \tag{15}$$

2. Detectors

Detectors transform the energy of the radiation into electrical form. The types of detector most commonly used in measurements are ionization chambers, G-M counters and scintillation counters.

An ionization chamber is a capacitor with an insulating gas filling. The radiation-produced ions drift under the influence of an external electric field, thus causing a current to flow in the circuit which depends on the circuit parameters, on the radiation intensity and on the voltage applied. Ionization chambers are used for measuring α-, β- and γ-ray intensities. With α-emitters the source is normally located inside the chamber. If placed outside, a small window is made in the chamber opposite the source. The chamber size is chosen to correspond with the maximum use of the α-particle range. The efficiency for α-particles of a chamber (detector), i. e., the ratio of the number of particles recorded to the total number passing through the working volume, is usually 100%.

With β-rays the source is placed outside the chamber and the efficiency is only a few percent. With γ-rays the wall material and thickness are very important. The efficiency is only a fraction of one percent. Special chambers can be made of somewhat higher efficiency. The efficiency also depends markedly on the nature, pressure and purity of the gas.

G-M counters operate by internal amplification of the weak primary ionization. The electric field has a high gradient near the thin wire anode. The negative ions generated by the radiation are rapidly accelerated near the wire and produce an intense ionization by collision. The counters are self-quenching if the discharge is extinguished on account of the properties of the gas filling, otherwise not. In the latter case special electronic quenching devices are used.

The efficiency of the G-M counter is determined by the probability that the radiation will produce one electron in the counter volume, according to the formula

$$c = 1 - e^{-X_m} \tag{16}$$

where X_m is the mean number of electrons ejected along the track of the ionizing particle in the counter.

X_m can be determined as the product of the specific ionization k_i, the particle path length in the counter l_c, and the gas pressure P:

$$X_m = k_i \, l_c P. \tag{17}$$

The efficiencies of G-M counters for γ-rays vary from a fraction of a percent to several percent, depending on the γ-ray energy and the cathode material.

Scintillation counters use the luminescence stimulated in certain organic and inorganic crystals (phosphors) by radiation. Zinc sulfide, silver or copper activated, is used with α-particles. The α-particle efficiency can be 100%. Cadmium sulfide, silver activated, is used for β-particle detection. The β-particle efficiency is also 100%. The scintillation pulse duration is about $2 \cdot 10^{-8}$ sec. The method is particularly efficient for recording soft γ-rays. This is because the crystal thickness is tens of times greater than the effective wall thickness in other counters. NaI(Tl) crystals are most frequently used for γ-ray detection. The efficiency can then be 20%. Pulse length is 0.25 μsec.

3. Radioisotopes

Radioisotopes decay steadily by internal change and lose their activities uniformly according to an exponential law

$$A = A_0 e^{-\lambda t},$$

where A_0 is the initial activity, A the activity after time t and λ the decay constant for that isotope.

If λ is given, we can easily find $T = \frac{\ln 2}{\lambda}$, which is the time taken for the activity to fall to one-half (half-life). All radioisotopes are also typified by the type of emission (α, β and γ) and by the particle or quanta energies, in addition to the half-life.

Below we give a table of certain radioisotopes most commonly used in automatic measurements.

Symbol	Name	Radiations	Half-life	Energy (Mev)	
				Particles	Quanta
Tl^{204}	Thallium	β, γ	2.7 years	0.76	0.76
Sr^{90}	Strontium in equili-	β	20 years	0.54	—
Y^{90}	brium with yttrium	β	2.54 days	2.27	—
Cs^{137}	Cesium	β, γ	33 years	0.52	0.66
Co^{60}	Cobalt	β, γ	5.3 "	0.31	1.3
Po^{210}	Polonium	α, γ	138 days	5.3	0.8
Ir^{192}	Iridium	β, γ	74 days	0.67	0,13 — 0.88
W^{185}	Tungsten	β	73 "	0.43	—
Ce^{144}	Cerium	β	290 days	0.3	—
Ru^{106}	Ruthenium in equili-	β	1 years	0.039	—
Rh^{106}	with rhodium	β, γ	40 sec.	3.5	0.5
Pu^{239}	Plutonium	α	2.4×10^4 years	5.1	—

II. AUTOMATIC PROCESS CONTROL

Nuclear radiations extend our means of automatic control considerably and enable us to solve many new problems arising in automation. Here they have several advantages over other methods on the measurement side, such as being contactless, the source being unaffected by external factors, no reaction between the object and the measuring instrument, high stability and long life in the radiation sources, rapid response, etc.

Passing to a review of the main trends in automatic methods using nuclear emission, we note that some uses are already firmly established. We refer to methods based on scattering or absorption by the material, or on ionization produced in it by the radiation, and several such others.

In addition to the above there are other trends which, while well known to physicists, are only just beginning to be used in instrumentation. These are nuclear radiation spectroscopy used for technical process control, use of neutron fluxes for the same purpose, and several other such contemporary physical techniques. These methods are particularly promising because they can in some cases be used for continuously checking the compositions of mixtures.

1. Automatic Gaging of Thicknesses, Densities, Weights, etc.

The gaging of thicknesses, weights, densities and other parameters uses the phenomena of β- or γ-ray absorption, which are described quite accurately by (4), (7) and (9) above. The errors of measurement of process parameters using radiation absorption can be analyzed in a general form [1] which is independent of the particular method and apparatus used. The error in measuring the mean flux of an emission results from the operation of two independent factors: the imperfections in the measuring unit and the statistical nature of radioactive decay:

$$\Delta J = \pm \sqrt{(\Delta J_{ap})^2 + (\Delta J_f)^2}. \tag{18}$$

Here ΔJ is the root mean square error in measuring the radiation flux, ΔJ_{ap} that due to imperfections in the measuring apparatus.

$$\Delta J_f = \sqrt{J\tau\varepsilon} \tag{19}$$

is the error due to statistical fluctuation in the decay (J being the flux emerging from the absorber of thickness d, τ the measurement time, ϵ the radiation detection efficiency).

Differentiating (4) or (9) we get the absolute error of thickness measurement:

$$\Delta d = \frac{\Delta J}{\mu J} = \frac{\sqrt{(\Delta J_{ap})^2 + (\Delta J_f)^2}}{\mu J_0 e^{-\mu d}} . \tag{20}$$

The minimum ΔJ_f occurs when

$$\mu = \frac{2}{d} . \tag{21}$$

The radiation source is chosen to give the best approximation to fulfilling (21) for the thickness range to be measured.

The source activity required to give this accuracy is found in general from

$$A = \frac{1.08 \times 10^{-7} e^{\mu d}}{\Delta d \mu d \sqrt{\tau\varepsilon}\, q\Omega} \left[\frac{1}{2\Delta d \mu \sqrt{\tau\varepsilon}} + \sqrt{\frac{1}{4(\Delta d)^2 \mu^2 \tau\varepsilon} + (\Delta J_{ap})^2 \tau\varepsilon} \right] , \tag{22}$$

where Ω is the solid angle subtended by the detector at the source and q is the number of β-particles or γ-ray quanta emitted per decay.

Balance methods are most commonly used in measurements as in this way errors due to changes in the external conditions, supply voltage, radioactive decay etc., can thereby be much reduced. Figure 1 shows a balancing device for measuring the thickness of rollings [2]. Here a differential ionization chamber 1 and two independent sources 2 and 3 are used. The shutter 4 is displaced to balance the radiation fluxes received from 2 and 3. The servo system contains a vibratory converter 5 and servomotor 6. The shutter is driven in till the fluxes reaching the two halves of the chamber are equal.

In most cases scintillation counters are much more efficient than other detectors and require much lower source activities. But they are relatively unstable, and unequal changes in the responses of the two counters in practice prevent their being used in balanced circuits such as of Figure 1. Hence balanced systems with a single common detector are required. Two methods have been proposed [3].

In the first the measured and balancing radiation fluxes fall on the same phosphor in turn, the source being alternately uncovered by rotating lead choppers. The sign of the unbalance can be determined from the phase of the photomultiplier output and balancing effected. The heavy lead choppers restrict the design in this system.

In the second (Figure 2) the measured and balancing fluxes, F_1 and F_2 respectively, fall on separate phosphors P_1 and P_2 joined by a common light-guide C to the common multiplier. The light fluxes from the phosphors are chopped by the opaque thin half-circular disc A and fall alternately on the photocathode. The use of two separate inputs (phosphors) is somewhat of a disadvantage as they may drift differently in response. The most unstable component, the photomultiplier, being common to both, has no effect on the operation.

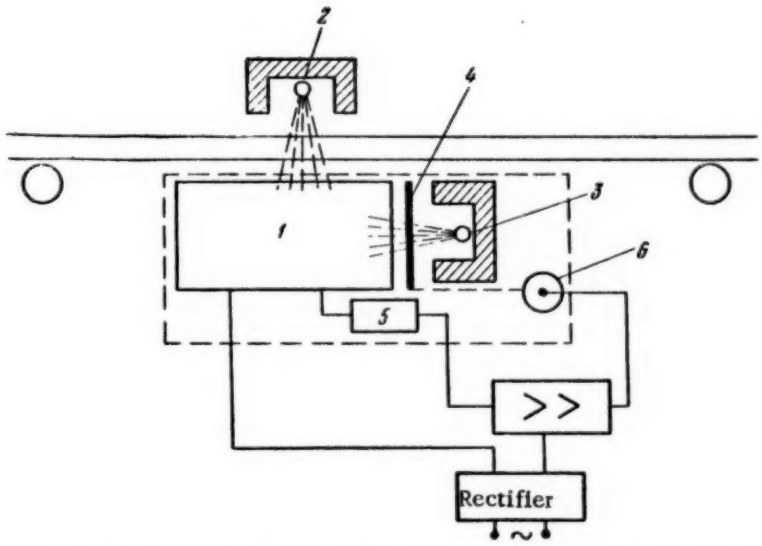

Fig. 1. Schematic diagram of an automatic thickness gaging and control device for steel sheet.

The next advance was the use of vibrating sources [4] which were developed for use in automatic density gaging. Here two radiation sources are used with a common detector system and a balancing wedge inserted in the balancing flux. The sources are fitted to the ends of two electromagnetic vibrators working in phase opposition. The out-of-balance modulated signal controls the movement of the balancing wedge in accordance with the out-of-balance phase.

There are no heavy moving parts in this system.

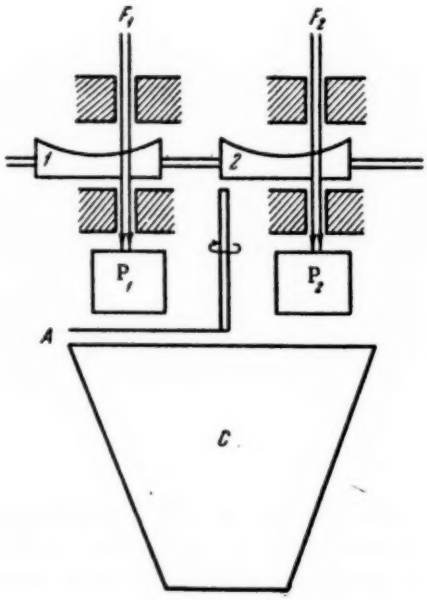

Fig. 2. System using two phosphors: 1) Part under test, 2) standard part.

Yet another interesting balance system has been developed [5]: this is shown in Figure 3. Its main feature is that it is the first to produce balance using a single source and receiver, thereby enabling one to reduce apparatus errors to a great extent. In this device, which was intended for density measurements, the radioisotope is deposited on a rotating disc and the radiation passes alternately via the medium and the balancing wedge to the same scintillation counter.

In the device for automatically gaging and controlling the thickness of steel rollings (Figure 1) a recorder can be fitted to record the readings or else the roll pressure in the mill can be automatically controlled.

Three models of the thickness gage for steel during rolling have been developed.

The following ways of arranging the primary measuring units are possible: a) for measuring the mean thickness of a sheet across its width a single source and receiver are used, of lengths equal to the width of the material; b) for point measurements across the width several sources and detectors are placed, say, at the edges and the center. A single head with source and detector rigidly connected

together can be used, this being traversed across the material. The use of thickness gages at the Leningrad Steel Rolling Works and at the "Zaporozhstal" works [6] halved the rejection of material on thickness grounds and reduced the idle time of the mills to a tenth.

Studies have been made [7, 8] of γ-ray attenuation in coal and rock. These tests led to a radiometric separator being produced which is intended to separate coal and rock lumps, which differ in density. A rapid method of determining the mineral content (ash in particular) of coal was developed and tested under laboratory conditions.

Type	Thickness range	Isotope	Activity, curies	Error of measurement	Minimum strip width, mm	Working life
I	5 — 150 μ	Tl^{204}	10×10^{-3} 5×10^{-3}	±3%	50	5years
II	50 — 1 mm	Ce^{144}	5×10^{-3} 3×10^{-3}	±2%	60	2 years
III	2 — 10 mm	Ir^{192} W^{185}	5 20×10^{-3}	±2%	300	5 months

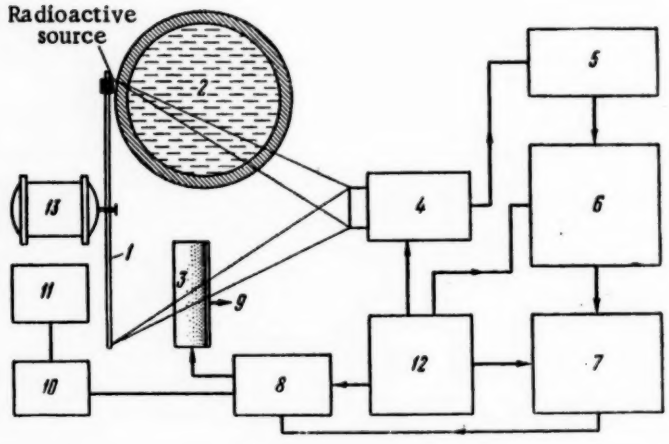

Fig. 3. The PZhR-2 density gage; 1) disc, 2) measured vessel, 3) balancing wedge, driven normal to the section, 4) scintillation counter, 5) integrator, 6) amplifier, 7) phase-sensitive device, 8) reversible motor, 9) indicator arrow, 10) induction coil, 11) secondary equipment, 12) power supply, 13) synchronous motor.

Devices for recording nonuniformities and weight of a moving thread have been used in the textile industry [9]. Figure 4 shows the design of a device for measuring and recording unevenness in thread products. A differential ionization chamber and a balanced measuring circuit are used, the coefficient of variation being computed automatically.

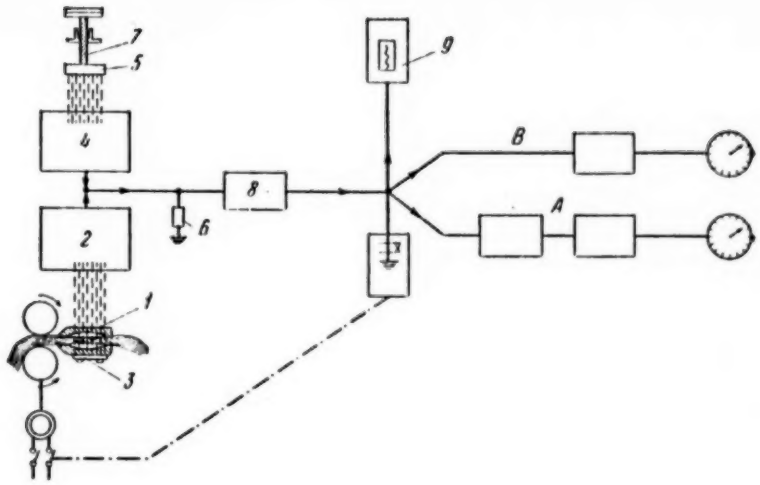

Fig. 4. Structural design of the apparatus for measuring and recording unevenness in spun products: A) Square-law integrating channel, B) linear integrating channel. 1) Shaper unit, 2) working chamber, 3) main source, 4) balance chamber, 5) auxiliary source, 6) chamber load resistor, 7) micrometer screw for adjusting the auxiliary source, 8) electrometer amplifier, 9) recorder.

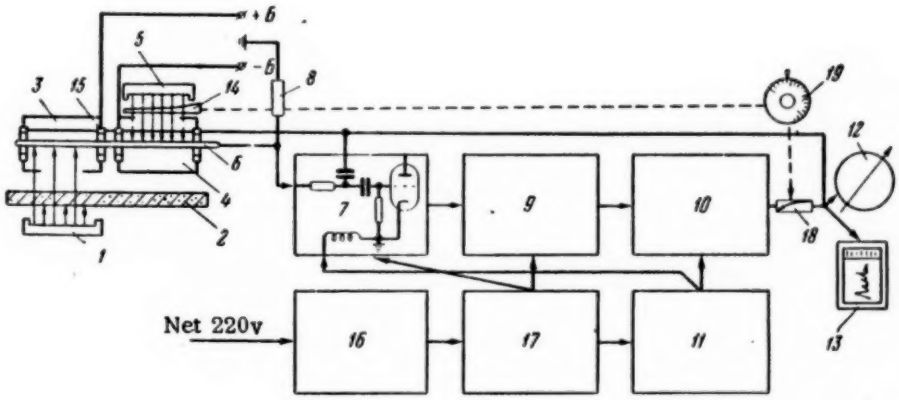

Fig. 5. Block diagram of the "Gosnak Vesomer" (Gosnak weight gage): 1) Working source, 2) absorber (paper), 3) working ionization chamber, 4) balancing ionization chamber, 5) balancing source, 6) collector electrode, 7) electrometer, 8) input resistance of 10^9 ohms, 9) amplifier, 10) phase detector, 11) generator, 12) dial gage, 13) recorder, 14) profile stop, 15) guard rings, 16) power supply, 17) stabilizer, 18) graded slide-wire, 19) weight indicator.

A balanced system is also used for automatic thickness gaging on moving cloth. Tl^{204} and Sr^{90} are used as sources. The ranges are 150-800 g/m² and 800-5000 g/m². Ionization chambers are used as the detectors. The error in the weight does not exceed 1%.

Devices using radioactive transducers for automatically controlling scutching machines have been designed and tested.

The "Gosnak Vesomer" [10] was developed in the paper industry; it checks the weight of paper using ray absorption. The design (Figure 5) uses balance methods with a differential ionization chamber, a vibrating-reed electrometer and a graded slide-wire, which provides high accuracy and sensitivity with good scale linearity. Tl^{204} is used as the source. The error in weight measurement does not exceed 1%.

A radiometric thickness gage has been developed in the fur industry [11]: this uses β-ray absorption. Tests have been made on continuous gaging of milk product and condensed milk quality in the milk industry [12] using β-ray and γ-ray absorption. Work has been done on a contactless method of gaging densities from 0.75-3.35 g/cm³ on refractory parts in the refractories industry.

A device for gaging leather thickness using the absorption of Ce^{144} β-rays [13] has been developed in the leather industry. Balance methods are used (Figure 6), the balancing source being on the needle of the indicator unit. Halogen counters working on average current (i. e., high-current counters) are used as detectors.

Dredgers fitted with γ-ray mud gages are widely used in river dredging and other such operations. The γ-ray gage enables the dredger foreman to check the soil content of the slime continuously by remote control and thereby to operate the dredger most effectively [14].

The Thermal Equipment Research Institute of the Ministry of Apparatus Construction and Automation has developed and introduced the PZhR-1, PZhR-2 and PZhR-3 density gages for general industrial use in recent years [5].

The RKM-1 concentration gage [15] uses β-ray back-scattering from the solution. The current produced in the ionization chambers by the back-scattering β-particles from a mixture is approximately

$$I = \sum_{n=1}^{n} I(Z_k) C_k, \tag{23}$$

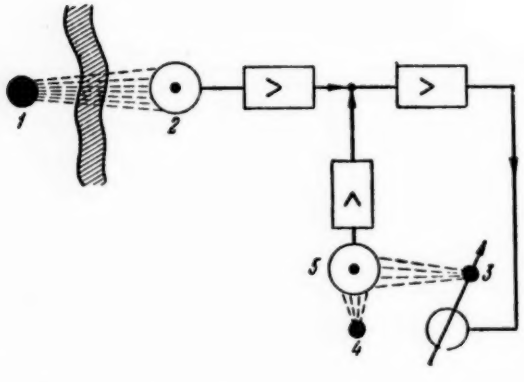

Fig. 6. Block diagram of the device for measuring leather thickness: 1) Main source, 2) main receiver, 3) balancing source, 4) accessory radiation source (for shifting the zero), 5) balancing receiver.

where $I(Z_1), \ldots I(Z_n)$ are the currents produced by reflection from the separate components and $C_1, \ldots C_n$ are the weight contents of the components.

For a binary mixture (n = 2) the sensitivity is given by

$$S = \frac{dI}{dC} = I(Z_1) - I(Z_2). \tag{24}$$

2. Automatic Gaging and Control of Liquid Levels

The main methods of liquid level gaging on closed vessels using radioisotopes are as follows:

the float method;
axial radiation passage;
diametrical radiation passage.

All automatic liquid level gages, with but few exceptions, use γ-rays, Co^{60} being mostly used.

Very simple float-type ones using γ-rays are shown in Figure 7.

The radioisotope 1 is sealed in the float 2 and is displaced relative to the detector 3 as the level alters; 3 transforms the radiation flux into an electrical signal. The faults of those shown in a and b in Figure 7 are that the readings are essentially nonlinear.

The radiation flux, and hence the detector current, is inversely proportional to the square of the source-detector separation, i. e.,

$$I = \frac{A}{(D-h)^2}, \tag{25}$$

where A and D are constants.

To straighten out the characteristic a differential float level gage design was developed [16] (Figure 7c). In this the electrical signals from two detectors are subtracted in the electronic unit 4, which makes the characteristic linear to about ± 3% over a range of about 1 m. If a float at the surface cannot be used, axial irradiation of the liquid in bulk can be employed (Figure 9). A fault here is that the readings are nonlinear, as (25) shows.

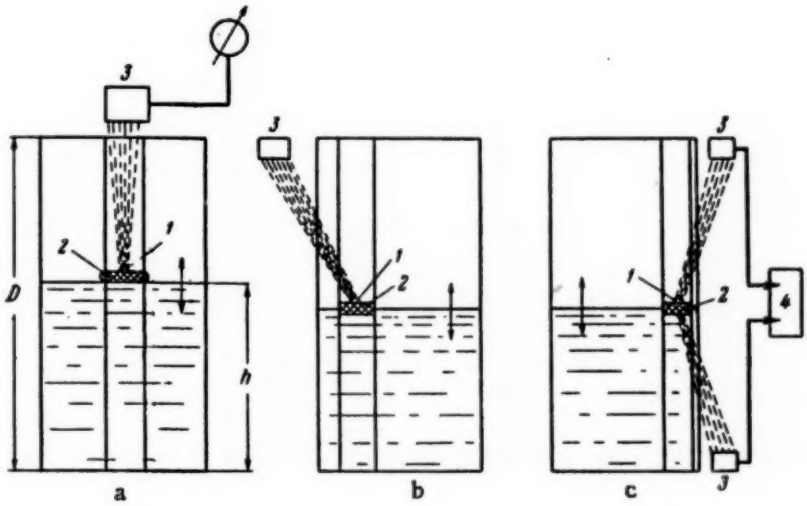

Fig. 7. Level gages using γ-rays (float type, schematic).

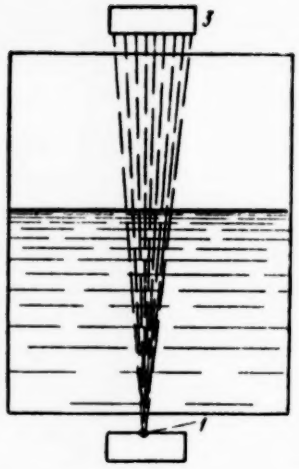

Fig. 8. Diametrical irradiation of bulk liquid in level gages.

The best method of automatic radiometric level gaging is the diametrical irradiation of bulk liquid. Figure 8 shows the commonest method used with closed vessels [16-19]. Figure 9a shows a device for automatically locating a liquid level or interface using a servo system [16]. This can be used with gas/liquid, liquid/liquid and gas/solid interfaces. The γ-ray source 1 and receiver 3 are moved synchronously by the selsyns 5. The selsyns are actuated by a signal from unit 4. When the interface shifts relative to the source-counter line the unit produces a signal (because the media differ in density) which actuates the selsyns. The source and countercarriages follow the liquid level in synchronism. This device is intended to measure levels in the 1-6 m range with object diameters from 6-8 cm to 5-7 m with wall thicknesses up to 100 mm of steel. The absolute error is less than 3 mm.

A level gage for closed vessels using a different principle is shown in Figure 9b [17]. There is no servo system, which is an advantage. On one side of the vessel there is an extended source 1, on the other the detector 2, both extending the full height to be covered. The output current I from the detector depends on the liquid height as the liquid absorbs more strongly than the air or gas above. The current is

$$I = I_0 - ah,^* \qquad (26)$$

where a is a constant and I_0 the current at the minimum level.

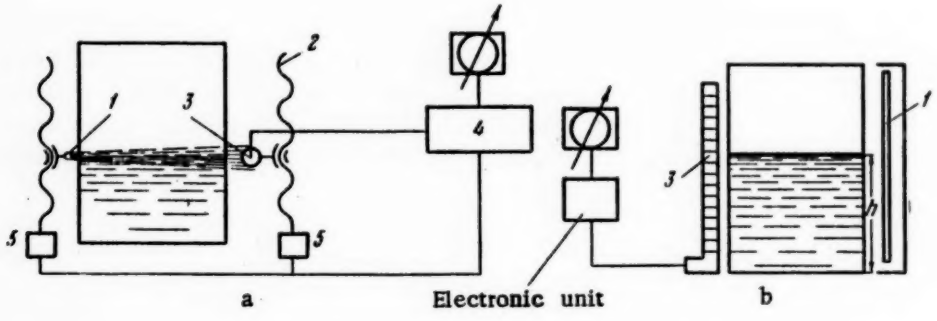

Fig. 9. Level gages with axial irradiations.

Continuous level measurement is very often not required, the level having only to be kept at some present value.

A two-position regulator type IU-2, as shown in Figure 10, can be used for this purpose.

The accuracy of level maintenance is 40-50 mm. The level is adjusted automatically (the actuator 4, which controls the valve, being coupled to the electronic unit 3).

* This formula is approximate; the real scale is rather nonlinear at the ends of the range.

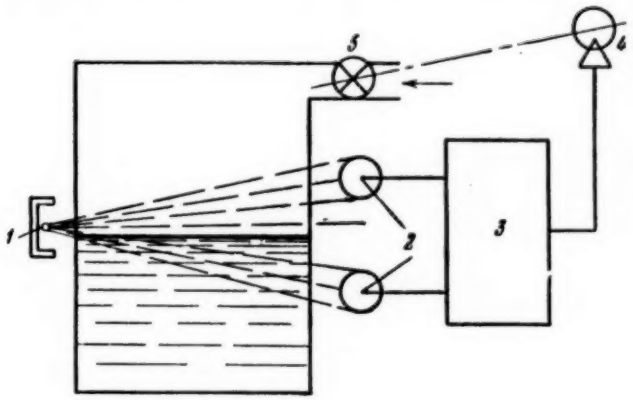

Fig. 10. IU-2 level gage. 1) Source, 2) detector, 3) amplifier, 4) servometer, 5) valve.

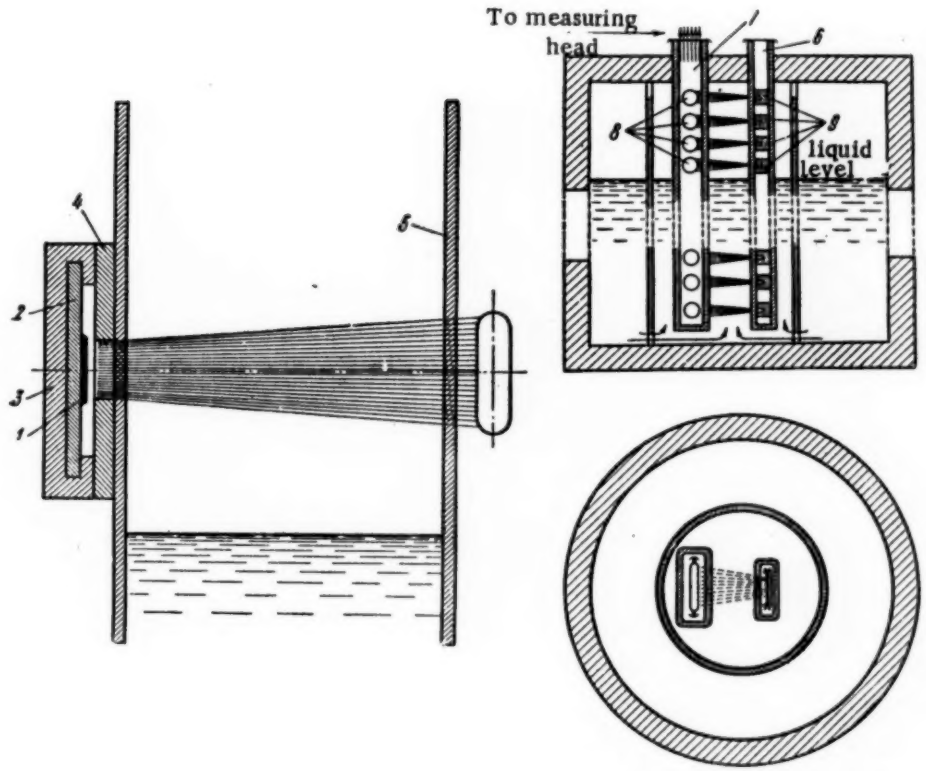

Fig. 11. Schematic level gage using β-ray absorption: 1) Source, 2) aluminum backing, 3) container, 4) steel or aluminum collimator, 5) aluminum screen, 6) source cassette, 7) counter cassette, 9) sources.

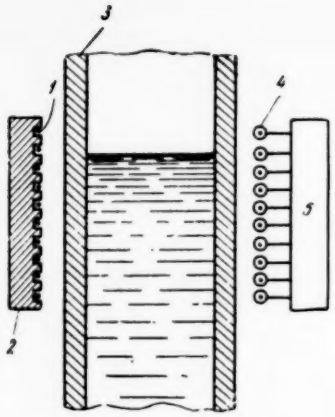

Fig. 12. Schematic diagram of the RU-2 level regulator: 1) γ-source, 2) shielding, 3) crystallizer, 4) counters, 5) thyratron relay control circuit.

A contactless method of checking when the liquid level has reached a set height was developed at the Institute of Automation and Remote Control, Academy of Sciences of the USSR: in this β-ray absorption in the liquid is used (Figure 11). Here the liquid level can be checked to 0.5 mm. The detector output must be coupled to a servomotor which operates the supply line valve if automatic control is required.

This indicator has the advantage of small size and weight. One such unit (source, collimator, detector, electronic relay), less power supplies, weighs about 200 g. Several units with the detectors operating from a single power supply can be used if a certain range of levels has to be covered.

Liquid metal levels are gaged and controlled in metallurgical industries, including the level in the crystallizer in continuous steel casting [20]. Figure 12 shows the RU-2 system used for level regulation with steel in a crystallizer.

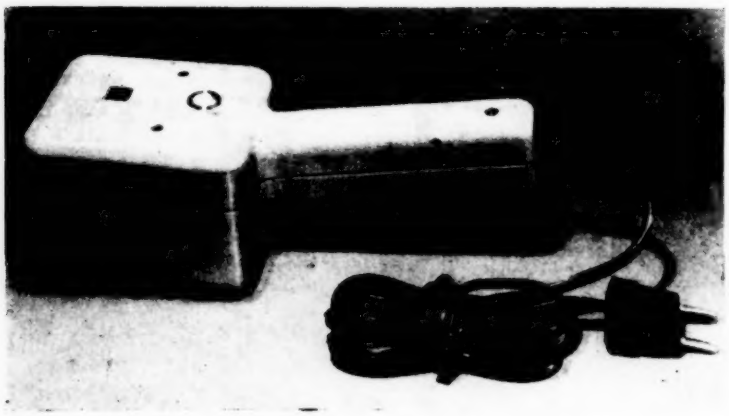

Fig. 13. Exterior view of the RIU-3 radiation level indicator.

A circuit using a scintillation counter fed with a pulsed voltage has been used for measuring ore levels in nonferrous metallurgy [21]. The required source activity was reduced by a factor of ten by this circuit

The Institute of Physics, Academy of Sciences of the Latvian SSR, has developed a portable radiation level gage, RIU-3 (Figure 13) meant for use with liquids in vessels of large diameter and with tank vehicles, which uses a float containing a radioactive source [22]. The unit contains only one tube and is very small and compact. Radiation level gages have also been used in the oil [23], food, chemical and other industries.

3. Automatic Gas and Liquid Flow Measurement and Control

Automatic gas flow measurement. Methods of gas flow metering using radioisotopes can be divided into amplitude and time types. Amplitude types are those based on ion removal and recombination. Figure 14 explains methods using ion removal.

Two electrodes are inserted in the flow [24, 25] opposite one another and a potential applied between them. One also carries a layer of radioactive material R to ionize the interelectrode space. The ions move with a velocity which is the sum of two components: V_y along the y axis (lines of electric field)

$$V_y = k\epsilon, \tag{27}$$

where k is the ion mobility, ϵ the field strength; and V_x along the x axis (gas flow rate). The greater V_x the more ions are removed from the interelectrode space, so the current passed decreases.

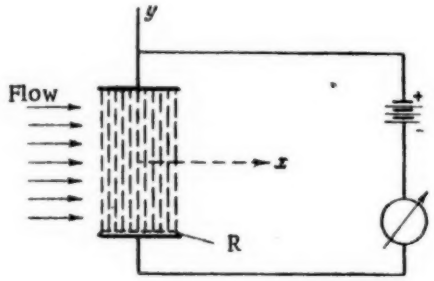

Fig. 14. Theoretical circuit of the ion removal flowmeter.

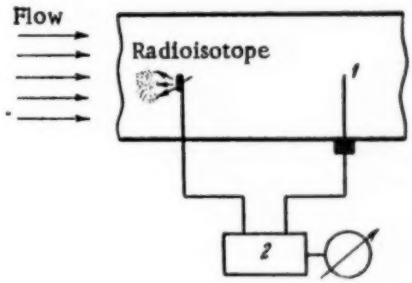

Fig. 15. Theoretical circuit of the flowmeter using ion recombination.

The formula defining the relation of ionization current I to gas flow rate V_x for flat electrodes and the linear section of the voltage-current curve is [26]:

$$I = 2en_0\left[k\varepsilon - \frac{2V_x k\varepsilon}{\sqrt{V_x^2 + 4l^2\alpha N_0}\coth \omega y + 2l\alpha n_0 + V_x}\right]. \tag{28}$$

Here

$$\omega = \frac{\sqrt{V_x^2 + 4l^2\alpha N_0}}{2k\varepsilon l}, \tag{29}$$

e is the electronic charge, l the electrode length, α the ion recombination coefficient, N_0 the radiation intensity, n_0 the number of ions per unit volume (at $\epsilon = 0$ and $V_x = 0$) and y is the distance from the electrode.

Formula (28) shows that the current depends on several quantities in addition to the flow rate, in particular on k and α, which are mainly determined by the state of the gas: temperature, motion, humidity, chemical composition etc. Hence the measurements are of low accuracy. The accuracy can be raised by using differential circuits. But it is difficult to raise the accuracy very greatly in practice. Figure 15 shows a design in which ion recombination is used [27] which is suitable for use at low gas speeds (and hence low flows). Some potential relative to the tube is applied to the receiving electrode 1 from a rectifier in the measuring head 2. This unit also contains an electrometer circuit connected to the receiving electrode. If there is no flow in the region adjacent to the receiving electrode there are no ions there, and the current is zero. At low flow rates a current flows in the circuit, but this is small because most of the ions have time to recombine in transit between the site of production and the receiving electrode. The ion transport time falls as the speed rises, so the ion density near the receiving electrode rises and with it the current. At high speeds the transport time is so low that recombination scarcely occurs and the current is velocity-independent.

β-emitters are used and so volume recombination occurs.

The ion concentration time variation is given by

$$n = \frac{n_0}{1 + \alpha n_0 t}, \tag{30}$$

where t is time, n_0 the number of ion pairs at t = 0, n the number at a later time t and α the recombination coefficient.

The electrode current is proportional to the number of ions in the space around the electrode. The time t is determined by the ratio of the distance s from ionizer to electrode to V_x. For the current-speed relation to be linear we must have

$$\alpha n_0 t \gg 1. \tag{31}$$

Hence (30) becomes

$$n = \frac{1}{\alpha t} = \frac{V_x}{\alpha s}. \tag{32}$$

The calibration curve [27] is a straight line at low speeds. The upper limit of velocity usable in this method with a given ionizer is defined by (31). Formulas (30) and (32) imply a direct relation between the readings and the recombination coefficient, and hence the state of the gas.

The time methods are based on velocity determinations from the formula

$$V_x = \frac{s}{t}, \tag{33}$$

where s is the path length traversed by the gas particles in time t. The main problem is thus to label some section of the gas and measure the time for it to pass over a fixed distance. This time is determined only by the flow speed and is independent of pressure, temperature, humidity, chemical composition, etc.

Tracer atom methods are a classical example of this [28]. But we will not pause over this because it involves introducing radioactive material into the pipe and is difficult to make automatic.

In 1955 the Institute of Automation and Remote Control, Academy of Sciences of the USSR, developed a new contactless method of automatic gas flow metering using modulated radioactive emissions which had decided advantages over the methods considered above [29, 30].

Figure 16 shows the design used.

The radioisotope lies in the special container 1 outside the tube and has no direct contact with the gas. The radiation falling on the tube is chopped by a special unit 2 so that it only falls on the tube for short intervals separated by pauses. A section of the gas inside the tube is periodically ionized, giving an ion marker which moves with the flow. The detector 3 placed further along determines the instant when the ion marker passes, the special measuring unit 5 computing the time between mark production and detection. The ion marker occupies the whole flow cross-section and takes on the velocity distribution curve shape 4, so the mean flow velocity can be measured as the time when the maximum number of ions is transferred from the marked volume.

Unit 2 is a magnetic or mechanical chopper. In the simplest case it is just a shutter which uncovers the isotope for a short time. Vibratory choppers can also be used. In some cases (mainly when the harder radiations are used) it is convenient to have a fixed diaphragm and move the isotope.

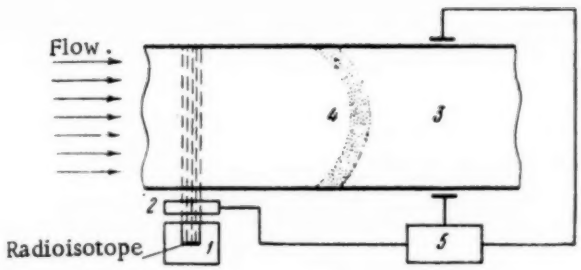

Fig. 16. Schematic diagram of the flowmeter using modulated radiation.

The detector 3 is two insulated plates which produce a transverse electric field in the pipe. This field is necessary to reveal the electrical properties of the ion markers which are as a whole electrically neutral (they contain equal numbers of positive and negative ions). The ion displacement produced by the field results in a current pulse in the detector plates. The plates may be insulated from the flow but must not be screened from it, so insulating inserts must be fitted in the metal walls with the plates attached to the inserts. The repetition frequency is usually some tens per second, so automatic continuous gas metering is easy. An engineer's design method for such flow meters has been developed [31, 32].

Notable features of this method are a) the measuring elements have no contact with the gas, b) the results are unaffected by change in the radiation flux or gas properties (the measurement is absolute, the accuracy being determined solely by the accuracies of the time and distance measurements).

The Heat Equipment Research Institute of the Ministry of Apparatus Construction and Automation has designed a standard flow meter, RGR-1, for general industrial use, which uses the above principle [33]. Balance methods are used for measurements, the transport time being kept constant by varying the source-detector spacing. Figure 17 gives an exterior view of the flowmeter. The range is 1-3 m^3/hour, error not exceeding ± 2.5%.

Automatic liquid flow metering and control. The need to meter flows of liquid automatically when the liquid is aggressive or in a pipeline under pressure or heated to a high temperature often arises in many technical processes. It has so far been very difficult to solve such problems by existing methods.

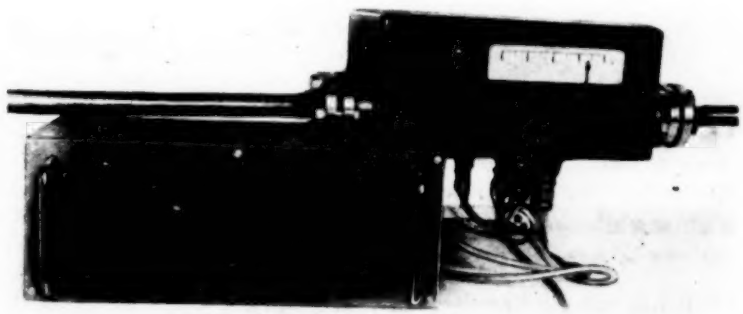

Fig. 17. Exterior view of the RGR-1 flowmeter.

A solution is much facilitated by using radioisotopes and flow measurement technique in which the measuring parts are mechanically completely disconnected from the primary transducer, which is immersed in the flow.

The Institute of Automation and Remote Control, Academy of Sciences of the USSR, has developed one species of such flowmeter [34]. Figure 18 illustrates the method. Here the absorption of γ-rays in the collimator 4 is used to produce a modulated radiation flux. The primary transducer is a rotating vane with one or several blades carrying small Co^{60} sources (1-2 millicuries). Outside the tube the radiation detector 2 (halogen counter) lies behind a screen: it receives a modulated radiation flux. The required modulation depth $\underline{m}$ is determined by the screen length l, in accordance with the formula:

$$l_s = \frac{\ln m}{\mu}, \qquad (34)$$

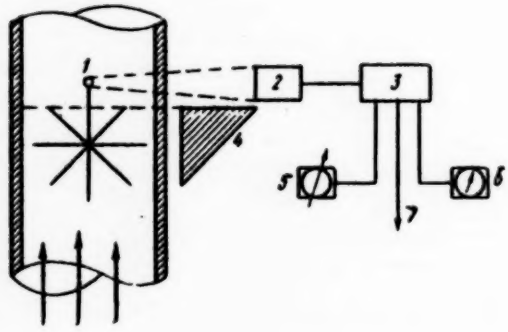

Fig. 18. Schematic diagram of the vane flowmeter.

where μ is the linear absorption coefficient for the γ-rays in the screen.

The vane rotation rate varies with the flow speed, so the frequency of the current pulses from the output of 2 varies also. The measuring head 3 has an electromechanical register 6 which reads the total flow and a needle instrument 5, which shows the instantaneous flow rate. The measuring head contains one tube and can be connected to a recorder. The maximum flow rate measurable is determined by the maximum permissible rotation frequency for the vane, f_{max}, with a given source strength A and detector sensitivity:

$$f_{max} = \frac{N\alpha}{360 N_{min}} \text{ rps} \qquad (35)$$

where N is the maximum number of γ-quanta the G-M counter can record per second, α is the working angle, which indicates the part of the source path seen directly from the counter and N_{min} is the minimum permissible number of pulses in a bunch which will ensure normal operation of the measuring circuit.

When the source activity for this sytem is calculated the following relationship may be used:

$$A = \frac{4\pi R^2}{S_r n \epsilon k} N e^{\mu_a R + \mu_w t} \text{ mC} . \qquad (36)$$

R is the source-counter distance in cm, given by the screen thickness if the pipe diameter is small. The number of counters n and the working area of a single counter S (cm^2) determine the total working area of the detector; ϵ is the counter efficiency, which indicates what fraction of the quanta reaching the counter area is recorded; k is the number of quanta emitted per decay (for Co^{60} k = 2); μ_a and μ_w are the linear absorption coefficients for air and tube wall for the γ-rays, respectively; t is the pipe thickness and N is the maximum number of counts that can be recorded per second.

Tests showed that line voltage variations of ± 20% did not affect the operation. The accuracy of the total flow, read from the register, is 0.5%. The lower limit of readings in this instrument is 5 cycles/second. The accuracy of flow measurement is 2.5%. The instrument also includes an output 7 for connecting an automatic flow regulator. It is made up of two separate units joined by a cable. The measurement and control units can be up to 150-200 m away from the measuring point. This instrument may find extensive use in the very many branches of industry where the technical processes involve transferring explosive and highly corrosive liquids since no connection to the object is required.

4. Automatic Indication of Impurities in a Gas

If the gas composition varies in a chamber receiving a fixed radiation flux the output will alter. This effect is used to monitor for impurities in the gas automatically. The chamber operating conditions must be chosen to suit the impurity concentration [35].

At low impurity concentrations (tenths or hundredths of a percent) the initial linear section of the ionization chamber characteristic should be used. Then the chamber current expression takes the form

$$I_p = \frac{2eS\,k}{h}\sqrt{\frac{n_0}{\alpha}}\,U, \tag{37}$$

where e is the charge on an ion, S is the chamber electrode area, h is the interelectrode separation, k is the ion mobility, α the recombination coefficient, n_0 the number of ion pairs produced in unit volume per unit time, and U the potential difference between the chamber electrodes.

α varies little with gas composition. n_0 is proportional to the gas density at constant pressure, the density being practically constant at low impurity concentrations. But the ion mobility varies very markedly when small traces of smoke, ammonia, chlorine, sulfur dioxide, etc., are present in the air or other gas.

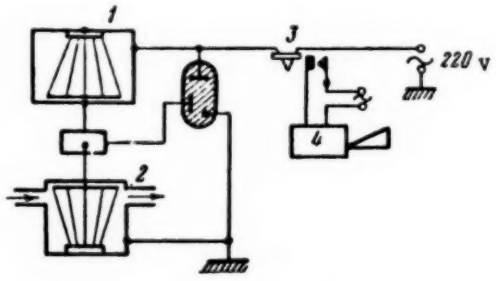

Fig. 19. Automatic indicating unit for smoke in the air.

This property of an ionization chamber is used in fire alarms and industrial health work to indicate the presence of smoke or injurious impurities in the air automatically.

Figure 19 shows the circuit of such an alarm [36], using a cold-cathode tube.

The two ionization chambers 1 and 2 are connected differentially, one being sealed off and the other open to the atmosphere. When impurities are present in the air the output currents become unbalanced, the relay in the plate circuit operates and the alarm 4 rings.

When high impurity concentrations are to be measured it is better to work in the saturation range. Here the current is proportional to the molecular weight of the gas [35], so concentrations of impurities differing in molecular weight from the principal gas can be measured and recorded.

5. Automatic Gaging and Control of Gas Pressures

The current from an ionization chamber containing an internal α-source is proportional to the chamber pressure (recombination neglected) [36, 37]:

$$I = 3.7 \times 10^7 A\eta e n l_e \frac{P}{760}, \tag{38}$$

where A is the source activity in millicuries, η the source utilization coefficient, e the electronic charge, n the number of ion pairs produced by one α-particle in 1 cm, l is the chamber dimension and P is the gas pressure in mm Hg.

This effect can be used to develop a device for automatic gaging and control of gas pressures.

The source activity at any given current measurement sensitivity I_T can be found from

$$A = 1.4\frac{10^{14} I_T}{npl\eta}. \tag{39}$$

The activity must be calculated for the lower bound of the working pressure range, where the activity required is highest. At very low pressures the limit of measurement is set by the currents caused by secondary electrons ejected from the chamber walls by the α-particles.

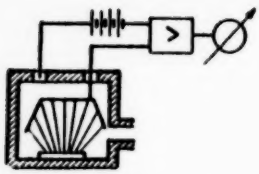

Fig. 20. Scheme used in gage (indicator style).

At high pressures the chamber dimensions are restricted and must be very small since the constant ionization region has to be used (the chamber dimensions must be much less than the particle range at that pressure). On this basis two types of gage were developed [37]; an indicator type, for use at 10^{-3} to 10 mm Hg (with three subranges) and a recording one with a range of 10^{-2} to 10 mm Hg. Accuracy of pressure measurement is 2%.

Figure 20 shows the system used, no special explanation being needed. We only note that 100% feedback is used on the electrometer amplifier to ensure high stability.

Figure 21 shows the design of a recording type of this instrument. Here the ionization chamber signal is modulated at 50 cycles/second and amplified by a normal ac amplifier. The amplifier feeds a servomotor which drives a special self-balancing potentiometer fed from a separate stabilized power supply. The potentiometer produces a balance signal of sign the reverse of the amplifier output.

When the two signals balance, the system is at rest and the angle of rotation of the potentiometer shaft serves to measure the gas pressure. The pressure is recorded on a distant recorder.

When coupled to auxiliary equipment, automatic control can be effected as well.

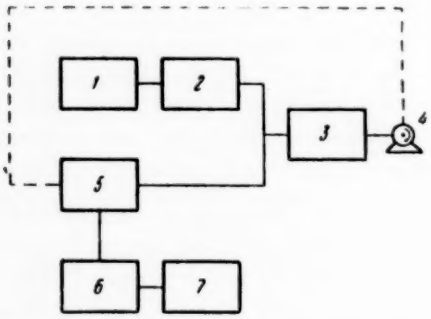

Fig. 21. Gage scheme (recording style): 1) Ionization chamber, 2), 3) amplifiers, 4) servomotor, 5) balancing device, 6) converter, 7) recorder.

6. Relay Systems Using Contactless Radioactive Relays

Contactless radioactive relays find a place in many automatic metering and control devices as they enable one to improve and simplify the systems greatly. A particular feature of relay circuits is that the magnitude of the radiation flux (if above the operating threshold) has no effect on the result, this being in addition to their simplicity.

A typical relay circuit produced by the Institute of Physics, Academy of Sciences of the Latvian SSR (Figure 22) works on ac and is widely used, for instance, for positional voltage control* [22]. The Central Ferrous Metallurgy Research Institute thyratron relay (Figure 23) is mainly used for liquid metal gaging.

The **γ-relays** with transistors (Figure 24) and scintillation counters (Figure 25) developed at VUGI [38] are of interest.

Relay type temperature controller. A relay used for furnace temperature control [39] is described below.

The furnace temperature is measured by a thermocouple plus millivoltmeter. The millivoltmeter needle carries a small vane bearing an α-emitter which lies opposite the slit of an ionization chamber. The latter is connected to an electrometer amplifier, which controls the furnace switching relay. When the vane no longer overlaps the slit, the furnace is switched off. The vane moves as the temperature falls, and the radiation again enters the chamber and the furnace is switched on. If the permissible insensitive range at the needle Δl is given the insensitive range can be expressed in current terms as

$$\Delta I = I \frac{\Delta l}{b},$$

*Here the source is fixed to the indicator needle. If the needle goes beyond the limits of a screen, the width of which determines the voltage maintenance accuracy, the radiation falls on one of the counters GC_1, GC_2, which cut in appropriate relays in the voltage control circuit.

where I is the chamber current when the radiation enters and b is the slit width.

$\Delta I = 10^{-10}$ amp when $\Delta l = 0.05$ mm.

If the operation is to be stable the electrometer stage grid current must be much lower, i. e., around 10^{-11} amp: this presents no special difficulties.

The chamber capacitance plus the high input resistance in the grid circuit determine the relay time-constant (above 1 sec). The actuator section is a thyratron plus mercury contact relay. Prolonged tests gave good results and the relay system should find many uses in automatic control of various production processes.

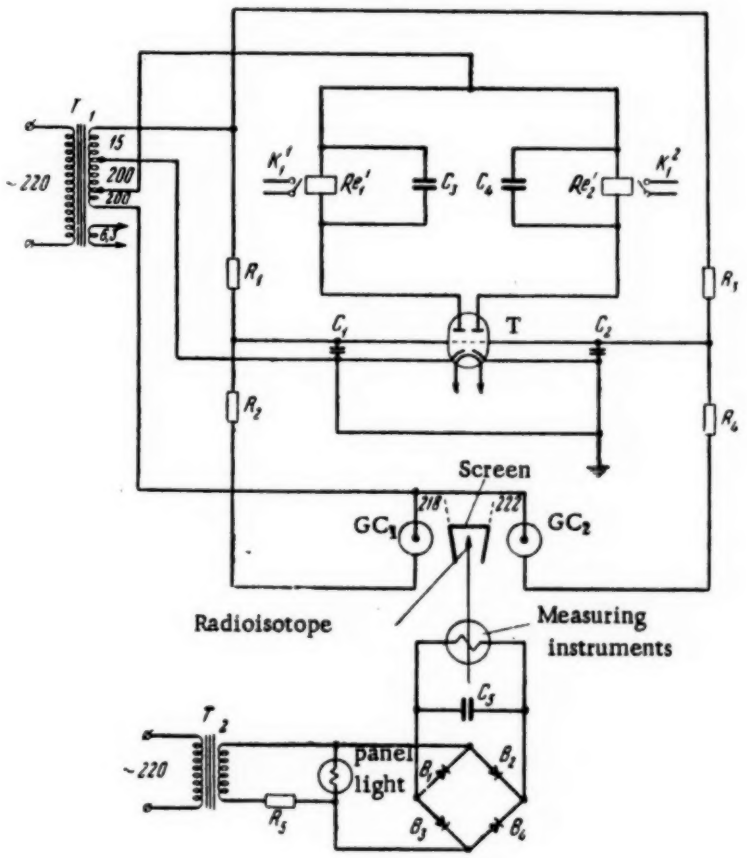

Fig. 22. A typical relay circuit produced by the Institute of Physics, Academy of Sciences of the Latvian SSR.

Relay systems for counting and marking products. The combined contactless relay circuits developed by the Institute of Physics, Academy of Sciences of the Latvian SSR [22] are of considerable interest.

Devices for counting product items on conveyors are primarily involved. On one side of the conveyor is a radiation source, on the other a detector which passes a pulse to the counting head each time the beam is interrupted.

Another system is designed to switch over cineprojectors when the reel finishes. For this the end of each reel is marked by a small amount of active material. When the mark passes before the detector a pulse is produced which switches off that projector and switches on the next one.

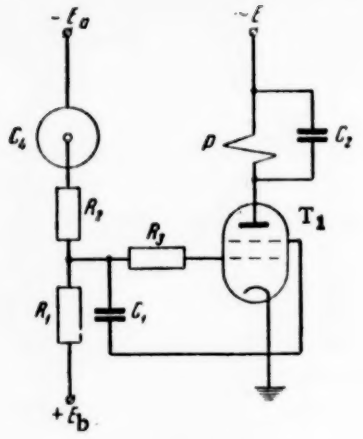

Fig. 23. The TsNII Chermet thyratron relay.

A relay system of marking steel rollings has also been developed [18]. Sheets rolled from steels of different grades are marked with radioactive labels. When the sheets are passed before a detector a pulse is produced from which the steels can be sorted automatically. The relay circuits developed by the Institute of Physics, Academy of Sciences of the Latvian SSR are used to count cans moving along a conveyor in the meat industry, for checking the filling of aluminum tubes with cream in the cosmetic industry and for many other purposes.

Relay systems have been developed in the coal mining industry for counting and checking the loading of mine carts, for producing contactless control pedals in electric trains, for automatic stopping of trains on red signals, and for loading etc., devices [38].

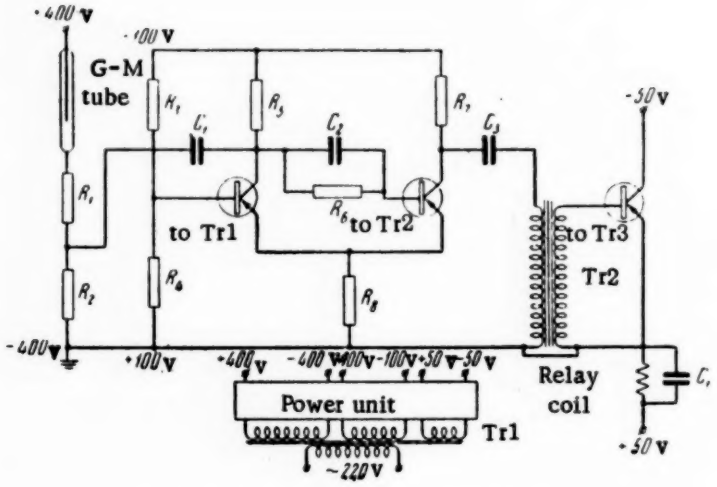

Fig. 24. The transistorized VUGI relay.

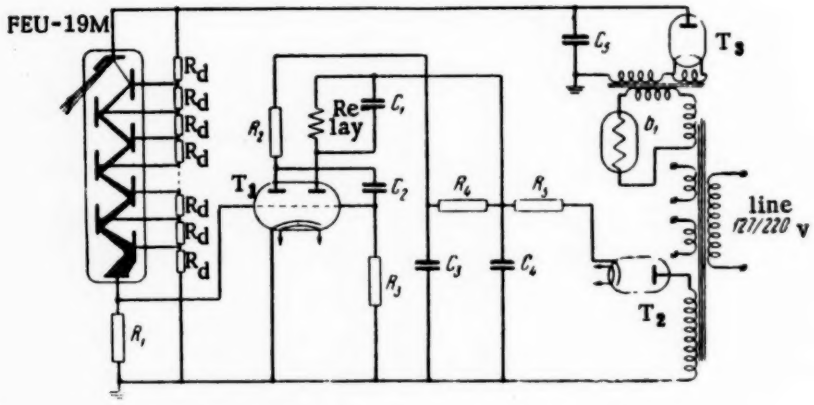

Fig. 25. The scintillation counter VUGI relay.

7. The Future Development of Automatic Gaging Methods

The methods of automatic gaging using radioisotopes reviewed above have found practical applications. But work is also being done on using nuclear radiation spectroscopy in automatic devices, in which the individual components of the energy spectrum are utilized or the scattered radiation intensity is selectively detected using γ-ray spectroscopy.

A considerable advance in spectroscopic methods could be made by using the bremsstrahlung generated when β-particles pass through matter. A device and circuits developed by the Institute of Physics, Academy of Sciences of the Latvian SSR, for determining the thicknesses of parts by working from one side only represents a practical step in this direction: the intensity of the Cs^{137} backscattered γ-rays is used, the energy of these γ-rays differing markedly from that of the primary ones. This type of work deserves very serious attention.

Attention should also be given to using neutrons and the absorption, scattering and moderation of the neutrons in media. Neutron methods can be used to determine moisture contents, for unilateral level gaging on hydrogeneous media, for temperature measurement, etc.

Automatic composition testing using neutrons [40] by activation analysis or by using nuclear reactions such as (n, γ), etc., is of particularly great interest, since these are often not accompanied by radioisotope formation and demand much lower neutron fluxes. The fluxes can then readily be produced from low-power Po-Be sources, etc.

The data presented here indicate the wide range of work on the use of nuclear radiations in automatic devices going on in the Soviet Union and the great prospects which have already been revealed for further advance in this branch of technology.

LITERATURE CITED

[1] A. M. Bogachev, B. I. Verkhovskii and A. N. Makarov, "Theory of a method of thickness gaging with radioactive emissions," Zavodskaya Lab. 21, 7 (1955).

[2] A. M. Bogachev, B. I. Verkhovskii and A. N. Makarov, "Method and apparatus for thickness gaging on steel rolled sections with radioactive emissions," Zavodskaya Lab. 21, 7 (1955).

[3] B. I. Verkhovskii, V. A. Sotkinov and V. V. Iakushin, "Scintillation-counter measurements on radioactive emissions; a method of reducing apparatus errors."*

[4] G. I. Birger, B. I. Verkhovskii and I. Ia. Ovcharenko, "A new type of radiation density meter."*

[5] G. G.Iordan and K. S. Furman, "Measurement of liquid density with γ-rays."*

[6] L. N. Baskin, A. M. Bogachev, I. A. Brodskii, B. I. Verkhovskii, A. N. Makarov, N. S. Novoshenia, and L. A. Rubinshtein, "Tests on introducing gages for thicknesses of rollings and coatings."*

[7] V. D. Goroshko, "Use of radiations in coal enrichment processes," Vestnik Akad. Nauk SSSR 1956, No. 2.

[8] V. D. Goroshko, "Use of radiations for enriching coal and checking its quality."*

[9] S. S. Shvyrev, A. N. Slatinskii, and K. D. Pismannik, "Use of radioisotopes in the textile industry."*

[10] E. A. Nekhaevskii, "An experiment on using radioisotopes for continuous checking of the weight of a moving paper strip."*

[11] V. A. Pchelin, and T. A. Shmeleva, "A radiometric method of determining the hair covering thickness on furred pelts."*

[12] A. Ia. Vainberg, "An experiment on using radiations for automatically checking and controlling technical processes in producing milk products."*

*Report to the All-Union Scientific-technical Conference on the use of radioactive and stable isotopes and radiations in the national economy and science, Moscow, April 4-12, 1957.

[13] S. M. Smirnov, "Use of radioisotopes in the leather industry."*

[14] S. N. Dediukov, "Use of radioisotopes in river transport."*

[15] G. G. Iordan, and T. G. Neiman, "β-ray measurements of densities of solutions."*

[16] G. G. Iordan, "Use of radioisotope emissions for controlling technical processes," Priborstroenie 1956, No. 1.

[17] L. K. Tatochenko and S. V. Medvedev, "Use of radioisotopes for liquid level measurement," Zavodskaya Lab. 1955, No. 10.

[18] G. G. Iordan, V. B. Brodskii and B. S. Sotskov, "Use of radioisotopes for controlling technical processes." (Report to the Geneva Conference on the Peaceful Uses of Atomic Energy), 1955.

[19] L. K. Tatochenko, "Liquid metal level gaging with γ-rays," Problemy metallov i fiziki metallov, 1955,No. 4.

[20] L. K. Tatochenko, "Automation of continuous steel casting," Stal' 1956, No. 3.

[21] B. Ia. Orcharenko, "Use of electronically modulated scintillation counters in industrial radiation indicators."*

[22] A. Ia. Auzan, V. E. Banashek, Kh. E. Gunne, I. M. Taksar, A. D. Tumul'kan, P. E. Chaplinskii, A. I. Eimanis, and V. A. Ianushkovskii, "Devices for automation and checking using a contactless radiation relay."*

[23] Iu. S. Zaslavskii, and G. N. Shor, 'Use of atomic energy in the oil industry, [in Russian] (Gostekhizdat, 1956).

[24] S. A. Samoilov, Authors certificate No. 75354 (1947).

[25] J. E. Lovelok, and E. N. Wasilewska, "An ionization anemometer," J. Sci. Instr. 26, 11 (1949).

[26] N. I. Shteinbok," The main problems in using radioactive emissions in measurement," Uspekhi Fiz. Nauk 54, 2 (1954).

[27] J. Kohl, "Radioisotopes in process instrumentation," Chem. Eng. Prog. 48, 12 (1952).

[28] E. W. Voice," Radioactive determination of gas flow in large ducts," J. Iron Steel Inst. 177, 4 (1954).

[29] N. N. Shumilovskii, and L. V. Mel'ttser, "Use of radioisotopes for gas velocity gaging and for automatically recording gas flows by the 'marked molecule' method," Proc. Akad. Sci. SSSR 106, 4 (1956).

[30] N. N. Shumilovskii, and L. V. Mel'ttser, "Automatically recording gas flows by the 'marked molecule' method," Priborstroenie 1956, No. 3.

[31] N. N. Shumilovskii, and L. V. Mel'ttser, "An engineer's method of designing flowmeters using the 'marked molecule' method," Priborstroenie 1956, No. 11.

[32] L. V. Mel'ttser, 'Use of radioisotopes," Dissertation for the science degree of Candidate in Technical Sciences, Inst. Automation and Remote Control, Akad. Nauk SSSR, 1956.

[33] G. G. Iordan, K. S. Furman, and T. G. Neuman, "A device for automatically checking a gas flow with β-rays."*

[34] N. N. Shumilovskii, Iu. V. Gushchin, and M. I. Tolokonnikov, "Use of radioisotopes for automatically recording liquid flows."*

[35] N. I. Shteinbok, 'The operative principle in α-ionization gas analyzers," J. Tech. Phys. (USSR) 26, 1 (1956).

[36] V. B. Brodskii, "Measurement of gas pressure by a radioactive method," Inform. nauch.-tekh. biul., NII Labpribor, No. 5, 1954.

---

*Ibid.

[37] V. B. Brodskii, "Vacuum gaging by a radioactive method," Priborstroenie 1956, No. 7.

[38] V. G. Segalin, Use of Radiation Gaging Methods and Automation in the Coal Industry [in Russian] (Ugletekhizdat, 1956).

[39] A. S. Matveev, I. N. Ermolov and M. F. Kranovian, "A contactless radiation relay," Priborstroenie 1956, No. 1.

[40] V. A. Korotkova, "Analysis methods using radiation."*

[41] M. B. Neiman, "Radioisotopes in measurement," Izmeritelnai tekhnika 1955, No. 1.

[42] N. N. Shumilovskii, and L. V. Mel'ttser, "Use of radioisotopes in automatic control devices," (Report to the Conference on current instrument design in the measurement field) (F. E. Dzerzhinsk Moscow Branch Sci. Tech. Propaganda Press, 1956).

[43] N. I. Shteinbok, "The principal characteristics of ionization chambers," J. Exptl.-Theoret. Phys. (USSR) 27, 5 (1954).

[44] N. N. Shumilovskii, "Use of radioisotopes in measurement. Trans. Conf. on Electrical measurements," Izd. Akad. Nauk. Ukr. SSR (in press).

[45] B. Z. Votlokhin, A. Z. Dorogochinskii, and N. P. Mel'nikova, "An industrial test of gaging the sequence of pumping of oil products using a radioactive material."*

[46] V. I. Kuznetsov, "Determination of leak site on underground gas-pipes using radioisotopes."*

[47] T. B. Abramova, " Determination of leak sites in the lead covering of a telephone cable."*

[48] V. S. Medvedev, and I. S. Roizen, "Use of radioactive materials in accident prevention."*

Received September 4, 1956

*Ibid.

EVALUATION OF ELECTRONIC INTEGRATORS

B. Ia. Kogan

(Moscow)

The three main types of electronic integrators are compared as regards the minimum permissible integration frequency for a sinusoidal input signal and the largest permissible integrating time for a step signal.

The three main types [1] of electronic linear computing units, classified according to operating principle, are

1) those with passive amplifier input circuits (Figure 1a),

2) those with parametric error compensation (Figure 1b),

3) those with negative feedback (Figure 1c).

The advantages or otherwise of the various types have already been dealt with fully [2, 3].

In defining their various fields of use it is of considerable value to compare the devices with one another. The minimum permissible frequency of a sinusoidal input ω_{min} and the maximum permissible integrating time t_{max} for a step input are fundamental to such a comparison, being applicable to digital computer and analog problems. ω_{min} and t_{max} are restricted in principle to linear units by the requirement that the error of their operation shall not exceed some preset value, and by the extent of the dynamic range. By dynamic range we here mean the ratio of the output signal at the linearity limit to the minimum input signal which can be distinguished from the noise.

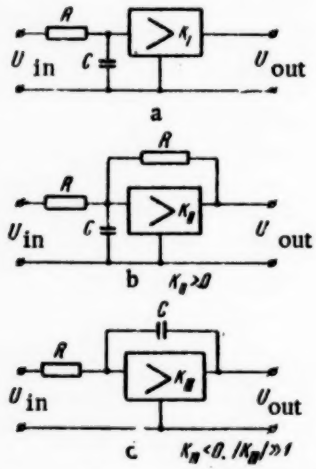

Fig. 1. Linear electronic integrators.

These types of unit have not been fully compared in the literature (e. g., [2-5]). In addition, improvements in computer amplifiers have resulted in some earlier deductions becoming invalid. The present note aims to evaluate and compare ω_{min} and t_{max} for these three types of integrators and to establish how ω_{min} and t_{max} are affected by the various primary errors and by the finiteness of the dynamic range.

1. The Minimum Permissible Sinusoidal Input Frequency

We estimate ω_{min} from the permissible systematic error and the finiteness of the dynamic range. The equations for these types of integrators can be put into operator forms as

$$\bar{U}_{out\ I} = \frac{K_I}{Tp+1}\bar{U}_{out\ I},\quad \bar{U}_{out\ II} = \frac{\frac{1}{\alpha}K_{II}}{\frac{1}{\alpha}Tp+1}\bar{U}_{in\ II},$$
$$\bar{U}_{out\ III} = \frac{K_{III}}{(1+K_{III})Tp+1}\bar{U}_{in\ III}, \tag{1}$$

where $0 < \alpha \leq 1$ is a coefficient which allows for the degree of error compensation, K_I, K_{II} and K_{III} being the gains of the amplifiers in the integrators I, II and III without feedback and T = RC is the time-constant of the passive circuit. T is taken as being the same for all three types.

All such units can integrate if, over the operating frequency range, the inequalities $|Tj\omega| \gg 1$, $|T \cdot 1/\alpha \cdot j\omega| \gg 1$, $|(1 + K_{III}) Tj\omega| \gg 1$ hold.

In principle these inequalities can be complied with by increasing T and restricting the least permissible ω.

In practice it is not desirable to make T larger than 1-10 sec. Hence we are restricted to some minimum permissible input frequency ω_{min}.

We estimate ω_{min} from the accuracy with which integration is performed. With a sinusoidal input ($p = j\omega$) the input and output voltage amplitudes are related by

$$U_{out\ I} = \frac{K_I}{T\omega} \frac{U_{in\ I}}{\sqrt{1 + \frac{1}{(T\omega)^2}}} \approx \frac{K_I}{T\omega}\left[1 - \frac{1}{2}\frac{1}{(T\omega)^2}\right] U_{in\ I},$$

$$U_{out\ II} \approx \frac{K_{II}}{T\omega}\left[1 - \frac{\alpha^2}{2}\frac{1}{(T\omega)^2}\right] U_{in\ II}, \qquad (2)$$

$$U_{out\ III} \approx \frac{1}{T\omega}\left[1 - \frac{1}{2}\frac{1}{(1 + K_{III})^2 (T\omega)^2}\right] U_{in\ III}.$$

The second terms in the square brackets determine the systematic amplitude errors in the output voltages due to the principles of the integrators. Denoting this error by Δ we get an expression for the minimum permissible frequency of the processes

$$(\omega_{min})_I = \frac{1}{T}\sqrt{\frac{1}{2\Delta}}, \quad (\omega_{min})_{II} = \frac{\alpha}{T}\sqrt{\frac{1}{2\Delta}}, \qquad (3)$$

$$(\omega_{min})_{III} = \frac{1}{(1 + K_{III})T}\sqrt{\frac{1}{2\Delta}}.$$

Comparing the ω_{min} in (3) we see that at given T and Δ the type III unit will have the least permissible ω. But phase as well as amplitude errors are present with a sinusoidal input.

Let us determine the minimum permissible ω for a given permissible phase error $\Delta\varphi$. From (2) we have

$$(\omega_{min})^{\bullet}_{I} = \frac{1}{T}\tan\left(\frac{\pi}{2} - \Delta\varphi\right),$$

$$(\omega_{min})^{\bullet}_{II} = \frac{\alpha}{T}\tan\left(\frac{\pi}{2} - \Delta\varphi\right), \qquad (4)$$

$$(\omega_{min})^{\bullet}_{III} = \frac{1}{(1 + K_{III})T}\tan\left(\frac{\pi}{2} - \Delta\varphi\right).$$

Since $1 < \frac{1}{\alpha} < (1 + K_{III})$ normally the least permissible ω will occur in type III at given T and $\Delta\varphi$.

Let us determine ω_{min} from the finiteness of the dynamic range $K_d = \frac{(U_{out})\ max}{(U_{in})_{min}}$. We here suppose that the unit integrates ideally, i. e.,

$$U_{\text{out I}} = \frac{K_I}{T\omega} U_{\text{in I}}, \quad U_{\text{out II}} = \frac{K_{II}}{T\omega} U_{\text{in II}}, \quad U_{\text{out III}} = \frac{1}{T\omega} U_{\text{in III}}. \tag{5}$$

Equation (5) implies that the output amplitude will rise as the frequency falls and that at some value $\omega = \omega_{min}$ the linearity limit $(U_{out})_{max}$ will be reached. Of course, the lower the minimum U_{in} the lower the permissible ω without going beyond the linear range. But $(U_h)_{min}$ is limited by the noise at the input.

Remembering that K_d has a perfectly definite finite value for any given unit, (5) gives

$$(\omega_{min})_I^{**} = \frac{K_I}{TK_d}, \quad (\omega_{min})_{II}^{**} = \frac{K_{II}}{TK_d}, \quad (\omega_{min})_{III}^{**} = \frac{1}{TK_d}. \tag{6}$$

Since $K_I > K_{II} > 1$, it follows that unit III again gives the lowest permissible ω. In many cases one can assume $(U_{out})_{max} = 100$ v, $(U_{in})_{min} = 0.1$ v and hence $K_d = 1000$.

Thus we get three conditions to determine ω_{min} for each type of unit. It is clear that the decisive condition will be the one that gives the highest frequency. Which of these conditions it will be is determined by the values of Δ, $\Delta\varphi$, T, α, K_d, K_I, K_{II} and K_{III} for the unit.

TABLE 1

Unit type	Condition for ω_{min}			Remarks
	error		$K_d = 1000$	
	$\Delta = 0.001$	$\Delta\varphi = 1°$		
I	22.4	57.3	0.01	$K_I = 10$
II	0.224	0.573	0.002	$K_{II} = 2$, $\alpha = 0.01$, $T = 1$
III	4.5×10^{-4}	1.15×10^{-3}	0.001	$K_{III} = 50000$
	4.5×10^{-6}	1.15×10^{-5}	0.001	$K_{III} = 5\times10^{6}$

In Table 1 we give the calculated ω_{min} for values of the above parameters frequently found in computer devices.

Thus for units of types I and II, ω_{min} is determined by the need to keep the phase error down, and for I by the finiteness of K_d.

2. Permissible Integrating Time for a Step Input

Let us estimate t_{max}, allowing as before for the various primary errors and the finite dynamic range.

If only systematic error is considered the outputs resulting from a step input will vary according to the laws

$$U_{\text{out I}} = K_I U_{\text{in I}} (1 - e^{-\frac{t}{T}}) \approx K_I U_{\text{in I}} \frac{t}{T}\left(1 - \frac{t}{2T}\right),$$

$$U_{\text{out II}} = \frac{K_{II}}{\alpha} U_{\text{in II}} (1 - e^{-\frac{\alpha t}{T}}) \approx K_{II} U_{\text{in II}} \frac{t}{T}\left(1 - \frac{\alpha t}{2T}\right),$$

$$U_{\text{out III}} = K_{\text{III}} U_{\text{in III}} \left(1 - e^{-\frac{t}{(1+K_{\text{III}})T}}\right) \approx \frac{K_{\text{III}}}{K_{\text{III}}+1} \frac{t}{T} U_{\text{in III}} \left(1 - \frac{t}{2(1+K_{\text{III}})T}\right). \quad (7)$$

These formulas show that the integration error Δ, given by the second terms in the parentheses, will increase most slowly for type III units.

Formula (7) gives

$$(t_{\max})_{\text{I}} = 2T\Delta, \; (t_{\max})_{\text{II}} = \frac{2T\Delta}{\alpha}, \; (t_{\max})_{\text{III}} = 2T\Delta(1+K_{\text{III}}). \quad (8)$$

Integrating capacitor leakage and zero drift in the amplifier, as well as the systematic error, affect the permissible integrating time.

The above two factors are of secondary importance relative to the systematic error for the first two types. Allowing for them we get the expressions

$$t_{\max} = \delta U_{\text{out}} 2RIC \text{ and } t_{\max} = \frac{\delta U_{\text{out}} T}{\frac{(e_{\text{dr}})_{\text{ref}}}{(U_{\text{out}})_{\max}}},$$

where R_l is the capacitor leakage resistance in megohms, δU_{out} is the permissible relative error and $(e_{\text{dr}})_{\text{ref}}$ is the voltage drift referred to the input.

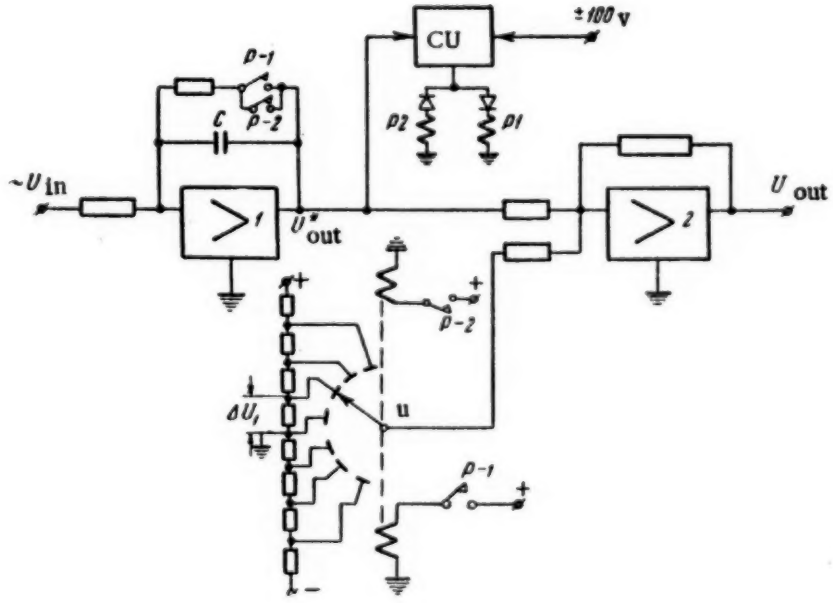

Fig. 2. Stepwise integrator circuit.

Let us estimate $t_{\max}$ from the finiteness of the dynamic range. Supposing, as before, that the integrators are ideal, we have

$$(t_{max})_I = \frac{K_d}{K_I} T, \qquad (t_{max})_{II} = \frac{K_d}{K_{II}} T, \qquad (t_{max})_{III} = K_d T. \tag{9}$$

Table 2 gives t_{max} computed for the Δ, K_d, K_I, K_{II}, K_{III} most commonly found.

TABLE 2

Unit type	Condition determining t_{max}, sec: error: Systematic $\Delta = 0{,}001$	Capacitor leakage $\delta U_{out} = 0{,}001$	Zero drift $\delta U_{out} = 0{,}001$	$K_d = 1000$	Remarks
I	0.002	—	—	100	$K_I = 10$
II	0.2	—	—	500	$K_{II} = 2$
III	100	800	100	1000	$K_{III} = 5\times10^4$ $(e_{dr})_{ref} = 1$ mv $R_l = 4\times10^5$ m Ω
	10 000	800	2000	1000	$K_{III} = 5\times10^6$ $(e_{dr})_{ref} = 50$ μv $R_l = 4\times10^5$ mΩ

The data of Table 2 show that at the parameter values assumed and with a permissible error of 0.1% the decisive factors are the systematic error for types I, II and III (when $K_{III} = 5 \cdot 10^4$) and the finite dynamic range for type III when $K_{III} = 5 \cdot 10^6$. Other things being equal, type III allows of much larger integration times.

To increase the permissible integration time further in a stabilized amplifier (at $K_{III} = 5 \cdot 10^6$) we require a greater dynamic range. This can be effected both by reducing the amplifier error and by increasing the linear output range. The latter has been very ingeniously realized in Korolkov and Bubnov's proposed stepwise integrator [6] (Figure 2). The basic idea in this device is that the amplifier integrates only for the permissible time $(t_{III})_{max}$. When U^*_{out} reaches $(U_{out})_{max} = \pm 100$ v, which is determined by the comparator unit CU, the wiper on the reversible uniselector U steps once along the divider and the voltage $\pm \Delta U_1$ is stored. The capacitor C is simultaneously discharged by the contacts on relays P-1 or P-2, and integration begins again. U_{out} is taken from the accessory summing unit 2, which combines the voltages from the uniselector divider and the integrator output. This gives a piecewise-linear curve instead of a stepped one. Hence after $\underline{n}$ steps the divider output is $n\Delta U_1$, which corresponds as it were to an n-fold increase in the linear limit of the amplifier, and hence in K_d. Thus the maximum permissible integrating time is now $\underline{n}$ times larger:

$$(t_{max})_{III} = K^*_d T,$$

where $K^*_d = K_d n$ ($\underline{n}$ being the number of steps on the divider for a voltage of one sign only).

The errors due to zero drift and capacitor leakage are reduced at the same time as the dynamic range is extended because the real integrating time of the electronic integrator is reduced by a factor $\underline{n}$ as compared with $(t_{max})_{III}$.

SUMMARY

This comparison shows that it is desirable to use passive integrating circuits with the amplifier at input frequencies of 10 cps and above. If signals of very low frequency have to be integrated an operational amplifier has to be used. The minimum permissible frequency will then be $(1 + K_{III})$ times less than with passive networks.

The factor which determines W_{min} in all three types is the phase error. Integrators using stabilized operational amplifiers are excluded, as the decisive factor is here K_d.

The maximum permissible integrating time for a step input for all three types (except ones using stabilized operational amplifiers) is determined by the systematic error. The operational amplifiers give the longest integrating times.

In integrators using stabilized operational amplifiers the decisive factors are the capacitor leakage and the finite dynamic range. In such amplifiers t_{max} does not exceed 1000 sec when $K_d = 1000$ and $R_l = 4 \cdot 10^5$ megohms.

A further increase in permissible integrating time can be obtained by using the stepwise integrator system.

Received March 6, 1957

LITERATURE CITED

[1] V. A. Trapeznikov and B. Ia. Kogan, "The design principles of analogs for studying automatic control processes," Automation and Remote Control (USSR) 13, 6 (1952).

[2] G. Korn and T. Korn, Electronic Analog Computers (IL, 1955) [Russian Translation].

[3] B. Ia. Kogan, "Analogs to automatic control systems," Trudy Akademii oboronnoi promyshlennosti, 1955, No. 2.

[4] I. M. Tetel'baum, "Electrical analogs to physical systems," Konspekt lektsii, Vol. 1, (MEI*, 1955).

[5] G. M. Zhdanov, Computer automatics. Konspekt lektsii, razdel II, "Integrating differentiating devices," (MEI*, 1954).

[6] I. V. Korolkov and I. A. Bubnov, A stepwise integrator. Author's certificate as of 1954.

*Moscow Institute of Energetics.

A MAGNETIC RELAY USING FERRITES

G. D. Kozlov

(Moscow)

A magnetic amplifier operating as a relay which uses ferrite cores is considered; the relative relay load current change is 100-200. A calculation method for the relay is presented.

Ferrite cores have several advantages over strip laminated ones prepared from high-grade magnetic materials. The specific resistance of a ferrite is about $5 \cdot 10^6$ ohms mm^2/m. The amplifier supply frequency can then be raised to 200-500 kilocycles/sec.

Unlike strip cores ferrites are practically insensitive to vibration and require no housings. It is also easier to make ferrite cores, which are in addition very much cheaper. Although the magnetic properties of ferrites are much worse than those of high-permeability alloys (see, for instance, Figure 1), it is often more convenient to use ferrites at supply frequencies of 10-20 kilocycles/sec. One method of producing relay characteristics in any type of amplifier is to use strong positive feedback. We take the feedback coefficient as being

$$K_{fb} = \frac{H_{fb}}{H_{\sim av}} \tag{1}$$

where $H_{\sim av}$ is the mean alternating field strength (i. e., that computed from the half-wave mean of the alternating current, $I_{\sim av}$), H_{fb} is the field produced by the feedback current in the same part of the magnetic circuit as H.

When $K_{fb} > 1$ relay mode operation occurs [1, 2] and the characteristic shown in Figure 2 obtains, where Δ is the hysteresis loop width, which depends on K_{fb} (the width increasing with K_{fb}) and H_k is the ac field strength at maximum magnetizing field after the relay has operated:

$$H_k = \frac{I_k W_\sim}{l_{av}} \tag{2}$$

(I_k being the working circuit current after the relay has operated), H_0 is the ac field strength with no magnetizing field (relay not operated);

$$H_0 = \frac{I_0 W_\sim}{l_{av}} \tag{3}$$

(I_0 being the minimum relay current).

The bias determines whether the working point is A or A'. The operate field component produced by the control current $I_{c\,op}$ will be

$$H_{c\,op} = H_A - H_B = I_{c\,op} W_c / l_{op} \tag{4}$$

and the drop-off field component produced by the control current $I_{c\,off}$ will be $H_{c\,off} = H_{B'} - H_{A'} = I_{c\,off} W_c / l_{op}$.

The working point is selected to give operation stable against fluctuations in supply voltage and frequency, load resistance, temperature, etc.

The current gain of the relay is $K_I = I_K / I_{c\,op}$.

In practice the amplifier is sometimes operated in circuits where only the rising branch of the characteristic is significant. This case will be considered here. The calculation parameters will then be I_k, I_0, H_B, H_A and $I_{c\,op}$. The load current change factor is defined as $K = I_k / I_0$.

Since the minimum current in the feedback amplifier corresponds to the no-load current of the amplifier without feedback and occurs when the magnetizing field $H_=$ is zero, I_0 can be determined as follows:

$$I_0 \approx \frac{U_{0\sim}}{2X_0} = \frac{U_{0\sim}}{2 \times 2\pi f \mu_0 4\pi S W^2 / l_{av} 10^9}, \tag{5}$$

where U_0 is the voltage (in volts) on the working windings, connected as in Figure 3, with zero magnetizing field, $2X_0$ is the reactance of these windings (ohms) with zero magnetizing field, f is the supply frequency in cycles/sec, S is the cross-sectional area of each core in cm^2, l_{av} is the average length of a line of force, in cm, W is the number of terms on each working winding and μ_0 is the zero magnetizing field magnetic permeability of the core.

The voltage drop in the working winding resistance is neglected in (5).

One of the main points in designing a magnetic relay is the choice of magnetic conditions in the core for magnetizing fields present and absent. To obtain a high load current change factor the largest possible permeability drop produced by the magnetizing field changing from zero to its maximum value must be used. The maximum drop is of course obtained if $\mu_0 = \mu_{max}$ (Figure 4).

Magnetic amplifier design usually begins with selecting the core volumes. With resistive loads the formula used is [3]:

$$V_c = \frac{1.6 \times 10^7 P \sqrt{1 - \frac{1}{K^2}}}{f H_k \sqrt{B_0^2 - B_k^2}}, \tag{6}$$

where V_c is the core volume in cm^3, P is the total power dissipated in the load and rectifier resistances, the windings and the internal resistance of the supply,* in watts, B_0 is the core induction at zero magnetization in oersted and B_k is the core induction at the maximum magnetizing signal.

This formula has to be transformed because in calculating for magnetic relays it is more convenient to use the permeabilities. Remembering that $H_k = H_0 K$, $B_0 = \mu_0 H_0$, $B_k = \mu_k H_k$ (μ_0 and μ_k being the permeabilities at zero and maximum magnetizing fields) and using (6), we get

*The latter component is neglected in amplifiers operating at industrial frequency. The source internal resistance is often comparable with the load resistance when other frequencies are used, and has to be allowed for.

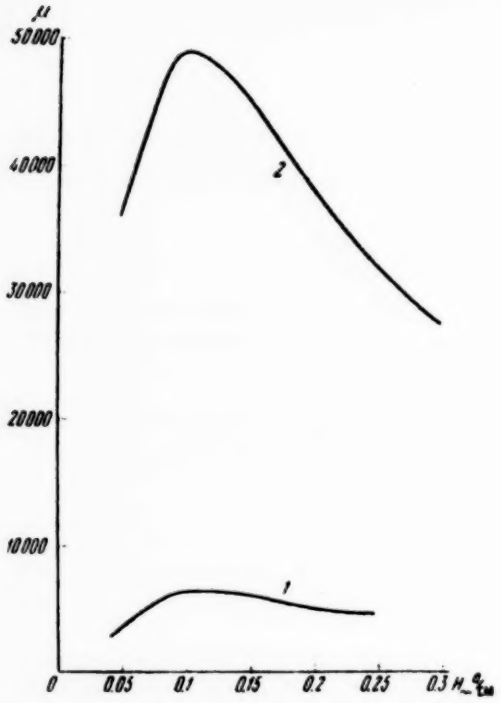

Fig. 1. Magnetic permeabilities of materials at f = 10 kilocycles/sec and $H_{=} = 0$; 1) Ferrite 2) 79-NM5, δ = 0.01 mm.

$$V_c = \frac{1.6 \times 10^7 P \sqrt{1 - \frac{1}{K^2}}}{fKH_0^2 \sqrt{\mu_0^2 - \mu_k^2 K^2}}. \qquad (7)$$

Bearing in mind that K >> 1 this expression can be put as

$$V_c = \frac{1.6 \times 10^7 P}{fKH_0^2 \sqrt{\mu_0^2 - \mu_k^2 K^2}}. \qquad (8)$$

Since magnetic permeabilities cannot be less than one ($\mu_k = 1$ is normally only obtained at very high magnetizing fields) (8) can give the condition for minimum possible core volume at a given power and relative load current change

$$V_c > \frac{1{,}6 \times 10^7 P}{fKH_0^2 \sqrt{\mu_0^2 - K^2}}. \qquad (9)$$

Equation (9) can be used to determine the core volume approximately. If a selection of ready-made cores (e. g., ferrites) is available then if P, μ_0, K and H_0 are known, a core of adequate volume can be selected by using (9).

If V_c is known the permeability at maximum magnetization and K can be determined from (8):

$$\mu_k = \frac{1}{K} \sqrt{\mu_0^2 - \left(\frac{1{,}6 \times 10^7 P}{V_c f K H_0^2}\right)^2}. \qquad (10)$$

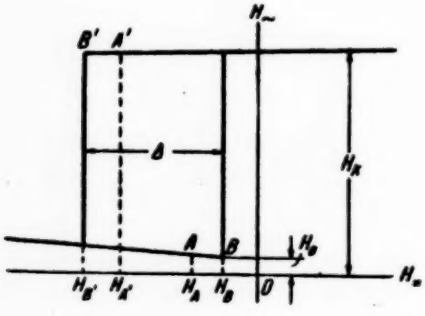

Fig. 2.

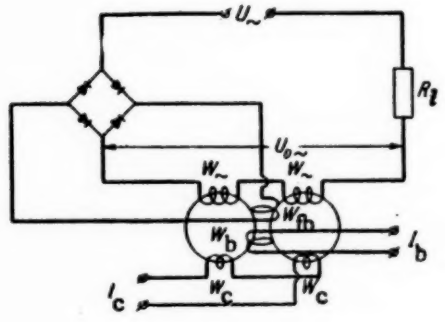

Fig. 3.

The required $H_=$ can be determined for known μ_k and H_k by using the $\mu_\sim = f(H_\sim, H_=)$ family of curves for the material (Figure 4).

But in approximate calculations, particularly when Δ is not important, or in order to increase the stability and reliability of the relay, $H_=$ can be selected somewhat high. The choice can be made from the empirical formula

$$H_= = \theta H_k, \tag{11}$$

where θ is an empirical coefficient. For F-200 ferrites working at 10-15 kilocycles/sec we can take θ = 1.2-1.3.

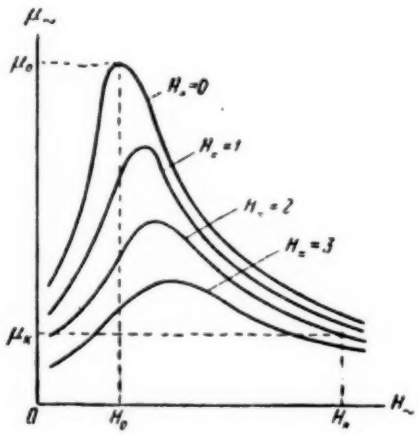

Fig. 4.

The fixed magnetizing field is mainly produced by the feedback winding in the relay mode. So, putting $H_= = H_{fb}$ we get the number of feedback winding turns:

$$W_{fb} = \frac{H_{fb}\, l_{av} K_f}{I_k K_r}, \tag{12}$$

where K_f and K_r are form and rectification factors for the rectifiers, respectively.

The numbers of turns on the working coils are given by (3).

The supply voltage is selected to give the maximum permeability at no load and zero fixed magnetization. Neglecting the resistance R, the voltage can be found from

$$U_\sim \approx U_{0\sim} = 4.44 f S 2 W_\sim B_0 10^{-8}, \tag{13}$$

where $U_\sim$ is the source voltage, $B_0 = \mu_0 H_0$ being taken from the $\mu_\sim = f(H_\sim)$ curve at $H_= = 0$.

Let us consider the sequence in computing the control circuit.

The bias field H_A, which determines the working point on the relay characteristic at zero signal, is selected from stability considerations. Knowing H_A the requisite bias ampere-turns can be determined:

$$(IW)_b = H_A l_{av}. \tag{14}$$

The "operate" ampere-turns are given by

$$(IW)_{cop} = (H_A - H_B)\, l_{av} \tag{15}$$

where

$$H_r = \frac{I_{fb}\, W_{fb}}{l_{av}} = \frac{I_0 W_{fb}\, K_r}{l_{av} K_f} \tag{16}$$

Then

$$(IW)_{c\,op} = \left(H_A - \frac{I_0 W_{fb} K_r}{l_{av} K_f}\right) l_{av} \tag{17}$$

The control coil power for operate can be found from

$$P_{c\,op} = \frac{(IW)^2_{c\,op}\, \rho l_{W_c}}{S'_c K_u}, \tag{18}$$

where ρ is the specific resistance of the winding wire in ohm-mm^2/m, l_{W_c} is the mean length of a control turn, S'_c is the control coil window area, in cm^2, and K_u is the utilization factor.

An Example

Data. Core dimensions: D_{out} = 1.55 cm, D_{in} = 1.1 cm, h = 0.3 cm, l_{av} = 5.5 cm, S = 0.0675 cm^2, V_c = 0.37 cm^3; core material F-200 ferrite; supply frequency f = 10 kilocycles per second; source resistance R_i = 15 ohms; rectifier type DG-Ts 24; load resistance R_l = 20 ohms; relative load current change K = 100; I_k = 200 ma, I_0 = 2 ma, $I_{c\,op}$ = 0.5 ma.

Order of calculation. 1. Using the curve of Figure 4 for $H_= = 0$, we get μ_0 and H_0 as $\mu_0 = 6300$, H_0 = = 0.14 oersted = 0.11 amp-turns per cm.

2. Total power: $P = I^2_k R'_l = I^2_k (R_l + R_i + R_r) = 1.6$ watts, where R_r = 5 ohms is found from the rectifier characteristic.

3. Using (9) we check that the core volume is sufficient for K = 100 and P = 1.6 watts:

$$V_c = 0.37 > \frac{1.6 \times 10^7 \times 1.6}{10^4\, 100\, (0.11)^2 \sqrt{(6300)^2 - (100)^2}} \approx 0.34,$$

so the core is in fact adequate.

4. From (3) we get the number of turns on the working coil: $W_\sim$ = 214 turns.

5. To find $H_=$ we use (11) with θ = 1.2: $H_= = 1.2\, H_k = 1.2 H_0 K$, or $H_=$ = 13.2 amp-turns/cm.

6. From (12) we get the feedback turns: $W_{fb} \approx 300$ turns, assuming that $H_{fb} = H_=$; K_r = 0.95, K_f = 1.11.

7. Putting $B_0 = \mu_0 H_0$ in (13) we get $U_\sim$ as 11.3 volts.

We now calculate the bias and control circuit parameters.

8. The total core window area $S_0 = \pi/4 D^2_{in}$ = 95 mm^2.

9. The window area taken up by the working coil: $S_{0\sim} = W_\sim S_w / K_u$, where K_u = 0.3, being the utilization factor, S_w = 0.028 mm^2 being the cross-sectional area of the PELShO wire of diameter 0.12 mm. This gives $S_{0\sim}$ = 20 mm^2.

10. The window area taken up by the feedback coil: $S_{0fb} = W_{fb} S_w / K_u$.

Using the same values for K_u and S_w we get S_{fb} = 28 mm^2.

Thus the following area remains for the control and bias windings: $S_{0c} + S_{0b} = S_0 - (S_{0\sim} + S_{0fb})$ = 47 mm^2.

To determine $H_{c\,op}$ we have first to find H_B and determine H_A in accordance with Figure 2.

11. H_B is found from $H_B = I_0 W_{fb} K_r / l_{av} K_f$, assuming $K_r = 0.95$; $H_B \approx 0.093$ amp-turns/cm.

12. The stability condition gives $H_A = 0.15$ amp-turns/cm.

13. The bias winding turns W_b are determined from (14).

W_b is usually determined by selecting the bias source current. We here assume $I_b = 30$ ma; then $W_b = 17$ turns.

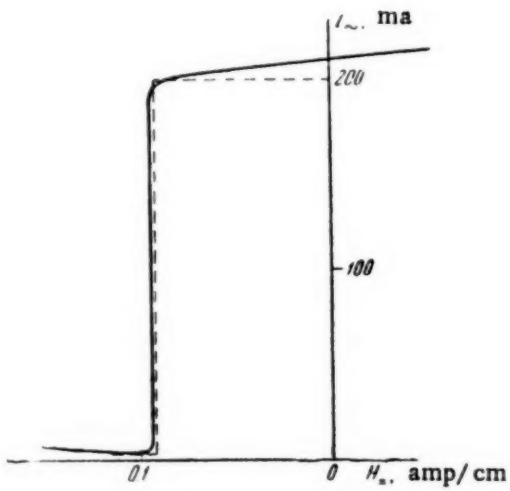

Fig. 5.

14. From $S_{0\,b} = W_b S_w / K_u$ we get the window area taken up by the bias coil.

Since the bias source power is unimportant the bias winding wire area is chosen from the permissible current density. For our PELShO wire of 0.12 mm diameter, assuming $K_u = 0.3$, we get $S_{0b} \approx 16$ mm^2.

15. From (4) we determine $H_{c\,op} = 0.15 - 0.093 = 0.057$ amp-turns/cm.

16. From (4) we also get the control turns, $W_c \approx 627$ turns.

17. The control winding window area is found as $S'_{0c} = W_c S_w / K_u \approx 38$ mm^2, where $S_w = 0.018$ mm^2, being the cross sectional area of the PELShO wire.

18. From (4) and (18), using $K_u = 0.3$, $\rho = 0.0175$ ohm mm^2/m and $l_{wc} = 3.5$ cm we get the control winding power required to operate the relay.

The numerical values, when substituted, give $P_{c\,op} \approx 0.4 \cdot 10^{-3}$ watt.

19. The power gain is determined: $K_p = P_l / P_{c\,op} = 2000$.

An amplifier was built from the above calculation. Figure 5 shows its characteristic. The computed curve is shown dashed, the full line being the experimental one.

Received August 31, 1956

LITERATURE CITED

[1] I. B. Negnevitskii, "The relay mode in a magnetic amplifier," Elektrichestvo 1949, No. 4.

[2] S. A. Dokhman and M. A. Rozenblat, "A contactless magnetic relay," Automation and Remote Control (USSR) 15, 1 (1954).

[3] N. P. Vasil'eva and O. A. Sedykh, "Calculation of choke magnetic amplifiers with complex loads," Automation and Remote Control (USSR) 16, 1 (1955).

REVIEW

EXTREMUM REGULATION

Iu. I. Ostrovskii

(Moscow)

The extremum controllers described in the Soviet and foreign literature are classified and the main designs presented.

Khlebtsevich [1] and Kazakevich [2, 3] first proposed extremum control principles; Drapper and Li [4] have described such principles, as have others [5-13]; particular topics have also been considered [14-16].

The problem in extremum control differs from that in ordinary control, which amounts to maintaining equality between the actual and preset values of some controlled quantity with the requisite accuracy. This controlled quantity can be either constant (automatic stabilization) or variable (program control, servo systems).

In extremum control systems the extreme value of the controlled quantity is not known in advance and is not preset. The problem then amounts to locating and maintaining the extremum with the required accuracy when the controlled quantity changes in time according to an unknown law. Not all the functional relationships which determine the quantity and the extremum position need be known. We only need to know that an extremum exists.

The Basic Types of Extremum Regulators

Such regulators can be divided into the following four types in accordance with the method of locating the extremum.

Those reacting to the sign of the derivative of the output coordinate with respect to the input coordinate or with respect to time. Figure 1 illustrates the sequence of operations in this type. The state of the object at the instant when the regulator is cut in is specified by point A on the static characteristic $y = f(x)$.

The input coordinate x is forcibly changed at a constant rate (Fig. 1d). The corresponding changes in y (if the object shows no lag) are shown in Figure 1b. If a maximum is being approached dy/dt is positive (Fig. 1c), the sign changing on passing through the extremum. When dy/dt, being negative, reaches some preset value δ the input coordinate drive is reversed. The motion is then again towards the extremum so dy/dt is positive, the sign again changing on passing through the extremum, and the process repeats. Thus the system hunts about the extremum.

Figure 1 clearly shows that $T_x = 2T_y$, where T_x and T_y are the oscillation periods of the input and output coordinates.

The difference between the maximum possible value y_{max} and the mean effective value y_{ef} during hunting specifies the loss involved in the search loss $\Delta y = y_{max} - y_{ef}$.

Those with extremum "storage". Figure 2 illustrates the sequence of operations in this type. Here again x is forcibly driven at a constant rate. The maximum y, being reached at time t_M, is noted by a special

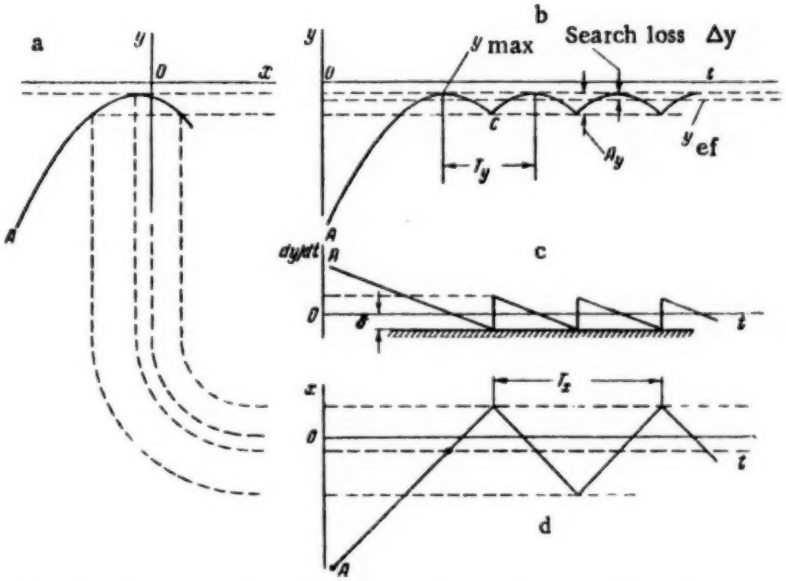

Fig. 1. Sequence of operations in an extremum regulator which reacts to the sign of the output coordinate derivative.

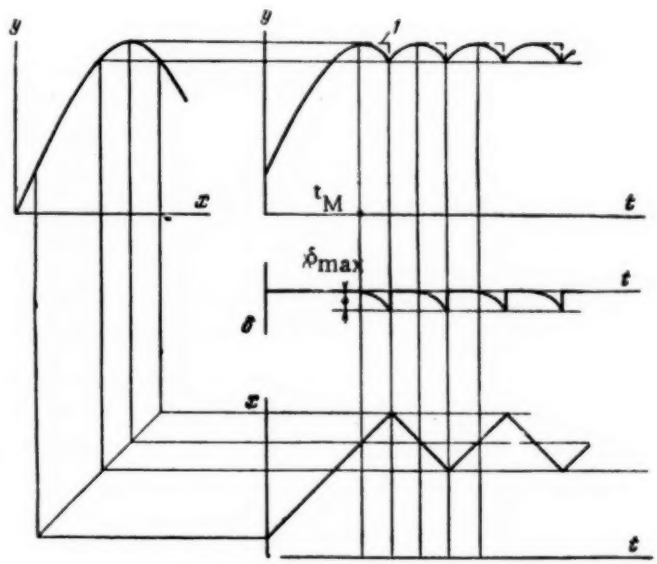

Fig. 2. Sequence of operations in an extremum regulator which "remembers" the extremum: 1) Value of y_{max}, recorded in the memory unit.

memory device. When the maximum has been passed the current $\underline{y}$ is compared with the extreme value and the direction in which $\underline{x}$ is being driven is reversed when the difference $\delta = y_{max} - y$ reaches some limit δ_{max}, the memory being wiped out. $\underline{y}$ again increases, approaches the extremum from the other side, and the process repeats.

Those with phase discriminators. Figure 3 illustrates the sequence of working states in this type. The signal $\underline{x}$ at the input (Fig. 3b) is added to the control signal Δx (Fig. 3g) and the harmonic signal δx (Fig. 3a) produced by a special generator.

The harmonic component δy (Fig. 3e) is separated from the output coordinate $\underline{y}$ (Fig. 3d) by a band filter. The phase of this component changes by 180° on passing through the extremum.

δy and δx are supplied to a phase discriminator. The sign of $\underline{z}$ (Fig. 3f) at the discriminator input is determined by the position on the static characteristic (Fig. 3c) and the amplitude defines the distance from the extremum. The averaged value of $\underline{z}$ (γ in Fig. 3f) is used to effect control.

Those with stepwise input coordinate change. Figure 4 shows the sequence of operations in an extremum regulator which operates in this way. The input coordinate is periodically altered by a discrete amount $\pm \Delta x$. When the transient has died away the steady-state output $\underline{y}$, averaged over a time Δt, is evaluated.

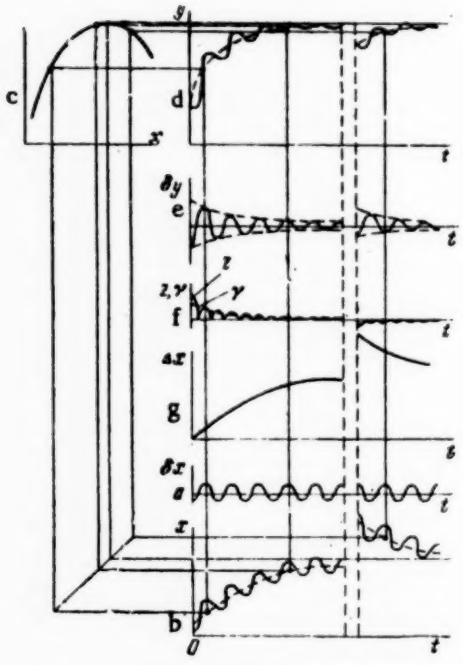

Fig. 3. Sequence of operations in an extremum regulator using a phase discriminator.

TABLE

Sign of Δx_n	Sign of Δy_n	Sign of Δx_{n+1}
+	+	+
+	−	−
−	+	−
−	−	+

The quantity so obtained, y_n, is compared with y_{n-1}, which was the value obtaining before the change Δx_n and which is stored in the memory unit. Then a new change, Δx_{n+1} is applied, of sign determined by that of Δx_n and that of $\Delta y_n = y_n - y_{n-1}$ (see table). The stored value y_{n-1} is erased, and y_n recorded. The cycle then repeats.

Two types of regulator can be differentiated on the basis of how they hunt about the extremum.

1. Those in which the hunting zone is symmetrical about the extremum (e. g., BD in Fig. 5).

2. Those in which the hunting zone is displaced relative to the extreme (e. g., zone BC or CD in Fig. 5).

In type 1, derivatives of both input and output coordinates have to be formed. Thus, if the regulator works in zone BC the control device changes its direction of motion at the following times:

When $dx/dt > 0$ the switch-over occurs when $dy/dt = \delta_1 > 0$; and when $dx/dt < 0$ it occurs when $dy/dt = \delta_2 < 0$; $|\delta_2| > |\delta_1|$.

The need for type 2 devices arises when for some reason it is undesirable to operate in a region to right or left of the extremum. Thus in turbine drilling of oil wells the relation of boring rate to axial load is unsymmetrical. The boring rate drops sharply if the limiting axial load is exceeded with solid rocks, and sometimes only a slight excess load over that giving the maximum boring speed may cause complete stoppage. A regulator for turbine boring in which the working zone corresponds to load somewhat below the extremum has been described [9].

If the extremum shifts fairly frequently (or continuously) the regulator must seek the extremum continually. But cases where the extremum drifts very slowly are also common. Then the ordinary regulator can be returned with an extremum device. A single extremum regulator can then look after several parameters [2, 4, 17].

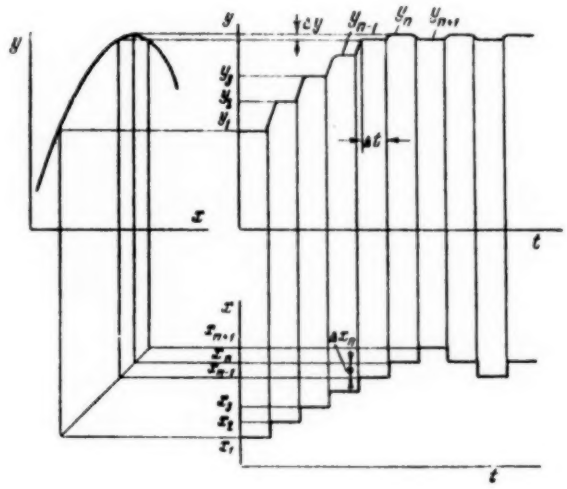

Fig. 4. Sequence of operations in an extremum regulator using stepwise input coordinate change.

The main indices to be looked for in a high-grade extremum regulator are

1) the search loss, equal to the difference between the mean effective value of the output coordinate prevailing during operation and the extreme value on the steady-state characteristic;

2) the follow-up rate when the extremum shifts, which is determined by the rate of change of the input coordinate during the search for the extremum.

The search loss is mainly a function of the noise in the system, of the properties of the object and the rate of input coordinate change.

The noise level determines the oscillation amplitude in the output coordinate, A_y, which is the minimum required for the regulator to operate properly.

It is not our purpose here to compare the various principles of extremum control. We only note that high-frequency noise components are accentuated by differentiating with respect to time. This makes extremum regulator design difficult, particularly if the static characteristic is flat around the extremum. Those using extremum "storage", and particularly those using stepwise input coordinate change, are less noise-sensitive.

Regulator Circuits

Various such circuits have been described [3-13]. We only mention certain of them here.

Figure 6 shows the circuit of one which reacts to change in the sign of the output coordinate derivative. A voltage u_y, proportional to the output coordinate $\underline{y}$ of the object O, is fed to the polarized relay A via the differentiating capacitor C_1. The motor M, which acts on the control unit CU, changes the input coordinate $\underline{x}$ at a constant rate. When the change in $\underline{x}$ causes $\underline{y}$ to increase du_y/dt is positive. Then contact a_2 on relay A is open. On passing through the maximum (point C in Fig 5) du_y/dt becomes negative, a_2 closes, and the stepping seeker S moves on one tooth, reversing M. Then $\underline{y}$ again begins to increase, du_y/dt becomes positive, and a_2 opens. The cycle then repeats.

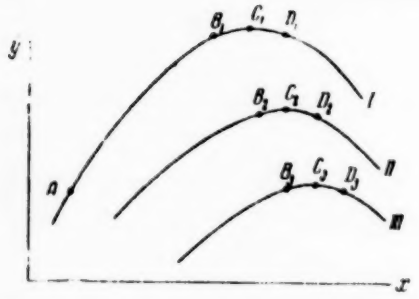

Fig. 5. Typical static characteristic for a controlled object having one extremum.

If the noise causes S to operate when it should not while the system is moving towards the extremum, the motor reverses and the motion moves away from the maximum, e. g., in the direction BA (Fig. 5). Then $du_y/dt < 0$ and S will remain cut in. Here contact b_1 on relay B serves to cut it out as this relay operates and opens the contact a certain time after the seeker has operated and closed contact S_1.

The circuit given in [3] differs from that given here mainly in using a special device (sign transducer) for determining the sign of the derivative.

The needle N in this sign transducer (Fig. 7) is friction-coupled to the axle O of the unit which measures y; it can move in the narrow gap between K_1 and K_2. K_1 and K_2 are also stops limiting the needle motion. If rise in $\underline{y}$ corresponds to clockwise motion K_1 will be closed when $dy/dt > 0$ and K_2 when $dy/dt < 0$. A similar system has been described [7].

The system shown in Figure 8 [10] also belongs to this type. A distinguishing feature of this is the use of derivatives of both input and output coordinates. The dx/dt transducer (the speed-voltage generator T) is fed to the polarized relay A, dy/dt to one of the two coils on the polarized relay B, which reverses the electric motor M.

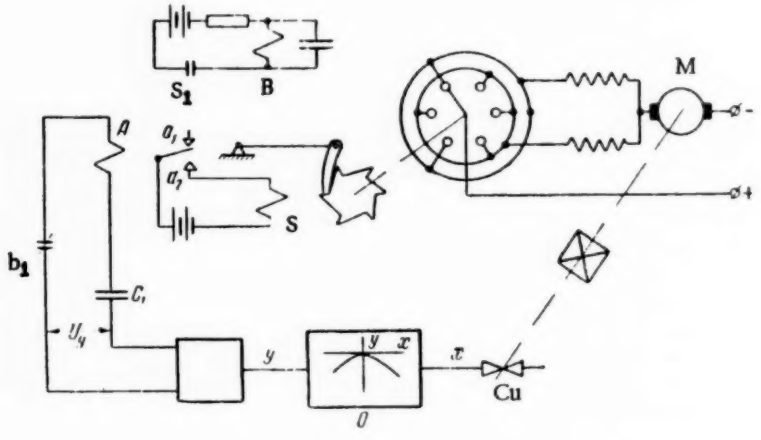

Fig. 6.

The following states are possible.

a) $dx/dt > 0$, $dy/dt > 0$ during motion from B to C (Fig. 5). Contacts a_1 and b_1 are closed. The motor rotates in the same sense as the torque applied to the rotor.

b) In region CD $dx/dt > 0$, $dy/dt < 0$. a_1 and b_2 are closed. The motor reverses.

c) In region DC $dx/dt < 0$, $dy/dt > 0$. a_2 and b_2 are closed. The motor rotation and torque directions coincide.

d) In region CB $dx/dt < 0$, $dy/dt < 0$. a_2 and b_1 are closed. The motor reverses. The system thus oscillates about the extreme point C.

An analogous system using the sign transducer is given in [8].

A pneumatic extremum regulator of analogous type is described in [11].

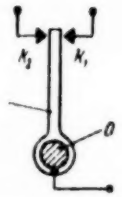

Fig. 7. The sign transducer.

Let us consider, as an example, the system proposed by Drapper and Li [4] for controlling carburation in an internal combustion engine. In the experimental setup they described the regulator alternately acted on the excess air coefficient and the spark advance angle, maintaining the shaft power at its maximum. An electric generator was used as load. The generator voltage was kept constant, so maximum motor power corresponded to maximum generator current. This current passes through the resistor R_3 = 0.02 ohms (Fig. 9). The potential difference produced is applied to the control grid of the pentode T_6. The bias, taken from the potentiometer R_2, balances out the fixed component of the input. The sensitivity is thereby increased.

Passing through a filter and the cathode follower (triode T_5) the signal reaches the double diode T_4. When the signal increases it raises the voltage on C_4(1μ F) used as "memory". When the signal drops the voltage across C_4 stays the same.

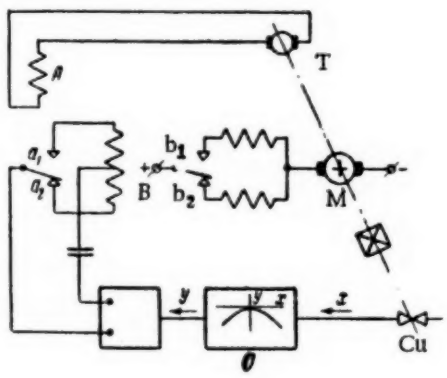

Fig. 8. Extremum regulator using input and output coordinate derivatives.

The memory capacitor voltage is fed via the cathode follower double triode T_3 to the grid of the thyratron T_2, the current value of the signal being applied to the thyratron cathode. Potentiometer R_1 sets the insensitive range (δ_{max} in Fig. 2).

When the difference between the above two voltages reaches a set value T_2 fires. C_1 is then discharged and the pulse produced passes to a trigger circuit (double triode T_1). When current flows in the right plate circuit of T_1 the left half is shut off and relay P_1 is dead. When the left half of T_1 is on the plate current passes through P_1. The right half of T_1 is then shut off. The switch-over occurs at the instant when T_2 fires. P_1 reverses the motor M when the switch-over occurs; this motor controls the changes in the input coordinate.

When C_1 is discharged, C_2 is charged, being connected between ground and the cathode of T_2. Then thyratron T_7 fires and operates relay P_2, which has a delay on drop-off brought about by C_3. The left contact of P_2 is normally closed, the right two normally open. When the latter contacts close C_4 ("memory") is discharged, together with the filter capacitor C_5.

The left contact breaks the plate circuit of T_1, this going out, and the circuit returns to its initial condition.

The "maximum storage" principle has also been used in a pneumatic regulator developed at the Institute of Automation and Remote Control, Academy of Sciences of the USSR. This regulator will be described in a special article.

A regulator with stepwise input coordinate change has been developed in the Automation Laboratory of the Central Institute of the Ministry of the Oil Industry for selecting the optimum bit loads in turbine boring of oil boreholes.

The output coordinate is here the penetration rate of the boring tool, while the noise level is many times greater than the accuracy required on maximum holding. The mean speed is determined by measuring the time required for the tool to penetrate a given depth.

The measuring head includes two shafts which rotate in turn at a constant speed during the set interval. The angle of rotation is inversely proportional to the mean penetration rate. "Memory" is effected by recording

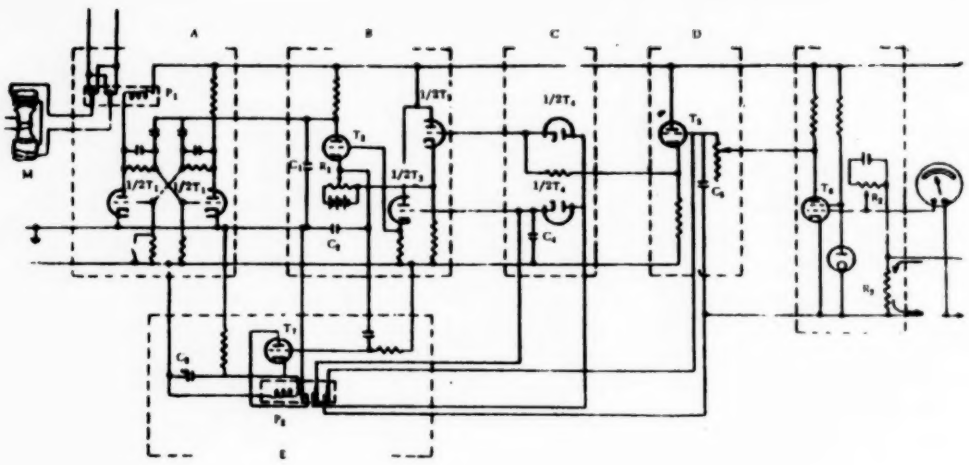

Fig. 9. Circuit of Drapper and Li's extremum regulator; A) Switch-over section, B) compensator section, C) memory section, D) noise filter and cathode follower, E) memory erase section.

the rotation angle of the corresponding shaft. After the sign and magnitude of the speed change from the shaft which performed the previous measurement have been determined it is restored to its initial position, and the position of the second shaft remains fixed. Relays record the sign of the input coordinate (axial load on bit) change.

The regulator and operational test results on it have been described [9]. Circuits for extremum regulators of this type have been given [10, 13].

Received January 1, 1957

LITERATURE CITED

[1] Iu. S. Khlebtsevich, An electrical economy regulator. Author's certificate No. 231496 of April 4, 1940.

[2] V. V. Kazakevich, An extremum regulator. Author's certificate No. 66335. Priority as of November 25, 1943. Bulletin Izobretenii 1946, No. 10.

[3] V. V. Kazakevich, Extremum Control. Dissertation for the science degree of candidate in technical sciences, Moscow Higher Technical College (1945).

[4] C. S. Drapper, J. T. Li, "Principles of optimalizing control systems and an application to internal combustion engine," ASME, Vol. 70 (1951).

[5] J. R. Shull, "An automatic cruise control computer for long range aircraft," Trans. IRE (Electronic Computers) Vol. 1, 1 (December, 1952).

[6] N. H. Joung, "An automatic control system with provision for scanning and memory," Trans. AIEE 72, Part I (1953).

[7] B. Farber, "Computer circuit finds peaks automatically," Control Eng. 1, 2 (October, 1954).

[8] R. Gosgriff, "Servos that use logic can optimize," Control Eng. (September 1955).

[9] Iu. I. Ostrovskii and M. G. Eskin, An extremum regulator for turbine boring of oil boreholes. Automation and Remote Control (USSR) 17, 9 (1956) [See C. B. Translation].

[10] A. G. Ivakhenko, "The problems of extremum control," Automatkia, Izd. Akad. Nauk Ukr. SSR 1956, No. 3.

[11] L. A. Zalmanzon,"Some arguments for the production of extremum regulators," Automation and Remote Control (USSR) 18, 1 (1957).

[12] A. G. Ivakhenko, Self-Adjusting Automatic Control Systems, Izd. Akad. Nauk Ukr. SSR, 1957.

[13] Byron White,"The Quarie Optimal Controller," Instr. and Automation, 29, 11 (November 1956).

[14] V. V. Kazakevich, Theory of an ideal analog to an extremum regulator. Trudy Central Scientific Research of Aircraft Engines, 1939, No. 165.

[15] H. S. Tsien and S. Serdengecti, "Analysis of peak-holding optimalizing control" J. Aeronaut. Sci. 22, 8 (1955).

[16] H. S. Tsien, Engineering Cybernetics (Izd. Inost. Lit., 1956).

[17] J. T. Li, "Optimalizing System for Process Control," Instruments 25, 1, 2, 3 (1952).

BIBLIOGRAPHY

A LIST OF SOVIET AND FOREIGN LITERATURE ON COMPUTER TOPICS FOR 1955

I. Books

G. Korn and T. Korn, Electronic analog computers (direct current). Moscow, Foreign Literature Press, 1955, 420 pp.

A brief description of a dynamic analog to electrical systems. Moscow, 1955, 143 pp. with illustrations (Molotov Power Institute, Moscow, Research Division).

I. M. Tetel'baum, Electrical analogs to physical systems, A course of lectures. Vol. I, Moscow, 1955, 166 pp., with illustrations (Molotov Power Institute, Moscow).

H. M. Paynter, A Palimpset on the Electronic Analog. Part I. Boston Mass. Philbrick Researches, Inc., 1955, 270 pp.

F. H. Raymond, Calcul analogique et machines electroniques. Paris, Societe de la revue optique, 1955, 129 pp.

A. W. Wance, E. C. Hutter, J. Lehman and M. I. Wadlin, Analog Computers. In: Advances in Electronics and Electron Physics, 1955, Vol. 7, pp. 363-398, 20 figures, 62 bibliographies.

C. A. A. Wass, An Introduction to Electronic Analogue Computers. London, Pergamon Press Ltd., 1955, 237 pp.

II. Transactions of Meetings and Conferences

Association for Computing Machinery Meeting (Philadelphia, September 14-16, 1955). Titles of Papers and Abstracts. Computers and Automation, 1955, November, Vol. 4, No. 11, pp. 17-33.

Eastern Joint Computer Conference. Proceedings. N. Y., Americ. Institute of Electric Engineers, 1955, 29 figures, 92 pages.

Eastern Joint Computer Conference. Proc. IRE, 1955, October, Vol. 43, No. 10, p. 1545.

Electronic Computers. In: Summaries of Technical papers (1955, IRE, National Convention Program). Session 27 and 35. Proc. IRE, 1955, March, Vol. 43, No. 3, pp. 362 and 366.

International Analogy Computation Meeting (Brussels, September 24-October 10, 1955). Regelungstechnik, 1956, No. 2, p. 50.

Journees de Calculs analogiques de Septembre 1955. Mesures et Controle Industriel, 1955, Ann. 20, No. 222, Nov., p. 806.

F. H. Raymond, Compte-rendu des "Journees Internationales du Calcul Analogique", organisees par la S. I. T. E.L. a Bruxelles. L'Onde electrique, 1955, Nov., 35, No. 344, p. 1116.

Transactions of the Symposium on Computing Mechanics, Statistics and Partial Differential Equations. London Interscience Publishers, 1955, 216 pp.

The University of Wisconsin Conference "The Computing Laboratory in the University" Mathematical Tables and Other Aids to Computation, 1955, April, Vol. 9, No. 50, p. 84.

Wescon Computer Sessions. Proceedings. Proc. IRE, 1955, April, Vol. 41, Pt. I, No. 4, p. 513.

Western Computer Conference and Exhibit (Los Angeles, March 1-3, 1955). Titles of papers and abstracts. Computers and Automation, 1955, Vol. 4, No. 4, pp. 38-40.

III. General Theoretical Topics

1. General topics

V. A. Venikov, and A. V. Ivanov-Smolenskii, Development of electrical analogs to power systems. Elektrichestvo, 1955, No. 8, pp. 1-10. 10 references.

B. Ia. Kogan, Analogs to automatic control systems. Trudy Akad. oboronnoi prom., 1955, No. 2, pp. 80-124, 28 figures, 9 references.

V. A. Trapeznikov, Mathematical analogs to dynamical systems. Elektrichestvo, 1955, No. 8, pp. 20-26, 11 figures, 8 references.

I. I. Eterman, and M. I. Obuvalin, A method of solving characteristic equations on electrical analog equipment. Automation and Remote Control (USSR) 16, 6, 554-555 (1955).

W. Allison, A broad look at analog computers. Control Engng., 1955, February, Vol. 2, No. 2, p. 53.

H. Andre, Aspects generaux d'un calculateur analogue. Ingrs et techniciens, 1955, No. 76, pp. 27, 29, 30; Abs. J. Math. 1955, No. 4, p. 146.

R. Brown, Review of Electronic Computer Progress, 1954. Trans. IRE, 1955, March Vol. EC-4, No. 1, pp. 33-38.

Communique concernant la creation de l'Association internationale pour le calcul analogique. L'Ohde Electrique, 1955, Nov. Vol. 35, No. 344, pp. 1116-1117.

Data processing machines. Ferranti to collaborate with Powers. Samas in computer production. Engineering, 1955, Vol. 179, No. 4647, pp. 218-219; Abs. J. Math. 1956, No. 7, p. 106.

B. E. Davis and I. H. Swift, Analogue Computer Technique Using Magnetic Amplifiers. Trans. Amer. Inst. Electr. Engrs, 1955, Jan. Vol. 74, Pt. I, No. 16, pp. 635-639.

Electronic computing — its many applications. Brit. Petrol. Equipm. News. 1954-1955, Vol. 4, No. 3, pp. 34-37.

J. Hult, Automatiska raknemaskiner i Sverige. Tekn. Tidskr., 1955, March 29, Vol. 95, No. 13, pp. 273-281, 14 figures, 10 bibliographies.

N. L. Irvine and L. Davis, Simulation by modeling. Proc. West. Joint Comput. Conf., 1955, pp. 13-16; Abs. J. Math. 1956, No. 9, p. 118.

E. F. Johnson, Analogs as Aids in Process Studies, Industr. and Engng. Chem., 1955, March, No. 3, p. 396.

C. E. Jones, Factors in Evaluating Electronic Analog Computers. Machine Design, 1955, February, Vol. 27, No. 2, pp. 218-220.

W. J. Kapplus, The use of electronic analogue computers with resistance network analogues. Brit. J. Appl. Phys., 1955, October, Vol. 6, No. 10, pp. 356-357, 3 figures.

D. A. Lieberman, A Complex or nonlinear design problems can often be simplified with an analog approach. Machine Design 1955, February, Vol. 27, No. 2, pp. 162-166.

J. Malecki, Development and application of electromechanical analogies in technology. Nauka, Polska, 1956, (13), pp. 15-36.

Y. Paschkis, Electric analog computers: classification, design and application. Ann. N. Y. Acad. Sci. 1955, Vol. 60, pp. 884-904. 9 bibliographies.

M. Salamon, Electrical methods of performing the simple mathematical operations. — Slaboproudy obzor, 1955, Sv. 16, Cis. 3, pp. 126-131; 16 Obr.

J. Schulze, Mathematische Maschinen in Schweden. Feingerätetechnik, 1955, Juli, No. 7, S. 315-317, 4 Abb. Bibliogr. 12.

J. D. Strong, Practical approach to analog computers. Instruments and Automation, 1955, Apr., Vol. 28, No. 4, pp. 602-610.

R. E. Vowels, Computers. El. Engr. and Merchandiser, 1955, Jan. 15, Vol. 32, No. 3 pp. 82-84.

L. B. Wadel and A. W. Wortham, Survey of Electronic Analog. Installations. Trans. IRE 1955, June, Vol. EC-4, No. 2, pp. 52-55.

2. Methods of solving problems with analog devices

P. M. Honnel and R. E. Horn, Matrices in Analogue Mathematical Machines. J. Frankl. Inst., 1955, Sept., Vol. 260, No. 3, pp. 193-207, 8 figures, 3 bibliographies.

F. H. Raymond, Sur la realisation d'un coefficient de transfert donne. L'Onde electrique, 1955, Fevr., No. 335, pp. 105-112, figures 14.

3. Operational accuracy of analog device components

V. A. Shetnikov, Dynamic accuracy of friction-type integrators. In "computer equipment", Collection No. 49, Moscow, Oborongiz, 1955, pp. 13-72, 59 figures (MVTU).

W. Allison, It pays to use error analysis during design. Control Engng, 1955, May, Vol. 2, No. 5, p. 51.

IV. Electronic Analog Equipment Built Up From Separate Units

Session of the Scientific Council of the Institute of Automation and Remote Control, Academy of Sciences of the USSR on analog problems. Automation and Remote Control (USSR) 16, 2, 206-207 (1955).

B. Ia. Koga, Electronic analog equipment at the Institute of Automation and Remote Control, Academy of Sciences of the USSR. Trans. 2nd All-Union Conference on the Theory of Automatic Control, 1955, Vol. 3, pp. 47-69, 25 figures, 10 references.

G. M. Petrov, Linear analog equipment produced by the Ministry of Machine Construction, and tests on its use. Trans. 2nd All-Union Conference on the Theory of Automatic Control, 1955, Vol. 3, pp. 39-46, 5 figures, 4 references.

French electronic computers. Express-information, Institute of Scientific Information, Academy of Sciences of the USSR, 1955, May 16, No. NBT-5, p.2.

AGE and Lockheed computers. Cornell Engr. 1955, Vol. 21, No. 2, 50, 52, 54; Abs. J. Math. 1956, No. 9, p. 121.

AGWAG Electronic analogue Computer. Common Wealth Engnr. 1955, March, Vol. 42, No. 8, pp. 299-300.

Analog computers features 30 amplifiers. Electronics, 1955, Vol. 28, No. 1, pp- 270-271; Abs. J. Math. 1956, No. 5 p. 116.

G. Andre, Les operateurs mathematiques electroniques de la S. E. A.; L'ensemble Standard O. M. E. P 2. Mesures et Controle Industriel, 1955, Nov., No. 222, 781-787, 6 figures.

N. N. Bismas, V. N. Chiplunkar and V. C. Rideaut, Design and Construction of High Speed Electronic Differential Analyzers. J. Indian Inst.-Science. Section B, 1955, July, Vol. 37, No. 3, pp. 186-199, 5 suppl. plates.

E. W. Burdette, Computers at Oak Ridge. J. Instrum. Soc. America, 1955, February, Vol. 2, No. 2, pp. 42-44.

Le calculateur analogique S. E. A. type O. M. E. L. 2 — Ingrs et techniciens, 1955, No. 75, pp. 49, 51; Abs. J. Math. 1956, No. 7, p. 108. O. M. E. L. 2 S. E. A. Computer for universal application. — Electr. Times, 1955, Vol. 127, No. 3303, pp. 319-320; Abs. J. Math. 1956, No. 7, page 107.

Desk Model Analog Computer Light Enough to be Carried. Control Engng, 1955, Dec. Vol. 2, No. 12, p. 87, 1 figure.

Differential analysis at high speed. Electr. Times, 1955, Vol. 127, No. 3310, pp. 613-614.

"Djinn" electronic analogue computer. Interavia Air Letter, 1955, No. 3269, p. 9; Abs. J. Math. 1956, No. 9, page 117.

A. B. Johnson, Miniature Analogue Computer. Electronic Engng, 1955, Aug., Vol. 27, No. 330, pp. 348-349; Brit. Commun and Electronics, 1955, Vol. 2, No. 8, p. 69; Abs. J. Math. 1956, No. 5, ctp. 116.

S. Kitsopoulos, Ein photoelektrisches Analogiegerät für die Berechnung von Faltungsintegralen, Sci. electrica, 1955, Bd. 2, Nr. 1, S. 1-29; Abs. J. Math. 1956, No. 7 pp. 109-110.

S. Kistopoulos, Ein photoelektrisches Analogierechnengerät zur Untersuchung des dynamischen Verhaltens von linearen Systemen. Bull. Scweiz. elektrot. Ver., 1955, Bd. 46, Nr. 15, pp. 690-693, 11 figures.

H. R. Loos, J. Pelnaz, Analysis of electron integrator for integrators of durable processes. Slaboproudy obzor 1955, 16, 6, 316-320, 8 figures, 7 bibliographies.

L. Lofgren, Analogimaskiner med separata minnen och prediktorer. Tekn. Tidskr., 1955, 29 Mars, vol. 85, No. 13, pp. 296-300, 4 figures.

Low-Cost Analog Computer. Instrument and Automation, 1955, Nov. Vol. 28, No. 11, pp. 1914-1915, 5 figures.

D. M. MacKay, High-Speed Electronic-Analogue Computing Techniques. Proc. Inst. Electr. Engrs. Part B, 1955, Sept. Vol. 102, No. 5, pp. 609-620, 18 figures, 9 bibliographies.

New developments in aviation computers. Aviation Week, 1955, Vol. 62, No. 20, p. 37; Abs. J. Math. 1955, No. 9, pp. 128-129.

M. J. Pelegrin, Les machines a calculer electroniques. Electricite, 1955, Oct. Ann. 39, No. 220, pp. 259-265, 29 figures.

R. Peretz, Calculateur analogique electronique. Ensemble analogique electronique de l'Universite libre de Bruxelles, destine a l'etude des systemes phisiques. Revue E, 1955, Vol. 1, No. 7, pp. 157-161; No. 8, pp. 173-191; Abs. J. Math. 1956, No. 7 page 109.

I. Williard, At Purdue Electronic Computers. Purdue Engnr., 1955, Vol. 50, No. 4, pp. 46-47; Abs. J. Math. 195 , No. 2, page 162.

H. Winkler, Über eine elektronische Analogiemaschine zur Losung von Differential-gleichungen höherer Ordnung zur Untersuchung von Problemen der Regelungstechnik. Wiss. Z., Hochschule fur Elektrotechn. Ilmenau, 1954-1955, Nr I, S. 15-27, 21 Abb. Bibliogr. 16.

D. Wray, An introduction to electronic computers. Irish Build. Constr. and Engng. J., 1955, Vol. 5, No. 8, pp. 486-489; Abs. J. Math. 1956, No. 9, page 125.

V. Amplifier Elements in Electronic Analog Equipment

1. D-c electronic amplifiers

I. G. Gurvich and V. S. Ivanov, An electrometer amplifier with 100% feedback. Zavod. Lab., 1955, No. 3, p. 365.

A. A. Sokolov, Balanced repeaters in parallel. Automation and Remote Control (USSR) 1955, 16, No. 2, pp. 196-202, 6 figures, 3 references.

A. A. Sokolov, Electronic summators. In "Some problems in electronics", Moscow, Mashgiz, 1955, pp. 121-131, 9 figures.

J. L. Cederbaum and P. Balaban, Automatic Drift Compensation in dc Amplifiers. Rev. Sci. Instrum. 1955, Aug., Vol. 26, No. 8, pp. 746-747.

B. E. Davis and I. H. Swift, An Analogue Computer Technique Using Magnetic Amplifiers. Commun. and Electronics, 1955, No. 16, pp. 635-640; Abs. J. Math. 1956, No. 5, page 119.

H. Fuchs, Some Aspects of the Design of a dc Amplifier for Use with a Slow Analogue Computer. Electronic Engng., 1955, Jan., Vol. 28, No. 335, pp. 22-25, 6 figures, Bibliogr. 3.

H. Hamer and I. D. Kennedy, Testing of Operational Amplifiers. J. Assoc. Computing Machinery, 1955, April, Vol. 2, pp. 92-94.

A. B. Johnson, Gain Measurements on Computing Amplifiers. Electronic Engng, 1955, March, Vol. 27, No. 325, pp. 127-129, 14 figures.

2. Tubeless computer amplifiers

G. M. Ettinger, Transistor Amplifiers for Analog Computers. Electronics, 1955, July, Vol. 28, No. 7, pp. 119-121, 6 figures.

3. Integrating and differentiating units.

I. G. I. Michell, Errors of Friction Wheel Integrators. J. Sci. Instrum., 1955, February, Vol. 32, No. 2, pp. 43-44.

J. G. Thomason, Feedback Integrators and Differentiators. In: Linear Feedback Analysis. L., Pergamon Press Ltd. 1955, pp. 290-327, 17 figures.

H. Wittke, Elektrische Integrationsverfahren. Frequenz, 1955, Vol. 9, No. 2, pp. 49-57, 12 figures. 3 bibliographies.

4. Multiplying and dividing units.

L. Lukashevich, A multiplying system using double amplitude modulation. Bull. Pol. Akad. Sci. 1955, Section IV, Vol. 3, No. 3, pp. 147-151, 4 figures, 5 references.

S. A. Davis, 31 Ways to Multiply. Control Engng., 1954, Nov., Vol. 1, No. 3, pp. 34-46.

M. Lilamand, Multiplieurs a decoupage temporel. L'Onde electrique, 1955, Fevr., Vol. 35, No. 335, pp. 142-158, 13 figures.

M. A. Meyer and H. W. Fuller, Two New Electronic Analog Multipliers. Rev. Sci. Instrum., 1954, Dec., Vol. 25, No. 12, pp. 1166-1172.

I. A. Miller, A. S. Soltes and R. E. Scott, Wide-Band Analog Function Multiplier. Electronics, 1955, Febr., Vol. 28, No. 2, pp. 160-163, 4 figures.

D. H. Schaeffer, A Static Magnetic Transistor Analogue Divider. Commun. and Electronics, 1955, Nov., No. 21, pp. 652-655. 10 figures, 2 bibliographies.

S. Sternberg, An accurate electronic multiplier. RCA Review, 1955, Dec., Vol. 16, No. 4, pp. 618-634, 14 figures.

R. L. Van Allen, Four Quadrant Multiplication with Transistors and Magnetic Cores. Commun. and Electronics, 1955, Nov. No. 21, pp. 643-648, 7 figures, 6 bibliographies.

5. Functional convertors.

I. Sh. Pinsker, Representation of functions of many variables using summing, multiplying and very simple functional units. Trudy Inst. Mashinovedeniia Akad. Nauk SSSR. Seminar on accuracy in machines and apparatus construction, 1955, No. 8, pp. 35-51, 10 tables, 6 references.

V. V. Shershun, More accurate functional potentiometers for computer devices. Trudy Leningr. Inst. Aviats. priborstroen, 1954, No. 6, pp. 63-72, 4 figures.

D. F. Bearick, Function Generation on Differential Analyzer Extended to Analog Computer. Trans. IRE, 1955, Aug., Vol. TRC-1, No. 3, pp. 8-12.

J. R. Brathovde and J. D. Breazeale, Linear-to-log converter. Rev. Sci. Instrum., 1955, Vol. 26, No. 9, pp. 892-893.

B. E. Davis and I. H. Swift, An Analogue Computer Technique Using Magnetic Amplifiers. Commun. and Electronics, 1955, Jan., No. 6, pp. 635-640, 13 figures.

H. F. Meissinger, An Electronic Circuit for the Generation of Function of Several Variables. IRE Convention Record, 1955, Pt. 4, pp. 150-161, 13 figures.

E. E. Newhall, Waveform generator uses pulse techniques. Electronics, 1955, June, Vol. 28, No. 6, pp. 149-151, 4 figures, 1 bibliography.

P. N. Nikoforuk, A Technique for Non-Linear Function Generation. Electronic Engng, 1955, March, Vol. 27, No. 325, pp. 118-119.

A. S. Robinson, Electronic Analog Computing Technique for Solution of Trigonometric Problems. Trans. IRE 1955, Sept., Vol. EC-4, No. 3, pp. 95-101.

J. W. Sauber, Square-Law Detector for RMS Voltages. Electronics, 1955, Nov., Vol. 28, No. 11, pp. 170-172, 5 figures.

A. S. Soltes, Wide-Band Square-Law Circuit Element.-Trans. IRE, 1955, April, Vol. ED-2, pp. 32-39.

H. Winkler, Über Funktionstransformatoren mit Bildabtastrohre und einer Photozelle mit Sekundarelektronen-verfielfacher fur die Verwendung in grosser Arbeitsgeschwindigkeit. Wissenschaftlche Z. der Hochschule fur Electrotechnik. Ilmenau, 1954-1955, H. 2, S. 93-98, 7 figures.

6. Other computer components.

M. S. Libkind, Inductors with ferromagnetic cores for computing machines and analogs. Moscow, Institute of Technical and Economic Information. Akad. Nauk SSSR, 1955, 21 pp. illus. (Periodical Information, Subject No. 29, No. K-55-44).

C. D. Bock, Make the most of good components. Control Engng., 1955, April, Vol. 2, No. 4, p. 60.

G. M. Davidson, Basic Math. with ac analogs. Control Engng, 1955, March, Vol. 2, No. 3, pp. 57-66, 10 figures 3 bibliographies.

H. Eisenpress, J. L. McPherson and J. Shiskin, Charting on Automatic Data Processing Systems. Computers and Automation, 1955, Vol. 4, Aug., No. 8, pp. 21-23, 2 charts.

M. H. Hayes and J. L. West, Potentiometer Characteristics. Tele-Tech, 1955, Febr., No. 2, pp. 97, 126, 127.

R. A. Henle, A Multi Stable Transistor Circuit. Commun. and Electronics, 1955, Nov., No. 21, pp. 568-571, 8 figures, 1 bibliography.

T. J. Keefe, Truer Input Functions in Electronic Analog Computers. Computers and Automation, 1955, Vol. 4, No. 1, pp. 27-30.

L. Knight, Stabilized dc Supplies Using Grid-Controlled Rectifiers. Electronic Engng., 1955, Jan., Vol 27, No. 323, pp. 16-19.

G. Meyer, Elektromechanische Analogien. Physikalische Deutung. Schaltungsbegriff und Klemmenvorstellung in der Mechanik. Frequenz, 1955, Bd. 9, Nr. 7, Juli, S. 27.

G. H. Royer, A Switching Transistor dc to ac Converter having an Output Frequency Proportional to the dc Input Voltage. Commun. and Electronics, 1955, July, No. 19, pp. 322-326, 7 figures, 2 bibliographies.

J. Schwartz and R. Solomonoff, Photoelectric dc Chopper for Guided Missiles. Electronics, 1954, Nov., Vol. 27, No. 11, pp. 162-163.

VI. Electromechanical Analogs (Nondigital Electromechanical Computers)

V. A. Karabanov, et al., An electrodynamic analog. Moscow, Institute of Technical and Economic Information Akad. Nauk SSSR, 1955, pp. 3-21, 10 figures (Pribory i stendy. Subject No. 10, No. PS-55-494).

S. A. Levitan and V. Iu. Kaganov, An electromechanical analog to a hot object for studying automatic control systems. Institute of Technical and Economic Information, Akad. Nauk SSSR, 1955, pp. 30 (Pribory i stendy).

C. M. Davis, Electromechanical Analogue Simulates Transient Phenomena and Governor Action in 10 kc Network Analyzer Generators. Proc. Nat. Electron. Conference, Vol. 10, Chicago, 1955, pp. 533-542, 5 figures, bibliographies 7.

N. L. Fritz, Analog Computer for Nonlinear Coordinate Transformation. Rev. Sci. Instrum., 1955, Jan., Vol. 26, No. 1, pp. 23-27, 5 figures.

G. R. Marner, High Precision Computer for Automatic Solution of the Celestial Triangle. IRE Convention Record, 1955, Part 5, pp. 115-118, 9 figures.

Mechanical Integrator. Rev. Sci. Instrum., 1955, Vol. 26, No. 6, p. 628; Abs. J. Math., 1956, No. 7, 110 pages.

J. G. L. Michel, Errors of friction wheel integrators. J. Sci. Instrum., 1955, Vol. 32, No. 2m pp. 43-44.

F. S. Preston, Analog Computer for Solution of Tangents. Trans. IRE, 1955, Sept. Vol. EC-4, No. 3, pp. 101-106.

J. E. Walker, Electro-Mechanical Integration to be Featured at Machine-Tool Show. Machinery, N. Y., 1955, Aug., No. 12, pp. 185-186.

VII. Specialized Analog Computers

1. Devices for solving systems of algebraic equations. Root locators.

L. I. Gutenmakler, G. K. Kuz'minok, and L. S. Klabukova, A method of solving linear algebraic equations on electronic integrator. In "Computer mathematics and computing technique". Vol. 2, Moscow, Akad. Nauk SSSR, 1955, pp. 230-246, 17 illus., 7 references.

L. Lofgrin, An analog computer for determining the roots of algebraic equations. In "Mashinstroenie", 1955, No. 2, pp. 16-26, 5 illus., 10 refs.

Calculatrice analogique resolvant les systemes d'equations linearies et les problemes connexes. Revue general de l'electricite, 1955, Nov., Ann. 39, t. 64, No. 11, p. 576.

A. Choudhury, The Isograph — an Electronic Root Finder. Indian J. Physics, 1955, Oct., Vol. 29, No. 10, pp. 468-473.

N. L. Fritz, Analog computer for nonlinear coordinate transformation. Rev. Sci. Instrum., 1955, Vol. 26, No. 1, pp. 23-27; Abs. J. Math., 1956, No. 6, p. 138.

M. Henon, Machine analogique pour le calcul de l'indice complexe d'un corps a partir de son purvoir reflecteur. C. R. Acad. Sci., 1955, t. 240, No. 12, pp. 1305-1306.

R. Janin, Resolution de Systemes D'Equations Algebriques Lineaires d'Ordre Eleve, A l'Aide des Methodes Mecanographiques. Rech. Aeronaut., 1955, No. 44, pp. 47-50.

S. K. Mitra, Electrical analog computing machine for solving linear equation and related problems. Rev. Sci. Instrum., 1955, Vol. 26, No. 5, pp. 453-457, 5 figures.

G. Röntsch, Uber die Berechnung linearer Gleichungssysteme mit vollautomatischen Rechenmaschinen. Bauplannung u. Bautechnik, 1955, Bd. 9, Nr. 2, S. 88-89; Abs. J. Math., 1956, No. 6 p. 137.

F. L. Ryder, Linear algebraic computation by multi-winding transformers. J. Franklin Inst., 1955, May, Vol. 259, No. 5 pp. 427-439, 5 figures, 3 bibliographies.

B. H. Stowens, New computing facility. Sperry Engng. Rev., 1955, March-Apr., Vol. 8, No. 2, pp. 19-21.

N. P. Tolinson, M. Horowitz and C. H. Reynolds, Analog Computer Construction of Conformal Maps in Fluid Dynamics. J. Appl. Phys., 1955, Febr., Vol. 26, No. 2, pp. 229-232, 5 figures, 9 bibliographies.

2. Correlators

K. W. Goff, An Analog Electronic Correlator for Acoustic Measurements. J. Acoust. Soc. America, 1955, March, Vol. 27, No. 2, pp. 223-236, 13 figures.

V. S. Haneman and J. W. Senders, Correlation Computation on Analog Devices. J. Assoc. Computing Mach., 1955, Oct., Vol. 2, pp. 267-279.

F. Smith, Analog equipment for processing randomly fluctuating data. Preprints Ann. Meeting Inst. Aeronaut. Sci., 1955, No. 545, 18 p., 11 figures. Aeronautic Engng. Rev., 1955, Vol. 14, No. 5, pp. 113-119; Abs. J. Math., 1956, No. 1, p. 168.

3. Trainers.

G. V. Amico, Synthetic Training for Space Flight. IRE Convention Record, 1955, Part 10, pp. 49-54.

R. C. Dehmel, The Flight Simulator Modification Problem. Aeron. Engng. Rev., 1955, May, Vol. 14, No. 5, pp. 102-108, 17 figures.

J. J. Gait and F. R. I. Spearman, Simulators. J. Inst. Electr. Eng., 1955, Nov., Vol. 1, No. 11, pp. 684-686, 6 figures.

M. Krakauer and R. J. Bibberg, Modular Simulator Tests Missile Radar., Electronics, 1955, July, Vol. 28, No. 7, pp. 127-129, 3 figures.

W. J. Perking, Electronic Simulators for Physiological Use. Electronic Engng., 1955, Oct., Vol. 27, No. 332, pp. 434-440, 10 figures, 4 bibliographies.

Reactor Simulator. Instruments and Automation, 1955, Vol. 28, No. 11, p. 1923.

Silent simulator for jet engine testing at Northrop. Control Engng., 1955, May, Vol. 2, No. 5, p. 80.

Supersonic flight simulator. Control Engng., 1955, May, Vol. 2, No. 5, p. 22.

U. S. Air Force Demonstrates First Supersonic Flight Simulator. Electronic Engng., 1955, Vol. 74, May, No. 5, p. 413.

Universal Flight Trainer. Electronic Engnr., 1956, Jan., Vol. 28, No. 335, p. 15.

G. J. Wheeler, A Broadband Electronic Doppler Simulator. IRE Convention Record, 1955, Part 8, Commun. and Microwave, pp. 75-77, 4 figures.

Wright Air Development Center to Have Largest Flight Simulation Center in the World. Control Engng., 1955, Oct., Vol. 2, No. 10, p. 21.

VIII. Devices for Converting from Digital Code to Physical Quantities and Conversely

Analog-to-digital Converter. Instruments and Automation, 1955, Dec., Vol. 28, No. 12, pp. 2132-2134, 1 figure.

Analog-digital Converter. Rev. Sci. Instrum., 1955, Vol. 26, No. 4, p. 408.

Data Handling Instrument. Rev. Sci. Instrum., 1955, Vol. 26, No. 4, pp. 405-406; Abs. J. Math., 1956, No. 5,page 120.

D. E. S. Isle, Analogue to Digital Conversion in Data Processing Systems. Instrum. Practice, 1955, Nov., Vol. 9, No. 11, pp. 1061-1065, 5 figures.

IX. Comparison of Digital Machines and Analogs

E. J. Galli and C. C. Wang, Electronic computation. Sperry Eng. Rev., 1955, Jan.-Febr., No. 1-2, pp. 21-28.

X. Accessory Equipment

A. M. Petrovskii, A review of methods of generating infrasonic fluctuation emfs. Trans. 2nd. All-Union Conference on the Theory of Automatic Control, 1955, Vol. 3, pp. 105-107, 2 figures, 3 references.

V. B. Ushakov, Ultralow-frequency apparatus for recording dynamic responses of automatic control systems. Trans. 2nd. All-Union Conference on the Theory of Automatic Control, 1955, Vol. 3, pp. 147-162, 14 figures.

J. C. Balchen and J. H. Mo, An Instrument for the Simultaneous Recording of Several Magnitudes. Takn. ukeblad, 1955, Sept. 15, Vol. 102, No. 33, pp. 712-716.

Z. Czajkowski, A harmonic response plotter. Electronic Engng., 1955, May, Vol. 27, No. 327, pp. 207-211, 6 figures , 4 bibliographies.

A. Linek, Mathematical machine for calculating Fourier transformations. Czechoslov. J. Phys. 1955, 5, 2, 212-220, 5 figures, 9 bibliographies.

H. B. Mohanti and A. D. Booth, A Simple Electronic Fourier Synthesizer. J. Sci. Instrum., 1955, Nov., Vol. 32, No. 11, pp. 442-444, 5 figures, 9 bibliographies.

J. Pottier, Un Analyseur Harmonique Analogique. L'Onde electrique, 1955, Oct., Ann. 35, No. 343, pp. 847-866, 14 figures, 8 bibliographies.

T. S. Tox, A Waveform Synthesizer for Technical Training. Electronic Engng., 1955, Vol. 27, No. 331, pp. 374-378, 11 figures.

XI. Analog Applications

1. Use of analog devices for solving automatic control problems.

Iu. E. Golubchin, Units representing typical nonlinearities for use in an automatic control system analog. In: "Collected papers of the Student Scientific Society at Moscow Power Institute", Moscow, 1955, pp. 173-190.

B. Ia. Kogan, Analogs to automatic control systems when typical nonlinearities are present. Automation and Remote Control, 16, 2, 113-128 (1955), 12 figures, 10 references.

G. M. Kuz'michev, Electrical analog studies of electromechanical relay servo systems. In "Papers from the Student Scientific Society, Penza Industrial Institute, 1955, pp. 24-66, illus., 36 references.

S. A. Levitan and V. Iu. Kaganov, An electromechanical analog model to a hot object for studying automatic control systems. Moscow, Institute of Technical and Economic Information, Akad. Nauk SSSR, 1955, pp. 28, 19 figures (Pribory i stendy).

A. A. Malinin, Study of relay system motion on an electrical analog. Automation and Remote Control (USSR) 1955, No. 6, pp. 542-547.

G. M. Fialko, Analogs and optimum parameter calculations for automatic control systems for the chemical industry. Trans. 2nd. All-Union Conference on the Theory of Automatic Control, 1955, Vol. 2, pp. 514-522, 11 figures, references, pp. 521-522.

H. Bohler, Modell zur Darstellung und Ausmessung der Reguliervorhaltnisse von Synchrongeneratoren, zwecks Bestimmung der gunstigsten Spannungsregelung. Bull. Oerlikon, 1955, Febr., No. 308, S. 9-14, 18 figures.

Computer Analysis of Industrial Control Regulating Sustems. Product. Engng., 1955, June, Vol. 26, No. 6, pp. 314-315.

Discussion on "An Analogue Computer for use in the Design of Servo Systems," Proc. Inst. Electr. Engnrs, 1955, July, Part 13, Vol. 102, No. 4, p. 411.

T. Dunnegan and J. D. Harnden, Cyclic Integrator Measures Frequency Response. Electr. Engng., 1955, Apr., Vol. 74, No. 4, p. 285, 1 figure.

V. Ferner, Über die Darstellung und Untersuchung von Regelungsvorgangen mit Hilfe von Modellregelstrecken. Bergakademie, 1955, Apr., Bd. 7, Nr. 4, S. 171-181, 27 Abb.

E. F. Johnson and T. Bay. Application of Pneumatic Analog. Ind. Engng. Chem., 1955, Vol. 47, No. 3, Part 1, pp. 403-408.

R. C. Klein, Analog Simulation of Sampled Data Systems. Trans. IRE, 1955, Vol. TRC-1, No. 2, pp. 2-7.

J. H. Laning and R. H. Battin, An Application of Analog Computers to the Statistical Analysis of Time-Variable Networks. Trans. IRE, 1955, March, Vol. CT-2, No. 1, pp. 44-49, 7 figures.

J. T. Miller, Control handbook. Section 5. Electrical analogies in process control. Instrument Practice, 1955, Vol. 9, No. 5, pp. 441-444, 8 figures, 7 bibliographies.

J. Pack and W. E. Phillips, Analog Study of Interacting and Noninteracting Multipleloop Control Systems for Turbojet Engines. Nat. Adv. Committee Aeronautics Rep. 1212, Washington, 1955, 13 p., 14 figures, 4 bibliographies.

J. B. Reynolds, An Analog Machine Approach. Control Engng., 1955, Oct., Vol. 2, No. 10 p. 60.

D. Singer, Application of miniaturized equipment for calculating control problems. Praha, Ceskoslovenska Akad. Ved. 1955, Str. 244-266, 20 Obr. Bibliogr. 12.

L. B. Wadel, Analysis of combined sampled and continuous-data systems on an electronic analog computer. IRE Convention Record., 1955, Part 4, pp. 3-14, 8 figures.

2. Use of analogs and components thereof in aviation.

Analog computer designed for use by aircraft engineers. Electric. Engng, 1955, Vol. 74, No. 4, p. 335.

Analog computers simulate engines. Electronics, 1955, Vol. 28, No. 5, pp. 214, 216; Abs. J. Math., 1956, No. 7, page 119.

Computers for aviation research and development. Aviation Age, 1955, Vol. 23, No. 6, pp. 266-271; Abs. J. Math., 1956, No. 9, page 115.

H. J. Curfman, Theoretical and Analog studies of the effects of nonlinear stability derivatives on the longitudinal motions of an aircraft in response to step control deflections and the influence of proportional automatic control. NACA Report 1241, 1955, 21 p., 17 figures, 19 bibliographies.

K. V. Diprose, Analogue Computing in Aeronautics. J. Roy. Aeron. Society, 1955, July, Vol. 59, No. 535, pp. 479-493, 7 figures, 20 bibliographies.

J. J. Foody, Analogue Computation. Its Place in Aircraft Design. Flight, 1955, July 29, Vol. 68, No. 2427, pp. 168-170, 4 figures.

J. R. Forester and C. I. Sullivan,* Flight Simulation with a Computer. Automatic control, 1955, Dec., No. 12, pp. 16-17.

J. R. Forester and O. J. Sullivan,* Integrating a computer into a simulator program. Proc. Nation. Electron. Conference, 1955, Vol. 11; Chicago, 1956, pp. 620-626, 4 figures.

A. H. Kuhnel, Test-flight analysis speeded with computer. Control Engng, 1955, March, Vol. 2, No. 3, p. 81.

W. R. Monroe, Application of Electronic Simulation Techniques to the Development of Airplane Flight Control Systems. Aeron. Engng. Rev., 1955, Vol. 14, No. 5, pp. 91-101, 20 figures.

F. E. Nixon, What Can Electronic Simulators Do for the Designer? Aeron. Engng. Rev., 1955, May, Vol. 14, No. 5, pp. 109-112, 1 figure.

K. E. Wood and I. V. Hansford, A Flutter Computer with Low Gain Amplifier. Electronic Engng, 1955, Nov., Vol. 27, No. 333, pp. 477-481.

3. Use of analogs and components thereof for solving various problems.

A. E. Krushevskii, Some applications of the ELI-14 electrical integrator. In "Students' papers, No. 2" Minsk, Izd. Akad. Nauk Beloruss. SSR, 1955, pp. 10-16, 1 figure, 4 references (Beloruss. Polytech. Inst).

V. I. Motiakov and Iu. A. Babich, Experimental studies on secondary methods of developing oil deposits using the EM-8 UMNP electrical analog. Izv. Akad. Nauk Azerb. SSR, 1955, No. 10, pp. 33-40, figures.

E. A. Papernyi and R. Ia. Berkman, A computer device for continuously measuring the efficiency of a steam boiler. In "Sci. Rep. Lvov. Polytech. Inst.", 1955, No. 32, heat engineering series, No. 1, pp. 163-175, 7 figures.

A computer for calculating the directional actions of antennae. Vestn. inform., 1955, No. 23, pp. 9-13, 6 figures.

N. I. Chelnokov and I. M. Tetel'baum, Solution of some ordinary differential equations with an electronic analog computer. Jubilee Scientific-Technical Conference. Summaries of Reports. Moscow, 1955, pp. 5-6 (MVO SSSR, Moscow Power Institute).

G. H. Amber, Analog computers for machine control. Elec. Mfg., 1955, Aug., Vol. 56, No. 2, pp. 70-76; Oct., No. 4, pp. 145-153.

Analog Computer for Mine Ventilation Problems. Mining Mag., 1955, Febr., Vol. 92, No. 2, pp. 123-125.

F. R. Berry, Electrical analog solution of certain nonlinear problems in vibrations and elastic stability. Proc. Soc. for Experimental Stress Analysis, 1955, Vol. 13, No. 1, pp. 1-10, 10 figures.

P. Braffort, Machines analogiques, simulateurs de pile. L'Onde electrique, 1955, Oct., Ann. 35, No. 343, pp. 888-889, 10 figures, 7 bibliographies.

R. P. Burr and J. P. White, Simple color computer gives tristimulus values. Electronics, 1955, Oct., Vol. 28, No. 10, pp. 166-169, 5 figures, 1 bibliogrphy.

Computer for machining problems. Machinery, L. 1955, Sept., Vol. 87, No. 2236, p. 728, 1 figure.

M. C. Crowley-Milling, A computer for solving some problems in connection with travelling-wave particle accelerators. Metropolitan-Vickers Gazette, 1955, Apr., Vol. 26, No. 429, pp. 127-131, 7 figures, 2 bibliographies.

---

*As in original – Publisher's note.

D. F. Early, C. L. Smith and D. Schoder, "Early bird" guides system loading. Electr. World, 1955, Vol. 143, No. 2, pp. 62-64; Abs. J. Math., 1956, No. 5, p. 117.

E. D. Early, W. E. Phillips and W. T. Shreve, Incremental Cost of Power-Delivered Computer. Trans. Americ. Inst. Electr. Engrs., 1955, June, Vol. 74, Part 3 (Power Apparatus and Systems), No. 18, pp. 529-535.

Electronic computer determines machinability. Machine Design, 1955, Vol. 27, No. 8, p. 24.

M. I. Fornaseri, Calcolatori and logici per analisi rontgenografica X-RACeS—DaC. — Ric. Scient. 1955, Vol. 25, No. 3, pp. 544-552, 4 figures, 1 bibliography.

N. E. Friedmann, Analog Methods for Study of Transient Heat Flow in Solids with Temperature-Dependent Thermal Properties. J. Appl. Phys., 1955, Vol. 26, No. 1, pp. 129-130.

Gas network computer. Control Engng., 1955, Apr., Vol. 2, No. 4, p.13.

H. Grover, Analog Helps Solve Suspension Problems. SAE-Journ., 1955, Apr., Vol. 63, No. 4, pp. 44-46, 8 figures.

House analog. Electronics, 1955, Vol. 28, No. 8, p. 206.

R. L. Hovious, C. D. Morrill and N. P. Tomlinson, Industrial Uses of Analog Computers. Instruments and Automation, 1955, Vol. 28, No. 4, pp. 594-601; No. 7, pp. 1108-1113.

C. E. Howe and R. M. Howe, Application of the Electronic Differential Analyzer to the Oscillation of Beams, Including Shear and Rotary Inertia. J. Appl. Mech., 1955, March, Vol. 22, No. 1, pp. 13-19, 8 figures, 12 bibliographies.

P. Huard de la Marra, Three-dimensional electrical analogue models for studying drainage by free-surface filtration. C. R. Acad. Sci., Paris, 1955, June 6, Vol. 360, pp. 2203-2205.

A. J. Kennedy, The physical and computing significance of an electrical analogue of creep and recovery. Brit. J. Appl. Phys., 1955, Febr., Vol. 6, No. 2, pp. 49-58, 11 figures, 24 bibliographies.

A. H. Kugnel, Industrial Uses of Special-Purpose Computers. Instruments and Automation 1955, Vol. 28, No. 7, pp. 1108-1113, 5 figures.

G. N. Lange and E. C. Deland, On the differential analyzer solution of the water bells problems. Proc. Phys. Soc. Section B, 1955, Vol. 68, No. 421, pp. 54-55, 3 figures.

J. H. Laning and R. H. Battin, An application of analog computers to the statistical analysis of time-variable networks. Trans. IRE, 1955, March, Vol. CT-2, No. 1, pp. 39-44, 7 figures.

D. C. Leckie and R. E. Cain, Application of Consolidated computer to solution of metallurgical regression problems. Indus. Quality Control, 1955, June, Vol. 11, pp. 3-8.

G. Liebmann, The solution of plane stress problems by an electrical analog method. Brit. J. Appl. Physics, 1955, May, Vol. 6, No. 5, pp. 145-157, 19 figures, 16 bibliographies.

B. F. Logan and others. Analog study of electron trajectories. J. Assoc. Comput. Machinery, 1945, Jan., Vol. 2, No. 1, pp. 28-41; Abs. J. Math., 1956, No. 2, page 162.

J. T. Miller, Control handbook. Section 4. Simple computing devices in process measurement and control. Instrument Practice, 1955, IV, Vol. 9, No. 4, pp. 342-348, 18 figures, 10 bibliographies.

R. C. Moore, McElroy Fluid Network Analyzer. Instruments and Automation, 1955, March, Vol. 28, No. 3, pp. 428-429.

J. E. Nolan, Analog computers and their application to heat transfer and fluid flow. Part 3. Computers and Automation, 1955, Vol. 4, No. 1, pp. 31-35, 37. Bibliogr. 153.

J. Nowinski and S. Turzki, Solving Lame's problems for nonhomogeneous cylinder using a machine for solving differential equations. Archivum Mechaniki Stosowanej, 1955, 7, 3, 419-424, 7 figures 6 bibliographies. (Polska Akademia Nauk).

Ohio Edison power system will be controlled by computer. Control Engng., 1955, Oct., Vol. 2, No. 10, p. 20.

W. Paul, Analog computer for ac oximetry. J. Sci. Instruments, 1955, July, Vol. 32, No. 7, p. 286.

A. Piatt, Computing Mechanisms integrate Process Control Elements. Automation, 1955, June, Vol. 2, No. 6, pp. 61-64.

H. E. Rose, Electronic computer for color printing. Commun. and Electronics, 1955, May, No. 18, pp. 268-272, 5 figures, 5 bibliographies..

E. S. Shire, Analog computer for nuclear reactions. J. Sci. Instrum., 1955, Vol. 32, No. 10, pp. 391-392, 3 figures.

J. D. Strong, A practical approach to analog computers. Instruments and Automation, 1955, Apr., Vol. 28, No. 4, pp. 602-610, 28 figures.

This computer trims ships. Control Engng., 1955, Oct., Vol. 2, No. 10, pp. 90-91, illus.

L. C. Vogel and R. F. Krueger, Analog computer for studying heat transfer during thermal recovery process. J. Petrol. Techn. 1955, Vol. 7, No. 12, pp. 205-212.

XII. Bibliography

Calculating machines. History, principles of structure, new types. Recommended list of literature. Moscow Central Polytechnic Library 1955, 11 pages.

J. Bonn, Books and other publications. Computers and Automation, 1955, Vol. 4, No. 9, p. 36; Abs. J. Math., 1956, No. 9, page122.

J. Bonn and G. Spenser, Books and other publications. Computers and Automation, 1955, Vol. 4, No. 8, pp. 28-32; Abs. J. Math., 1956, No. 9, page 122.

J. E. Nolan, Analog computers and their application to heat transfer and fluid flow. Computers and Automation 1955, Jan., Vol. 4, No. 1, pp. 31-37.

G. Spenser, Books and other publications. Computers and Automation, 1955, Vol. 4, No. 7, pp. 26-28.

A METHOD OF PRODUCING COMPLEX CONTROL LAWS USING ONLY THE ERROR SIGNAL OR CONTROLLED COORDINATE PLUS THEIR FIRST DERIVATIVES

S.V. Emel'ianov

(Moscow)

A method of producing various control laws using only the error signal plus its first derivative is presented.

The efficacy of such correction is shown to be the same for different scale changes in the disturbance for linear control systems.

One possible method of producing a nonlinear corrector which effects various control laws is presented.

INTRODUCTION

Correction devices are important in improving the performance of automatic control systems. These devices transform the error signal, or the deviation of the controlled quantity, according to some functional law, usually termed the control law [1] which, in particular, can be put in the form

$$v(t) = N(p)\,x(t) = \sum_{i=-l}^{k} n_i p^i x(t), \tag{1}$$

where x(t) is the error signal (corrector input), n_i is a constant factor,

$$p^{-l}x(t) = \int_0^t dt \ldots \int x(t)\,dt, \quad p^k x(t) = \frac{d^k x(t)}{dt^k},$$

and v(t) is the corrector output.

The law can be nonlinear, e.g.,

$$v(t) = \varphi[x(t), px(t), \ldots], \tag{2}$$

where φ is some given nonlinear function of x(t), px(t), ... [2, 3].

Converters are used in which various devices have a stepwise change in gain on closed circuit [4—8].

Methods of system stabilization have recently been developed using pulsed devices and digital computers [9, 10]. It is difficult to produce a unit which realizes Law(1) above because high-order derivatives are difficult to produce with sufficient accuracy.

Automatic control systems (ACS) having nonlinear control laws, as in (2), have the disadvantage that when the perturbation $f(t)$ deviates from the calculated one the nonlinear converter which produces the control law must be adjusted in order to maintain the required properties of the system (optimal ACS being excluded [3]). If not reset the corrector sometimes makes the system response worse; stability may be lost.

Ways of stabilizing systems using stepwise changes in gain have been considered [4—8]; the efficacy of this corrector method has been demonstrated. The idea is a very fruitful one, and if realized can greatly improve the transient response. But the above papers consider converters which effect particular forms of control law.

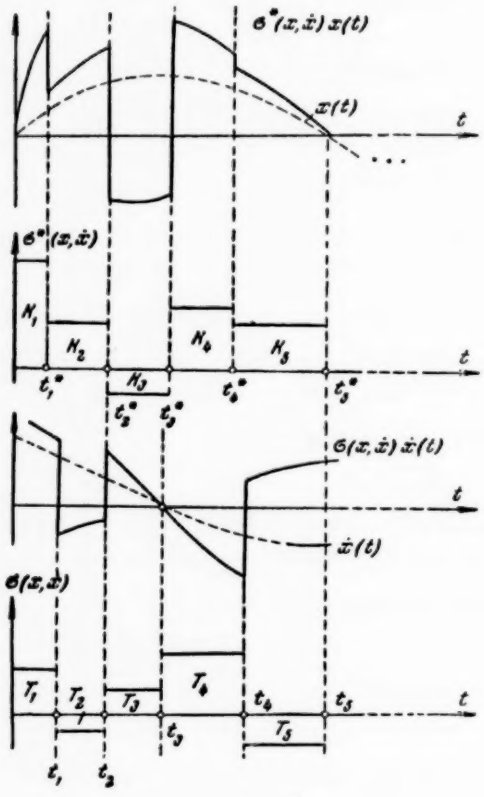

Figure 1.

Here we present a method by which, by relatively simple means, it is possible to produce quite an extensive range of control laws which satisfy preset requirements as to transient response. Such laws are those of the form

$$v(t) = Kx(t) + w(t), \tag{3}$$

where K is a constant nonnegative coefficient, x(t) is the controlled coordinate,

$$w(t) = \sigma^*(x, \dot{x})x(t) + \sigma(x, \dot{x})\dot{x}(t), \tag{4}$$

$\sigma^*(x, \dot{x})$, $\sigma(x, \dot{x})$ being step functions having constant values within defined sectors of the x, $\dot{x}$ plane and having first-order discontinuities at the sector boundaries.

This functional transformation uses only the controlled coordinate x and its first derivative $\dot{x}$ in producing the control law, as (4) shows. During the finite time intervals between the instants when the control system switches, it is described by equations with constant coefficients (for a linear object and linear effector). In any interval the coefficients of x(t) and $\dot{x}(t)$ in the control law can be chosen arbitrarily. For a given form of perturbation and zero initial conditions the switching times in the transients are independent of the scale coefficient A (scale of perturbation change). This ensures that some properties of a linear system are retained; in particular, that the control law is equally effective at different A values.

Figure 1 shows examples of $\sigma^*(x, \dot{x})x(t)$ and $\sigma(x, \dot{x})\dot{x}(t)$, which go to form w(t). The symbols K and T denote the coefficients of the perturbations of the control coordinate and its derivative in the corresponding time intervals, t^* and t being the instants when K and T are switched. The structural diagram of an automatic control system using this form of correction is shown in Figure 2, where $\mu(t)$ denotes the control unit coordinate, g(t) the perturbation and p is the differential operator.

A nonlinear converter which effects a transform of the type of (4) can be represented as an assembly of 2N switches with differing transfer coefficients (Figure 3). The signal x(t) is supplied to the first N, and $\dot{x}(t)$ to the second N. Switches $S_1^*, S_2^*, \ldots S_N^*$ and $S_1, S_2, \ldots S_N$ are closed by signals from the control unit. The output signal from the control unit is produced in relation to the signs of x(t) and $\dot{x}(t)$ and to the ratio between them, consisting of the sequence of pulses required to control the switches S_i^* and S_i. The efficacy of this correction method will be illustrated by an example.

A method of producing the nonlinear functional relationship:

$$w(t) = \sigma^*(x, \dot{x})x(t) + \sigma(x, \dot{x})\dot{x}(t).$$

Let us consider the production of the function $\sigma(x, \dot{x})\dot{x}(t)$. We note that $\sigma^*(x, \dot{x})x(t)$ is produced analogously. Assume the transient curve x(t) and the curve $\dot{x}(t)$ (Figure 4). Divide the transient time into two groups of intervals. To the first we assign intervals in which x(t) and $\dot{x}(t)$ are of the same sign, i.e., $x > 0$, $\dot{x} > 0$ or $x < 0$, $\dot{x} < 0$, or in other words, those where $x\dot{x} > 0$. To the second we assign intervals when $x\dot{x} < 0$.

Let us write the expression $T_i\dot{x}(t)$, where T_i is a constant coefficient, in the form of the sum of two nonlinear functions, $\Phi_i(x, \dot{x})\dot{x}(t)$ and $\bar{\Phi}_i(x, \dot{x})\dot{x}(t)$ (Figure 4), $\Phi_i(x, \dot{x})\dot{x}(t)$ is a nonlinear function equal to $T_i\dot{x}(t)$

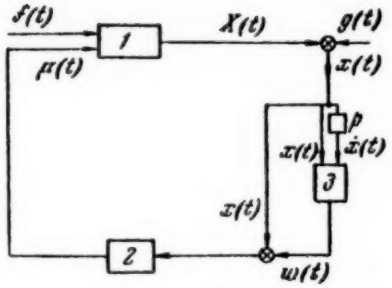

Figure 2. 1)Object, 2)effector mechanism, 3)nonlinear converter.

during group one intervals and zero during group two, and $\overline{\Phi}_i(x, \dot{x})\,\dot{x}(t)$ is a nonlinear function equal to $T_i\dot{x}(t)$ during group-two intervals and zero during group one.*

The nonlinear coefficients $\Phi_i(x, \dot{x})$ and $\overline{\Phi}_i(x, \dot{x})$ can be represented as follows (Figure 5):

$$\Phi_i(x, \dot{x}) = \begin{cases} T_i & \text{when } x\dot{x} > 0, \\ 0 & \text{when } x\dot{x} < 0, \end{cases}$$

$$\overline{\Phi}_i(x, \dot{x}) = \begin{cases} T_i & \text{when } x\dot{x} < 0, \\ 0 & \text{when } x\dot{x} > 0. \end{cases}$$

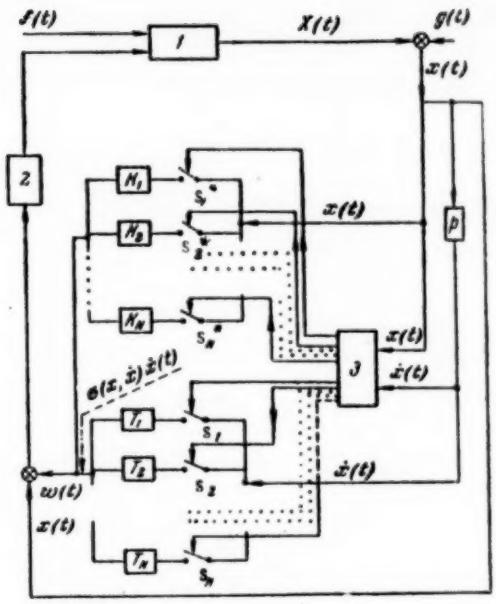

Figure 3. 1)Object, 2)effector mechanism, 3)control unit.

By subjecting $\Phi_i(x, \dot{x})\,\dot{x}(t)$ and $\overline{\Phi}_i(x, \dot{x})\,\dot{x}(t)$ to additional conditions we get new nonlinear functions $\Psi_{ij}(x, \dot{x})\,\dot{x}(t)$ and $\overline{\Psi}_{ij}(x, \dot{x})\,\dot{x}(t)$, from which the function $\sigma(x, \dot{x})\,\dot{x}(t)$ can be derived.

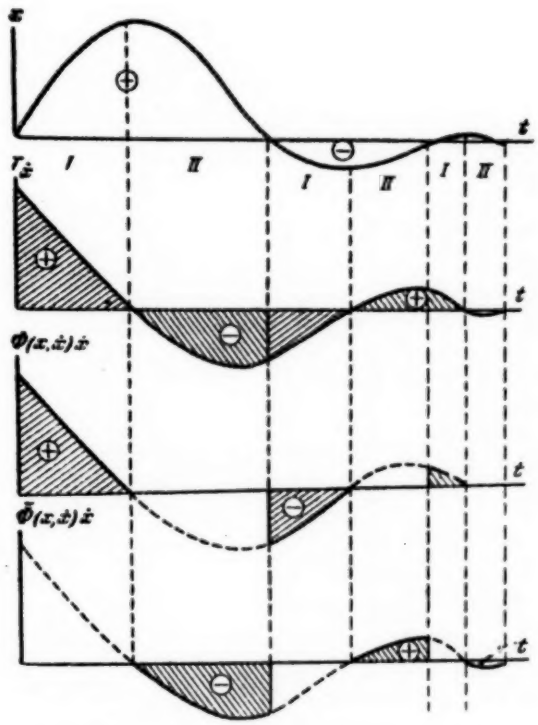

Figure 4. I)Group one intervals, II)group two intervals.

* The nonlinear functions can be assigned the values of the functions either to the right or left at the boundaries of the intervals.

Suppose we require that $\Psi_{ij}(x, \dot{x})\,\dot{x}(t)$ coincides with $\Phi_i(x, \dot{x})\,\dot{x}(t)$ when $\left|\frac{x}{\dot{x}}\right| > K_j$ applies and is zero when $\left|\frac{x}{\dot{x}}\right| < K_j$, where K_j is a constant positive coefficient.

Let us also require that the nonlinear function* $\overline{\Psi}_{ij}(x, \dot{x})\,\dot{x}(t)$ coincides with $\overline{\Phi}_i(x, \dot{x})\,\dot{x}(t)$ when $\left|\frac{x}{\dot{x}}\right| > K_j$ applies and is zero when $\left|\frac{x}{\dot{x}}\right| < K_j$. The expression for nonlinear coefficients $\Psi_{ij}(x, \dot{x})$ and $\overline{\Psi}_{ij}(x, \dot{x})$ is found as follows (Figure 6).

For $\infty > K_j > 0$

$$\Psi_{ij}(x, \dot{x}) = \begin{cases} \left.\begin{matrix} T_i \text{ when } x\dot{x} > 0 \\ 0 \text{ when } x\dot{x} < 0 \end{matrix}\right\} & \text{when } \left|\frac{x}{\dot{x}}\right| > K_j, \\ 0 & \text{when } \left|\frac{x}{\dot{x}}\right| < K_j, \end{cases}$$

$$\overline{\Psi}_{ij}(x, \dot{x}) = \begin{cases} \left.\begin{matrix} T_i \text{ when } x\dot{x} < 0 \\ 0 \text{ when } x\dot{x} > 0 \end{matrix}\right\} & \text{when } \left|\frac{x}{\dot{x}}\right| > K_j, \\ 0 & \text{when } \left|\frac{x}{\dot{x}}\right| < K_j; \end{cases}$$

For $K_j = 0$

$$\Psi_{ij}(x, \dot{x}) = \Phi_i(x, \dot{x}),$$
$$\overline{\Psi}_{ij}(x, \dot{x}) = \overline{\Phi}_i(x, \dot{x});$$

For $K_j = \infty$

$$\Psi_{ij}(x, \dot{x}) = 0,$$
$$\overline{\Psi}_{ij}(x, \dot{x}) = 0.$$

$\Psi_{ij}(x, \dot{x})\,\dot{x}(t)$ and $\overline{\Psi}_{ij}(x, \dot{x})\,\dot{x}(t)$ are determined by T_i and K_j. The index $\underline{i}$ denotes the corresponding value of T_i, $\underline{j}$ the corresponding value of K_j. By subtracting a $\Psi_{ij}(x, \dot{x})\,\dot{x}(t)$ [or $\overline{\Psi}_{ij}(x, \dot{x})\,\dot{x}(t)$] with K_j large from a $\Psi_{ij}(x, \dot{x})\,\dot{x}(t)$ [or $\overline{\Psi}_{ij}(x, \dot{x})\,\dot{x}(t)$] with a lesser K_j (T_i being the same for both) we get the functions $S_i(x, \dot{x})\,\dot{x}(t)$ and $\overline{S}_i(x, \dot{x})\,\dot{x}(t)$.

The values of the coefficients $S_i(x, \dot{x})$ and $\overline{S}_i(x, \dot{x})$ are expressed as follows:

$$S_{ipq}(x, \dot{x}) = \Psi_{ip}(x, \dot{x}) - \Psi_{iq}(x, \dot{x}) \text{ при } K_p < K_q,$$
$$\overline{S}_{ipq}(x, \dot{x}) = \overline{\Psi}_{ip}(x, \dot{x}) - \overline{\Psi}_{iq}(x, \dot{x}) \text{ при } K_p < K_q.$$

Thus T_i, K_p and K_q determine $S_{ipq}(x, \dot{x})$ in the sector of the $x, \dot{x}$ plane delimited by the rays K_p and K_q Figure 7a). Over the rest of the plane $S_{ipq} = 0$.

To determine $\sigma(x, \dot{x})$ over the whole of the $x, \dot{x}$ plane we form the sum of the $S_{ipq}(x, \dot{x})$ which differ in their T_i values and apply the condition that the boundaries of adjacent sectors defined by the K_p and K_q rays are common:

$$\sigma(x, \dot{x}) = \sum_{i=1}^{m} S_{iTq}(x, \dot{x}) + \sum_{i=1}^{m} \overline{S}_{ipq}(x, \dot{x}),$$

where $\underline{m}$ is the number of sectors into which each quadrant of the $x, \dot{x}$ plane is divided by the rays K_j (Fig. 7b).

* When $\left|\frac{x}{\dot{x}}\right| = K_j$ is fulfilled the values of $\Psi_{ij}(x, \dot{x})\dot{x}(t)$ and $\overline{\Psi}_{ij}(x, \dot{x})\dot{x}(t)$ can be taken as their values when either $\left|\frac{x}{\dot{x}}\right| > K_j$ or $\left|\frac{x}{\dot{x}}\right| < K_j$.

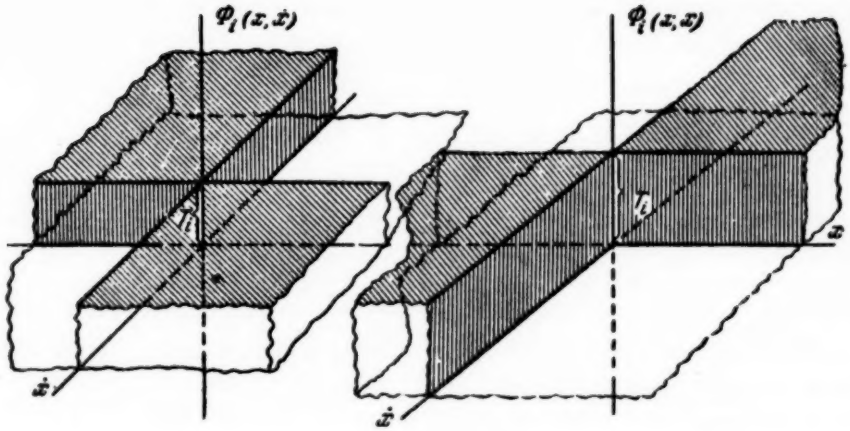

Figure 5

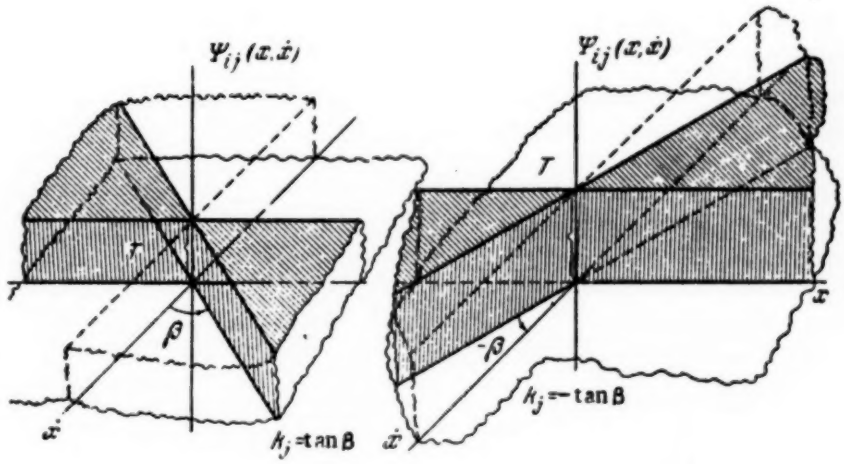

Figure 6

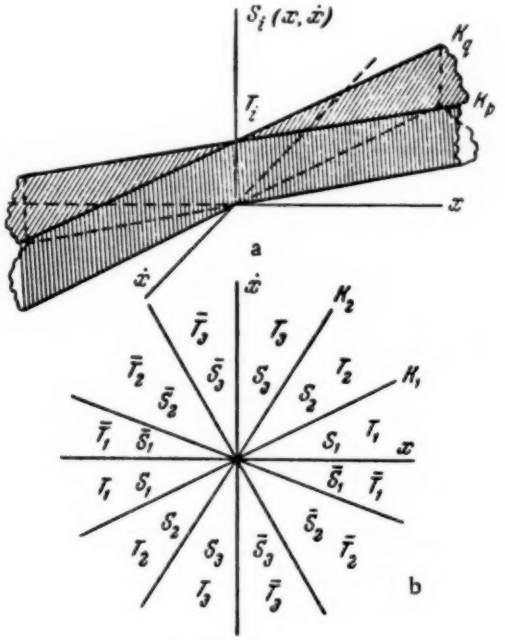

Figure 7.

By analogy we get the function

$$\sigma^*(x,\dot{x})=\sum_{i=1}^{m} S^*_{ipq}(x,\dot{x})+\sum_{i=1}^{m}\overline{S}^*_{ipq}(x,\dot{x}).$$

Figure 8 shows a typical graph of $\sum_{i=1}^{m} S_{ipq}(x,\dot{x})\dot{x}(t)$.

The nonlinear function w(t) in the control law is

$$w(t)=\left[\sum_{i=1}^{m} S^*_{ipq}(x,\dot{x})+\sum_{i=1}^{m}\overline{S}^*_{ipq}(x,\dot{x})\right]\dot{x}(t)+$$
$$+\left[\sum_{i=1}^{m} S_{ipq}(x,\dot{x})+\sum_{i=1}^{m}\overline{S}_{ipq}(x,\dot{x})\right]\dot{x}(t).$$

This expression shows that our method can give quite complex control laws.

The expressions for $\sigma(x, \dot{x})$ and $\sigma^*(x, \dot{x})$ can be derived in a somewhat different way, by assuming the $\Psi_{ij}(x, \dot{x})$ and $\overline{\Psi}_{ij}(x, \dot{x})$ and selecting the T_i values within the sectors of the $(x, \dot{x})$ plane such that the sum comes to a given value of the coefficient of $x(t)$ or $\dot{x}(t)$ in the region in question, i.e., by taking

$$\sigma(x, \dot{x}) = \sum_{i=1}^{m} \Psi_{ij}(x, \dot{x}) + \sum_{i=1}^{m} \overline{\Psi}_{ij}(x, \dot{x}),$$

$$\sigma^*(x, \dot{x}) = \sum_{i=1}^{m} \Psi^*_{ij}(x, \dot{x}) + \sum_{i=1}^{m} \overline{\Psi}^*_{ij}(x, \dot{x}).$$

We can derive a functional transform which is effective for nonlinear automatic control systems analogously, and can determine the structure of the appropriate correcting unit. Here the values of T_i and K_j, which determine the $\Psi_{ij}(x, \dot{x})$ or the $S_{ipq}(x, \dot{x})$, can be made different in the various regions of the $(x, \dot{x})$ plane. We can, for instance, change their values when x attains the values x_1, x_2, x_3, x_4, etc., and $\dot{x}$ the values $\dot{x}_1$, $\dot{x}_2$, $\dot{x}_3$, $\dot{x}_4$, etc., (Figure 9).

T, T* and T**, and K, K* and K** in Figure 9 denote the constant coefficients of x and $\dot{x}$ respectively in regions of the $(x, \dot{x})$ plane corresponding to the three fixed values of the coefficients in the nonlinear equations.

In conclusion we note that the choice of control law and corresponding corrector setting must be made in each particular case in dependence on the properties of the system and the demands on control response.

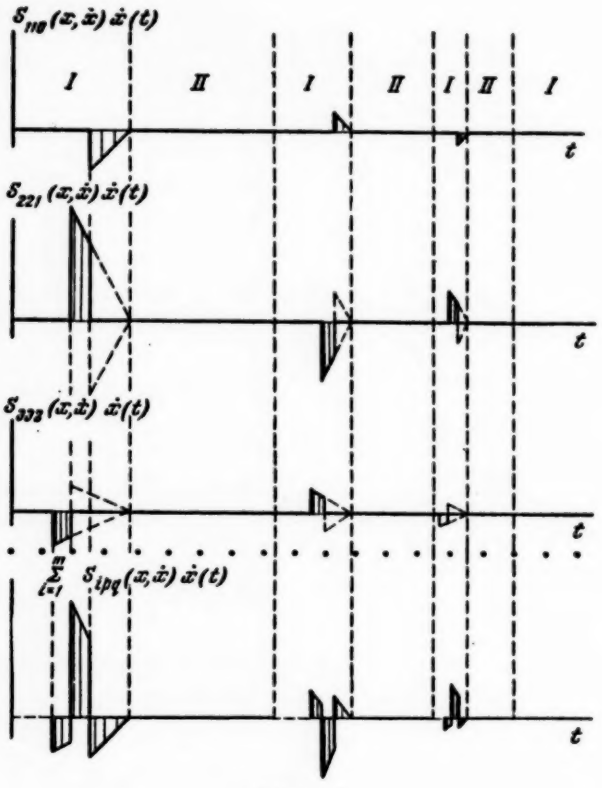

Figure 8

$$S_{110}(x, \dot{x})\dot{x}(t) = \Psi_{11}(x, \dot{x})\dot{x}(t) - \Psi_{10}(x, \dot{x})\dot{x}(t)$$
$$(T = T_1, K = K_1) \quad (T = T_1, K = K_0)$$
$$S_{221}(x, \dot{x})\dot{x}(t) = \Psi_{22}(x, \dot{x})\dot{x}(t) - \Psi_{21}(x, \dot{x})\dot{x}(t) \text{ when } K_1 > K_2$$
$$(T = T_2, K = K_2) \quad (T = T_2, K = K_1)$$
$$S_{332}(x, \dot{x})\dot{x}(t) = \Psi_{33}(x, \dot{x})\dot{x}(t) - \Psi_{32}(x, \dot{x})\dot{x}(t) \text{ when } K_2 > K_3$$
$$(T = T_3, K = K_3) \quad (T = T_3, K = K_2)$$

The development of a method of deriving the required control law is an independent problem and is not considered here.

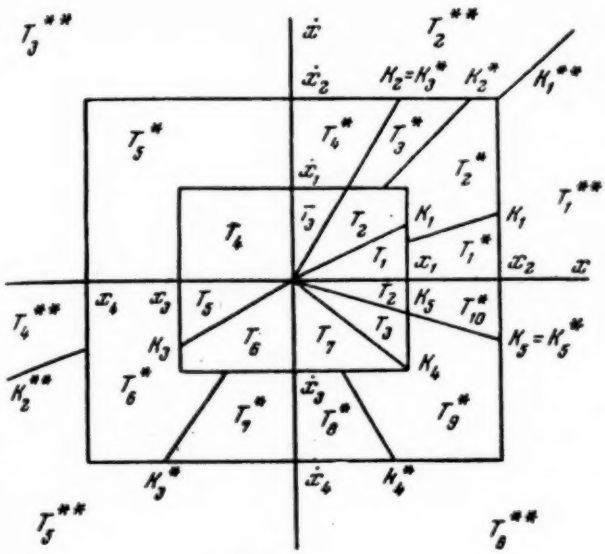

Figure 9

Construction of circuits producing nonlinear functions of two variables, x and $\dot{x}$.

Figure 10 shows one of the possible circuits for a device producing nonlinear functions of the form $\Phi_i(x, \dot{x})\,\dot{x}(t)$, $\Psi_{ij}(x, \dot{x})\,\dot{x}(t)$, $\overline{\Phi}_i(x, \dot{x})\,\dot{x}(t)$ and $\overline{\Psi}_{ij}(x, \dot{x})\,\dot{x}(t)$. It consists of the double-wound relay type RP-4 and two 6Kh-2P diodes.* To produce the nonlinear function $\Phi_i(x, \dot{x})\,\dot{x}(t)$, a voltage proportional to x(t) is applied to one of the relay coils, and a voltage proportional to $\dot{x}(t)$ applied to the changeover contact.

The signal proportional to x(t) closes one of the contacts, thereby directing the signal proportional to $\dot{x}(t)$ via one diode, which latter passes the half-wave of the same sign as x(t) and not the half-wave of opposite sign.

When the sign of x(t) changes the relay directs the $\dot{x}(t)$ signal into the other diode circuit, this second diode doing the same as the first. Hence the nonlinear function $\Phi_i(x, \dot{x})\,\dot{x}(t)$ appears at the output. The nonlinear function $\overline{\Phi}_i(x, \dot{x})\,\dot{x}(t)$ is produced in an analogous fashion, but the diode actions are somewhat different. One is connected so as to pass the half-wave of opposite sign to $\dot{x}(t)$ and not the other half-wave. The nonlinear functions $\Psi_{ij}(x, \dot{x})\,\dot{x}(t)$ and $\overline{\Psi}_{ij}(x, \dot{x})\,\dot{x}(t)$ are derived by feeding in an additional signal, proportional to $-K_j\dot{x}(t)$ to the second coil to give $\Psi_{ij}(x, \dot{x})\,\dot{x}(t)$, or to $+K_j\dot{x}(t)$ to give $\overline{\Psi}_{ij}(x, \dot{x})\,\dot{x}(t)$. By subtracting the signals proportional to $\Psi_{ij}(x, \dot{x})\,\dot{x}(t)$ and $\overline{\Psi}_{ij}(x, \dot{x})\,\dot{x}(t)$ we get $S_i(x, \dot{x})\,\dot{x}(t)$ and $\overline{S}_i(x, \dot{x})\,\dot{x}(t)$; by adding these we get the required nonlinear function w(t).

Thus our nonlinear corrector can be produced by connecting m elementary circuits of the above type in parallel, the output voltages being summed.

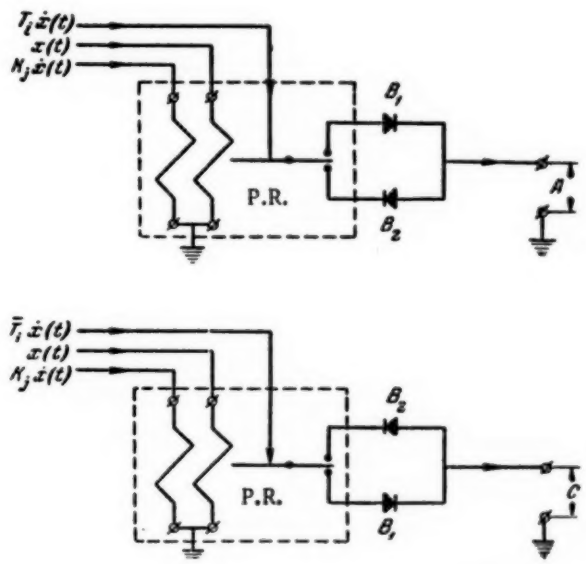

Figure 10. PR) polarized relay type RP-4 or RP-5; B_1, B_2) rectifiers (6Kh-2P diodes); A) nonlinear functions $\Psi_{ij}(x, \dot{x})\,\dot{x}(t)$, $\Phi_i(x, \dot{x})\,\dot{x}(t)$; C) linear functions $\overline{\Psi}_{ij}(x, \dot{x})\,\dot{x}(t)$, $\overline{\Phi}_i(x, \dot{x})\,\dot{x}(t)$.

*[6Kh-2P ≡ diode with E_f = 6.3v, I_f = 0.3 amp, ep_{eff} = 150v, E_{inv} = 450v, I_m = 90ma, I_{dc} = 18 ma, C_{a-k} = 3.8 μμ f—Ed.]

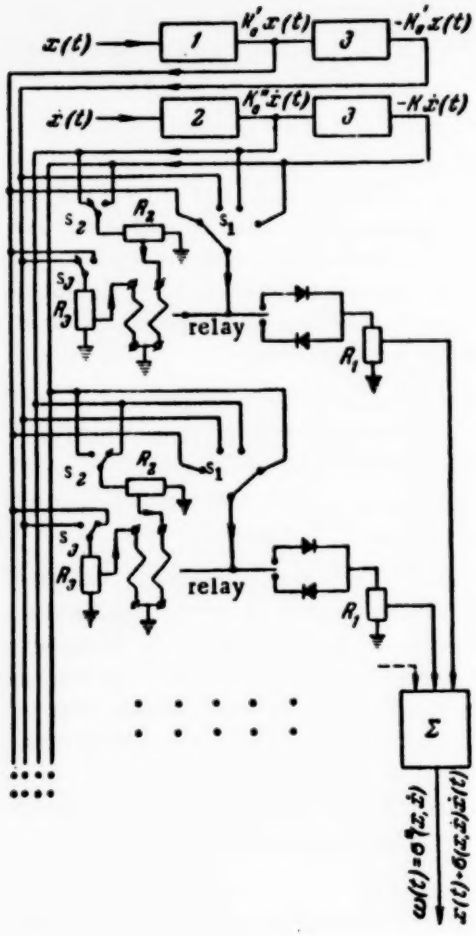

Figure 11. 1) amplifier K_0'. 2) amplifier K_0'', 3) inverters.

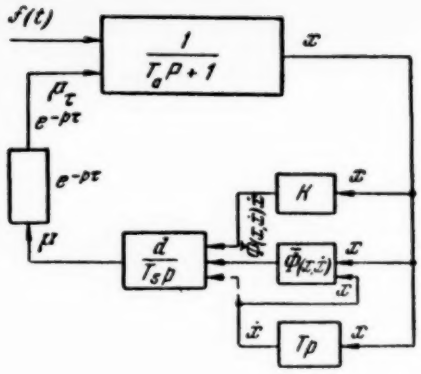

Figure 12.

Figure 11 shows the theoretical circuit of a nonlinear corrector. It consists of two amplifiers with gains of K_0' and K_0'', two inverters to change the signs of $K_0'x(t)$ and $K_0''\dot{x}(t)$, m units of the type mentioned above, in parallel, and a summing unit. The corrector is set up using the switches S_1, S_2, S_3 and the potentiometers R_1, R_2, R_3.

Example. Existing automatic control systems containing delay elements have low critical gains. Attempts to increase the critical gain by introducing derivative feedback from the controlled coordinate do not produce desirable results. We will illustrate the efficacy of our method of correction by an example.

Let us consider a second-order automatic control with a delay (Figure 12):

a) equation for the controlled object:

$$T_a\ddot{x} + \dot{x} = d\mu_\tau + f(t), \qquad \mu_\tau = \mu(t-\tau);$$

b) regulator equation:

$$T_s\dot{\mu} = Kx,$$

where x is the relative pressure change in a pipe at the point where the transducer is inserted, μ is the relative displacement of the controller, T_a, d, T_s, K are constants and τ is the delay time.

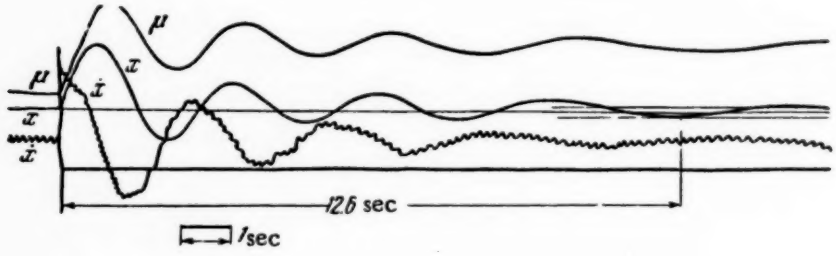

Figure 13.

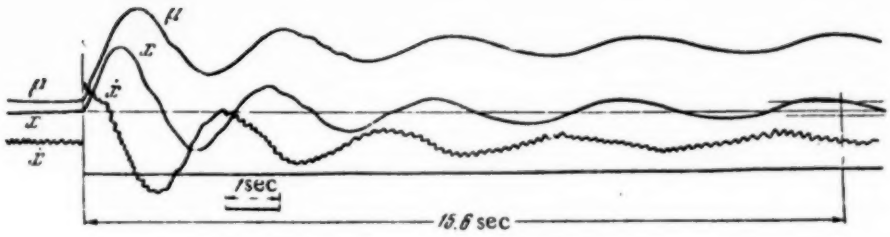

Figure 14.

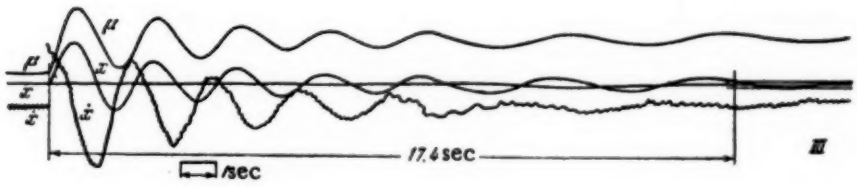

Figure 15.

The numerical values of the system constants are $T_a = 0.9$ sec, $K = 52$, $d = 0.05$, $T_s = 1$ sec, $\tau = 0.5$ sec.

These linearized equations can describe approximately a control system in which the object is a compressor with a long pipeline and the regulator transducer is at a considerable distance from the compressor.

The transient duration will be taken as an index of the efficacy of our correction method. Let us consider the stabilization systems for two types of regulator:

a) in which the control law contains a derivative

$$T_g\dot{\mu} = Kx + T\dot{x},$$

b) in which the control law contains a nonlinear function $\Phi_i(x, \dot{x})\,\dot{x}$

$$T_s\dot{\mu} = Kx + \Phi_i(x, \dot{x})\,\dot{x}.$$

The automatic control svstems were studied on an electrical analog. The coefficient T of the derivative was determined for which the transient duration was minimal. By giving T various values it was found that when T = 38 sec the transient duration was 12 sec (Figure 13). All other values of T gave worse results (Figure 14: T < 38 sec; Figure 15: T > 38 sec).

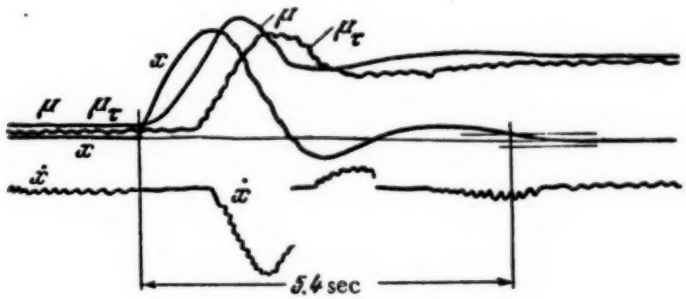

Figure 16.

When the nonlinear function $\Phi_i(x, \dot{x})\,\dot{x}$ was introduced into the control law (Figure 16) the transient duration dropped sharply to 5.4 sec, which demonstrates the efficacy of our method as applied to this system.

The result obtained on the analog was verified by Bashkirov's graphical method.

SUMMARY

A method is presented for producing various control laws by using only the error signal or the output coordinate plus their first derivatives. A method of producing quite complex control laws is demonstrated, which laws can be used in solving stabilization problems and effecting high-grade control. In a linear automatic control system the introduction of a functional transform of the type of (4) into the control law gives identical efficacy with varying scale changes in the perturbation.

It is shown that a functional transform of the type of (4) can be effected by a nonlinear corrector devised from very simple relay circuits.

The author is indebted to B.N. Petrov for considerable assistance in the present work, and thanks A.M. Letov and Ia. Z. Tsypkin for valuable discussion and advice.

APPENDIX

We shall show that in a linear automatic control system with nonlinear correction of the above type the efficacy of the corrector is the same for varying perturbations of the same form which differ only in magnitude (scale factor) when the initial conditions are zero, i.e., when $x_2(t) = Ax_1(t)$ is correct, $x_2(t)$ being a solution to the nonlinear equation of the system when the perturbation $f(t)$ acts, $x_1(t)$ being the same when a perturbation $Af(t)$ acts.

To prove this we must show that, firstly, the above relation is correct in the intervals between the stepwise changes in the coefficients in the equation, and secondly, that these instants of stepwise change (switching), and hence the duration of each interval in which the coefficients are constant, are independent of A. We assume that the control response in the k-th interval between two adjacent steps is described by the following linear differential equation with constant coefficients: $(a_0p^n + a_1p^{n-1} + \ldots + a_n)x(t) = (b_0p^m + b_1p^{m-1} + \ldots + b_m)f(t)$ where $p = d/dt$, a_i and b_j being constants and $f(t)$ the perturbation. The time t is reckoned from the beginning of the interval. We assume that at $t = 0$ the initial conditions have the values $x(0)$, $\dot{x}(0)$ .... $x^{(n-1)}(0)$ and $f(0)\dot{f}(0)$ $f^{(m-1)}(0)$.

The Laplace transform for the controlled quantity, $x(s)$, will be

$$x(s) = \frac{M(s)}{D(s)} f(s) + \frac{M_{init}(s) - M_f(s)}{D(s)},$$

where

$$M(s) = b_0s^m + b_1s^{m-1} + \ldots + b_m, \quad D(s) = a_0s^n + a_1s^{n-1} + \ldots + a_n,$$

$$M_{init}(s) = A_1(s)\,x^{(n-1)}(0) + A_2(s)\,x^{(n-2)}(0) + \ldots + A_n(s)\,x(0),$$

$$M_f(s) = B_1(s)\,f^{(m-1)}(0) + B_2(s)\,f^{(m-2)}(0) + \ldots + B_m(s)\,f(0).$$

Here $A_i(s)$ and $B_j(s)$ are polynomials in s which depend on the coefficients in the equation.

Let us compare the control actions when the perturbations $f_1(t)$ and $f_2(t) = Af_1(t)$ act (A being a constant), assuming for the first case $x(t) = x_1(t)$. For the first interval, the initial conditions being zero, we have $x_2(t) = Ax_1(t)$. The initial conditions for the second interval will be the finite values for $x(t)$ and $f(t)$ at the boundary between the intervals, i.e., at $t = t_1$. The instant of stepping (boundary between the intervals) t_1 will be the same for both processes because the step occurs when one of the following conditions is fulfilled:

$$x\dot{x} = 0 \text{ or } \left|\frac{x}{\dot{x}}\right| = K_j,$$

and the conditions for these to be fulfilled do not depend on A (since $x_2 = Ax_1$ and $\dot{x}_2 = A\dot{x}_1$). Hence the initial conditions for the second interval will in both cases be proportional;

$$x_2(0) = A\,x_1(0),\quad \dot{x}_2(0) = A\dot{x}_1(0), \ldots, x_2^{(n-1)}(0) = Ax_1^{(n-1)}(0) \text{ and}$$

$$f_2(0) = Af_1(0),\quad \dot{f}_2(0) = A\dot{f}_1(0), \ldots, f_2^{(m-1)}(0) = Af_1^{(m-1)}(0) \text{ or}$$

$$M_{init_2}(s) = AM_{init_1}(s) \;\&\; M_{f_2}(s) = AM_{f_1}(s).$$

The transient reponse in the second interval will be defined by

$$x_1(t) = \frac{1}{2\pi j}\int_{\sigma-j\infty}^{\sigma+j\infty} \frac{M_2(s)}{D_2(s)} f_2(s)\, e^{st} ds + \frac{1}{2\pi j}\int_{\sigma-j\infty}^{\sigma+j\infty} \frac{M_{init_2}(s) - M_{f_2}(s)}{D_2(s)}\, e^{st} ds,$$

$$x_2(t) = \frac{A}{2\pi j}\int_{\sigma-j\infty}^{\sigma+j\infty} \frac{M_2(s)}{D_2(s)} f_1(s)\, e^{st} ds + \frac{A}{2\pi j}\int_{\sigma-j\infty}^{\sigma+j\infty} \frac{M_{init_1}(s) - M_{f_1}(s)}{D_2(s)}\, e^{st} ds$$

or $x_2(t) = Ax_1(t)$ in the second interval, and hence $x_2(t_2) = Ax_1(t_2)$. By continuing this argument the above hypothesis is readily confirmed.

LITERATURE CITED

[1] V.V. Solodvnikov, Some methods of correcting the dynamic properties of automatic control systems. Fundamentals of automatic control. Theory (Ed.,V.V. Solodovnikov), [in Russian] (Mashgiz, 1954) Ch. 16.

[2] A. Ia. Lerner, Improvement of the dynamic properties of automatic control systems using nonlinear links. Fundamentals of automatic control. Theory (Ed.,V.V. Solodovnikov), [in Russian] (Mashgiz, 1954) Ch. 31.

[3] A.A. Fel'dbaum, Phase-space synthesis of optimal systems. Automation and Remote Control (USSR), 16, No. 2, (1955).

[4] V.A. Maslennikov, Qualitative control of a neutral object by an astatic regulator. Automation and Remote Control (USSR), 17, No. 2 (1956).*

[5] V.A. Trapeznikov, V.A. Kotel'nikov and A.P. Puchkova, Improvement in ACS** stabilization at restricted servo-drive speeds by using a storage device. Report of the Institute of Automation and Remote Control, Academy of Sciences of the USSR, [in Russian] No. 27,(1956).

[6] S.V. Ol'man, Ia. I. Solov'ev and V.P. Tokarev, Autopilots [in Russian](Oborongiz, 1946).

[7] J.M.L. Janssen and J.C. Vermeulen. Behandlung zweier Regelungsprobleme mit Hysteresis und Reibung nach der Methode der BeschriebungsFunktion, Nichtlineare Regelungsvorgänge (Vorträge). Verlag R. Oldenbourg, München. 1955.

[8] M. Schuler. Einfuhrung in die Theorie der selbsttätigen Regler. Leipzig, 1956.

[9] Ia. Z. Tsypkin, A frequency method of analyzing discontinuous control systems. Automation and Remote Control (USSR), 14, No. 1 (1953).

[10] Ia. Z. Tsypkin, Correction of pulsed systems of adjustment and control. Report of the Institute of Automation and Remote Control, Academy of Sciences of the USSR, [in Russian] No. 29 (1955).

Received January 1, 1957

* See C.B. Translation.

** Automatic Control System.

THE EFFECT OF CERTAIN NONLINEAR CHARACTERISTICS IN THE ELEMENTS OF AN ISODROME REGULATOR ON THE TRANSIENT RESPONSE OF AN AUTOMATIC CONTROL SYSTEM

E. K. Krug and O. M. Minina

(Moscow)

The way range restriction in the regulating unit, and nonlinearities in the regulator components which produce the proportional and integral terms in the control law influence the transient response is demonstrated using as example an automatic control system with a very simple object and an isodrome regulator.

INTRODUCTION

Isodrome regulators are widely used in industry to produce high-grade control; these are comprised of pneumatic, hydraulic or electrical devices. Linear approximation equations are very often used to study automatic control systems (ACS) using isodrome regulators. Isodrome regulators contain elements with nonlinear characteristics, hence the linear approximation is only correct at small perturbations.

Here we consider the effects of certain nonlinear characteristics in the isodrome regulator on the transient response.

Such a regulator (Figure 1) as a rule consists of a comparator unit, integrating and proportional links and an effector mechanism. The comparator determines the deviation y of the controlled quantity x from its set value X:

$$y = k_1 (X - x), \tag{1}$$

where k_1 is the conversion coefficient.

The effector mechanism operates in accordance with the signals from the integrating and proportional units. In an isodrome regulator the relation between y and the control device position μ can be expressed as

$$\mu = k_3 y + k_2 \int y dt + c, \tag{2}$$

where k_2 is the integrating unit coefficient, k_3 the proportional unit coefficient and c a constant determined by the initial conditions. $1/k_2$ is a measure of the time required to eliminate the deviation, being termed the "isodrome time." $1/k_3$ is termed the statism coefficient.

In a real ACS the displacement of the control device (throttle, valve, etc.) is restricted by limiting stops, the limiting values being μ_1 and μ_2. Hence a nonlinear element NE_1 is inserted in the structural scheme of Fig. 1. In the integrating element the relation between y and the output $\eta = k_2 \int y\, dt$ applies to a limited range in y. In an electrical isodrome regulator with an electromechanical integrating element [1] the speed of the motor in the nonintegrating element is constant for $|y| > y_0$, i.e., no matter what y is the integral increases at a constant rate, so $\eta = \pm k_2 y_0 t$ when $|y| > y_0$. The nonlinear element NE_2 is inserted in Fig. 1 to allow for this nonlinear relation in the integrator.

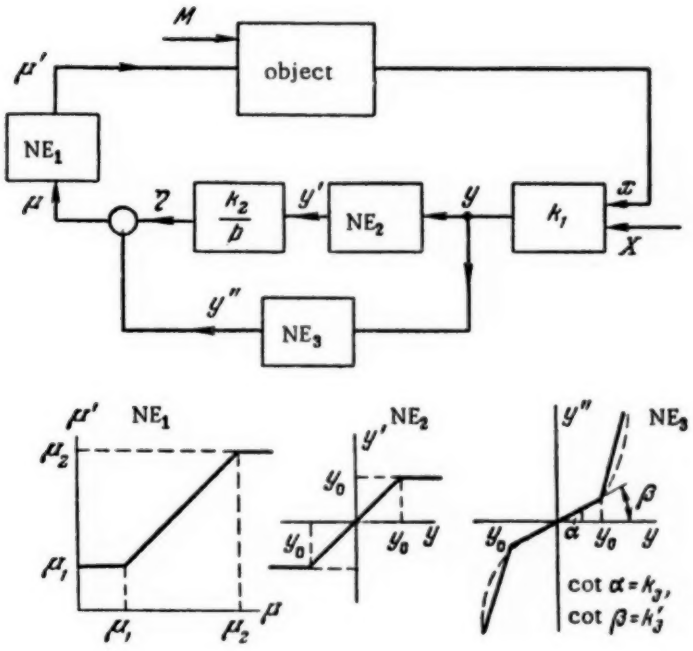

Fig. 1. Structural system of an ACS and characteristics of its components.

It will be shown later that the nonlinear converter element NE_3 has to be introduced to improve the transient response. The way to select the characteristics for this converter will be demonstrated in Section 2.

An isodrome regulator can therefore be described by the following system of equations:

$$y = k_1(X - x), \quad y' = \Phi_1(y), \quad y'' = \Phi_2(y),$$
$$\mu' = \Phi_3(\mu), \quad z = \frac{k_2}{p}y', \quad \mu = \eta + y'', \tag{3}$$

where y', y", η, and μ' are coordinates of the system and Φ_1, Φ_2, Φ_3 are single valued nonlinear functions (Fig. 1).

The transients in an ACS are here studied for two types of perturbations (stepwise at the comparator input and stepwise at the load) assuming the system to be in a steady state prior to the perturbation; $y_{ss} = 0$, $(dy/dt)_{ss} = 0$. Since we do not here consider improving the transient responses of linear systems the choice of design parameters, i.e., the numerical values of k_1, k_2, k_3, is made in accordance with the transient response of the object and with certain recommendations [2-5]. Here we deal with systems having objects described by first- and third-order differential equations Sections 1 and 3) and those having objects described by first-order differential equations plus a delay (Sections 2 and 3).

1. Phase-plane Study of a System with a Controlled Object Described by a First-Order Differential Equation

In the region $|y| < y_0$, (1)—(3), neglecting the restriction on the control device position, pass over to the following linear approximation equations for an ACS with a first-order object:

$$T\frac{dx}{dt} + x = k_0(M - \mu),$$
$$\mu = k_3 y + k_2 \int y\,dt + \mu_{ss} \qquad (4)$$
$$y = k_1(x - X),$$

where T is the time-constant of the object, k_0 the amplification of the object, μ_{ss} the position of the control device at equilibrium and M the perturbation to the load.

The coordinate y is found from

$$T\frac{dy}{dt} + (1 + k_0k_1k_3)\,y + k_0k_1k_2\int y\,dt = \qquad (5a)$$
$$= k_0k_1M - k_0k_1\mu_{ss} - k_1X - Tk_1\frac{dX}{dt}.$$

In the region $|y| > y_0$ the equation of motion will be as follows when the restriction on the isodrome element alone is allowed for;

$$T\frac{dy}{dt} + (1 + k_0k_1k_3)\,y + k_0k_1k_2y_0t = \qquad (5b)$$
$$= k_0k_1\,M - k_0k_1\mu_{ss} - k_1X - Tk_1\frac{dX}{dt}.$$

Let us study the properties of the system in the phase plane y, dy/dt = z. The differential equations for the phase trajectories and their solutions are given in Table 1.

TABLE 1

Case	Differential equations for the phase trajectories	Equations for the phase trajectories
$\|y\| < y_0$	$z\frac{dz}{dy} + 2hz + \omega_0^2 y = 0$	$(z+hy)^2 + (\omega_1 y)^2 = c_1 e^{-2\frac{h}{\omega_1}\tan^{-1}\frac{z+hy}{\omega_1 y}}$ when $h^2 < \omega_0^2$
$\|y\| > y_0$	$z\frac{dz}{dy} + 2hz = -\omega_0^2 y_0$	$(z+q_1y)^{q_1} = c_2(z+q_2y)^{q_2}$ when $h^2 > \omega_0^2$
		$y = -\frac{z}{2h} + \frac{\omega_0^2}{4h^2}\ln\left(-z - \frac{\omega_0^2}{2h}y_0\right) + c_3$ when $z < -\frac{\omega_0^2}{2h}y_0$
		$y = -\frac{z}{2h} + \frac{\omega_0^2}{4h^2}\ln\left(z + \frac{\omega_0^2}{2h}y_0\right) + c_3$ when $\infty > z > -\frac{\omega_0^2}{2h}y_0$
		$y = -\frac{z}{2h} - \frac{\omega_0^2}{4h^2}\ln\left(-z + \frac{\omega_0^2}{2h}y_0\right) + c_4$ when $-\infty > z > \frac{\omega_0^2}{2h}y_0$
		$y = -\frac{z}{2h} - \frac{\omega_0^2}{4h^2}\ln\left(z - \frac{\omega_0^2}{2h}y_0\right) + c_4$ when $z > \frac{\omega_0^2}{2h}y_0$

In Table 1

$$2h = \frac{1 + k_0 k_1 k_3}{T}, \quad \omega_0^2 = \frac{k_0 k_1 k_2}{T},$$

$$\omega_1^2 = \omega_0^2 - h^2, \quad q_{1,2} = -h \pm \sqrt{h^2 - \omega_0^2},$$

c_1, c_2, c_3, and c_4 being constants determined by the initial conditions.

Let us choose the initial values of certain coordinates (y_i, z_i, μ_i). If the load changes stepwise $M = M_0 + M_1$, $X = X_0$, where M_1 is the load change, M_0 and X_0 being the load and set coordinate prior to the perturbation,

$$y_i = 0, \; z_i = \frac{k_0 k_1 M_1}{T}, \; \mu_i = M_0 - \frac{X_0}{k_0}.$$

When the set position changes stepwise,

$$X = X_0 + X_1, \quad dX_1/dt = 0 \text{ when } t > 0, \; M = M_0,$$

where X_1 is the change in the controlled quantity,

$$y_i = -k_1 X_1, \; z_i = \frac{k_0 k_1 k_3}{T} k_1 X_1, \; \mu_i = M_0 - \frac{X_0}{k_0} - k_1 k_3 X_1.$$

We will thus assume that the locus of the initial coordinate values in the y,z plane when the load changes stepwise is the ordinate axis, and when the set position changes stepwise it is the straight line

$$z_i = -\frac{k_0 k_1 k_3}{T} y_i$$

The design parameters for a second-order linear system are best selected from the condition of least mean square error $4h^2 = \omega_0^2$ [5]. Figures 2 and 3 show the phase diagrams for this case and Table 2 gives the transient duration* t_p for various perturbations.

TABLE 2

Parameter	For the ACS of Fig. 2					For the ACS of Fig. 3			
Perturbation in the load									
$k_0 k_1 M$	±6.25	±12.5	±18.75	±25	±37.5	±6.25	±12.5	±18.75	±25
t_p/T	0.61	1.2	1.83	2.4	3.55	0.6	1.13	1.22	1.34
Perturbation in the set position									
$k_1 X$	±5	±6	±8	±10	±12	±4.25	±8.5	±12.75	
t_p/T	1.48	1.55	1.67	1.83	2	1.1	1.57	1.61	

* t_p is the time from the moment the perturbation is applied to that when y = 0.2 .

Let us compare the transient responses of the ACS allowing for the bounded isodrome element (Figure 2) and in the linear approximation (Figure 3). When the load changes stepwise the bounded speed of the isodrome element causes the overshoot to increase and reduce the subsequent oscillations considerably, and also increases the transient duration. When the set position changes stepwise the limiting in the isodrome unit causes the overshoot to be lower while the transient duration is nearly unchanged.

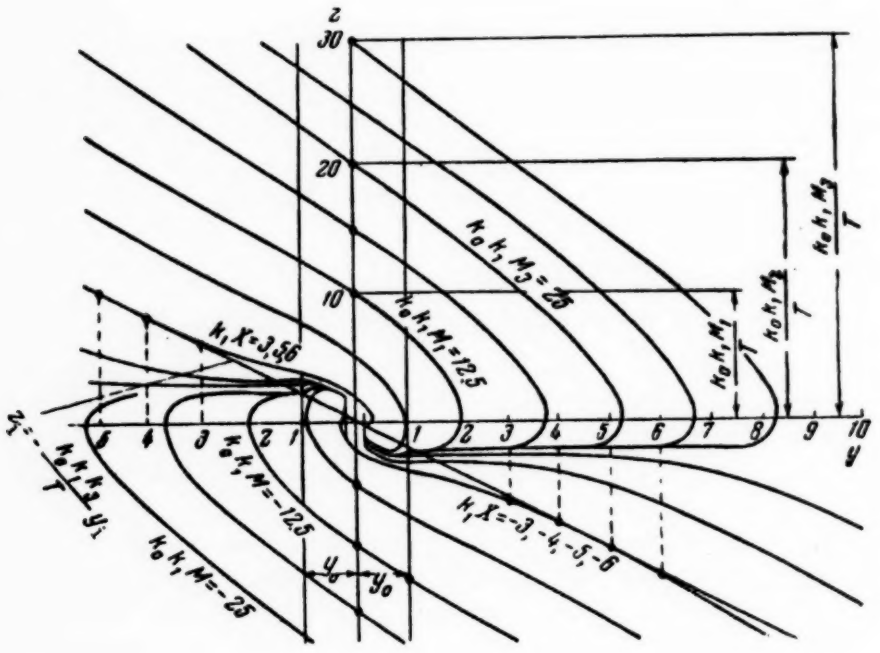

Fig. 2. Phase diagram for the system, allowing for NE_2. Parameters $k_0k_1k_3 = 2.5$, $k_0k_1k_2 = 10$, $T = 1.25$, $y_0 = 1$.

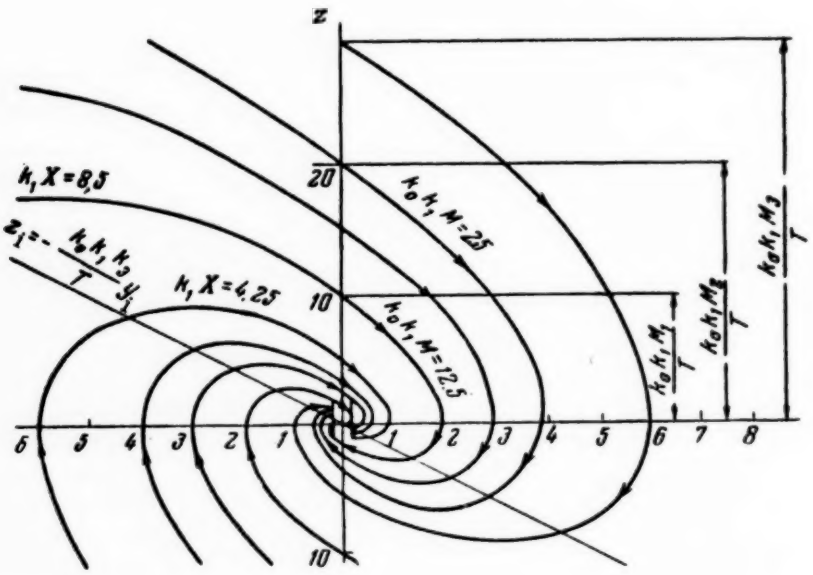

Fig. 3. Phase diagram for the system in the linear approximation. Parameters $k_0k_1k_3 = 2.5$, $k_0k_1k_2 = 10$, $T = 1.25$.

Let us see how the motion of the system is affected by allowing for the limited range of displacement in the control device (from μ_1 to μ_2). In such a system the permissible perturbations to the load M_{per} and to the set position X_{per} will depend on the possible control device positions, i.e.,

$$\mu_2 - M_0 + \frac{X_0}{k_0} > M_{per} - \frac{X_{per}}{k_0} > \mu_1 - M_0 + \frac{X_0}{k_0}.$$

While the controlled quantity is taking up its new value, or while the ACS is dealing with any other perturbation when the control device is in one of its extreme positions, the equation of motion for the ACS is

$$T\frac{dx}{dt} + x = k_0(M - \mu_2) \text{ when } \mu > \mu_2 \tag{6a}$$

or

$$T\frac{dx}{dt} + x = k_0(M - \mu_1) \text{ when } \mu < \mu_1, \tag{6b}$$

while the phase trajectory equation in the y,z plane will be of the form

$$z = c_5 - \frac{y}{T}, \tag{7}$$

where c_5 is a constant determined by the initial conditions.

In such a system z_i (initial rate of change of the controlled quantity) will be bounded, so the locus of the initial coordinate values on a stepwise perturbation to the set position in the y,z plane will lie on a kinked line having three sections:

$$\begin{aligned}
z_i &= -\frac{k_0 k_1 k_3}{T} y_i && \text{when } \mu_1 - M_0 + \frac{X_0}{k_0} < k_3 y_i < \mu_2 - M_0 + \frac{X_0}{k_0}, \\
z_i &= \frac{k_0 k_1}{T}\left(M_0 - \frac{X_0}{k_0} - \mu_1\right) && \text{when } k_3 y_i < \mu_1 - M_0 + \frac{X_0}{k_0}, \\
z_i &= \frac{k_0 k_1}{T}\left(M_0 - \frac{X_0}{k_0} - \mu_2\right) && \text{when } k_3 y_i > \mu_2 - M_0 + \frac{X_0}{k_0}.
\end{aligned} \tag{8}$$

After the perturbation has been applied to the set position ($M = M_0$, $X = X_0 + X_1$, $dx/dt = 0$ at $t > 0$), if X_1 is chosen such that μ takes the initial values*

$$\mu_i = M_0 - \frac{X_0}{k_0} - k_1 k_3 X_1 > \mu_2$$

or

$$\mu_i = M_0 - \frac{X_0}{k_0} - k_1 k_3 X_1 < \mu_1,$$

then $\underline{z}$ changes according to (7) while the conditions

$$k_2 \int y\,dt + k_3 y > \mu_2 \text{ when } k_2 \int y\,dt + k_3 y < \mu_1,$$

are fufilled.

Further, when $k_2 \int y\,dt + k_3 y < \mu_2$ or $k_2 \int y\,dt + k_3 y > \mu_1$, the linear approximation phase trajectories (Table 1 with $|y| < y_0$, Figure 4) will be correct for systems in which the isodrome element is not bounded.

* In other cases of setpwise change in set position or load the motion of the system will not depend on the restrictions on the control device position.

The points where the linear approximation straight-line trajectories cut the other trajectories at varying X_1 can be found from the following transcendental equations:

$$\ln \frac{k_0k_1\left(\mu_2 - M_0 + \frac{X_0}{k_0}\right) + k_1X_1 + y^*}{k_0k_1\left(\mu_2 - M_0 + \frac{X_0}{k_0}\right)} = \frac{\left(\mu_2 - M_0 + \frac{X_0}{k_0}\right) + k_1k_2TX_1 - y^*(k_3 - k_2T)}{k_2T\left[k_0k_1\left(\mu_2 - M_0 + \frac{X_0}{k_0}\right) + k_{11}X\right]}. \tag{9}$$

Here y^* is the value of y at the intersection point.

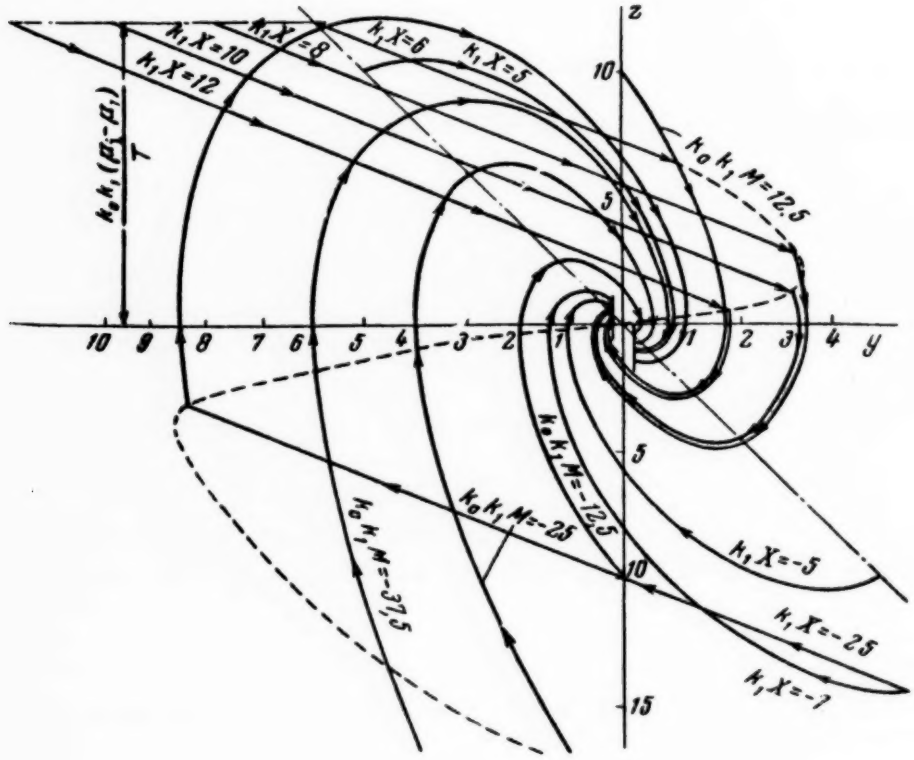

Fig. 4. Family of phase trajectories in which NE_1 is allowed for when stepwise perturbations are applied to set position and load. Parameters: $k_0k_1k_3 = 2.5$, $k_0k_1k_2 = 10$, $T = 1.25$, $k_0k_1(\mu_1 - \mu_1) = 15$, $k_0k_1(\mu_1 - \mu_2) = 37.5$.

If the isodrome element is bounded, the intersections with the rectilinear trajectories can occur on the linear approximation trajectories, if $|y^*| < y_0$, and on trajectories of logarithmic type (Table 1 with $|y| > y_0$, Figure 5), if $|y^*| > y_0$. In the first case the switch-over lines are defined by the transcendental equation

$$\ln \frac{k_0k_1\left(\mu_2 - M_0 + \frac{X_0}{k_0}\right) + k_1X_1 + y^*}{k_0k_1\left(\mu_2 - M_0 + \frac{X_0}{k_0}\right)} =$$

$$= \frac{\left(\mu_2 - M_0 + \frac{X_0}{k_0}\right) + k_2Ty_0 + k_2T\left[k_0k_1\left(\mu_2 - M_0 + \frac{X_0}{k_0}\right) + k_1X_1 + y_0\right]}{k_2T\left[k_0k_1\left(\mu_2 - M_0 + \frac{X_0}{k_0}\right) + k_1X_1\right]} \times \tag{10}$$

$$\times \ln \frac{k_0k_1\mu_2 + k_1X_1 + y_0}{k_0k_1\left(\mu_2 - M_0 + \frac{X_0}{k}\right)} - y^*(k_3 - k_2T),$$

and in the second by

$$\ln \frac{k_0 k_1 \left(\mu_2 - M_0 + \frac{X_0}{k_0}\right) + k_1 X_1 + y^*}{k_0 k_1 \left(\mu_2 - M_0 + \frac{X_0}{k_0}\right)} = \frac{k_3 y^* - \left(\mu_2 - M_0 + \frac{X_0}{k_0}\right)}{k_2 T y_0} . \qquad (11)$$

Figures 2-5 and Tables 2-3 show that the overshoot and transient duration are increased by the restrictions on the control device position when a fresh set position is being taken up.

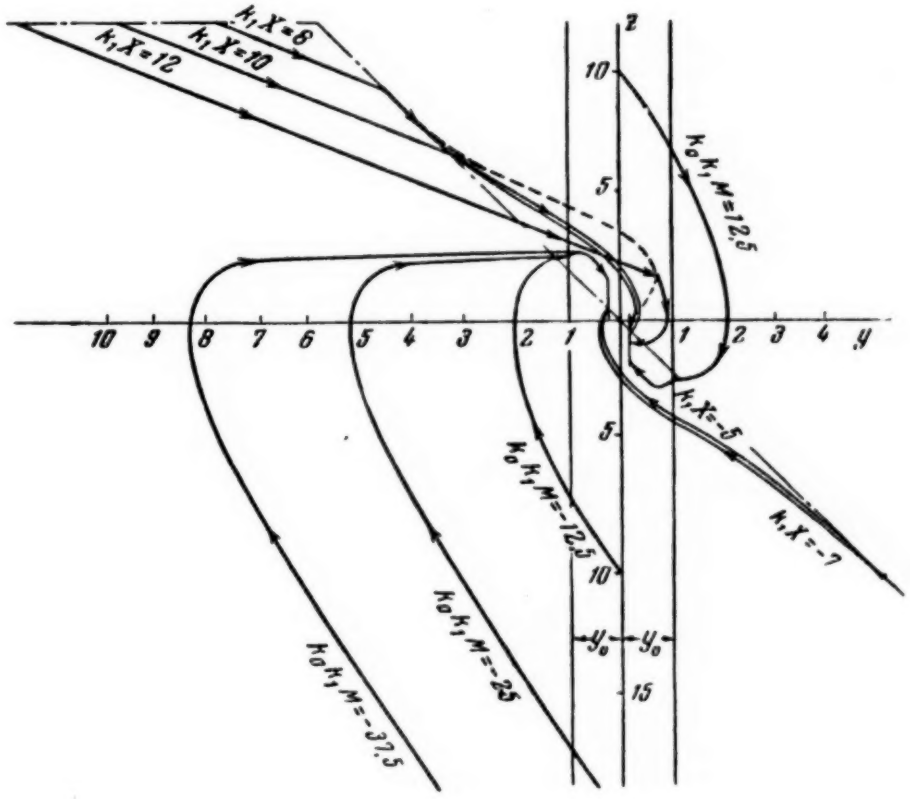

Fig. 5. Family of phase trajectories in which NE_1 and NE_2 are allowed for when stepwise perturbations are applied to set position and load. Parameters: $k_0k_1k_3 = 2.5$, $k_0k_1k_2 = 10$, $T = 1.25$, $k_0k_1(\mu_1 - \mu_1) = 15$, $k_0k_1(\mu_1 - \mu_2) = 37.5$, $y_0 = 1$.

If the control device has a restricted range of positions and the isodrome unit speed is also restricted (Fig. 5) the controlled quantity takes up its new value more rapidly and with less overshoot; and when the perturbation is to the load, outage of the control device is less probable than in a system (Fig. 4) in which only the control device position is restricted.

TABLE 3

Parameter			For the ACS of Fig. 4		For the ACS of Fig. 5			
$k_1 X$	6	8	10	12	6	8	10	12
t_p/T	1.9	2.5	3.56	3.93	1.55	1.73	2.2	3

Thus speed limitation in the isodrome unit here reduces the transient duration when new set positions are being taken up, but when the perturbation is to the load the transient duration is increased even if the control device is not required to open fully.

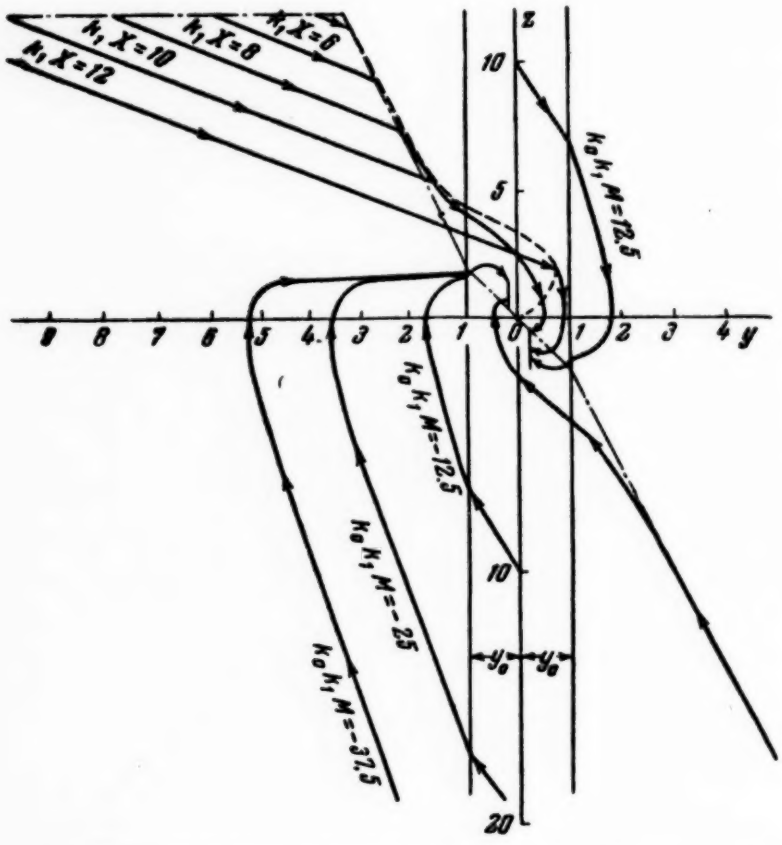

Fig. 6. Family of phase trajectories in which NE_1, NE_2 and NE_3 are allowed for when stepwise perturbations are applied to set position and load. Parameters: $k_0k_1k_3 = 2.5$, $k_0k_1k_3' = 5$, $k_0k_1k_2 = 10$, $T = 1.25$, $k_0k_1(\mu_1-\mu_1) = 15$, $k_0k_1(\mu_1-\mu_2) = 37.5$, $y_0 = 1$.

To improve the transient response of the ACS to load changes a nonlinear converter was introduced into the proportional unit in the regulator. A piecewise straight curve (Fig. 1) was selected for the nonlinear converter characteristic. When $|y| \le y_0$ the statism coefficient remains as before ($1/k_3$), being chosen from the least-square error criterion. Studies show that the statism coefficient must be reduced when $|y| > y_0$.* To simplify the calculations for $|y| > y_0$ the coefficient was changed stepwise instead of smoothly.

In complete analogy to the above a system subject to two forms of limiting (in isodrome element speed and control device position) was studied with a nonlinear converter inserted in the isodrome element.

Figures 6 and 7 show families of phase trajectories for various perturbations to set position and load, subject to the condition that the system was at balance prior to the perturbation; Table 4 gives the t_p values.

The nonlinear converter at the proportional unit input causes the fluctuations in the controlled quantity to be lower when the load changes, and the transient duration to be shorter if k_3' is chosen appropriately. The fluctuations will be smaller the larger k_3'. When the system is taking up a new set position the nonlinear converter affects the transient response very slightly (duration somewhat reduced – see Tables 3 and 4).

* Nonlinear converters are easily introduced into electrical regulators.

TABLE 4

Parameter	For the ACS of Fig. 6			For the ACS of Fig. 7		
Perturbation to load						
k_0k_1M	+12,5	−25	−37.5	+12.5	−25	−37.5
t_p/T	1.08	1.69	2.48	1.07	2.2	3.26
Perturbation to set position						
k_1X	6	8	10	12	6	8	10	12
t_p/T	1.55	1.73	2.2	3	1.28	1.56	1.85	2.6

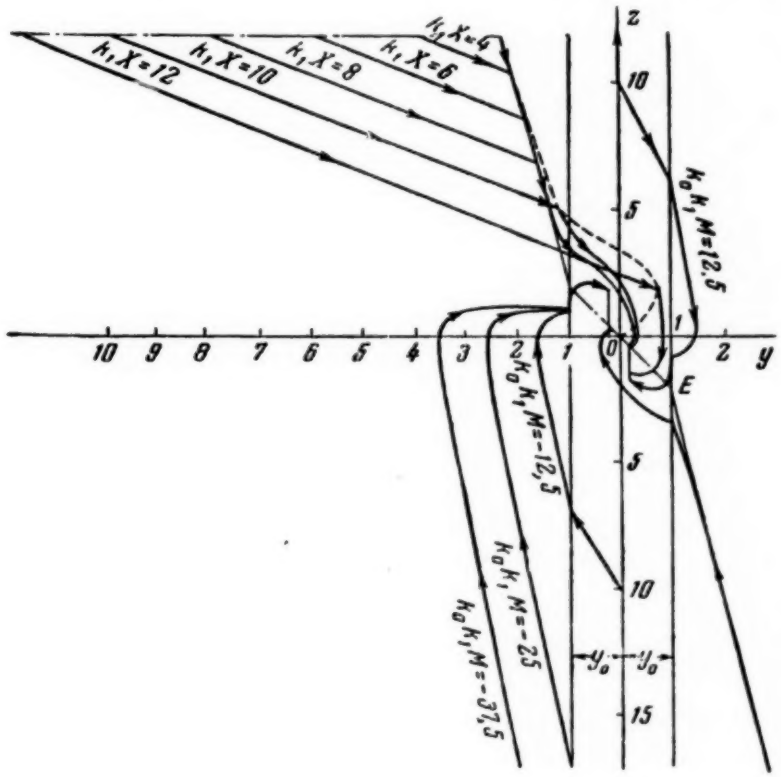

Fig. 7. Family of phase trajectories for the system, allowing for NE_1, NE_2 and NE_3, with stepwise perturbations to set position and load. Parameters: $k_0k_1k_3 = 2.5$, $k_0k_1k_3' = 10$, $k_0k_1k_2 = 10$, $T = 1.25$, $k_0k_1(\mu_1-\mu_1) = 15$, $k_0k_1(\mu_1-\mu_2) = 37.5$, $y_0 = 1$.

2. ACS Stability when the Nonlinear Characteristics of the Elements are Allowed for

The effects of the nonlinear characteristics of the elements on the stability can be visualized by constructing the stability boundary for the linear system in the plane of parameters which describe the nonlinear elements, and by considering the harmonic coefficients of these elements in this plane.

Let us consider the stability boundary for a system consisting of a first-order controlled object with a delay and an isodrome regulator. The equations of motion will take the form:

for a nonself-balancing object

$$\frac{dx}{dt} = \frac{k_0}{T}\mu(t-\tau) - \frac{k_0}{T}M(t-\tau), \mu = k_3y + k_2\int y\,dt + \mu_{ss}, y = k_1(X-x); \qquad (12a)$$

for a self-balancing object

$$T\frac{dx}{dt} + x = k_0\mu(t-\tau) - k_0M(t-\tau), \mu = k_3y + k_2\int y\,dt + \mu_{ss}, y = k_1(X-x). \qquad (12b)$$

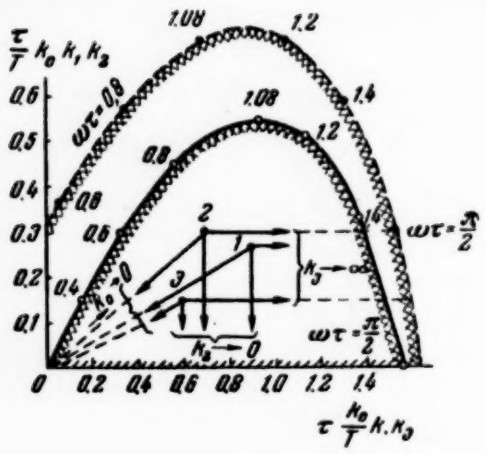

Fig. 8. Stability boundary curves in the parameter plane for an isodrome regulator. The full curve is for a nonself-balancing object, the dashed one for a self-balancing object when $\mu/T = 0.2$.

The characteristic equation of the system can be determined from (12a) and (12b) and the stability boundary equation. The expression for the stability boundary is conveniently put in the form:

for a nonself-balancing object

$$\frac{k_0}{T}\tau^2 k_1 k_2 = (\omega\tau)^2 \cos\omega\tau,$$
$$\frac{k_0}{T}\tau k_1 k_3 = \omega\tau \sin\omega\tau; \qquad (13a)$$

for a self-balancing object

$$\frac{k_0}{T}\tau^2 k_1 k_2 = (\omega\tau)^2 \cos\omega\tau + \frac{\tau}{T}\sin\omega\tau,$$
$$\frac{k_0}{T}\tau k_1 k_3 = \omega\tau \sin\omega\tau - \frac{\tau}{T}\cos\omega\tau. \qquad (13b)$$

Figure 8 shows the stability boundary curves in dimensionless coordinates proportional to the regular design parameters.

As we have already noted, the use of these coordinates enables us to establish the effects of the nonlinear elements on the stability characteristics and to find the relative disposition of the stability boundaries and points on the plane corresponding to values of the regulator parameters recommended by various workers. In Fig. 8 point 1 corresponds to Ziegler and Nichols recommendations [3], and 2 and 3 to those of Chien et al., [4], 2 defining a response with 20% overshoot and 3 an aperiodic response.

In this system the nonlinear relationships are of a single type (bounding or saturation). The harmonic coefficients for such elements can be represented as a reduction in their gains as compared with the values selected on considering the system as linear.

Let the design parameters be chosen and the system coefficients correspond to points 1, 2 or 3. Then, as Fig. 8 shows, limiting in the integrating element speed-reduction in k_2 brings these points close to the abscissa. When $k_2 = 0$ the system shows a static error, but no hunting occurs. A bounded motion in the control device – reduction in k_0 – brings points 1, 2 and 3 near the origin and no traversal of the stability boundary occurs. Hence limiting in the control device and the integrating unit do not cause hunting in objects with positive self-balancing or without it.

The introduction of the nonlinear converter into the proportional term of the control law will be considered as a change (increase) in k_3. Figure 8 shows that increase in k_3 relative to the values selected from the recommendations [3, 4] (points 1, 2 or 3) can cause instability. To ensure stability we must then make the nonlinear converter coefficient lie within preset or calculated limits.

The above studies only enable one to evaluate the effects of each nonlinear element on the stability separately in an approximate fashion.

3. Examples of Transients in High-Order Automatic Control Systems when Nonlinear Relationships are Present in the Regulator

As controlled objects we consider those in which the dynamic properties are characterized by equations for several first-order links joined in series or by equations of first-order plus delays. Various relationships between the parameters (k_0, τ, T_1, T_2,...) were used. k_2 and k_3 were selected in accordance with the recommendations of [3]. The transient responses were found by graphical construction [6] and by using analogs [7] in which the controlled object and isodrome regulator plus their nonlinearities were reproduced. The stepwise perturbations were applied to the load and to the set position.

Differential equations and parameters of the systems	Transient responses to stepwise perturbations	
	in the set position	to the load
$T\frac{dx}{dt}+x=k_0\mu(t-\tau)-k_0M(t-\tau),\ \mu=k_3y+k_2\int ydt+\mu_{ss}$ $y=k_1(X-x);$ $\tau=0{,}2;\ T=1.25;\ k_0k_1=1;\ k_2=10;\ k_3=5;\ y_0=1;\ k_3'=9$	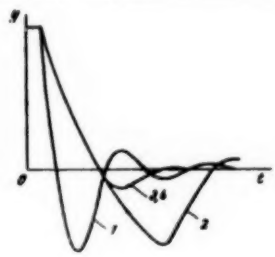	
$T_1T_2T_3\frac{d^3x}{dt^3}+(T_1T_2+T_2T_3+T_1T_3)\frac{d^2x}{dt^2}+(T_1+T_2+T_3)\frac{dx}{dt}+x-k_0(\mu-M),$ $\mu=k_3y+k_2\int ydt+\mu_{ss}\quad y=k_1(X-x);$ $T_1=0.1;\ T_2=0.25;\ T_3=0.25;\ k_0k_1=1;\ k_2=20;\ k_3=5;\ y_0=1;\ k_3'=9$	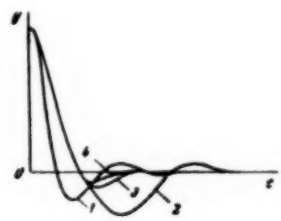	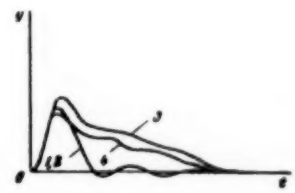
$\frac{dx}{dt}=\frac{k_0}{T}y(t-\tau)-\frac{k_0}{T}M(t-\tau),$ $\mu=k_3y+k_2\int ydt+\mu_{ss}\quad y=k_1(X-x);$ $\tau=0{,}2;\ \frac{k_0k_1}{T}=1;\ k_2=10;\ k_3=5;\ y_0=1;\ k_3'=9$	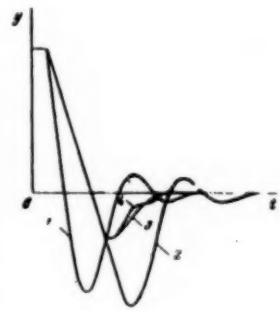	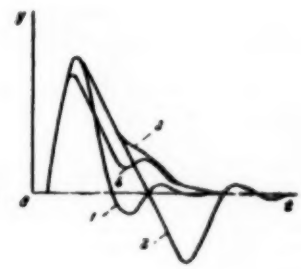

Fig. 9. Transient responses to setpwise perturbations in the set position and in the load. 1) linear system, 2) system with a bounded control device motion (NE_1), 3) system with a bounded control device motion and bounded isodrome element (NE_1, NE_2), 4) system with nonlinear relationships in accordance with the structural scheme of Fig. 1 (NE_1, NE_2, NE_3).

NE_3 (Fig. 1) was introduced into the proportional element and increased the efficacy of the proportional term in the control law by about a factor of two.

In all cases the nonlinear isodrome characteristic altered the transient response shape in a quite definite manner. Figure 9 shows several examples of transients which illustrate these effects.

The numerous examples we considered and an analysis of the results lead us to the following conclusions.

1. An ACS with an isodrome regulator having a bounded range in the control device has worse transients in response to both load and set position perturbations (see Curves 1 and 2 in Fig. 9 and Figs. 3 and 4).

2. Speed limitation in the isodrome element (when the load is perturbed) reduces the transient duration relative to that in the system in the linear approximation (see Curves 1 and 3 in Fig. 9 and Figs. 2 and 3).

3. Speed limitation in the isodrome element (when the set position is perturbed) makes the transient response worse in systems with bounded control device range in those described by linear equations (see Curves 1, 2 and 3 in Fig. 9 and Figs. 2, 3, 4 and 5).

In an ACS where set position changes are frequent the nonlinear converter should therefore be associated with the integrating element NE_2.

4. The use of the nonlinear converter with the proportional element NE_3 improves the transient response to load perturbations in an ACS in which the control device range and isodrome element speed are bounded (see Curves 3 and 4 in Fig. 9 and Figs. 5 and 6). When selecting a nonlinear converter the stabilities of high-order systems and those with delays must be checked.

LITERATURE CITED

[1] S. N. Diligenskii, E. K. Krug, O. M. Minina and D. E. Polonnikov, Electronic devices for checking and controlling in combined automation of production processes. Report of the Institute of Automation and Remote Control, Academy of Sciences of the USSR [in Russian] No. 51, (1955).

[2] V. F. Kaganov, Design of automatic regulators. Collection "Technique of automation control of production processes," [in Russian] (Mashgiz, 1951).

[3] J. G. Ziegler and N. B. Nichols, Optimum settings for automatic controller. Trans. ASME, vol. 64, (1942).

[4] K. L. Chien, J. A. Hrones and J. B. Reswick, On the automatic control of generalized passive systems. Trans. ASME, vol. 74, (1952).

[5] C. von Kessler, Über die Vorausberechnung optimal abgestimmter Regelkreise. Regelungstechnik, Heft. 2, 1955.

[6] D. A. Bashkirov, A graphical method of deriving processes in automatic control systems, [in Russian] (Izd. LKVVIA, 1952).

[7] V. V. Gurov, Ia. B. Kogan, A. D. Talantsev and V. A. Trapeznikov, The new analog equipment at the Institute of Automation and Remote Control, Academy of Sciences of the USSR. Automation and Remote Control (USSR) 17, No. 1 (1956).*

Received March 25, 1957

*See C.B. Translation.

SINGLE-INPUT NONLINEAR CONVERTERS

L. V. Medvedev, A. A. Fel'dbaum and L. N. Fitsner

(Moscow)

Ways of designing single-input nonlinear converters are considered.

Circuits developed for the main types of nonlinear converter are presented: the types being diode, diode-triode, combined and balancing. Their uses are indicated.

1. The Main Types of Single-Input Nonlinear Converter

Units to perform nonlinear conversions are required in nonlinear analogs, differential equation integrators and other computing devices. A single-input nonlinear converter has to effect the relationships

$$y = f(x), \tag{1}$$

where x is the input and y the output, f being, in general, a nonlinear function. Such converters are denoted by NP-1. In electronic computers x and y are usually voltages.

A universal-type nonlinear converter must have set up within it various single-valued continuous functions f(x) belonging to some fairly broad class. In specialized NP-1 units one definite functional relationship is set up (e.g., a backlash characteristic, an insensitive zone, etc.), and only the parameters in the relationship can be adjusted, without the form being alterable. Universal NP-1 devices are considered below.

The solution used in developing a universal NP-1 is largely determined by the way in which f(x) is set up. Various methods are possible, the following four being the main ones.

1) Analytic, as a power or trigonometric series, or as a function in exponents, Legendre polynomial, etc.

2) As a template or curve traced on paper or film, as a tape-recording, etc.

3) The value of the function is given at a series of values of x; the converter must then be capable of interpolating to find y at other points.

4) A differential equation for f(x) is supplied which is integrated by an auxiliary integrator, or else a time-function f(t) is supplied and converted to f(x).

In the first method the number of series terms must not be large; otherwise the computer becomes complicated. But if only few terms are used the class of functions that can be adequately approximated becomes narrow. The series method is frequently inconvenient because the desired relationship is supplied as a curve or table. Additonal calculations, sometimes very complex ones, are then required.

The second method is very convenient; but a fresh template is required for f(x) if any changes or corrections are made, and this makes the device more complicated to use. In this type of NP-1 the error is usually greater or the design of the moving parts more complex.

In the third method the function is supplied in punch-card form (or on perforated tape).

When the values at the points x_i (i = 1,2,...,n) are set by means of dials on the instrument, one function can rapidly and simply be replaced by another, no calculations being needed. But if the x_i are excessively numerous the circuit becomes complicated. If the function can be represented sufficiently accurately by fairly few x_i (10-40) the third method is most convenient.

The number of points to be supplied is related to the method of approximation. Linear approximation is most frequently used. There are also methods of effecting square-law approximation between adjacent points [1]. The number of points required can then be reduced, but the circuit is more complicated, and the method has so far not become common.

A consideration of the various ways of producing a NP-1 using various ways of supplying the function shows that the best way to combine the requirements of accuracy, simplicity of design, flexibility and general utility is to use the third method [2]. Here we give some ways of using the third method, and results from apparatus development.

2. Diode Nonlinear Converter Circuits

The first known nonlinear universal diode converter circuit was developed by Kogan (ENIN*). In this circuit the set function was approximated by straight lines. But it was not commonly used, and had some disadvantages. A separate supply was required for each converter of this type. It was not possible to produce several functions of a single variable.

Figure 1 shows a diode nonlinear converter circuit which is free from the above mentioned faults [2, 3]. The circuit contains subcircuits of identical design, denoted by A_i and B_i (i = 1,2...,n). The number n of these subcircuits in the converter is determined by the preassigned number of intervals into which the function is divided on approximation (Fig. 1 shows only one subcircuit A_i and one subcircuit B_i). Each contains a diode D_i, voltage dividers R_{1i} and R_{2i}, and two potentiometers P_{1i} and P_{2i}. The source of stabilized voltage E is connected to the common points on the dividers.

The voltages from the potentiometer sliders are passed to the adding units Y_1-Y_4 (see, for instance, [4]). Two nonlinear functions of one variable can be obtained with this system. $f_1(x)$ is taken from Y_2, $f_2(x)$ from Y_4 (Fig. 1).

Suppose voltages x and −x are applied to the inputs of the A_i and B_i. Then the cathode voltages of the A_i diodes will be positive, no current being passed; hence the potentials on the sliders of P_{1i} and P_{2i} will be zero. In the B_i subcircuits current will only pass through those diodes on which the bias voltage x_b is less in absolute value than the input x. When the input polarity changes, current will only flow in the corresponding A_i. The voltages from the sliders coupled to the conducting diodes pass via resistors to the output adding units of the converter.

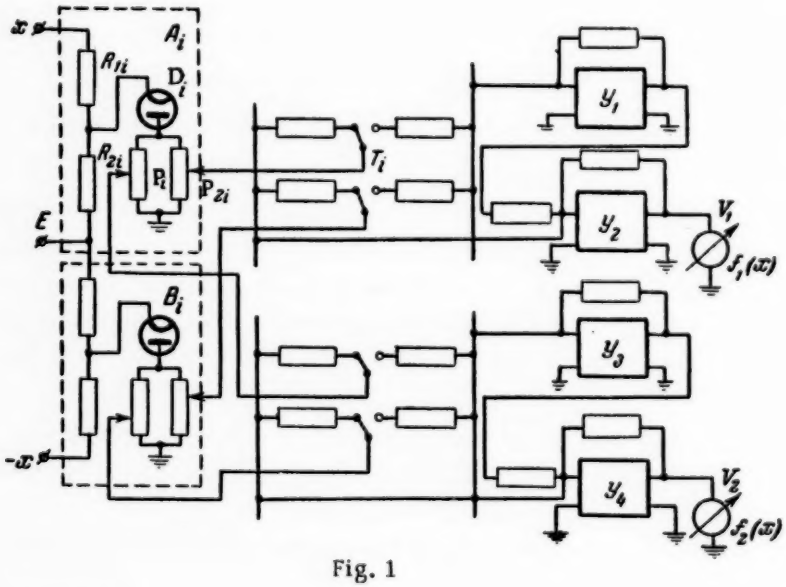

Fig. 1

*Institute of Power Engineering.

Figure 2 shows the resistors R_1 and R_2 of the diode subcircuit voltage dividers, the center points of these being connected (via diodes not shown) to resistors R_0, of value equal to the sum of the resistances of P_{1i} and P_{2i}, which are connected in parallel. If we put $R_1 + R_2 = R = \text{const}$ for all subcircuits, then the bias voltage x_b at which a diode begins to conduct is given by

$$xR_2 + ER_1 = 0, \tag{2}$$

so that

$$x_b = -E\frac{R_1}{R_2}. \tag{3}$$

The summing amplifiers Y_1 and Y_2 reverse the signs of the voltages fed to them. These units enable one to reproduce the given functional nonlinear species with both rising and falling first derivatives (Fig. 3, sections 1-2 and 2-3, respectively).

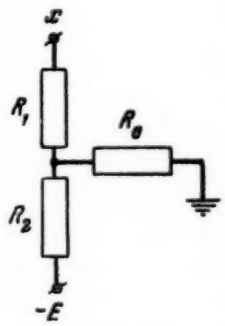

Fig. 2

When the diode circuits have to reproduce the function in regions where the first derivative is increasing, the voltages from their sliders should be connected to Y_2 and Y_4; and if the derivative is falling, to Y_1 and Y_3. The connections from the sliders to the output amplifiers are taken via the switches T_1 (Fig. 1). The converter is set up (potentiometer sliders set) using the input and output voltmeters (V_1, V_2).

In some cases the converter must reproduce a function of completely defined type. A specialized converter of this type is best made with fixed settings, the potentiometers and switches in the diode circuits being omitted and the total number of resistors in the circuit reduced. Figure 4 shows a particular case of the circuit of Fig. 1, being the circuit of one diode subcircuit coupled to the input of an operational amplifier, this being suitable in a specialized NP-1.

Talantsev has proposed to use such circuits in specialized NP-1 units and has given a method for calculating them [5].

In these circuits the diodes tubes can be replaced by crystal diodes, which are more reliable and require no heater power.

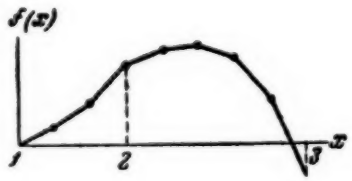

Fig. 3

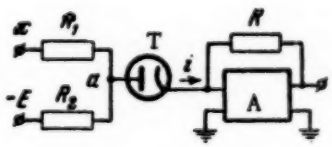

Fig. 4

If several functions of one variable have to be reproduced simultaneously on specialized NP-1 units it may be advantageous to use the diode circuits of Fig. 1. These circuits are also useful in designing nonlinear converters with two inputs [6]. Multiplication [7], division [2] and the production of analogs to typical nonlinearities [8, 9] can also be effected with specialized nonlinear converters.

3. Diode-Triode Nonlinear Converters

The diode converters are simple and reliable, but they cannot be used to reproduce functions f(x) with sharp changes of slope and steep leading edges, i.e., large values of dy/dx, without the output voltage drift being greatly increased. In theory very steep characteristics can be obtained by using output amplifiers with sufficiently high gains. But the output drift is thereby also increased in proportion; it may become quite large

in relation to the scale of the nonlinear conversion. The maximum permissible dy/dx is then restricted by the maximum output drift that can be tolerated.

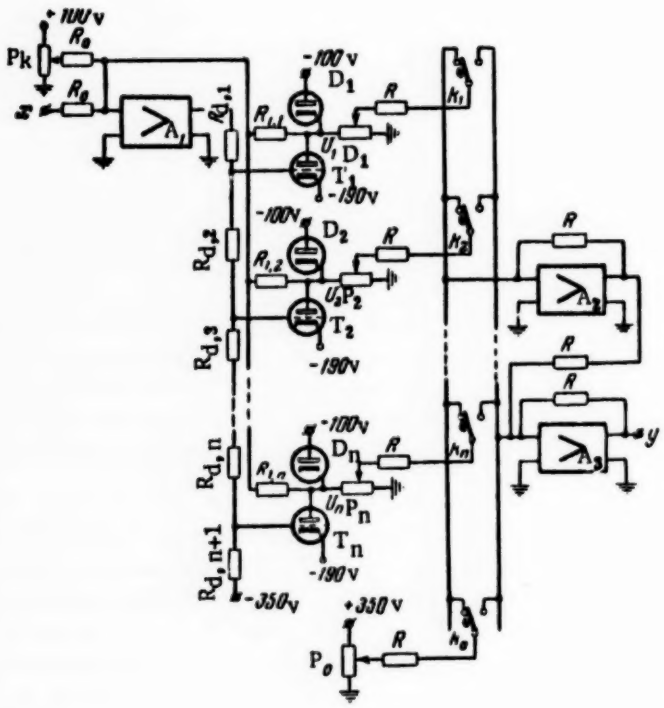

Fig. 5

The drift is also increased when the derivatives change sharply and alternate in sign in adjacent sections. To reduce the drift in such cases one should therefore use a balance method, if only partially. The theoretical circuit of a diode-triode converter using this method [10] is shown in Fig. 5. A voltage $\underline{x}$ is fed to the input of the two-stage dc amplifier A_1 via a resistor R_0. A_1 is of high gain, a divider R_d — $R_{d_{n+1}}$ being connected to the output. The output voltages from the various points of the divider are fed to the grids of tubes T_1–T_n. The divider resistors are so chosen that T_1–T_n are cut off when $\underline{x}$ has its minimum value (e.g., – 100 volts).

Thus T_1–T_n are, as it were, an additional (third) output stage of A_1. The tube plates are connected back to the amplifier input via feedback resistors $R_{1,1}$–$R_{1,n}$, as in any operational dc amplifier. Hence the relations between the output voltages of the circuit U_1, U_2,...U_n and the input $\underline{x}$ are completely determined by the feedback resistances. Let us consider the case where these resistances $R_{1,i}$ are equal, although this is not a necessary condition.

Suppose that $\underline{x}$, being intially minimal, begins to increase while remaining within some range $x_{min} < x < x_{min} + \Delta x_m$. Only one of the output tubes then conducts (i.e., T_1), the feedback loop being then closed via $R_{1,1}$. The potentials on the plates of the other tubes are then zero as the plate resistors P_1–P_n are connected to ground.

The change in U_1 at the plate of the conducting tube, denoted by U_1, is given by

$$\frac{\Delta U_1}{\Delta x} = -\frac{R_{1,1}}{R_0}, \tag{4}$$

where Δx is the input voltage change.

Hence

$$\Delta U_1 = -\Delta x \frac{R_{1,1}}{R_0}. \tag{5}$$

When U_1 attains −100 volts diode D_1 begins to conduct, this being connected to the plate of T_1; further change in U_1 then ceases and the voltage is frozen at the value $U_1 = U_{1max} = -100$ volts. This voltage will correspond to an input $x = x_{min} + \Delta x_m$, where Δx_m is given by (4) when we substitute $\Delta U_1 = -100$ v:

$$\Delta x_m = \frac{R_0}{R_{1,1}} 100. \tag{6}$$

Hence Δx_m depends on the ratio between $R_{1,1}$ and R_0 selected.

T_2 is still cut off, but if $\underline{x}$ is increased slightly above the value $x_{min} + \Delta x_m$ the output voltage from A_1 jumps suddenly because the feedback circuit via T_1 is effectively opened, and without this feedback A_1 will have a very high gain. Then T_2 conducts instantaneously, since it is connected to the output divider, and the feedback is restored via $R_{1,2}$. U_2 (at the plate of T_2) beings to change in this second range just as did U_1 in the first:

$$\frac{\Delta U_2}{\Delta x} = -\frac{R_{1.2}}{R_0}, \tag{7}$$

the limiting value $U_{2max} = -100$ volts being reached at the end of the second interval, the diode limiter D_2 then beginning to conduct.

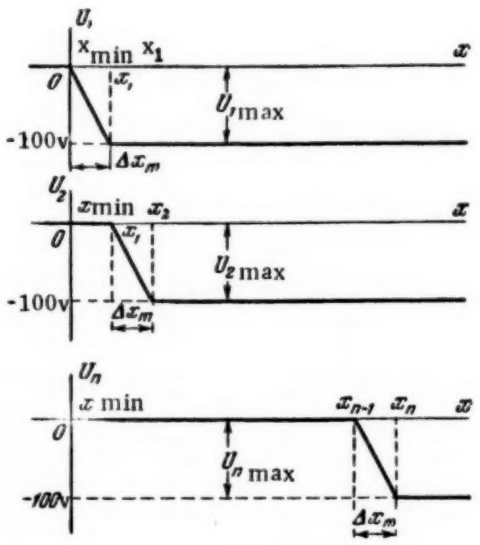

Fig. 6

Since T_1-T_n are all connected to the amplifier input via their feedback resistors $R_{1,1}-R_{1,n}$, similar arguments can be applied to T_3-T_n. The output voltages U_1-U_n will change as shown in Fig. 6. Voltages proportional to U_1-U_n are taken from the potentiometers P_1-P_n and fed to the summing amplifiers A_2 and A_3 via the switches K_1-K_n. A resistor is connected at the input and in the feedback circuits of these amplifiers. The output voltage from A_3 is the output $\underline{y}$ of the nonlinear converter. A_2 is used to change the sign of dy/dx when necessary. f(x) is compiled by summing voltages of trapezoidal form (shown in Fig. 6) in such a way that at the ends of the intervals the function has the set values and within the intervals a piecewise-linear approximation is performed. U_0, which corresponds to the values of the function at $x = x_{min}$, is set by a separate potentiometer P_0 and switch K_0.

If the function is defined for $x < x_{min}$ it can be reproduced by supplying a positive zero-shift voltage to the input from the potentiometer P_k, as shown in Fig. 5, the point where the first diode-triode circuit begins to conduct being then displaced to the left from x_{min}. The sequence of conduction, and hence the course of the function, must always be from left to right, beginning at the lowest value of $\underline{x}$.

Another method of supplying the values of f(x) for $x < 0$ can be used. Here an extra input integrator amplifier A_4 plus a range-switching device are required; the circuit is illustrated by Fig. 7. A_4 serves to derive the modulus of $\underline{x}$ and supply it to the input of A_1. When $x > 0$ the operation is as for the diode-triode circuit described above (Fig. 5).

If $\underline{x}$ changes sign relay R_1 operates and interchanges the common leads to the grids of the output amplifiers A_2 and A_3; meanwhile the input to A_1 is only supplied with the modulus $|x|$. The values of f(x) for $x < 0$ are set with the potentiometers $P_1'-P_n'$ connected in parallel with P_1-P_n.

This enables one to use the diode-triode circuits twice, as they begin to conduct once when $\underline{x}$ changes from zero to positive, and a second time when $\underline{x}$ goes from zero to minus. Hence the number of tubes required in the subcircuits can be halved.

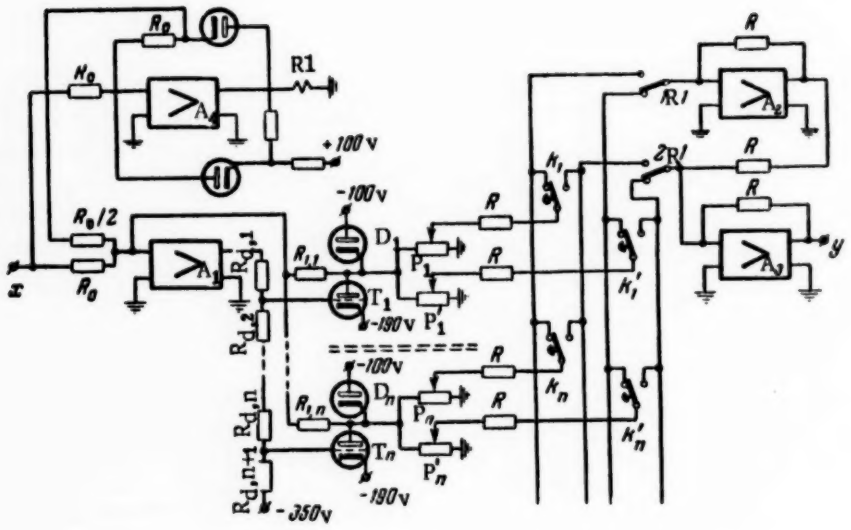

Fig. 7

Relay switching is shown in Fig. 5 for simplicity in explaining the operation; electronic diode switches attached to the inputs of A_2 and A_3 normally do the switching. If the intervals along the x axis have to be unequal the procedure is simply to make the feedback resistors $R_{1,i}$ unequal.

The piecewise linear curves shown in Fig. 6 can also be obtained without using D_1-D_n by utilizing the grid currents of T_1-T_n. But the points where transfer between the approximating straight lines occurs are then less stable.

The above principle was used in constructing the NP-1-II converter, designed at the Special Design Bureau, Ministry of Apparatus and Automatic Equipment Construction. All the Δx_m were set at 5 v in this type of converter. The range of x from 0 to +100 v was split up into 20 intervals; i.e., 20 diode-triode circuits containing one diode and one triode each were used.

To use the range of x from 0 to −100 v the diode-triode circuits were switched using another amplifier plus relay. In one of the modifications electronic switches were used for the same purpose.

This circuit provided steep fronts and sharp changes between sections of the approximating function. Here the output amplifiers A_2 and A_3 were of low gain, so the output voltage drifts were small.

4. Combined Two-Stage Nonlinear Converter

Diode-triode nonlinear converters, in which circuits of balance type are partially used, enable one to provide a selection of nonlinear functions f(x) showing sharp slope changes and high dy/dx values.

The converter circuits are more complex than in the diode case, both as regards number of components and tubes, and as regards adjustment. One way of reducing the number of components in diode-triode units is to use diode-triode subcircuits in which the interval widths are adjustable, so the total number of such subcircuits can be reduced. But range-switching cannot then be used when $x<0$ has to be covered since the functions f(x) are usually asymmetrical about the x axis. Best use is then not made of the facility for setting the interval widths at will. Twice as many tubes and an extra (third) amplifier are required, as compared with the diode circuits.

The diode-triode system is simplified by using a combined circuit in which two degrees of approximation are used. This design retains the advantages of the diode-triode system and enables one to provide functions having sharp slope changes and large dy/dx values. Also the ordinary diode circuits are used in the second

approximation, which simplifies the design. The error due to the scatter in the potentials at which the diodes begin to conduct is thereby somewhat reduced. The widths of the intervals along the $\underline{x}$ axis can also be adjusted. The whole range of variation of $\underline{x}$ is broken up into a few large intervals using the diode-triode system (first approximation), finer subdivision within the intervals being effected by diode circuits (second approximation).

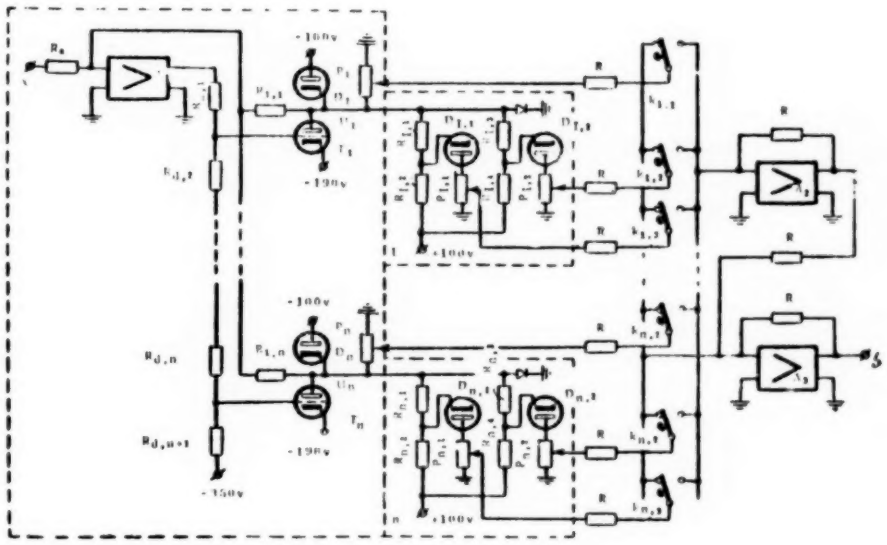

Fig. 8

Consider the circuit shown in Fig. 8. The subunit A is here analogous to the diode-triode converter circuit considered above. When the input varies from 0 to +100 volts the voltages $U_1 - U_n$ all vary from 0 to −100 volts, as shown in Fig. 6. Then the output $U_1 - U_n$ are passed to diode subunits, denoted by 1,2...,n in Fig. 8. Each diode subunit contains several diode circuits like those used in the diode NP-1 (see § 2). $U_1 - U_n$ are the inputs, varying from 0 to −100 v, for these subunits.

The reference bias voltage in the diode subunits can be taken as +100 v. The circuit contains the dividers $R_{I,1}$, $R_{I,2}$, $R_{I,3}$, and $R_{I,4}$, so calculated that diodes $D_{I,1}$ and $D_{I,2}$ each begin to conduct at their own set values of input U_I. Thus if the number of diode circuits in a subunit is two (using a 6 × 6 C double diode) and Δx_m is divided into three equal parts, then $D_{I,1}$ must begin to conduct at $U_I' = -33\frac{1}{3}$ volts, and $D_{I,2}$ at $U_I'' = -66\frac{2}{3}$ volts.

Assuming divider resistances $R_{I,1} + R_{I,2} = R = \text{const}$ for each of the two diode circuits, we have

$$-\frac{U_1}{E_1} = \frac{R_{I.1}}{R_{I.2}}. \tag{8}$$

When $U_1 = -33\frac{1}{3}$ volts we have

$$\frac{R_{I.1}}{R_{I.2}} = \frac{33\frac{1}{3}}{100} = \frac{1}{3}$$

and hence

$$R_{I.1} = \frac{1}{4} R, \tag{9}$$

$$R_{I.2} = \frac{3}{4} R. \tag{10}$$

When $U_1 = -66\frac{2}{3}$ volts we have

$$\frac{R_{I,3}}{R_{I,4}} = \frac{66\frac{2}{3}}{100} = \frac{2}{3}$$

and hence

$$R_{I,3} = \frac{2}{5}R, \tag{11}$$

$$R_{I,4} = \frac{3}{5}R. \tag{12}$$

In a combined nonlinear converter the wide intervals should be of adjustable width. The width of an interval is defined by $R_0/R_{1,i}$, where $R_{1,i}$ is the feedback resistance and R_0 the first-stage input resistance (Fig. 5). Since R_0 is common in the NP-1 each width can be adjusted separately via $R_{1,i}$. It is very convenient to vary the width in steps of 1 volt up to 63 volts. The resistance steps must then have a definite relationship, i.e., must diminish in geometrical progression $R_1 = 2R_2 = 4R_3 = 8R_4 = 16R_5 = 32R_6$. Any required width is set by switching in the corresponding resistors $R_1 - R_6$ (not shown in Fig. 5). Each large interval should be divided up into equal nonadjustable sections using diode subunits.

An example of a combined two-stage nonlinear converter is the BN-4 nonlinear device developed at the Special Design Bureau of the Ministry of Apparatus and Automatic Equipment Construction in 1953. It contains eight diode-triode circuits, the range in $\underline{x}$ being split up into eight main intervals, each of which can be varied in 1 v steps from 3 v to 45 v. Each main interval is split up into three equal parts by two diode circuits.

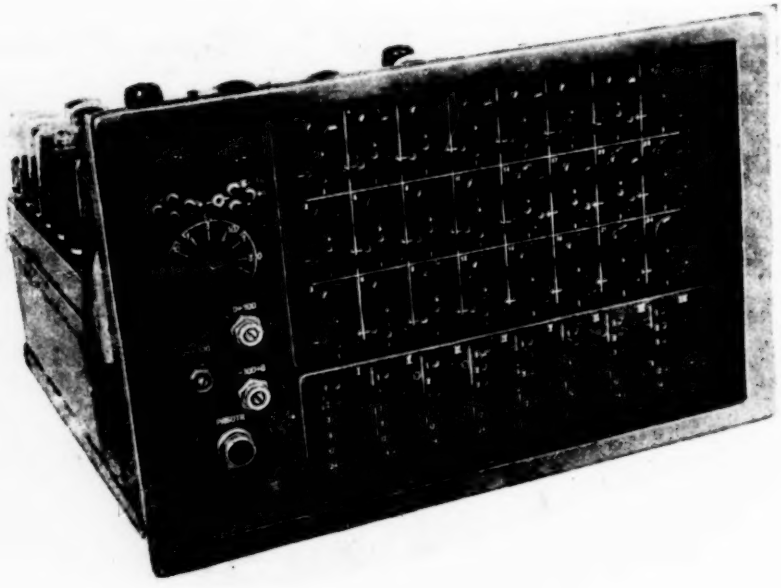

Fig. 9

The unit contains the following interchangeable subunits:

a) input amplifier A_1 with the diode-triode stages at the output,

b) feedback bank of the diode-triode circuit,

c) diode subcircuits,

d) two output amplifiers A_2 and A_3.

The maximum dy/dx which f(x) can have is 33 volts/volt, or sharp bends involving twice this change in the derivative. A bias facility to shift the zero either to −50 v or to −100 v is provided for use with $x<0$. A fixed component can also be added to the output voltage. The maximum number of intervals into which x can be split is $3 \times 8 = 24$.

Figure 9 gives a general view of the BN-4 nonlinear converter.

Prolonged use of the BN-4 units has shown them to be satisfactory. One fault is that the BN-4 is complicated compared with diode converters. Although the combined NP-1 contains less tubes than the NP-1-II (diode-triode type) the number of components is quite large and some of them require preadjustment. The complex feedback circuit prevents the unit from being used at input frequencies above 10-15 cycles/sec.

An advantage is that functions with dy/dx large can be generated, which is not possible with the ordinary diode NP-1 units.

5. Balancing Nonlinear Converters

The elementary "kinks" used in the above types of NP-1 units can be produced as high-stability curves independent of the diode characteristics if pure balance circuits are used (see [11]). One of the simplest forms of such a circuit is shown in Fig. 10. The diode D is inserted in the feedback circuit of the high-gain amplifier A; the essential difference in this circuit is that the output is taken from the point M, the input U_0 is such that if the potential at N (the amplifier input) is below zero, the output U_2 from the amplifier will be so large that D will be shut off. Only three resistances (R_1, R_2 and R_3) have then to be considered; the relation of U_3 to U_0 is then a nearly horizontal straight line for $U_0 < U_{01}$ (Fig 10b). When the potential at N rises slightly above zero U_2 becomes negative, D begins to conduct and the feedback circuit is completed via R_2. A normal amplifying link is produced and the relation of U_3 to U_0 is expressed by a straight line of slope determined by R_2/R_1 (line for $U_0 > U_{01}$ in Fig. 10b). The break thus produced is independent of the diode characteristics, should these fluctuate, for the same reason as when the gain in an amplifier link is independent of any changes in the resistance of the last stage.

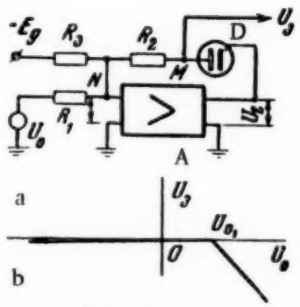

Рис. 10.

Fig. 10

An additional subcircuit enables one to keep the potential at N approximately zero when $U_0 < U_{01}$, the left branch of the curve then being strictly horizontal.

The curves produced by the above system are very stable if wire-wound resistors are used (constancy ~ 0.01%). But here we require an amplifier in each subunit responsible for an elementary "kink" so the system as a whole is cumbrous. The design is only suitable for use when a fairly small number of sections can be used in the approximation and high stability is required.

SUMMARY

The operative principles of the devices have been considered and NP-1 type apparatus has been described which is the result of many years development and which has given good results in use. The problem of providing enhanced accuracy and stability, and of extending the class of functions which can be reproduced was solved by using balance principles. The circuit complexity naturally increases as higher accuracy is demanded. Hence any one circuit is not suitable for every application. The diode NP-1 units are best used for the less exacting requirements; if curves of high slope with sharp breaks have to be reproduced the diode-triode or combined NP-1 units are best used. Finally, when high stability coupled to few piecewise-linear intervals are required the pure-balance circuits are the best to use.

LITERATURE CITED

[1] A. A. Fel'dbaum and A. I. Manukhin, A nonlinear converter with square law approximation. Authors' Certificate No. 98096, (1952).

[2] A. A. Feldbaum and L. N. Fitsner, Diode nonlinear converters. Nauchnotekhnicheskii sbornik NII MPSS,* No. 12 (1951).

[3] A. A. Fel'dbaum, A nonlinear converter with a diode circuit. Authors' Certificate No. 86673, (1950).

[4] G. Korn and T. Korn, Electronic analog equipment [Russian translation] IL, (1955).

[5] A. D. Talantsev, Designing diode functional converters. Automation and Remote Control (USSR) 17, No. 2 (1956).**

[6] A. I. Manukhin, A. A. Fel'dbaum and L. N. Fitsner, Nonlinear converters with two inputs. Pribory i tekhnika eksperimenta, No. 4 (1957).

[7] L. N. Fitsner, A device for multiplying two quantities. Authors' Certificate No. 100505, (1952).

[8] A. I. Manukhin, Electronic analog circuits for typical nonlinearities. Nauchno-tekhnicheskii sbornik NII MRTP, No. 5 (13) (1955).

[9] B. Ia. Kogan, Analogs to automatic control system with typical nonlinearities. Automation and Remote Control (USSR), 16, No. 2 (1955).

[10] A. A. Fel'dbaum, A diode-triode nonlinear converter. Authors' Certificate No. 98305, (1951).

[11] A. A. Fel'dbaum, An electronic functional device. Authors' Certificate No. 100152 (1952).

Received July 16, 1956

* Scientific Research Institute of the Ministry of the Communications Equipment Industry.

**See C.B. Translation.

INPUT CIRCUIT DESIGN FOR ELECTRONIC AMPLIFIERS IN SELF-BALANCING DEVICES*

D. E. Polonnikov

(Moscow)

The importance of interference generated by the heater circuit is demonstrated for self-balancing device amplifiers; its level is estimated and selection of parameters for the amplifiers is recommended. The interference sources arising on isolating the input circuits are demonstrated and a method of eliminating them suggested.

The optimum ratio for the input transformer (that providing maximum sensitivity) is determined.

The amplifier parameters in a self-balancing device to a large extent determine the performance of the whole equipment. Some topics in the design of such amplifiers have so far been inadequately considered and have scarcely been mentioned in the literature.

This paper deals with input circuit design for such amplifiers, with the end of reducing the interference to some set value. We only consider ac amplifiers operating at 50 cycles/sec, which are used in nearly all self-balancing units (including those with dc signal inputs).

Various types of noise or interference appearing at the input or generated within the amplifier frequently restrict the overall sensitivity and increase the error. It is therefore particularly important to depress the interference to some set value when designing the amplifier.

1. The Main Interference Sources

The noise and interference found in the amplifiers of self-balancing devices is of very varied origin and nature. Certain sources have been much studied, so we shall only enumerate them and briefly state methods of dealing with them. These types are as follows:

a) That caused by internal and external ac electric fields. This type is easily eliminated by electrostatic screening.

b) That caused by alternating magnetic fields. This is attenuated by magnetic screening, by removing the input circuits from near the field sources, by reducing the areas of loops between input leads, by grounding to a single point and by special designs of input transformer.

c) That related to ripple on the plate circuit supplies. This is eliminated by extra filtering in the plate circuits of the first stages or by improving the smoothing circuit filter.

d) That caused by the slider links. This source is only present if the design is done incorrectly. It can only be eliminated by separating the input circuits from the currents in the ac circuits, and by grounding to one point.

*Self-balancing devices here means various types of self-balancing potentiometers, bridges and the like, in which continuous automatic self-balancing is used.

e) That caused by external high-frequency fields, microphonics and pulsed noise. This group is of no practical importance in this type of amplifier, where the useful signal is at 50 cycles/sec.

f) Fluctuation noise, mostly determined by the input circuit parameters and by the first tube. It sets a theoretical limit to the overall sensitivity, for given input circuit parameters and passband width.

Interference originating in the ac heater circuit and in isolating the input circuit has been much less studied. This paper deals with this topic in detail.

2. Noise Originating in Isolating the Input Circuits

In some cases it is necessary to ground the amplifier input when the amplifier proper cannot be grounded (e.g., if no isolating transformer is used in the plate supply circuit). Sometimes, conversely, it is impermissible to ground the input when the amplifier circuit is grounded. In such cases an isolating input transformer is required. It is less satisfactory to use differential circuits in these amplifiers. But ordinary isolating transformers with an electrostatic screen between windings do not give the desired result. Let us consider a simple example. Suppose we have to provide an input device with grounded input to an amplifier fed directly from the power line (no power isolating transformer). The input transformer primary is then grounded while the secondary is at line voltage with respect to ground. Replace the distributed capacitance between windings by two equivalent capacitors connected to the ends of the windings (Fig. 1).

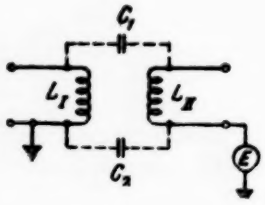

Fig. 1. Equivalent circuit of an input transformer lacking a screen between windings.

It is clear that a parasitic voltage appears at the transformer output because of the currents flowing through the secondary and C_1 to ground. Its value is given approximately by

$$U_p \approx E\omega^2 C_1 L_{II}, \qquad (1)$$

where E is the voltage to ground on the secondary, C_1 is the equivalent capacitance between the ends of the windings, L_{II} is the secondary inductance and ω is the angular frequency of E.

If we use values frequently found in input transformers, i.e., L_{II} = 500 henries, $C_1 = 50\mu\mu f$ and assume E = 127 v and ω = 314 we get U_p = 300 mv. A parasitic signal at the input as large as this is impermissible. The normal grounded electrostatic screen between windings cannot be used here because the capacitance from secondary to screen remains and so the current producing the parasitic signal continues to flow.

If the screen is joined to the secondary (Fig. 2) we have

$$U_p \approx \frac{E\omega^2 L_{II} C_1'}{n}, \qquad (2)$$

where n is the transformer ratio.

If n>1, as is usual, the interference is attenuated by a factor n (assuming $C_1 = C_1'$).

To eliminate this interference completely, double screening can be used [1, 2]. Each winding is fitted with its own electrostatic screen, the screens being joined to points in the circuits at the same potentials to ground as the corresponding windings (Fig. 3). Capacity currents then flow only between screens and cause no interference. Interference attenuation by more than a factor of 10^5 relative to ordinary transformers was thereby achieved. At E = 127 v the ripple, referred to the primary, was less than 1 μv.

This method of screening can be used in any case where capacity currents between windings are troublesome, e.g., in supplies to various bridge circuits [2], and is not restricted to amplifiers.

3. Interference Caused by ac Filament Heating, and Methods of Reducing It

In amplifiers designed to operate at 50 cycles/sec the heater circuit is one of the main interference sources if ac heating is used. The pickup is often much above the permissible value, and recourse is made to

rectifiers plus cumbrous filters with capacitors of ~ 1,000 μf. Hence in amplifier design it is important to be able to estimate the pickup and to choose an appropriate heater supply, in particular to design a filter which is not of excessive size. Various methods of dealing with heater circuit interference are known but no quantitative relations have been established, and the pickup is usually eliminated empirically.

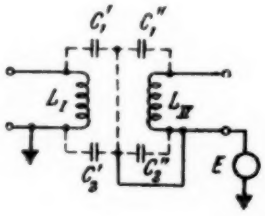

Fig. 2. Equivalent circuit of an input transformer with a screen joined to the secondary.

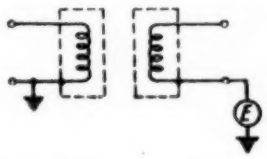

Fig. 3. Double-screened windings; parasitic signal eliminated.

We studied this pickup on numerous tubes of various types. Figure 4 shows the pickup referred to the grid vs the total grid circuit resistance Z_c when the heater pin nearest the grid one is grounded in 6N9S, 6N2P, 6Zh1Zh and 6Zh1P tubes.* Each curve is the average from 10 tubes of each type. The values differed by 20-30% between specimens, but in all cases the U_p vs Z_c relation was linear. Figure 5 shows the U_p vs Z_c relations for four 6N2P tubes with the filament center grounded. Analogous curves were obtained for the other tube types. Figure 6 shows a typical curve relating interference level to heater supply frequency.

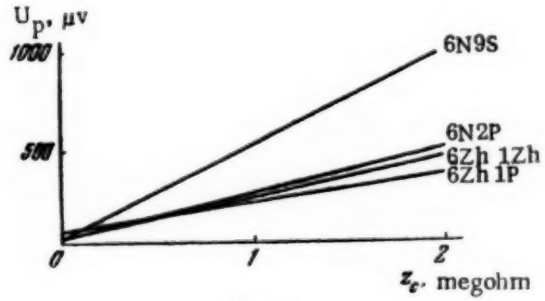

Fig. 4

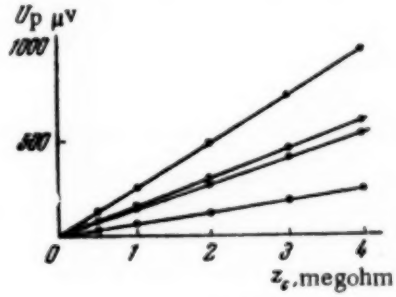

Fig. 5

A detailed study of the pickup of heater origin showed it to have two components. The first was proportional to the grid circuit resistance and is caused by capacitance between the grid and heater circuit wires (within the tube and tube-base, and in the external circuit). The second did not depend on the resistance and was caused by the magnetic field modulating the electron flux, by resistive leaks and partially by capacity between plate and heater circuits. That caused by direct electron emission from the heater was not detected in any of our tubes (this type of pickup was frequently found in the older batches of tubes). The following formula is proposed for estimating pickup from the heater circuit

$$U_p = aU_h + Z_c\omega_h C_{1g} U_h, \qquad (3)$$

where U_p is the pickup voltage referred to the input, U_h is the ac component of the heater supply voltage

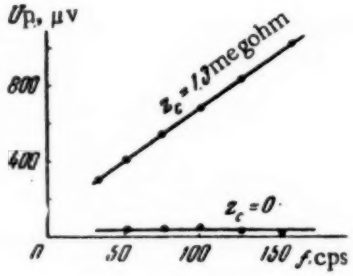

Fig. 6

*[6N9S ≡ 6SL7; 6N2P: E_f = 6.3v, I_f = 0.345 amp, E_p = +250v, I_p = 2.3 ma, E_{c_1} = − 1.5v, gm = 2000μ mho, Γ_p = 50k, R_L = 10k, P_p = 1w; 6Zh1Zh ≡ 954 (Acorn); 6Zh1P ≡ 6AK5 − Ed.]

for the input tube (the effective heater voltage being assumed constant whatever U_h), $\underline{a}$ is the coefficient of proportionality between U_h and U_p when the grid is short-circuited (constant for a given tube), Z_c is the modulus of the grid circuit impedance, which includes the input impedance of the first tube, ω_h is the angular frequency of the ac component in the heater current and C_{lg} is the equivalent capacitance between the ungrounded heater lead and the grid circuit.

In (3) both components are added without regard to any phase relationships, since we are interested in the worst case, where the phases are the same. The table gives the mean values of $\underline{a}$ and C_{lg} from tests on 10 tubes of each type from three different batches, and the maximum values.

TABLE

Parameter	Tube type			
	6N9S	6N2P	6Zh1P	6Zh1Zh
C_{lg} av, μμf	0.25	0.12	0.09	0.11
C_{lg} max, μμf	0.50	0.18	0.12	0.20
a_{av}	5×10^{-6}	5×10^{-6}	2×10^{-6}	2.5×10^{-6}
a_{max}	1×10^{-5}	8×10^{-6}	3×10^{-6}	4×10^{-6}

From the $\underline{a}$ and C_{lg} values for a given tube type we can determine the maximum permissible U_h for a given Z_c and permissible pickup level Up from (3).*

Knowing U_h we can choose the heater supply and compute the filter if a rectifier has to be used. If U_h is greater than or equal to 6.3 v, ac can reasonably be used for the heaters. If $4.2 \leq U_h < 6.3$ v a full-wave rectifier without filter is required. If $U_h < 4.2$ v a smoothing circuit of parameters determined by the value of U_h is required. The use of rectifiers is not the sole way of dealing with the interference: in some cases heater supply from a higher frequency lying outside the amplifier passband can be used with advantage.

In calculations the maximum values of $\underline{a}$ and C_{lg} are to be recommended, so that the pickup will not exceed the permissible limit even for the worst specimens. It should be remembered that C_{lg} is reduced by about a factor five when the center of the heater is grounded (which is desirable in reducing the pickup). But the scatter in C_{lg} between specimens is then large.

4. Determination of the Optimum Ratio for an Input Transformer

The relation of pickup from the heater circuit at the input to Z_c was given above. The relation of fluctuation noise to input circuit parameters is also known. This clearly imposes additional conditions on the choice of the optimum $\underline{n}$ for the input transformer. A solution is only obtainable by obtaining the maximum transfer coefficient K_T for a given signal-to-noise ratio, or by producing the maximum signal-to-noise ratio, i.e., attaining the limiting sensitivity. The optimum $\underline{n}$ also depends on the ratio between amplifier input and signal transducer (measuring circuit) impedances.

Let us first determine the transformer parameters which provide maximum K_T, i.e., maximum ratio of grid signal at the input tube U_c to transducer emf E_c, when no conditions are imposed on the input impedance (Fig. 7).

We assume we are given R_i (the transducer internal impedance); E_c, the signal voltage corresponding to the required sensitivity threshold; α, the minimum permissible signal-to-noise ratio; β, the minimum permissible ratio of signal to fluctuation noise; $U_{h0} = aU_h$, the pickup voltage independent of the grid resistance; $I_h = \omega_h C_{lg} U_h$, the pickup current determined by the component proportional to Z_c; Δf, the effective amplifier passband [4]; I_c, the grid current in the first tube; and R_n, the equivalent noise resistance of the input tube.

* The permissible U_p depends on the noise frequency. At 50 cycles/sec U_p must not exceed the insensitive zone width. At other frequencies the permissible value is greater because the motor in the amplifier output responds only to the 50-cycle component. But U_p must not exceed the linear range of the amplifier at ω_h.

Leakage is slight in input transformers and so will in future be neglected. We may assume in approximation that the input impedance of a transformer tuned to resonance is proportional to the square of the number of turns [3]. Then K_T for the input circuit (Fig. 7) may be expressed as

$$K_T = \frac{nR_0}{R_0 + R_i (1+n)^2}, \tag{4}$$

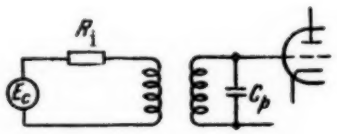

Fig. 7. Input circuit with a transformer tuned to resonate at the signal frequency.

where R_0 is the circuit resistance at resonance with the capacitor in parallel with the transformer winding having the maximum number of turns that can be fitted onto the core, and n is the transformer ratio.

By equating $\partial K_T/\partial n$ to zero we get the optimum n:

$$n_{opt} = \sqrt{1 + R_0/R_i}. \tag{5}$$

Then

$$K_{T\,max} = \frac{R_0}{2R_i(1+\sqrt{1+R_0/R_i})}. \tag{6}$$

Hence it is clear that to increase K_T we must make R_0 as large as possible. Henceforth we assume $n \gg 1$, so $R_0 \gg R_i$. But the requisite signal-to-noise ratio cannot be provided for all R_0.

The useful signal voltage at the tube grid is

$$U_c = E_c \frac{R_0 n}{R_0 + R_i (1+n)^2}. \tag{7}$$

The pickup voltage at the same point is

$$U_p = U_{h0} + I_h Z_c = U_{h0} + \frac{I_h R_i R_0 n^2}{R_0 + R_i (1+n)^2}. \tag{8}$$

The noise voltage, referred to the grid, may be determined approximately as follows [2, 4]:

$$U_n = \sqrt{\frac{4kTR_0R_i n^2\Delta f}{R_0 + R_i(1+n)^2} + 4kTR_n\,\Delta f + 2eI_c \frac{R_i^2 R_0^2 n^4 \Delta f}{[R_0 + R_i(1+n)^2]^2}}, \tag{9}$$

where k is Boltzmann's constant, T the absolute temperature of the input circuit and e the electronic charge.

The conditions of the problem imply that we must observe the relations

$$\frac{U_c}{U_h} \geqslant \alpha, \quad \frac{U_c^2}{U_n^2} \geqslant \beta^2. \tag{10}$$

Substituting (7), (8) and (9) into (10) we get the conditions imposed on R_0:

$$R_1 \leqslant R_0 \leqslant R_2, \quad R_3 \leqslant R_0 \leqslant R_4, \tag{11}$$

where

$$R_{1,2} = \left[\frac{E_c}{2\alpha I_h \sqrt{R_i}} \pm \sqrt{\left(\frac{E_c}{2\alpha I_h \sqrt{R_i}}\right)^2 - \frac{2U_{h\cdot}}{I_h}}\right]^2, \tag{12}$$

$$R_{3,4} = \frac{E_c^2}{160\,kTR_i I_c \Delta f \beta^2} - \frac{1}{20I_c} \pm \sqrt{\left[\frac{E_c^2}{160\,kTR_i I_c \Delta f \beta^2} - \frac{1}{20I_c}\right]^2 - \frac{R_n}{5I_c}}. \tag{13}$$

For $R_{1,2}$ and $R_{3,4}$ to be real the following conditions must be fulfilled:

$$\left(\frac{E_c}{\beta}\right)^2 \geqslant 8\,kTR_i\,\Delta f\,(1 + 2\sqrt{20 I_c R_n}), \tag{14}$$

$$U_h \leqslant \frac{E_c}{\alpha\sqrt{8\,a\omega_h C_{1g} R_i}}. \tag{15}$$

Thus to get the maximum transfer coefficient subject to the above conditions R_0 must be taken as large as will satisfy (11) and the transformer ratio must be chosen from (5). The input resistance is then

$$R_{in} = \frac{R_0}{(1+n)^2} \approx R_i. \tag{16}$$

If technical requirements force us to use $R_{in} >> R_i$ we have $K_T \approx n$ (independent of R_0).

The optimum transformer ratio corresponding to the limiting sensitivity, i.e., the minimum E_c, is found analogously. We assume we are given $R_{in} >> R_i$, R_i, α, β, Z_c, U_{h0}, I_{h0}, Δf, I_c. Since the following inequality must apply

$$E_c \geqslant \sqrt{\alpha^2 U_p^2 + \beta^2 U_n^2}, \tag{17}$$

to find E_{cmin} we must find the minimum of $\alpha^2 U_p^2 + \beta^2 U_n^2$. Substituting for U_p and U_n from (8) and (9) into (17) and solving for the minimum we get

$$n_{opt} = \sqrt[4]{\frac{U_{h\cdot}^2 \alpha^2 + 4\,kTR_n\,\Delta f \beta^2}{(I_h R_i \alpha)^2 + 4\,kTR_i\,20\,I_c R_i \beta^2}}$$

and (18)

$$E_{c\min} = \{4\,kTR_i\,\Delta f \beta^2 + 2[U_{h\cdot} I_h R_i \alpha^2 + \sqrt{(U_{h\cdot}^2 \alpha^2 + 4\,aTR_n\,\Delta f \beta^2)(I_h^2 R_i^3 \alpha^2 + 4\,kTR_i\,\Delta f\,20\,I_c R_i \beta^2)}]\}^{1/2}.$$

Thus when $R_{in} >> R_i$ the limiting sensitivity is independent of R_0 and the optimum transformer ratio is determined by the relation between the various components of the interference.

LITERATURE CITED

[1] D. E. Polonnikov, A small-size electronic amplifier. Author's certificate No. 103197, May 19, 1954.

[2] D. E. Polonnikov, Input Devices for Electronic Amplifiers in Automatic Self-balancing Equipment, Dissertation for the science degree of candidate in technical sciences, Institute of Automation and Remote Control, Academy of Sciences of the USSR (1956).

[3] G. S. Tsykin, Low-frequency Transformers* (Gosenergoizdat, Moscow, 1950).

[4] S. Goldman, Harmonic Analysis, Modulation and Noise* (Gosenergoizdat, Moscow, 1951).

[5] A. J. Williams, "The input transformer problem," Rev. Sci. Instr. Vol. 17, (May, 1946).

Received February 5, 1957

* In Russian.

DESIGN OF MAGNETIC CIRCUITS AND AC COILS IN ACCORDANCE WITH SET PARAMETERS

B. K. Bul'

(Moscow)

A method of computing the electrical, magnetic and structural parameters of circuits and ac coils is given. The ohmic impedance of the coil is allowed for, as is the steel loss and nonlinearity in magnetic characteristics. The method is shown to be also applicable to dc circuits. The calculation of a number of species with various initial data is considered. A numerical example is given.

The method of calculating magnetic circuits and coils to various initial conditions (induction, power, etc.) proposed here can be used for circuits without air-gaps (or with small ones) when the leakage flux can be neglected [1, 2, 7-9]. When the coil and steel parameters are being determined the relations between the electrical, magnetic and structural parameters of magnetic circuit and winding must be derived. The induction, magnetic circuit length or cross-section and number of turns are determined by calculation (see cases 1 and 2 in Table 1).

The current density is chosen from the condition of normal temperature conditions. For continuous operation the current density is taken as 2.5 amps/mm^2, for intermittent operation as 10-15 amps/mm^2, and for millisecond operation as 30 amps/mm^2 [3]. The current and flux are assumed to vary sinusoidally. All electrical and magnetic quantities are expressed in practical units, the effective values being used for current, emf, magnetic impedance and conductivity, and the peak ones for flux and induction.

We also assume the steel characteristic given:

$$\rho_R = f(B) \quad \text{or} \quad \rho_z = f(B) \tag{1}$$

and that of the winding wire:

$$f_M = f(d). \tag{2}$$

Here ρ_R and ρ_Z are the resistive and total magnetic impedances of the steel (Fig. 1) [2, 4], B is the induction in the core, f_M the coefficient giving the fraction of winding window filled with copper [5] and d is the wire diameter.

For a closed magnetic circuit the magnetizing force of the coil is

$$F = IW = \Phi Z_\mu = Bl\rho_z, \tag{3}$$

where I is the coil current and Φ the flux in the core.

TABLE 1

Case	Given	Chosen	Determined
1a	U (or I), P, S	i_q, H	I, Z, d, f_M, B, Θ, W, l, R_0, X, φ
1b	U (or I), P, S, δ	i_q, H	I, Z, d, f_M, B, W, b, R_0, X, φ
2a	U (or I), P, l, a	—	B, ρ_R, Θ, I, i_q, P, $R_\sim$, X, Z, φ
2b	U (or I), P, l, a, δ	—	B, ρ_R, Θ, $R_\sim$, X, Z, U, P, φ
3	U, l, S, W, H, d, δ	B	R_0, $R_\sim$, Z, φ, U, P, V, S, l, q
4	I, l, S, W, H, d, δ	B	R_0, $R_\sim$, Z, φ, I, P, V, S, l, q
5	I, L, Q, f		
6	U, L, Q, f		

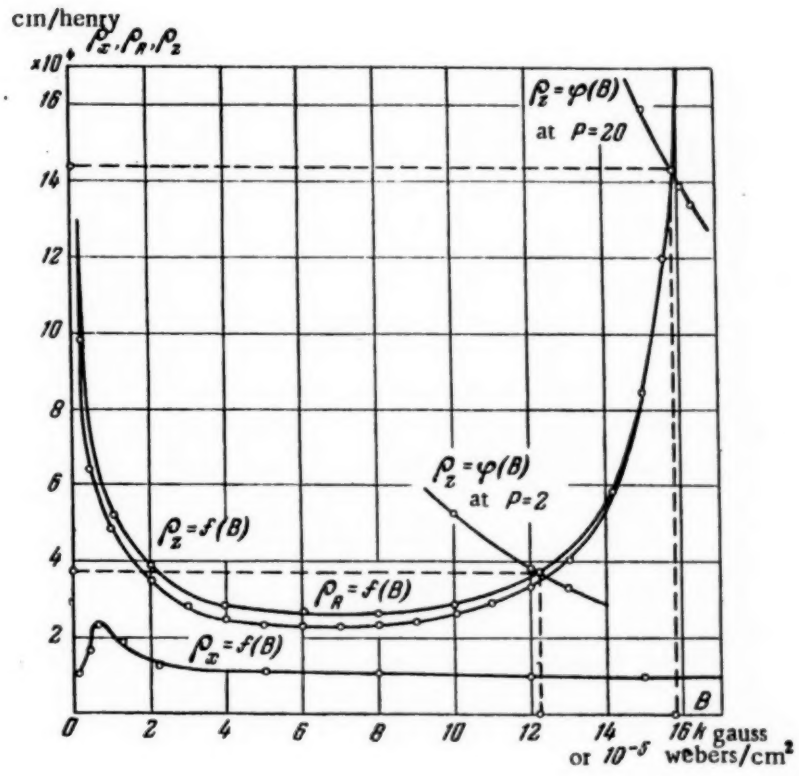

Fig. 1. Specific (effective) resistive, reactive and total impedances of E_1 – AA steel vs induction for a strip thickness of 0.5 mm and f = 50 cycles/sec; $\rho_z = f(B)$ is the magnetic characteristic of the material, $\rho_z = \varphi(B)$ that of the projected circuit.

If the core has an air gap

$$F = IW = \Phi \sqrt{(R_{\mu\delta} + R_\mu)^2 + X_\mu^2} = B \sqrt{\left(\frac{\delta}{\sqrt{2}\,\mu_0} + \rho_R l\right)^2 + (\rho_x l)^2}\,, \qquad (4)$$

where R_μ, X_μ and Z_μ are the ohmic, reactive and total impedances of the steel, $R_{\mu\delta}$ is the magnetic resistance of the air gap δ, ρ_X is the reactive specific magnetic impedance of the steel (Fig. 1), l is the mean length of the core, $\mu_0 = 0.4\pi 10^{-8}$.

Allowing for the wire resistance and steel loss, the number of turns is determined from a formula given previously by the author [6]:

$$W = \frac{U}{\sqrt{c_1^2 + c_2^2 + 2c_1c_2 \sin\theta}}, \tag{5}$$

where

$$c_1 = \rho i_q l_{av}, \quad c_2 = \frac{\omega\Phi}{\sqrt{2}}, \quad l_{av} = 2(a_1 + b_1) + \pi H, \tag{6}$$

$$S = abk_3, \quad a_1 = 2(a + \Delta_3), \quad b_1 = b + 2\Delta_3. \tag{7}$$

Here ρ is the specific electrical resistance of the wire, i_q the current density, S the core cross section, a and b the core dimensions (Fig. 2), l_{av} the mean length of a turn, k_3 the iron fill-in coefficient for the core area, a_1 and b_1 the dimensions of the former.

The steel loss angles with and without a gap are given respectively by

$$\tan\theta = \frac{\rho_x}{\rho_R}, \qquad \tan\theta = \frac{\rho_x l}{\frac{\delta}{\sqrt{2}\mu_0} + \rho_R l}. \tag{8}$$

If the steel loss is small ($\theta = 0$) (5) becomes

$$W = \frac{U}{\sqrt{c_1^2 + c_2^2}}. \tag{9}$$

If the coil resistance is neglected

$$W = \frac{U}{c_2} = \frac{\sqrt{2}U}{\omega BS} \tag{10}$$

The mean core length can be expressed as

$$l = 2(c + l_0) + \pi a = 2L + \\ + E = 2lW\lambda + E, \tag{11}$$

where

$$c = H + \Delta_1 + \Delta_3, \quad l_0 = L + 2\Delta_2, \quad \lambda = \frac{1}{i_q l_M H}; \\ E = 2(\Delta_1 + 2\Delta_2 + \Delta_3 + H) + \pi a. \tag{12}$$

Here c and l_0 are the width and height of the core window. Figure 2 shows Δ_1, Δ_2, Δ_3. The bare wire diameter is

$$d = \sqrt{\frac{4I}{\pi i_q}}. \tag{13}$$

Table 1 gives the possible types of initial data available when designing electromagnetic devices.

The calculation will be considered for each case separately.

Case IA. Let us determine the relations between ρ_z, the magnetic induction B and the other electrical and dimensional parameters of the circuit and winding. Solving (3), (5) and (11) for ρ_z we get

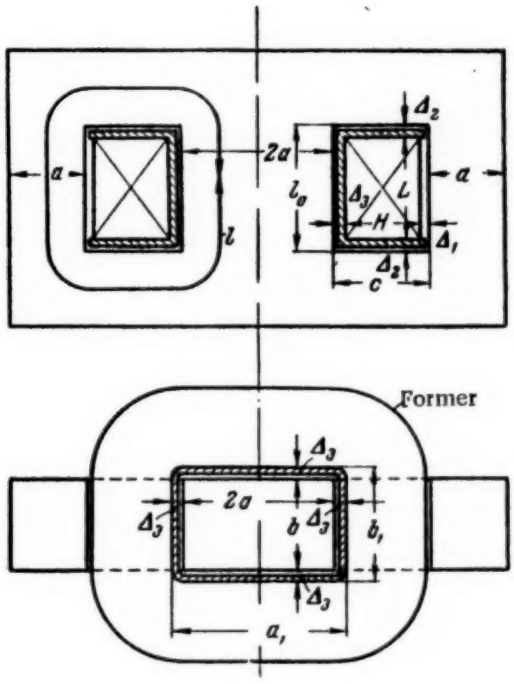

Fig. 2. Steel cored choke coil.

$$\rho_z = \frac{-b_5 \pm \sqrt{b_5^2 + 4 a_5 c_5}}{2 a_5}. \tag{14}$$

Here

$$a_5 = B^2 (m_2 + m_3 B^2),\ b_5 = B (m_1 + m_4 B^2),\ c_5 = P^2, \tag{15}$$

$$m_1 = 4 \lambda P^2, \quad m_2 = (c_1 E)^2 - m_1 \lambda, \quad m_3 = \left(\frac{\omega S E}{\sqrt{2}}\right), \quad m_4 = \frac{2}{\sqrt{2}} c_1 \omega E^2 S \rho_x. \tag{16}$$

Calculation steps. 1. The coil current and total impedance are given by

$$I = \frac{P}{U}, \qquad Z = \frac{U}{I}. \tag{17}$$

2. From (13) the diameter of the bare wire is found, i_q being given; f_m is found for the insulation type used from the $f_m = f(d)$ curve [5].

3. E, λ, m_1, m_2, m_3 and m_4 are determined from (12) and (16). Assigning values to B, we use $\rho_z = f(B)$ (Fig. 1) to derive the curve $\rho_z = \varphi(B)$ in the same scale from (14) (see numerical example). The point where the curves cross gives the desired B and ρ_z.

4. Using (3), (11) and (12) we get a formula for the coil turns:

$$W = \frac{E B \rho_z}{I (1 - 2\lambda B \rho_z)}. \tag{18}$$

The number of turns can also be determined from (5).

5. From (3) we get l, and then L = ½ (l − E), l_0 and c (Fig. 2).

6. From [6] we get the resistive and reactive coil impedances (neglecting the steel loss) as

$$R_0 = c_1 \frac{W}{I}, \qquad X_0 = \frac{\omega W^2}{\sqrt{2} R_\mu}, \tag{19}$$

where

$$R_\mu = \rho_R \frac{l}{S}. \tag{20}$$

For E1-AA steel ρ_R is found from Fig. 1 using the induction (already known). The magnetic characteristics of other steels are given in [2].

Allowing for steel loss we have

$$R = R_0 + R_\sim = R_0 + X_0 \sin\Theta \cos\Theta, \quad X = X_0 \cos^2\Theta, \tag{21}$$

$$Z = \sqrt{R^2 + X^2}. \tag{22}$$

This value of Z must equal the Z from (17). The angle between current and voltage is found from

$$\tan\varphi = \frac{X}{R_0 + R_\sim}. \tag{23}$$

When R_0 and the steel loss are small, and so can be neglected, (14) becomes much simpler:

$$\rho_z = \rho_R = \frac{\sqrt{2} P}{(\omega E S B + 2\sqrt{2}\lambda P) B} = \varphi(B). \tag{24}$$

As previously, we assign B a series of values and construct the curve $\rho_R = \varphi(B)$. The point where this intersects $\rho_R = f(B)$ gives the B and ρ_R required to correspond to the set power P.

Case 1B. The calculation is performed for $R_0 = 0$ and $\theta = 0$ (if these are allowed for an equation of high order results). From (3), (10) and (11) the core length is found in the form

$$l = E + 2\lambda I \frac{\sqrt{2} U}{\omega S B}. \tag{25}$$

Substituting the values of W and l from (10) and (25) into (4) we get

$$\rho_R = \frac{-b_6 \pm \sqrt{b_6^2 + 4a_6 c_6}}{2a_6}. \tag{26}$$

Here

$$a_6 = (B\xi)^2, \quad b_6 = 2SB^2 R_{\mu 8} \xi, \quad c_6 = \left(\frac{\sqrt{2} P}{\omega S B}\right)^2, \tag{27}$$

$$\xi = E + \frac{2\sqrt{2}\lambda P}{\omega S P}. \tag{28}$$

Giving B values in accordance with (26) we construct $\rho_R = \varphi(B)$. The point where this intersects $\rho_R = f(B)$ gives the values of B and ρ_R required. Knowing these we can easily determine all the other quantities.

Case 2A. This calculation can be performed when the dimensions of the core strips (stampings) are given and the thickness of the core has to be found.

From (3) and (11) we have

$$\rho_z = \frac{(l - E)}{2\lambda l} \frac{1}{B} = \varphi(B). \tag{29}$$

As above we determine B and ρ_z. From (3) we get the number of turns:

$$W = \frac{lB}{I} \rho_z. \tag{30}$$

The core thickness is found from (5) and (6) [6]:

$$b = \frac{-b_3 \pm \sqrt{b_3^2 - 4a_3c_3}}{2a_3}. \tag{31}$$

Here

$$a_3 = \tau_1^2 + \tau_2^2 + 2\tau_1\tau_2 \sin\Theta, \quad b_3 = n_2(\tau_1^2 + \tau_1\tau_2 \sin\Theta), \tag{32}$$

$$c_3 = \left(\frac{n_2\tau_1}{2}\right)^2 - \left(\frac{U}{W}\right)^2, \tag{33}$$

where

$$\tau_1 = 2\rho i_q, \quad \tau_2 = n_1 B, \quad n_1 = \frac{\omega n}{\sqrt{2}} k_3, \quad n_2 = \pi H + 2(a_1 + 2\Delta_3).$$

If the steel loss is negligible ($\theta = 0$), (31) becomes

$$b = \frac{\sqrt{4(U/W)^2(\tau_1^2 + \tau_2^2) - (n_2\tau_1\tau_2)^2}}{2(\tau_1^2 + \tau_2^2)}. \tag{34}$$

If $R_\theta = 0$ the core thickness is given by (31) or (10):

$$b = \frac{\sqrt{2}U}{\omega W a B k_3}. \tag{35}$$

Knowing the effective core cross section from (7) we can calculate R_μ, X_θ, X and $\tan\varphi$.

Case 2B. From the value of I we find d and f_m, and from (12), λ. From (11) we have

$$W = \frac{l - E}{2\lambda l}. \tag{36}$$

Using (4) we get the relation between specific resistance and induction as

$$\rho_R = \frac{-b_7 \pm \sqrt{b_7^2 - 4a_7c_7}}{2a_7} = \varphi(B). \tag{37}$$

Here

$$a_7 = l^2, \quad b_7 = 2l\left(\frac{\delta}{\sqrt{2}\mu_0}\right), \quad c_7 = \left(\frac{\delta}{\sqrt{2}\mu_0}\right)^2 + (\rho_x l)^2 - \left(\frac{lW}{B}\right)^2. \tag{38}$$

At zero steel loss (37) becomes

$$\rho_R = \frac{1}{l}\left(\frac{IW}{B} - \frac{\delta}{\sqrt{2}\mu_0}\right). \tag{39}$$

As previously, the point where $\rho_R = \varphi(B)$ and $\rho_R = f(B)$ intersect gives ρ_R and B. From (31), (34) or (35) we calculate b, and then all the other quantities (see Table 1).

Case 3. Here the calculation is performed when a preexisting electromagnetic device (choke, relay, etc.) must work with a changed air-gap and all the electrical and magnetic parameters have to be determined. The relation between ρ_R and B is here determined from (3) – (5) in the form:

$$B = \frac{U}{SW\sqrt{0{,}5\omega^2 + \frac{k_0 Z_\mu}{W}\left(\frac{k_0 Z_\mu}{W} + \frac{2}{\sqrt{2}}\frac{\omega}{\rho_z}\rho_x\right)}}, \tag{40}$$

where

$$Z_\mu = \sqrt{\left(\rho_R \frac{l}{S} + R_{\mu\delta}\right)^2 + X_\mu^2}\ , \quad k_0 = \rho \frac{l_{av}}{q}. \tag{41}$$

By inserting values of ρ_R in (40) we determine B and construct the $\rho_R = \varphi(B)$ curve. Then as before we get the required values of ρ_R and B.

Z_μ is calculated from (41), θ from (8). The coil current is

$$I = \frac{BSZ_\mu}{W}. \tag{42}$$

The $R_0 = 0$ calculation is very simple. (40) takes the form of (10) ($k_0 = 0$).

Case 4. If (4) is used the relation of B to ρ_z is determined from (37). Determining B and ρ_R as above we get all the other quantities (see Table 1).

Let us determine the requisite relationships for computing low-power chokes (Cases 5 and 6)

The Q of a steel-cored coil is

$$Q = \frac{X}{R_0 + R_\sim} = \frac{X}{R} \tag{43}$$

or

$$\frac{1}{Q} = \frac{R_0 + R_\sim}{X} = \frac{R_0}{X} + \frac{R_\sim}{X} = \frac{1}{Q_W} + \frac{1}{Q_M} = \frac{Q_M + Q_W}{Q_M Q_W}, \tag{44}$$

whence

$$Q = \frac{Q_M Q_W}{Q_M + Q_W}. \tag{44a}$$

Here the winding Q is

$$Q_W = \frac{X}{R_h} \tag{45}$$

and the Q of the magnetic material

$$Q_M = \frac{X}{R_\sim} = \frac{X_0 \cos^2\theta}{X_0 \sin\theta\cos\theta} = \frac{R_\mu}{X_\mu} = \frac{\rho_R}{\rho_x}, \tag{46}$$

$$R_0 = \rho \frac{l_{av} W}{q}. \tag{47}$$

Results which have been given [6] enable us to find the relation of core volume (in cm^3) to power, induction, etc., in the form

$$V = \frac{V\overline{2}P\sin\varphi}{\omega B^2\rho_R}. \tag{48}$$

Here the coil resistance and steel loss are allowed for. When $R_0 = 0$

$$V = \frac{V\overline{2}P\cos\varphi}{\omega B^2\rho_R}. \tag{49}$$

Neglecting the steel loss,

$$V = \frac{V\overline{2}P}{\omega B^2\rho_R}. \tag{50}$$

Case 5. 1. Since the power consumed must be small we take B small [7, 8]. Using this B we determine ρ_R and ρ_X from Fig. 1, and Q_M and Q_w from (46) and (44a).

If the frequency is other than 50 cycles/sec ρ_X must be recalculated, e.g., from the formulas given in [6].

2. From (45), (46), (22) and (23) we calculate R_0, $R_\sim$, Z and φ.

3. From (48) we get the steel volume, since $P = I^2Z$.

4. Having V we select suitable dimensions for the stampings. We thus get a, b and l.

5. Using (3), (47) and (6) we calculate W and q.

Case 6. The course of the calculation is as before. The coil power is found from $P = V^2/Z$.

DC Magnetic Circuit Calculation

A circuit with a small gap (leakage neglected) can be calculated using (3), (4), (11) – (13). Here we have to assume $\rho_X = 0$ for the steel and $\rho_R = 1/\mu$, where μ is the permeability of the steel [4, 6]. Let us consider an example using case 1B (Table 1).

The number of turns is determined from (19):

$$W = \frac{R_0 I}{\rho l_{av} i_q} = \frac{U}{\rho l_{av} i_q}.$$

From I (given) d and f_m are found. From (11) we get l

From (4) we get

$$\rho_R = \frac{1}{l}\left(\frac{IW}{B} - \frac{\delta}{\mu_0}\right) = \varphi(B).$$

As previously, the point where $\rho_R = \varphi(B)$ intersects $\rho_R = 1/\mu = f(B)$ gives the required B and ρ_R.

Numerical example. We are given the choke voltage U = 100 v, the power P = 2 volt-amps, the core cross section S = 1.98 cm^2 (Fig. 3), that the steel is type E1-AA and that the wire is type PShD.

We choose a current density i_q = 250 amps/cm^2 and a winding height H = 10 mm.

The distance between the winding and core is chosen as Δ_1 = 1 mm (Fig. 2), the former wall thickness plus air space between former and core Δ_2 = 1.5 mm, Δ_3 = 2 mm.

Let us determine W and l, the wire diameter d, B, the steel and winding power loss P_a, the loss angle 0, Z, R_0, $R_\sim$, and X, plus the angle between current and voltage φ.

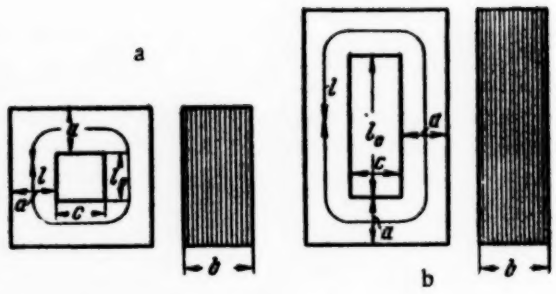

Fig. 3. Magnetic circuit for a given power: a) P = 2 volt-amps, a = 12, b = 16.5, c = 13, l = 88.2, l_0 = 12.3; b) P = 20 volt-amps, a = 12, b = 16.5, c = 13, l = 139.5, l_0 = 37.9 (dimensions in mm).

Sequence of calculation. 1. The current and total impedance are found:

$$I = \frac{P}{U} = \frac{2}{100} = 0.02 \text{ a}, \quad Z = \frac{U}{I} = \frac{100}{0.02} = 5000 \text{ ohms}.$$

2. The bare diameter of the wire is found from the current and current density:

$$d = \sqrt{\frac{4I}{\pi i_q}} = \sqrt{\frac{4 \times 0.02}{\pi \times 2.5}} = 0.1 \text{ mm}.$$

The $f_m = f(d)$ curve [5] gives $f_m = 0.17$.

(7), (6), (12) and (16) then give $a_1 = 1.6$ cm, $b_1 = 2.05$ cm, $l_{av} = 10.44$ cm, $c_1 = \rho\, l_{av} i_q = 5.16 \times 10^{-3}$ volts, E = 6.97 cm, $\lambda = 2.35 \times 10^{-2}$ cm/amp, $m_1 = 37.6 \times 10^{-2}$ cm-amp-volt^2, $m_2 = -75.6 \times 10^{-4}$ cm^2 volt^2, $m_3 = 7.7 \times 10^6$ cm^6/sec^2, $m_4 = 2 \times 10^6$ amps-cm^5/sec^2.

TABLE 2

Data for $\rho_z = \varphi(B)$

$B \times 10^{-4}$, webers/cm^2	a_s	b_s	$\rho_z \times 10^4$, cm/henry	Note
10	6.94	39.6	5.24	$c_s = P^2 = 4$
12	14.9	48.5	3.84	
13	20.7	53.2	3.29	

Using the values of B (Table 2) we calculate a_s and b_s from (15) and then ρ_z from (14). The curve $\rho_z = \varphi(B)$ is drawn up from the data of Table 2. The point where this curve intersects the characteristic for E1-AA steel gives $B = 12.2 \times 10^{-5}$ webers/cm^2 and $\rho_z = 3.7 \times 10^4$ cm/henry.

4. From (18) we get W = 1990.

5. The magnetizing force and the mean core path length are F = 39.8 amp-turns and l = 8.82 cm,

respectively. The former length and core window dimensions are

$$l = 0.93 \text{ cm}, \quad l_0 = 1.23 \text{ cm}, \quad c = 1.3 \text{ cm}.$$

6. The ohmic and reactive impedances of the coil (neglecting steel loss) from (19) are $R_0 = 513$ ohms, $X_0 = 5.07 \times 10^3$ ohms.

Here $\rho_R = 3.53 \times 10^4$ cm/henry was found from Fig. 1 with $B = 12.2 \times 10^{-5}$ webers/cm^2.

When the steel loss is allowed for R = 1828 ohms, $X = 4.7 \times 10^3$, tan $\varphi = 2.57$, so $\varphi = 68° 45'$ [from (21) and (23)].

Here θ is determined from $\sin \theta = 0.27$: $\theta = 15° 40'$.

The coil and steel power loss is $P_a = 0.732$ watts.

The total impedance $Z' = 5 \times 10^3$ and is almost exactly that found from $Z = U/I = 100/0.02 = 5 \times 10^3$ ohms. A sketch of the magnetic system is given in Fig. 3a. For comparison, a system for P = 20 volt-amps (Fig. 3b) is also given. The calculated induction is $B = 15.8 \times 10^{-5}$ webers/cm^2 (Fig. 1).

LITERATURE CITED

[1] B. K. Bul', "An analytic method of calculating inductances and resistances of coils in electromagnetic mechanisms, Automation and Remote Control (USSR) 14, 2 (1953).

[2] B. K. Bul', "Methods of calculating magnetic circuits with allowance for the magnetic impedance of the steel" Elektrichestvo 1952, No. 11.

[3] N. A. Livshits, D. V. Spitsyn and A. V. Danilin, Theory and Calculation of Automatic Control System Elements* (GONTI, 1939).

[4] B. K. Bul', "An analytic method of determining magnetic impedances and steel losses," Elektrichestvo 1950, No. 5.

[5] B. S. Sotskov, Fundamentals of Calculating and Designing Elements in Automatic and Remote Control Devices* (Gosenergoizdat, 1953).

[6] B. K. Bul', "A method for calculating steel-cored coils carrying ac " Elektrichestvo 1954, No. 8.

[7] L. I. Iaroslavskii and N. A. Iablonovskii, Multiple-Frequency Telegraphy* (ONTI, 1935).

[8] G. S. Tsykin, Low-Frequency Transformers (Sviaz'izdat**, 1950).

[9] A. I. Rutskii, "Use of dynamic magnetization curves for calculating steel-cored reactor coils," Collected scientific papers of the Byelorussian Polytechnical Institute No. 53 (1956).

* In Russian.

**State Publishing House of Literature on Communications and Radio Problems.

CHARACTERISTICS OF MAGNETIC MATERIALS FOR USE IN MAGNETIC AMPLIFIERS OPERATING AT AUDIOFREQUENCIES

G. V. Subbotina

(Moscow)

The characteristics of some Soviet soft magnetic alloys are given, for use in magnetic amplifier calculations. The characteristics were taken on strips 10 and 20 μ thick at frequencies from 500 to 20,000 cycles/sec.

Higher supply frequencies result in reduced dimensions in magnetic amplifiers and in more rapid response. But the need for special power supplies restricts their use. As reliable high-frequency generators can be built around transistors the audiofrequency supply problem can be solved, so magnetic amplifiers operating at audiofrequencies are now of greater interest.

The cores in amplifiers operating at above 1,000 cycles/sec are made from thin strips of soft magnetic alloys or from ferrites.

At low frequencies the magnetic properties of the core are mainly determined by the static magnetic characteristics of the alloy; these properties become much poorer in materials of thicknesses in the micron range.

At 10-20 kilocycles/sec eddy current losses are of more importance, as they reduce the apparent magnetic permeability. The reduction increases with the thickness of the material. Hence thinner materials should be used at 10-20 kilocycles/sec (10-20μ) although these have worse static characteristics.

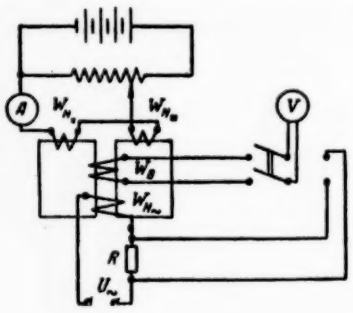

Fig. 1. Circuit for recording $B_{\sim} = f(H_{\sim}, H_{=})$ characteristics for soft magnetic materials.

At present alloys 79NMA, 79NM4, 80NKhS, 50NP, 50NKhS, 65NP and N34K29MZP are produced as unannealed strip 20-100 mm wide in lengths not less than 5 m and of thicknesses 20μ and less. The dc magnetic properties (at a thickness of 10μ) of certain alloys which are guaranteed to comply with the technical requirement of ChMTU*-5010-55 and ChMTU*-4680-54 [1] are given in Table 1.

The difficulty of preparing a torus from strip 10μ or less thick compels us to use ferrites, which are available ready-made and require no additional annealing or the use of formers.

The dc magnetic properties of ferrites are much worse than those of metal cores, as can be seen from Table 2 [2].

The principle magnetization characteristics of a material used in designing magnetic amplifiers for audiofrequency working are those taken with ac and dc fields acting together, $B_{\sim} = f(H_{\sim}, H_{=})$, taken at the appropriate supply frequency with a suitable induction or field strength curve shape. The set of $\mu = f(H_{\sim}, H_{=})$ curves, where $\mu = f(B_{\sim}, H_{=})$, is more useful in some cases and can be constructed if the set of $B_{\sim} = f(H_{\sim}, H_{=})$ curves is available.

*Ferrous Metallurgy Technical Specifications.

TABLE 1

Alloy	thickness mm	initial permeability μ_0 (gauss/oersted), not less than	maximum permeability μ max (gauss/oersted), not less than	Coercive force H_c, oersted	saturation induction B_s, gauss, not less than	B_r / B_s, %
79MNA	0.01	15 000	65 000	0.07	7 500	—
80NK1S	0.01	12 000	40 000	0.10	7 000	—
50NP	0.01	700	20 000	0.5	15 000	83
N34K29MZP	0.01	200	20 000	0.65	15 000	95

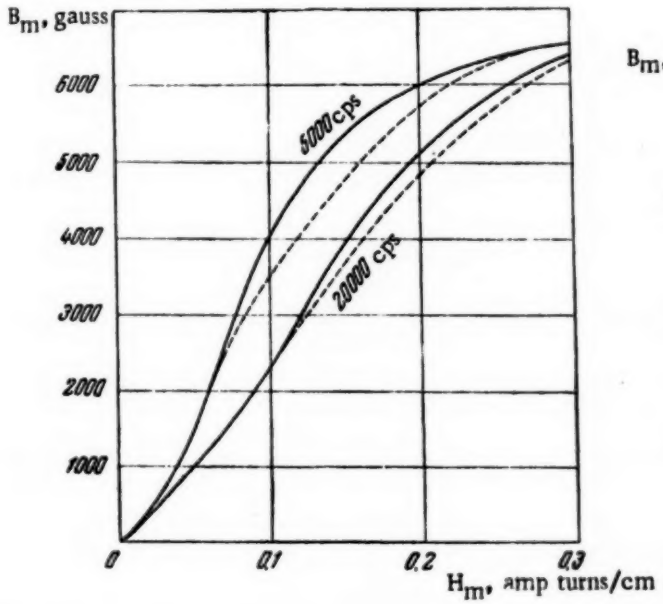

Fig. 2. Effect of number of turns of strip on properties. Full lines for six turns, dashed for three.

Such curves, taken at 50 and 400 cycles/sec, have been given [3, 4] for several Soviet alloys at thicknesses of 50μ and above. The curves given here were taken on 10 and 20μ strip at 500, 1,000, 5,000, 10,000 and 20,000 cycles/sec [5].

The circuit of Fig. 1 was used, the ac field strength being measured by the voltage drop across R (1.5 ohms) in the ac circuit. To measure the mean values of emf and voltage drop in R a LV9-2 vacuum-tube voltmeter was used.

A ZG-10 electronic generator plus an amplifier delivering up to 5 watts with a sinusoidal waveform were used as power supply.

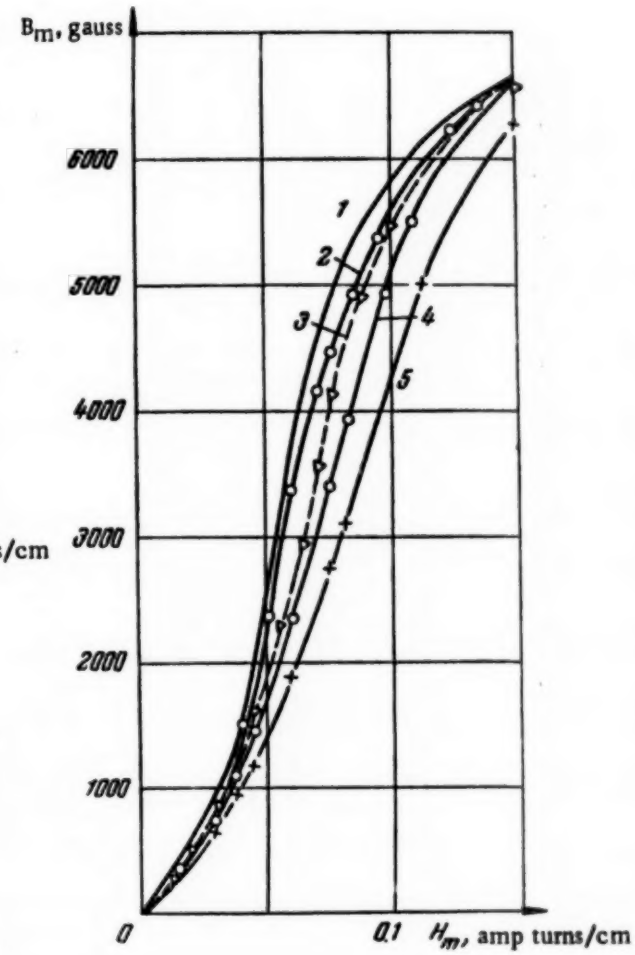

Fig. 3. The principle magnetization curves for alloy 79NMA. Strip thickness 10μ: 1) at 500 cycles/sec; 2) 1,000 cycles/sec; 3) 5,000 cycles/sec; 4) 10,000 cycles/sec; 5) 20,000 cycles/sec.

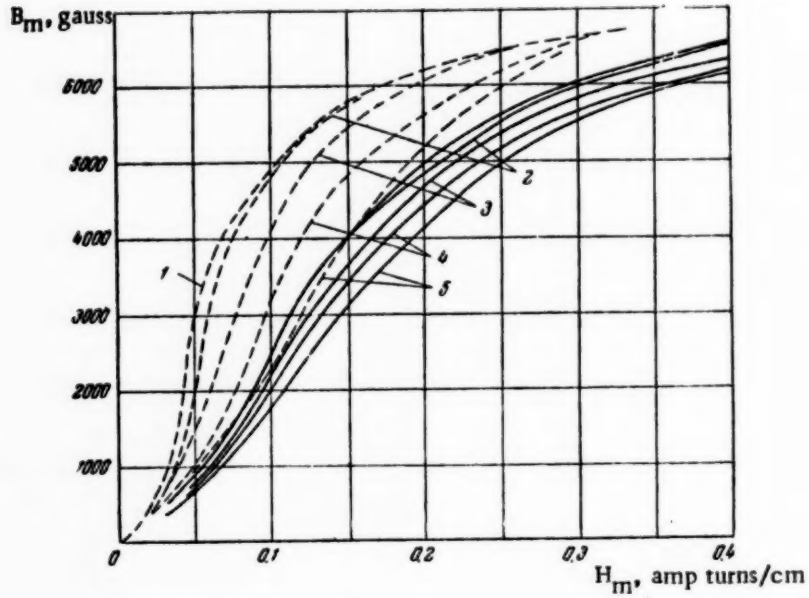

Fig. 4. The principle magnetization curves for alloy 80NKhS. The full curves are for a strip thickness of 20μ, the dashed for 10μ: 1) at 500 cycles/sec; 2) 1,000 cycles/sec; 3) 5,000 cycles/sec; 4) 10,000 cycles/sec; 5) 20,000 cycles/sec.

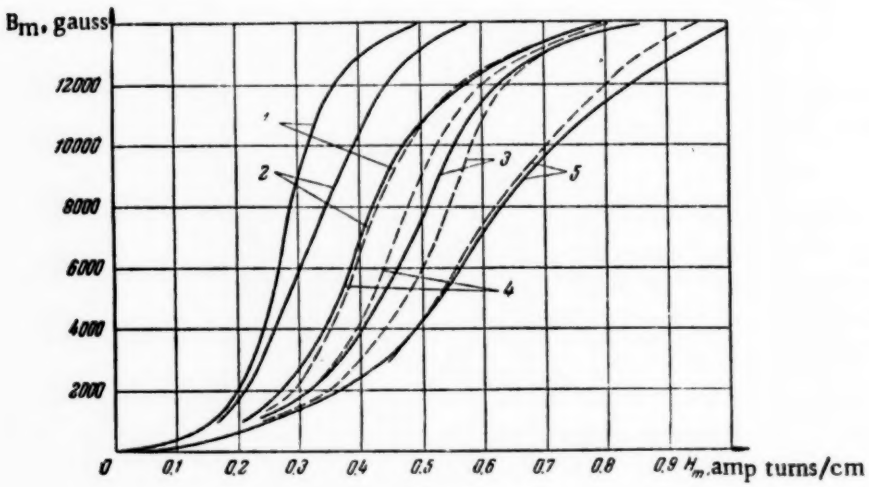

Fig. 5. The principle magnetization curves for alloy 50NP. The full curves are for a strip thickness of 20μ, the dashed for 10μ: 1) at 500 cycles/sec; 2) 1,000 cycles/sec; 3) 5,000 cycles/sec; 4) 10,000 cycles/sec; 5) 20,000 cycles/sec.

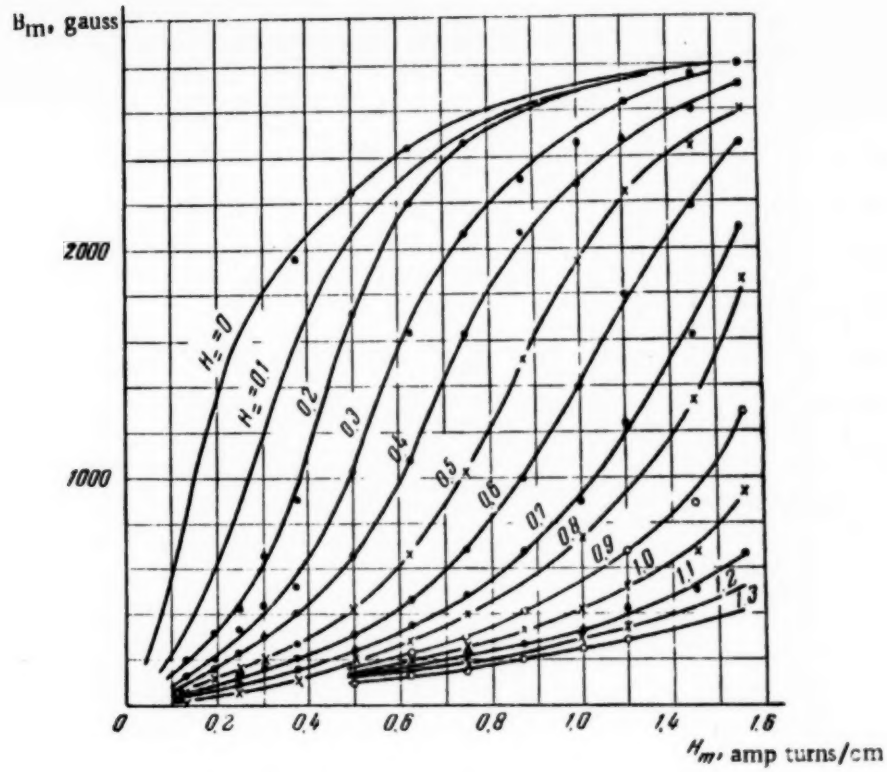

Fig. 6. Curves taken with ac and dc fields acting together on an oxifer-2,000 core at f = 5,000 cycles/sec.

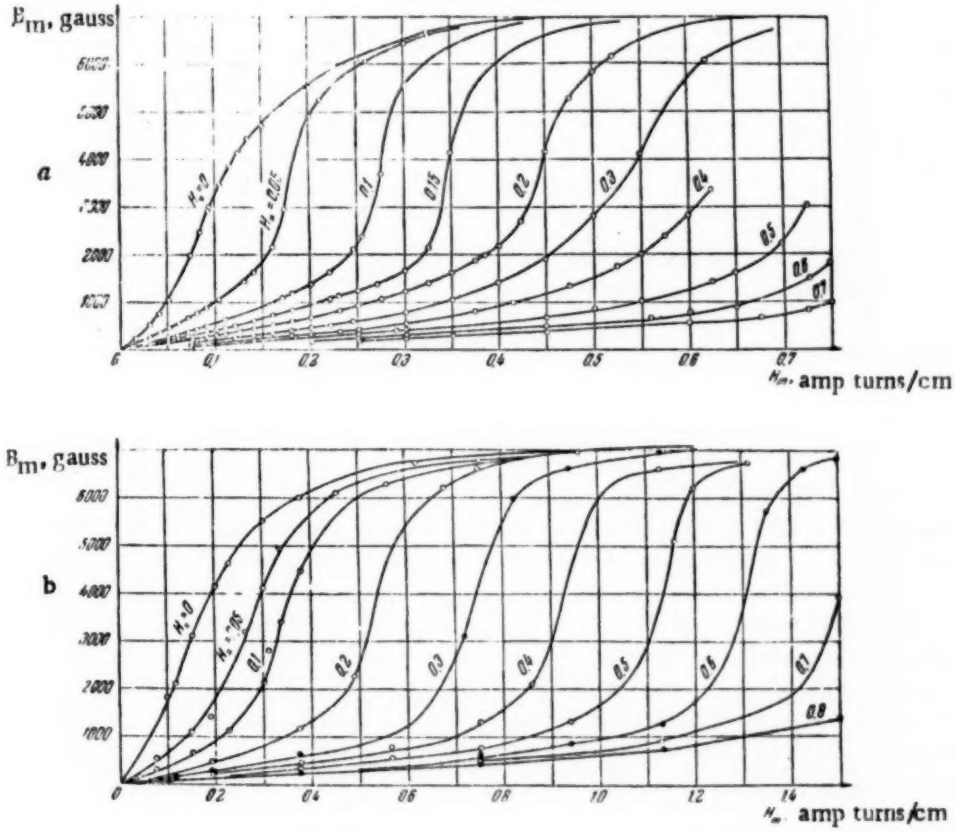

Fig. 7. a) 80NKhS alloy, thickness 20μ, f = 10,000 cycles/sec; b) thickness 10μ, f = 20,000 cycles/sec.

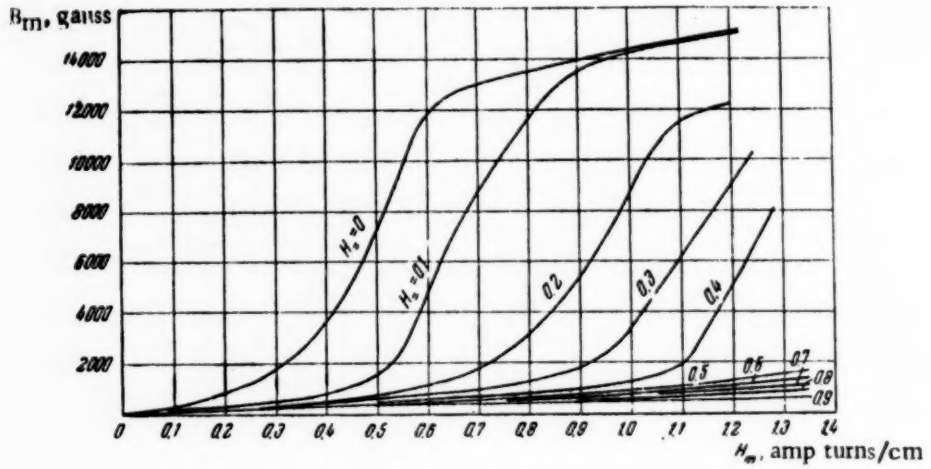

a

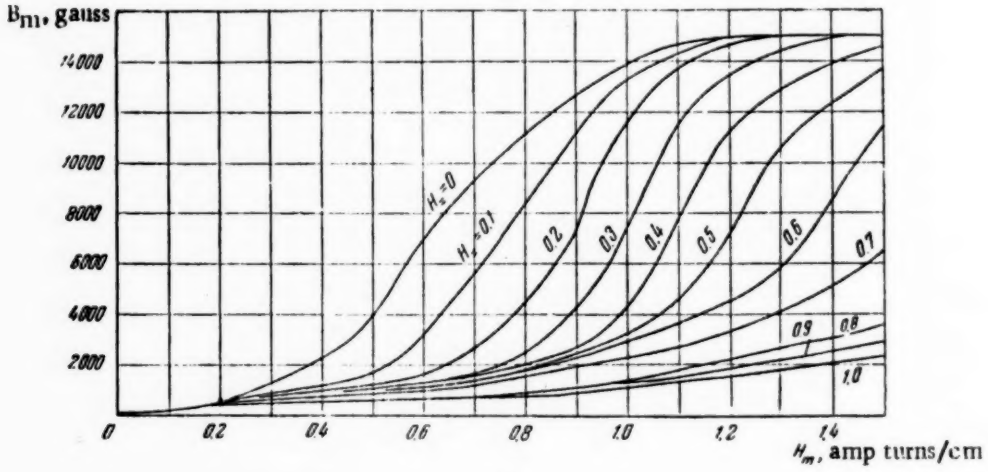

b

Fig. 8. a) 50NP alloy, 20μ thick, f = 10,000 cycles/sec; b) 10μ thick, f = 20,000 cycles/sec.

The cuves were drawn up in B_m, H_m coordinates, with

$$H_m = \frac{\sqrt{2}\,U_R W_{H\sim}}{R l_{av}},$$

where B_m is the maximum induction, U_R the voltage drop across the resistance, H_m the maximum field strength, $W_{H\sim}$ the number of turns on the magnetizing winding and l_{av} is the is the average length of a line of force.

TABLE 2

Ferrite type	μ_0 gauss/ oersted	μ max gauss /oersted	H_c oersted	B_s, gauss
Oxifer -2000	2000	7000	0.1	2500
Oxifer -1000	1000	3000	0.25	3200

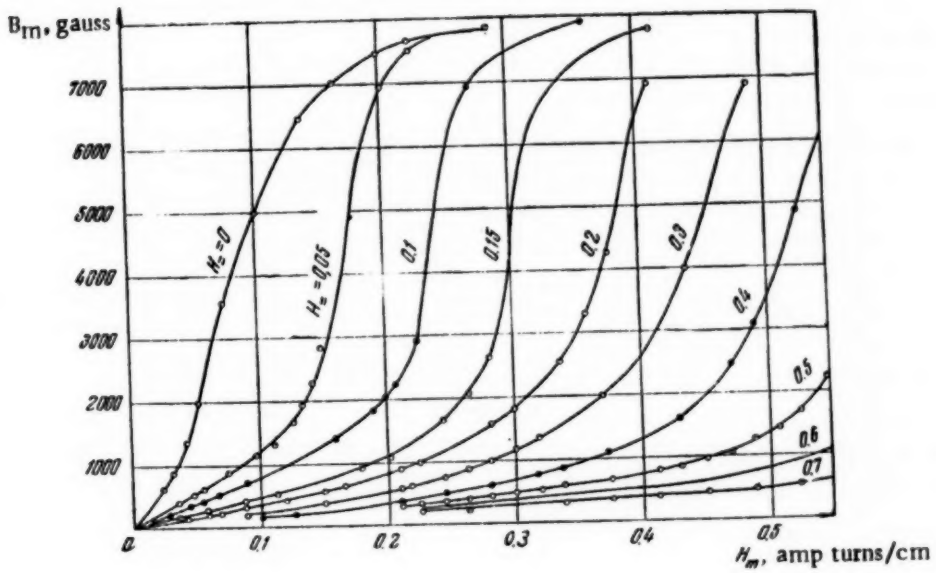

a

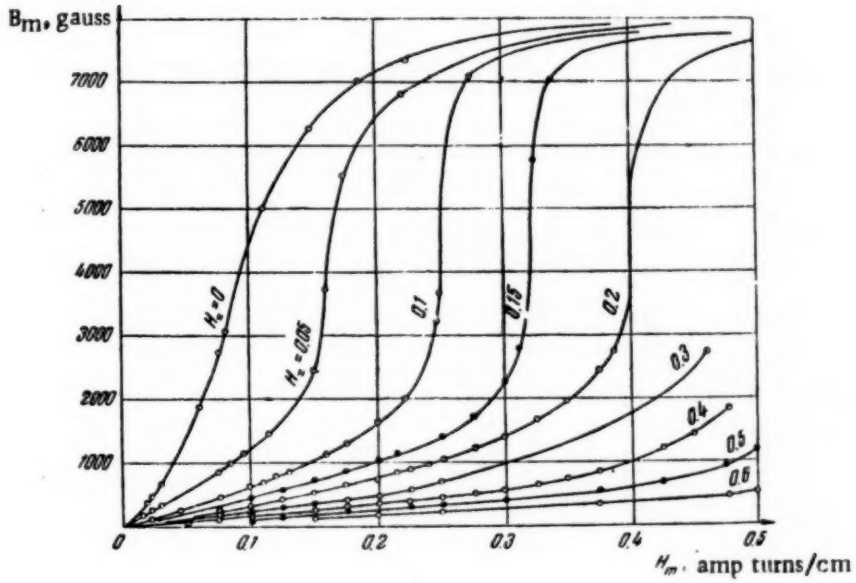

b

Fig. 9. a) 79NMA alloy 10μ thick, f = 10,000 cps; b) f= 20,000 cps.

The metal cores of high-frequency magnetic amplifiers are of small size and frequently have few turns of strip. Tests show that if the number of turns is less than five the air gaps between the turns begin to have an appreciable effect on the core quality. There is practically no difference between cores having unequal (large) numbers of turns. Figure 2 shows the principle curves for cores consisting of three and six turns of 80NKhS strip of thickness 20μ prepared from the same batch of material. The curves were taken at 5,000 and 20,000 cycles/sec. The differences increase at high inductions, where leakage has the greatest effect. The differences become less as the frequency is raised because the effects of losses begin to predominate over those of the air gaps.

Cores prepared at the Institute of Precision Alloys, Central Ferrous Metallurgy Research Insitute, were used in the tests. The cores had six turns of strip 10 mm wide and 10 or 20μ thick. The strip was wound on a ceramic former of 10 mm internal diameter; the core and former were annealed together.

The cores were tested for matching by comparing the principal magnetization curves, taken at 5,000 cycles/sec. A subsequent comparison of the hysteresis loops on an oscillograph at 50 and 500 cycles/sec gave the same result. In this way core selection for use at high frequencies was much simplified by using a device for recording hysteresis loops at industrial frequencies.

Figures 3-5 constitute a set of principle magnetization curves taken at 500-20,000 cycles/sec with 79NMA, 80NKhS and 50NP alloys. The curves enable one to evaluate the effect of increasing the frequency. The maximum magnetic permeability of 20μ 80NKhS strip falls by a factor 2.2 between 500 and 20,000 cycles/sec (Fig. 4). The 10μ strip shows a permeability lower by a factor 1.3 in the same frequency range. For 50NP (Fig. 5) the 500 and 1,000 cycles/sec curves practically coincide, at high frequencies the 10 and 20μ curves come closer together, the 10μ running slightly higher at 20,000 cycles/sec. Thus, while the 10μ 50 NP strip is somewhat worse than the 20μ up to about 10,000 cycles/sec, above this they are comparable, and above 20,000 cycles/sec the 10μ is to be preferred.

Figure 6 shows simultaneous ac and dc magnetization curves for oxiter-2,000. The curves are practically unaltered up to 20,000 cycles/sec. In this range the characteristics of 1μ strip of 79NMA, 80NKhS and 50NP (iron-nickel alloys) remain considerably better.

Similar curves are given for 80NKhS and 50NP at 10,000 cycles/sec for 20μ strip (Figs. 7a and 8a) and at 20,000 cycles/sec for 10μ (Figs. 7b and 8b). Curves taken at 10,000 and 20,000 cycles/sec for 10μ strip are given (Fig. 10).

LITERATURE CITED

[1] Technical conditions for iron-nickel alloys of the Ministry of Ferrous Metallurgy, Ferrous metallurgy technical specification 5010-55 and 4680-54.

[2] N. I. Sholts and K. A. Piskarev, "Oxide Ferromagnetics: Oxifers," Nauchno-tekhn. sbornik, No. 2 (OTI, Leningrad, 1954).

[3] I. B. Negnevitskii, I. K. Panina and V. P. Mishchenko. "Simultaneous ac and dc Magnetization Curves," Elektrichestvo 1953, No. 3-4.

[4] O. I. Aven, "Magnetic alloys for magnetic amplifier cores and their simultaneous ac and dc magnetization curves," Automation and Remote Control (USSR) 17, 4 (1956).*

[5] G. V. Subbotina, "Magnetic amplifiers fed at higher frequencies," Report of the Institute of Automation and Remote Control, Acad. Sci. USSR (1955).

Received September 29, 1956

*See C.B. Translation.

A RADIO REMOTE CONTROL SYSTEM FOR OIL FIELDS

K. V. Belevich, R. P. Demeskin, R. A. Il'in and G. B. Suvorov

(Moscow)

A radio remote control system using narrow channels for centralized well control in an oil field is described.

The oil extraction process used in eastern areas where gusher or deep-pumped wells are employed does not in principle require staff at the wellhead. But as the equipment may not operate properly, and thus cause large oil losses, and the wells are perhaps 0.5-1 km apart in eastern areas, many operators have to be present (about one per well). The producing fields in these areas cover several hundred square kilometers. Since the plants number over ten thousand it is clear that remote control methods should be widely introduced.

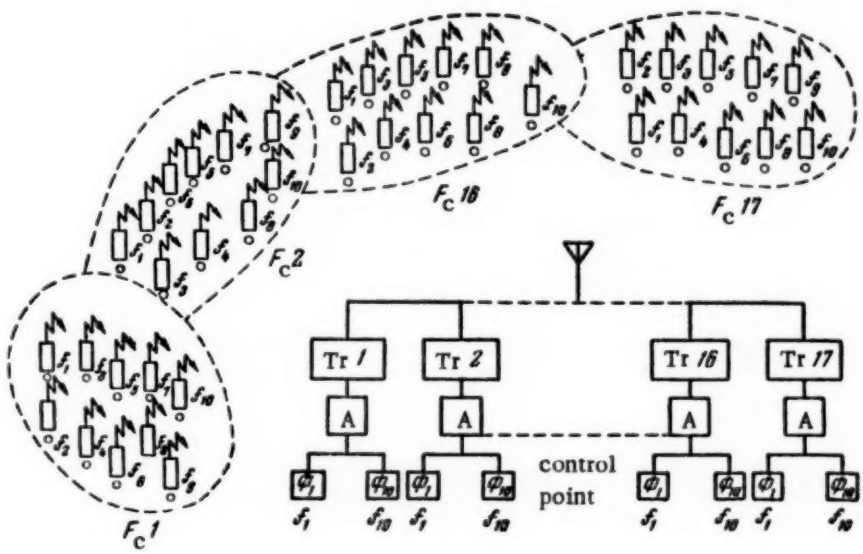

Fig. 1. Well grouping scheme, the signals being differentiated by frequency.

The Institute of Automation and Remote Control, Academy of Sciences of the USSR, in collaboration with the Oil Equipment Design Bureau (KBNP), has developed a radio remote control system using narrow channels for centralized well control, in accordance with its analysis of the principles on which systems for dealing with distributed objects are designed.

The system provides the following for each well:

1) automatic transmission of an alarm signal to the control point if the equipment does not function properly;

2) measurement of the oil flow by transmission of signals regarding the filling of the automatized measuring vessel;

3) a two-way radiotelephone link with the control point operator.

Figure 1 illustrates the principle on which the system is designed. The wells are split up into groups, each group being assigned a separate carrier frequency.

The R-106 radio transmitter, intended to replace field telephones, is used in the system; this has 18 fixed frequencies in the range 46.1-48.5 megacycles /sec. Its range is 10-12 km with beamed antenna in medium-rough country.

The signals from the individual wells are differentiated by assigning them separate subcarrier frequencies. The 300-3,000 cycles passband of the transmitter is split up into 20 channels. By making the frequency band for each well narrow the noise-stability is improved without introducing complexities. By using a frequency method of separating the well signals an apparatus of a single type became accessible, no matter what the number of wells in the field, and interchangeable unit principles could be used.

One of the 18 fixed frequencies was used for the radiotelephone link; therefore the maximum number of wells in the system is 17 × 20 = 340.

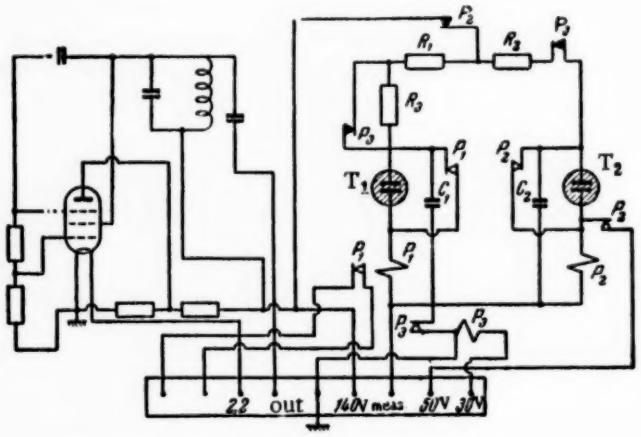

Fig. 2. Theoretical circuit of the remote control unit at the well.

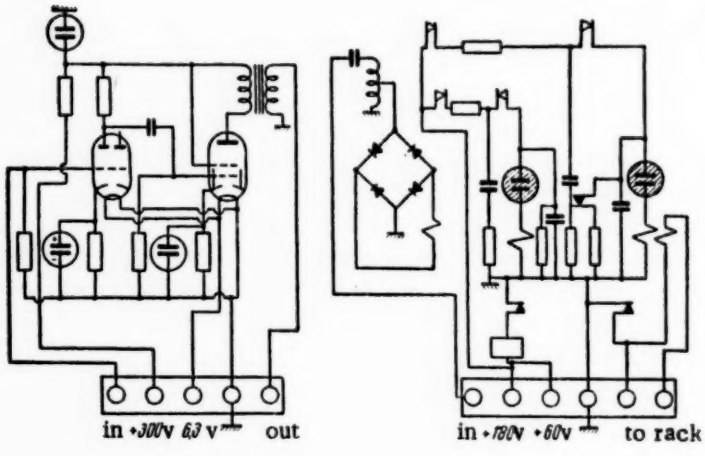

Fig. 3. Theoretical circuit of the group amplifier and decoder at the well.

All signals are transmitted as pulses of about 100 msec duration on the carrier and subcarrier frequencies. The alarm signal is simply single pulses repeated once per minute, while the filling signal is a single code group consisting of two pulses spaced 0.3 sec apart.

Figure 2 shows the circuit of the transmitter unit. The subcarrier generator has a normal transitron circuit; the subcarrier amplitude modulates the transmitter. The coding unit consists of two RC relaxation oscillators using gas-discharge tubes. Cold-cathode MTKh-90 thyratrons are used. The windings of the electromechanical relays P_1 and P_2 are connected in series with the thyratrons.

When the measuring vessel is full a contact closes which cuts in the common supply to the transmitter and remote control unit. The two relaxation generators begin to operate. The first (R_1, C_1, T_1) produces pulses at 0.3 sec intervals which key the transmitter. The second (R_2, C_2, T_2) is of longer period; when T_2 fires, P_2 operates and cuts off the circuit. Two pulses are generated up to the time P_2 operates.

The second generator is cut out when the alarm signal is sent and the frequency of the first is much reduced by inserting the resistance R_3.

The remote control apparatus at the well is insensitive to tube changes and works from -50°C to +50°C. The mean service life at the well without tube or other component changes has been increased to 2-3 years by choosing working conditions in which the apparatus is only switched on briefly while the remote control signals are being transmitted. This is less than 2% of the total time.

Figure 3 shows the output group amplifier circuit plus individual filters and decoders for the wells, which are established at the control point. The components are the same as in the coding device. A telephone register is included in the decoder output to record the number of vessel fillings, and a lamp to signal the alarm for the well. The control-point apparatus operates continuously.

The wellhead apparatus is built as a separate enclosed unit, while at the group point the equipment is rack-mounted with interchangeable units, one per 10 wells, plus a panel to cover the 10 wells. The number of units used is determined by the number of wells in the field.

An experimental setup of the apparatus was successfully tested in the "Tuimazaneft" field; it has been put into production. The Technical Committee of the Ministry of the Oil Industry of the USSR discussed it and resolved to put the system into large-scale use.

Wide use of the system will raise productivity by reducing the number of operators required considerably, increase the oil flow by ensuring early detection and rectification of faults, and improve the technical standard of work.

The system could also be used for remote control in other branches of the national economy.

Received May 14, 1957

REVIEW

THROTTLE – CONTROLLED HYDRAULIC AMPLIFIERS

V. A. Khokhlov

(Moscow)

The throttle-controlled hydraulic power amplifiers used in electrohydraulic servo systems and automatic controls are reviewed. The review was compiled from results published in the Soviet and foreign periodical literature and from results obtained at the Institute of Automation and Remote Control, Academy of Sciences of the USSR.

INTRODUCTION

Electrohydraulic systems are now widely used in automatic control. The success of such systems is largely determined by the use of hydraulic power amplifiers. Hydraulic devices which actuate the valves or other control devices of hydraulic effector mechanisms while simultaneously amplifying the input signal power are termed hydraulic amplifiers. By using such amplifiers the control step from electronic or magnetic amplifiers to the hydraulic effector is effected in a single unit. The distinctive features of hydraulic amplifiers are that the forces acting on the valves, including the flow reaction from the liquid, have no major effect on the comparatively low-power electromechanical converters and torque motors controlling the hydroamplifiers.

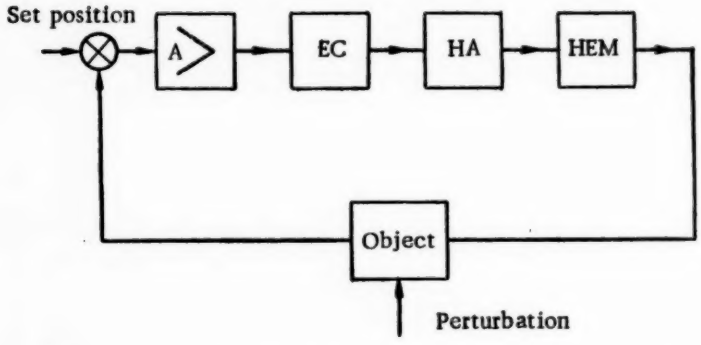

Fig. 1. Typical structural diagram of an electrohydraulic control system. A) an electronic or magnetic amplifier, EC) an electromechanical converter, HA) a hydraulic amplifier, and HEM) a hydraulic effector mechanism.

The advantages of hydraulic over other power amplifiers lie in their fast response, reliability, simplicity and compactness, together with high output power from small units, etc.

Figure 1 shows a typical structural diagram of an electrohydraulic control system containing a hydraulic amplifier.

Two types of this amplifier are used in control engineering, i.e., ones with throttle and with jet control. The first is more commonly used as it is simple and faster in response. Figure 2 shows the classification of throttle hydraulic amplifiers.

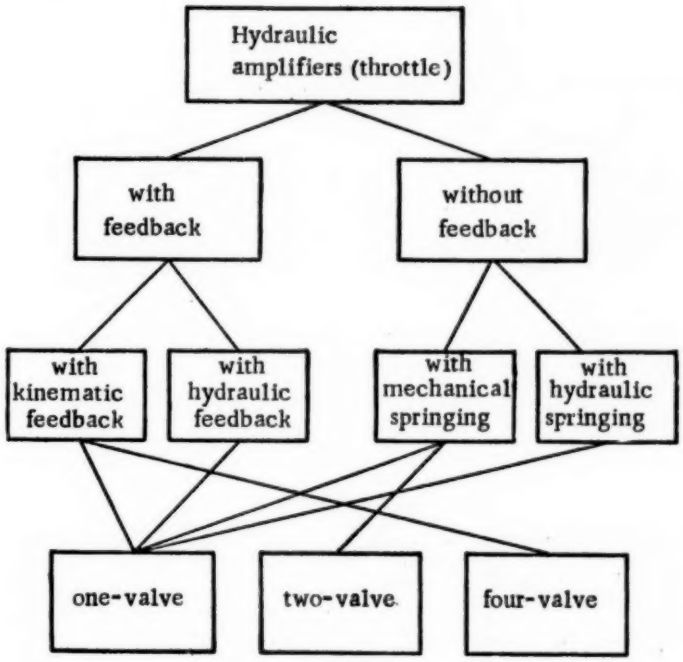

Fig. 2

1. Hydraulic Amplifiers with Feedback

One-valve amplifiers. The general system of a one-valve feedback amplifier used in one of the early makes of the Siemens electrohydraulic autopilot is shown in Fig. 3a. The main components are the control needle 1, the diaphragm 2, the needle block 3, the plunger 4 and the throttle insert constriction 5. Let us consider its operative principles. The oil at pressure P_0 enters the accessory chamber 7 and also chamber 8 via 5. The oil flows out into the return line from the working chamber via valve 6. The pressure in 7 remains constant at P_0. The pressure in the working chamber depends on the relation between the pressure losses in 6 and in the throttle 5. Thus the needle block is acted on by two forces: on the left, that generated by the pressure in the working chamber acting on the end face of the slide, and on the right, that produced by the pressure in the accessory chamber acting on the plunger. The slide comes to balance under these forces. This can only occur for a certain definite spacing between the control needle 1 and the diaphragm 2. If, for instance, the needle is displaced leftwards the pressure in the working chamber falls because more of 6 is uncovered. The accessory chamber pressure is unchanged. The block will therefore be displaced to the left by the plunger. The motion will continue till the working chamber pressure is restored to the original value. This will clearly occur when the slide has been displaced by the same amount as the control needle. A reverse displacement of the needle produces a motion to the right. Hence our hydraulic amplifier is a servo system with motion of the needle block following that of the needle. The feedback is effected via the slide valve.

In a later make of Siemens autopilot the hydraulic amplifier unit, which was very troublesome to make, was replaced by a simpler one. Fig. 3b shows the system. The response was improved along with the design. The improved response was achieved by increasing the working valve length and reducing the unbalanced forces exerted on the control needle 1 by the oil.

These amplifiers are designed to control flows bearing power up to 250 watts.

An amplifier using a similar principle and intended to control powers up to 5 kw has been developed at

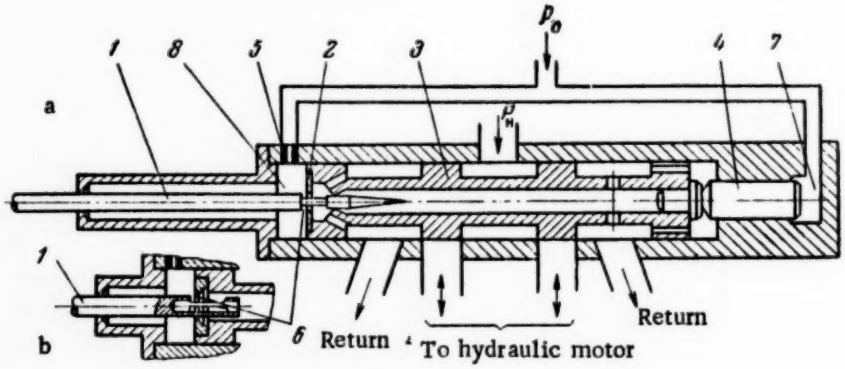

Fig. 3. Siemens hydraulic amplifier. P_H is the supply head pressure, P_0 the amplifier supply pressure.

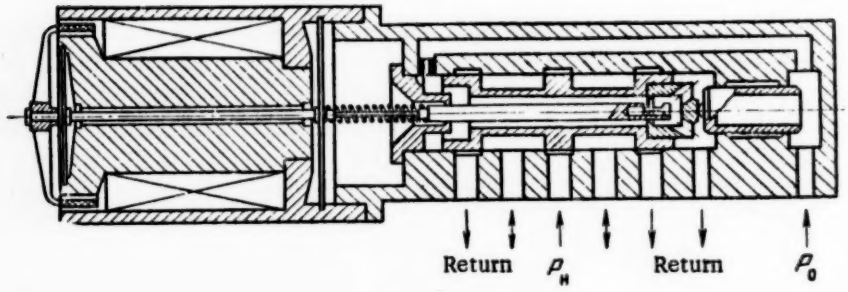

Fig. 4. Hydraulic amplifier designed at the Institute of Automation and Remote Control, Academy of Sciences of the USSR.

the Institute of Automation and Remote Control, Academy of Sciences of the USSR [1], the maximum electrical control power being practically the same as in the Siemens autopilot amplifiers.

Figure 4 shows the general design of this amplifier, together with the electromechanical converter. The amplifier specifications are as follows: maximum pressure fed to slide valve 50 atm; maximum liquid flow controlled by slide 50 liters/min; slide diameter 22 mm; amplifier time-constant 2 msec; control current range 20 ma; coil resistance 5000 ohms; resonant frequency of converter system 110 cycles/sec.

Figure 5 shows the amplitude and phase characteristics.

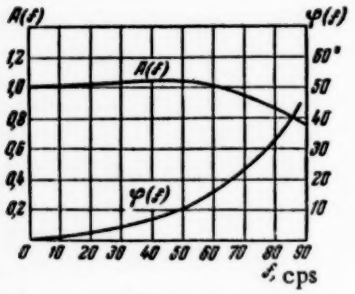

Fig. 5

Figure 6 shows a general view of a similar amplifier by AEG [2]. It is stated that the amplifier controls flows up to 6 kw. Time-constant 5-20 msec. The AEG unit is intended for program control, for controlling the rolls in rolling-mills, for use in copying machines and in power plant control.

A somewhat different design of single-valve amplifier is used in electrohydraulic regulators for water turbines [3].

Figure 7 shows the amplifier design used for this

purpose. The operative principles do not differ from those considered above, but a number of special design features occur. Control is via the stepped piston 2, and so the effector mechanism valve is not controlled by a needle or control slide but by the sleeve valve 1 coupled to the electromechanical unit 4. To relieve 1 from being forced by the oil pressure onto 2, and hence to reduce friction, the centering apertures 3 are provided. The special shape of these apertures, which become wider at the edge of the unit, reduces the oil thrust on 1 on the one hand, and also ensures a uniform hydrostatic pressure within, on the other.

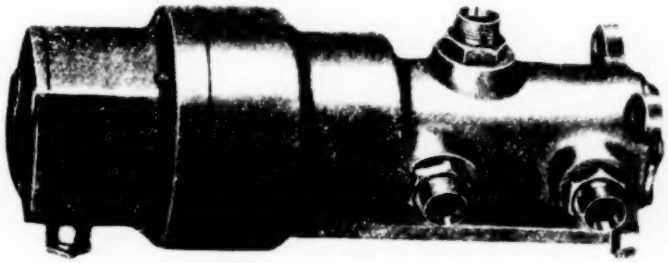

Fig. 6. General view of the AEG hydraulic amplifier.

Experiment shows that a force of about 1 kg is required to force 1 onto the piston. In this design the force produced by 2 is about 30 kg for a 0.1-mm displacement relative to 1. The hydraulic reaction on the slide valve does not then exceed 3 g. The maximum displacement speed of 2 is 30 mm/sec. The amplifier response characteristics are illustrated by Fig. 8.

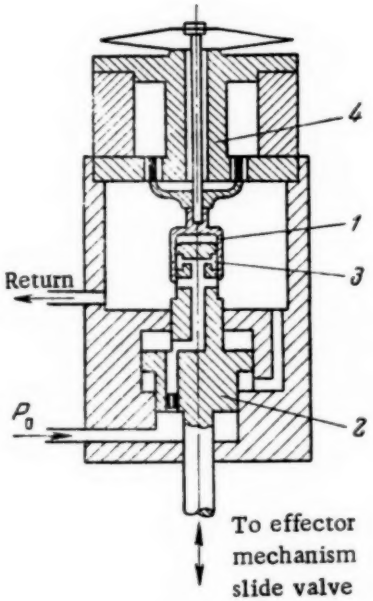

Fig. 7. Hydraulic amplifier for water turbine hydraulic regulators.

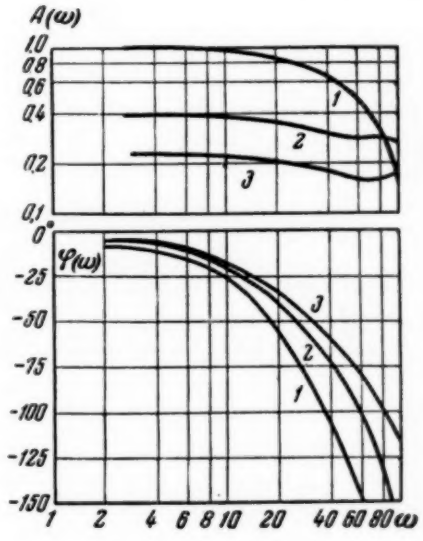

Fig. 8. Frequency characteristics of the water turbine hydraulic amplifier plus electromechanical unit. Curve 1: spring rigidity 20 g/mm; curve 2: 40 g/mm; curve 3: 88 g/mm.

The amplifier shown schematically in Fig. 9 is of some interest [4]. It is distinguished by the original rigid feedback, effected hydraulically. The operative principle is as follows. Suppose that at zero control signal, slide 1 is centered, i.e., that the working cylinder of the hydraulic motor is disconnected from both supply and return lines. The forces exerted by the oil on the left and right ends of slide 1 are then equal.

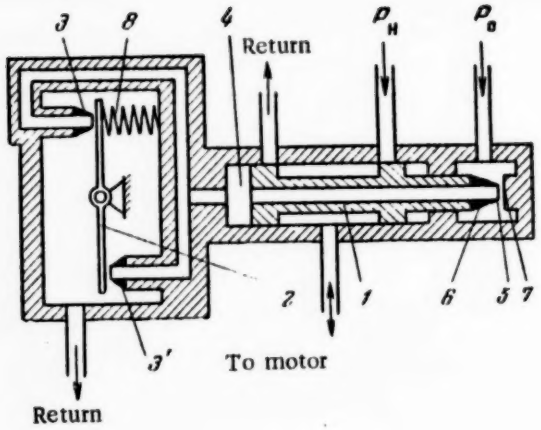

Fig. 9. Amplifier with rigid hydraulic feedback.

When a control signal is applied the electromechanical unit rotates the vane 2. Suppose the rotation to be clockwise. Since this increases the effective openings at 3 and 3'* the working chamber pressure falls. An unbalanced force will act from right to left on the slide and move it from the center position. The liquid flow through the throttle slot 5 (formed by the nipple 6 and the face 7) increases as the slide moves. The pressure drops at 3 and 3' increase; so does the pressure in the working chamber 4. Hence when the slide moves from right to left the pressure drops at the control throttles increase while that at the feedback one decreases. When the pressure in 4 reaches the initial value the slide ceases to move. The slide displacement is clearly determined by the displacement of the vane 2. If a control signal of opposite sign is applied the slide is similarly displaced to the right from the center position. Spring 8 serves to balance the pressures applied to 3 and 3' when there is no control signal.

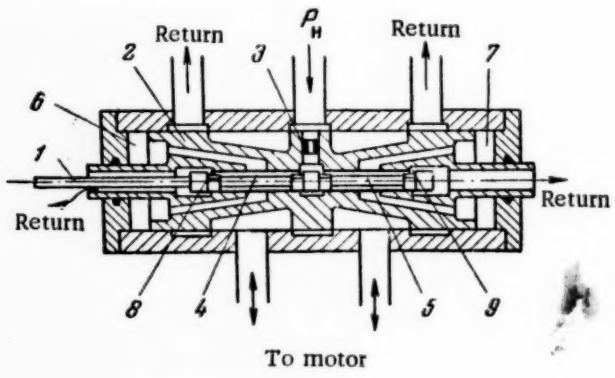

Fig. 10. Four-valve hydraulic amplifier (Institute of Automation and Remote Control, Academy of Sciences of the USSR).

The flaws in this amplifier are that the slide position is not linearly related to the control signal and that the liquid flow is inadequate. It is best used at small slide displacements (± 0.2-0.3 mm).

Four-valve hydraulic amplifiers. These have four control ports. This improves the response, sensitivity and accuracy, as compared with those considered above. But the construction is sometimes more complicated and adjustment difficult..

* Two throttles in parallel were used to reduce the motion required of 2.

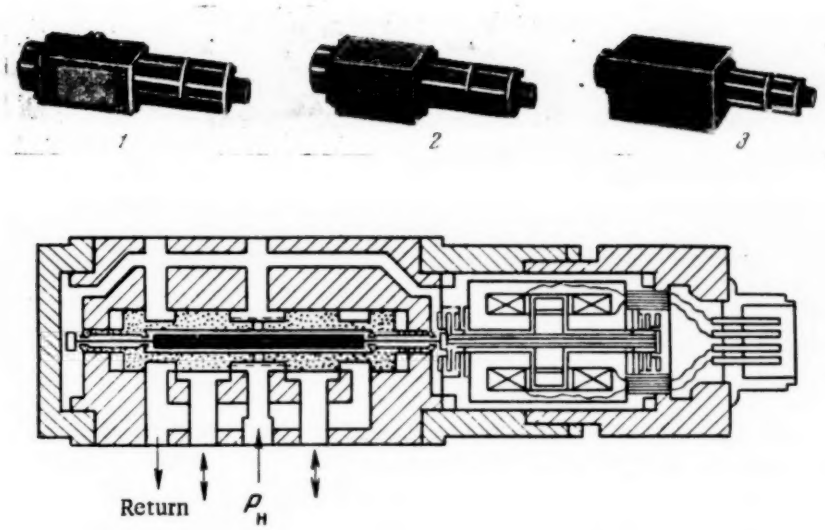

Fig. 11. Layout and exterior views of Pegasus hydraulic amplifiers.
1) Model 120; 2) model 140; 3) model 160.

One type of four-port amplifier has been developed in the Hydroautomatics Laboratory at the Institute of Automation and Remote Control, Academy of Sciences of the USSR. Figure 10 shows the system. The operative principle is as follows. The oil from the supply line enters the central cylindrical recèss in the control slide 1 via a fixed throttle 3. As there are axial gaps between the flange and the internal hole in the working slide 2 the oil enters the cavities 4 and 5. On the one hand these cavities are connected via internal channels to chambers 6 and 7, and on the other via the axial gaps 8 and 9 to return. The design is such that the gaps between the shoulders on 1 and the recess shoulders in the working slide 2 are equal when these are both in their center positions. The pressures in chambers 6 and 7 are then equal and the working slide is at equilibrium. It is clear that if the control slide is displaced from the center position the pressures in 6 and 7 are altered, one rising, the other falling. Then 2 is displaced by the unbalanced forces. It moves until the pressures in 6 and 7 become equal. Then 2 again occupies a position central with respect to 1. If 1 continues to move 2 will follow it.

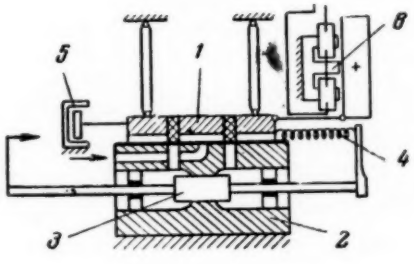

Fig. 12

Data have recently been published on four-port hydraulic amplifiers abroad. Pegasus states [5] that a series of such amplifiers has been put into production. Figure 11 shows the general design and an exterior view of the amplifiers this firm produces. The amplifiers are stated to have been designed especially for industrial use. They are compact, strong and reliable. Electronic or magnetic amplifiers can be used to control the hydraulic amplifiers. It is claimed that they are suitable for use in copying machines, power regulation equipment and for controlling pumps when complex problems of position, speed and load control are encountered.

The table gives the technical details of the Pegasus electrically controlled amplifiers.

A minature four-port amplifier with a flat slide is also of interest [6]. Figure 12 shows the general design. It consists of a flat control slide 1 tensioned by flat springs, the body 2, the working piston 3, the feedback

spring 4 and the damper 5. The amplifier is controlled by the torque motor 6. The design is such that the gap between 1 and 2 is 0.005 mm. The piston rod 3 is to be joined to the control device on the hydraulic effector (e.g., to its slide valve).

Parameter	Model		
	120	140	160
Working pressure in supply line, kg/cm^2	14—210	14—210	14—70
Maximum flow at 70 kg/cm^2, in liters/min	19	38	76
Slide diameter, mm	6.4	9.5	16
Internal consumption at 70 kg/cm^2, cm^3/sec	8	13	16.5
Range of change of control current, ma	±40	±40	±40
Time-constant, sec	0.001	0.00175	0.0025
Dimensions, mm	51×51×152	51×64×152	76×76×230

Consider the operation. Let us first assume that the torque motor control current is constant and that the force exerted by the feedback spring is balanced by that from the torque motor. A change in torque motor current causes the slide to be displaced and the working fluid is directed from chamber 7 to one of the working cylinders, the other being joined to the return. Piston 3 is displaced by the liquid pressure and alters the feedback spring tension. It will continue to move until the force from the spring equals that from the motor.

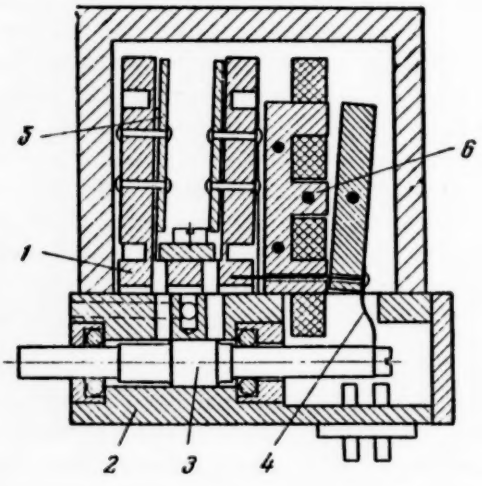

Fig. 13

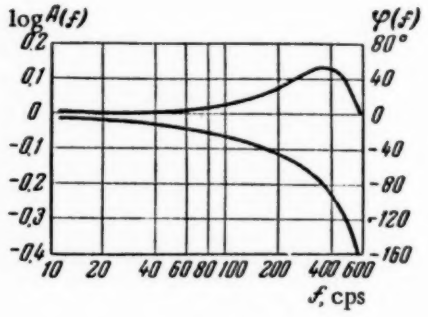

Fig. 14

Thus in the steady state any given force exerted by the torque motor will correspond to a quite definite position of the piston. The damper 5 is essential to ensure stability. Figure 13 shows the design.

The amplifier parameters are maximum slide displacement ± 0.1 mm, supply pressure 140 kg/cm^2, effective area of piston 0.16 cm^2, piston diameter 5.5 mm, maximum force on piston rod 22.7 kg, maximum speed of unloaded piston 45 cm/sec, liquid flow 8.2 cm^3/sec and control current 40 ma.

Figure 14 shows the amplitude and phase frequency characteristics, taken in combination with the torque motor and electronic amplifier.

An evident advantage of these hydraulic amplifiers, as being one variety of servo, is that their response is independent of supply pressure over a wide range. Their faults consist in the errors caused by reactive forces acting on the slide and also that the gain with respect to displacement is nonadjustable. The value of the latter is usually not greater than 1. An exception occurs in amplifiers where the feedback is either via elastic or hydraulic springs. In these the gain with respect to displacement can be greater than 1 if the parameters are suitably chosen.

The calculation of feedback hydraulic amplifiers and their equations of motion have been considered in [1].

2. Hydraulic Amplifiers without Feedback

One-valve amplifiers. Fig. 15a shows the design of a one-valve amplifier without feedback [7]. Let us consider its operation. At balance the force exerted on the slide 1 due to oil in the working chamber 2 pressing on its end face is balanced by the force from the spring 3. The pressure in 2 is then the same as that in chamber 4 between the throttles, being determined by the tension in the spring 5 on the ball valve. When a control signal is applied the moment developed by the electromechanical unit 6 alters the force on the ball. The force exerted by the arm 7 is assumed to coincide in direction with that exerted by 5. The pressure drop across the ball valve is then increased, and that across the throttle 8 decreased, if the supply pressure is constant. Hence the pressures in 2 and 4 rise and the slide begins to move to the right, compressing the spring 3. The new balance position will clearly be determined by the new pressure in 2 and by the stiffness of 3. If the direction of the force exerted by the electromechanical unit reverses due to change of sign in the control signal the slide will be displaced to the other side of the neutral position. Throttle 9 serves to hasten the damping of the natural oscillations of 1 during the transient period.

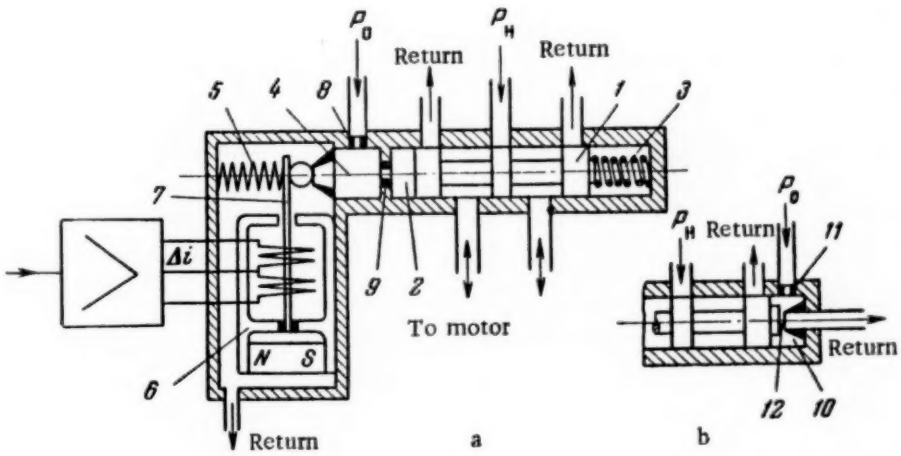

Fig. 15. Single-valve no-feedback amplifier.

The following are some parameters of this amplifier. It is designed to operate at working pressures up to 105 kg/cm^2 at flows of up to 16 liters/min. Slide diameter 6.4 mm. Diametrical gap between slide and case 5μ. The pressure in chamber 4, and hence in 2, changes by 42 kg/cm^2 when the ball is moved 18μ. Tests showed that in the working range of displacements the slide displacement was proportional to the control current. Figure 16 shows the frequency characteristics of electromechanical unit plus hydraulic amplifier. Total weight not more than 0.5 kg.

Let us consider an amplifier similar to the one above, but with the coil spring 3 replaced by a "hydraulic spring" (Fig. 15b). Oil under pressure from the supply line here enters chamber 10 via the fixed throttle 11. Because the oil continually escapes from 10 via the variable throttle 12 the pressure in 10 when 1 is at its equilibrium position will equal that in 2. When the pressure in 2 rises the slide may move to the right, reducing the area of 12 and hence increasing the pressure in 10. The slide ceases to move when the pressures in 2 and 10 are equal.

The use of hydraulic springs is advantageous when the slide motion is small (not more than 0.2-0.3 mm).

Two-valve hydraulic amplifiers. Figure 17 shows the general design of such an amplifier by Moog [8]. The operative principle is as above except that here the slide is controlled by two valves 1 and 2 simultaneously (Fig. 17). It is stated that this amplifier is highly sensitive, has linear characteristics, is of good response, and is reliable. The amplifier slide distributes the liquid at pressures of 70-210 kg/cm^2 at flows of 0.4-19 liters/min. The amplifier is controlled by an electromechanical converter. Maximum control current 40 ma.

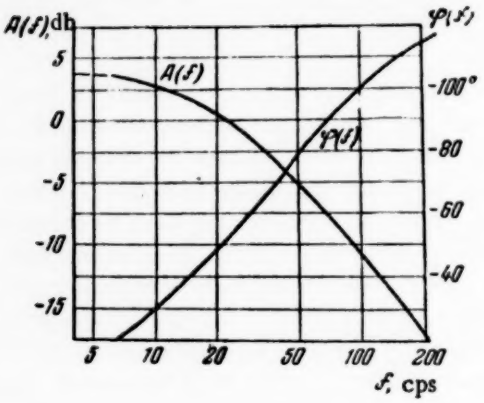

Fig. 16.

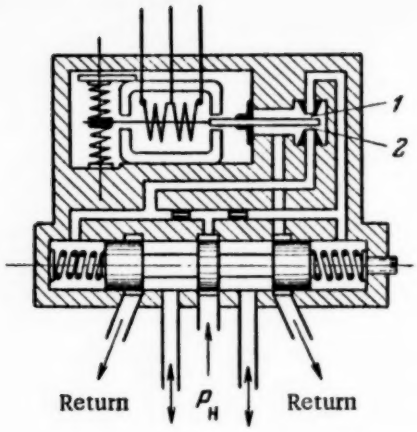

Fig. 17. General design of a two-valve no-feedback hydraulic amplifier by Moog.

It is stated that the amplifier is used in control systems in rockets, aircraft, radar equipment, copying machines and automatic packing devices.

An advantage of a hydraulic amplifier without feedback is that the gain with respect to displacement can be varied widely and can, in particular, be made greater than unity. This is because a large displacement of the slide occurs for a comparatively small movement in control throttle. The operation is also unaffected by reaction from oil flowing through the slide. •

A disadvantage is that the slide displacement depends on the supply pressure.

This review demonstrates that hydraulic amplifiers are high-grade devices as regards response and power in relation to size.

LITERATURE CITED

[1] V. A. Khokhlov, "Calculation and analysis of the dynamics of throttle hydraulic amplifiers," Automation and Remote Control (USSR) 17, 10 (1956).••

[2] Advertisement by AEG in Regelungstechnik, 1954, No. 2.

[3] E. A. Hardey, "An electrohydraulic regulator for water turbines," in Automatic Control (reports from a conference in Cranfield, 1951) (IL 1954) [Russian translation].

[4] D. P. Eckman, C. K. Taft and R. Schuman, Electrohydraulic Servomechanism with an Ultrahigh Frequency Response (Paper read at Am. Soc. Mech. Engrs.) 56-IRD-8, (1956).

[5] Advertisement by Pegasus Laboratories, Inc. in Control Engineering, 1955, No. 9.

[6] S. J. Lee and J. L. Shearer, "Development of a miniature electrohydraulic actuator," Trans. ASME 77, 7 (1955).

[7] W. R. Ahrendt, Servomechanism Practice (New York, 1954).

[8] Advertisement by Moog Valve Co., Inc., in Instruments and Automation, 1955, No. 5.

[9] S. J. Lee and I. F. Blackburn, "Contributions to hydraulic control, I; steady-state axial forces on control-valve pistons," Trans. ASME 74, 6 (1952).

Received December 27, 1956

• The flow reaction varies linearly with slide displacement, according to [9], and hence can be compensated by appropriate change in the return spring rigidity.

•• See C.B. Translation.

CHRONICLE

LENINGRAD SEMINAR ON AUTOMATIC CONTROL THEORY (1955-1956)*

E. N. Fomina

On January 21, 1955, P. A. Lebedev read a paper entitled "The stability of nonsteady-state motion during a finite time interval," in which it was shown that in studying the general case of nonsteady-state motion when the right hand sides of the perturbed motion equations

$$\frac{dx_i}{dt} = P_i(t, x_1, \ldots, x_n) \quad (i = 1, \ldots, n)$$

depend explicity on time but are not periodic time functions and are given only in the range $0 \leq t \leq T$, the problem of stability may be formulated in a form somewhat different from Liapunov's classical one.

Arguments were considered from which G. V. Kamenkov and another proposed to determine the stability in a finite time interval (see G. V. Kamenkov and A. A Lebedev, Comments on "Stability in a finite time interval," Applied Mathematics and Mechanics (USSR) 18, No. 4, 1954).

The paper was concluded with a statement of the principles of contructing the Liapunov functions for solving the above problem.

The paper has been published in full in the Transactions of the Moscow Aviation Institute, No. 50 (Oborongiz, 1955).

On February 24, 1955, T. N. Sokolov presented a paper "Quality indices in automatic control theory" in which indices to specify transient response in linear automatic control and servo systems with allowance for the type of external perturbation were proposed. Approximate expressions for the unbalance in terms of derivatives of the perturbation, the roots of the characteristic equation and the initial conditions were given, the error was estimated in terms of the system Q, and it was shown how system parameters could sometimes be chosen from the relations between the parameters and the error coefficients. This paper has been published in the Transaction of the Leningrad Polytechnical Institute (Radiophysics, No: 181, 1955).

In D. A. Bashkirov's paper of March 31, 1955 "Finding the roots of algebraic equations by successive division" Lin Nge-Shi's proposed integration method of finding the roots of algebraic equations was considered and the conditions for it to converge were given. Lin Nge-Shi's method consists in sucessive division of the initial equation by polynomials of first and second degree; it has the advantage of simplicity and requires less calculation than other methods of finding the roots. But some types of equation cannot be solved because the calculations diverge. The conditions for convergence show that divergence can occur if the roots differ little in modulus and some are complex. Then the equations have to be transformed to give new equations with roots differing greatly in modulus. A very simple method of estimating the roots directly from the coefficients in the equations was given; this is applicable to the roots which differ considerably in modulus from the others.

On June 9, 1955, I. A. Orurk** presented a paper "Use of integral equations for studying transients in complex linear and nonlinear systems." Part of the material has been published in the Transactions of the Krylov Naval Academy of Shipbuilding and Armament (No. 12, 1956). A method of studying complex systems using the Volterra integral was presented, using a series in the form of the polynomial

* The report for 1953-4 appeared in Automation and Remote Control (USSR), No. 3, 1955.

** Transliteration of Russian — Publisher's note.

$$x(t)+\int_0^t \sum_{k=1}^{n} a_k \frac{(t-s)^{k-1}}{(k-1)!} x(s)\,ds = f(t)+\sum_{k=1}^{n} b_k \frac{t^k}{k!},$$

where x (t) is the relevant co-ordinate of the dynamic system.

For a linear system with constant lumped parameters the integral equation is written directly from the coefficients a_k and b_k, where f (t) = 0. In systems with variable parameters and nonlinear elements the a_k are the coefficients of a general differential equation and are functions of time, of the coordinates, and of their derivatives; the b_k depend on the coordinates and the initial conditions.

The resulting integral equations are used for system analysis and synthesis. In numerical analysis a number of particular values of x (t_k) are found using three or four simple formulas with any order of equation for the system. The computational formulas for linear and nonlinear systems are analogous.

In linear system synthesis m unknown parameters can be selected in such a way that the transient response differs as little as possible from optimal. A system of m equations has to be solved for the m parameters, these equations being linear in a_k and b_k, which is not the case when integral methods are used.

This method gives a means of solving very diverse problems, is not laborious and requires no special training; the calculation is formulated as a series of algorithms which can also be used to program computers. It was stated that an approximate equation of algebraic form for the transient response of a linear system can be obtained from the integral equation.

At the same session N. G. Barinov presented a paper "Transient response construction for automatic control systems." The original differential equation for an automatic control system is transformed to a second-order Volterra integral equation with a series of the same form as in Orurk's method. The trapezium method is used, the ends of sections being joined up by using approximate values of the (n-1)-th order derivatives (n being the order of the differential equation).

In this way the input x_1 (t) and output x_2 (t) from the links of an automatic control system can be related in the following form:

$$x_{2(m)} = \beta_0 x_{2\,(m-1)} + \beta_1 x_{1(m)} + \beta_2 x_{1\,(m-1)}$$

for a link of transfer function

$$\frac{x_2(p)}{x_1(p)} + \frac{c_0 p + c_1}{a_0 p + a_1};$$

$$x_{2(m)} = \beta_0 x_{2\,(m-1)} + \beta \sum_{j=0}^{m-1} x_{2\,(j)} + \beta_2 x_{1(m)} + \beta_3 x_{1\,(m-1)} + \beta_4 \sum_{j=0}^{m} x_{1\,(j)}$$

for a link of transfer function

$$\frac{x_2(p)}{x_1(p)} = \frac{c_0 p^2 + c_1 p + c_2}{a_0 p^2 + a_1 p + a_2};$$

$$x_{2(m)} = \beta_0 x_{2\,(m-1)} + \beta_1 x_{2(m-2)} + \beta_2 \sum_{j=0}^{m-1} x_{2(j)} + \beta_3 x_{1(m)} + \beta_4 x_{1\,(m-1)} +$$

$$+ \beta_5 x_{1\,(m-2)} + \beta_6 \sum_{j=0}^{m} x_{1\,(j)}$$

for a link of transfer function

$$\frac{x_2(p)}{x_1(p)} = \frac{c_0p^3 + c_1p^2 + c_2p + c_3}{a_0p^3 + a_1p^2 + a_2p + a_3}.$$

The coefficients β are related to the transfer function parameters by simple algebraic relations. The formulas are used for deriving the transient response by proceeding from link to link. They are quite simple and give good accuracy.

The session of September 27, 1956 heard E. P. Popov's paper "Approximate study of transients in some nonlinear automatic systems by harmonic linearization." A method of studying oscillations of nearly sinusoidal form with rapidly changing amplitudes (heavily damped oscillations) was proposed. The method the author had previously described in "One generalization of Bogoliubov's asymptotic method in the theory of nonlinear oscillations" (Doklady Akad. Nauk USSR, 111, No. 2, 1956) was extended.

The first approximation formulas were deduced in the form

$$x = a \sin u, \quad \frac{da}{dt} = a\alpha(a), \quad \frac{du}{dt} = \omega(a),$$

where a is the oscillation amplitude (variable), α (a) and ω (a) being the damping and frequency parameters respectively, these being constant in a linear system, but here varying slowly with time. Since α can be large the amplitude may drop rapidly. It was shown that when the harmonic linearization coefficients q(a) and $q_1(a)$ vary slowly and smoothly, α (a) and ω (a) can be found as the roots of the characteristic equation of the harmonically linearized nonlinear system. The applied aspect of the method has been dealt with by Popov in Izv. Akad. Nauk SSSR, Otdel. Tekh. Nauk (Nos. 9 and 12, 1956),* where examples of high-order nonlinear systems are given. The method is extremely convenient for choosing the structure and parameters of nonlinear automatic systems of a certain class to conform with set requirements as to transient response.

On November 1, 1956 A. A. Voronov presented a paper "An approximate method of determining how self-oscillations are set up in certain nonlinear systems;" an approximate method of deriving the transient response in systems with one nonlinear element subject to stepwise perturbations was considered. The approximate solution is written in the form x = a sin ($\Omega t + \psi$), where a and ψ are time-functions, Ω being a constant, taken as the angular frequency of the steady-state self-oscillations.

After harmonically linearizing the nonlinear element equation and applying the displacement theorem to the equation, it is assumed that the higher derivatives are comparatively small in the displaced equations

$$\frac{d^k a}{\Omega^k dt^k} \ll \frac{da}{\Omega dt}, \quad \frac{d^k \psi}{\Omega^k dt^k} \ll \frac{d\psi}{dt} \quad (k = 2, 3, \ldots)$$

and a system of two shortened first-order nonlinear differential equations in a and ψ is obtained, the variables in the equation for a being separable. Using piecewise linear approximation to the nonlinear functions the solution is obtained in quite a simple form.

On November 29, 1956 A. D. Maksimov presented his paper "Improvement in the first approximation in vibrational linearization of nonlinear automatic systems." A method of finding the harmonics higher than the second when forcing perturbations are present was presented. Methods proposed by Pospelov and Popov were extended. The equation considered was

$$N(p)x + M(p)F(x, px) - H(p)x_f = 0,$$

where N (p), M (p) and H (p) are operator polynomials and F (x, px) a nonlinear function.

*See C.B. Translation.

The forcing action x_f was represented in series form

$$x_f = \sum_{k=1}^{m} c_k \sin k\omega_f t.$$

The solution is written as $$x = \sum_{k=1}^{m} a_k \sin (k\omega_f t + \varphi_k).$$

A method of calculating the amplitudes and phases of the higher harmonics was given. The behavior of the system in response to a comparatively low-frequency control signal when the linearizing action was of high frequency was examined. Two types of linearizing oscillation were considered, sawtooth and sinusoidal. Solutions were found with nonlinearities of backlash type in a generalized relay characteristic and square-law friction $F(x, px) = kx^2 \operatorname{sign} x$. It was concluded that vibrational linearization in systems with backlash type nonlinearities makes it possible to consider them as linear (in relation to low-frequency perturbations) with any type of linearizing vibration; a relay characteristic is linearized by sawtooth oscillations, while square law friction is not linearized.

The seminar program continues. Those desiring to participate should write to the secretary. Address: Leningrad, nab. Fontanki, d. 25., Institute of Electromechanics, Academy of Sciences of the USSR.

SEMINAR ON THE ENGINEERING APPLICATIONS OF MATHEMATICAL LOGIC (1955-1957)

N. S. Koval'

In October 1955, this seminar was begun at Moscow State University on the initiative of Professor S. A. Ianovskii. The meetings were arranged by V. I. Shestakov from the Physics Faculty.

Scientific workers, aspirants and engineers from research institutes and organizations participated, including ones from The Institute of Automation and Remote Control (IARC), Academy of Sciences of the USSR, the All-Union Insitute of Scientific and Technical Information, the Steklov Mathematical Institute of the Academy, the Laboratory for Scientific Problems of Telephony, the All-Union Polytechnical Correspondence Institute, the Moscow Electrotechnical Communications Institute, etc., plus also certain foreign scientists.

In 1955-1957 mostly problems of structural analysis and synthesis of contactor and electronic relay circuits were discussed. In all, 45 meetings were held, dealing with 37 papers. The original work of the participants and of certain others was reported.

The following original papers were presented and discussed.

G. N. Povarov (Institute of Automation and Remote Control) read his paper "Systematics of Boolean functions" on October 25, 1955, which dealt with the current state of the theory of types of Boolean functions and their applications in contactor circuit theory. Jevons considered the concept of Boolean function type in the 19th century, and later by D. Pol (J. Symb. Logic, Vol. 5, No. 1, 1940). Such functions of one type are realized by physically identical circuits. In this way, for instance, the synthesis of circuits with four receiver elements can be reduced to using tables of 402 type circuits (G. N. Poverov, Dissertation, Institute of Automation and Remote Control, 1954). An asymptotic estimate of the number of types of Boolean functions of n variables was presented and hence the number of physically distinct contactor two-terminal networks which realize these functions determined.

In Povarov's paper of October 25, 1955, "Synthesis method for symmetrical contact circuits with one input and k outputs" a graphical method for the purpose, also applicable to similar quasi-symmetrical circuits, was demonstrated. This is a modification of the author's earlier "stages" method, presented in algebraic form (Dokl. Akad. Nauk SSSR, 100, No. 5, 1955). After discussion the paper was published in "Avtomatika" No. 4 1956. The engineering presentation was published in "Priborostroenie" (No. 12, 1956).

V. N. Roginskii (Laboratory of Scientific Telephony Problems) read his paper "Graphical synthesis method for multiterminal contact circuits" (February 17, 1956) concerning the extension of Povarov's method (proposed October 25, 1955) to any (1, k)-terminal network. The conductivity between terminals is given as the numbers of states in which the circuit must or can be closed. This graphical method enables one to construct circuits without recourse to algebraic manipulations; the indistinguishable states which, when added considerably simplify the circuit, are taken into account automatically.

On March 15, 1957 G. N. Povarov read his paper "Extension of the 'stages' method to contactless relay circuits," in which part of his paper from Automation and Remote Control (USSR) 18, No. 2, 1957* was dealt with.

Problems of circuit synthesis for multicycle systems designed around contactless elements with relay actions were dealt with by N. S. Revunova (Laboratory of Scientific Telephony Problems). A class of multicycle

*See C.B. Translation.

asynchronous circuits built round contactless relay-action elements with internal pulse production, i.e., where the pulses are due to circuit (trigger) state changes, was considered. Equations describing the operation of such circuits were given together with a method of structural synthesis based on switching tables adapted to the operation of that class of system. Formulas were deduced for use in designing the circuits, and it was shown that the circuits could be simplified in structure by transforming the formulas corresponding to the structures.

Academician Gr. K. Moisil (Rumanian Peoples' Republic) gave two papers on the work of Rumanian scientists on relay systems theory. In the first (March 23, 1956) he reported analysis and synthesis methods for circuits with multi-position elements developed by himself together with Engineer G. Joanin (Academy of Sciences, Rumanian Peoples' Republic). Recurrent equation methods were used. Such methods for three-position relays were reported in the second paper (work done with G. Joanin and M. Nedelka). Three-valued logic was used in this method. The reports aroused great interest and led to a lively discussion.

A. N. Iurasov and T. L. Maistrova (VZPI) read a paper on "Methods of synthesizing circuits with reacting components" (April 20, 1956). Iurasov presented a method of equivalent transformations for circuits containing relay coils as well as contacts. Partial subtractions, bridge connections and windings with opposed magnetic fluxes were used in the method. Maistrova dealt with the use of implication operations for expressing the relations between the contact circuits and the relays controlling them.

In papers on "Circuits with contacts and resistances" (May 4, 1956) and "Synthesis of coding circuits with least numbers of contacts" (December 14, 1956) B. M. Rakov (All-Union Institute of Scientific Information) presented a method of synthesizing contact circuits containing resistors, used instead of rectifiers for separating various circuit currents. Matrix calculus was used to describe four-terminal networks. The method is applicable, in particular, to coding circuits (coders and decoders) containing fewest possible contacts. An example where an existing coding circuit was simplified by this method was described.

V. I. Ivanov (Institute of Automation and Remote Control) described his work on "A circuit for automatically seeking and recording results from searches" (October 12, 1956). This session was held at the above Institute. The apparatus developed by the speaker was demonstrated. The circuit was basically similar to Shannon's "mouse in labyrinth" circuit.

P. P. Parkhomenko (above Institute) described the principles and block system of his relay contact analyzer and compared its functions with that of the Shannon-Moore analyzer.

V. N. Roginskii, V. G. Lazarov and A. A. Arkhangelskaia (Laboratory of Scientific Telephony Problems) described a "Machine for designing multi-terminal contact networks" (November 16, 1956) and presented its main operating principles in relation to (1, k) − networks; this was produced at the above Institute on the basis of Roginskii's graphical method, reported on February 17, 1956.

B. M. Rakov and V. P. Cherenin reported on the "Experimental information machine at the Institute of Scientific Information" (February 15, 1957 and March 1, 1957). Cherenin dealt with the general problems in mechanizing documentation and information searches: the history of the subject, the information language problem, and methods of coding information. Rakov presented the main functional aspects of the E. I. M. information machine and its general structure; this machine was designed on the basis of an S80-1 sorting machine. The paper concluded by considering examples of using Boolean algebra for designing some relay circuits which control the sorting of punched cards in the machine.

S. M. Iakovlev (Institute of Automation) dealt with the use of Boolean algebra for synthesizing mechanical relay-action devices: "A method of analyzing and synthesizing combiner mechanisms" (November 30, 1956). He described a method he developed in 1947 for this purpose using Boolean algebra. The idea of combiner mechanisms was introduced; this covers various devices with a common functional structure (mechanical devices for centralized train signal control, mechanical coders and decoders in telegraph equipment, program units for weaving machines, etc).

V. I. Ivanov (above Institute) described "A circuit for establishing priorities in sequences of external actions" (April 5, 1957).

Synthesis problems for such circuits arose in connection with lifts for high buildings and filters at water stations. Examples were given of circuits designed to establish the sequence of on- and off- operations on

controlled objects in relation to externally applied sequences, and formulas for the general case were deduced.

A. D. Kharkevich (Institute of Scientific Telephony Problems) dealt with the classification of routing circuits and posed certain problems in the mathematical theory of such circuits in "Routing circuits and their use in automatic telephony" (December 7, 1956).

G. N. Povarov "An attempt at constructing a theory of combiner switching circuits" (December 28, 1956), formulated the main definitions and postulates in the abstract theory of such circuits, and briefly considered how this theory was related to those of logical networks and relay-contact circuits.

A. A. Markov (Mathematics Institute, Academy of Sciences) in "The invertor complexity of systems of functions" (December 21, 1956 and January 4, 1957) considered the minimization of the number of invertors in circuits consisting of conjunctors (units effecting the logical operation of conjunction), disjunctors (units effecting the logical operation of disjunction), and invertors (units effecting negativing). It was shown that in circuits effecting one given Boolean function this minimum number was dependent in a definite fashion on the properties of the sign variation of the function in increasing sequences of Boolean vectors. Circuits realizing systems of Boolean functions of $\underline{n}$ variables were also considered. It was shown that any such system can be produced from a circuit with a number of invertors not exceeding the number of digits resulting when $\underline{n}$ is expressed in binary notation. It was also shown that this estimate of the number of invertors cannot be reduced.

In Markov's second paper "Minimal contact – rectifier circuits for monotonic symmetrical functions" (March 22, 1957) such circuits containing only fixed contacts and rectifiers were considered which effect the above functions, i.e., those of the form

$$S_{n,m}(x_1 x_2 \ldots x_n) = \sum_{1 \leqslant i_1 < i_2 < \ldots < i_m \leqslant n} x_{i_1} x_{i_2} \ldots x_{i_m},$$

where Σ is the Boolean sum sign.

A theorem which states that the minimum number of contacts in a circuit realizing a function $S_{n,m}$ is $m(n - m + 1)$ was proved.

V. M. Grebenshchikov (Moscow State University) dealt with "The synthesis of a (1, k) network by Lunts' method" (April 19, 1957) and considered his own interpretation of Lunts' characteristic function. This function is considered as an expression in Boolean algebra for some two-terminal circuit contained in the multiterminal network. The variable a_{ij} in the function for the two-terminal circuit corresponds to some contact. The variable x_i corresponds to the wire joining contact a_{ij} to the upper terminal and x_j the wire joining the same contact to the lower. This interpretation was used in a commentary on some of Lunts' theorems.

On April 26, 1957 A. V. Kuznetsov spoke on "Interpretation of Lunts' characteristic function" the interpretation proposed being the reverse of Lunts' function. Each terminal M_i ($i = 1,2,\ldots,n$) of a network A stands in correspondence with the variable x_i, equal to unity when a voltage is applied to M_i, and zero otherwise. A function $G_A(x_{11}\ldots x_n)$ is introduced which is unity for any choice of $x_1,\ldots x_n$ possible with the conductors in the circuit, and zero if the choice is impossible. It was shown that $G_A(x_1,\ldots,x_n) = \Pi (x_i \longrightarrow x_j)$, where the product Π is taken over all pairs i, j for which the direct conductivity from M_i to M_j is unity, and $\longrightarrow$ is the implication sign. G_A is clearly the reverse of Lunts' characteristic function.

On May 10, 1957 V. N. Grebeneshchikov spoke on "A method of synthesizing multiterminal contact circuits," the proposed method being based on the sucessive removal of extraneous contacts. The parameters of the part remaining after removing each extraneous contact were determined on each occasion by solving certain systems of equations in Boolean algebra.

A number of participants spoke on topics from their published work. V. M. Ostianu (Institute of Automation) spoke on "Design of contact circuits using stepping switches" (October 21, 1955 – Dokl. Akad. Nauk SSSR, 103, No. 5, 1955). V. I. Ivanov (above Institute) dealt with "Cyclic relay systems and relationships in them" (Dokl. Akad. Nauk. 104, No. 2, 1955). O. B. Lupanov (Mathematics Institute, Academy of Sciences) dealt with "Possibilities of synthesizing circuits from arbitrary elements" (Dokl. Akad. Nauk SSSR, 103, No. 4, 1955).

Several review papers were also given: V. M. Ostinau on the work of Academician Moisil and his school on relay systems theory (July 10, October 14, December 13, and December 20, 1955, and April 13, 1956)

G. N. Povarov on the work of Czech scientists on contact circuit synthesis (February 24, and March 2, 1956); G. K. Moskatov on synthesis of magnetic switching circuits (February 22, and February 29, 1955); A. V. Kuznetsov on nonreduplicated circuit synthesis (December 27, 1955); G. N. Povarov (May 18, and May 25, 1956) on the use of the theory of Boolean function types in linguistics, from the work of V. Belevich; V. A. Purto (September 14, 1956) on the Bar-Khillel* logical method for analyzing language structure; G.N. Povarov (September 26, and October 5, 1956) on the cryotron, a super-conducting switching element, and on cryotron circuit synthesis; and V. N. Grebenshchikov on Lunts' method of synthesizing a (1, k) – network (April 12, 1957).

Most of the original work presented at the seminars has been published or is in press.

The success of the meetings over two years, which have brought together specialists from many research institutes and organizations, has facilitated the development and technical application of relay systems theory.

*Transliteration of Russian – Publisher's note.

GROWTH OF AUTOMATION IN THE USSR

(1917-1957)

The forty years since the Great October Socialist Revolution have been years of socialist growth unprecedented in history. Backward Russia has been transformed into a powerful industrial empire.

The October Revolution created the conditions for the rapid development of all branches of science and technology. During these years, along with other scientific disciplines, automation has developed intensively.

On the eve of the fortieth anniversary of the Great October Socialist Revolution, the Soviet Union has attained very significant success in the theoretical development and the practical utilization of automation. Planned development and systematic application of automation in different branches of the national economy began at the end of the first five year plan.

Industry, transportation, and communications of the USSR mastered in a series of important steps advanced means and methods of automation in only 25 years, of which 5 years were eliminated by the Great Patriotic War.

Let us cite several examples and comparisons which convincingly portray the accomplishments attained in this field during such a short historical period.

In 1932 in Erevan the first automated hydroelectric station having a power capacity of 2000 kw was put into operation. At the present time all regional hydroelectric stations in the USSR are automated, the total power capacity of which is over 6 million kw. Fifteen hydroelectric stations, each of which greatly exceeds the power capacity of the Erevan station, function unattended, that is, without constant attending personnel.

Some of these stations are equipped with auto operators. Taking into account the total load and pressure of the hydroelectric station, this equipment automatically turns on those units which ensure the greatest efficiency of the station as a whole. At the end of the first five year plan we did not have a single automated steam boiler, but now 75% (according to steam production) of the regional electric steam plant boilers are supplied with automatic combustion regulators. In 1950 in the USSR only one power system was capable of being controlled from a central dispatch point and equipped with means of remote control. This system included only 3.1% of the total power capacity of the power systems under the Ministry of Electric Stations.

At the present time, power systems which include 2/3 of the established power capacity are controlled from central dispatching points, having at their disposal modern automatic and remote control equipment.

In 1931 the Khar'kov Electromechanical Factory achieved at one of their blast furnaces the first successful experiment involving the mechanization and automation of feed, mixing and preparation of raw materials for smelting. At the present time the overwhelming majority of the blast furnaces (smelting over 90% of the pig iron) are not only mechanized but also have equipment for the automatic control and regulation of draft temperature and humidity.

Two hundred and thirty six Martin open hearth furnaces, producing approximately 90% of the country's steel, are equipped with means of automatic control and furnace thermal control.

In 1936-37 the first attempts at automating a blooming mill were made at the S. M. Kirov Makeevka Metallurgical Combine and now the basic mechanisms of three blooming mills are controlled automatically. Also a number of rolling mills were automated to a great degree. Among these are the No. 300 sorting mill of the Magnitogorsk Metallurgical Combine, the pipe rolling unit of the Pervouralsk New Pipe Factory, and

No. 70 MZMA triple shaft mill for the rolling of periodic profiles and others.

Soviet machine designers have achieved considerable success in the field of automation. The first small automatic production line consisting of five lathes was put into operation at the Stalingrad Tractor Factory in 1940.

Today many machine construction factories are successfully operating hundreds of automatic lines. This is amply illustrated by the following automatic lines: cylinder finishing, ball and roller bearings, motor shafts and rotors, plowshares and moldboards, hook and ship chains, rake teeth, bodies, valves , nuts and bolts, knitting needles, safety razor blades and other products. It should be emphasized that modern automatic lines, in contrast to the first ones, are more complex and incorporate various technological and transport operations.

At the First Government Ball Bearing Factory, which this year celebrated its 25th anniversary, a complex automatic shop produces ordinary bearings. The shop combines two lines for the production of ball bearings and conical roller bearings. All production processes, starting with the loading of primary materials and ending with packaging of the finished products, are automated. A group of engineers under the leadership of N. A. Volchek was awarded a Lenin prize for the creation of this shop.

Automation of railroad dispatching functions is becoming widespread, making possible control of switching and signaling at all stations extending over a distance of 150 to 200 kilometers. At a number of large stations a centralized electric relay-routing switching control system has been incorporated which determines the train's route after two push buttons on a panel corresponding to the starting point and the destination have been depressed. All available switches distributed along one of the possible routes of the train are transferred to the required positions, after which the necessary signal is automatically turned on. River transportation in a number of cases is automated by controlling flood gates and automatic vessel control equipment is being incorporated. Considerable success has been achieved in automating communications, in particular, telephone stations and radio-relay lines.

Automatic equipment has also been placed at the disposal of agriculture (automation of small hydroelectric stations, small power stations, elevators, mills etc).

The economic life of the city has become a serious consumer of automatic and remote control equipment (automation of water, gas and lighting systems).

Automation elements and means are utilized in trade and commerce (coin automats, weighing, packaging and sorting automats etc.), in banking (calculating machines), in office operations (office machines).

Automation has become an inseparable element in the life of the Soviet citizen. Automation elements and equipment play a vital role in the construction of refrigerators, gas hot water heaters, washing machines, radio receivers, telephones and automobiles.

It would be difficult to find a branch of technology in which there would be no application of automation and remote control. For instance, it is well known that the achievments of atomic power would have been impossible without automation. Automation plays a significant role in scientific research, particularly in interplanetary space research. One of the greatest accomplishments of modern science and technology, the launching of the first artificial earth satellite, would have been impossible had not some difficult problems of automation been solved.

Success in the field of automation would have been unthinkable without the requisite development of instrument and apparatus construction facilities in the USSR.

Prior to the Great October Socialist Revolution, automation and remote control equipment was made in single units in special workshops at Kronstadt, at the factories of Duflon and Konstantinovich, Tenishev, Ericson, Heisler, Gordeenko in Petrograd, but at the present time tens of large instrument and apparatus manufacturing plants located throughout the USSR manufacture in large production quantities a varied assortment of automation elements and equipment. Almost every large factory, every regional electric station and many oil enterprises have their own instrument and automation workshops and laboratories.

During the years of Soviet rule giant production centers were created in Moscow, Leningrad, Kiev, Kharkov, Sverdlovsk, specializing in the automating of leading branches of the national economy.

Automation instruments and equipment of advanced technical design have been created and put into use.

All of these paractical results would have been unthinkable without corresponding successes in the science of automation, without the proper organization of scientific research work in that field. Describing the condition of the present day network of scientific research institutes and laboratories, solving problems of automation, remote control and instrument construction, it is impossible not to remember that only during the start of the second five year plan, before the creation in the Academy of Science, USSR system of a special automation and remote control commission (1934), there was only one scientific research institute specializing in this firld in the USSR: the Scientific Research Institute of Remote Control (NIIT) and one institute of the field of instrument construction (Institute of Pyrometry in Leningrad), seven branch institutes whose structure consisted of automation laboratories and five factory laboratories where research and development work was conducted to automate production processes.

In 1957 the USSR possesses a branch system of scientific research institutes, laboratories and special construction bureaus solving scientific problems in the field of automation. In the recent past automation research institutes and laboratories have been organized in all the soviet republic acadamies of science, whereas before the war they used to be concentrated aroung Moscow and Leningrad. Scientific research institutes, laboratories and project-construction organizations were also created in the Ukrainian SSR, Uzbek SSR, Azerbaijan SSR, Georgian SSR and in other industrial centers such as Sverdlovsk, Novosibirsk, Gorky and others.

The condition of the science of automation before 1917, when it was in its infant stage, could be characterized by the presence of only a few initial works on the theory of automatic regulation, but in 1957 a foundation has been created for the formation of the theoretical principles of automation as a science dealing with self controlling equipments and systems.

A large group of scientific workers are successfully occupied with the problems of the theory of regulation, theory of relay circuits, automatic drive, automatic control, automatic protection, remote control, telemetering, theory and design of automation elements, and the theory of complex automation of production processes.

Suffice it to point out that over the last 20 years more than 1500 candidates' and doctors' dissertations have been defended in the previously mentioned fields. Over 90% of these dissertations have been completed during the last 12 years. The statistics of the scientific and technical publications (books and periodical publications) in the field of automation, remote control and instrument construction are indicative.

During the period of 1917 through 1956, 14,000 works including 3000 books and brochures were published.

These figures eloquently portray the unprecedented scope of the scientific research work in this field, especially during the post war period. It is notable that during the first post war five year plan the average yearly publication figure was 312 works and during the second post war five year plan it was 1380 works; in 1956, however, approximately 4000 works, including 600 books and brochures, were published.

It should be noted that a series of books, monographs, textbooks and articles dealing with various aspects of automation and remote control have been translated into other languages: English, German, Czech, Chinese, Rumanian, Polish, Bulgarian and others. Books and articles of soviet scientists and specialists have been translated not only in the national democracies but also in the USA, West Germany, and England. The journal "Automation and Remote Control" is systematically translated and distributed in the USA. Soviet automation has been represented at a series of international conventions and conferences dealing with questions of automation, cybernetics and automatic regulation. The reports of soviet scientific workers in the field of automation have provoked great interest and a lively exchange of opinions. The comments pertaining to the reports of USSR representatives show that our researches in the field of automation and, in particular, the theory of automatic regulation are at the world level of achievement.

In 1956 the Munich publisher R. Oldenburg published a book "Nichtlineare Regelungsvorgänge" containing the reports of a number of German and Dutch scientists in the field of regulation. It is notable that 50% of the quoted literary sources were Russian authors. Many such examples of references to Soviet works could be cited.

Analyzing the results of scientific investigations in the field of automation, it is necessary to single out the following results.

In the theory of automatic regulation methods of analyzing the stability of linear systems with lumped and distributed parameters and systems with delay have been developed. Methods of constructing stability regions have been developed. Methods of synthesizing linear automatic regulation systems with given quality requirements and considering external distrubances, including those of a random nature, have also been developed. A general theory of pulse control of linear systems has been worked out. An autonomous theory of regulation has been created and a theory of multicoupled, multinetworked and combined systems is being developed. Methods of solving stability problems of a wide class of nonlinear automatic regulation systems on the basis of regular methods of Liapunov function formation have been proposed. A series of effective approximation methods for the construction of transient processes in linear and nonlinear automatic regulation systems have been developed. The study of automatic regulation systems by means of phase planes has been brought to the engineering level. The same can be said of approximate methods for the analysis of nonlinear systems (the small parameter method, harmonic balance and others). Theory and design methods of automatic regulating relay systems have been developed. Methods of forming optimum automatic regulating systems have been developed. Effective experimental research methods for the study of automatic regulation systems have been proposed; in particular, methods widely using means of modern computing technology.

In the theory of structure of relay action systems, methods of analyzing relay circuits have been developed, a basis has been formed for the theory of structure of relay action systems, and a qualitative theory for the formation of remote control signals has been suggested.

New methods based on the theory of random functions for studying self-regulating systems are being successfully developed, as well as electronic simulation methods of these systems.

In other fields of automation, methods for the formation of automated drives (electric, hydraulic and pneumatic) have been developed. Principles for the formation of automatic control systems are being developed, passive as well as active.

General theoretical principles of the theory of construction of automation elements (transducers, relays, distributors, amplifiers and others) are being developed. A unit system of building instruments for automatic control and regulation has been proposed. Principles for the building of wire and wireless remote control systems have been developed. Contactless systems of remote control, utilizing semiconductor and magnetic elements, have been created.

During the period under discussion several schools have crystallized in the USSR, developing definite scientific trends and directions in automation. The majority of them are in the sphere of automatic regulation, which, as is known, constitutes one of the most important parts of the theoretical foundations of modern automation.

One of the first Soviet schools to be formed was that of Corresponding Member of the Academy of Sciences, USSR I. N. Voznesenskii which started in 1934 when the well known investigation on the theory of autonomous regulation was published. It is important to note that the object of this school's scientific activity was the study of complex systems with several regulated quantities (multicoupled) which are being widely used by modern technology. This school was born and developed at the I. I. Polzunov Central Boiler-Turbine Institute (TsKTI), and solved practical problems of boiler and turbine regulation.

Analogous problems were solved at the F. E. Dzerzhinskii All Soviet Heat Technology Institute (VTI). Starting in the thirties, a group of scientific workers and engineers of this institute grouped itself aroung Corresponding Member of the Academy of Sciences, USSR A. V . Shchegliaev and Professor S. G. Gerasimov and developed the theory of steam turbine and boiler regulation.

The schools at TsKTI and VTI had as their ultimate goal the study of the regulation of heat processes, whereas the group of scientific workers, created at the same time, at the V. I. Lenin All-Union Electrotechnical Institute (VEI) under the leadership of S. A. Lebedev and A. V. Mikhailov concentrated their main attention upon the automatic regulation of electrical machines and systems.

The VEI school made an important contribution to science by its development and application of frequency methods, which, as is known, received its greatest use in the theory of automatic regulation. Although the VEI did not maintain the leading role it played in the thirties and forties, many of its representatives, however,

became important scientific investigators and initiators of several directions of development in the theory of automatic regulation, which led subsequently to the development of a new class of equipment and regulating systems based upon the application of computer techniques.

The latter schools investigated thermal and electrical processes; the school of Corresponding Member of the Academy of Science, USSR B. V. Bulgakov, which appeared in the early forties at the Lomonosov Moscow State University, studied primarily mechanical processes, in particular, dissipative systems (gyroscopy, autopiloting and others).

The efforts of this school were directed towards the creation of analytical apparatus for the investigation of self oscillating nonlinear systems in the field of automatic regulation. Simultantously, this group of scientific workers and engineers, guided by the ideas of B. V. Bulgakov, made its contribution to the problem of dynamic accuracy of an automatic regulation system with disturbing forces of limited modulus.

Aviation technology has long attracted the attention of investigators working in the field of automation. At the end of the thirties, groups of scientific workers and engineers appeared at a series of our aviation organizations and dedicated their efforts to the study of stability, quality and dynamic accuracy of regulation. The N. E. Zhukovskii VVIA* played the leading role amongst these groups.

One of the important studies of this school, which was headed by Professor N. D. Moiseev in the forties, was the development of the so called technical stability theory in which regulation systems with a finite deviation and a finite time interval were investigated. This theory is very closely related to the problem of dynamic accuracy of systems with disturbing forces of limited modulus.

A definite contribution was also made by the VVIA in the development of a method for the evaluation of a regulation system by quadratic integrals. A great deal of attention, especially in the last few years, has been given by this school to nonlinear problems of regulation, in particular, to the damping of self oscillations in automatic regulation systems.

One of the newest and most effective schools of automatic regulation is that formed by Academician A. A. Andronov at Gorky. This group of scientific workers, under the leadership of A. A. Andronov, and with his close participation, investigated the phase space of an automatic regulation system with the aid of a method developed by him (point transformation of surfaces) and solved several fundamental problems in the theory of automatic regulation postulated during the second half of the last century.

Besides the relatively large schools mentioned, smaller scientific groups exist and thrive in a number of scientific research and learning institutes and organizations, developing theory of automatic regulation problems. Among these are the chairs of automation at the A. F. Mozhaisky LKVVIA,** M. I. Kalinin Leningrad Polytechnical Institute, the Moscow Power Institute and others. The largest group of scientific workers in the field of theory of automatic regulation is concentrated at the Institute of Automation and Remote Control of the Academy of Science, USSR (IAT AN SSSR). Being the central academic institute in the field of automation, the IAT AN SSSR has not limited its activity to the confines of one of the schools. In the process of solving actual problems in the theory of automatic regulation, the IAT AN SSSR has used and is using methods of various schools and, simultaneously, is developing new methods.

Scientific workers of the IAT AN S SSR have published tens of monographs and books and several hundred articles dealing with actual questions in the theory of automatic regulation, which not only summarize scientific results obtained in this field, but also present new concepts, principles and methods.

Among the works of IAT AN SSSR in this field, the following investigations should be singled out: stability of nonlinear automatic regulation systems, relay and pulse automatic regulation systems, statistical dynamics of automatic regulation systems, utilizing methods and systems of mathematical simulation to analyze automatic regulation systems, optimum automatic regulation systems, combination automatic regulation systems and others. The IAT AN SSSR has achieved considerable success in the theory of relay circuits. Development of the scientific principles of automation elements and equipment is being furthered.

*Translator's note: Military Aeronautical Engineering Academy.

**Translator's note: This is also a Military Aeronautical Engineering Academy, probably located in Leningrad.

The Academy of Science, USSR devotes a great deal of attention to the development of scientific efforts in the field of automation. Starting with 1935, a number of conferences in the Academy of Science, USSR system were held dealing with automation questions, including the First All-Union Conference of Automation, Remote Control and Dispatching (1935), the Second All-Union Conference on Automatic Regulation Theory (1953), the AN SSSR Session on Scientific Problems of Automation (1956). Not only the Academy itself but the branch scientific research institutes and laboratories actively participated in all the conferences. The results of the conferences graphically show that during the last two decades the theory of automatic regulation has been transformed from a small branch of mechanics into an independent scientific discipline which at the present time constitutes one of the basic branches of automation as a science of self controlling equipments and systems.

On the basis of scientific accomplishments, highly effective automatic and remote control elements, equipments and systems have been created and put into use.

Experienced scientific and technical personnel in the field of automation and remote control have been trained. A system of scientific investigation, design and construction, and instrument construction organizations has been created, the cooperation of which insures the planned growth of automation in the leading sectors of the national economy.

However, no matter what our successes have been in the field of automation, they still do not correspond to the rapidly growing demands of production. Describing the condition of the science of automation as a whole, it is necessary to point out the unevenness of the development of certain branches and, in particular, the lag in automatic control theory, theory of construction of automation elements and the theory of complex automation. It is also important to note that insufficient attention has been given to the general questions of automation, to the scientific classification of automation elements and equipment and to the problem of economic efficiency of automation.

The directives of the Twentieth Congress of the Communist Party of the Soviet Union define the direction and the work program for the automation of production processes for the period of 1956 to 1960, presenting new demands and placing new problems before our science.

Automation must become one of the basic means for the sharp increase in the productivity of labor in all the important sectors of our national economy. It would be difficult to overestimate the role of science in the solution of this problem.

Successes achieved during the previous years in all sectors of socialist growth inspire Soviet scientists towards newer creative exploits which will bring the country of socialism to even greater accomplishments in all spheres of science and technology.

ON THE THEORY OF OPTIMUM REGULATION

N. N. Krasovskii

(Sverdlovsk)

Problems of optimum regulation (at high speed) are constantly assuming greater importance. Substantial results were obtained in this field by A. A. Fel'dbaum [1-3] and recently L. S. Pontriagin, V. G. Boltianskii, and Gamkrelidze [4]. The formulation of the problem given below differs somewhat from the formulation of the problems investigated in the papers [1-6], where it was assumed that during each moment t of the transient process, the magnitudes of the controlling values of $u_k(t)$ were limited. Here it is assumed that the controlling value, whose magnitude is determined, generally speaking, by the behavior of the function $u_k(t)$ during the full interval of the transient process, is limited (an accurate formulation is given in Part 1). Along with the case of limiting of $u_k(t)$ during each moment t, such a formulation of the problem includes a series of other cases. An example could be the problem of maximum speed with limited average (in a specific sense) values of $u_k(t)$ during the transient process. The last condition corresponds to the limiting of such characteristics of the controlling values as average power, pulses, etc.

The effective method developed in [4] can be generalized for these cases also. The formulation described above also makes another approach to the problem appropriate. That approach is presented in this article. In the cases coinciding with those investigated in the quoted works, the method chosen below leads to analogous results. Some sufficient conditions for the existence of optimum trajectories are given in this article; approximate methods for the determination of these trajectories are described.

In the formulation of the problem used in this article it is assumed, as in [1-6], that the basic part of the system has given constant parameters [the form of function X_i in Equation (1.1)]. The problem of optimum high speed when these parameters can be selected is investigated in N. G. Chetaev's article [7] (when $u = 0$).

1. Let the behavior of the regulated system be described by the equation

$$\frac{dx_i}{dt} = X_i(x_1, \ldots, x_n, t, u_1, \ldots, u_r) \quad (i = 1, \ldots, n), \tag{1.1}$$

where $x_1, \ldots, x_n$ are coordinates of a describing point in a phase space of the system, and $u_1, \ldots, u_r$ are controlling values. Given: the time $t = t_0$, the point $\{x_{10}, \ldots, x_{n0}\} \equiv x_0$ and the moving point $x_i = \xi_i(t)$ ($\xi_i(t)$ are continuous functions).

The trajectory of the (1.1) system, where functions $\eta_k(t)$ are substituted in place of values u_k, we will designate by the symbol $x_i(x_0, t_0, \{\eta_k\}, t)$, at the same time $x_i(x_0, t_0, \{\eta_k\}, t_0) = x_{i0}$.

It is necessary to determine the function $u_k^0(t)$ so that the trajectory of $x_i(x_0, t_0, \{u_k^0\}, t)$ coincides with the point $x_i = \xi(t)$ in the shortest possible time $T = t - t_0$. Piecewise continuous functions $u_k(t)$ are permitted, restrained by the condition

$$g_T(u_1(\tau), \ldots, u_r(\tau)) \leqslant N. \tag{1.2}$$

Here N is a constant value or a function of the variables $x_{10}, \ldots, x_{n0}$, T, g_T, the given functional corresponds to that type of limiting on the function $u_k(t)$ which occurs in the problem under investigation; that is, g_T is a value whose magnitude is computed according to the definite rule corresponding to the functions $u_1(\tau)$, $\ldots$, $u_r(\tau)$, given at the segment $t_0 \leq \tau \leq t_0 + T$.* For instance, in the case of limiting

$$|u_k(t)| \leqslant N \quad \text{for.} \quad t \geqslant t_0, \quad k = 1, \ldots, r \tag{1.3}$$

it is necessary to place $g_T(u_1(\tau), \ldots, u_r(\tau)) = \max |u_k(\tau)|$ when $t_0 \leq \tau$, k = 1, . . ., r; if the sum of the average squares of the functions of u_k is limited by the number N during the time of the transient process, then

$$g_T(u_1(\tau), \ldots, u_r(\tau)) = \frac{1}{T} \int_{t_0}^{t_0+T} \left[\sum_{k=1}^{r} u_k^2(\tau)\right] d\tau \leqslant N.$$

We will call the formulated problem the optimum regulation problem. The trajectory $x_i(x_0, t_0, \{u_k^0\}, t)$, which satisfies the conditions of this problem we will call the optimum trajectory; the functions $u_k^0(t)$ will be the optimum controlling functions, and T will be the optimum time of the transient process.

We will describe one method of solving the problem. Let $t > t_0$ be an arbitrary but fixed moment of time and $\eta_k(\tau)$ be functions satisfying the conditions

$$x_i(x_0, t_0, \{\eta_k\}, t) = \xi_i(t) \quad (i = 1, \ldots, n). \tag{1.4}$$

At this point no other conditions are placed upon η_k.

Considering the value of t fixed, we find

$$F(t) = \min g_T(\eta_1(\tau), \ldots, \eta_r(\tau)) \quad (t_0 \leqslant \tau \leqslant t) \tag{1.5}$$

under the conditions of (1.4). Obviously, the optimum time of the transient process T will be the smallest of the numbers $\theta = t - t_0$ satisfying the condition

$$F(t) = F(t_0 + \theta) \leqslant N, \tag{1.6}$$

and corresponding to this value of $t = t_0 + T$ are solutions of the variational problem (1.5)-(1.4); functions $\eta_k(\tau)$ will be the optimum controlling functions $u_k^0(\tau)$ $(t_0 \leq \tau \leq t_0 + T)$.

2. Let us investigate the problem of optimum regulation with Condition (1.2) in the form

$$\int_{t_0}^{t_0+T} G[u_1(\tau), \ldots, u_r(\tau), \tau]\, d\tau \leqslant N \quad (N = \text{const}), \tag{2.1}$$

*We will designate time by the letter τ also.

where $G[u_1, \ldots, u_r, \tau]$ is a nonnegative function differentiated with respect to u_k.

To solve the problem (1.5)-(1.4) it is necessary, as is known [8], to calculate the variation δh of the functional

$$h[\{\eta_k\}] = \int_{t_0}^{t} G[\eta_1(\tau), \ldots, \eta_r(\tau), \tau]\, d\tau + \sum_{i=1}^{n} \lambda_i x_i(x_0, t_0, \{\eta_k\}, t), \tag{2.2}$$

where $\lambda_i = \lambda_i(t) = \text{const}$ with $t = \text{const}$, and solve the equation

$$\delta h = \int_{t_0}^{t} \left[\sum_{k=1}^{r} \frac{\partial G}{\partial \eta_k} \delta\eta_k \right] d\tau + \sum_{i-1}^{n} \lambda_i \delta x_i(t) = 0. \tag{2.3}$$

The variations $\delta x_i(t)$, corresponding to the variations $\delta\eta_k$, can be considered solutions of a linear system of first approximation:

$$\frac{d\delta x_i}{dt} = \sum_{j=1}^{n} \frac{\partial X_i}{\partial x_j} \delta x_j + \sum_{k=1}^{r} \frac{\partial X_i}{\partial u_k} \delta\eta_k \quad (\delta x_i(t_0) = 0, \quad i = 1, \ldots, n), \tag{2.4}$$

where the values $\partial X_i / \partial x_j$, $\partial X_i / \partial u_k$ are calculated at the points of the curve $x_i(x_0, t_0, \{\eta_k\}, t)$ when $u_k = \eta_k$. We will designate by $\varphi_{ji}(t)$ the fundamental matrix elements of the solutions [9] of the homogeneous system (2.4) (when $\delta\eta_k = 0$);* $\psi_{ij}(t)$ are the inverse matrix elements of the matrix $\| \varphi_{ji} \|$. Using the formula for the solutions of linear heterogeneous systems [9], the variation $\delta x_i(t)$ can be written as

$$\delta x_i(t) = \int_{t_0}^{t} \left[\sum_{j,l=1}^{n} \sum_{k=1}^{r} \varphi_{ij}(t) \psi_{jl}(\tau) \frac{\partial X_l}{\partial u_k} \delta\eta_k(\tau) \right] d\tau \quad (i = 1, \ldots, n). \tag{2.5}$$

Substituting the value $\delta x_i(t)$ in Condition (2.3) and breaking this condition up into r conditions, because the variations $\delta\eta_k$ are arbitrary ([8], page 210), we obtain the system of equations

$$\frac{\partial G}{\partial \eta_k} + \sum_{i,\, j,\, l=1}^{n} \lambda_i(t) \varphi_{ij}(t) \psi_{jl}(\tau) [\partial X_l / \partial u_k] = 0 \quad (k = 1, \ldots, r), \tag{2.6}$$

which in conjunction with Conditions (1.4) can determine the value $\lambda_i(t)$ and the functions $\eta_k(\tau)$.

Let us examine a linear case. Let the system (1.1) have the form

$$\frac{dx_i}{dt} = \sum_{j=1}^{n} p_{ij}(t) x_j + \sum^{r} q_{ik}(t) u_k + f_i(t) \ (i = 1, \ldots, n), \tag{2.7}$$

*That is, the functions $\delta x = \varphi_{ji}(t)$ $(i = 1, \ldots, n)$ are solutions for the system (2.4) (for each fixed value of j), where $\delta\eta_k = 0$; besides this, $\varphi_{ii}(t_0) = 1$, $\varphi_{ij}(t_0) = 0$ when $i \neq j$.

where $p_{ij}(t)$, $q_{ik}(t)$, $f_i(t)$ are continuous functions of time; the function $G[u_1, \ldots, u_r, \tau]$ is a positive definite quadratic form:

$$G[u_1, \ldots, u_r, \tau] = \sum_{k,m=1}^{r} a_{km}(\tau)\, u_k u_m > 0 \text{ where } \sum_{k=1}^{r} u_k^2 \neq 0. \tag{2.8}$$

The Condition (2.1) with the G of (2.8) can be encountered when the average power (useful or dissipated) is limited and when the controlling factor is current amplitude. In cases (2.7) and (2.8) Equations (2.6) become a linear system

$$2\sum_{m=1}^{r} a_{km}\eta_m + \sum_{i,j,l=1}^{n} \lambda_i(t)\,\varphi_{ij}(t)\,\psi_{jl}(\tau)\,q_{lk}(\tau) = 0 \quad (k = 1, \ldots, r) \tag{2.9}$$

Conditions (1.4) in the linear case assume the form (according to a formula in [8]):

$$\sum_{j=1}^{n} \varphi_{ij}(t)\,x_{j0} + \int_{t_0}^{t} \Big[\sum_{j,l=1}^{n} \sum_{k=1}^{r} \varphi_{ij}(t)\,\psi_{jl}(\tau)\,(q_{lk}(\tau)\,\eta_k(\tau) + f_l(\tau)) \Big] d\tau = \xi_i(t), \tag{2.10}$$

where $\varphi_{ij}(t)$ are fundamental matrix elements of homogeneous system (2.7) (with $u_k = 0$, $f_i = 0$).

After substitution of the solutions of System (2.9)

$$\eta_k(\tau) = -\frac{1}{\Delta}\Big[\sum_{m=1}^{r} \Delta_{mk} \sum_{i,j,l=1}^{n} \lambda_i(t)\,\varphi_{ij}(t)\,\psi_{jl}(\tau)\,q_{lm}(\tau) \Big],$$

where Δ is the determinant of System (2.9), Δ_{mk} is the minor of the determinant,* into the conditions of (2.10) we obtain a linear equation of the form

$$\begin{aligned} \sum_{s=1}^{n} \gamma_{is}(t)\,\lambda_s(t) = \xi_i(t) - \sum_{j=1}^{n} \varphi_{ij}(t)\,x_{j0} - \\ - \int_{t_0}^{t} \Big[\sum_{j,l=1}^{n} \varphi_{ij}(t)\,\psi_{jl}(\tau)\,f_l(\tau) \Big]\, d\tau, \end{aligned} \tag{2.11}$$

in which γ_{is} are known functions of t, $i = 1, \ldots, n$. From (2.11) it is necessary to determine the value of $\lambda_i(t)$.

The second variation $\delta^2 h$ in the given case has the form

$$\delta^2 h = \int_{t_0}^{t} \Big[\sum_{k,m=1}^{r} a_{km}(\tau)\,\delta\eta_k(\tau)\,\delta\eta_m(\tau) \Big] d\tau$$

*The determinant of System (2.9) $\Delta \neq 0$ because of the definite positiveness of the form of (2.8).

and because of (2.8), is positive when $(\delta\eta_1)^2 + \ldots + (\delta\eta_n)^2 \not\equiv 0$. Thus, sufficient conditions to show that the optimum regulation problem has a solution in this case will be the fact that the determinant of System (2.11) is not equal to zero when $t > t_0$ and the point $x_i = \xi_i(t)$ of the trajectory (2.7) can be reached for at least one value of $t = t_1 > t_0$ (with the limits (2.1) placed on the function u_k). In effect, with these conditions the problem (1.5)-(1.4) has with each $t > t_0$ a single solution and the value $F(t)$ [Equation (1.5)] is a continuous function of t. Since, when $t = t_1$ the trajectory $x_i(x_0, t_0 \{u_k\}, t)$ falls on the curve $x_i = \xi_i(t)$, then $F(t_1) \leq N$. On the other hand, $\lim F(t) = \infty$ when $t \to t_0$; therefore a minimum value of $t = t_0 + T$ exists, when the equality $F(t_0 + T) = N$ is fulfilled. This minimum value of T is equal to the optimum time of the transient process.

Let us investigate, for illustrative purposes, a simple example:

$$\frac{d^2x}{dt^2} = u, \tag{2.12}$$

$$x_0 = 0, \quad y_0 = (dx/dt)_{t=0} = 0, \quad x = \xi_1(t) = 1 + t,$$

$$y = (dx/dt) = \xi_2(t), \quad t_0 = 0, \int_0^T u^2(\tau)\,d\tau \leqslant 28. \tag{2.13}$$

When the trajectory $x(x_0, y_0, t_0, u, t)$ of Equation (2.12) falls on the point $x = \xi_1(t)$ it is also necessary for the velocities to coincide, i. e., $y = dx/dt = \xi_2(t)$.

The fundamental matrix $\|\varphi_{ji}\|$ of the homogeneous system $dx/dt = y$, $dy/dt = 0$, equivalent to Equation (2.12) and the inverse matrix $\|\psi_{ij}\|$ have the form:

$$\|\varphi_{ij}(t)\| = \begin{pmatrix} 1 & t \\ 0 & 1 \end{pmatrix}; \quad \|\psi_{ij}(t)\| = \begin{pmatrix} 1 & -t \\ 0 & 1 \end{pmatrix}.$$

System (2.9) becomes

$$2\eta(\tau) + \lambda_1\tau + \lambda_2 = 0 \quad \text{or} \quad \eta(\tau) = a\tau + b \quad (a, b = \text{const}), \tag{2.14}$$

and System (2.11) becomes

$$\int_0^t [a\tau^2 + b\tau]\,d\tau = -1, \int_0^t [a\tau + b]\,d\tau = 1. \tag{2.15}$$

Solving Equation (2.15) and substituting the obtained value in (2.14) and (2.13) we obtain the inequality $\frac{1}{t^3}[4t^2 + 12t + 12] \leq 28$.

The smallest positive root of the equation $28t^3 - 4t^2 - 12t - 12 = 0$ is $t = 1$.

Consequently, the optimum regulation time is $T = 1$, and the optimum controlling function $u(\tau)$ [Equation (2.14)] has the form $k = 10 - 18\tau$.

Let us note, in conclusion, that in the solution of the optimum regulation problem, for a wide class of linear systems with constant coefficients, in the case of limiting (for definiteness $r = 1$)

$$\int_{t_0}^{t_0+T} u^2(\tau)\,d\tau \leqslant N \tag{2.16}$$

we obtain a picture, analogous in a certain sense, to the same problem but with limits [1-3]

$$|u(\tau)| \leqslant N \quad \text{for} \quad \tau \geqslant t_0. \tag{2.17}$$

In particular, although in (2.16) the functions $u^0(\tau)$ are continuous, in contrast to (2.17), the intervals in which the sign of $u^0(\tau)$ changes are similar: in the case of real roots of the characteristic equation of system (2.7) (when $p_{ij} = \text{const}$, $u_k = 0$, $f_i = 0$) the number of sign changes of the optimum controlling function $u^0(t)$ is less than or equal to the order $\underline{n}$ of the system; in the case of complex roots of the characteristic equation the number of sign changes can be arbitrarily large.

Let us also note the following. As is known [2, 11], the determination of the value u_k^0 in the form of functions of time $\underline{t}$ for many regulation problems is only the first stage of solving the problem.

In order to synthesize an autonomous regulation system, that is, a system whose behavior is determined only by the values of $x_1(t), \ldots, x_n(t)$, it is necessary to determine u_k^0 in the form of functions of the arguments $x_1, \ldots, x_n$. With limits of the (2.17) type, this second problem, after determining $u_k^0(t)$, is solved comparatively easily. In the case of limits of the (2.17) type, the second problem, generally speaking, is not capable of solution; here, only a representation of the value u_k^0 in the form of functions of $x_1, \ldots, x_n, x_{10}, \ldots, x_{n0}$, is possible, which makes a synthesis exceedingly complicated. However, in an instance where some coincidence of starting disturbances x_{j0} is more probable (because of some probability characteristic), then here also a synthesis of the autonomous system can be effected, starting with the conditions of minimum time for the transient process with the more probable disturbances. Synthesis problems of this type are a subject for independent investigation.

3. Let us now investigate the problem of optimum regulation under Conditions (1.3). We will utilize the designations introduced in Parts 1 and 2. The problem (1.5)-(1.4) becomes in this case a more troublesome variational problem of minimum and maximum: to find the smallest maximum value of the functions $|\eta_k(\tau)|$ ($k = 1, \ldots, r$), determined during the interval $t_0 \leq \tau \leq t$, under the condition that this function satisfies Equation (1.4). We will investigate here only the linear System (2.7). Let us first note that multiplying both sides of Equation (2.10) by $\psi_{si}(t)$ and integrating with respect to $\underline{i}$, this system of Equations can then be replaced by the conditions

$$\int_{t_0}^{t} \left[\sum_{k=1}^{r} y_{sk}(\tau)\,\eta_k(\tau)\right] d\tau = c_s(t) \quad (s = 1, \ldots, n), \tag{3.1}$$

where

$$y_{sk}(\tau) = \sum_{l=1}^{n} \psi_{sl}(\tau)\, q_{lk}(\tau), \tag{3.2}$$

$$c_s(t) = \sum_{i=1}^{n} \psi_{si}(t)\,\xi_i(t) - x_{s0} - \int_{t_0}^{t} \left[\sum_{l=1}^{n} \psi_{sl}(\tau)\, f_l(\tau)\right] d\tau. \tag{3.3}$$

Therefore, the problem (1.5)-(1.4) can be formulated here in the following manner: find

$$F(t) = \min\,[\max|\eta_k(\tau)| \text{ when } t_0 \leqslant \tau \leqslant t,\ k = 1, \ldots, r] \tag{3.4}$$

under the Conditions (3.1). This problem is a particular case of a general problem, investigated in [10] as the "L-problem in abstract space." In the future we shall assume that functions y_{sk} [Equation (3.2)] satisfy the following condition (A):* linear combinations

*This condition is needed later as proof of the statement that the optimum regulation problem has a single solution.

$$\sum_{s=1}^{n} \lambda_s y_{sk}(\tau)\ (\lambda_s = \text{const},\ \lambda_1^2 + \cdots + \lambda_n^2 \neq 0,\quad k = 1, \ldots, r)$$

can become zero only during certain values of τ, whose number in each interval $t_0 \leq \tau \leq t$ is limited. Since the functions (3.2) are determined by elements of the fundamental matrix of System (2.7), which are linearly independent [9], the condition can be considered natural and practically fulfilled almost always. Krein's results [10] are given (statements 2°, 7°, 8°, pp. 173-178) in a general form; in the case under investigation here they are formulated in the following manner.

(L). A solution of Problem (3.4), (3.1) exists for all $t > t_0$. The value of function $F(t)$ can also be determined by the following equality

$$\lambda(t) = \frac{1}{F(t)} = \min \int_{t_0}^{t} \left[\sum_{k=1}^{r} \left| \sum_{s=1}^{n} \lambda_s y_{sk}(\tau) \right| \right] d\tau, \tag{3.5}$$

where λ_s are constant numbers, satisfying the equality $\lambda_1 c_1 + \ldots \lambda_n c_n = 1$. The value of $\lambda(t)$ is a continuous function of $c_1, \ldots, c_n$. Solutions of Problem (3.4), (3.1) – functions $\eta_k(\tau)$ – are determined solely* from the condition

$$-\eta_k(\tau) \left[\sum_{s=1}^{n} \lambda_s y_{sk}(\tau) \right] = \max,\quad |\eta_k| \leqslant F(t). \tag{3.6}$$

where λ_s are constants which supply a solution to Problem (3.5).

From (3.6) we conclude that function $\eta_k(\tau)$ has the form

$$\eta_k(\tau) = F(t)\, \operatorname{sign} \left[\sum_{s=1}^{n} \lambda_s y_{sk}(\tau) \right]. \tag{3.7}$$

Using these results it is not difficult to verify the following statements. To solve the problem of optimum regulation for system (2.7) for the case of limits (1.3), two mutually exclusive cases are possible: 1) the curve $x_i = \xi_i(t)$ is unattainable for $t > t_0$; 2) a single optimum trajectory $x_I(x_0, t_0; \{u_k^0\}, t)$, exists, while the optimum controlling function u_k^0 is computed by the formula

$$u_k^0(\tau) = N \operatorname{sign} \left[\sum_{s=1}^{n} \lambda_s y_{sk}(\tau) \right] \quad (t_0 \leqslant \tau \leqslant t_0 + T).$$

---

*To be more precise, the functions $\eta_k(\tau)$ have a single value solution with high accuracy to values approaching zero, that is, almost for the whole interval $t_0 \leq \tau \leq t$ with the exception of some values of τ, lying within the combination of intervals $\tau_\alpha < \tau < \tau_\beta$, the sum of the lengths of which can be selected to be as small as desired. It is obvious that this condition should simply be neglected in the problem under investigation. Let us note also that the problem (2.7)-(2.8) of Part 2 can also be made into an "L-problem" [10].

where the constants λ_s are solutions for the problem (3.5) when $t = t_0 + T$, $\lambda(t_0 + T) = 1/N$ and T is the smallest root of the equation $\lambda(t_0 + \theta) = 1/N$. In effect, if the trajectory $x_i(x_0, t_0, \{u_k\}, t)$ exists and falls on the curve $x_i = \xi_i(t)$ when $t = t_1$, then $F(t_1) \leq N$. On the other hand, from (3.5) it follows that $F(t) \to \infty$ when $t \to t_0$. We will show that F(t) is a continuous function of $\underline{t}$. In fact, on the one hand, when c_i is constant we have

$$\left| \min_{\Sigma c_s \lambda_s = 1} \left[\int_{t_0}^{t+\Delta t} \left(\sum_{k=1}^{r} \left| \sum_{s=1}^{n} y_{sk} \lambda_s \right| \right) d\tau \right] - \min_{\Sigma c_s \lambda_s = 1} \left[\int_{t_0}^{t} \left(\sum_{k=1}^{r} \left| \sum_{s=1}^{n} y_{sk} \lambda_s \right| \right) d\tau \right] \right| \leqslant \leqslant \int_{t}^{t+\Delta t} \left(\sum_{k=1}^{r} \left| \sum_{s=1}^{n} y_{sk} \lambda_s^0 \right| \right) d\tau \quad (\Delta t > 0), \tag{3.8}$$

where λ_s^0 are solutions to the problem

$$\min \int_{t_0}^{t} \left(\sum_{k=1}^{r} \left| \sum_{s=1}^{n} y_{sk}(\tau) \lambda_s \right| \right) d\tau \text{ for } \sum_{s=1}^{n} c_s \lambda_s = 1, \tag{3.9}$$

and, consequently, when c_s is constant, the left side of Inequality (3.8) approaches zero when $\Delta t \to 0$. On the other hand, the solution of Problem (3.5) is a continuous function of c_s ([10], pp. 172-173), but the values $c_s(t)$ [Equation (3.3)] are continuous functions of time, which proves the continuity of the function F(t) with $\underline{t}$. Thus, the equation $F(t_0 + \theta) = N$ has a minimum root $\theta = T$, which is the minimum time of the transient process. Now, the truth of our statement follows immediately from result (L) given above.

Conditions (3.6) and (3.7) coincide with the condition which is obtained here for the problem under consideration by utilizing the maximum principle formulated in [4] for fixed (that is, not being clearly a function of time) Equations (1.1). It should be noted, however, that this principle has a greater general significance than the particular method of solving the problem described above.

Let us consider the case where $p_{ij} = \text{const}$, $q_{ij} = \text{const}$, $\xi_i(t) = 0$ and $f_i(t) = 0$. To synthesize the autonomous regulation system in this case (see the comment on page 1010) it is necessary to find the value of u_k^0 as a function of $u_k^0(x_1, \ldots, x_n)$. Obviously, in order to determine $u_k^0(x_{10}, \ldots, x_{n0})$ it is necessary, according to the rule described above, to determine $u_k^0(t)$ and substitute $t_0 = 0$. According to the latter we have

$$u_k^0(x_1, \ldots, x_n) = N \operatorname{sign} \left[\sum_{s=1}^{n} \lambda_s y_{sk}(0) \right], \tag{3.10}$$

where the constants $\lambda_s(x_1, \ldots, x_n)$ are determined from the condition

$$\frac{1}{N} = \min \int_{0}^{T(x_1, \ldots, x_n)} \left(\sum_{k=1}^{r} \left| \sum_{s=1}^{n} \lambda_s y_{sk}(\tau) \right| \right) d\tau \text{ for } \sum_{s=1}^{n} \lambda_s x_s = -1. \tag{3.11}$$

Let us consider for illustrative purposes a simple example:

$$\frac{d^2x}{dt^2} + 2l \frac{dx}{dt} + \omega^2 x = u, \quad l < \omega, \quad l > 0. \tag{3.12}$$

The starting point is $x_0,\ y_0 = (dx/dt)_{t=-0};\ \xi_1(t) = \xi_2(t) = 0$; Condition (1.3) has the form:

$$|u| \leqslant N. \tag{3.13}$$

The fundamental matrix of the homogeneous system $dx/dt = y,\ dy/dt = -\omega^2 x - 2ly,$ equivalent to Equation (3.12), has the form:

$$\| \varphi_{ij}(t) \| = \begin{pmatrix} e^{\alpha t}\left(\cos \beta t - \frac{\alpha}{\beta} \sin \beta t\right) & \frac{1}{\beta} e^{\alpha t} \sin \beta t \\ e^{\alpha t}\left(-\frac{\alpha^2}{\beta} - \beta\right) \sin \beta t & e^{\alpha t}\left(\cos \beta t + \frac{\alpha}{\beta} \sin \beta t\right) \end{pmatrix}, \tag{3.14}$$

$$\| \psi_{ij}(t) \| = \| \varphi_{ij}(-t) \|,$$

where $\alpha \pm i\beta$ are roots of the characteristic equation for (3.12). Function $y_{sk}(\tau)$ [Equation (3.2)] and numbers c_s [Equation (3.3)] have the form:

$$y_{11}(\tau) = -\frac{1}{\beta} e^{-\alpha\tau} \sin \beta\tau, \quad y_{21}(\tau) = e^{-\alpha\tau}\left[\cos \beta\tau - \frac{\alpha}{\beta} \sin \beta\tau\right],$$

$$c_1 = -x_0, \quad c_2 = -y_0.$$

Therefore, in order to solve the problem it is necessary to solve the equation

$$\min \int_0^T \left| (-\lambda_1/\beta) \sin \beta\tau + \lambda_2 \left(\cos \beta\tau - \frac{\alpha}{\beta} \sin \beta\tau\right)\right| e^{-\alpha\tau} d\tau = \frac{1}{N} \tag{3.15}$$

when $\lambda_1 x_0 + \lambda_2 y_0 = -1$.

Equation (3.15), obviously, can be solved only for any x_0, y_0 and $N > 0$, since

$$\lim \left[\min_{x_0\lambda_1 + y_0\lambda_2 = -1} \left(\int_0^t |\lambda_1 y_{11} + \lambda_2 y_{21}|\, d\tau\right)\right] = \infty \text{ when } t \to \infty.$$

Therefore, the problem under consideration can be solved and the optimum controlling function has the form $u^0(\tau) = N \operatorname{sign} [\lambda_1^0 y_{11}(\tau) + \lambda_2^0 y_{21}(\tau)]$, where the constants λ_1^0, λ_2^0 are determined from (3.15). The function $u^0(x, y)$ is computed by means of Equation (3.10) and consequently

$$u^0(x_0, y_0) = N \operatorname{sign} [\lambda_1^0 y_{11}(0) + \lambda_2^0 y_{21}(0)].$$

We note that in this case it would have been possible to dispense with the calculation of the values of λ_1^0, λ_2^0 from (3.15) since we have $u^0(\tau) = N \operatorname{sign} |\sin(\beta\tau + \gamma)|$ and the fact of the uniqueness of the solution is sufficient to determine $u^0(x, y)$, starting with simple geometric considerations which lead to a phase plane picture of optimum regulation, obtained for this case by Bushau [11].

4. We will describe approximate methods of obtaining the optimum regulation functions $u_k^0(t)$. In the case where a sufficiently simple and clear form of the fundamental matrix $\| \varphi_{ij}(t) \|$ is not known, it is possible

to use numerical integration in the solution, and solve the variational problem and Inequality (1.6) approximately. The approximate solution obtained will not, generally speaking, fall on the point $x_i = \xi_i(t)$; however, an approximate trajectory will come sufficiently close to the region of this point. *

The computational method described in Part 2 for linear systems can also be used in the instance of nonlinear equations to determine an approximate optimum trajectory. Assume a given nonlinear system (1.1) and that it is required to solve the problem of optimum regulation with Conditions (2.1). Let us assume, further, that the trajectory $x_i(x_0, t_0, \{u_k^{(1)}\}, t)$, is known and it approaches sufficiently close to the point $x_i = \xi_i(t_1)$ at the moment $t_1 = t_0 + T_1$. Let us determine the functions $\delta u_k^{(1)}(\tau)$ $(k = 1, \ldots, r)$, satisfying the conditions

$$\int_{t_0}^{t_1-\delta} G[u^{(1)} + \delta u^{(1)}, \ldots, u^{(n)} + \delta u^{(n)}, \tau]\, d\tau \leqslant N \tag{4.1}$$

($\delta > 0$ is a sufficiently small constant),

$$\int_{t_0}^{t_1-\delta} \left[\sum_{j,l=1}^{n} \sum_{k=1}^{r} \varphi_{ij}^{(1)}(t_1 - \delta)\, \psi_{jl}^{(1)}(\tau) \frac{\partial X_l}{\partial u_k}\, \delta u_k^{(1)}(\tau) \right] d\tau = \tag{4.2}$$

$$= \xi_i(t_1 - \delta) - x_i(x_0, t_0, \{u_k^{(1)}\}, t_1 - \delta).$$

Here $\varphi_{ij}^{(1)}(t)$ are elements of the fundamental matrix of the solutions for the system of equations of the first approximation (2.4), the coefficients of which $\partial X_i / \partial x_j$, $\partial X_i / \partial u_k$ are computed at the trajectory points $x_i(x_0, t_0, \{u_k^{(1)}\}, t)$, ψ_{jl} — are inverse matrix elements of $\| \varphi_{ij} \|$. Functions $\delta u_k^{(1)}$ can be determined if the solution of the variational problem

$$F(t_1) = \min \int_{t_0}^{t_1-\delta} G[u_1^{(1)} + \eta_1, \ldots, u_n^{(1)} + \eta_n, \tau]\, d\tau, \tag{4.3}$$

where $\eta_k = \delta u_k^{(1)}$ under Condition (4.2) satisfies the condition

$$F(t_1) \leq N. \tag{4.4}$$

Let us select a new trajectory as a point of departure: $x_i(x_0, t_0 \{u_k^{(1)} + \delta u_k^{(1)}\}, t)$ and repeat the same operations with this trajectory as with curve $x_i(x_0, t_0, \{u_k^{(1)}\}, t)$, shortening the time $T_2 = T_1 - \delta$ still further by the value δ. We shall repeat this process as long as it is possible to shorten the time by δ. The accuracy can be increased by continuing to decrease the time by $\delta/2$, etc.

In an analogous manner, it is also possible to use successive computations of the optimum trajectory in a problem where the limits are of the form (1.3). It should be noted, however, in a general case of a nonlinear system, the described method results in unwieldy calculations. Besides this, it is difficult to prove that the computation process is approaching the ultimate optimum trajectory, since, as is evident from the description of the

* See [3] in this connection.

method, as the computation progresses, we reach a certain number of steps and come to a trajectory, relative to which in a linear approximation it is impossible to diminish the time T_m by a given quantity $\delta > 0$ by varying $u_k^{(m)}$. However, a linear approximation can be effected only in the region of small separation from the given trajectory.

We note that for the general case of the nonlinear system (1.1) no theorem concerning the existence of an optimum trajectory has yet been proven.* We shall explain the difficulties that arise here. Let us consider, for example, the system

$$dx_i / dt = X_i(x_1, \ldots, x_n, t) + b_i u \quad (b_i = \text{const}), \tag{4.5}$$

$$|u| \leqslant N. \tag{4.6}$$

Assume that a sequence of numbers $T_1, \ldots T_m, \ldots$ exists such that $\lim T_m = T$ as $m \to \infty$, and that $T_m > T$; assume also that there exist a sequence of piecewise continuous functions $u^{(1)}, \ldots, u^{(m)}, \ldots$ such that $x_i(x_0, t_0, u^{(m)}, t_0 + T_m) = x_{i1}(x_{i0}, x_{i1}, t_0$ are quantities given beforehand), but no piecewise continuous function $u(t)$ satisfying Condition (4.6) and for which $x_i(x_0, t_0, u, t_0 + \theta) = x_{i1}$ for $\theta < T$. It is not difficult to prove, with sufficient general assumptions, that the sequence of curves

$$z_i^{(m)}(\tau) = x_i(x_0, t_0, u^{(m)}, \tau) \quad (t_0 \leqslant \tau \leqslant t_0 + T)$$

approaches the continuous curve $z_i^0(\tau)$. The difficulty here, however, is to prove that a piecewise continuous curve $u^0(\tau)$ exists and satisfies Condition (4.6) and is such that $x_i(x_0, t_0, u^0, t_0 + T) = x_{i1}$.

We were successful in proving this for only some particular assumptions; specifically, if a system of first approximation (2.4) computed for Equation (4.5) along curve $x_i = z_i^0(\tau)$ satisfies Condition (A) (page 1010). We note also that function $u^0(\tau)$ satisfies in this case the maximum rule formulated in [4]. The equation $d^2x/dt^2 + X(x) = u$, where $\partial X / \partial x > l > 0$, for instance, satisfies this last condition.

In the case of the problem, considered in Part 3, concerning the linear system (2.7) when $p_{ij} = \text{const}$, $q_{ij} = \text{const}$, $f_i = 0$, there exists an accurate solution. However, a concrete computation of the functions $u_k^0(t)$ and especially the computation of the quantity u_k^0 in the form of functions $u_k^0(x_1, \ldots, x_n)$ is difficult. To do this, as was shown in Part 3, it is necessary to be able to solve Problem (3.11). Here it is possible to use the approximation method of computation which replaces Integral (3.11) with a sum of a sufficient number of component items. Then the rule for computing u_k^0 will be read in the following manner: the approximate value of the optimum controlling function $u_k^0(x_1, \ldots, x_n)$ is computed by the formula

$$u_k^0(x_1, \ldots, x_n) = N \operatorname{sign}\left[\sum_{s=1}^{n} \lambda_s y_{sk}(0)\right],$$

where the constant $\lambda_s(x_1, \ldots, x_n)$ is a solution of the problem

$$\min_{\Sigma \lambda_s x_s = -1} \left[\sum_{m=0}^{\mu} \sum_{s=1}^{n} \left| \sum_{s=1}^{n} \lambda_s y_{sk}(m\delta) \right|\right] \delta \geqslant \frac{1}{N}. \tag{4.7}$$

*The author learned from L. S. Pontriagin's report at the AN SSSR Session on Scientific Problems of Production Automation (Moscow, 1956) that a series of theorems on the existence of optimum trajectories were proven recently by R. V Gamkrelidze; however, the author does not know the exact formulation of these theorems because the results have not been published.

Here $y_{sk}(\tau)$ has the same meaning as above [(3.2), (3.3)], $\delta > 0$ and is a sufficiently small constant and μ is the smallest integral positive number for which Condition (4.7) is fulfilled. Such a method of computation results in simple arithmetic operations, although a great many are required.

In conclusion, the author considers it his duty to note that he became acquainted with problems of optimum regulation at seminars under the leadership of L. S. Pontriagin and also from conversations with A. A. Fel'dbaum, which were most useful to the author.

Received January 7, 1957

LITERATURE CITED

[1] A. A. Fel'dbaum, "Optimum processes in automatic regulation systems," Automation and Remote Control (USSR) 14, No. 6 (1953).

[2] A. A. Fel'dbaum, "On the synthesis of optimum systems with the aid of phase space," Automation and Remote Control (USSR) 16, No. 2 (1955).

[3] A. A. Fel'dbaum, "On the question of synthesizing optimum automatic regulation systems," Proceedings of the Second All-Union Automatic Regulation Theory Conference, Vol. 2, [in Russian] (Izd. AN SSSR 195)*.

[4] V. G. Boltianskii, R. V. Gamkrelidze and L S. Pontriagin, "On the theory of optimum processes," Proc. Acad. Sci. USSR 110, No. 1 (1956).

[5] A. Ia. Lerner, "On the high speed limit of automatic control systems," Automation and Remote Control (USSR) 15, No. 6 (1954).

[6] L. M. Sil'va, "Regulation with anticipation, providing optimum functioning of an automatic regulation system," Trans. ASME, 70, No. 8 (1955).

[7] N. G. Chetaev, "On the selection of parameters of a stable mechanical system," [in Russian] PMM, 15, No. 3 (1951).

[8] V. I. Smirnov, Course in Higher Mathematics, Vol. 4 [in Russian] (State Technical Press, 1951).

[9] V. V. Nemytskii and V. V. Stepanov, A Qualitative Theory of Differential Equations [in Russian] (StateTechnical Press, 1949).

[10] N. Akhiezer and M. Krein, "On some questions of the theory of moments," Article 4 [in Russian] (State United Scientific and Technical Press-NTVU, 1938).

[11] H. S. Tsien, Engineering Cybernetics (Russian translation) (IL, 1956).

*As in original — Publisher's note.

INTEGRAL CANONICAL REPRESENTATION OF RANDOM FUNCTIONS AND THEIR APPLICATION IN DERIVING OPTIMAL LINEAR SYSTEMS

V. S. Pugachev

(Moscow)

The theory of integral canonical representations of random functions and their use in determining the optimal linear operator is presented. Use of this method leads to a formula for the weighting function of an optimal one-dimensional linear system for the case where the observation interval is unlimited (infinite memory in the system), when the observed random function is the result of passing white noise through some linear system. Formulas previously given by Wiener [5] and Booton [8] are derived as special cases.

1. Integral Canonical Representations of Random Functions

The problem in such representations is to find an expression for an arbitrary random function in terms of very simple ones, namely, those which are not cross correlated for differing values of the argument. For brevity we will in future term a random function of zero mathematical expectation and uncorrelated values, "white noise", no matter what the nature of its argument.

In the theory of canonical expansions of random functions I have developed [1, 2] we seek an expression for an arbitrary random function in terms of uncorrelated random quantities which can be considered as values of pulsed white noise (i. e., white noise with a discrete argument). In practical problems it is frequently convenient to express the arbitrary function in terms of continuous white noise (i. e., white noise with a continuous argument). This latter type of expression we shall term an integral canonical representation of a random function.

I have shown [3] that any three functions $x(t, \lambda)$, $a(t, \lambda)$ and $G(\lambda)$ which satisfy

$$x(t, \lambda) = \frac{1}{G(\lambda)} \int_T K_x(t, s)\, a(s, \lambda)\, ds, \tag{1}$$

$$\int_T x(t, \lambda)\, \overline{a(t, \mu)}\, dt = \delta(\lambda - \mu), \tag{2}$$

$$\int_\Lambda x(t, \lambda)\, \overline{a(s, \lambda)}\, d\lambda = \delta(t - s), \tag{3}$$

where $K_X(t, s)$ is the correlation function of the random function $X(t)$, and T and Λ are certain ranges of the argument t and the parameter λ respectively, defining the integral canonical representation of $X(t)$:

$$X(t) = m_x(t) + \int_{\Lambda} Z(\lambda)\, x(t, \lambda)\, d\lambda. \tag{4}$$

Here $m_x(t)$ is the mathematical expectation of $X(t)$, and $Z(\lambda)$ is the white noise, of correlation function

$$K_z(\lambda, \mu) = G(\lambda)\, \delta(\lambda - \mu). \tag{5}$$

$Z(\lambda)$ is expressed in terms of the centered random function

$$X^0(t) = X(t) - m_x(t) \tag{6}$$

by the formula

$$Z(\lambda) = \int_T X^0(t)\, \overline{a(t, \lambda)}\, dt. \tag{7}$$

The canonical representation (4) for X and (5) give the integral canonical representation of the correlation function for X as

$$K_x(t, s) = \int_{\Lambda} G(\lambda)\, x(t, \lambda)\, \overline{x(s, \lambda)}\, d\lambda. \tag{8}$$

$G(\lambda)$ can be termed the dispersion density of $Z(\lambda)$. It can be a generalized function, i. e., may contain linear combinations of δ-functions. Karhunen [4] has shown that for X to be represented in terms of $Z(\lambda)$ by (4) it is both necessary and sufficient that its correlation function be given by (8).

This shows that to find the integral canonical representation of X (in the region T) it is sufficient to find the $x(t, \lambda)$, $a(t, \lambda)$ and $G(\lambda)$ which satisfy (1)-(3). Unfortunately we as yet have no method of solving (1)-(3) if the random function and T are arbitrary. This greatly restricts the practical use of integral canonical forms. It is easy to solve the corresponding equations for finding the canonical representation of X in series form (i. e., the expression in terms of pulsed white noise) [2] for any random function and any T, and this in innumerable ways. This is the great advantage of series forms for canonical representations of random functions (canonical expansions) over the integral canonical forms.

In the particular case where X is a stationary random function of the scalar variable t, the range of which is the whole numerical axis $|t| < \infty$, $K_X(t, s) = k_X(t - s)$ depends only on $t - s$, and the functions satisfying (1)-(3) are

$$a(t, \lambda) = \frac{e^{i\lambda t}}{2\pi}, \quad x(t, \lambda) = e^{i\lambda t}, \qquad G(\lambda) = \frac{1}{2\pi} \int_{-\infty}^{\infty} k_x(\tau)\, e^{-i\lambda\tau}\, d\tau, \tag{9}$$

where λ is a scalar parameter of range of change $|\lambda| < \infty$. Hence any stationary random function X has the integral canonical representation

$$X(t) = m_x + \int_{-\infty}^{\infty} Z(\lambda)\, e^{i\lambda t}\, d\lambda, \tag{10}$$

the coordinate functions of which are the exponential functions of imaginary argument $e^{i\lambda t}$. This, together with the particular importance of exponential functions to stationary linear systems, is why the spectral theory of stationary random functions is of such great practical importance. Formula (8) shows that there are no nonstationary random functions for which the Fourier integral is the integral canonical representation. This is why attempts to generalize spectral theory to such nonstationary functions are fruitless.

Let us now consider some linear system with a random input of white noise Z(t). The output will be a random function given, for any semi-infinite range $-\infty < t < T$, by the formula

$$X(t) = \int_{-\infty}^{T} Z(\lambda)\, w(t, \lambda)\, d\lambda, \tag{11}$$

where $w(t, \lambda)$ is the weighting function of the linear system. Equation (11) gives the integral canonical representation of X in any semi-infinite range $-\infty < t < T$. Thus if the input is white noise, the output random function is expressed by the integral canonical representation, the coordinate functions of which will be values of the weighting function for all values of the second argument λ lying in the range $-\infty < \lambda < T$, considered as a function of the first argument t.

Equation (11) gives an expression for Z in terms of X:

$$Z(\lambda) = \int_{-\infty}^{T} X(t)\, w^{-}(\lambda, t)\, dt, \tag{12}$$

where $w^{-}(\lambda, t)$ is the weighting function of the inverse system, i. e., of a system which, if joined in series with our system in either order, gives output and input identical. In this case (1-3) are satisfied by the functions *

$$a(t, \lambda) = w^{-}(\lambda, t), \quad x(t, \lambda) = w(t, \lambda). \tag{13}$$

If the linear system is described by the differential equation

$$FX = HZ, \tag{14}$$

where F and H are linear differential operators (polynomials in the differentiation operator), then w and w^{-} are given by the differential equations

$$F_t w(t, \lambda) = H_t \delta(t - \lambda), \tag{15}$$

$$H_t w^{-}(t, \lambda) = F_t \delta(t - \lambda). \tag{16}$$

The w and w^{-} can be determined for a given value of the first argument by integrating the corresponding conjugate differential equations [3].

Thus to find the integral canonical representation of a random function of one scalar variable it is sufficient to find a linear system which gives white noise at the output when the random function is applied to the input.

* Since any real system has a real weighting function, w and w^{-}, and hence x and a, must here be real.

If in particular, X is stationary with a rational-fraction spectral density $s_X(\omega)$, then, representing this latter in the form

$$s_x(\omega) = c\left|\frac{H(i\omega)}{F(i\omega)}\right|^2, \tag{17}$$

where c is a certain constant and F(x) and H(x) are polynomials, F(x) having no zeros in the right half-plane, we get a differential equation with constant coefficients of the form of (14), which expresses the centered random function X^0 in terms of the stationary white noise Z. Here w and w^- depend only on $t-\lambda$ and are determined by the normal methods for integrating linear equations with constant coefficients. Thus for a random function of the above type the problem of finding the integral canonical representation in any semi-infinite interval reduces to integrating two linear equations with constant coefficients.

N. M. Sotskii was the first to put forward in explicit form the idea of a canonical representation of a random function of a scalar argument, the coordinate functions of which are values of the weighting functions of some linear system. This idea appears implicity in Weiner's earlier work [5].

The range Λ in which λ varies can be a range in the proper sense, or consist of several ranges not in contact. In the latter case the integrals with respect to λ in (3), (4) and (8) will become sums of integrals for the various parts of Λ. All parts of Λ can be brought into coincidence by appropriate change of variables, so we get the integral canonical representations of X and its correlation function as sums of integrals covering the same range Λ_0. Since these representations can always be transformed to the forms of (4) and (8) by changing the variables they are of no interest from the point of view of theory. They are sometimes useful in practice, though (cf [3]).

The argument t (or s) in (1)-(8) can be any scalar or vector variable. Hence (1)-(8) are also applicable to vector random functions. To apply these to vector random functions we must consider a component of the vector function as a scalar function of its argument and number. Then the argument t in (1)-(8) will become a set of arguments and numbers for the components of the vector random function, and s a set of variables of integration and summation indices, and the corresponding integrals in (1)-(8) should be taken as the sums of integrals corresponding to all components of the vector random function.

Example 1. Consider the stationary random function X, of correlation function given by

$$k_x(\tau) = D_x e^{-a|\tau|} \tag{18}$$

The spectral density of this random function can be expressed in the form

$$s_x(\omega) = \frac{D_x}{\pi}\frac{a}{a^2+\omega^2} = \frac{D_x a}{\pi}\left|\frac{1}{a+i\omega}\right|^2. \tag{19}$$

Hence from the above argument the centered random function X^0 is related to white noise Z of spectral density $s_X(\omega) = D_X a/\pi$ and dispersion density* $G(\lambda) = 2D_X a$ by the differential equation

$$\frac{dX^0}{dt} + aX^0 = Z. \tag{20}$$

*The correlation function of $Z(\lambda)$ of spectral density s_0 is given (see [3], Section 77, example 1) by

$$k_z(\lambda-\mu) = 2\pi s_0 \delta(\lambda-\mu).$$

Comparing this with (5) we get the dispersion density of $Z(\lambda)$: $G(\lambda) = 2\pi s_0$.

Hence $\underline{w}$ is given by the differential equation

$$\frac{\partial w(t, \lambda)}{\partial t} + aw(t, \lambda) = \delta(t - \lambda). \tag{21}$$

Integrating this equation we get

$$w(t, \lambda) = e^{-a(t-\lambda)}(t > \lambda). \tag{22}$$

For the inverse system w^- is given by

$$w^-(t, \lambda) = \delta'(t - \lambda) + a\delta(t - \lambda). \tag{23}$$

Applying (11) to X^0 we get the integral canonical representation of X:

$$X(t) = m_x + \int_{-\infty}^{t} Z(\lambda)\, e^{-a(t-\lambda)} d\lambda. \tag{24}$$

Example 2. In just the same way, when X is related to Z by the differential equation with variable coefficients

$$a_1(t)\, X' + a_0(t)\, X = Z, \tag{25}$$

we get $\underline{w}$ and w^-

$$w(t, \lambda) = \frac{1}{a_1(\lambda)}\, e^{-\int_{\lambda}^{t} \frac{a_0(\tau)}{a_1(\tau)} d\tau}, \tag{26}$$

$$w^-(t, \lambda) = a_1(t)\, \delta'(t - \lambda) + a_0(t)\, \delta(t - \lambda) \tag{27}$$

and (11) for X becomes

$$X(t) = \int_{-\infty}^{t} \frac{Z(\lambda)}{a_1(\tau)}\, e^{-\int_{\lambda}^{t} \frac{a_0(\tau)}{a_1(\tau)} d\tau} d\lambda. \tag{28}$$

Example 3. Consider the stationary random function X, of correlation function given by

$$k_x(\tau) = D_x e^{-a|\tau|} \cos \omega_0 \tau. \tag{29}$$

The spectral density of this random function can be expressed in the form

$$s_x(\omega) = \frac{D_x a}{\pi} \left| \frac{b + i\omega}{b^2 + 2ai\omega + (i\omega)^2} \right|^2, \tag{30}$$

where

$$b = \sqrt{a^2 + \omega_0^2}. \tag{31}$$

Hence X^0 is expressed in terms of stationary white noise of spectral density $D_X a/\pi$ and dispersion density $2D_X a$ by

$$\frac{d^2X^0}{dt^2} + 2a\frac{dX^0}{dt} + b^2X^0 = \frac{dZ}{dt} + bZ. \tag{32}$$

Here $\underline{w}$ and w^- are given by

$$\frac{\partial^2 w(t, \lambda)}{\partial t^2} + 2a\frac{\partial w(t, \lambda)}{\partial t} + b^2 w(t, \lambda) = \delta'(t-\lambda) + b\delta(t-\lambda), \tag{33}$$

$$\frac{\partial w^-(t, \lambda)}{\partial t} + bw^-(t-\lambda) = \delta''(t, \lambda) + 2a\delta'(t-\lambda) + b^2\delta(t-\lambda). \tag{34}$$

Integrating these equations, we get

$$w(t, \lambda) = e^{-a(t-\lambda)}\left\{\cos\omega_0(t-\lambda) + \frac{b-a}{\omega_0}\sin\omega_0(t-\lambda)\right\} \quad (t \geqslant \lambda), \tag{35}$$

$$w^-(t, \lambda) = \delta'(t-\lambda) + (2a-b)\,\delta(t-\lambda) + 2b(b-a)\,e^{-b(t-\lambda)} \quad (t \geqslant \lambda). \tag{36}$$

Applying (11) to X^0 we get the integral canonical representation of X:

$$X(t) = m_x + \int_{-\infty} Z(\lambda)\, e^{-a(t-\lambda)}\left\{\cos\omega_0(t-\lambda) + \frac{b-a}{\omega_0}\sin\omega_0(t-\lambda)\right\} d\lambda. \tag{37}$$

2. Determination of the Optimal Linear Operator

The determination of the optimal linear operator A by minimizing the root mean square error amounts in general [3, 6] to solving the equation

$$A_t K_x(t, u) = f(s, u) \quad (u \in T), \tag{38}$$

which must be satisfied for all values of $\underline{u}$ lying in the range T of the argument $\underline{t}$ of the observed random function X, to which is extended the operation of the operators of the class in which there is an optimal operator.

When the mathematical expectation of X is exactly zero, function $\underline{f}$ in (38) is the mutual correlation function of the random function to be reproduced Y(s) and the observed random function X(t):

$$f(s, u) = K_{yx}(s, u). \tag{39}$$

If we reproduce the random function

$$W(s) = \sum_{r=1}^{N} U_r \psi_r(s) + Y(s) \tag{40}$$

by applying a linear operator to the random function

$$V(t) = \sum_{r=1}^{N} U_r \varphi_r(t) + X(t), \tag{41}$$

where $\varphi_1, \ldots, \varphi_N$, $\psi_1, \ldots, \psi_N$ are given functions, $U_1, \ldots, U_N$ random quantities, and X and Y are random functions of exactly zero mathematical expertation uncorrelated with $U_1, \ldots, U_N$, $\underline{f}$ in (38) is given by

$$f(s, u) = K_{yx}(s, u) + \sum_{r=1}^{N} \lambda_r \overline{\varphi_r(u)}. \tag{42}$$

Here $\lambda_1, \ldots, \lambda_N$ are accessory unknowns which are determined after solving (38) from the system [3, 6]

$$\psi_p(s) - A\varphi_p(t) = \sum_{r=1}^{N} c_{rp}\lambda_r \quad (p = 1, \ldots, N), \tag{43}$$

in which the coefficients c_{rp} are elements of a matrix which is the inverse of that for the second-order moments of $U_1, \ldots, U_N$.

The determination of the optimal linear operator by finding the extremum in the mathematical expectation and error dispersion (error correlation matrix, if a vector) leads also to (38), (42) and (43) [3, 7]. In this case the c_{rp} are functions of the mathematical expectations, dispersions and correlation moments of $U_1, \ldots, U_N$ and some accessory parameters, to determine which an appropriate system of algebraic or transcendental equations is found. These parameters are found by seeking the extremum of the function directly in a class of linear operators, dependent on these parameters and obtained by solving (38) and (43) [3, 7].

To solve (38) we express X via some integral canonical representation (4). Then $\underline{a}$, $\underline{x}$ and G, which satisfy (1)-(3), will be determined. We seek an operator to satisfy (38) in the form

$$Az(t) = \int_{\Lambda} \xi(s, \lambda)\, d\lambda \int_{T} \overline{a(t, \lambda)}\, z(t)\, dt, \tag{44}$$

where $\xi(s, \lambda)$ is a function to be determined. Remembering (1), and that the correlation function is symmetrical, we get

$$\begin{aligned} A_t K_x(t, u) &= \int_{\Lambda} \xi(s, \lambda)\, d\lambda \int_{T} \overline{a(t, \lambda)}\, K_x(t, u)\, dt = \\ &= \int_{\Lambda} G(\lambda)\, \xi(s, \lambda)\, \overline{x(u, \lambda)}\, d\lambda. \end{aligned} \tag{45}$$

Substituting this expression into (38) we get

$$\int_{\Lambda} G(\lambda)\,\xi(s,\lambda)\,\overline{x(u,\lambda)}\,d\lambda = f(s,\ u)\ (u \in T). \tag{46}$$

Multiplying this by $a(u, \mu)$, integrating with respect to $\underline{u}$ within the range T and using (2) we get

$$G(\mu)\,\xi(s,\mu) = \int_{T} f(s,u)\,a(u,\mu)\,du. \tag{47}$$

This formula defines the unknown function ξ. Substituting (47) into (46) and using (3) we see that the ξ given by (47) satisfies (46). Hence (44) and (47) define the solution to (38).

Substituting for ξ from (47) into (44) we get the final form for the optimal linear operator

$$Az(t) = \int_{\Lambda} \frac{d\lambda}{G(\lambda)} \left\{ \int_{T} f(s,u)\,a(u,\lambda)\,du \int_{T} \overline{a(t,\lambda)}\,z(t)\,dt \right\}. \tag{48}$$

If $\underline{f}$ is determined from (39), (48) gives an expression for the optimal linear operator directly.

If $\underline{f}$ is determined from (42), (48) gives an expression for the optimal linear operator in terms of the accessory unknowns $\lambda_1, \ldots, \lambda_N$. Substituting this expression into (43) we get, as in [2], a system of linear algebraic equations for determining $\lambda_1, \ldots, \lambda_N$. When $\lambda_1, \ldots, \lambda_N$ have been determined (48) and (42) define the optimal linear operator completely.

If the optimal linear operator is found from the extremum of the mathematical expectation and error dispersion (error correlation matrix, if a vector), (48) and (42), after (43) has been solved, give an expression for the optimal linear operator in terms of an accessory parameter θ (a vector if the system error is a vector). If this parameter is determined by one of the two methods given by Andreev [7] the problem of finding the optimal linear operator is solved completely.

3. Particular Cases of the Optimal Linear Operator

Equation (48) is of great generality. The arguments $\underline{s}$ and $\underline{t}$ (and correspondingly $\underline{u}$) can be any scalar or vector variables, some of their components being discrete variables. Hence (48) also defines the optimal linear operator when X and Y are vector random functions.

If $\underline{t}$ is a continuously changing variable, operator A can be written in the form

$$Az(t) = \int_{T} g(s,t)\,z(t)\,dt. \tag{49}$$

Comparing this with (48) we get

$$g(s,t) = \int_{\Lambda} \frac{\overline{a(t,\lambda)}\,d\lambda}{G(\lambda)} \int_{T} f(s,u)\,a(u,\lambda)\,du. \tag{50}$$

In the special case where $\underline{s}$ and $\underline{t}$ are different instants in time (50) defines the weighting function of an optimal one-dimensional linear system.

If X is an n-dimensional vector random function, $\underline{t}$ is a combination of the continuous variable τ and the number $\underline{p}$ of the components of X. In the same way, if Y is an m-dimensional vector random function, $\underline{s}$ is a combination of the variable σ and the number $\underline{q}$ of the components of Y. Hence $\underline{a}$ and $\underline{z}$ will be n-dimensional vector functions, and $\underline{f}$ a set of nm functions (i. e., a rectangular matrix). Equation (48) takes the form

$$\{Az\}_q = \int_\Lambda \frac{d\lambda}{G(\lambda)} \left\{ \sum_{l=1}^{n} \int_T f_{gl}(\sigma, u)\, a_l(u, \lambda)\, du \times \right.$$
$$\left. \times \sum_{p=1}^{n} \int_T \overline{a_p(\tau, \lambda)}\, z_p(\tau)\, d\tau \right\} \quad (q = 1, \ldots, m). \tag{51}$$

Expressing A as

$$\{Az\}_q = \sum_{p=1}^{n} \int_T g_{qp}(\sigma, \tau)\, z_p(\tau)\, d\tau \quad (q = 1, \ldots, m) \tag{52}$$

and comparing this with (51) we get the following formula for the weighting functions g_{qp}:

$$g_{qp}(\sigma, \tau) = \sum_{l=1}^{n} \int_\Lambda \frac{\overline{a_p(\tau, \lambda)}\, d\lambda}{G(\lambda)} \int_T f_{ql}(\sigma, u)\, a_l(u, \lambda)\, du \quad \begin{pmatrix} q = 1, \ldots, m \\ p = 1, \ldots, n \end{pmatrix}. \tag{53}$$

In the special case where σ and τ are different instants in time (53) determines the weighting functions of an optimal multidimensional system with $\underline{n}$ inputs and $\underline{m}$ outputs.

Since the formulas are so general they are applicable to many problems other than those of automatic control theory. In particular, (50) and (53) can be used to solve problems of optimal linear extrapolation and interpolation for random functions of vector arguments. They can, for instance, be used to provide the best linear extrapolation and interpolation in time and space for the parameters of the atmospheric state, which are random functions of the space and time coordinates, and can thus be used in weather forecasting.

Equations (48), (50) and (53) define the optimal linear operator in a closed form. This is an advantage of our method over that of canonical expansions [2], which gives the optimal linear operator in series form. But the use of (48), (50) and (53) is restricted in practice to cases where the integral canonical representation of X can be found for the given region T. The canonical expansion method is, on the other hand, always applicable, since an unlimited set of canonical expansions can always be found for any random function [2].

4. Optimal Linear System When the Observation Interval is Infinite and the Observed Random Function Results From White Noise Acted on by Some Linear System

We now apply (50)to determine the weighting function of an optimal linear system which must, from observations on the random function X [or V, given by (41)] in an infinite time interval $-\infty < t \leq T$, provide the best approximation to a random function Y [or to W given by (40), correspondingly]. We restrict ourselves to cases where X results from white noise acted on by some linear system of weighting function $w(t, \tau)$. As we saw in Section 1, the random function λ is here expressed by the integral canonical representation (11), the range Λ in which λ varies being the semi-infinite one $-\infty < X \leq T$, and $a(t, \lambda)$ is the weighting function of the inverse linear system $w^{-}(\lambda, t)$ [Formula (13)]. Hence (13), for the weighting function of an optimal linear system, here becomes

$$g(s,t)=\int_{-\infty}^{T}\frac{w^{-}(\lambda,t)\,d\lambda}{G(\lambda)}\int_{-}^{T}f(s,u)\,w^{-}(\lambda,u)\,du. \tag{54}$$

From the known properties of the weighting functions of linear dynamic systems, (54) can also be written as

$$g(s,t)=\int_{-\infty}^{T}\frac{w^{-}(\lambda,t)\,d\lambda}{G(\lambda)}\int_{-\infty}^{\infty}f(s,u)\,w^{-}(\lambda,u)\,du. \tag{55}$$

This formula is a generalization of Wiener's [5] and Booton's [8] earlier results. Booton's formula is found from (55) when the end of the interval of observation T coincides with the argument s, f is defined by (39) and X is stationary. Wiener's formula is a particular case of Booton's, when Y is also stationary and has a stationary relation to X.

To deduce Booton's formula from (55) we represent the spectral density of X (stationary) in the form

$$s_x(\omega)=|\Phi(i\omega)|^2, \tag{56}$$

which is always possible, since the spectral density is inherently a positive function. Then from Section 1 we can consider X as white noise of unit spectral density transformed by a stationary linear system of transfer function $\Phi(p)$. If the use of (56) is to be valid we must define $\Phi(p)$ in such a way that it has no poles in the right half-plane. The dispersion density of white noise of unit spectral density is 2π [3]. Hence, putting $T = s$ in (55) and remembering that w^- here depends only on the difference of the arguments, we have

$$g(s,t)=\frac{1}{2\pi}\int_{-\infty}^{s}w^{-}(\lambda-t)\,d\lambda\int_{-\infty}^{\infty}f(s,u)\,w^{-}(\lambda-u)\,du \tag{57}$$

or, introducing new variables $\xi = s-\lambda$, $\eta = s-u$:

$$g(s,t)=\frac{1}{2\pi}\int_{0}^{\infty}w^{-}(s-t-\xi)\,d\xi\int_{-\infty}^{\infty}f(s,s-\eta)\,w^{-}(\eta-\xi)\,d\eta. \tag{58}$$

We now use the known relationships between the weighting and transfer functions of a linear system. Since the transfer function of the inverse system is $1/\Phi(p)$ and w^- is real, we get

$$w^{-}(\tau)=\frac{1}{2\pi}\int_{-\infty}^{\infty}\frac{e^{i\mu\tau}d\mu}{\Phi(i\mu)}=\frac{1}{2\pi}\int_{-\infty}^{\infty}\frac{e^{i\mu\tau}d\mu}{\overline{\Phi(i\mu)}} \tag{59}$$

and

$$\int_{-\infty}^{\infty}f(s,s-\eta)\,w^{-}(\eta-\xi)\,d\eta=$$

$$= \frac{1}{2\pi} \int_{-\infty}^{\infty} \int_{-\infty}^{\infty} \frac{f(s, s-\eta)\, e^{-i\mu(\eta-\xi)}}{\overline{\Phi(i\mu)}}\, d\mu\, d\eta = \int_{-\infty}^{\infty} \frac{\chi(s, \mu)\, e^{i\mu\xi}}{\overline{\Phi(i\mu)}}\, d\mu, \tag{60}$$

where

$$\chi(s, \mu) = \frac{1}{2\pi} \int_{-\infty}^{\infty} f(s, s-\eta)\, e^{-i\mu\eta}\, d\eta. \tag{61}$$

From (59) and (60) we give (58) the form

$$g(s, t) = \frac{1}{2\pi} \int_{-\infty}^{\infty} \frac{e^{i\omega(s-t)}\, d\omega}{2\pi\Phi(i\omega)} \int_{0}^{\infty} d\xi \int_{-\infty}^{\infty} \frac{\chi(s, \mu)\, e^{i(\mu-\omega)\xi}}{\overline{\Phi(i\mu)}}\, d\mu. \tag{62}$$

This is Booton's formula when $\underline{f}$ is given by (39).

If Y is also stationary and has a stationary relationship to X, then

$$f(s, u) = K_{yx}(s, u) = k_{yx}(s-u) \tag{63}$$

and χ is the mutual spectral density of X and Y:

$$\chi(s, \mu) = \frac{1}{2\pi} \int_{-\infty}^{\infty} k_{yx}(\eta)\, e^{-i\mu\eta}\, d\eta = s_{yx}(\mu). \tag{64}$$

Formula (62) is then the same as Wiener's formula [5].

We note that Wiener's deduction of (62), then applied to a more general case by Booton, is in essence implicitly based on an integral canonical representation of X. To see this it is sufficient to show that the Wiener-Booton deduction is based on representing the correlation function of a stationary random function in the form

$$k_x(t-t') = \int_{-\infty}^{\infty} \psi_1(t-\sigma)\, \psi_2(\sigma-t')\, d\sigma, \tag{65}$$

where $\psi_1(\tau)$ is a function zero for $\tau < 0$, and $\psi_2(\tau)$ is a function zero for $\tau > 0$; it is an integral canonical representation of the type of (8). This is a direct consequence of the expressions for ψ_1 and ψ_2 in terms of $\Phi(p)$ derived by Wiener [5] (see also [9]):

$$\psi_1(\tau) = \frac{1}{\sqrt{2\pi}} \int_{-\infty}^{\infty} e^{i\omega\tau}\, \Phi(i\omega)\, d\omega,$$
$$\psi_2(\tau) = \frac{1}{\sqrt{2\pi}} \int_{-\infty}^{\infty} e^{i\omega\tau}\, \overline{\Phi(i\omega)}\, d\omega. \tag{66}$$

In fact, these formulas imply that

$$\psi_2(-\tau) = \frac{1}{\sqrt{2\pi}} \int_{-\infty}^{\infty} e^{-i\omega\tau}\, \overline{\Phi(i\omega)}\, d\omega = \overline{\psi_1(\tau)} \tag{67}$$

and (65) takes the form

$$k_x(t-t') = \int_{-\infty}^{\infty} \psi_1(t-\sigma)\,\overline{\psi_1(t'-\sigma)}\, d\sigma = \int_{-\infty}^{T} \psi_1(t-\sigma)\,\overline{\psi_1(t'-\sigma)}\, d\sigma, \tag{68}$$

where T is any quantity exceeding the lesser of t and t'. Comparing (68) and (8), we see that (68) gives an integral canonical representation of the correlation function of X. Then Wiener's function ψ_1 differs only by a factor $\sqrt{2\pi}$ from the weighting function $w(\tau)$.

Example 1. Let us find the weighting function of an optimal linear system intended for extrapolating a linear function of time with random coefficients when the perturbation X(t) is a random function related to white noise Z by the first-order differential Equation (25). As criterion of optimum we use the root mean square error.

Here the observed random function is expressed by a formula of the type of (41):

$$V(t) = U_1 + U_2 t + X(t), \tag{69}$$

and the random function to be reproduced by one of the type of (40):

$$W(s) = U_1 + U_2 s. \tag{70}$$

Hence here $\underline{f}$ is given by a formula of the type of (42):

$$f(s, u) = \lambda_1 + \lambda_2 u. \tag{71}$$

Here (27) defines w^-. The white noise density dispersion $G(\lambda)$ can without loss of generality be taken as unity, since the general case is readily reduced to this one by dividing (25) by $\sqrt{G(\lambda)}$. Substituting (27) and (71) for w^- and $\underline{f}$ into (54) we get

$$\begin{aligned} g(s, t) = [a_0^2(t) - a_0(t)\, a_1'(t) - a_0'(t)\, a_1(t)]\,(\lambda_1 + \lambda_2 t) - \\ - 2\lambda_2 a_1(t)\, a_1'(t) + a_1(T)\,[\lambda_2 a_1(T) + (\lambda_1 + \lambda_2 T)\, a_0(T)]\,\delta(T-t). \end{aligned} \tag{72}$$

To determine the accessory unknowns λ_1 and λ_2 we substitute (72) into (43), which equations here take the form

$$\begin{aligned} 1 - \int_{-\infty}^{T} g(s, t)\, dt &= c_{11}\lambda_1 + c_{21}\lambda_2, \\ s - \int_{-\infty}^{T} t g(s, t)\, dt &= c_{12}\lambda_1 + c_{22}\lambda_2. \end{aligned} \tag{73}$$

Determination of λ_1 and λ_2 completes the solution.

Example 2. Let us find the weighting function of a system optimal from the point of view of the minimum mathematical expectation for the function $1-e^{-k^2\Delta^2}$ of the error Δ, which is designed for extrapolating a linear function of time with random coefficients when the perturbation X(t) is a random function of normal distribution with correlation function given by (29). Denoting the mathematical expectation and the dispersion of the error Δ by m_Δ and D_Δ, respectively, we get a quantity taken as the criterion of optimum:

$$M[1-e^{-k^2\Delta^2}] = 1 - \frac{1}{\sqrt{2\pi D_\Delta}} \int_{-\infty}^{\infty} e^{-k^2z^2 - \frac{(z-m_\Delta)^2}{2D_\Delta}} dz =$$

$$= 1 - \frac{1}{\sqrt{2k^2D_\Delta + 1}} e^{-\frac{2k^2D_\Delta - 3}{2D_\Delta(2k^2D_\Delta+1)} m_\Delta^2} \tag{74}$$

It is clear that this criterion is equivalent to the condition that we have a maximum in

$$\varphi(m_\Delta^2, D_\Delta) = \frac{1}{\sqrt{2k^2D_\Delta + 1}} e^{-\frac{2k^2D_\Delta - 3}{2D_\Delta(2k^2D_\Delta+1)} m_\Delta^2} \tag{75}$$

This quantity is a function of the mathematical expectation and the dispersion of the error in the system. Hence to determine the optimal linear system we can use Andreev's [7] theory. We deduce, following Andreev, the accessory parameter

$$\theta = \frac{\frac{\partial\varphi}{\partial D_\Delta}}{\frac{\partial\varphi}{\partial m_\Delta^2}}, \tag{76}$$

where the derivatives must be taken at values of m_Δ and D_Δ corresponding to the optimal system sought, and get (38) as the operator of this system, where $\underline{f}$ is defined by (71) from the conditions of the problem, and to determine the unknowns λ_1 and λ_2 we have the same system of equations as in the previous example (73), but here the c_{pq} will not be elements of a matrix which is the inverse of the matrix of second-order moments of U_1 and U_2, but will be given by

$$c_{11} = \frac{m_2^2 + \sigma_2^2\theta}{m_1^2\sigma_2^2 - 2m_1m_2\sigma_1\sigma_2 r + m_2^2\sigma_1^2 + \sigma_1^2\sigma_2^2(1-r^2)\theta},$$

$$c_{12} = c_{21} = -\frac{m_1m_2 + \sigma_1\sigma_2\theta}{m_1^2\sigma_2^2 - 2m_1m_2\sigma_1\sigma_2 r + m_2^2\sigma_1^2 + \sigma_1^2\sigma_2^2(1-r^2)\theta}, \tag{77}$$

$$c_{22} = \frac{m_1^2 + \sigma_1^2\theta}{m_1^2\sigma_2^2 - 2m_1m_2\sigma_1\sigma_2 r + m_2^2\sigma_1^2 + \sigma_1^2\sigma_2^2(1-r^2)\theta},$$

where m_1, m_2, σ_1, σ_2, r are mathematical expectations, root mean square deviations and correlation coefficient for u_1 and u_2.

The weighting function w^- for X, the correlation function of which is given by (29), as in Example 3 in Section 1 is defined by (36). Substituting for w^- and $\underline{f}$ from (36) and (71) into (54) we get

$$g(s,t) = \frac{1}{2D_x a}\left\{b^2(\lambda_1+\lambda_2 t) - 2b(b-a)\left(\frac{2a}{b^2}\lambda_2 + \lambda_1 + \right.\right.$$

$$\left.\left. + \lambda_2 T\right) e^{-b(T-t)} + \left[\frac{2a-b}{b}\lambda_2 + b(\lambda_1 + \lambda_2 T)\right]\delta(T-t)\right\} \tag{78}$$

To determine λ_1 and λ_2 we substitute (78) into (73). Then, from (77), we obtain λ_1 and λ_2 in terms of of the parameter θ.

To set up the equation to determine θ we substitute in (76) the expressions for the derivatives of φ obtained by differentiating in (75). Then we have

$$0 = \frac{2k^2 D_\Delta}{2k^2 D_\Delta - 3} + \frac{3 + 12k^2 D_\Delta - 4k^4 D_\Delta^2}{D_\Delta(3 - 4k^2 D_\Delta + 4k^4 D_\Delta^2)} m_\Delta^2. \tag{79}$$

Here m_Δ and D_Δ are determined in an elementary fashion from the general formulas in the theory of the linear transformations of random functions. From the formulas of (69), (70) and the equations of (38) and (73) we get

$$m_\Delta = m_1(c_{11}\lambda_1 + c_{21}\lambda_2) + m_2(c_{12}\lambda_1 + c_{22}\lambda_2), \tag{80}$$

$$D_\Delta = \sigma_1^2(c_{11}\lambda_1 + c_{21}\lambda_2)^2 + 2\sigma_1\sigma_2 r(c_{11}\lambda_1 + c_{21}\lambda_2)(c_{12}\lambda_1 + c_{22}\lambda_2) +$$

$$+ \sigma_2^2(c_{12}\lambda_1 + c_{22}\lambda_2)^2 + \lambda_1 + \lambda_2 s - c_{11}\lambda_1^2 - 2c_{12}\lambda_1\lambda_2 - c_{22}\lambda_2^2. \tag{81}$$

Since λ_1 and λ_2 are given by (73), and, as we have seen, are functions of θ, m_Δ and D_Δ given by (80) and (81) will be functions of θ. Hence the right half of (79) is a function of θ, so to determine this we need only to solve (79). Any approximate method of solving equations can be used for this. For instance, a graphical method can be used. Here a graph for the right half of (79), considered as a function of θ, is drawn up and the point where the curve intersects the bisectrix of the angle between the axes determined. The abscissa and ordinates of the point give the sought value of θ.

To determine θ we can also find the maximum of (75) directly, considering this as a function of θ. To do this we calculate m_Δ and D_Δ for various θ, after which we can find the functions φ corresponding to these values of θ from (75). The value of θ at which φ is maximal gives the solution.

Received March 11, 1957

LITERATURE CITED

[1] V. S. Pugachev, "The general theory of random function correlation," Izvest. Akad. Nauk SSSR, Ser. Matem. 17, No. 5 (1953).

[2] V. S. Pugachev, "Use of canonical expansion of random functions to derive optimal linear systems," Automation and Remote Control (USSR) 17, No. 6 (1956).*

[3] V. S. Pugachev, Theory of Random Functions and its Application to Problems of Automatic Control [in Russian] (Gostekhizdat, 1957).

* See C. B. Translation.

[4] K. Karhunen, Uber lineare, Methoden in der Wahrscheinlichkeitsrechnung Ann. Acad. Sci. Fennicae, AI Nr. 37 (Helsinki, 1947).

[5] N. Wiener, Extrapolation, Interpolation and Smoothing of Stationary Time Series (John Wiley, New York, 1949).

[6]V. S. Pugachev, "The general condition for minimum mean square error in a dynamic system," Automation and Remote Control (USSR) 17, No. 4 (1956).*

[7] N. I. Andreev, "Derivation of an optimal linear dynamic system from the criterion of an extremum of a certain functional," Automation and Remote Control (USSR) 18, No. 7 (1957).*

[8] R. C. Booton, "An optimization theory for time-varying linear systems with nonstationary statistical inputs," Proc. IRE 40, 8 (1952).

[9] V. V. Solodovnikov, Introduction to the Statistical Dynamics of Automatic Control Systems [in Russian] (Gostekhizdat, 1952).

* See C. B. Translation.

DETERMINATION OF THE DISTRIBUTION LAW PARAMETERS FOR A RANDOM FUNCTION FROM LIMITED A PRIORI DATA

Iu. P. Leonov and L. A. Tel'ksnis

(Moscow)

A method for the determination of the distribution law parameters for a random function from limited a priori data is considered. It is shown that the a priori data on the parameters required can be reduced if the correctness of any hypothesis concerning the parameters can be checked.

One of the possible methods is considered, as is the circuit of a device with which the correctness of any hypothesis can be checked.

1. Preliminary Remarks

The current theory of optimal systems, which has mainly been developed in [1-3], is to a considerable extent an extension of problems in the mathematical statistics of random functions.

One of the main problems in mathematical statistics is to estimate the distribution law parameters for a random quantity from a given random sample.*

If this problem is extended to random functions we have therefore to determine the parameters of the distribution laws of the random functions. The task is here more complex, since the parameters are functions of one or more variables. The n-th sample consists of n values of the random function X(t) deriving from n independent tests undertaken in identical conditions.

It might be said that the current theory of optimal systems deals with just this problem, were it not that a restriction deriving from physical feasability is applied.

In most practical problems the required parameter has to be found continuously as a function of its argument (e. g., time). Hence in the current theory of optimal systems it is supposed that the estimate is not obtained as any formula (as in mathematical statistics), but only as one on which a real physical device (the optimal system) can be based. But if we suppose that the course of X(t) can be recorded in advance on some recording instrument and used as required for determining the parameter, we can without reservation say that determination of the parameters of a random function is a problem in mathematical statistics.

Two main trends in the development of mathematical statistics as applied to determining distribution law parameters can be discerned. In the first, which is associated with Fisher [4], the problem considered is how to obtain an estimate of the parameter which is (in a certain sense) the most exact, using a given fixed sample. In the second, developed by Neyman and Pearson [4] and also by Wald [5], the problem considered is how to reduce the a priori information on the random function, and how to use this information most completely and efficiently.

* By random sample of a random quantity X we mean a sequence of n observations giving values $x_1, x_2, \ldots x_n$ for X which derive from n independent experiments.

Additional a priori data on the distribution law or on the parameter itself simplify the problem considerably. An example is [2] the determination of the best unbiassed estimate (best being taken to mean minimum dispersion) for the mathematical expectation of a random function from data on the mathematical expectation in the form of an unknown linear combination of known functions and from a consideration of filters with finite memories. Here the a priori data are the noise correlation function $R_\eta(t)$, the degree $\underline{r}$ of the polynomial and the memory T of the system, and the condition that in the interval (t-T, t) the mathematical expectation is exactly represented by a polynomial of degree $\underline{r}$. But at present few real steps in developing the second trend have been taken. Except for [6, 7] in which only the possible general ways of reducing the a priori data are considered following [5], we know of no papers dealing with real systems enabling one to reduce the data required.

One of the possible ways of solving this problem is considered here.

2. Determination of the Mathematical Expectation of a Random Function

Let us consider the following problem.

We are given the random function

$$y(t) = g(t) + n(t), \quad M[y(t)] = g(t). \tag{2.1}$$

It is known a priori that g(t) can be represented by a Taylor series at any point, and that n(t) is a stationary random function with a known correlation function $R_\eta(t)$.

We have to find what is in a certain sense the best estimate $g^*(t)$ for the mathematical expectation of the random function y(t).

To find $g^*(t)$ we proceed as follows.

Suppose we are given some numbers $r \geq 0$ ($\underline{r}$ being an integer) and $T > 0$ and from our knowledge of $R_\eta(t)$ we construct a filter which is optimal in the Zadeh and Ragazzini sense [2], in which T and $\underline{r}$ will be the memory and order of astatism, respectively.

Then, using this filter, in which T and $\underline{r}$ were chosen at will, we perform the following operations on y(t):

1) determine the filter output signal:

$$x(t) = \int_0^T k(\tau)\,[g(t-\tau) + n(t-\tau)]\,d\tau = g_1(t) + n_1(t), \tag{2.2}$$

where $k(\tau)$ is the pulse transfer function of a filter optimal in the sense of [2] having an arbitrarily chosen $T > 0$ and given $\underline{r}$.

$$g_1(t) = \int_0^T k(\tau)\,g(t-\tau)\,d\tau \tag{2.3}$$

and

$$n_1(t) = \int_0^T k(\tau)\,n(t-\tau)\,d\tau; \tag{2.4}$$

2) determine the difference

$$\varepsilon(t) = x(t) - y(t) = g_1(t) - g(t) + n_1(t) - n(t); \tag{2.5}$$

3) find the mean over the set of values of the function for $\epsilon^2(t)$, i. e., $M[\epsilon^2(t)] = \overline{\epsilon^2}(t)$;

4) find the function

$$\lambda_1^2(t) = M[\varepsilon^2(t)] + 2\int_0^T k(\tau) R_n(\tau)\, d\tau; \tag{2.6}$$

5) finally choose T > 0 (for a given r) such that the maximum of $\lambda_1^2(t_M, T, r)$ at $t = t_M$ is least in value.

Figure 1 shows a device which can effect this series. It consists of a filter I, in which T and r can be varied, a unit II for calculating $\epsilon(t)$, a unit III for calculating $\epsilon^2(t)$, a device IV for averaging over the set (or time-averaging) the random function $\epsilon^2(t)$, a device V for generating the function k(t) (in which r and T are changed together with the parameters of I), a multiplication unit VI and an integrating unit VII.

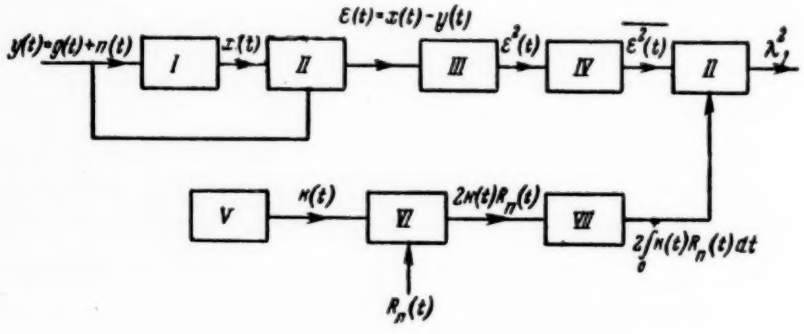

Fig. 1.

These operations can be performed because of our knowledge of y(t) and our a priori information on g(t) and n(t).

We now use the function x(t) as the best estimate of the mathematical expectation of y(t), i. e., $x(t) \equiv g^*(t)$ if the filter memory T is chosen as above and we consider in what sense the estimate of g(t) will be the best.

Since we are given that g(t) can be expanded in a Taylor series at any point, we may write the function $g_1(t)$ as

$$g_1(t) = \int_0^T k(\tau)\left\{g(t) - \frac{g'(t)}{1!}\tau + \ldots + \frac{g^{(r)}(t)}{r!}(-1)^r\tau^r + \right.$$

$$\left. + \frac{1}{r!}\int_0^\tau (\tau - u)^r g^{(r+1)}(t-n)\, du\right\} d\tau =$$

$$= \sum_{k=0}^{r} g^{(k)}(t)\,\mu_k + \frac{1}{r!}\int_0^T k(\tau)\,d\tau \int_0^{\tau} (t-n)\,g^{(r+1)}(t-n)\,dn, \tag{2.7}$$

where

$$g^{(r)}(t) = \frac{d^r g(t)^0}{dt^r} \text{ and } \mu_k = \frac{(-1)^k}{k!}\int_0^T k(\tau)\,\tau^k\,d\tau.$$

Here r is the degree of the polynomial for which the system was calculated to be optimal in the sense of [2]. Since we are speaking of filtering, the conditions that the estimate of the mathematical expectation for t > T be unbiassed imply that

$$\mu_0 = 1, \quad \mu_k = 0 \quad (0 < k \leqslant r). \tag{2.8}$$

For ϵ (t) we have

$$\varepsilon(t) = \varepsilon_d(t) + \varepsilon_r(t), \tag{2.9}$$

where

$$\varepsilon_d(t) = g_1(t) - g(t) \text{ and } \varepsilon_r(t) = n_1(t) - n(t). \tag{2.10}$$

Further

$$M[\varepsilon^2(t)] = \varepsilon_d^2(t) + M[\varepsilon_r^2(t)]. \tag{2.11}$$

Remembering that

$$M[\varepsilon_r^2(t)] = M\left\{\int_0^T k(\tau)\,n(t-\tau)\,d\tau - n(t)\right\}^2 =$$

$$= \int_0^T\int_0^T k(\tau_1)\,k(\tau_2)\,R_n(\tau_1-\tau_2)\,d\tau_1\,d\tau_2 - 2\int_0^T k(\tau)\,R_n(\tau)\,d\tau + D_n,$$

where $D_n = M[n^2(t)]$, we get the expression for $\lambda^2(t)$ as

$$\lambda^2(t) = \varepsilon_d^2(t) + \int_0^T\int_0^T k(\tau_1)\,k(\tau_2')\,R_n(\tau_1-\tau_2)\,d\tau_1\,d\tau_2 + D_n. \tag{2.12}$$

Thus the memory T is defined by applying the sequence 1-5 to y(t) from the condition that the maximum $\lambda^2(t_M)$ has a minimum value, given by (2.12), i. e., from the condition that the second moment of ϵ (t) is maximal. But it is also readily seen that if we apply as criterion of best estimate of the mathematical expecta-

tion of y(t) the condition $\lambda_1^2(t) = M[\epsilon_1(t)]^2$, where $\epsilon_1(t) = x(t) - g(t)$, or

$$\lambda_1^2(t) = \varepsilon_d^2(t) + M[n_1(t)]^2 = \min, \tag{2.13}$$

we get from (2.12) and (2.13) the same value of T for our filters in the class in which the filter memory is finite.

Thus we get the best estimate of the mathematical expectation of y(t) in the sense that $\lambda_1^2(t_M)$ is minimal in the class of filters with finite memories.

It is important to remark that the estimate we have so obtained is best in the sense of (2.13), not simply for linear filters with fixed parameters and finite memories, but also for the class of filters considered in [2]. Hence, generally speaking, we can construct a filter of finite memory which can give us an estimate best in the (2.13) sense.

However, it is clear that the class of filters considered in [2] is sufficiently broad for us to be able to obtain in general an estimate extremely close to that attainable with finite-memory filters by changing the T and r of various functions $R_n(t)$ for sufficiently smooth g(t).

Certain features of this estimate are noteworthy. Firstly, much less a priori data on g(t) is required to derive the estimate. All we need to know a priori about g(t) is that it is a sufficiently smooth function of t. We require the same data as in [2] on the statistical characteristics of n(t). Unlike the estimates derived in [2], these are biassed. This is clear from Condition (2.13). The bias is $\epsilon_d(t) = g_1(t) - g(t)$, which remains unknown, since to find the estimate we do not need to know g(t).

Certain complexities in finding $g^*(t)$ are related to the need to average the $\epsilon^2(t)$ in the general case over the whole set (and not over time), although n(t) is a stationary random function. This is because averaging the $\epsilon^2(t)$ over time and over the assembly do not give identical results. In fact, if $\epsilon^2(t)$ is averaged over time, (2.9) and (2.10) give

$$\lim_{T\to\infty} \frac{1}{T}\int_0^T \varepsilon^2(t)\,dt = \lim_{T\to\infty} \frac{1}{T}\int_0^T \varepsilon_d^2(t)\,dt + M[\varepsilon_r^2(t)]. \tag{2.14}$$

The ergodic hypothesis for stationary functions implies that on averaging the second term in (2.14) over time and over the assembly we get the same result. But the first component may pass through zero for some functions g(t), and hence, in general, time-averaging cannot be used.

But we may have

$$\lim_{T\to\infty} \frac{1}{T}\int_0^T \varepsilon_d^2(t)\,dt \neq 0. \tag{2.15}$$

If this additional information is provided we can use time-averaging instead, which greatly simplifies finding $g^*(t)$.[1] In particular, (2.15) is fulfilled by any periodic function g(t).

[1] The estimate will then be best not in the (2.13) sense, but in the sense that we have a minimum in the functional

$$\lambda_2^2 = \lim_{T\to\infty} \frac{1}{T}\int_0^T \varepsilon_d^2(t)\,dt + M[\varepsilon_r^2(t)]^2.$$

We must once again remark on some features of producing $g^*(t)$ using the system of Figure 1 which are related to averaging $\epsilon^2(t)$ over the assembly. It is clear that if it is possible to estimate the mathematical expectation of y(t) by averaging in this way we can use the well-known formula $g^*(t) = M_n[y(t)]$, where the subscript n denotes that the averaging is done over the n realizations of y(t).

Of course when $n \to \infty$, $g^*(t) = g(t)$, i. e., the problem of finding an estimate is only meaningful for some finite n, as in practice. Thus we can always find $g^*(t)$ by such averaging, no a priori data on y(t) being then required. Why therefore do we use the complex system proposed in Section 2 for finding an estimate?

The circuit of Figure 1 is of value in that it can provide a more precise estimate. This estimate can be obtained by averaging simultaneously over time and over the set of values. The estimate will be more accurate than that obtained by either method in isolation. An example where time-averaging alone is used is the problem of [2], while for averaging over a set of values formulas from the theory of estimates can be used. An important point is that only time-averaging can provide optimal filters, from the outputs of which we derive an estimate of the parameter continuous in time. Averaging over a set or combined averaging do not enable us to construct optimal filters, and hence only enable us to estimate the distrubution law parameters under laboratory conditions, where records of the random function realization are available. But much more precise estimates are then obtained.

Thus the system considered in Section 2 is of value in that it provides a more precise estimate by combined averaging. This, as we saw, reduces the a priori data on g(t) required as compared with that in [2].

When time-averaging can replace averaging over a set, the system of Figure 1 enables one to construct an optimal self-adjusting filter which only requires very restricted data on g(t).

We also note that since in averaging over a set we can only average over a finite number of realizations we must take as estimate of g(t) the function

$$g^*(t) = \frac{1}{n} \sum_{k=1}^{n} x_k(t).$$

To find the increase in accuracy resulting from combined averaging, let us consider the following simple example.

Suppose we have to find an estimate of the mathematical expectation of $y(t) = g(t) + n(t)$, where $g(t) = a + b(t)$ and n(t) is a gaussian stationary random process of correlation function $R_n(t) = D_n e^{-\alpha|t|}$.

The filters of [2] are used for the time-averaging estimate, this giving an unbiassed estimate of g(t) for $t > T$ (T filter memory). In this case the pulse transfer function of the optimal filter is $k(t) = A_0 + A_1 t + k_1 \delta(t) + D_1 \delta(t - T)$.

The dispersion of the estimate in time-averaging is [2]:

$$D_{g_t^*} = \frac{(\alpha^2 T^2 + 3\alpha T + 3)}{(\alpha^2 T^2 + 6\alpha T + 12)(\alpha T + 2)} D_n.$$

If an estimate is required at t = 1 sec we must put T = 1 and with a = 20 we get $D^*_{gt} = 0{,}32\, D_n$. If we also average over n realizations D^*_{gt} is clearly reduced by a factor n. Thus in combined averaging we have $D^*_{gMt} = 0{,}32\, D_n/n$. If we only average over the set we have $D^*_{gM} = D_n/n$, from which it is clear that time-averaging improves the accuracy the better the larger T.

In conclusion we observe that we have here estimated the mathematical expectation of y(t). The method is readily extended to cases where one has to determine the best estimate (in the sense of (2.13)) of any linear operator from the function g(t).

3. Estimates when n(t) is Nonstationary

The estimate best in the (2.13) sense may formally be said to be obtained in exactly the same way when n(t) is nonstationary. Here the problem of [2] must be extended to n(t) nonstationary. In this case we obtain an optimal system with variable parameters [8, 9], i. e., the pulse transfer function $k(t, \tau)$ depends on time.

When n(t) is nonstationary Condition (2.13) takes the form

$$\lambda_1^2(t) = \varepsilon_d^2(t) + D_{n_1}(t), \tag{3.1}$$

the dispersion of the nonstationary random function $n_1(t)$ at the filter output, $k(t, \tau)$, then depending on time. Unfortunately the expression for $k(t, \tau)$ can only be found in a closed form for quite a narrow class of nonstationary random functions. Hence the published [8] method of deriving estimates can only be extended to this narrow class. It has been shown [8, 9] that this class contains functions which are the solutions to stochastic differential equations with variable coefficients and right-hand sides which are white noise.

But we can often use optimal filters of finite memory designed for a stationary n(t) for estimating the parameters of nonstationary random functions.

Consider, for instance, the estimate of the mathematical expectation

$$g^*(t) = \int_0^T k(\tau)\, y(t-\tau)\, d\tau,$$

where k(t) is the pulse function of a filter designed for n(t) stationary.

Since the no-bias condition still applies, the dispersion of the estimate is

$$D_d(t) = \int_0^T \int_0^T k(\tau_1)\, k(\tau_2)\, R_n(t-\tau_1, t-\tau_2)\, d\tau_1 d\tau_2, \tag{3.2}$$

where $R_\eta(t_1, t_2)$ is the correlation function of n(t) (nonstationary).

It can be shown that for $D_d(t)$ to be sufficiently small it is sufficient that the mean value of $R_\eta(t_1, t_2)$ be sufficiently small within a square of side (t − T, t) (Figure 2). This condition will be fulfilled if $R_\eta(t_1, t_2)$ differs essentially from zero only within the band $|t_2 - t_1| < \tau_0$, where $\tau_0 \ll T$, and is sufficiently small outside it.

The physical meaning of this requirement is that the useful component g(t) of the random function y(t) = g(t) + n(t) must change more smoothly in time than does n(t).

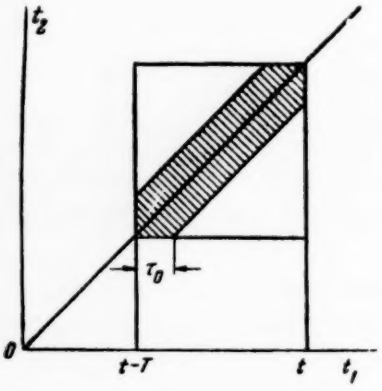

Fig. 2.

In fact here T can be chosen quite large so as to fulfill $T \gg \tau_0$ without materially distorting g(t) appreciably as this is a sufficiently slowly varying function of t and hence can be represented quite accurately by a polynomial of degree r in the range $T \gg \tau_0$.

Thus for Zadeh and Ragazzini's very simple filter, designed for white noise and r = 0, $D_d(t)$ is

$$D_d(t) = \frac{1}{T^2} \int_{t-T}^{t} \int_{t-T}^{t} R(t_1, t_2)\, dt_1 dt_2, \tag{3.3}$$

Since here the pulse function of the system optimal in the sense of [2] is

$$k(t) = \frac{1}{T} \qquad \text{for} \qquad 0 \leqslant t \leqslant T$$

and

$$k(t) = 0 \qquad \text{for} \qquad t < 0 \text{ и } t > T.$$

If we suppose that

$$| R(t_1, t_2) | < \varepsilon \quad \text{for} \quad | t_1 - t_2 | > \tau_0$$

and

$$R(t_1, t_2) \approx D_n(t) \quad \text{for} \quad | t_1 - t_2 | < \tau_0,$$

where $t = t_1 = t_2$, the estimate of the integral in (3.3) is easily obtained [10]:

$$D_d(t) \leqslant \frac{\tau_0 D_0(t)}{T} + \varepsilon. \tag{3.4}$$

Analogous estimates of $D_d(t)$ can be derived for other forms of k(t).

Thus when n(t) is nonstationary we can use optimal filters designed for the stationary case only if the noise is weakly correlated and g(t) varies sufficiently smoothly in time.

4. Estimate of a Correlation Function

Since by definition a correlation function is the mathematical expectation of a random function U(t), i. e., $M[U(t, \tau)] = R(t, \tau)$, where $U(t, \tau) = n(t)\, n(t + \tau)$ and τ can be reckoned as parameters, the methods considered in Sections 2 and 3 as suitable for estimating mathematical expectations can also be used to get an estimate of a correlation function $R(t, \tau)$.

But it is shown in Section 5 that this method of estimating $R(t, \tau)$ is not uniquely possible.

5. Determination of the Distribution Law Parameters for a Random Function From Limited A Priori Data

Most work dealing with parameter estimates for the distribution laws of random functions normally start from some fixed a priori data. Such a priori data are frequently unavailable, however. Thus when we need to estimate the mathematical expectation of the random function $y(t) = g(t) + n(t)$, i. e., $M[y(t)] = g(t)$ we do not usually know $R_n(t)$, and when we need to estimate $R_n(t)$ we do not know the mathematical expectation g(t), which is needed for calculating the correlation function.

We therefore have in the problem of [2] to reduce the requirements for a priori data on n(t), as the solution becomes unsuitable for deriving $g^*(t)$. This is one of the main shortcomings [1-3]. To eliminate it we need a method of checking the hypothesis as to y(t) made when sufficient a priori data are lacking.

We shall show that the method of Section 2 can be used for checking the correctness of any hypothesis as to g(t) and n(t). In fact the system considered in Section 2 in general is as follows. We have determined the linear positive functional $\lambda_1^2\{y(t), \mu_k, A, B, C, D, \ldots\}$ on a known set of random functions $y(t) \in Y$.

But to calculate λ_1^2, which is needed for the estimate, it is insufficient to know y(t), because we need also some a priori data μ_k on g(t) and n(t) plus also certain hypotheses A, B, C, D, . . ., which we are obliged to make about these functions, since to calculate λ_1^2 some of the μ_k are inadequate.

λ_1^2 only has a minimum when our hypotheses on g(t) and n(t) are true, i. e., when they are equivalent to being given precise a priori data on y(t) sufficient to calculate λ_1^2. This scheme clearly enables one to check any hypothesis as to y(t) and also to establish how close it is to the true characteristics of y(t), which were initially unknown.

Let us now turn to the system of Figure 1. Here λ_1^2 is given by (2.13). To calculate it we need, as we have seen, not only y(t), but also the following μ_k:

μ_1 – the function g(t) is sufficiently smooth (condition of expansibility in a Taylor series);

μ_2 – n(t) is stationary and of correlation function $R_n(t)$.

But the precise μ_1 and μ_2 on the properties of y(t) are insufficient to calculate λ_1^2, and additional hypotheses on how g(t) changes must be made ("degree of smoothness" of the change). The various hypotheses as to how g(t) behaves in $0 < t < T$ correspond to different values of T and $\underline{r}$, the correctness of the choice being determined from the values of λ_1^2 for the various hypotheses (various T and $\underline{r}$).

It is clear that here the amount of μ_k can be reduced. In particular we need only suppose that g(t) is sufficiently smooth and n(t) a stationary random function. Then, as well as checking our hypotheses as to the behavior of g(t) we have also to check the various hypotheses as to the statistical characteristics of n(t), i. e., to check the various expressions for $R_n(t)$ which we may be given for correctness. This is also done using the extremum in λ_1^2.

As noted in Section 2, the k(t) giving a minimum λ_1^2 is in general different from the optimal functions considered in [2]. This function is readily determined using the extremum in λ_1^2. But for this we need to know g(t). Also the functions considered in [2] sometimes give values of λ_1^2 very close to the minimum, but to determine these functions we do not need g(t), only its local properties around the point $\underline{t}$ being required. The conditions under which the functions considered in [2] give values of λ_1^2 very close to the minimum amount to a choice of T for the filter such that the function is sufficiently accurately represented by a polynomial of degree $\underline{r}$ for which the filter of [2] was designed in the range $(t - T, t)$. In fact, if g(t) is precisely a polynomial of degree $\underline{r}$ (2.13) takes the form $\lambda_1^2 = M[n_1^2(t)]$, which shows that λ_1^2 is only a minimum when the $R_n(t)$ for which the filter of [2] was designed coincides with the correlation function of the noise applied to the input. If g(t) differs from a polynomial we can always choose T such that g(t) is sufficiently accurately represented by a polynomial of degree $\underline{r}$ in the range $(t - T, t)$. With this choice of T we get a value of λ_1^2 very close to the minimum. Calculations show that the method of choice considered in Section 2 gives a value of λ_1^2 very close to the minimum so the k(t) considered in [2] can then be considered as an approximate solution to the problem of (2.13).

Hence this method not only enables us to make a determination of the distribution law parameters for a random function from limited a priori data on y(t), but also to check the various hypotheses on y(t) for correctness. Hence the a priori data on y(t) required may be much reduced. We can thus proceed from a position of knowing little about y(t) to one of more complete knowledge.

In particular, the scheme of Figure 1 enables us to get estimates for the mathematical expectation and correlation function of y(t); then the a priori data are only conditions on the smoothness of g(t) and the stationary nature of n(t).

Such estimates cannot be made by other methods which have been given [1-3]. This is the main advantage of our method.

To derive λ_1^2 [y(t), μ_k, A, B, C, D, . . .] we used the filters considered in [2]. But this is clearly only one of the possible ways of finding λ_1^2 to satisfy set requirements. The convenience of filters of finite memory lies in our being able to write down explicity how the functional depends on the hypotheses and a priori data on g(t) and n(t).

Let us consider a simple example of calculating the mathematical expectation of a random function y(t) by the method of Section 2.

We assume that to calculate an estimate best in the sense of (11) we have the following a priori data on g(t) and n(t):

a) we know $y(t) = g(t) + n(t)$;

b) g(t) is sufficiently smooth;

c) n(t) is a stationary random function of known correlation function $R_n(t) = c^2\delta(t)$.

We have thus to find T and $\underline{r}$ from the condition that (2.13) is a minimum.

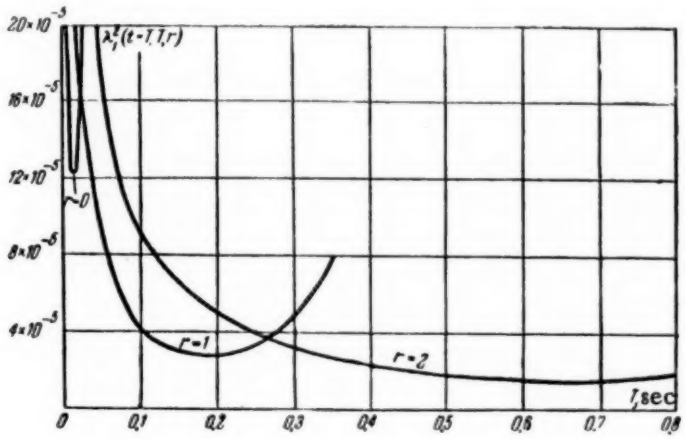

Fig. 3.

Of course, we must here be given g(t) in order to find T and $\underline{r}$. But when estimating using the model of Section 2 we need only know that g(t) is sufficiently smooth (Condition b).

Suppose

$$g(t) = \begin{cases} e^{-\alpha t}, & t > 0, \\ 0, & t \leqslant 0. \end{cases}$$

Then we have

$$\varepsilon_d(t) = g_1(t) - g(t) = \int_0^T k(\tau)\, g(t-\tau)\, d\tau - g(t).$$

In our case

$$\varepsilon_d(t) = \int_0^T k(\tau)\, e^{-\alpha(t-\tau)} d\tau = e^{-\alpha t}[A(T) - 1],$$

where

$$A(T) = \int_0^T k(\tau)\, e^{\alpha\tau} d\tau$$

and

$$\varepsilon_d^2(t,\ T,\ r) = e^{-2\alpha t}\,[A(T) - 1]^2.$$

We note that $\lim_{T \to 0} \varepsilon_d(t,\ T,\ r) \to 0$, and also $\lim_{r \to \infty} \varepsilon_d(t,\ T,\ r) \to 0$.

It is readily seen that in our special case ϵ_d^2 (t, T, r) is maximal at t = T. Hence we get

$$\lambda_1^2(T,\ r) = e^{-2\alpha T}\,[A(T) - 1]^2 + M\,[n_1(t)]^2.$$

The following table gives λ_1^2 for various r:

r	$k(\tau)$ for $0 \leqslant \tau \leqslant T^*$	$M\,[n_1(t)]^2$	$\lambda_1^2(t = T,\ T,\ r)$
0	$\frac{1}{T}$	$\frac{c^2}{T}$	$e^{-2\alpha T}\left[\frac{1}{\alpha T}\left(e^{\alpha T} - 1\right) - 1\right] + \frac{c^2}{T}$
1	$\frac{4}{T} - \frac{6}{T^2}\tau$	$\frac{4}{T}c^2$	$e^{-2\alpha T}\left[\frac{6}{\alpha^2 T^2}\left(e^{\alpha T} - 1\right) - \frac{2}{\alpha T}\left(e^{\alpha T} + 2\right) - 1\right]^2 + + \frac{4}{T}c^2$
2	$\frac{9}{T} - \frac{36}{T^2}\tau + \frac{30}{T^3}\tau^2$	$\frac{9}{T}c^2$	$e^{-2\alpha T}\left\{e^{\alpha T}\left[\left(\frac{20}{\alpha^2 T^2} - \frac{8}{\alpha T} + 1\right) - \frac{20}{\alpha^2 T^2} - \frac{12}{\alpha T} - - 3\right] - 1\right\}^2 + \frac{9}{T}c^2$

*$k(\tau) = 0$ when $0 < \tau$ and $\tau > T$.

Figure 3 gives λ_1^2 (T, r) curves for $\alpha = 1$ and $c^2 = 10^{-6}$.

These show that the larger r the more exact the estimate (the less λ_1^2). But the increase in accuracy leads to T being increased. This means that the more exact estimates are only available at later times. Thus if we want estimates for t < 0.1 sec we must here (Figure 3) have r = 0, and if we want estimates for 0.1 < t < 0.3 sec we must have r = 1, etc. Hence the choice of r is decided by the time when the estimate is required. Figures 4 and 5 show $\lambda_1^2(r)$ curves for $T = T_{opt}$ and $T_{opt}(r)$ curves for $\lambda_1^2 = \lambda_{1\min}^2$.

SUMMARY

It has been shown that, being provided with very limited data on the function y(t) we can get more complete information by checking various hypotheses and rejecting the incorrect.

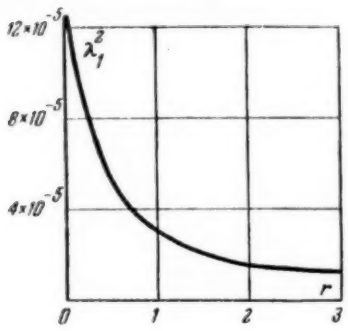

Fig. 4.

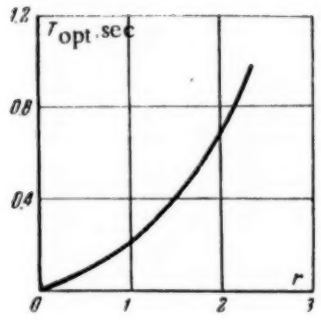

Fig. 5.

A self-adjusting system can be designed around this principle. In particular, the system of Figure 1 can act as a part of it. Figure 6 shows the design of such a system.

Suppose we only know that g(t) is sufficiently smooth and that n(t) is stationary, and that we have to determine the best estimate (in some sense) of y(t) = g(t) + n(t). Then if time-averaging is possible we can connect in paralliel several elements based on Figure 1 and designed on some hypothetical correlation function $R_m(t)$ common to all with different memory values $T_{1,m}$, $T_{2,m}$, . . . $T_{n,m}$ (the first subscript denoting the memory

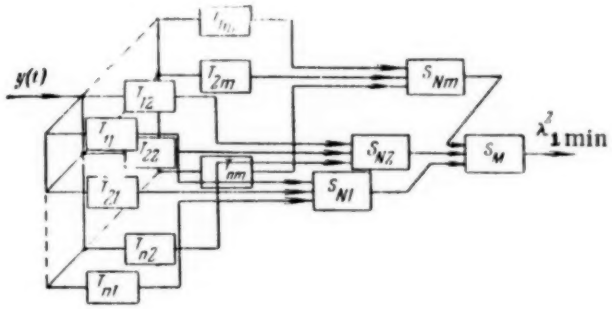

Fig. 6.

time, the second the correlation function number). In all we have m such blocks of n elements each, each block corresponding to one of the m hypothetical correlation functions we seek to find. In series with each block we have to connect a unit which passes the one out of the n signals which correspond to the minimal value λ^2_{1n}. In all there are m such units (corresponding to the m correlation functions). The output elements S_{nm} supply the input of the element S_m, which passes the one out of the m signals which corresponds to the minimal value $\lambda^2_{1m} = \min$.

This type of system gives the best estimate of the mathematical expectation and of the correlation function this occurring when $\lambda^2_{1n,m} = \min$. The system is clearly self-adjusting in the sense that it adjusts itself best to g(t) and n(t) in accordance with (2. 13) and the properties of the functions. At first the characteristics of g(t) and n(t) are unknown to us, as we only have very limited a priori data. The amount of such a priori data can always be reduced by feeding in, in turn, hypotheses to be checked. The amount of a priori data can thereby be reduced without limit. But the process for deriving estimates then becomes lengthier and more complex.

If the properties of g(t) and n(t) alter, the system of Figure 6 adjusts itself in such a way that $\lambda^2_{in,m}$ has the minimum possible value in the new conditions.

Received May 15, 1957

LITERATURE CITED

[1] N. Wiener, Extrapolation, Interpolation and Smoothing of Stationary Time Series (New York, 1949).

[2] L. A. Zadeh and J. R. Ragazzini, "An extension of Wiener's theory of prediction," J. Appl. Phys. 21, No. 7 (1950).

[3] R. C. Davis, "On the theory of prediction of nonstationary stochastic processes," J. Appl. Phys. 23, No. 9 (1952).

[4] H. Cramer, Mathematical Methods of Statistics [Russian translation] Edited by A. N. Kolmogorov (IL 1948).

[5] A. Wald, Statistical Decision Functions (New York, 1950).

[6] D. Van Meter and D. Middleton, "Modern statistical approaches to reception in communication theory," Trans. IRE, PGOT-4 (September, 1954).

[7] P. M. Woodward and I. L. Davies, "A theory of radar information," Phil. Mag., Vol. 41 (October, 1950) pp. 1001-1007.

[8] Dolph and Woodbury, "Of the relation between Green's function and covariances of certain stochastic processes of linear prediction," Trans. ASME (May, 1952).

[9] J. H. Laning and R. H. Battin, Random Processes in Automatic Control (New York, 1956).

[10] V. S. Pugachev, Theory of Random Functions and its Application to Automatic Control Problems [in Russian] (Gostekhizdat, 1957).

APPROXIMATE DETERMINATION OF THE OUTPUT COORDINATE PROBABILITY CHARACTERISTICS FOR NONLINEAR AUTOMATIC CONTROL SYSTEMS

B. G. Dostupov

(Moscow)

A method is presented for determining approximately the moments of the integral of a system of ordinary differential equations from the given moments of the relation for the random parameters appearing in the equations. The method is based on using finite sections of the expansion of the integral of the system in powers of the random parameters.

INTRODUCTION

A number of important topics in current automatic control theory require the random perturbations applied to the input of an automatic control system to be allowed for, as also scatter in the system parameters. These problems are encountered, e. g., in determining the probability characteristics of the error at the outputs of automatic control and servo systems. Mathematically speaking, they amount to determining these characteristics for the integral of a system of ordinary differential equations from the known probability characteristics of the random quantities and functions appearing in the equations.

Fairly simple methods have only so far been found for the differential equations to linear or linearizable systems [1-7, 11]. General but very complex methods involving large-scale laborious calculations have been given for nonlinear systems [2, 8]. An approximate method, based on so-called "statistical linearization," has been developed for nonlinear systems [9, 10].

Here a new approximate method for the probability characteristics of solutions to systems of ordinary differential equations containing random parameters is presented. The method is an extension of certain ideas of Pugachev's. In particular, he has proposed [2] a method for this purpose based on canonical expansions for the random functions appearing in the right halves of the equations. The partial derivatives of the solution with respect to the random parameters have then to be calculated. To calculate these derivatives it is proposed [2] to integrate special systems of differential equations in which the derivatives are the functions sought after. The partial derivatives do not have to be calculated explicitly in the method given here, and the calculations are simple.

1. The Problem

Suppose we are given a system of ordinary differential equations

$$\frac{dX_\nu}{dt} = f_\nu(X_1, X_2, \ldots, X_n, V_1, V_2, \ldots, V_m, t) \quad (\nu = 1, 2, \ldots, n), \tag{1.1}$$

which has a unique solution in the region D of interest, that the initial conditions and the change in the argument t are given, that $f_1, f_2, \ldots, f_n$ are given nonrandom functions, that $V_1, V_2, \ldots, V_n$ are random parameters and that $X_1, X_2, \ldots, X_n$ are the desired random functions.

Since, very broadly speaking, the random functions can be represented sufficiently accurately as a set of random parameters via expansion in certain (say, canonical [1, 2]) series which converge the probability, it is sufficient to consider differential equations which contain only random parameters, i. e., those as (1.1). The number m of such parameters is assumed finite. Without loss of generality we may assume the mathematical expectations of the V_r as zero:

$$M[V_r] = 0 \quad (r = 1, 2, \ldots, m). \tag{1.2}$$

We further suppose that the relation moments up to the q-th order inclusive are given for the V_r, i. e., we know the quantities

$$\mu_{r_1 r_2 \ldots r_k} = M[V_{r_1} V_{r_2} \ldots V_{r_k}] \quad \begin{pmatrix} k = 1, 2, \ldots q, \\ r_1, r_2, \ldots, r_k = 1, 2, \ldots, m \end{pmatrix}. \tag{1.3}$$

Finally we assume that the integrals of (1.1) can be expanded in Maclaurin series in terms of the V_r with a residual term of (q + 1)-th order, this latter being negligibly small. The determination of the moments for solving (1.1) will be carried out within the framework of the above assumptions.

2. Determination of the Mathematical Expectations of the Solutions to (1.1)

The solutions to (1.1) are certain functions of the time t, of the V_r, and of the initial conditions, $X_1^0, X_2^0, \ldots, X_n^0$, some of the X_i^0 (and sometimes all) being random. The random X_i^0 can be included with the V_r. Then, striking out the nonrandom X_i^0 for simplicity, we can write the solutions to (1.1) in the form

$$X_\nu = \varphi_\nu(t, V_1, V_2, \ldots, V_m) \quad (\nu = 1, 2, \ldots, n). \tag{2.1}$$

Consider one of the X_ν, which, omitting the subscript, we write as

$$X = \varphi(t, V_1, V_2, \ldots, V_m). \tag{2.2}$$

We have already assumed that φ can be expanded as a Maclaurin series in the V_r. Limiting the series to the terms of the q-th degree and striking out the residual, we get

$$X = \varphi_0 + \sum_{k=1}^{q} \frac{1}{k!} \sum_{r_1=1}^{m} \sum_{r_2=1}^{m} \cdots \sum_{r_k=1}^{m} \left(\frac{\partial^k \varphi}{\partial V_{r_1} \partial V_{r_2} \ldots \partial V_{r_k}} \right)_0 V_{r_1} V_{r_2} \ldots V_{r_k}, \tag{2.3}$$

where

$$\varphi_0 = \varphi(t, 0, 0, \ldots, 0). \tag{2.4}$$

The subscripts zero to the partial derivatives indicate that they are taken at $(t, 0, 0, \ldots, 0)$.

Transferring from random quantities to mathematical expectations on right and left in (2.3), and incorporating (1.3), we have

$$\nu_1 = M[X] = \varphi_0 + \sum_{k=1}^{q} \frac{1}{k!} \sum_{r_1=1}^{m} \sum_{r_2=1}^{m} \cdots \sum_{r_k=1}^{m} \left(\frac{\partial^k \varphi}{\partial V_{r_1} \partial V_{r_2} \cdots \partial V_{r_k}} \right)_0 \mu_{r_1 r_2 \ldots r_k}. \tag{2.5}$$

If the calculations are pursued further with (2.5) great difficulties arise because the partial derivatives have to be determined explicitly. Hence ways of avoiding this are much to be desired. One such way is as follows. Substitute certain special values $\xi_{r,s}$ of the V_r into (2.2) and expand it in terms of these parameters. Then by analogy with (2.3) we have

$$x_s = \varphi_0 = \sum_{k=1}^{q} \frac{1}{k!} \sum_{r_1=1}^{m} \sum_{r_2=1}^{m} \cdots \sum_{r_k=1}^{m} \left(\frac{\partial^k \varphi}{\partial V_{r_1} \partial V_{r_2} \cdots \partial V_{r_k}} \right)_0 \xi_{r_1 s} \xi_{r_2 s} \cdots \xi_{r_k s}. \tag{2.6}$$

In all there are N distinct combinations of the $\xi_{r_k s}$, so s = 1, 2, . . . , N. Multiplying both sides of (2.6) by certain coefficients α_s and summing the result, we have

$$S = \sum_{s=1}^{N} \alpha_s x_s = \sum_{s=1}^{N} \alpha_s \varphi_0 + \sum_{k=1}^{q} \frac{1}{k!} \sum_{r_1=1}^{m} \sum_{r_2=1}^{m} \cdots \cdots \sum_{r_k=1}^{m} \left(\frac{\partial^k \varphi}{\partial V_{r_1} \partial V_{r_2} \cdots \partial V_{r_k}} \right)_0 \sum_{s=1}^{N} \alpha_s \xi_{r_1 s} \xi_{r_2 s} \xi_{r_k s}. \tag{2.7}$$

Comparing (2.5) and (2.7) we see that the sum S will be an approximate value of the mathematical expectation of the integral of (2.2) if the α_s and $\xi_{r_k s}$ satisfy this system of algebraic equations:

$$\sum_{s=1}^{N} \alpha_s = 1, \tag{2.8}$$

$$\sum_{s=1}^{N} \alpha_s \xi_{r_1 s} \xi_{r_2 s} \cdots \xi_{r_k s} = \mu_{r_1 r_2 \ldots r_k} \qquad \begin{pmatrix} k = 1, 2, \ldots, q \\ r_1 r_2, \ldots, r_k = 1, 2, \ldots, m \end{pmatrix}. \tag{2.9}$$

So, selecting for the α_s and $\xi_{r_k s}$ some real solution to the system of (2.8), (2.9) we have

$$S = \sum_{s=1}^{N} \alpha_s x_s = M[X]. \tag{2.10}$$

The x_s appearing in this formula can be calculated by integrating the initial system of (1.1) while substituting various combinations of the $\xi_{r_k s}$ in the right parts, instead of the V_r. In all (1.1) is integrated N times each time with new $\xi_{r_k s}$ values. Calculation of the derivatives in (2.5) is thereby obviated.

Let us consider certain features of the system in (2.8), (2.9). We first observe that N is not restricted by any special conditions. But as N increases so do the numbers of unknowns, α_s and $\xi_{r_k s}$, while the number of equations in (2.8), (2.9) is unaltered. We may therefore always in principle take N large enough to ensure that there is a solution to (2.8), (2.9). The number of distinct equations in (2.8), (2.9) can be shown to be $Z = C_{m+q}^{q}$.

The total number of unknowns in (2.8), (2.9) will clearly be mN + N = N(m + 1).

Hence, choosing N from the condition

$$N \geqslant \frac{1}{m+1} C_{m+q}^{q}, \tag{2.11}$$

we can in principle ensure that a solution exists to (2.8), (2.9). In any case, when

$$N = C_{m+q}^{q} \tag{2.12}$$

we can choose all the $\xi_{r_k s}$ such that the resulting set of linear algebraic equations has a determinant different from zero. Then we can ensure that there really are α_s which can be found by the usual methods for these equations. However, as a rule the number N of coefficients α_s is extremely large, so when using (2.10) we have to integrate (1.1) a correspondingly large number of times. In practical calculations it is desirable to choose the $\xi_{r_k s}$ such in each case that as many as possible of the α_s are zero. The number of integrations of (1.1) can then be substantially reduced.

3. Determination of the Higher-Order Moments

To determine the central moments of higher orders it is sufficient to find the corresponding moments about the origin, because the relations between the two are simple. We therefore only state how the latter moments can be found. Denote the moment of order p of the quantity X about the origin by ν_p:

$$\nu_p = M[X^p]. \tag{3.1}$$

The notations also to be used are

$$X^p = \varphi^p(t, V_1, V_2, \ldots, V_m) = \psi(t, V_1, V_2, \ldots, V_m). \tag{3.2}$$

The whole discussion for φ above applies to ψ. Expanding ψ in Maclaurin series in terms of the V_r and transferring to mathematical expectations we get an expression analogous to (2.5) with this difference alone, that instead of φ we have ψ:

$$\nu_p = M[X^p] = \psi_0 + \sum_{k=1}^{q} \frac{1}{k!} \sum_{r_1=1}^{m} \sum_{r_2=1}^{m} \cdots \sum_{r_k=1}^{m} \left(\frac{\partial^k \psi}{\partial V_{r_1} \partial V_{r_2} \cdots \partial V_{r_k}} \right)_0 \mu_{r_1 r_2 \ldots r_k}. \tag{3.3}$$

Substituting in (3.2) for the V_r the $\xi_{r_k s}$ previously found, and expanding in series, we have

$$x_s^p = \psi_0 + \sum_{k=1}^{q} \frac{1}{k!} \sum_{r_1=1}^{m} \sum_{r_2=1}^{m} \cdots \sum_{r_k=1}^{m} \left(\frac{\partial^k \psi}{\partial V_{r_1} \partial V_{r_2} \cdots \partial V_{r_k}} \right)_0 \xi_{r_1 s} \xi_{r_2 s} \cdots \xi_{r_k s}. \tag{3.4}$$

Multiplying the resulting equations by the α_s, summing over s, and using (2.8), (2.9) we obtain

$$\nu_p = M[X^p] = \sum_{s=1}^{N} \alpha_s x_s^p. \tag{3.5}$$

Hence to determine ν_p it is sufficient to calculate the p-th degree of the solutions previously found and substitute the result in (3.5). No additional integrations of (1.1) to determine the ν_p are required.

Any cross moments for the $X_1, X_2, \ldots, X_n$, defined by (2.1) can be found by analogy. Thus to calculate

$$\nu = M[X_{k_1} X_{k_2} \ldots X_{k_p}] \quad (k_1, k_2, \ldots, k_p = 1, 2, \ldots, n)$$

we consider the function

$$\Omega(t, V_1, V_2, \ldots, V_m) = X_{k_1} X_{k_2} \ldots X_{k_p} \quad (k_1, k_2, \ldots, k_p = 1, 2, \ldots, n).$$

Applying the same arguments to Ω as we did to φ and ψ, we get

$$\nu = M[X_{k_1} X_{k_2} \ldots X_{k_p}] = \sum_{s=1}^{N} \alpha_s x_{k_1 s} x_{k_2 s} \ldots x_{k_p s} \quad (k_1, k_2, \ldots, k_p = 1, 2, \ldots, n) \tag{3.6}$$

where the $x_{k_1 s}, x_{k_2 s}, \ldots, x_{k_p s}$ are solutions to (1.1) found for the particular values of the V_r equal to the $\xi_{rk} s$.

4. Derivation of the Mathematical Expectation and Dispersion of the Solutions to (1.1) for the Case q = 2

Consider the use of the above method when quantities of the second order in the V_r are allowed for in expansion of the integral of (2.2).

A particularly simple solution can be found when the previous system of parameters V_r can be referred to a canonical system, i. e., when the V_r are uncorrelated. We suppose this done. Then

$$M[V_{r_1} V_{r_2}] = 0. \tag{4.1}$$

We note that

$$M[V_r^2] = \sigma_r^2. \tag{4.2}$$

In this case (2.8), (2.9) have the form

$$\sum_{s=1}^{N} \alpha_s = 1, \tag{4.3}$$

$$\sum_{s=1}^{N} \alpha_s \xi_{r_1 s} = 0 \qquad (r_1 = 1, 2, \ldots, m), \tag{4.4}$$

$$\sum_{s=1}^{N} \alpha_s \xi_{r_1 s} \xi_{r_2 s} = 0 \qquad (r_1 \neq r_2, \quad r_1, r_2 = 1, 2, \ldots, m), \tag{4.5}$$

$$\sum_{s=1}^{N} \alpha_s \xi_{r s}^2 = \sigma_r^2 \qquad (r = 1, 2, \ldots, m) \tag{4.6}$$

Thus, if the $\xi_{r_1 s}$ and $\xi_{r_2 s}$ are chosen arbitrarily, we have to integrate (1.1) $N = \frac{1}{2}(m+2)(m+1)$ times. But many of the α_s can be made zero by suitable choice of the $\xi_{r_1 s}$ and $\xi_{r_2 s}$, and the number of integrations to (1.1) substantially reduced. The ξ_{rs} are chosen in accordance with Table 1.

TABLE 1

s	r						
	1	2	3	...	$m-2$	$m-1$	m
1	ξ_1	0	0	...	0	0	0
2	0	ξ_2	0	...	0	0	0
...	...	...	...	...	...	...	...
$m-1$	0	0	0	...	0	ξ_{m-1}	0
m	0	0	0	...	0	0	ξ_m
$m+1$	ξ_1	ξ_2	ξ_3	...	ξ_{m-2}	ξ_{m-1}	ξ_m
$m+2$	$-\xi_1$	$-\xi_2$	$-\xi_3$	...	$-\xi_{m-2}$	$-\xi_{m-1}$	$-\xi_m$

Here N = m + 2, and (4.3), (4.4) go over to

$$\sum_{s=1}^{m+2} \alpha_s = 1, \tag{4.7}$$

$$\alpha_r + \alpha_{m+1} - \alpha_{m+2} = 0 \qquad (r = 1, 2, \ldots, m). \tag{4.8}$$

Summing all m equations in (4.8) and using (4.7), we have

$$\sum_{s=1}^{m+2} \alpha_s + (m-1)\alpha_{m+1} - (m+1)\alpha_{m+2} = 0.$$

Hence

$$(m+1)\alpha_{m+2} = (m-1)\alpha_{m+1} + 1. \tag{4.9}$$

(4.5) and (4.6) become

$$\alpha_{m+1} + \alpha_{m+2} = 0 \tag{4.10}$$

and

$$(\alpha_r + \alpha_{m+1} + \alpha_{m+2})\,\xi_r^2 = \sigma_r^2. \tag{4.11}$$

(4.9) and (4.10) give

$$\alpha_{m+1} = -\frac{1}{2m}, \tag{4.12}$$

$$\alpha_{m+2} = \frac{1}{2m}. \tag{4.13}$$

Then from (4.8) we have

$$\alpha_r = \frac{1}{m} \qquad (r = 1, 2, \ldots, m). \tag{4.14}$$

Finally, we get the ξ_r from (4.11):

$$\xi_r = \sigma_r \sqrt{m}. \tag{4.15}$$

Let us denote by x_s the solutions to (1.1) obtained by replacing the random quantities V_r by the nonrandom ξ_r in accordance with Table 1. Then from (2.10), (4.12), (4.13) and (4.14) we can write

$$M[X] = \sum_{s=1}^{m+2} \alpha_s x_s = \frac{1}{m}\left(\sum_{s=1}^{m} x_s + \frac{x_{m+2} - x_{m+1}}{2}\right). \tag{4.16}$$

The dispersion D[X] will be given by

$$D[X] = \sum_{s=1}^{m+2} \alpha_s x_s^2 - (M[X])^2 = \frac{1}{m}\left(\sum_{s=1}^{m} x_s^2 + \frac{x_{m+2}^2 - x_{m+1}^2}{2}\right) - (M[X])^2. \tag{4.17}$$

5. Derivation of the Mathematical Expectation and Dispersion of the Solutions to (1.1) for the Case q = 3

We suppose that in deriving the mathematical expectation and dispersion of the solutions to (1.1) we have to allow for quantities of the third order in the V_r. We assume the V_r independent and that the third-order moments $M[V_r^3] = 0$. Then to (4.3)-(4.6) we add an equation of the form

$$\sum_{s=1}^{N} \alpha_s \xi_{r_1 s} \xi_{r_2 s} \xi_{r_3 s} = 0 \qquad (r_1, r_2, r_3 = 1, 2, \ldots, m), \tag{5.1}$$

since $M[V_{r1} V_{r2} V_{r3}] = 0$.

From (2.12) the number of integrations of (1.1) which will ensure solutions to (2.8), (2.9) is

$$N = C_{m+3}^3 = \frac{(m+3)(m+2)(m+1)}{1 \times 2 \times 3}.$$

This number can be very large. Even if m = 5 we have N = 56. But the ξ_{rs} can be selected so as to reduce the number of integrations substantially. The ξ_{rs} are chosen in accordance with Table 2.

TABLE 2

s	r					
	1	2	3	. . .	$m-1$	m
1	ξ_1	0	0	. . .	0	0
2	$-\xi_1$	0	0	. . .	0	0
3	0	ξ_2	0	. . .	0	0
4	0	$-\xi_2$	0	. . .	0	0
. . .	. . .	. . .	. . .	. . .	0	. . .
$2m-1$	0	0	0	. . .	0	ξ_m
$2m$	0	0	0	. . .	0	$-\xi_m$

Then we clearly have

$$N = 2m, \tag{5.2}$$

$$\xi_{r_1 s}\xi_{r_2 s} = 0 \quad (\text{when } r_1 \neq r_2), \tag{5.3}$$

$$\xi_{r_1 s}\xi_{r_2 s} = \xi_r^2 \quad (\text{when } r_1 = r_2 = r). \tag{5.4}$$

We conclude from (5.3) that all the equations of (4.5) are satisfied by this choise of the ξ_{rs}. As for (4.4), (4.6) and (5.1), they go over to

$$\alpha_{2r-1} - \alpha_{2r} = 0 \qquad (r = 1, 2, \ldots, m), \tag{5.5}$$

$$(\alpha_{2r-1} + \alpha_{2r})\,\xi_r^2 = \sigma_r^2 \qquad (r = 1, 2, \ldots, m). \tag{5.6}$$

Taking all the α_s equal, $\alpha_s = \alpha$, we satisfy (5.5), and from (4.3) and (5.6) get

$$\alpha_s = \alpha = \frac{1}{2m}, \tag{5.7}$$

$$\xi_r = \sigma_r \sqrt{m}. \tag{5.8}$$

Thus if we put the nonrandom quantities ξ_r and $-\xi_r$ into (1.1) instead of the random V_r and integrate, we get 2m values of the integrals of the form

$$x_r = \varphi(t, 0, \ldots, 0, \xi_r, 0, \ldots, 0), \quad x_r^* = \varphi(t, 0, \ldots, 0, -\xi_r, 0, \ldots, 0). \tag{5.9}$$

From (2.10), (5.7) and (5.9) M[X] will be given by

$$M[X] = -\frac{\sum_{r=1}^{m} (x_r + x_r^*)}{2m}. \tag{5.10}$$

As for the dispersion of X, it can be determined from

$$D[X] = M[X^2] - (M[X])^2 = \frac{\sum_{r=1}^{m} (x_r^2 + x_r^{*2})}{2m} - (M[X])^2. \tag{5.11}$$

This latter can easily be put in another form, more convenient for practical calculations, namely:

$$D[X] = M[(x - M[X])^2] = \frac{1}{2m} \sum_{r=1}^{m} [(x_r - M[X])^2 + (x_r^* - M[X])^2].$$

(5.10) and (5.11) become particularly simple if the right half of (1.1) contains only a single random parameter. Then we have

$$M[X] = \frac{x + x^*}{2}, \tag{5.12}$$

$$D[X] = \left(\frac{x - x^*}{2}\right)^2, \tag{5.13}$$

i. e., the mathematical expectation is half the sum of the solutions to (1.1), obtained by replacing V by σ and $-\sigma$, and the dispersion is the square of half the difference of these solutions.

When m is large it may be that the ξ_r will exceed the maximum possible values of the V_r. The error in (2.3) occaisoned by rejecting the residual term may then increase greatly. But formulas can easily be constructed for the mathematical expectation which do not require large values of the ξ_r to be substituted.

We choose the ξ_r in Table 2 proportional to the corresponding root mean square deviations σ_r:

$$\xi_r = \lambda\sigma_r \quad (r = 1, 2, \ldots, m), \tag{5.14}$$

where λ is a constant coefficient independent of r.

The following expression can be obtained for the mathematical expectation of X:

$$M[X] = \frac{1}{2\lambda^2} \sum_{r=1}^{m} (x_r + x_r^*) + x_0\left(1 - \frac{m}{\lambda^2}\right), \tag{5.15}$$

where x_r and x_r^* are given by (5.9) and $x_0 = \varphi(t, 0, 0, \ldots, 0)$. When $\lambda = \sqrt{m}$ this formula coincides with (5.10).

If all the V_r are covered by the normal distribution law it is frequently supposed that their limiting values do not exceed $3\sigma_r$. Taking $\lambda = 3$, (5.15) gives

$$M[X] = \frac{1}{18} \sum_{r=1}^{m} (x_r + x_r^*) + x_0\left(1 - \frac{m}{9}\right). \tag{5.16}$$

By analogy we could derive formulas for the probability characteristics of X for q = 4, 5, etc. These formulas are not deduced for reasons of space.

6. Example

In conclusion we consider an example illustrating the use of this method. The mathematical expectation and dispersion will be estimated for a random function given as a differential equation

$$\dot{X} = -f(X + V + 1) \tag{6.1}$$

with initial condition

$$X(0) = 0.$$

The function f(z) is given to be

$$f(z) = \begin{cases} 1 \text{ for } z > 1, \\ -1 \text{ for } |z| \leqslant 1, \\ z \text{ for } z < 1. \end{cases}$$

V is a random quantity following an equal probability law in the range $(-\frac{1}{4}, +\frac{1}{4})$. The probability density for V in this interval is p(V) = 2, being zero outside.

The mathematical expectation of V is zero, and its dispersionis

$$\sigma_v^2 = D[V] = 2\int_{-1/4}^{+1/4} V^2 dV = \frac{1}{48}.$$

It can be shown that when V > 0, beginning at t ≥ V, the integralof (6.1) has the form

$$X(t) = e^{V-t} - V - 1. \tag{6.2}$$

When V < 0 this integral is given by

$$X(t) = -(V + 1)(1 - e^{-t}). \tag{6.3}$$

Since $V \leq \frac{1}{4}$, the integral to (6.1) is given by (6.2) and (6.3) in any case for $t > \frac{1}{4}$. Using (6.2) and (6.3), we can determine the precise values of the mathematical expectation and dispersion for X(t):

$$M[X] = -2\int_{-1/4}^{0} (V + 1)(1 - e^{-t})\, dV +$$

$$+ 2\int_{0}^{1/4} (e^{V-t} - V - 1)\, dV = -1 + 1.0055\, e^{-t}, \tag{6.4}$$

$$D[X] = -2\int_{-1/4}^{0} (V + 1)^2 (1 - e^{-t})^2 dV +$$

$$+ 2\int_{0}^{1/4} (e^{V-t} - V - 1)^2\, dV - (M[X])^2 = 0.0208 - 0.0437\, e^{-t} + 0.0229\, e^{-2t}. \tag{6.5}$$

On the other hand, if we replace V in (6.2) and (6.3) by σ_V and $-\sigma_V$, we can determine M[X] and D[X] from (5.12) and (5.13).

Let us put

$$x_1 = X(\sigma_V, t) = e^{\frac{1}{4\sqrt{3}}t} - \frac{1}{4\sqrt{3}} - 1, \quad x_1^* = X(-\sigma_V, t) = -\left(-\frac{1}{4\sqrt{3}} + 1\right)(1 - e^{-t}).$$

Then the approximate values of M[X] and D[X] calculated from (5.12) and (5.13) will have the form

$$M[\tilde{X}] = \frac{x_1 + x_1^*}{2} = -1 + 0.0054\, e^{-t}, \tag{6.6}$$

$$D[\tilde{X}] = \frac{x_1^2 + x_1^{*2}}{2} - (M[\tilde{X}])^2 = 0.0208 - 0.0434\, e^{-t} + 0.0226\, e^{-2t}. \tag{6.7}$$

Comparison of (6.4) and (6.5) with (6.6) and (6.7) respectively shows that the results agree extremely well.

Received September 20, 1956

LITERATURE CITED

[1] V. S. Pugachev, "Fundamentals of the general theory of random functions," Trudy Akademii Art. Nauk (1952).

[2] V. S. Pugachev, "The general theory of random function correlation," AN SSSR, Ser. Matem. 17, No. 5 (1953).

[3] V. V. Solodovnikov, Introduction to the Statistical Dynamics of Automatic Control Systems [in Russian] (Gostekhizdat, 1952).

[4] V. I. Bunimovich, Fluctuation Processes in Radio Receiving Equipment [in Russian] (Sovetskoe Radio, 1952).

[5] N. I. Andreev, "Determination of the correlation function for the error at the output of a linear system with constant coefficients if a nonstationary perturbation is applied to the input," [in Russian]. Coll. of scientific papers from the N. E. Zhukovskii VVIA* 1 (1954).

[6] V. K. Krapivin, "Probability characteristics of linear automatic control systems subject to nonstationary perturbations" [in Russian] Coll. of scientific papers from the N. E. Zhukovskii VVIA* 1 (1954).

[7] B. G. Dostupov, "Determination of the probability characteristics of linearizeable integrals to systems of ordinary differential equations" [in Russian] Coll. of scientific papers from the N. E. Zhukovskii VVIA* 1 (1954).

[8] P. I. Kuznetsov, R. L. Stratonovich and V. I. Tikhonov, "Passage of random functions through nonlinear systems," Automation and Remote Control (USSR) 14, No. 4 (1953).

[9] I. E. Kazakov, "An approximate method for the static study of nonlinear systems" [in Russian] Trudy N. E. Zhukovskogo, VVIA* 1954, No. 394.

*Air Force Engineering Academy.

[10] I. E. Kazakov, "The study of dissipation in nonlinear automatic systems," [in Russian] Coll. of scientific papers from the Zhukovskii VVIA* 1 (1954).

[11] H. M. James, N. B. Nichols and R. S. Phillips, Theory of Servomechanisms [Russian translation] (IL, 1951).

*Air Force Engineering Academy.

THE DYNAMIC ACCURACY OF A SERVO SYSTEM CONTAINING A NONLINEAR LINK WITH A POLYNOMIAL CHARACTERISTIC

S. Ia. Raevskii

(Moscow)

The root-mean-square error of a servo system having a nonlinear link with a polynomial characteristic is calculated. The perturbations are supposed stochastic. The error is calculated in successive approximations by representing the higher moments approximately in terms of the lower.

The dynamic accuracy of a servo system to which perturbations of stochastic type are applied is estimated in terms of the mean square error. The latter is nonlinearly related to the input perturbations [1, 2]. Therefore no exact expression for the error in terms of some functional of the input can be derived, and so an approximate one must be sought. One way of doing this is to use successive approximation [1]. Another is to linearize the nonlinear functional which relates the error to the input perturbation [2]. In the latter case, however, it is impossible to allow for the effect of the oscillations occurring in nonlinear servos [3] on the mean square error, or for the higher (than second) moments of the perturbations. We use successive approximation in order to allow for such factors. To simplify the calculations involved in extracting the higher moments we represent them approximately in terms of the lower-order moments.

1. The Equation of the Nonlinear Servo System and its Solution

Figure 1 shows the structural diagram of a nonlinear servo.

The equation relating the system error $\epsilon(t) = x(t) - v(t)$ to the control and perturbation signals x(t) and z(t) in the nonsteady state is

$$\varepsilon(t) = x(t) - \int_0^\infty k(t') f[\varepsilon(t-t') + z(t-t')]\, dt' \tag{1.1}$$

or in short form

$$\varepsilon = x - \tilde{S}[\varepsilon + z], \tag{1.2}$$

where $\tilde{S}$ is the symbol for the nonlinear functional.

To decide on the zeroth approximation to the error we briefly consider how a nonlinear servo follows up an input signal.

We suppose that an approximately sinusoidal self-oscillation has been set up in the system, after which the perturbation u(t) = x(t) + z(t) is applied to the input. Thus up to the time of applying the perturbation the system error will be

$$\varepsilon_0 = a_0 \cos \omega_0 t, \tag{1.3}$$

where a_0 and ω_0 are determined in some way by the methods for use with self-oscillations in nonlinear controlled systems [3]. From the instant when the perturbation is applied the error will alter in accordance with the nature of the perturbation, and will of course depend on its initial value. It is therefore logical to take (1.3) as the zeroth approximation to the error. The relation to the type of perturbation will then appear in subsequent approximations. If there is no self-oscillation in the system we can take some steady-state error as our zeroth approximation.

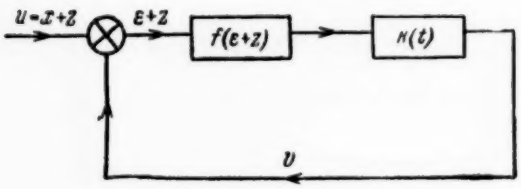

Fig. 1.

Thus from (1.2) our first approximation to the error is

$$\varepsilon_1 = x - \tilde{S}\,[\varepsilon_0 + z],$$

where ϵ_0 is given by (1.3).

The second approximation is of the form

$$\varepsilon_2 = x - \tilde{S}\,[\varepsilon_1 + z],$$

and the n-th approximation

$$\varepsilon_n = x - \tilde{S}\,[\varepsilon_{n-1} + z].$$

The successive approximations for the $\tilde{S}$, corresponding to the servo shown schematically in Figure 1 converge for a broad class of random functions [1] and the expression for the error in terms of the input can therefore in principle be found to any accuracy.

Let us now determine the form of the function $f(\xi)$ appearing in (1.1). We suppose that $f(\xi)$ can be represented as a polynomial of finite degree. This assumption is true of many automatic devices. Thus the characteristic of a bounded ac servo-motor, for which the approximation indicated by Curve 1 in Figure 2 is often used subject to the condition that the probability that ξ will take a value such that $|\xi| > \xi_0$ is small, may be represented by Curve 2, with the expression

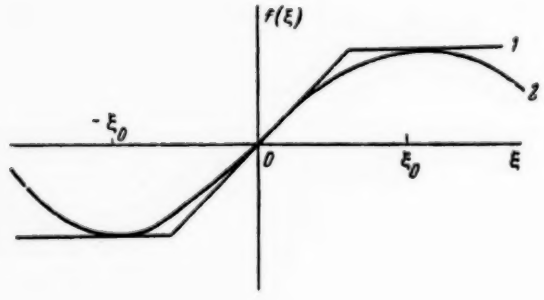

Fig. 2.

$$f(\xi) = A\xi - B\xi^3 \quad (A > 0, \quad B > 0). \tag{1.4}$$

In future we assume $f(\xi)$ given by (1.4).

2. Correlation Representation of the Higher Moments of Random Functions

To find the approximate mean-square error of our nonlinear servo we need to extract the higher moments of the perturbation. As the higher moments are cumbrous to handle we naturally seek a way of representing them approximately and reasonably simply as some function of the low-order moments, which can be handled with

simpler formulas. The lower-order moments we shall use are the second moments for even moments of any order, and the second combined with the first of the odd moments which differs from zero for odd moments.

As function of the lower-order moments we select for moments of the form

$$m_l(t_1, t_2, \ldots, t_l) = M[X_1(t_1) X_2(t_2) \ldots X_l(t_l)]$$

when the order of the index $l = 2n$ ($n = 1, 2, \ldots$) is even, the function

$$L_r(t_1, t_2, \ldots, t_l) = \sum_{p=1}^{N} a_p \Pi^{(p)} m_2^{(\alpha\beta)}(t_\alpha, t_\beta). \tag{2.1}$$

In (2.1) we have

$$\Pi^{(p)} m_2^{(\alpha\beta)}(t_\alpha, t_\beta) = m_2^{(\alpha_1\beta_1)}(t_{\alpha_1}, t_{\beta_1})\, m_2^{(\alpha_2\beta_2)}(t_{\alpha_2}, t_{\beta_2}) \ldots m_2^{(\alpha_n\beta_n)}(t_{\alpha_n}, t_{\beta_n});$$

the pairs of indices $(\alpha_1\beta_1), (\alpha_2\beta_2), \ldots, (\alpha_n\beta_n)$ being the p-th of $N = (2n-1)(2n-3)\ldots 1$ possible sequences comprised of pairs of integers from 1 to $l = 2n$ and which differ in at least one such pair $(\alpha_i\beta_i)$, where $\alpha_i \neq \beta_i$ for any i. For odd moments of order $l = 2n-1$ ($n = 1, 2, \ldots$) we select a function of the form

$$L_{\text{odd}}(t_1, t_2, \ldots, t_l) = \sum_{p=1}^{N} a_p m_{2k-1}(t_{\gamma_1}, t_{\gamma_2}, \ldots, t_{\gamma_{2k-1}})\, \Pi^{(p)} m_2^{(\alpha\beta)}(t_\alpha, t_\beta). \tag{2.2}$$

Here $m_{2k-1}(t_{\gamma_1}, t_{\gamma_2}, \ldots, t_{\gamma_{2k-1}})$ is the lowest odd moment which differs from zero,

$$\Pi^{(p)} m_2^{(\alpha\beta)}(t_\alpha, t_\beta) = m_2^{(\alpha_1\beta_1)}(t_{\alpha_1}, t_{\beta_1})\, m_2^{(\alpha_2\beta_2)}(t_{\alpha_2}, t_{\beta_2}) \ldots m_2^{(\alpha_{2(n-k)}\beta_{2(n-k)})} \times$$
$$\times (t_{\alpha_{2(n-k)}}, t_{\beta_{2(n-k)}});$$

the indices γ_i, α_j, β_k being all different from one another and forming the p-th of N possible combinations of the integers from 1 to $2n-1$, which differ in at least one of the indices $\gamma_i, \alpha_j, \beta_k$, $N = C_{2n-1}^{2k-1}(2n-2k-1)(2n-2k-3)\ldots 1$, C_{2n-1}^{2k-1} being a binomial coefficient.

The coefficients a_p appearing in the representations of (2.1) and (2.2) (which we shall term correlation representations) we arrange in order such that as representations of the higher moments they are the best in the least-squares sense. Hence these coefficients are determined from the condition that the quadratic functionals

$$I_e = \int_{-\infty}^{+\infty} \ldots \int_{-\infty}^{+\infty} \{m_{2n}(t_1, t_2, \ldots, t_{2n}) - L_e(t_1, t_2, \ldots, t_{2n})\}^2 dt_1 \ldots dt_{2n} \tag{2.3}$$

or

$$I_{\text{odd}} = \int_{-\infty}^{+\infty} \cdots \int_{-\infty}^{+\infty} \{m_{2n-1}(t_1, t_2, \ldots, t_{2n-1}) - \\ - L_{\text{odd}}(t_1, t_2, \ldots, -t_{2n-1})\}^2 dt_1 \ldots dt_{2n-1}. \tag{2.3a}$$

have a minimum.

Substituting (2.1) into (2.3) or (2.2) into (2.3a) we get a system of N equations to determine the N unknown coefficients a_p:

$$\sum_{p=1}^{N} b_{qp} a_p = c_q \quad (q = 1, \ldots, N), \tag{2.4}$$

where *

$$b_{qp} = \int_{-\infty}^{+\infty} \cdots \int_{-\infty}^{+\infty} \Pi^{(q)} m_2^{(\alpha\beta)}(t_\alpha, t_\beta)\, \Pi^{(p)} m_2^{(\gamma\delta)}(t_\gamma, t_\delta)\, dt_1 \ldots dt_{2n},$$

$$c_q = \int_{-\infty}^{+\infty} \cdots \int_{-\infty}^{+\infty} m_{2n}(t_1, t_2, \ldots, t \qquad \Pi^{(q)} m_2^{(\gamma\delta)}(t_\gamma, t_\delta)\, dt_1 \ldots dt_{2n}$$

for even-order moments. The coefficients for odd-order moments have analogous expressions.

Since the terms in the sums of (2.1) and (2.2) are linearly independent the determinant of this system differs from zero [4], and so the a_p are uniquely defined.

(2.4) implies that to determine the a_p we need to know the higher moments, since they appear in the expressions for the c_q. But having once calculated the a_p for a given random function the higher moments are henceforth excluded from consideration, only their correlation representations being used. The statistical properties of the random function, as expressed by the higher moments, will be taken care of approximately by the a_p.

On the other hand the a_p may sometimes be determined without calculation by using the scheme above. If $a_p \equiv 1$ for any $\underline{p}$ ($p = 1, 2, \ldots, N$) then (2.1) is the moment of order 2n for a normal random function of statistical mean equal to zero and having correlation functions $R^{(\alpha_i \beta_i)}(\xi_1, \xi_2) = m_2^{(\alpha_i \beta_i)}(\xi_1, \xi_2)$. Clearly, all random functions similar to this normal one will have $a_p \approx 1$ for all $\underline{p}$. In general the correlation representations of (2.1) and (2.2) will be close to the true values for random processes in which paired correlations predominate. In other circumstances they may be far from the true values, and hence correlations of higher order may need to be allowed for.

The moments of random processes which have been transformed by nonlinear devices with polynomial characteristics can be expressed in terms of the moments of the initial random processes [1]. If the correlation representations of the latter are known the moments of the transformed processes are expressible in terms of the second and lowest-order odd moments appearing in the correlation representations of the moments of the initial random process.

The moments of random processes transformed by linear systems are obtained as linear ones by linear transformation from the moments of the initial random processes. The correlation representation of the moments of the transformed process then has the same structure and coefficients as for the initial process, only the second and lowest-odd moments will now refer to the transformed process, and not to the initial one.

Thus by using correlation representations we can replace the consideration of higher moments by that of the second and lowest-odd moments with any linear or nonlinear transformations on random processes.

* The obliteration of part of the equation occurs in the original — Publisher.

3. Mean-Square Error of a Nonlinear Servo System

The successive approximations to the mean-square error of the nonlinear servo shown schematically in Figure 1 will be found by the method described in Section 1. The first approximation to the error is

$$\varepsilon_1 = x(t) - \int_0^\infty k(t') \{A[a_0 \cos \omega_0 (t - t') + z(t - t')] - B[a_0 \cos \omega_0 (t - t') + z(t - t')]^3\} dt',$$

and the mean-square error in the first approximation

$$\overline{\varepsilon_1^2} = m_{2x}(t, t) - 2\int_0^\infty k(t') \left\{ \sum_{n=0}^{3} \beta_n (t - t') M[x(t) z^n (t - t')] \right\} dt' + \int_0^\infty \int_0^\infty k(t_1) k(t_2') \left\{ \sum_{n=0}^{3} \sum_{m=0}^{3} \beta_n (t - t_1') \beta_m (t - t_2') \times M[z^n (t - t_1') z^m (t - t_2')] \right\} dt_1' dt_2', \tag{3.1}$$

where

$$\beta_0(t) = \left(Aa_0 - \frac{3}{4} a_0^3 B\right) \cos \omega_0 t - 4Ba_0^3 \cos 3\omega_0 t,$$

$$\beta_1(t) = A - 3Ba_0^2 \cos^2 \omega_0 t, \quad \beta_2(t) = -3Ba_0 \cos \omega_0 t, \quad \beta_3(t) = -B.$$

The signal and the noise are produced in different ways and are therefore statistically independent. The second term on the right-hand side in (3.1) therefore drops out. The noise moments appearing in (3.1) (the noise being assumed a normal random process) are represented as combinations of correlation functions:

$$M[z^2 (t - t_1') z(t - t_2')] = M[z(t - t_1') z^2 (t - t_2')] = 3R_z (t_2' - t_1') R_1 (0),$$
$$M[z^2 (t - t_1') z^2 (t - t_2')] = 2R_z^2 (t_2' - t_1') + R_z^2 (0),$$
$$M[z^3 (t - t_1') z^3 (t - t_2')] = 6R_z^3 (t_2' - t_1') + 9R_z^2 (0) R_z (t_2' - t_1').$$

The odd moments are zero because the noise is normal and its mathematical expectation zero.

Substituting the values of the moments into (3.1), we get

$$\begin{aligned} \overline{\varepsilon_1^2} = m_{2x}(t, t) + \int_0^\infty \int_0^\infty k(t_1') k(t_2') \{ & \beta_0 (t - t_1') \beta_0 (t - t_2') + \\ & + \beta_1 (t - t_1') \beta_1 (t - t_2') R_z (t_2' - t_1') + R_z^2 (0) [\beta_0 (t - t_1') \beta_2 (t - t_2') + \\ & + \beta_0 (t - t_2') \beta_2 (t - t_1')] + 3R_z (t_2' - t_1') R_z (0) [\beta_1 (t - t_1') \beta_3 (t - t_2') + \\ & + \beta_1 (t - t_2') \beta_3 (t - t_1')] + [2R_z^2 (t_2' - t_1') + R_z^2 (0)] \beta_2 (t - t_1') \beta_2 (t - t_2') + \\ & + [6R_z^3 (t_2' - t_1') + 9R_z (t_2' - t_1') R_z^2 (0)] \beta_3 (t - t_1') \beta_3 (t - t_2')\} dt_1' dt_2'. \end{aligned} \tag{3.2}$$

The second approximation is calculated on the simplifying assumption that z(t) (noise) is small compared with x(t) (control action). Neglecting the effect of the low noise, we get the first approximation to the error as

$$\varepsilon_1 = x(t) - \varphi(t),$$

where $\varphi(t)$ is a regular function of time with the expression

$$\varphi(t) = \left\{Aa_0 - \frac{3}{4} Ba_0^3\right\} \{\mathrm{Re}\,[Y(j\omega_0)] \cos \omega_0 t + \mathrm{Im}\,[Y(j\omega_0)] \sin \omega_0 t\} - \\ - \frac{1}{4} Ba_0^3 \{\mathrm{Re}\,[Y(j3\omega_0)] \cos 3\omega_0 t + \mathrm{Im}\,[Y(j3\omega_0)] \sin 3\omega_0 t\}. \tag{3.3}$$

Here

$$Y(j\omega) = \int_0^\infty k(t')\, e^{j\omega t'}\, dt'$$

is the transfer function of the linear part of the servo.

The expression for the second approximation to the error is

$$\varepsilon_2 = x(t) - \int_0^\infty k(t') \{A[x(t - t') - \varphi(t - t')] - \\ - B[x(t - t') - \varphi(t - t')]^3\}\, dt',$$

its mean square being

$$\overline{\varepsilon_2^2} = m_{2x}(t, t) - 2\int_0^\infty R_{xy}^{(1)}(t, t - t')\, k(t')\, dt' + \\ + \int_0^\infty \int_0^\infty k(t_1')\, k(t_2')\, R_{yy}^{(1)}(t - t_1', t - t_2')\, dt_1'\, dt_2', \tag{3.4}$$

where we have

$$R_{xy}^{(1)}(t_1, t_2) = M\{x(t_1) A[x(t_2) - \varphi(t_2)] - x(t_1) B[x(t_2) - \varphi(t_2)]^3\},$$
$$R_{yy}^{(1)}(t_1, t_2) = M\{A^2[x(t_1) - \varphi(t_1)][x(t_2) - \varphi(t_2)] - AB[x(t_1) - \varphi(t_1)]^3 \times \\ \times [x(t_2) - \varphi(t_2)] - AB[x(t_1) - \varphi(t_1)][x(t_2) - \varphi(t_2)]^3 + \\ + B^2[x(t') - \varphi(t_1)]^3 [x(t_2) - \varphi(t_2)]^3\}.$$

We suppose all the odd moments of the control action up to the fifth inclusive to be zero. Then only the even moments remain in the expressions for $R_{xy}^{(1)}(t_1, t_2)$ and $R_{yy}^{(1)}(t_1, t_2)$; we can consider the correlation representations of these known. Calculating $R_{xy}^{(1)}(t_1, t_2)$ and $R_{yy}^{(1)}(t_1, t_2)$, we get

$$R^{(1)}_{yy}(t_1, t_2) = P_{00}(t_1, t_2) + P_{11}(t_1, t_2) R_x(t_1, t_2) + P_{20}(t_1, t_2) R_x(t_1, t_1) +$$
$$+ P_{02}(t_1, t_2) R_x(t_2, t_2) + P_{31}(t_1, t_2) R_x(t_1, t_1) R_x(t_1, t_2) +$$
$$+ P_{13}(t_1, t_2) R_x(t_2, t_2) R_x(t_1, t_2) + P_{22}(t_1, t_2) \{2R_x^2(t_1, t_2) +$$
$$+ R_x(t_1, t_1) R_x(t_2, t_2)\} + P_{33}(t_1, t_2) \{6R_x^3(t_1, t_2) +$$
$$+ 9R_x(t_1, t_2) R_x(t_1, t_1) R_x(t_2, t_2)\},$$
$$R^{(1)}_{xy}(t_1, t_2) = Q_{13}(t_1, t_2) R_x(t_1, t_2) R_x(t_2, t_2) + Q_{11}(t_1, t_2) R_x(t_1, t_2).$$

The notation used here is

$$P_{00}(t_1, t_2) = B^2\varphi^3(t_1)\varphi^3(t_2) - AB[\varphi^3(t_1)\varphi(t_2) + \varphi(t_1)\varphi^3(t_2)] + A^2\varphi(t_1)\varphi(t_2),$$
$$P_{11}(t_1, t_2) = 9B^2\varphi^2(t_1)\varphi^2(t_2) - 3AB[\varphi^2(t_1) + \varphi^2(t_2)] + A^2,$$
$$P_{20}(t_1, t_2) = 3B^2\varphi^3(t_2)\varphi(t_1) - 3AB\varphi(t_1)\varphi(t_2),$$
$$P_{02}(t_1, t_2) = 3B^2\varphi^3(t_1)\varphi(t_2) - 3AB\varphi(t_1)\varphi(t_2),$$

$$P_{31}(t_1, t_2) = \{3B^2\varphi^2(t_2) - AB\} a_{31}, \quad P_{13}(t_1, t_2) = \{3B^2\varphi^2(t_1) - AB\} a_{13},$$
$$P_{22}(t_1, t_2) = \{9B^2\varphi(t_1)\varphi(t_2)\} a_{22}, \quad P_{33}(t_1, t_2) = B^2 a_{33},$$
$$Q_{13}(t_1, t_2) = -Ba_{13}, \quad Q_{11}(t_1, t_2) = A - 3B\varphi^2(t_2).$$

The constants a_{31}, a_{13}, a_{22}, a_{33} are determined by the method described in Section 2. These constants are, as it were, corrections to the correlation representation to allow for the deviations from normal in the real random process. The subsequent approximations to the mean square error can, in principle, be found in the same way.

Taking (3.4) together with (3.5), we see that the self-oscillations affect the mean-square error insofar as the expression for this error contains higher harmonics of the self-oscillation frequency. Even higher harmonics will appear in subsequent approximations, so the complete picture of how the self-oscillation affects the true mean-square error will be very complex. The higher moments of the perturbation also have a considerable influence on the mean-square error. In the second approximation moments up to the sixth inclusive are allowed for. In subsequent approximations moments of still higher order are incorporated.

This method of calculating the mean-square error of a servo with a nonlinearity of polynomial type enables one to determine the effect of self-oscillations and of higher moments of the perturbation on the dynamic accuracy approximately. This effect is extremely important and must be allowed for in practical cases.

This method can also be applied to certain nonlinear problems in electronics, in particular to fluctuations in tube oscillators.

Received September 27, 1956

LITERATURE CITED

[1] P. I. Kuznetsov, R. L. Stratonovich and V. I. Tikhonov, "Passage of random functions through nonlinear systems," Automation and Remote Control (USSR) 14, No. 4 (1953).

[2] I. E. Kazakov, "Approximate probability analysis of the operational accuracy of essentially nonlinear automatic systems," Automation and Remote Control (USSR) 17, No. 5 (1956).*

*See C. B. Translation.

[3] Fundamentals of Automatic Control [in Russian], Ed. by V. V. Solodovnikov (Mashgiz, 1954).

[4] S. G. Mikhlin, Direct Methods in Mathematical Physics [in Russian] (Gostekhizdat, 1950).

SOME ASPECTS OF THE SWITCHOVERS IN NONLINEAR AUTOMATIC CONTROL SYSTEMS WITH PIECEWISE-SMOOTH NONLINEAR ELEMENT CHARACTERISTICS

M. A. Aizerman and F. R. Gantmakher

(Moscow)

We consider automatic control systems in which the processes are described by the equations

$$\dot{x}_i = \sum_{j=1}^{n} \alpha_{ij} x_j + \lambda_i y \qquad (i = 1,2,\ldots,n),$$
$$y = f(x), \quad x = \sum_{j=1}^{n} \beta_j x_j - \varkappa y, \tag{1}$$

where α_{ij}, β_j, λ_i and $\varkappa$ are numbers (some of which may be zero).

As regards the characteristic $y = f(x)$, we suppose it composed of two single-valued smooth curves $y = f_1(x)$ and $y = f_2(x)$, termed in future branches I and II of the characteristic. The correspondence points P_1 and P_2 on these curves are given (Figure 1).

If the image point moves in the x, y plane along one branch and reaches a correspondence point at $t = t^*$ it instantaneously transfers to the other branch. This transfer is termed a switchover.

It will further be shown that in some cases of switchover $\underline{x}$ may change continuously, and in others discontinuously. The image point then passes from P_1 on one branch to Q on the other, P_1Q not necessarily being parallel to the y-axis.

Equations (1) usually enable one to determine the position of Q uniquely. But sometimes (see below) the position of Q cannot be determined from (1) alone, either at all, or at any rate uniquely. The switchover is then said to be undetermined. To compute the switchover in such special cases we must allow for minor parameters neglected in drawing up (1). When Q is given uniquely by (1), the switchover can occur in two ways.

1. At $t = t^*$, P_1 instantaneously jumps to Q and moves along this second branch for a certain time. No matter whether the direction of motion (i. e., the sign of dx/dt) is retained or not, and no matter when the next switchover, this type of switchover is termed normal.

2. At $t = t^*$ the point jumps to the other branch, but only instantaneously, i. e., it does not move along the other branch or remain on it for a finite time, dropping back at once to the former branch.

No matter what the subsequent motion (whether along its old branch, or whether a fresh jump to the second occurs) this mode is termed sliding.

As well as P_1 and Q, we further consider Q^*, lying on the second branch and having the same $\underline{x}$ as P_1 (Figure 1).

To determine the conditions for sliding switchover and the pecularities thereof we assume that when Q does not coincide with Q^* the instantaneous jump from P_1 to Q can be considered as a continuous and theoretically instantaneous process (in practice it is very fast) in which the point initially moves vertically from P_1 to Q^* and then along the second branch to Q. If P_2 is reached on the way, Q is not attained as "slipping-back" occurs, i. e., an instantaneous return to the first branch.

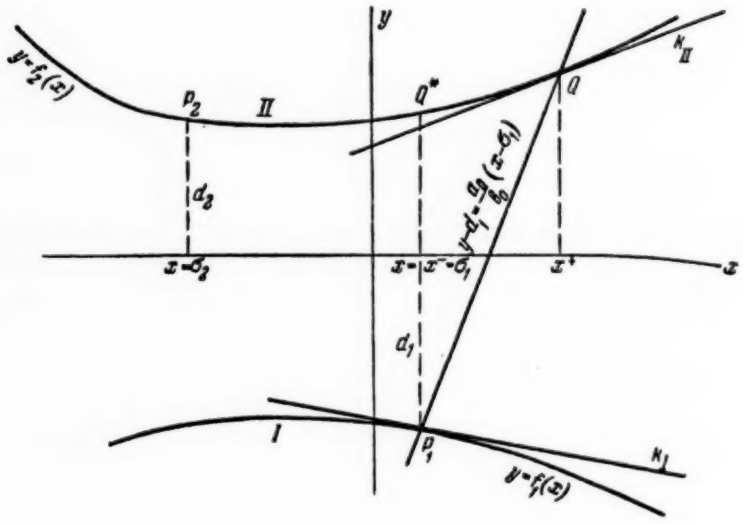

Fig. 1.

Sliding switchovers have so far been encountered in relay systems, and many papers have been devoted to sliding modes in relay systems.[1] Here we deal with the conditions where sliding and undetermined switchovers occur in systems with nonsmooth characteristics of a general type, which may be discontinuous or continuous. It will be shown that in general, and also in the special case of relay systems, two distinct types of sliding switchover can exist (only one has so far been considered in relay systems theory). Undetermined switchovers, impossible in relay systems, are evidently considered for the first time here. This is also the first time that it has been shown that sliding switchovers can occur in systems with continuous but kinked characteristics.

We will in future start from the system

$$D(p)x = K(p)y, \qquad y = f(x), \qquad p = \frac{d}{dt}, \tag{2}$$

instead of from (1); here[2] $D(p) = a_0p^n + a_1p^{n-1} + \ldots + a_n$, $K(p) = b_0p^n + b_1p^{n-1} + \cdots + b_n$.

(2) is derived from (1) by eliminating all unknowns except $\underline{x}$ and $\underline{y}$. It serves to determine $\underline{x}$ only prior to the correspondence point being reached. Function $\underline{x}$ and some of its derivatives are discontinuous at the jump point. The values of $\underline{x}$ and its derivatives before and after the breaks are determined by the step conditions

[1] Reviewed up to 1955 in [1]. Papers we have found appearing after 1955 are [2-4].

[2] If the degree $\underline{m}$ of the polynomial K(p) is less than $\underline{n}$, some of the coefficients in K(x) become zero.

$$
\begin{aligned}
a_0\xi_0 &= b_0\eta_0,\\
a_0\xi_1 + a_1\xi_0 &= b_0\eta_1 + b_1\eta_0,\\
&\cdots\cdots\cdots\cdots\\
a_0\xi_{n-1} + a_1\xi_{n-2} + \cdots + a_{n-1}\xi_0 &= b_0\eta_{n-1} + b_1\eta_{n-2} + \cdots + b_{n-1}\eta_0,
\end{aligned}
\tag{3}
$$

where

$$\xi_0 = x^+ - x^-,\ \xi_1 = \dot{x}^+ - \dot{x}^-, \ldots \text{and } \eta_0 = y^+ - y^-,\ \eta_1 = \dot{y}^+ - \dot{y}^-, \ldots$$

and the discontinuities in function $\underline{x}$, its derivatives, $\underline{y}$, and its derivatives, respectively.

The peculiarities of the switchovers follow directly from a consideration of the above conditions. Their deduction is given in [5]. They are reproduced in brief in the appendix in order to render this paper complete without reference to [5].

1. Switchovers with Characteristics Comprised of Infinite Curves

To consider further normal characteristics comprised of sections from curves, we first consider a case (Figure 1) where the curves are $y = f_1(x)$ and $y = f_2(x)$ (infinite curves). P_1 and P_2 have abscissas σ_1 and σ_2 and ordinates d_1 and d_2. The motion along both branches is supposed possible in both directions about the correspondence points up to the points themselves.

Suppose the image point lies on branch I and that at time $t = t^* - 0$ it coincides with P_1. It then instantaneously jumps to branch II. To find its position after the jump (at $t = t^* + 0$), we use the first equality in (3), $a_0\xi_0 = b_0\eta_0$, or

$$a_0(x^+ - x^-) = b_0(y^+ - y^-). \tag{4}$$

Putting $x^- = \sigma_1$, $y^- = d_1$ for point P_1, we get, to determine the x^+, y^+ corresponding to Q the equation

$$a_0(x^+ - \sigma_1) = b_0(y^+ - d_1). \tag{5}$$

x^+ and y^+ must also satisfy the equation for branch II of the characteristic:

$$y^+ = f_2(x^+). \tag{6}$$

Hence Q is determined by the intersection of this branch with the straight line

$$y - d_1 = \frac{a_0}{b_0}(x - \sigma_1). \tag{7}$$

This line passes through P_1 and is of gradient a_0/b_0 (Figure 1).

Construction and (7) show directly that when $b_0 = 0$, i. e., when the degree $\underline{m}$ of the polynomial $K(p)$ is less than $\underline{n}$ for the polynomial $D(p)$, $x^- = x^+ = \sigma_1$, i. e., $\underline{x}$ is continuous (Q and Q* coincide) and normal switchover occurs. If $b_0 \neq 0$, i. e., $n = m$, three cases can occur: a) line (7) intersects $y = f_2(x)$ at one point only; b) there are several such intersections; c) the line and curve do not meet.

The latter two cases are undetermined switchovers, since (1) and the main hypothesis introduced at the beginning are insufficient to define the nature of the switchover. We must allow for the minor parameters or introduce additional hypotheses from which to select one definite intersection from the several available, or if such points are lacking, to determine the subsequent behavior of the system.

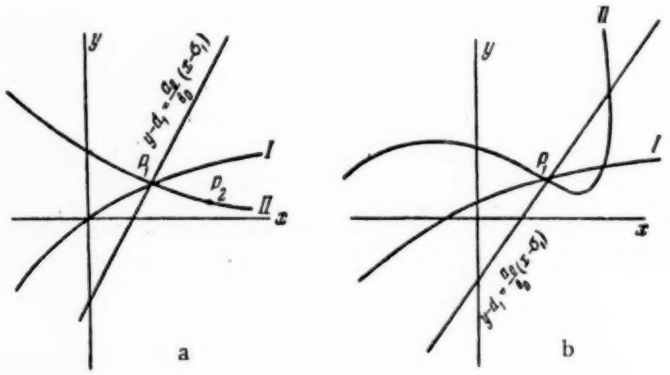

Fig. 2.

In the first case the switchover will be normal if P_2 lies outside the section of branch II between Q and Q*, and sliding if P_2 is between Q and Q*

The case where P_1 lies at the point where the branches intersect will be specially examined (Figure 2); P_2 can coincide with P_1 or lie at some other point on branch II. If (7) (passing through P_1 and of slope a_0/b_0) has no other intersections with branch II (Figure 2a) it will only intersect it at P_1, and the switchover will be both normal and continuous. If (7) has other intersections with II (Figure 2b) the switchover is undetermined, since (1) does not contradict either a continuous transition to II from P_1 or a jump to an intersection point. The behavior is then not solely determined by (1) and must be defined.

2. Switchovers with Characteristics Comprised of Sections of Curves

We suppose the branches given as semi-infinite curves; the transfer to the other branch occurs when the point reaches the end of one branch, i. e., P_1 and P_2 lie at the ends of the branches (Figure 3).

If P_1 and P_2 do not lie on a line parallel to the y-axis, all the above discussion for the I-II transfer conditions for infinite curves applies here completely. Thus, for instance, in the case of the characteristics shown in F gure 3, normal switchover involving a jump (Figure 3b) occurs when $a_0/b_0 > (d_2 - d_1)/(\sigma_2 - \sigma_1)$ (since for these a_0/b_0 values the bundle passes through P_2) and undetermined when the sign of the inequality is reversed (Figure 3a).

When defining the conditions for a step in the latter case it is, of course, most natural to expect a sliding switchover; the image point passes instantaneously from P_1 via Q_1^* to branch II, moves on to P_2 and drops back to branch I.

We now consider the case where P_1 and P_2 have the same abscissa, i. e., $\sigma_1 = \sigma_2 = \sigma$ (Figure 4).

Here two cases are distinguishable: characteristics continuous for $x = \sigma$ (Figure 4a) and discontinuous for $x = \sigma$ (F gure 4b).

When n = m the fact that P_1 and P_2 have the same abscissa gives rise to no special features in determining the type of switchover if P_1 and P_2 do not coincide (Figure 3b). But when n = m and n > m this case differs essentially from those considered above if P_1 and P_2 coincide (Figure 3a).

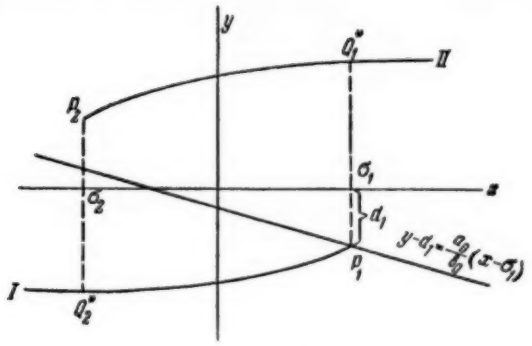

Fig. 3.

Previously the steps in dx/dt on switchover played no part. But here the steps in dx/dt influence the switchover type materially if the ends of the semi-infinite curves lie on a line parallel to the y-axis. Here we use the second of the conditions in (3):

$$a_0\xi_1 + a_1\xi_0 = b_0\eta_1 + b_1\eta_0. \tag{8}$$

We now introduce the symbol $\underline{r}$ for dx/dt at the instant when the correspondence point P_1 on branch I is reached, and k_I and k_{II} for the slopes of the tangents at P_1 and Q respectively.

Then

$$\xi_0 = x^+ - \sigma_1, \quad \xi_1 = \dot{x}^+ - r, \quad \eta_0 = f_2(x^+) - d_1,$$
$$\eta_1 = \left[\frac{df_2(x)}{dx}\right]_{x=x^+}\dot{x}^+ - \left[\frac{df_1(x)}{dx}\right]_{x=x^-} r = k_{II}\dot{x}^+ - k_I r.$$

Substituting these values in (8) we get

$$a_0(\dot{x}^+ - r) + a_1(x^+ - \sigma_1) = b_0(k_{II}\dot{x}^+ - k_I r) + b_1[f_2(x^+) - d_1],$$

from which

$$\dot{x}^+ = \frac{a_0 - k_I b_0}{a_0 - k_{II} b_0} r + \frac{b_1 [f_2(x^+) - d_1] - a_1 (x^+ - \sigma_1)}{a_0 - k_{II} b_0}. \tag{9}$$

If Q is found by construction or known independently (e. g., if $n \neq m$) then x^+ and $y^+ = f_2(\dot{x}^+)$ and (9) uniquely determines $\dot{x}^+$, i. e., the speed along $\underline{x}$ at the point Q.

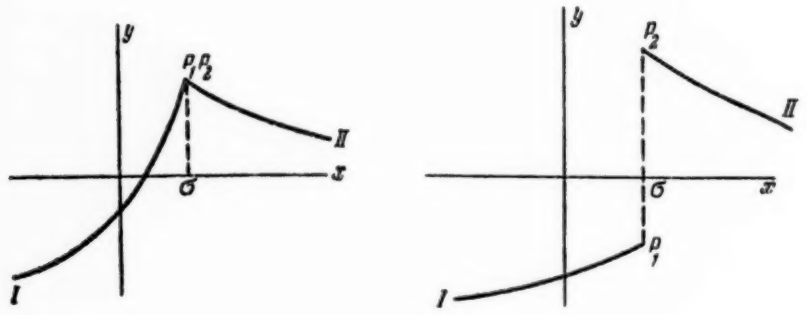

Fig. 4.

We now consider three cases in turn: $n - m > 1$; $n - m = 1$ and $n = m$.

When $n - m > 1$ we have $b_0 = b_1 = 0$, $x^+ = \sigma$ and so $\dot{x}^+ = r$. In this case not only is there no step on switchover but also no velocity change, i. e., the switchover is always normal.

2. Suppose now $n - m = 1$. Then $b_0 = 0$, $\dot{x}$ is continuous and so $x^+ = \sigma_1$, (9) being replaced by

$$\dot{x}^+ = r + \frac{b_1}{a_0} [f_2(\sigma_1) - d_1] = r + \frac{b_1}{a_0} \eta_0. \tag{10}$$

The sign of dx/dt changes after the switchover if

$$\operatorname{sign} r = -\operatorname{sign} \frac{b_1}{a_0} \eta_0, \quad |r| < \left| \frac{b_1}{a_0} \eta_0 \right|. \tag{11}$$

If (11) is fulfilled the image point slips back instantly from branch II to branch I.

After this jump the old value of $\dot{x} = r$ is restored, a jump to branch II occurs again, etc. In theory an oscillation of infinite frequency occurs at $x = \sigma_1$. In practice the presence of small loops results in a high frequency of oscillation between $y = f_1(\sigma_1)$ and $y = f_2(\sigma_1)$ at about $x \approx \sigma_1$. This type of sliding switchover has been considered in relay systems theory.

(11) can only be fulfilled if $\eta_0 \neq 0$. Hence these sliding switchovers can only occur at $n - m = 1$ if the characteristic is discontinuous (Figure 4b) and are impossible if it is continuous (Figure 4a).

When $n - m = 1$ and (11) is not fulfilled, in particular if the characteristic is continuous, the switchover will be normal.

3. Suppose, finally, that $n = m$. As above, if the characteristic is discontinuous (Figure 4b), nothing new is introduced by P_1 and P_2 lying on a line parallel to the y-axis, the switchover being normal or undetermined, a discontinuous sliding motion possibly occurring in the latter case, as above (Figure 3). But in the case as of Figure 4a the nature of the switchover is determined by the sign of the velocity.

Using (10) in relation to the case of Figure 4a, we put $x^+ = \sigma_1$, $f(x^+) = d_1$. Then (9) goes over to

$$\dot{x}^+ = \frac{a_0 - k_I b_0}{a_0 - k_{II} b_0} r. \tag{12}$$

dx/dt changes sign if

$$k_{II} > \frac{a_0}{b_0} > k_I. \quad \text{or} \quad k_{II} < \frac{a_0}{b_0} < k_I. \tag{13}$$

When (13) is fulfilled sliding switchovers occur although the characteristic is continuous. If (13) is not fulfilled the switchover will be normal.

3. Switchovers in Systems Containing Feedback Encompassing the Nonlinear Element

The above argument implies that we only find sliding and nonexistent switchovers if n = m or n − m = 1. These conditions are not merely due to the derivative action increasing the degree of K(p) but also to the feedback encompassing the nonlinear element.

Let us first consider the system of Figure 5. The equation is put as

$$D(p)\varphi = k_1(p)y, \quad x = \varphi + \rho y, \quad y = f(x),$$

where ρ may have either sign.

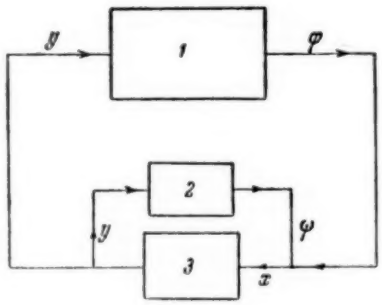

Fig. 5. 1) Linear section of system, 2) fixed feedback, 3) nonlinear element.

Elimination of φ gives

$$D(p)x = K(p)y, \quad y = f(x),$$

where $K(p) = K_1(p) + \rho D(p)$.

Even if the degree of $K_1(p)$ is much less than that of D(p), we still have K(p) of the same degree as D(p), i. e., n = m always. Therefore all the above discussion for n = m applies to any system in which the nonlinear coefficient is locked by fixed feedback.

We assume $K_1(p)$ to differ by not less than two units in degree from D(p). Then the first two coefficients in K(p) are $b_0 = \rho a_0$ and $b_1 = \rho a_1$, and $a_0/b_0 = 1/\rho$, i. e., the straight line used in the construction in Figure 1 passes through P_1 at an angle $\tan^{-1} 1/\rho$. The slope is determined only by the sign of the feedback around the nonlinear element.

Let us consider a system with the feedback having the transfer function $\frac{\rho}{Tp+1}$. The equation is

$$D_1(p)\varphi = K_1(p)y, \quad (Tp+1)\psi = \rho y, \quad x = \varphi + \psi, \quad y = f(x).$$

By eliminating φ and ψ we get

$$D(p)x = K(p)y, \quad y = f(x),$$

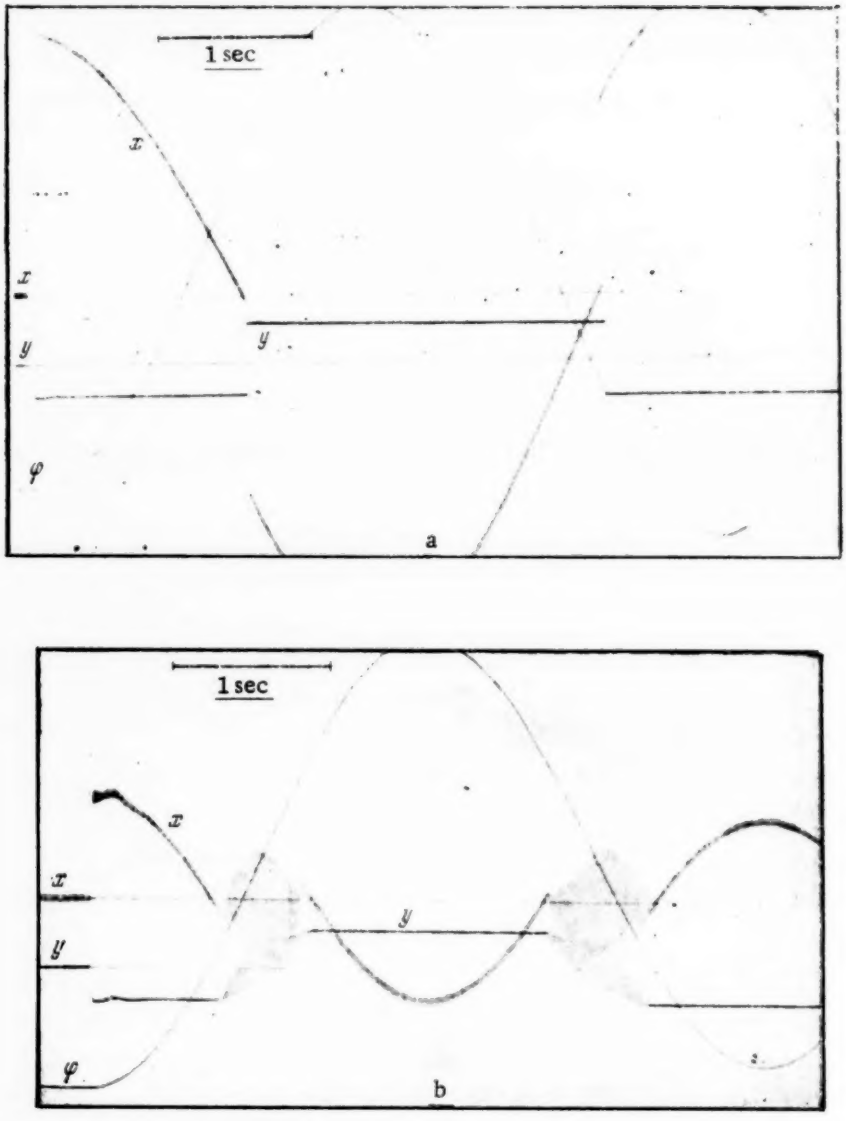

Fig. 6.

where

$$D(p) = (Tp + 1) D_1(p),$$
$$K(p) = \rho D_1(p) + (Tp + 1) K_1(p)$$

and D(p) is one unit higher in degree than K(p), and $b_1/a_0 = \rho/T$.

4. Analogs

Some of the above switchover processes were reproduced on an EMU-5 electronic analog [6]. The linear part was represented by the equation

$$\ddot{\varphi} + 0.1\dot{\varphi} + \varphi = -y. \tag{14}$$

Replacing by the equation

$$\dddot{\varphi} + 0.2\ddot{\varphi} + 2.2\ddot{\varphi} + 0.2\dot{\varphi} + \varphi = -y \tag{15}$$

did not alter the qualitative picture of the oscillogram.

A normal RN-4 relay was used as nonlinear element. The relay had fixed feedback with $\rho = \pm 1$, or derivative with transfer function $\rho/(Tp \pm 1)$, T being varied from 0.001 to 0.5 sec, so the relay input was supplied either with $x = \varphi + \rho y$ or $x = \varphi + \frac{\rho}{Tp + 1} y$.

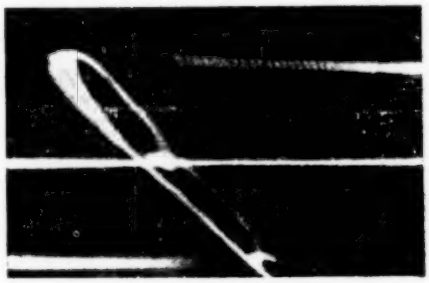

Fig 7.

Figure 6 shows oscillograms taken with (14) with direct feedback around the relay and when ρ and η_0 had the same signs (Figure 6a) or different ones (Figure 6b). The discontinuities in $\underline{x}$ are clearly seen, as also are the sliding switchovers accompanied by high-frequency (up to 400-600 cycles/sec) oscillations of appreciable amplitude in the second.

Figure 7 shows the pattern in the x,y plane for the sliding switchover case. The switchover occurs around loops inclined towards the inaccessible branches of the characteristic.

When feedback of transfer function $\rho/(Tp + 1)$ is used the nature of the sliding switchover, as seen on the oscilloscope, was determined by the magnitude of T.

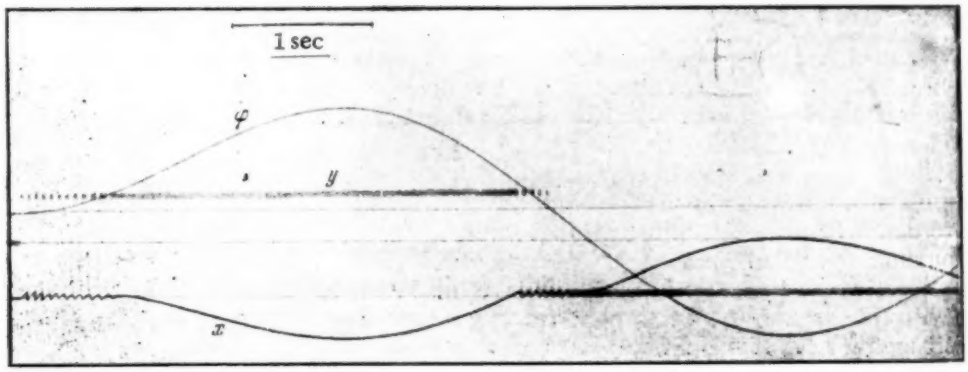

Fig. 8.

At T = 0.001 sec the picture was as for T = 0, but at T = 0.01 sec a change was seen. Oscillations of low frequency (5-6 cycles/sec) occurred practically at $x \approx 0$. The deviation from x = 0 was towards the characteristic. Figure 8 shows the oscillogram for T = 0.1 and the x, y plane picture is seen in Figure 9.

Comparison of Figures 7 and 9 shows clearly the differences in the sliding switchovers at T = 0 and at appreciable values of T.

Then the same linear part was used, but the relay was replaced by a nonlinear element comprised of two inclined straight lines intersecting at $x = \sigma_1 = \sigma_2 = \sigma$ (Figure 10). A RP-4 relay was used to change the gain of a linear amplifier at $x = \sigma$. Either negative ($\rho = -1$) or positive ($\rho = +1$) feedback round the nonlinear element was used.

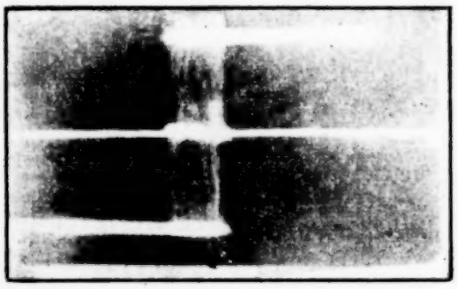

Fig. 9.

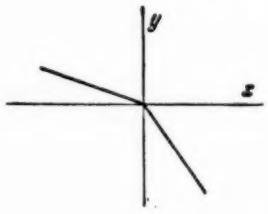

Fig. 10.

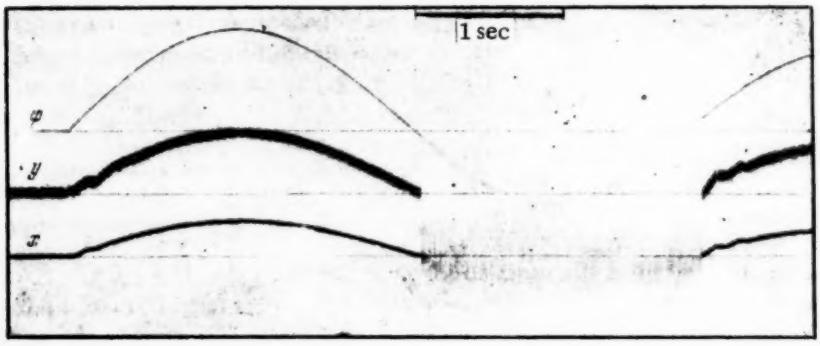

Fig. 11.

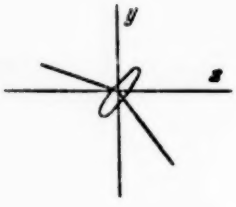

Fig. 12.

The angle between the straight lines was changed till no sliding switchovers occurred, here with a continuous but kinked characteristic.

Figure 11 shows the oscillograms, and Figure 12 the photo from the oscilloscope screen.

SUMMARY

So far sliding switchovers of the type of Figure 9 (little change in $\underline{x}$ during the sliding step along the y-axis) have been studied in relay systems theory. Our argument shows that for discontinuous characteristics, including those of relay systems, we get sliding switchovers which are different in principle and which correspond to Figure 7 (large change in $\underline{x}$ during steps along lines inclined to the y-axis and directed towards the nonexistent branches of the characteristics). In theory this new type of sliding switchover only occurs for $n = m$ (in particular for fixed feedback). In practice its realization in a system depends on the minor parameters, and sliding of Figure 7 type is actually observed in systems with a delay in the feedback if the time-constant is small.

Sliding is also observed with continuous but kinked characteristics.

In systems with discontinuous characteristics not of relay type we may get undetermined switchovers, i. e., ones involving steps which cannot be determined from the equations used alone; allowance for the minor parameters is required (or additional hypotheses) in order to determine them.

Thus the switchover phenomena in systems with piecewise-smooth characteristics are complex and of many aspects. The authors have not presented themhere in complete detail and have restricted themselves to the new results implied by the step conditions.

APPENDIX

All the unknowns except $\underline{x}$ and $\underline{y}$ are eliminated from (1). If $y = f(x)$ be continuous and sufficiently smooth the elimination will result in an equation of the type of (2).

If f(x) is not smooth the equations of (2) are meaningful only for the smooth regions. To describe the process as a whole the ordinary derivative operator $\underline{p}$ in (2) must be replaced by the generalized operator p^*:

$$D(p^*)x = K(p^*)y, \quad y = f(x).$$

p^* is defined by

$$p^*x(t) = px(t) + \sum_q \xi^q \delta(t - t_q),$$

where ξ^q is the magnitude of the q-th discontinuity in x(t), i. e., $\xi^q = x^+ - x^- = x(t_q + 0) - x(t_q - 0)$, $\delta(t)$ being Dirac's function, t_q the moment corresponding to the q-th discontinuity and the summation being carried over all points of discontinuity.

By successively applying the p^* operation we get

$$p^{*2}x(t) = p^2x(t) + \sum_q [\xi_0^q \delta'(t - t_q) + \xi_1^q \delta(t - t_q)],$$

. . . . . .

$$p^{2n}x(t) = p^n x(t) + \sum_q [\xi_0^q \delta^{(n-1)}(t - t_q) + \xi_1^q \delta^{(n-2)}(t - t_q) + \cdots + \xi_{n-1}^q \delta(t - t_q)].$$

Here $\delta', \delta'', \ldots, \delta^{(n-1)}$ are derivatives of δ, and $\xi_0^q, \xi_1^q, \ldots, \xi_{n-1}^q$ are the discontinuities in function $\underline{x}$ and the derivatives $\frac{dx}{dt}, \frac{d^2x}{dt^2}, \ldots, \frac{d^{(n-1)}x}{dt^{(n-1)}}$ at $t = t_q$, i. e.,

$$\xi^q = \dot{x}^+ - \dot{x}^- = \dot{x}(t_q + 0) - \dot{x}(t_q - 0), \ldots, \quad \xi_{n-1}^q = x^{(n-1)}(t_q + 0) - x^{(n-1)}(t_q - 0).$$

By analogy we determine the functions $p^*y, p^{*2}y, \ldots, p^{*(n-1)}y$.

For this purpose we need only replace $\underline{x}$ everywhere by y, and $\xi_0^q, \xi_1^q, \ldots, \xi_{n-1}^q$ by $\eta_0^q, \eta_1^q, \ldots, \eta_{n-1}^q$ the discontinuities in $\underline{y}$, $\frac{dy}{dt}, \ldots, \frac{d^{n-1}y}{dt^{n-1}}$ being determined in similar fashion.

Suppose

$$D(p^*) = a_0 p^{*n} + a_1 p^{*(n-1)} + \cdots + a_n.$$
$$K(p^*) = b_0 p^{*n} + b_1 p^{*(n-1)} + \cdots + b_n.$$

Substitute into $D(p^*)x$ and $K(p^*)y$ the above expressions for $p^*x, \ldots, p^{*(n-1)}x$, $p^*y, \ldots, p^{*(n-1)}y$. Equating terms not containing the δ-function and its derivatives, we get

$$D(p)x = K(p)y, \quad y = f(x).$$

Equating also for each t_q term containing $\delta(t-t_q)$, $\delta'(t-t_q)$ we get for each instant of discontinuity [3] $t = t_q$ the step conditions

$$\begin{gathered} a_0\xi_0 = b_0\eta_0, \\ a_0\xi_1 + a_1\xi_0 = b_0\eta_1 + b_1\eta_0, \\ \cdots\cdots\cdots\cdots\cdots\cdots \\ a_0\xi_{n-1} + a_1\xi_{n-2} + \ldots + a_{n-1}\xi_0 = b_0\eta_{n-1} + b_1\eta_{n-2} + \ldots + b_{n-1}\eta_0. \end{gathered}$$

(2) describes the motion where f(x) is a smooth function, and the step conditions relate the values of $x, \dot{x}, \ldots, x^{(n-1)}, y, \dot{y}, \ldots, y^{(n-1)}$ before and after $t = t_q$, i. e., determine the switchover conditions.

Received April 29, 1957

LITERATURE CITED

[1] Ia. Z. Tsypkin, Theory of Relay Automatic Control Systems [in Russian] (Gostekhizdat, 1055).

[2] Iu. I. Neimark, "Sliding regimes and oscillations in relay systems," Trudy GIFTI • i radiofizicheskogo fakul'teta GGU 30 (1956).

[3] N. A. Korolev, "Study of two methods of stabilizing relay automatic control systems," Dissertation for the degree of candidate in technical sciences, Institute of Automation and Remote Control, Academy of Sciences of the USSR (1956). ••

[4] J. André and Seibert, "Über Stückweise lineare Differentialgleichungen die bei Regelungsproblemen auftreten, I und II," Archiw der Mathematik, VII, No. 2, 3.

[5] M. A. Aizerman and F. R. Gantmakher, "Determination of oscillatory modes in nonlinear dynamic systems with piecewise-linear characteristics," Appl. Math. Mech. (USSR) 1956, No. 5.

[6] V. V. Gurov, B. Ia. Kogan, A D. Talantsev and V. A. Trapeznikov, "The new electronic analog equipment at the Institution of Automation and Remote Control, Academy of Sciences of the USSR," Automation and Remote Control (USSR) 17, No. 1, (1956).•••

[3] The subscripts q, y, ξ and η are omitted for simplicity.

• Gor'kii Research Institute of Physics and Technology.

•• In Russian.

••• See C.B. Translation.

METHODS OF EXTREMUM CONTROL

I. S. Morosanov

(Moscow)

The main methods of extremum control are considered. Systems are classified according to the method of seeking the extremum. Calculations on self-oscillation modes are demonstrated using relay systems as an example.

Brief suggestions on the practical use of the systems are made.

INTRODUCTION

Extremum control systems (ECS) are a form of very simple self-adjusting system. Unlike normal systems (with fixed settings) they can allow for the possible unforeseen changes in the properties of the controlled object. These changes are analyzed and the operation appropriately adjusted automatically, peak operating conditions being maintained. A necessary condition of such self-adjustment is a continuous search (in the simplest case, by scanning).

The following are examples of controlled objects showing extrema.

1. An aircraft on a maximum range flight with a given fuel reserve.

2. A well drilling turbine working at maximum penetration rate.

3. A heating furnace providing the maximum temperature from a given fuel consumption.

4. A klystron heterodyne in which the oscillation amplitude is kept constant while the generated frequency changes.

We will demonstrate that there are two possible types of changes in characteristics in the controlled object, using these typical examples, and illustrate the operating conditions.

The first type has a frequency spectrum falling below the scanning frequency; it results from drift in the object parameters and slow changes in the operating conditions. Examples are icing on an aircraft, wear in the bit in the drill and changes in hardness in the strata, changes in the draught and heat insulation of the furnace, slow changes in the supply voltages and ageing in the klystron.

This type of itself has occasioned and justified the construction of peak-holding systems.

The second type has a high-frequency spectrum and results from the fluctuating loads on the object; it determines the choice of system and the unit parameters. This type is usually termed noise or interference. In an aircraft gusts of wind produce it, in boring minor nonuniformities in the strata, in the furnace nonuniform conveyer loading. Klystron heterodynes do not show this type of fluctuation.

A constant setting which provides the peak output is possible if the object characteristics are fixed or if the extremum corresponds to a fixed value of some parameter.

Thus the maximum output current from any resonant system corresponds to zero phase shift. So any normal zero phase stabilization system, i. e., a system with a fixed setting, can act as peak-holding regulator no matter what the changes in the absolute value of the output or the form of the resonance response, although such a system is by no means extremal.

The main distinctive feature of an extremal control system is the continuous automatic follow-up of the changing object "tuning" (i. e., of the input which produces the peak output) as the result of an automatic search.

The search range in seeking the output peak is an index of the operations of ECS in the steady state. In transient states the time to attain the search range serves as quality index.

Draper and Li [1] have given the most complete presentation of extremum control principles. They proposed to classify ECS from the principle on which the input to the adjusting unit was derived. Two groups of regulators are considered.

In the first fall those which use signals proportional to the slope of the static characteristic. The systems in this group are named in accordance with the way of producing this signal:

1) those using direct differentiation (direct sensitivity controllers);

2) continuous test signal controllers;

3) discrete output regulators (output sampling controllers).

In the second fall peak-holding regulators, in which the deviation of the output from the extreme value is used.

In [1] preference is given to a peak-holding regulator, its electronic circuit and prototype test results being given.

Most of the foreign papers [2-6] deal with this type to a greater or less extent.

In [7] an extremum regulator using the logical elements "yes", "no" and "or" is used. The principle of analyzing the signs of the products of the input and output quantities is used. It would appear that stepping systems have begun to be developed in the USA [8].

Attention has mainly focussed on stepping regulators in the Soviet literature [9-11]. Unlike the others, in [11] a system with very small steps is considered. An attempt is made to classify objects and ECS in [9]. *

The following subdivisions are proposed.

1. Servo systems with preset nonlinear follow-up characteristics.

2. Systems with self-oscillating control: a) continuous-acting systems; b) ones operating discontinuously; c) systems with accessory scanning units.

3. Systems using forced oscillations: a) those with phase discriminators; b) those with peak voltmeters and memory units; c) stepping systems.

A brief survey of the proposed classifications shows that even Draper and Li's fairly detailed classification takes no account of the search method. Any classification must be based on the automatic se arch method, since this is the main distinctive feature of ECS.

Here we show that a classification on this basis covers all the numerous systems known having the two simplest structural designs, and leads fairly simply to a design method.

1. Design Principles

The functional diagram of any such system is shown in Figure 1. Here R is the regulator unit, T the extremum transducer, which determines some quantity to specify the position relative to the extreme point (search error signal), C is a control device, which reverses the scan direction, and E is an effector, which produces the automatic

* This position is expounded in more detail in [12].

search signal. Figure 2 gives a general illustration of the operation for a very simple system. Figure 2a shows the object output signal, Figure 2b the search error signal (output from T), Figure 2c the control signal (output from C) and Figure 2d the automatic search signal (output from E).

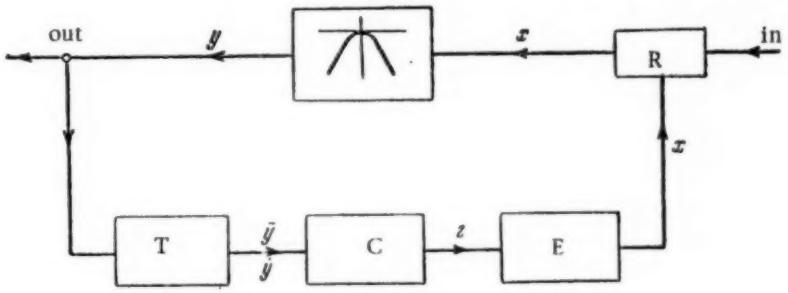

Fig. 1.

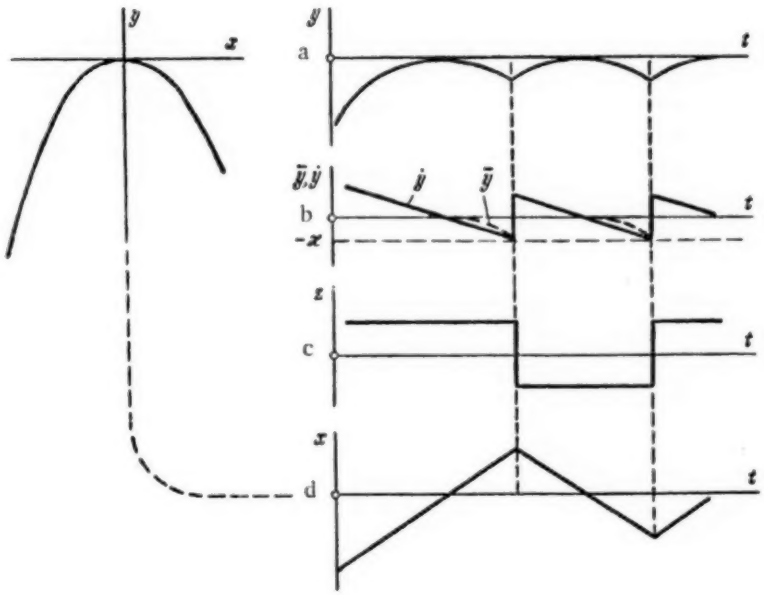

Fig. 2.

Let us consider sequentially the operation of each unit in this system.

Extremum transducer. Two parameters can be used as index to the extremum, i. e., the deviation of the output as reckoned from the extreme value ($\bar{y}$) or the derivative of the output with respect to the input (dy/dx).

Since by definition $\bar{y}$ can only be measured after the extremum has been passed, all transducers which provide the first parameter above must operate by determining the difference between the extreme and current outputs after each passage through the extremum.

If the second is used the position is determined independently at any point, no matter whether the extremum is passed through, the scan direction being allowed for.* The possible methods of forming the derivative are [1]:

* Since in practice it determines $\dot{y} = dy/dt = \pm\, a dy/dx$ at $x = \pm\, at$, where a = const (Figure 2).

a) direct differentiation (usually using elements showing delays, such as tachogenerators, servos, etc.):

b) an accessary test sinusoidal modulation, with subsequent phase detection;

c) approximate differentiation, the derivative being approximated via the first differences of the output.

If the characteristic is unsymmetrical the use of $\bar{y}$ as index to the extremum results in reversal on the steep and shallow branches occurring at differing y values. So the search will occur about some point displaced towards the shallow branch and not about the extremum itself. The search loss will clearly be thereby increased.

Control unit. This must determine either the time of scan reversal, or the sign of this reversal, or, finally, produce the automatic search signal, proportional to the search error signal, depending on the type of system. The design principles will be considered below.

Effector. This forms the search signal. The constant component of the search signal, about which the input oscillates with the search input amplitude, must correspond to the extremum in the output. It is determined by accumulating the changes proportional to the duration (or number of steps) in the $z(t)$ signal, allowing for sign. It must therefore be an integrator.

In real systems E is most frequently a reversible motor (continuous systems) or a reversible stepping motor (pulse systems). The direction of rotation (stepping) is determined by the sign of $z(t)$.

2. Classification of ECS

The above functional system covers certain extremum control systems having objects with one independent variable and one extremum.

Such systems use the simplest form of automatic search in a one dimensional region — a blind search [13]. The method of effecting the search, which is determined by the type of control unit used, is used below to classify ECS. The quantity used as index to the extremum is here unimportant. These systems may be subdivided into two classes in accordance with this principle as follows:

1) those with independent search signal variation, usually linear;

2) those with dependent proportional search signal change.

Systems with independent linear search (scanning) can be designed with relay or relay-pulse circuits. In relay systems the search is effected by changing the input at a constant rate, the scan direction being reversed when the output passes through the extremum. The switch-over point is determined by the relay control unit.

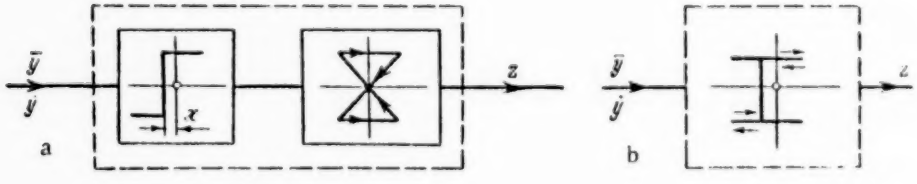

Fig. 3.

There are two relay device principles.

1. Switchover occurs when the extremum index is greater than some positive quantity $+\kappa$ (minimum) and less than some negative $-\kappa$ (maximum).

An important point is that the switchover conditions $\bar{y} \geq \kappa$, $\bar{y} \geq \kappa$ (minimum) and $\bar{y} \leq -\kappa$, $\bar{y} \leq -\kappa$ (maximum) do not depend on the scan direction, since scan sign reversal can only occur when the maximum has been passed (Fig. 2b). Thus there is no need to supply the sign of x to C, unlike what is stated in [9] and in [12].

A device using this principle can be built by joining an ordinary relay in series with a special nonlinear element of ratchet type, with response curve as of Figure 3a, this being equivalent to a nonlinear element with the response curve of Figure 3b. At the output we get a signal z(t) which is a train of pulses of alternating signs of repetition frequency half that of the input. The above conditions show this to be a switchover.

2. The signs of the combinations of $\dot{y}$ and $\dot{x}$ are analyzed. Of the four possible combinations two, $-\dot{y}$, $+\dot{x}$ and $-\dot{y}$, $-\dot{x}$ (maximum) or $+\dot{y}$, $+\dot{x}$ and $+\dot{y}$, $-\dot{x}$ (minimum) correspond to conditions after the extremum is passed, and hence indicate that switchover is due.

To establish reliably that the sign has changed the relay element must have hysteresis 2κ. This κ, as above, defines the output search range (search loss).

With an ideal lag-free object this device could be constructed as a relay amplifier effecting the operation

$$z(t) = k_p \frac{\operatorname{sign} \dot{y}(t)}{\operatorname{sign} \dot{x}(t)} . \tag{1}$$

where k_p is the relay control unit gain. But if the object has a lag cases can occur where a change in the sign to sign $\dot{y}$/sign $\dot{x}$ (which indicates the switchover point) does not correspond to correct operation. The cause is the delay τ_3 in $\underline{y}$ and $\dot{y}$ relative to $\underline{x}$ and $\dot{x}$.

For a time τ_3 after a switchover the sign combination gives a false idea of what is occurring, and hence causes a second (incorrect) switchover. Hence to define the moment and sign of the switchover we have to use four devices, and for each combination of signs of $\dot{y}$ and $\dot{x}$, and two delay elements after each unit which controls the switchovers (in accordance with the switchover conditions above). The scan sign is determined by units which record the combinations which have existed for some time, i. e., for times greater than τ_3.

For a maximum we have $z > 0$ when $\dot{y} > -\kappa$, $\dot{x} > 0$ and $z < 0$ when $\dot{y} > -\kappa$, $\dot{x} < 0$ (Fig. 2) [7].

The above discussion shows that a control unit which uses sign combinations cannot be superior to a relay control device because it is so complex. Without considering the circuits of T units in detail we note that in relay ECS two types are mostly used, i. e., those using deviations ($\bar{y}$) [5] or derivatives ($\dot{y}$) found by direct differentiation [14]. The use of derivatives determined by sinusoidal test signal methods is complicated by the need to balance out phase shifts in the object in order to get correct phase detection. This is particularly difficult at low frequencies. But if an extremum in two or more parameters has to be found it is the only method by which simultaneous control with respect to all parameters can be effected in relay systems [2]. This is done by selecting different test frequencies for the various inputs.

In relay-pulse systems the search is effected by varying the input continuously at a constant rate (by equal steps), the scan direction being reversed when the output has passed the extreme value.

A difference between these systems and pure relay ones is that the result of each step can be "discussed", so in systems showing inertia or lags the search loss or overshoot can be made less than in relay ones.

The "discussion" consists in determining the sign of each successive step in terms of the previous one without reference to passage through the extremum. So a relay-pulse control unit which determines the number of steps of variable sign must be designed round sign analysis applied to $\dot{y}$ and $\dot{x}$. The discrete nature of the processes greatly simplifies realization here. The delay τ_3 in the object is here simply allowed for by taking $\Delta y[n] = F(\Delta x[n-1])$, where $\Delta y[n] = y[n+1] - y[n]$ is the first difference. If the time t_p required for the system to settle down is less than T, the time between steps, delay effects are completely eliminated, and the control unit is simply designed to handle the equation

$$z[n] = k_i \frac{\operatorname{sign} \Delta y[n]}{\operatorname{sign} \Delta x[n-1]} . \tag{2}$$

Typical ECS with Independent Search

Class of system	Structural diagram	Index of extremum	Control unit	Effector unit	Object
Relay	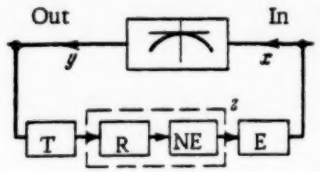	position	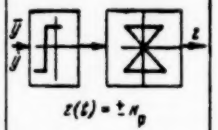 switchover condition or	Reversible motor	Low inertia with fluctuating load
		derivative $\dot{y}$ (direct differentiation)		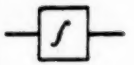	Low inertia, fixed load
Relay-pulse	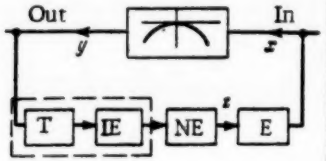	first difference	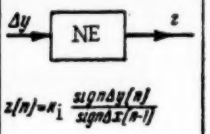		High inertia, fluctuating load

where k_i is the gain of the relay-pulse effector, so

$$x[n] = \sum_{m=0}^{n} z[m]. \tag{3}$$

In relay-pulse systems only the derivative can be used as extremum index. In general the derivative can be found in any way, but first differences are usually used.

The discussion of the first class of ECS is summarized as a table of typical systems with independent search.

ECS with dependent or proportional search can be divided into proportional and proportional-pulse classes. Proportional search is used to improve the response, i. e., to reduce the time to reach the set search range. t_s and to reduce the search loss Δ.

In ECS with dependent search the deviation from the extremum must be determined at every instant in both sign and magnitude. A control unit using computer principles to effect the operation

$$z(t) = k\frac{\dot{y}(t)}{\dot{x}(t)}. \tag{3a}$$

where $\underline{k}$ is the gain of the control unit, answers to these conditions.

Then any method of deriving the extremum index can be used. The accessory modulation method is most used. A steady small-amplitude perturbation is applied, and this prevents the feed-back being effectively open-circuited, as is general in proportional-search systems, since at the extremum $\dot{y}/\dot{x}$ is indeterminate, being 0/0.

When a pulsed element is introduced into the control circuit the system becomes a proportional-pulse one. Here it is best to derive the derivatives by using first differences. To prevent control breaking down at the extremum the system is set to accept not less than a certain minimum input signal. Then, as in proportional systems, a definite output search range is specially set.

ECS using prediction have a special place in this class.

The use of dependent search reduces t_s and Δ only with objects having near-parabolic static characteristics. If the characteristic can alter and become grossly unsymmetrical in real conditions the transient response is sometimes even worsened.

The unrealized possibilities of improving the transient response of ECS are in principle utilized by pulsed working. That the state of the system is known without reference to passage through the extremum enables one to intervene actively before the extremum is reached, appropriate correction signals being introduced at defined instants.

The operation of a pulsed extremal system with curvature prediction has been described [8]. At each control step the reaction is predicted which will correspond with a definite curvature to the static characteristic equal to that at the extremum in the controlled quantity. Since the actual state is not at the extremum, i. e., does not correspond to the set curvature, an automatic search signal is produced which is proportional to the actual and predicted object reactions. The system thus approaches the extremum.

Pulsed systems, in which the setting x_0 corresponding to the extremum is predicted, are also possible. After each control step x_0 is predicted assuming that the characteristic is approximated by sections of a parabola. An automatic search signal proportional to the difference between the actual position $\underline{x}$ and the x_0 predicted to correspond to the extremum is generated. Second as well as first differences have to be taken from the output, since $x - x_0 = \Delta y / \Delta^2 y$. This makes the design complex. Since the difference in quality is small the curvature prediction system is not one to be preferred.

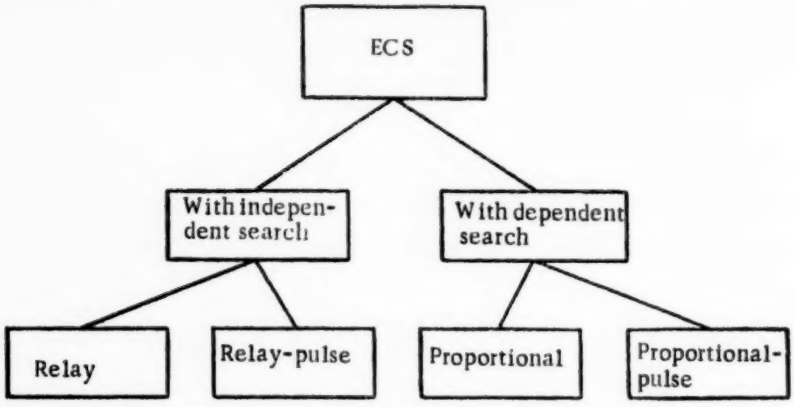

Fig. 4.

Very simple digital-type computers are used in the control units of predicting ECS.

Finally, we must emphasize one important property of predicting systems. Unlike all others, it is in principle possible to avoid searching about the extremum until some uncontrolled cause produces a disturbance.

Figure 4 shows the classification of ECS.

3. Design of Relay ECS

There must be two stages in calculating ECS, namely the calculation of the steady-state search mode, and that of the search for the extremum. The decisive stage is determined by the nature of the system. Thus in relay and relay-pulse systems the steady-state search mode is of most interest. The behavior of such systems while searching for the extreme value is completely determined if the rate of change of static characteristic position is less than the linear scan rate. Hence no special methods are required for class one ECS, those developed for relay [15] and relay-pulse [16] systems being usable.

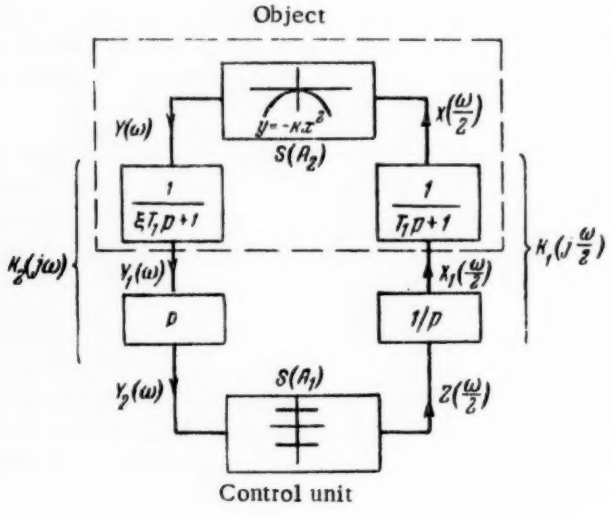

Fig. 5.

But in proportional systems the search for the extremum is the most important. The steady state calculation is of no practical interest, since the search loss is either very small, or completely absent.

Perturbations play a large part in analyzing ECS. The task of producing a signal proportional to the extremum index on a noise background may demand a substantial increase in the allowed search range. For instance, in relay systems the choice of κ which gives the search loss, must be defined in terms of the maximum noise amplitude in such a way that false scan reversals cannot occur. It is much more complicated to allow for noise in proportional systems.

Noise effects are not considered here.

To illustrate some aspects of ECS calculations we consider those for the steady-state search mode in relay ECS.

Let us first consider a system in which the derivative is the index.

The lag in the object is [3, 4] allowed for via two first-order inertial links at the input and output of an ideal inertialess object with characteristic $y = -kx^2$ (maximum).

The ECS is one with two nonlinear links (Fig. 5). Harmonic balance methods are used to determine the oscillation modes. Some difficulties arise in using the method because of the frequency – converting properties of the nonlinear links as the characteristics are double-valued. As two distinct oscillation frequencies exist in both halves of the control circuit it is possible to choose the main harmonic for the whole circuit, in the steady state. We take this to be the frequency ω at the object output. The frequency responses of the links before the object should be considered for $\omega/2$. The phase relationships in the object will in future be considered in the ωt scale.

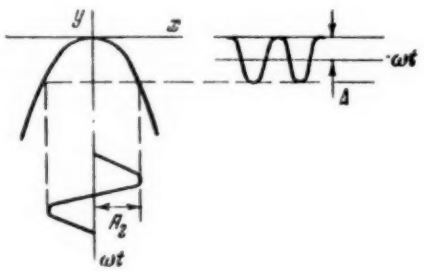

Fig. 6.

A certain difficulty is encountered in deducing the phase balance because there are phase shifts of two oscillations of different frequencies to allow for, although one frequency is a multiple of the other. Here the phase phenomena of one frequency change their relation to those of the other continuously, the phase difference thus depending on the initial conditions chosen. We must therefore specify more precisely what is meant by phase differences between the two oscillations. The two are considered synphasic if there is a definite periodically recurring instant when both begin together. By origin in this sense we mean a time when the time dependent variable passes through zero towards, say, positive values. This definition is correct if the frequencies are exact multiples, the repeat period then being the largest common divisor of the two frequencies, i. e., here $\omega/2$.

Thus this periodically repeating phase pattern, or, what is the same, the presence of a definite Lissajous figure on the oscillograph, enables one to give a definite value to the phase difference of two distinct frequencies. But the final determination of the phase difference depends on the notation used for the processes (sine or cosine). The double-valued result is unimportant if some one notation is adopted once and for all.

We now pass to determining the equivalent gains of the nonlinear links, $S(A_2)$ and $S(A_1)$.

By definition

$$S(A_n) = g(A_n) + jb(A_n), \tag{4}$$

where, for the lowest harmonic (n = 1, 2)

$$g(A_n) = \frac{2}{\pi A_n} \int_0^{\pi} \psi(A_n \sin \varphi) \sin n\varphi \, d\varphi, \tag{5}$$

and

$$b(A_n) = \frac{2}{\pi A_n} \int_0^{\pi} \psi(A_n \sin\varphi) \cos n\varphi \, d\varphi.$$

To make the arguments in $S(A_2)$ and $S(A_1)$ single-valued we calculate the coefficient of the lowest harmonic in the expansion of the output quantities while putting the input harmonics as sines, thus taking the origin as being at the negative-to-positive transition (Fig. 6).

With $y = -kx^2$ and $x = A_2 \sin\varphi$

$$\psi(A_2 \sin\varphi) = -kA_2^2 \sin^2\varphi.$$

Calculating $g(A_2)$ and $b(A_2)$, we get

$$g(A_2) = -\frac{2}{\pi A_2} \int_0^{\pi} kA_2^2 \sin^2\varphi \sin 2\varphi \, d\varphi = 0,$$

$$b(A_2) = -\frac{2}{\pi A_2} \int_0^{\pi} kA_2^2 \sin^2\varphi \cos 2\varphi \, d\varphi = \frac{kA_2}{2}.$$

Thus

$$S(A_2) = j\frac{kA_2}{2} = \frac{kA_2}{2} e^{j\frac{\pi}{2}}. \tag{6}$$

The constant in the expansion is deleted, since this is filtered out in the extremum index transducer and so takes no part in determining the periodic modes.

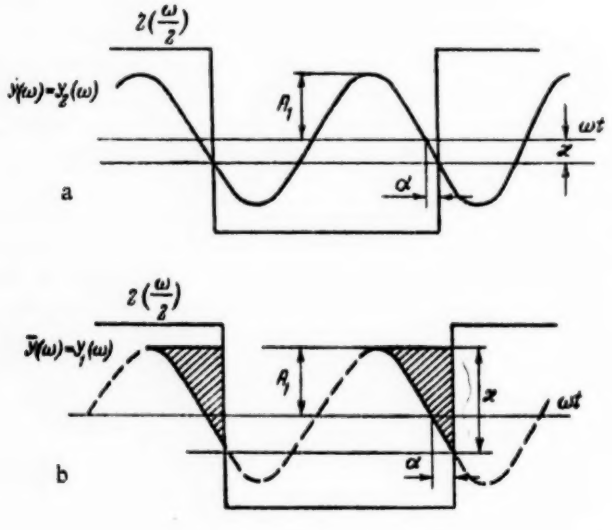

Fig. 7.

Using the same form for $S(A_1)$ (Fig. 7a) we get

$$g(A_1) = \frac{2}{\pi A_1} \int_{-\alpha/2}^{\pi-\alpha/2} k_p \sin\varphi d\varphi = \frac{4k_p}{\pi A_1} \cos\frac{\alpha}{2},$$

$$b(A_1) = \frac{2}{\pi A_1} \int_{-\alpha/2}^{\pi-\alpha/2} k_p \cos\varphi d\varphi = \frac{4k_p}{\pi A_1} \sin\frac{\alpha}{2},$$

where $\alpha = \arcsin \frac{K}{A_1}$.

Then

$$S(A_1) = \frac{4k_p}{\mu A_1}\left(\cos\frac{\alpha}{2} + j\sin\frac{\alpha}{2}\right) = \frac{4k_p}{\pi A_1} e^{j\frac{\alpha}{2}}$$

or in the ωt scale

$$S(A_1) = \frac{4k_p}{\pi A_1} e^{j \arcsin \frac{K}{A_1}}. \tag{7}$$

The frequency responses of the linear links are of the form *

$$K_1\left(j\frac{\omega}{2}\right) = \frac{4}{\omega\sqrt{\omega^2 T_1^2 + 4}} e^{-j2\left(\frac{\pi}{2} + \operatorname{arc\,tg}\frac{\omega}{2}T_1\right)},$$

$$K_2(j\omega) = \frac{\omega}{\sqrt{\omega^2 T_1^2 \xi^2 + 1}} e^{-j\left(\operatorname{arc\,tg}\omega T_1\xi + \frac{\pi}{2}\right)},$$

where $T_1\xi = T_2$.

The equation defining the frequency and amplitude characteristics of the closed-loop system is written as

$$S(A_1) K_1\left(j\frac{\omega}{2}\right) S(A_2) K_2(j\omega) = 1 \tag{8}$$

or, after substitution,

$$\frac{8k_p k}{\pi}\frac{A_2}{A_1}\frac{1}{\sqrt{\omega^2 T_1^2 + 4}\sqrt{\omega^2 T_1^2 \xi^2 + 1}} e^{j\left(\arcsin\frac{K}{A_1} - 2\operatorname{arc\,tg}\frac{\omega}{2}T_1 - \operatorname{arc\,tg}\omega T_1\xi\right)} = 1. \tag{8'}$$

But A_2 is related to A_1, as is clear from Figure 5, by

$$A_2 = A_1 S(A_1)\left|K_1\left(j\frac{\omega}{2}\right)\right| \quad \text{or} \quad A_2 = \frac{16k_p}{\pi\omega}\frac{1}{\sqrt{\omega^2 T_1^2 + 4}}. \tag{9}$$

*In this paper 'tg' ≡ 'tan' – Publisher.

Substituting (9) in (8'), we get

$$\frac{128k_p^2 k}{\pi^2 A_1} \frac{1}{\omega(\omega^2 T_1^2 + 4)\sqrt{\omega^2 T_1^2 \xi^2 + 1}} e^{j\left(\arcsin\frac{\varkappa}{A_1} - 2\operatorname{arc\,tg}\frac{\omega}{2}T_1 - \operatorname{arc\,tg}\omega T_1 \xi\right)} = 1.$$

Hence we get two equations, one for the amplitude balance:

$$\frac{128k_p^2 k}{\pi^2 A_1} \frac{1}{\omega(\omega^2 T_1^2 + 4)\sqrt{\omega^2 T_1^2 \xi^2 + 1}} \tag{10}$$

and one for the phase:

$$\arcsin\frac{\varkappa}{A_1} - 2\operatorname{arc\,tg}\frac{\omega}{2}T_1 - \operatorname{arc\,tg}\omega T_1 \xi = 0. \tag{11}$$

Equation (11) gives A_1:

$$A_1 = \varkappa\left[\sin\left(2\operatorname{arc\,tg}\frac{\omega}{2}T_1 + \operatorname{arc\,tg}\omega T_1 \xi\right)\right]^{-1}.$$

Using the relations

$$\sin(2\beta + \gamma) = \frac{\operatorname{tg} 2\beta + \operatorname{tg}\gamma}{\sqrt{1 + \operatorname{tg}^2 2\beta}\sqrt{1 + \operatorname{tg}^2 \gamma}}, \qquad \operatorname{tg} 2\beta = \frac{2\operatorname{tg}\beta}{1 - \operatorname{tg}^2\beta},$$

we get

$$A_1 = \varkappa \frac{(\omega^2 T_1^2 + 4)\sqrt{\omega^2 T_1^2 \xi^2 + 1}}{4\omega T_1(1 + \xi) - \omega^3 T^3 \xi}.$$

Substituting for A_1 in (10) we finally get

$$\frac{CT_1}{\varkappa} = \frac{\omega T_1(\omega^2 T_1^2 + 4)^2(\omega^2 T_1^2 \xi^2 + 1)}{4\omega T_1(1 + \xi) - \omega^3 T_1^3 \xi} \qquad \left(C = \frac{128k_p^2 k}{\pi^2}\right). \tag{12}$$

Systems in which the deviation from the extreme value is used can be considered in the same way. In contrast to the above there is here no differentiating link and the equivalent gain $S(A_1)$ of the control unit becomes

$$S(A_1) = \frac{4k_p}{\pi A_1} e^{j \arcsin\frac{\varkappa - A_1}{A_1}},$$

Since here $\alpha = \arcsin \frac{\varkappa - A_1}{A_1}$ (Fig. 7b).

The amplitude balance equation is then

$$\frac{128 k_p^2 k}{\pi^2 A_1} \frac{1}{\omega^2 (\omega^2 T_1^2 + 4) \sqrt{\omega^2 T_1^2 \xi^2 + 1}} = 1 \qquad (10')$$

and the phase balance equation is

$$\arcsin \frac{\varkappa - A_1}{A_1} - 2 \operatorname{arc\,tg} \frac{\omega}{2} T_1 - \frac{\pi}{2} - \operatorname{arc\,tg} \omega T_1 \xi = 0. \qquad (11')$$

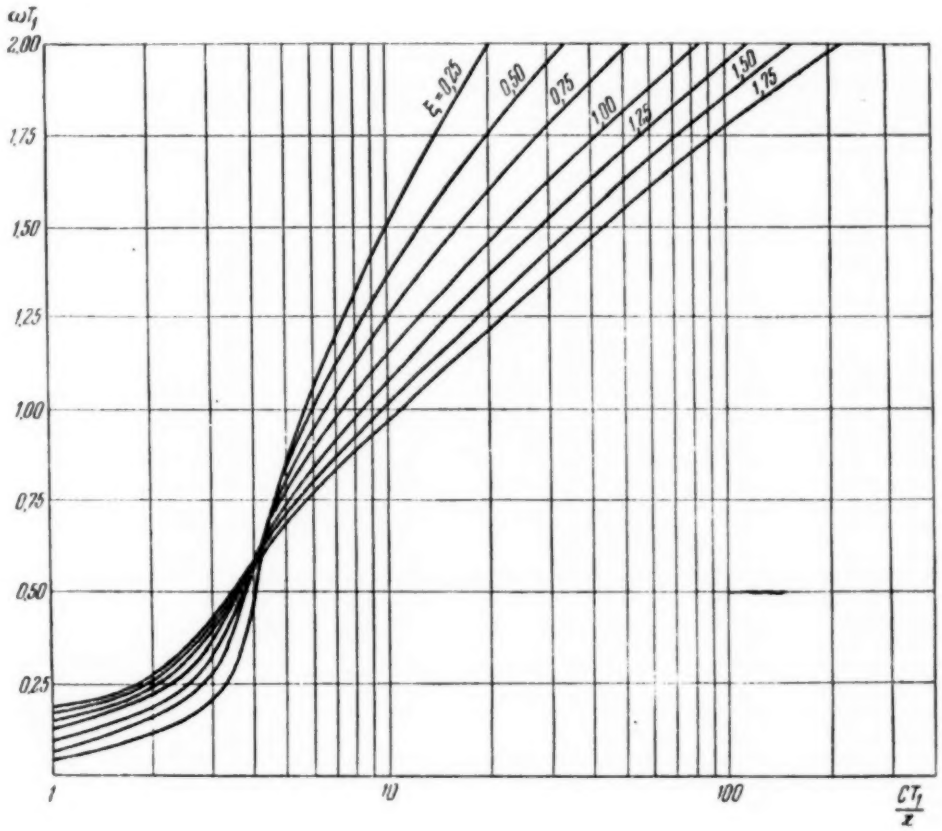

Fig. 8.

As before ,(11') gives an expression for A_1:

$$\frac{\varkappa - A_1}{A_1} = \cos\left(2 \operatorname{arc\,tg} \frac{\omega}{2} T_1 + \operatorname{arc\,tg} \omega T_1 \xi\right).$$

Remembering that

$$\cos(2\beta + \gamma) = \frac{1 - \operatorname{tg} 2\beta \operatorname{tg} \gamma}{\sqrt{1 + \operatorname{tg}^2 2\beta} \sqrt{1 + \operatorname{tg}^2 \gamma}},$$

we get

$$A_1 = \varkappa \frac{(4+\omega^2 T_1^2)\sqrt{1+\omega^2 T_1^2 \xi^2}}{(4+\omega^2 T_1^2)\sqrt{1+\omega^2 T_1^2 \xi^2}+4-\omega^2 T_1^2-4\omega^2 T_1^2 \xi}.$$

Substituting for A_1 in (10') we finally get

$$\frac{CT_1^2}{\varkappa} = \frac{\omega^2 T_1^2 (\omega^2 T_1^2+4)^2 (\omega^2 T_1^2 \xi^2+1)}{(4+\omega^2 T_1^2)\sqrt{1+\omega^2 T_1^2 \xi^2}+4-\omega^2 T_1^2-4\omega^2 T_1^2 \xi}, \qquad (12')$$

where $C = 128\, k_p^2\ k/m^2$.

Equations (12 and (12') can be solved from the graphs of Figure 8 (derivative case) or of Figure 9 (position case) at different $\xi = T_2/T_1$.

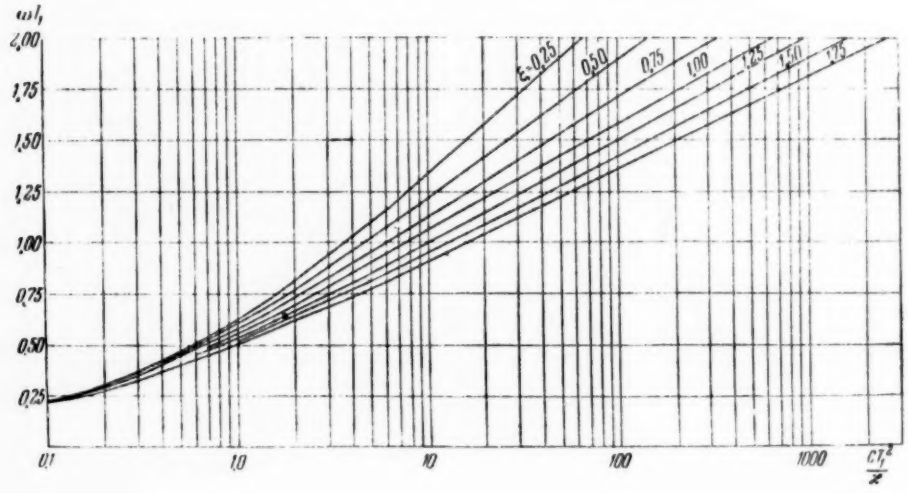

Fig. 9.

Having found ωT_1 from these graphs, we can get the basic quality index for ECS – the search loss Δ – from

$$\Delta = A_1 S(A_1) | k_1 \left(j\frac{\omega}{2} \right) S(A_2)$$

or, after substitution,

$$\Delta = CT_1^2 \frac{1}{\omega^2 T_1^2 (\omega^2 T_1^2+4)}.$$

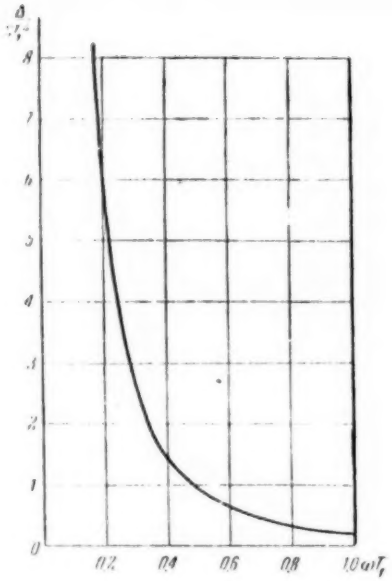

Fig. 10.

Figure 10 shows $\frac{\Delta}{CT_1^2} = f(\omega T_1)$, which is correct for both relay systems.

Consideration of Figures 8-10 gives the comparative characteristics of both systems. At low T_1, other things being equal, ωT_1 is larger in the second, and so Δ is less. At high T_1 this difference is absent. Since relay systems are generally best with low-lag objects, we may, in view of the above, only recommend the derivative system for the simplest unimportant cases, where simplicity is the predominant requirement. The relation of ωT_1 to $\xi = T_2/T_1$ (Figs. 8 and 9) shows that the less the lag at the output of the object (T_2) relative to that at the input (T_1) the higher the frequency and the less Δ. We must here point out that it is incorrect to assert, as in [4], that Δ does not depend on T_2. This is only true of the open-loop system.

The harmonic balance method for relay extremal systems gives the better approximation the stronger the inequality $\omega T_1 > 1$,, i. e., the closer the object approximates to a low-frequency filter in its properties.

Received March 13, 1957

LITERATURE CITED

[1] C. S. Draper and J. T. Li, Principles of Optimalizing Control Systems and an Application to Internal Combustion Engine (ASME publications, 1951).

[2] J. T. Li, "Optimalizing systems for process control." Instruments, 25, No. 1, 2, 3 (1952).

[3] H. S. Tsien and S. Serdengecti, "Analysis of peak-holding optimalizing control," J. Aeronaut. Sci., 1955, No. 8.

[4] H. S. Tsien, Technical Cybernetics [Russian translation] (IL, 1956).

[5] R. J. Shull, "An automatic cruise-control computer for long-range aircraft," Trans. IRE (Electronic Computer) 1952, No. 12.

[6] B. Farber, "Computer circuit finds peaks automatically," Control Engineering, 1954, No. 10.

[7] R. J. Dasgriff, "Servos that use logic can optimize," Control Engineering, 1955, No. 9.

[8] W. Byron, "The quarie optimal controllers," Instruments and Automation, 1956, No. 11.

[9] A. G. Ivakhnenko, "Problems of extremal control," Avtomatika, 1956, No. 3.

[10] Iu. I. Ostrovskii and M. G. Eskin, "An extremum regulator for turbine boring of oil wells," Automation and Remote Control (USSR), 17, 9 (1956). *

[11] L. A. Zalmanzon, "Some considerations on the production of pneumatic extremum regulators," Automation and Remote Control (USSR) 18, 1 (1957). *

[12] A. G. Ivakhnenko, Self-Adjusting Automatic Control Systems [in Russian] (Izd. AN Ukr. SSR, 1956). **

[13] A. A. Fel'dbaum, "The use of computers in automatic systems," Automation and Remote Control (USSR) 17, 11, (1956). *

* See C. B. Translation.

[14] S. Ratcliffe, "Automatic tuning in radar stations," [Russian translation]. Voprosy Radiolokatsionnoi Tekhniki, 1956, No. 6 (24).

[15] Ia. Z Tsypkin, Theory of Relay Automatic Control Systems, [in Russian] (Gostekhizdat, 1955).

[16] V. P. Kazakov, "Studies of the dynamics of relay-pulse automatic control systems," Automation and Remote Control (USSR) 18, 1 (1957).*

[17] E. Ia. Shchegolev, "The phase differences of periodic processes with a rational frequency ratio and their measurement on a cathode-ray oscillograph," J. Tech. Phys. (USSR) 4, 1 (1934).

* See C. B. Translation.

A PNEUMATIC EXTREMUM REGULATOR

Iu. I. Ostrovskii

(Moscow)

A pneumatic extremum regulator developed at the Institute of Automation and Remote Control, Academy of Sciences of the USSR, is described; laboratory test results are given.

1. The Operative Principle of the Regulator

This regulator operates by "remembering" the maximum. The search for the maximum is continuous, forced change in the input to the object X being used (Fig. 1a).

Figure 1c shows the change in air pressure P_x at the regulator output. P_x is proportional to the input to the object X (Fig. 2).

Figure 1b shows the corresponding change P_y, proportional to the output coordinate of the object Y. At time t_e the maximum in P_y, $P_{y\,max}$ is reached, further change in P_x resulting in a fall. If the object shows a lag $P_{y\,max}$ will be less than the $P'_{y\,max}$ given by the static characteristic.

A special device (memory unit) records $P_{y\,max}$ (Figs. 2 and 3). The pressure P_m in the memory chamber follows P_y when this increases. P_m remains fixed if P_y falls.

The comparator (Fig. 2) compares the current P_y with the maximum one, recorded in the memory chamber. When the difference δ_{max} reaches a set value $\delta = P_{y\,max} - P_y$ at time t_p the comparator output produces a pressure pulse P_u (Fig. 1d) which is passed on to the stepping valve (Fig. 2).

The pressure P_p at the stepping valve output (Fig 1f) can have two discrete values $P_p = 0$ and $P_p = P_{p1}$. Switching is effected when P_u arrives. The P_p produced by the previous pulse is maintained in the interval between pulses.

P_p is applied to the input of the "constant rate" unit (Fig. 2). If $P_p = P_{p1}$ the pressure P_x at the output of this unit rises at a constant rate. If $P_p = 0$, P_x falls at the same rate.

P_x controls the change in the controlled object input coordinate.

In addition to reversing the input coordinate, P_u also has the following functions:

a) it effects self-locking in the comparator,

b) wipes out the memory,

c) removes the self-locking in the comparator (via a delay unit).

The memory wipe-out is effected by connecting the memory chamber to the P_y line. P_m and P_y equalize, but because of the self-locking the output P_u from the comparator is retained.

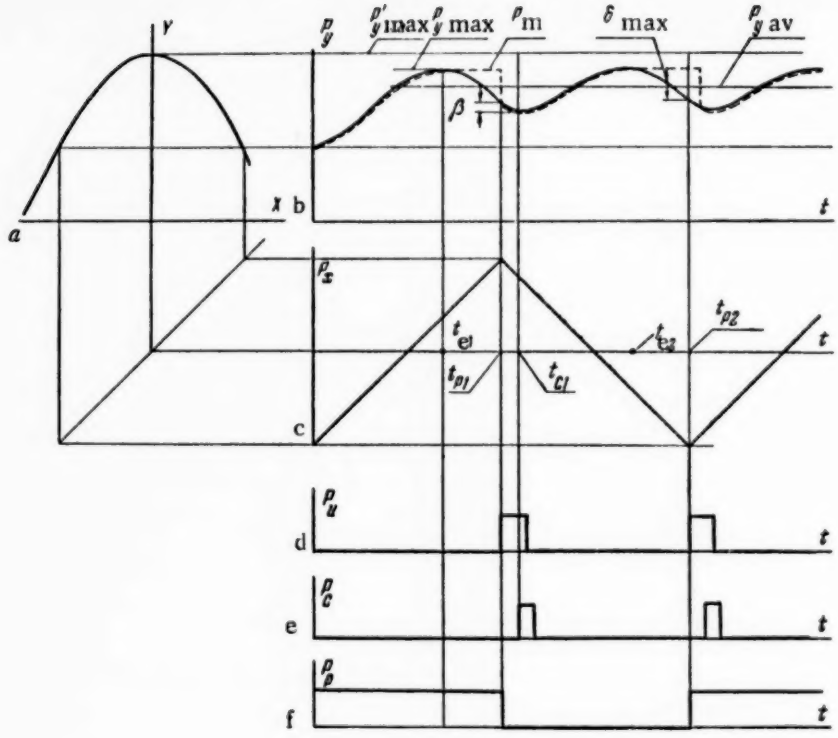

Fig. 1. Operational sequence in the pneumatic extremum regulator using maximum storage.

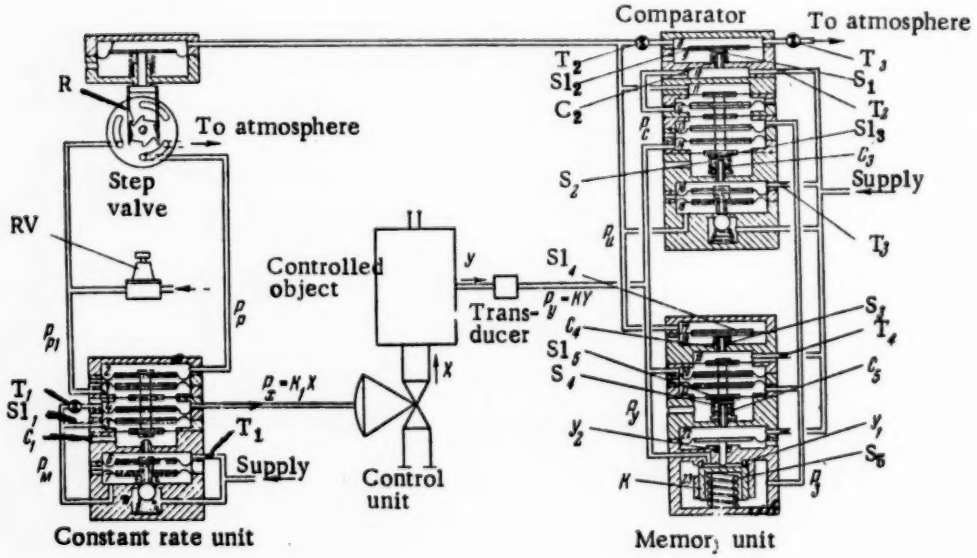

Fig. 2. Design of the pneumatic extremum regulator using maximum storage.

If the object lags the output Y (and P_y, proportional to it) will continue to fall for a certain time after reversing the input.

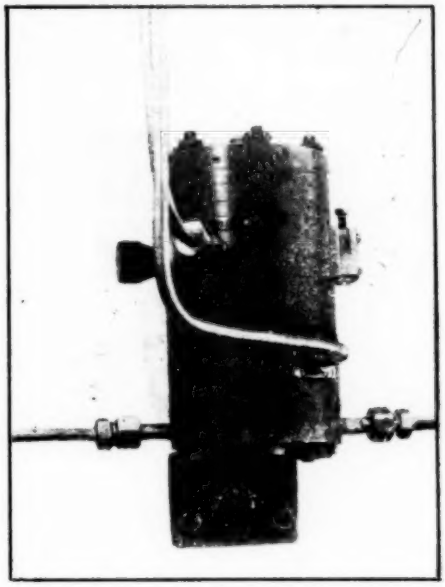

Fig. 3. Memory unit.

If the memory unit is again cut in at time t_p it will remember the corresponding P_y and in this case, if $\beta > \delta$ (Fig. 1b) a false reversal in the direction of change in P_x will occur. To avoid this P_u is applied with a certain delay.

At time t_c the delay unit produces an output pressure pulse P_c (Fig. 1e). This removes the comparator self-locking. The pressure in the P_u line falls to zero. As of this time the memory can again record the maximum P_y. The drop in P_u also causes a (delayed) drop in P_c.

At time t_{e2}, P_y again becomes maximal, the memory unit again records $P_{y\,max}$, and at time t_{p2} the direction of change in P_x is again reversed, and the cycle repeats.

2. Design of the Regulator

The design shown in Figure 2 is intended to utilize many of the standard components of pneumatic systems. There are four units: memory, comparator, step valve and constant rate. The naming is explained above.

P_y, which is proportional to the object output Y, is fed to chamber 20 in the memory and to chamber 14 in the comparator. When the valve K is open the P_y line is also connected to the memory chamber 23. K is closed by the spring S_5, and opens when a pressure appears in 22. The valve stem is sealed by the rubber ring Y_1. P_m from the memory chamber is fed to chambers 13 and 21, where it is compared with P_y.

The area of the valve C is considerably larger than that of the fixed throttle T. Hence if the gap between C and the slide Sl is large the pressure in the chamber between C and T will differ but slightly from atmospheric. The pressure rises as the gap is reduced.

When $P_y > P_m$, C_3 is open, so the pressure in chambers 8-12, 15-17 and 19 is atmospheric, Sl_5 covers C_5, which controls the opening of K. K opens, and P_y is applied to the memory chamber. Thus as the output coordinate increases the memory chamber pressure follows the rise in P_y. If the rise ceases the pressures in the memory chamber and the P_y line equalize. The spring S_4 then deflects the membrane, Sl_5 moves away from C_5, the pressure in chamber 22 falls, and K closes. As P_y falls K stays closed. Thus P_m is given by $P_y = P_{y\,max}$. When $\delta = P_{y\,max} - P_y$ reaches the set value δ_{max} (set by S_2) Sl_3 closes C_3 and the pressure P_u at the comparator output begins to rise. The positive feedback causes the P_u fed to chamber 11 in this unit to rise rapidly. The pressure is thus transmitted to Chamber 1, so the stepping valve rotates the ratchet R one step. In the position shown the valve connects the P_p line to the atmosphere. The next P_u pulse connects the P_p line to a line in which P_{p1} is maintained.

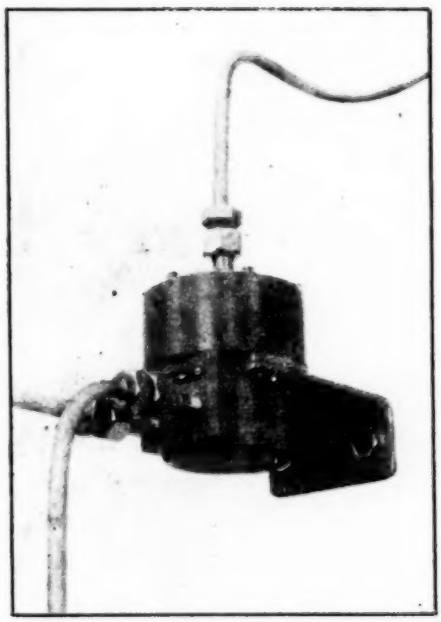

Fig. 4. Stepping valve with a flat gate.

P_u, fed to the memory, overcomes the force exerted by S_3 and closes C_4 by means of Sl_4. The pressure in 19 and 22 rises, K opens and connects the memory chamber to the P_y line. The pressures in 13 and 14 become equal, but C_3 remains closed because P_u is applied to chamber 11.

After a time determined by the areas of throttles T_2 and T_3 the pressure in 8 (delay element) overcomes spring S_1 and closes C_2 with Sl_2. Then the P_c pulse is passed to chamber 12, which opens C_3 and releases the P_u pulse. The initial state is then restored.

Let us now consider the operation of the constant rate unit. When there is no excess pressure in chamber 2 the pressure P_{p1} in chamber 3, set by the reducing valve RV, balances the difference of P_x and P_M in chambers 4 and 5, where $P_x > P_M$. The air then escapes from the control head of the control unit to the atmosphere. Since the pressure drop across T_1 remains constant, the regulator moves with constant velocity. Since the drop across T_1 is reduced the gap between Sl_1 and C_1 increases. The pressures in 5, 6 and 7 fall and the set pressure drop is restored. When P_p is applied to 2 the membrane head is filled at a constant rate, determined by the fixed drop across T_1.

The flat-gate stepping valve above (see also Fig. 4) differs considerably in design from the other units, which are based on pneumatic control systems.

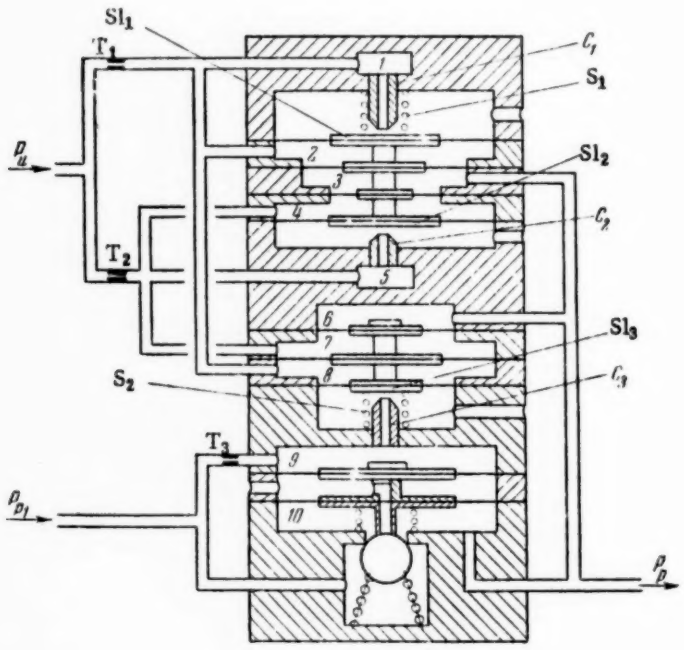

Fig. 5. Stepping valve designed round a pneumatic control system.

Figure 5 shows the design of a stepping valve designed round a pneumatic control system. The advantages of this are the absence of a ground-in slide and other parts subject to wear, and the small movements required of the moving parts, which results in quick response.

The operational sequence of this unit (Fig. 5) is as follows.

Initially, before the first P_u pulse is applied, C_1 and C_3 are open, due to S_1 and S_2. C_2 is closed by Sl_2. The pressure in cavities 1-10 is atmospheric.

Upon application of the P_u pulse, a pressure will appear in cavities 5, 4, and 7. Sl_3 shuts off C_3. P_p is fed to the constant rate unit. The same pressure is applied to cavities 3 and 6. When the pulse is received C_3 remains closed because of the pressure in 6. P_p is maintained. The pressure in 3 shuts off C_1 via Sl_1.

At the next P_u pulse the pressure enters 1, 2 and 8. C_3 is opened. The pressure in the P_p line falls to atmospheric. The initial state is restored when P_u is removed. The pressure in the P_p line remains atmospheric up to the next P_u pulse. The cycle then repeats.

3. Laboratory Test Results on the Regulator

Figure 6 shows the setup used to test a prototype regulator.

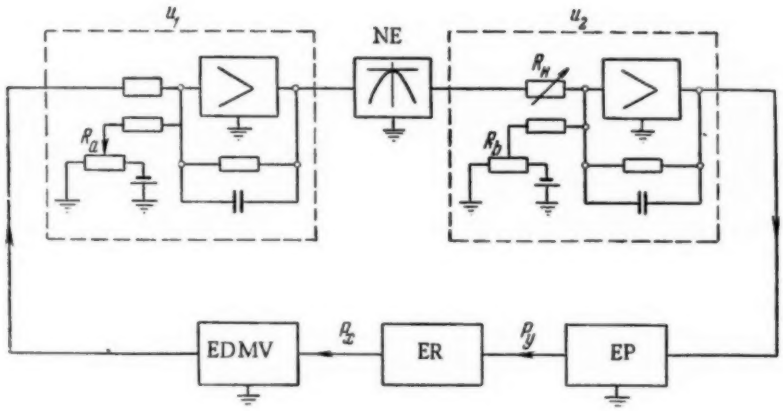

Fig. 6. Experimental circuit.

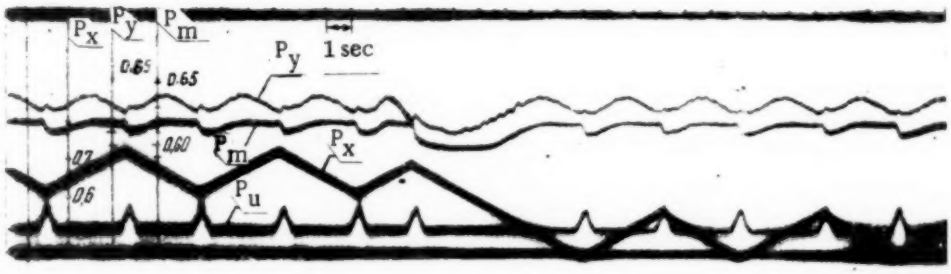

Fig. 7. Operation of the regulator when the peak suddenly shifts horizontally. (P in kg/cm^2.)

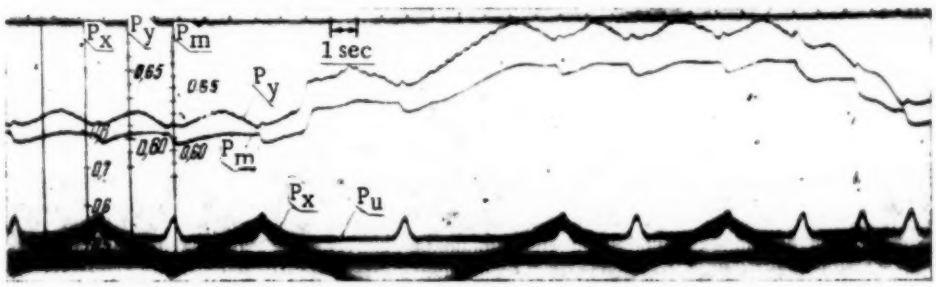

Fig. 8. Operation of the regulator when the peak suddenly shifts vertically. (P in kg/cm^2.)

A model of an object with the nonlinear static characteristic $Y = k(X - a)^2 + b$ was set up on an EMU-5 analog apparatus. The coefficients k, a and b could be changed during operation by adjusting the variable resistance R_k and the potentiometers R_a and R_b.

The analog consisted of a lagless nonlinear element NE with a parabolic response and two first-order delay links, u_1 and u_2.

P_x (output from the extremum regulator ER) was converted to an electrical signal by a type EDMU-1 potentiometric transducer. The output signal from the analog equipment was transformed to an air pressure P_y by the electropneumatic converter EP.

P_x, P_y, P_m and P_u (Fig. 1) were recorded with an oscillograph.

The oscillograms of Figures 7 and 8 illustrate the operation of a regulator with a lag-free object (time-constants of u_1 and u_2 zero). The steady-state oscillations about the maximum are seen, plus the transient response when b is altered (Fig. 7) or a (Fig. 8).

The test results give rise to the following conclusions.

1. The design provides good "recollection" of the maximum. The pressure drop in the memory chamber, starting from $P_m = 0.5$ atm and $P_y = 0$ was about 1 mm Hg per hour. The sealing could if necessary be improved.

2. The response was clear-cut at $\delta = 0.015$ kg/cm^2. (Working pressure range $P_y = 1$ kg/cm^2.) Further improvements to the regulator would clearly reduce δ.

3. The regulator follows slow changes in the maximum, and finds the new position when the maximum is sharply displaced horizontally (Fig. 7) or vertically (Fig. 8).

The system is at present the subject of more detailed study.

Received January 24, 1957

DESIGN OF MAGNETIC AMPLIFIERS TO A SET SUPPLY VOLTAGE

N. P. Vasil'eva and O. A. Sedykh

(Moscow)

It is demonstrated that at given supply and load voltages the amplifier volume is proportional to the ratio of these voltages if the magnetic conditions are unchanged.

Formulas and data, from which a choice can be made between an optimally designed amplifier with a separate matching transformer and one designed for a given supply voltage, are given.

Conclusions are drawn for amplifiers with and without feedback.

When a magnetic amplifier is designed for a given voltage, load power and gain, and minimum weight or size the supply voltage must have a definite value, which is often different from that of the standard supply sources [1]. Hence such amplifiers are commonly used with line or output transformers.

It is clearly important to determine within what limits it is best to deviate from the optimum amplifier design, so as to avoid using line or output transformers, particularly at medium or high powers.

Here we may either compare the overall sizes, or the weights, or the costs of an optimal amplifier plus transformer and one designed to a set supply voltage. All these problems can be solved by determining the iron volume required in the amplifier, since we can assume [2] that, if certain relations between the dimensions apply for an amplifier optimal for each case, the volume, weight and cost are proportional to the core volume.

In what follows we assume the currents and voltages in the amplifier sinusoidal. Then we can use the symbolic method, which gives good agreement with experience for materials of types E-310, E-320, 80NKhS and 50NP when the $B_{\sim} = \varphi(H_{\sim}, H_{=})$ characteristics are used. Calculations based on relationships for an ideal amplifier with rectangular magnetization curves and a resistive load agree precisely with those performed symbolically for a purely inductive load. The results are somewhat too high for an amplifier with a resistive load using the materials enumerated above.

For a single-phase amplifier with resistive load (Fig. 1) the specific steel volume can be expressed as [1]:

$$\frac{V_{st}}{P_a} = \frac{1.6\times10^7 \sqrt{1-\frac{1}{k^2}}}{fH_{mk}\sqrt{B_{m0}^2 - B_{mk}^2}}, \qquad (1)$$

where V_{st} is the steel volume in one core in cm^3, P_a is the resistive power, equal to the load power plus the copper loss in the working windings (watts), k is the load current ratio when the control (bias) field changes from zero to its maximum, f is the frequency in cycles/sec, H_{mk} is the ac field strength at maximum control field in amp-turns/cm, B_{mk} is the ac induction at maximum control field in gauss, and B_{m_0} is the same at zero control field, in gauss.

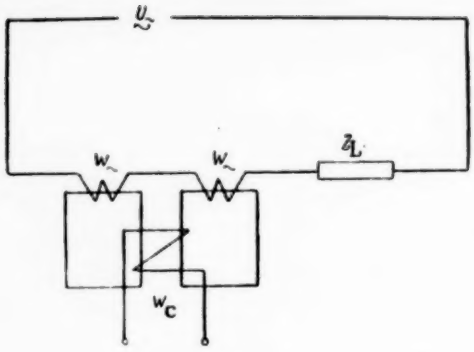

Fig. 1.

For an amplifier with an inductive load

$$\frac{V_{st}}{P_i} \approx \frac{1.6\times10^7 P_i\left(1-\frac{1}{k}\right)}{fH_{mk}(B_{m0}-B_{mk})}, \qquad (2)$$

where P_i is the apparent power in volt-amps, allowing for the copper loss in the working windings.

In (1) and (2) H_{mk}, B_{m_0} and B_{mk} are related by the principal magnetization curve for the material ($H_c = 0$) and by any other curve of the $B_{\sim} = \varphi(H_{\sim} H_c)$ family (Fig. 2). We have $H_{m_0} = H_{mk}/k$, where H_{m0} is the ac field strength at zero bias field.

Equations (1) and (2) are correct for any H_{mk} and H_c or B_{m0} and B_{mk}, but only if $H_{mk}/H_c = n_{opt}$ does this expression have a minimum value for each value of H_c = const [1]. For different materials n_{opt} varies from 1.4 to 1.6, being practically constant for any one material. Hence curves relating the minimum specific volumes of 50NP steel to the maximum dc control field H_c (Fig. 3) could be drawn up [1, 2].

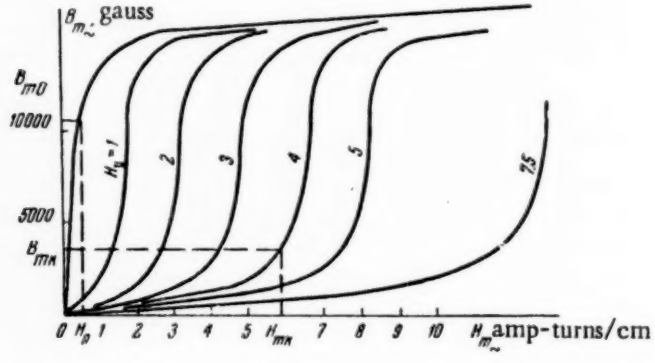

Fig. 2.

With these curves and the relations of the gain and copper volume to control field at hand it is simple to design an amplifier for minimum weight, size or cost. But, as above, in such an amplifier the $U_{\sim}/U_L$ ratio, where $U_{\sim}$ is the supply voltage and U_L the load voltage, is precisely determined (Fig. 3). It varies from 1.03 to 1.2 as H_c varies from low values to hundreds of amp-turns/cm.

Thus, if for a given voltage this ratio exceeds the optimum, we have to choose between an amplifier designed for minimum weight (size), plus a supply transformer, and one designed to a given supply voltage.

To find how the specific steel volume varies as the supply voltage deviates from optimal it is expressed in terms of $U_{\sim}/U_L$. For the circuit of Figure 1 we have

a) at zero control field:

with a resistive load

$$U_{\sim}^2 = U_0^2 + U_{L0}^2, \qquad (3)$$

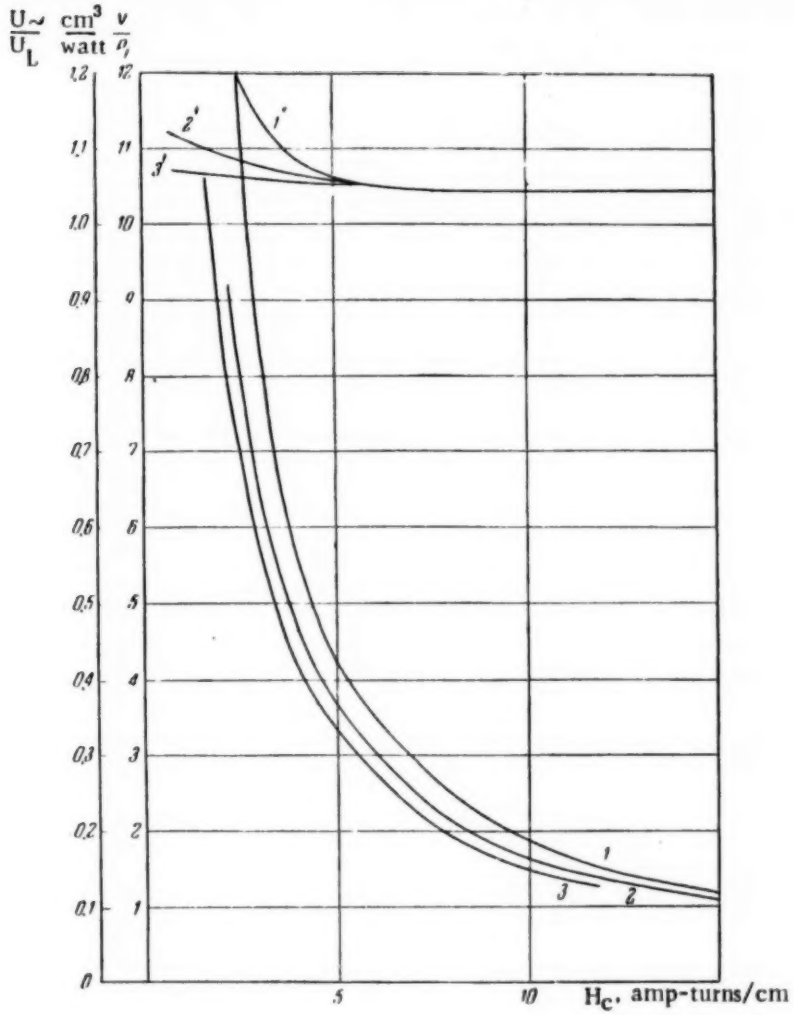

Fig. 3. 1, 2, 3) V/P curves; 1') $U_\sim/U_L$ for k = 20; 2') $U_\sim/U_L$ for k = 10; 3') $U_\sim/U_L$ for k = 5; f = 50 cycles/sec, cos φ_L = 1, δ = 0.1.

with an inductive load

$$U_\sim \approx U_0 + U_{L0}^2; \tag{4}$$

b) at maximum control field, as above

$$U_\sim^2 = U_k^2 + U_L^2, \tag{5}$$

$$U_\sim \approx U_k + U_L. \tag{6}$$

Here U_0 and U_k are the reactive voltages on the coil, and U_{L0} and U_L are the total voltages on load plus coil resistance, where $U_{L0} = U_L/k$.

Equations (3) and (4) give respectively

$$U_0 = U_L \sqrt{\left(\frac{U_\sim}{U_L}\right)^2 - \frac{1}{k^2}}, \tag{7}$$

$$U_0 \approx U_L \left(\frac{U_\sim}{U_L} - \frac{1}{k}\right). \tag{8}$$

We multiply by I_k and remember that $I_k = \frac{H_{mk} l_{st}}{\sqrt{2} W_\sim}$, $U_0 = 4.44 f 2W_\sim S_{st} B_{m0} 10^{-8}$, $l_{st} S_{st} = V_{st}$ and $U_L I_L = P_L$. Here l_{st} is the mean core circuit length, S_{st} the core section, $W_\sim$ the number of turns on the ac coil on one core. Then (8) gives, for a resistive load,

$$\frac{V_{st}}{P_a} = \frac{1.6 \times 10^7 \sqrt{\left(\frac{U_\sim}{U_L}\right)^2 - \frac{1}{k^2}}}{f B_{m0} H_{mk}} \tag{9}$$

and for an inductive load,

$$\frac{V_{st}}{P_i} = \frac{1.6 \times 10^7 \left(\frac{U_\sim}{U_L} - \frac{1}{k}\right)}{f B_{m0} H_{mk}}. \tag{10}$$

Similarly, (5) and (6) give

$$\frac{V}{P_a} = \frac{1.6 \times 10^7 \sqrt{\left(\frac{U_\sim}{U_L}\right)^2 - 1}}{f B_{mk} H_{mk}}, \tag{11}$$

$$\frac{V}{P_i} = \frac{1.6 \times 10^7 \left(\frac{U_\sim}{U_L} - 1\right)}{f B_{mk} H_{mk}}. \tag{12}$$

Dividing (9) by (11) and (10) by (12) we get, for a resistive load,

$$\frac{B_{m0}}{B_{mk}} = \frac{\sqrt{\left(\frac{U_\sim}{U_L}\right)^2 - \frac{1}{k^2}}}{\sqrt{\left(\frac{U_\sim}{U_L}\right)^2 - 1}}. \tag{13}$$

and for an inductive load,

$$\frac{B_{m0}}{B_{mk}} = \frac{\frac{U_\sim}{U_L} - \frac{1}{k}}{\frac{U_\sim}{U_L} - 1}. \tag{14}$$

So for a given $U_\sim / U_L$ the steel volume can be calculated from the $B_\sim = \varphi(H_\sim H_c)$ curves using (9)-(12) or (1), (2); but (13) or (14) must be allowed for. It is clear that for a given $U_\sim / U_L$ each H_c = const curve gives

only one point on the $B_\sim = \varphi(H_\sim H_c)$ curves satisfying (13) or (14). (Thus, for instance, only the point A in Figure 4 for which $k=H_{mk}/H_{m0}=5$ gives $B_{m0}/B_{mk}=2$. All other points on H_c = const give other values of B_{m0}/B_{mk}). So, by finding V/P for such points at various values of H_c, we can construct $V/P = F(H_c)$ curves for given values of $U_\sim/U_L$ and $\underline{k}$.

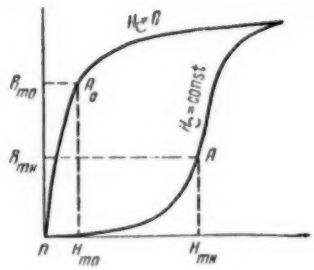

Fig. 4.

Taking $U_\sim/U_L$ as parameter and $\underline{k}$ as constant we can draw up a set of $V/P = f(H_c, U_\sim/U_L)$ curves. The lowest curve of all will be that of minimum specific steel volume, which has $U_\sim/U_L$ almost constant (Fig. 5). At higher $U_\sim/U_L$ the curve will run higher, in sequence. This follows readily from (9) and (10), if transformed to the form

$$\frac{V}{P}=\frac{U_\sim}{U_L}\frac{1.6\times10^7}{nfH_c B_0}\sqrt{1-\left(\frac{U_L}{U_\sim k}\right)^2}, \tag{15}$$

$$\frac{V}{P}=\frac{U_\sim}{U_L}\frac{1.6\times10^7}{nfH_c B_0}\left(1-\frac{U_L}{U_\sim k}\right). \tag{16}$$

Here $n = H_{mk}/H_c$.

In (15) and (16) $\underline{n}$ and B_0 alter very little with $U_\sim/U_L$ for any given H_c, if the $(U_L/U_\sim k)^2$ or $(U_L/U_\sim k)$ terms can be neglected relative to unity, so we may consider the specific volume directly proportional to $U_\sim/U_L$. If these terms cannot be neglected (if $\underline{k}$ is very small) the specific volume will rise more rapidly with $U_\sim/U_L$. In practice, with $k \geq 2$ and resistive loads, or $k \geq 4$ and inductive, we can assume V/P proportional to $U_\sim/U_L$, the error being less than 13%. Thus if the minimum specific steel volume curves are available an amplifier can be designed to a given supply voltage, if we remember that

$$\frac{V}{P_L}\approx\frac{U_\sim}{U_L}\Big/\left(\frac{U_\sim}{U_L}\right)_{opt}\times\left(\frac{V}{P_L}\right)_{min}, \tag{17}$$

where $(U_\sim/U_L)_{opt} = 1.03\text{-}1.2$.

This expression can be used to simplify the design to a given supply voltage. If high accuracy is needed we can use (1), (2), (9) and (10) or (11), (12) together with (13), (14) and the set of $B_\sim = \varphi(H_\sim H_c)$ curves. This (17) shows that at fixed H_c the steel volume is directly proportional to $U_\sim/U_L$. But to get our final estimate of the increase in steel volume on deviating from the optimum supply voltage we must compare the steel volumes at different gains (which depend on the amplifier dimensions as well as on H_c) and not at different H_L.

In the general case the power gain with and without feedback [1-3] is proportional to

$$\varkappa=\frac{S_0}{H_c^2 l_{st}^2 l_{w_{av}}(1+\beta)},$$

where S_0 is the winding area, l_{st} the mean core circuit length, $l_{w\,av}$ the average length of a control turn, and β the ratio of winding areas occupied by working and control coils.

Let us determine $\varkappa$ for an amplifier with toroidal cores. We express S_0, l_{st} and $l_{w\,av}$ in terms of V_{st}:

$$S_0 = a\sqrt[3]{V_{st}^2}\quad l_{st}=b\sqrt[3]{V_{st}},\ l_{w_{av}}=d\sqrt[3]{V_{st}} \tag{18}$$

$\underline{a}$, $\underline{b}$ and $\underline{d}$ being assumed optimal, i. e., such as to give the minimum weight or size. They then do not depend on changes in steel volume and are practically constant [2]. Substituting for S_0, l_{st} and $l_{w\,av}$ in the expression for k_p, we have

$$K_p = A \frac{a}{H_c^2 b^2 d \sqrt[3]{V_{st}} (1 + \beta)}. \quad (19)$$

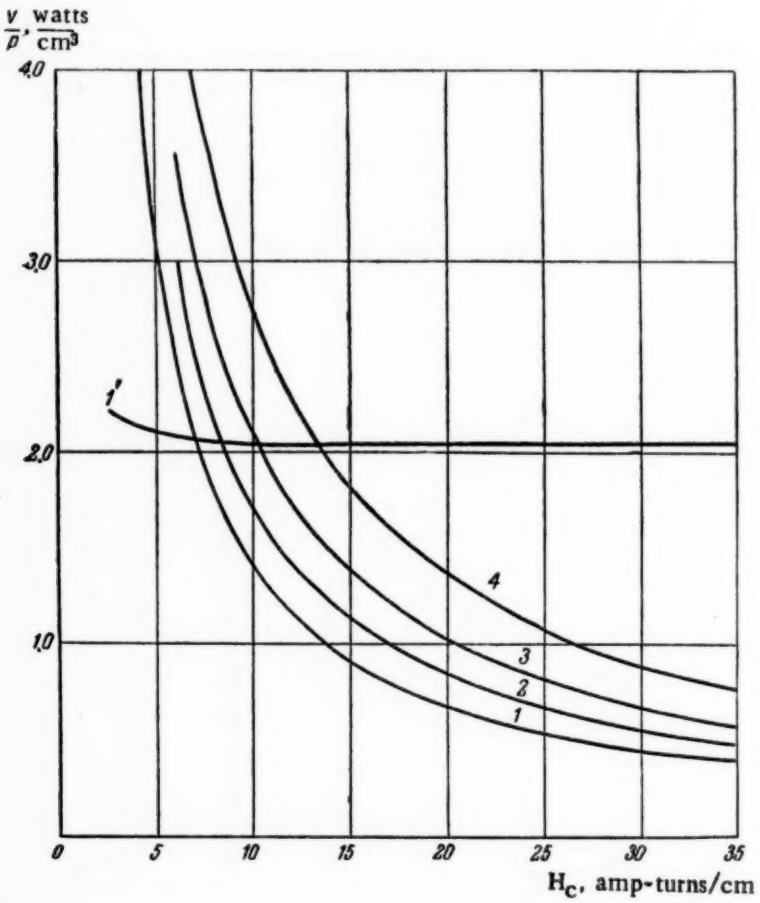

Fig. 5. Minimum volume curve, V/P_{min}: 1') $U_\sim/U_L$ for 1); 2) V/P for $U_\sim/U_L = 1.25$; 3) V/P for $U_\sim/U_L = 1.5$; 4) V/P for $U_\sim/U_L = 2$; f = 50 cycles/sec, cos $\varphi_L = 1$, k = 10, $\delta = 0.35$.

Here A is a coefficient dependent on P_L, the feedback, and certain other constants.

The subsequent treatment can be much simplified if an approximate analytic relation between H_c and V_{st} is used. It has been shown [2] that for several materials we have

$$\frac{V}{P_L} \approx \frac{c}{H_c}, \quad (20)$$

where c is a constant, which can be determined from $V/P = \varphi(H_c)$.

Since the specific volume at H_c = const is proportional to $U_\sim/U_L$, (20) indicates that

$$\frac{c_1}{c_2} = \frac{U_{1\sim}/U_L}{U_{2\sim}/U_L}. \qquad (21)$$

Substituting (20) into (19), we have

$$K_p = A\frac{aV^{4/3}}{c^2P_L^2b^2d(1+\beta)}. \qquad (22)$$

Two amplifiers with differing values of $U_\sim/U_L$ but equal gains will, using (22) and (21), have a steel volume ratio given by

$$\left(\frac{V_2}{V_1}\right)^{4/3} = \left(\frac{1+\beta_2}{1+\beta_1}\right)\left(\frac{c_2}{c_1}\right)^2. \qquad (23)$$

It is known [1] that

$$\beta = \left(\frac{S_0\sqrt{2}\Delta k_f}{nH_c\, l_{st}} - 1\right)^{-1}, \qquad (24)$$

where Δ is the current density in amps/cm^2 and k_f the fill-in factor. If we also assume the working windings of both to have identical current densities, and use (24), (18) and (20), we get yet another relationship for the steel volumes:

$$\left(\frac{V_2}{V_1}\right)^{4/3} = \frac{1+\beta_2}{1+\beta_1}\frac{\beta_1}{\beta_2}\frac{c_2}{c_1}. \qquad (25)$$

Solution of (23) with (25) does not give the relation of V_2/V_1 to $\frac{c_2}{c_1} = \frac{U_{\sim 2}/U_L}{U_{\sim 1}/U_L}$, explicitly, but it enables us to relate β_1, β_2 to c_1/c_2:

$$\frac{1+\beta_1}{1+\beta_2}\left(\frac{\beta_2}{\beta_1}\right)^8 = \left(\frac{c_1}{c_2}\right)^8. \qquad (26)$$

If β_1 is given V_2/V_1 can be determined.

For an amplifier with feedback (particularly internal) we can assume the working winding to occupy very much more of the space than the control one, i. e., $\beta >> 1$. Then (23) and (25) give

$$\frac{V_2}{V_1} = \left(\frac{U_2/U_L}{U_1/U_L}\right)^{4/3}. \qquad (27)$$

In low-power amplifiers without feedback the situation is usually reversed, i. e., $\beta << 1$. Then (23) and (25) give

$$\frac{V_2}{V_1} = \left(\frac{U_{2\sim}/U_L}{U_{1\sim}/U_L}\right)^{4/3} \tag{28}$$

Clearly, all intermediate values of β give V_2/V_1 within the limits

$$\frac{V_2}{V_1} = \left(\frac{U_{2\sim}}{U_{1\sim}}\right)^{4/3} \div \left(\frac{U_{2\sim}}{U_{1\sim}}\right)^{4/3}. \tag{29}$$

Since $U_{2\sim}/U_{1\sim}$ is always greater than one, V_2/V_1 is so also. Below we give a table for $(V_2/V_1)\cdot 100$ % for certain $U_{2\sim}/U_{1\sim}$ values with $\beta \ll 1$, $\beta = 1$ and $\beta \gg 1$.

β	$U_{2\sim}/U_{1\sim}$			
	1.25	1.50	1.75	2.00
$\ll 1$	133	160	191	235
1	125	150	175	200
$\gg 1$	119	137	153	170

Eq. (29) shows that amplifiers using feedback and designed to work at higher supply voltages have lower steel volumes, and hence lower weights and sizes relative to the minimum ones, than do those without feedback.

Using (29) or (23), (25) and (26), we can compare the overall weight (size) of an optimal amplifier plus transformer with that of an amplifier designed to the set supply voltage. No general rules can of course be given here, but we may, for instance, say that when $U_\sim/U_L$ is close to two the optimal amplifier plus transformer will be lighter and occupy less space than the other. Conversely, if $U_\sim/U_L$ is 1.25 the latter will be the better.

In push-pull magnetic amplifiers the question of design to a given supply voltage can only be posed in relation to bridge systems. All the conclusions drawn here are applicable to this case. The specific steel volume of a push-pull amplifier may [3] be expressed as a function of H_c in terms of the specific volume for a single-phase amplifier using

$$\left(\frac{V_{st}}{P_L}\right)_{II} \leqslant \frac{2}{\left(1-\frac{1}{k}\right)^2}\left(\frac{V_{st}}{P_L}\right)_I.$$

This expression is correct no matter whether the steel volume is calculated for the optimum supply voltage or a higher one. Thus we can assume that

$$\left(\frac{V_{st}}{P_L}\right)_{II} \leqslant \frac{2}{\left(1-\frac{1}{k}\right)^2}\frac{U_{\sim II}}{U_{opt\ II}}\left(\frac{V_{st}}{P_L}\right)_{I\,min}$$

where $U_{\sim II}$ is the set supply voltage of the bridge amplifier and $U_{opt\ II}$ the optimal supply voltage derived by the method given in [3].

Received April 18, 1957

LITERATURE CITED

[1] N. P. Vasil'eva and O. A. Sedykh, "Design of magnetic amplifiers with complex loads," Automation and Remote Control (USSR) 16, No. 1 (1955).

[2] O. A. Sedykh, "Design of power magnetic amplifiers using toroidal cores," Report of the Institute of Automation and Remote Control, Academy of Sciences of the USSR, No. 8, December (1955).

[3] N. P. Vasil'eva, "Design of push-pull power magnetic amplifiers," Automation and Remote Control (USSR) 17, No. 1 (1956).*

*See C. B. Translation.

TRANSIENT AND STEADY-STATE PROCESSES IN PULSE SYSTEMS WITH ABRUPTLY-CHANGING VARIABLE PARAMETERS

F.M. Kilin

(Leningrad)

This work describes one of the methods of determining the transient and steady-state processes in pulse systems with abruptly-changing variable parameters. To describe the phenomena in such systems one employs the formalism of step-functions in conjunction with continuous functions.

INTRODUCTION

Many modern electronic systems contain elements with variable parameters, which are changed abruptly by pulse signals applied to the inputs of these elements. Such a variation in parameters is describable by piecewise continuous functions.

Accordingly, we shall call such a change in system parameters a piecewise continuous variation. This is the only parameter variation that will be discussed below.

The use of such elements in pulse radio systems makes it possible to improve their technical characteristics. However, this complicates the character of the transients in the system, and leads therefore to certain difficulties in their analysis and in the engineering design of apparatus with such elements.

In some cases the absence of a clear conception of the influence of the parameters of the apparatus on the character of the transient makes it impossible to select suitable circuitry for the apparatus and determine correctly the values of its parameters.

A convenient theoretical formalism for the investigation and analysis of pulse apparatus and intermittent-regulation systems is the operational calculus of step functions [1-3]. However, this formalism was developed principally as applied to systems with constant parameters. For this reason it cannot be extended to include the systems considered here.

In Reference [4] are considered several particular cases of operation of pulse systems with piecewise continuous variation of parameters. Here the actual system is replaced by a continuous system with constant parameters. Below (Section 4) it will be shown that this substitution is possible and permissible only under certain conditions.

We shall determine in this work the transients in pulse systems with piecewise continuous variation using more general methods which are applicable to an extensive class of apparatus operating under a great variety of modes.

1. Description of Pulse System

Let us consider a pulse system with piecewise continuous variation of parameters, in which the processes are described by the following equation

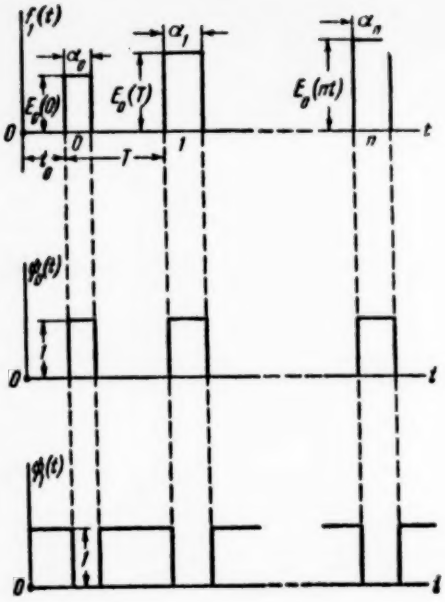

Fig. 1.

$$Dx_1 + \sum_{k=1}^{r} a_{1k}(t)\, x_k = f_1(t),$$

$$Dx_2 + \sum_{k=1}^{r} a_{2k}(t)\, x_k = 0,$$

$$\cdots\cdots\cdots\cdots\cdots$$

$$\cdots\cdots\cdots\cdots\cdots$$

$$Dx_r + \sum_{k=1}^{r} a_{rk}(t)\, x_k = 0. \qquad (1.1)$$

Here D = d/dt is the differentiation operator, and t is the independent variable (running time).

The quantity $f_1(t)$ is a pulse function of the form

$$f_1(t) = \sum_{k=0}^{\infty} E_0(kT)\,[H(t - t_0 - kT) - H(t - t_0 - \alpha_k - kT)]. \qquad (1.2)$$

Here H(t) is the unit step function, satisfying the following conditions:

$$H(t) = \begin{cases} 0 & \text{for } t \leqslant 0, \\ 1 & \text{for } t > 0, \end{cases}$$

$E_0(kT)$ is the height of the k'th pulse and T is the repetition period of the pulses, while α_k is the duration of the k'th pulse.

Thus, the function $f_1(t)$ describes a sequence of rectangular pulses, whose heights and durations vary with time (Figure 1).

The change in the system parameters is expressed by the equations

$$a_{jk}(t) = a^0_{jk}\,\psi_0(t) + a^1_{jk}\,\psi_1(t), \qquad (1.3)$$

where a^0_{jk} and a^1_{jk} are constant coefficients, while $\psi_0(t)$ and $\psi_1(t)$ are pulse functions of unit height of the form

$$\psi_0(t) = \sum_{k=0}^{\infty} [H(t - t_0 - kT) - H(t - t_0 - \alpha_k - kT)],$$

$$\psi_1(t) = H(t) - \psi_0(t). \qquad (1.4)$$

Plots of the pulse functions $\psi_0(t)$ and $\psi_1(t)$ are given in Figure 1. The pulses $\psi_0(t)$ coincide in time with the pulses $f_1(t)$, applied to the input of the system.

In matrix form, Equations (1.1) are written as

$$[DI + a(t)]X(t) = f(t). \qquad (1.5)$$

Here I is the unit matrix of order r, in which the principal diagonal consists of ones and all the remaining elements are zero,

$$a(t) = \psi_0(t)\, a^0 + \psi_1(t)\, a^1,$$

$$a^0 = \| a^0_{jk} \|, \quad a^1 = \| a^1_{jk} \| \quad (j, k = 1, 2, \ldots, r). \tag{1.6}$$

The quantities X(t) and f(t) are column matrices of the form

$$X(t) = \left\| \begin{matrix} x_1(t) \\ x_2(t) \\ \ldots \\ \ldots \\ x_r(t) \end{matrix} \right\|, \quad f(t) = \left\| \begin{matrix} f_1(t) \\ 0 \\ \ldots \\ \ldots \\ 0 \end{matrix} \right\|. \tag{1.7}$$

A system describable by Equations (1.1) or (1.5) will be henceforth called, for brevity, a pulsed system.

2. Transients and Steady-State Processes in Pulse Systems

When determining the characteristics of pulse systems, complex analysis methods, which call for the use of the formalism of step functions in conjunction with continuous functions, become significant. This corresponds to the character of the processes in such systems. Let us briefly describe the essence of such methods and obtain expressions for continuous step functions, determining the variation of certain quantities $x_j(t)$ ($j = 1, 2, \ldots, r$) with time.

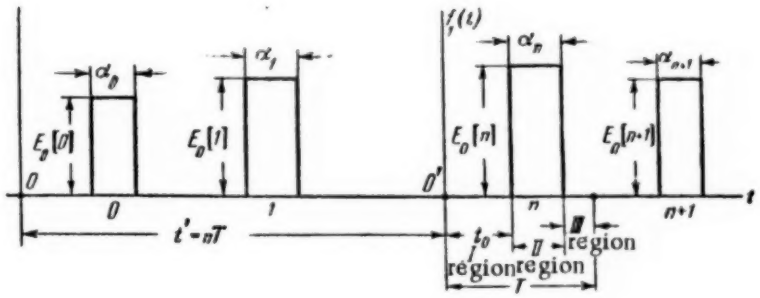

Fig. 2.

Let us apply certain transformations to Equation (1.1). For this purpose let us choose a new coordinate system, with the origin located at the point t' = nT (Figure 2). The height and duration of the n'th pulse will be denoted by $E_0[n]$ and α_n respectively. Let us find expressions for the function X(t) in the new coordinate system for the interval $0 < t \leq T$. This interval is broken up into three regions (Figure 2). Let us denote the initial conditions for $x_j(t)$ by $x_j[n]$, i.e.,

$$x_j(0) = x_j[n] \text{ when } t = 0 \tag{2.1}$$

or

$$X(0) = X[n]. \tag{2.2}$$

We shall determine X(t) below for each region.

Region I. The differential equation for X(t) in this region is of the form:

$$[DI + a^1]\, X(t) = 0 \qquad (0 < t \leqslant t_0). \tag{2.3}$$

The solution of the matrix Equation (2.3) leads to the following expression:

$$X(t) = \beta^1(t)\, X[n]. \tag{2.4}$$

The operational transforms of the matrix elements

$$\beta^1(t) = \|\beta^1_{jk}(t)\| \quad (j, k = 1, 2, \ldots, r)$$

are given by the equations

$$L[\beta^1_{jk}(t)] = \frac{A^1_{jk}(p)}{\Delta a_1(p)}, \tag{2.5}$$

where $\Delta a_1(p)$ and $A^1_{jk}(p)$ are, respectively, the determinant and the elements of the adjoint matrix for $a_1(p) = pI + a^1$. From the transforms (2.5) it is easy to determine the elements of the matrix $\beta^1(t)$.

Region II. The equation for X(t) is of the form

$$[DI + a^0] X(t) = f(t) \quad (t_0 < t \leqslant t_0 + \alpha_n). \tag{2.6}$$

Solving Equation (2.6), we obtain the following expression:

$$X(t) = \beta^0(t - t_0)\beta^1(t_0) X[n] + E_0[n] h(t - t_0). \tag{2.7}$$

The matrix h(t) is of the following structure:

$$h(t) = \left\| \begin{matrix} h_1(t) \\ h_2(t) \\ \ldots \\ \ldots \\ h_r(t) \end{matrix} \right\|. \tag{2.8}$$

The operational transforms of the elements of the matrices $\beta^0(t)$ and h(t) are obtained from the following formulas:

$$L[\beta^0_{jk}(t)] = \frac{A^0_{jk}(p)}{\Delta a_0(p)}, \quad L[h_j(t)] = \frac{A^0_{j1}(p)}{p\Delta a_0(p)}. \tag{2.9}$$

The operators $\Delta a_0(p)$ and $A^0_{jk}(p)$ are respectively the determinant and the elements of the adjoint matrix for $a_0(p) = pI + a^0$.

Region III. The equation for this region is of the form:

$$[DI + a^1] X(t) = 0 \quad (t_0 + \alpha_n < t \leqslant T), \tag{2.10}$$

i.e., the same form as (2.3) for the Region I and differs only in the initial conditions.

The solution of Equation (2.10) leads to the following expression:

$$X(t) = \beta^1(t - t_0 - \alpha_n)\beta^0(\alpha_n)\beta^1(t_0) X[n] + E_0[n]\beta^1(t - t_0 - \alpha_n) h(\alpha_n). \tag{2.11}$$

It is easy to see that if we put t = T in Equation (2.11) and if we use the notation

$$X[n+1] = X(T), \quad Q[n] = \beta^1(T - t_0 - \alpha_n)\beta^0(\alpha_n)\beta^1(t_0), \tag{2.12}$$

$$\eta[n] = E_0[n]\beta^1(T - t_0 - \alpha_n) h(\alpha_n),$$

then Equation (2.11) is transformed into an equation of the form

$$X[n+1] - Q[n] X[n] = \eta[n] \tag{2.13}$$

or in expanded form

$$x_j[n+1] - \sum_{k=1}^{r} Q_{jk}[n]\, x_k[n] = \eta_j[n] \quad (j = 1, 2, \ldots, r). \tag{2.14}$$

The quantities X[n], Q[n] and η[n] are stepped matrix functions. The independent variable n assumes only integral values 0, 1, 2, etc. To distinguish them from the ordinary functions, we shall place the independent variable n for the stepped functions in square brackets.*

The quantity Q(n) is a square matrix

$$Q[n] = \| Q_{jk}[n] \| \quad (j, k = 1, 2, \ldots, r).$$

According to (2.12), the elements of this matrix are found from the formulas

$$Q_{jk}[n] = \sum_{\nu=1}^{r} \sum_{\xi=1}^{r} \beta^1_{j\nu}(T - t_0 - \alpha_n)\, \beta^0_{\nu\xi}(\alpha_n)\, \beta^1_{\xi k}(t_0). \tag{2.15}$$

The stepped function η[n] is a column matrix whose elements are given by

$$\eta_j[n] = E_0[n] \sum_{k=1}^{r} \beta^1_{jk}(T - t_0 - \alpha_n)\, h_k(\alpha_n). \tag{2.16}$$

If the duration of the pulses is constant, Equation (2.13) becomes an equation with constant coefficients

$$X[n+1] - QX[n] = \eta[n],$$

where Q is a matrix independent of n.

In other words, if the pulse duration is constant, Equations (1.1) with variable coefficients

$$a_{jk}(t) = a^0_{jk}\, \psi_0(t) + a^1_{jk}\, \psi_1(t)$$

become equations with constant coefficients

$$x_j[n+1] - \sum_{k=1}^{r} Q_{jk}\, x_k[n] = \eta_j[n]. \tag{2.17}$$

The form of the stepped function η[n] depends on how the height E_0[n] and the duration α_n of the pulses vary with changing n. Consequently, if the function E_0[n] and $\alpha_n = \alpha$[n] are known, this determines also the stepped function η[n] in accordance with the corresponding formula in (2.12).

Solving Equation (2.13) determines the stepped function X[n], which characterizes the variation of the unknown quantity X(t) at discrete instants of time 0, T, 2T, etc. In the intervals between these discrete values of time, the variation of X(t) for the corresponding region is determined by the Expression (2.4), (2.7) and (2.11), provided one substitutes in them the values of the stepped function X[n], obtained by solving (2.13). Thus, knowledge of the stepped function X[n] and of the solutions of (2.4), (2.7) and (2.11) gives a complete representation of the character of the transient and steady-state processes produced in a system describable by Equations (1.1) in response to pulse signals.

For practical use, it becomes more convenient to rewrite Solutions (2.4), (2.7) and (2.11) in the following form:

*The definition of the stepped function is given in Reference [3], pages 9-14.

region I

$$X(t) = \beta^1(t - nT)\, X[n] \quad (nT < t \leqslant nT + t_0); \tag{2.18}$$

region II

$$X(t) = \beta^0(t - t_0 - nT)\, \beta^1(t_0)\, X[n] + E_0[n]\, h(t - t_0 - nT), \quad (nT + t_0 < t \leqslant nT + t_0 + \alpha_n); \tag{2.19}$$

region III

$$X(t) = \beta^1(t - t_0 - \alpha_n - nT)\, \beta^0(\alpha_n)\, \beta^1(t_0)\, X[n] + E_0[n]\, \beta^1(t - t_0 - \alpha_n - nT)\, h(\alpha_n) \quad (nT + t_0 + \alpha_n < t \leqslant (n+1)T). \tag{2.20}$$

3. Another Form of the Expression for the Transient and Steady-State Processes in Pulsed Systems

Solutions (2.18), (2.19) and (2.20) can be obtained in another form. For this purpose let us consider the matrix Equations (2.3), (2.6) and (2.10) as ordinary equations, in which the operator matrix ID is, so to speak, a simple operator D, and the matrices a^0 and a^1 are numbers. Let us find, in this new form, the solutions of the above-mentioned equations, and, by then changing over from the variable t to the variable $t - nT$, obtain for the corresponding regions the following expressions:

region I

$$X(t) = e^{-a^1(t-nT)}\, X[n] \quad (nT < t \leqslant nT + t_0); \tag{3.1}$$

region II

$$X(t) = e^{-a^0(t-t_0-nT)}\, e^{-a^1 t_0}\, X[n] + E_0[n]\, h(t - t_0 - nT) \quad (nT + t_0 < t \leqslant nT + t_0 + \alpha_n); \tag{3.2}$$

region III

$$X(t) = e^{-a^1(t-t_0-\alpha_n-nT)}\, e^{-a^0\alpha_n}\, e^{-a^1 t_0}\, X[n] + E_0[n]\, e^{-a^1(t-t_0-\alpha_n-nT)}\, h(\alpha_n) \quad (nT + t_0 + \alpha_n < t \leqslant (n+1)T). \tag{3.3}$$

Here

$$h(t) = \int_0^t e^{-a^0(t-\tau)}\, F(\tau)\, d\tau, \qquad F(t) = \begin{Vmatrix} H(t) \\ 0 \\ \cdots \\ \cdots \\ 0 \end{Vmatrix}.^{*} \tag{3.4}$$

The expressions for Q[n] and $\eta[n]$ in Equations (2.13) are written in the form

$$Q[n] = e^{-a^1(T-t_0-\alpha_n)}\, e^{-a^0\alpha_n}\, e^{-a^1 t_0}, \qquad \eta[n] = E_0[n]\, e^{-a^1(T-t_0-\alpha_n)}\, h(\alpha_n). \tag{3.5}$$

*Solutions (3.1), (3.2) and (3.3) can be obtained by a method given in Reference [5], pages 99-105.

Comparing (3.1) and (3.2) with (2.18) and (2.19) respectively, we get

$$e^{-a^0 t} = \beta^0(t) = \|\beta^0_{jk}(t)\|, \quad e^{-a^1 t} = \beta^1(t) = \|\beta^1_{jk}(t)\|. \tag{3.6}$$

In some cases it is more convenient to use another form of expressions for these matrices. In particular, they can be represented in the form of series*

$$\begin{aligned} e^{-a^0 t} &= I - \frac{a^0}{1!}t + \frac{(a^0)^2}{2!}t^2 - \ldots, \\ e^{-a^1 t} &= I - \frac{a^1}{1!}t + \frac{(a^1)^2}{2!}t^2 - \ldots \end{aligned} \tag{3.7}$$

This applies primarily to those cases when it is necessary to determine the values of the matrices on the initial portion of the time axes, i.e., when the terms containing t^2, t^3, . . ., etc. can be neglected as being of second and higher orders.

To determine the matrices $e^{-a^0 t}$ and $e^{-a^1 t}$ it is possible to use the Lagrange-Sylvester interpolation polynomial.

It is known,** that if the eigenvalues of the matrix a^0 are different and have values $\lambda^0_1, \lambda^0_2, \ldots, \lambda^0_r$, then a function of the matrix $f(a^0) = e^{-a^0 t}$ can be represented with the aid of the Lagrange-Sylvester interpolation polynomial in the following form

$$f(a^0) = e^{-a^0 t} = \sum_{k=1}^{r} \frac{(a^0 - \lambda^0_1 I)\ldots(a^0 - \lambda^0_{k-1} I)(a^0 - \lambda^0_{k+1} I)\ldots(a^0 - \lambda^0_r I)}{(\lambda^0_k - \lambda^0_1)\ldots(\lambda^0_k - \lambda^0_{k-1})(\lambda^0_k - \lambda^0_{k+1})\ldots(\lambda^0_k - \lambda^0_r)} f(\lambda^0_k). \tag{3.8}$$

The functions $f(a^1) = e^{-a^1 t}$ can be analogously represented.

In applications we can represent the matrices $e^{-a^0 t}$ and $e^{-a^1 t}$ by the form that is more suitable for solving the particular problem. The above procedure for the analysis of the processes is best combined with the structural transformations of the system under investigation, by which a simplification of the matrices $e^{-a^0 t}$ and $e^{-a^1 t}$ is attained. This will be illustrated below with an example.

Let us use the notation

$$e^{-c_n T} = e^{-a^1(T - l_* - \alpha_n)} e^{-a^* \alpha_n} e^{-a^1 l_*}. \tag{3.9}$$

Using these new symbols, Equation (2.13) can be rewritten as

$$X[n+1] - e^{-c_n T} X[n] = \eta[n]. \tag{3.10}$$

From this equation we get

$$X[n] = \left\{\prod_{\nu=0}^{n-1} e^{-c_{n-\nu-1} T}\right\} X[0] + \sum_{k=0}^{n-1} \left\{\prod_{\nu=1}^{n-k-1} e^{-c_{n-\nu} T}\right\} \eta[k], \tag{3.11}$$

where X[0] are the initial conditions for n = 0.

Expression (3.11) is readily determined by finding X[1], X[2], . . . , X[n] in sequence. Substituting (3.11) into (3.10), it is easy to verify that X[n], expressed in terms of Equation (3.11), satisfies Equation (3.10).

If the matrices c_n commute, i.e., if

---

*See Reference [1], pages 85-89.

**See Reference [5], pages 87-89.

$$c_n c_{n+1} = c_{n+1} c_n \quad (n = 0, 1, 2, \ldots, \infty),$$

then the expression for X[n] can be rewritten in a simpler form:

$$X[n] = e^{-T\sum_{\nu=0}^{n-1} c_{n-\nu-1}} X[0] + \sum_{k=0}^{n-1} e^{-T\sum_{\nu=1}^{n-k-1} c_{n-\nu}} \eta[k]. \tag{3.12}$$

And, finally, if c_n is independent of n, i.e.,

$$c_n = c,$$

then the equation for X[n] assumes the form

$$X[n] = e^{-cTn} X[0] + \sum_{k=0}^{n-1} e^{-cT(n-k-1)} \eta[k]. \tag{3.13}$$

To find the components $x_j[n]$ it is enough to represent (3.13) in expanded form and carry out the summation.

4. One Particular Case of Operation of a Pulse System

Let us assume that the amplitudes and the durations of the pulses are constant, i.e.,

$$E_0[n] = E, \quad \alpha_n = \alpha. \tag{4.1}$$

and in addition, that the elements of matrices a^0 and a^1 satisfy the conditions

$$|a^0_{jk}\alpha| \ll 1, \quad |a^1_{jk} T| \ll 1. \tag{4.2}$$

The symbol | | denotes here the absolute value of the product of the corresponding element by the duration of the pulse α and the repetition period T. When Inequalities (4.2) are satisfied, the matrices $e^{-a^0\alpha}$, $e^{-a^1 t_0}$, and $e^{-a^1(T-t_0-\alpha)}$ can be represented by the approximate expressions

$$\begin{aligned} e^{-a^0\alpha} &\approx I - a^0\alpha, \\ e^{-a^1 t_0} &\approx I - a^1 t_0, \\ e^{-a^1(T-t_0-\alpha)} &\approx I - a^1(T - t_0 - \alpha). \end{aligned} \tag{4.3}$$

Consequently

$$e^{-a^1(T-t_0-\alpha)} e^{-a^0\alpha} e^{-a^1 t_0} \approx e^{-cT}, \tag{4.4}$$

where

$$c = \frac{a^0\alpha + a^1(T-\alpha)}{T}. \tag{4.5}$$

Here the absolute values of the matrix elements c satisfy the inequalities

$$|c_{jk} T| \ll 1, \tag{4.6}$$

as follows from (4.2) and (4.5).

The equation for the stepped function X[n] is written in the form

$$X[n+1] - e^{-cT} X[n] = Eh(\alpha). \tag{4.7}$$

Let us assume that the characteristic equation

$$\Delta(pI + c) = 0$$

has simple roots, which will be denoted by $\lambda'_1, \lambda'_2, \ldots, \lambda'_r$. Here the symbol Δ denotes the determinant of the matrix pI + c. In this case

$$e^{-ct} = \| \beta_{jk}(t) \|, \quad \beta_{jk}(t) \sum_{\nu=1}^{r} b_{jk}^{\nu} e^{-\lambda_\nu t}, \quad \lambda_\nu = -\lambda'_{\nu}. \tag{4.8}$$

The operational transforms of the matrix elements $\| \beta_{jk}(t) \|$ are determined from the equations

$$L[\beta_{jk}(t)] = \frac{c^*_{jk}(P)}{\Delta(pI + c)},$$

where $c^*_{jk}(P)$ and $\Delta(pI + c)$ are, respectively, the elements of the adjoint matrix and the determinant, written for the matrix pI + c. For the case of simple roots of the characteristic equation, the coefficients b^{ν}_{jk} are readily determined by representing the operator expression $\frac{c^*_{jk}(P)}{\Delta(pI + c)}$ in the form of a sum of elementary fractions. Changing then from the transforms to the originals, we obtain expressions for $\beta_{ik}(t)$ in the form of (4.8). Consequently

$$e^{-cTn} = \left\| \sum_{\nu=1}^{r} b_{jk}^{\nu} e^{-\lambda_\nu Tn} \right\| \quad (j, k = 1, 2, \ldots, r). \tag{4.9}$$

Solving Equation (4.7) and representing the obtained expressions in expanded form, we get*

$$\begin{aligned} x_j[n] &= x_{j0}[n] + x_{je}[n], \\ x_{j0}[n] &= \sum_{\nu=1}^{r} e^{-\lambda_\nu Tn} \sum_{k=1}^{r} b_{jk}^{\nu} x_k[0], \\ x_{je}[n] &= E \sum_{\nu=1}^{r} \frac{1 - e^{\lambda_\nu Tn}}{1 - e^{-\lambda_\nu T}} \sum_{k=1}^{r} b_{jk}^{\nu} h_k(\alpha), \end{aligned} \tag{4.10}$$

Since

$$1 - e^{-\lambda_\nu T} \approx \lambda_\nu T, \quad h(\alpha) = \begin{Vmatrix} \alpha \\ 0 \\ 0 \\ \cdots \\ \cdots \\ 0 \end{Vmatrix},$$

the expression for $x_{je}[n]$ can be rewritten as:

$$x_{je}[n] = \frac{E\alpha}{T} \sum_{\nu=1}^{r} b_{j1}^{\nu} \frac{1 - e^{-\lambda_\nu Tn}}{\lambda_\nu}. \tag{4.11}$$

The stepped functions $x_j[n]$ for this case can be obtained from the continuous functions $x'_j(t)$, which satisfy

*To find Solutions (4.10) we made use of Equations (3.13).

the differential equation

$$[DI + c]\, X'(l) = \frac{Eh(\alpha)}{T},$$
$$X'(0) = X[0] \text{ for } t = 0, \tag{4.12}$$

using the formula

$$X[n] = \{X'(l)\}_{l=nT}. \tag{4.13}$$

Solving Equation (4.12) and forming the stepped function X[n], we obtain expressions for the components $x_{j0}[n]$ and $x_{jl}[n]$, coinciding with Formulas (4.10).

For this case the unknown functions $x_j(t)$ can be represented as

$$x_j(l) = x'_j(l) + \Delta x_j(l). \tag{4.14}$$

At the discrete points $t_n = nT$ ($n = 0, 1, 2, \ldots, \infty$) the following equations hold:

$$x_j(t_n) = x'_j(t_n), \quad \Delta x_j(t_n) = 0. \tag{4.15}$$

In the interval between these points, if Inequalities (4.2) are satisfied, the differences

$$\Delta x_j(l) = x_j(t) - x'_j(t) \tag{4.16}$$

assume small values, close to zero, which diminish with the degree to which Inequalities (4.2) are satisfied. Consequently, one can write

$$x_j(l) \approx x'_j(l). \tag{4.17}$$

This means that the processes in a pulse system subject to Conditions (4.2) reduce to continuous processes in a system with constant parameters. In case of necessity it is possible to estimate the differences (4.16) at the corresponding points, substituting in them the values $x_j(t)$ from Formulas (2.18), (2.19) and (2.20).

If the variable coefficients a(t) of the matrix are located only on the principal diagonal, i.e.,

$$c_{jj} = \frac{a^0_{jj}\alpha + a^1_{jj}(T - \alpha)}{T}, \tag{4.18}$$

then one can consider instead of a^0_{jj} and a^1_{jj} the time constants

$$\tau^0_j = \frac{1}{a^0_{jj}}, \quad \tau^1_j = \frac{1}{a^1_{jj}}. \tag{4.19}$$

The changeover to a system with constant parameters reduces,in this case, to the calculation of the equivalent time constant for the pulse elements, using the formula

$$\tau_e = \frac{1}{c_{jj}} = \frac{T}{\frac{\alpha}{\tau^0_j} + \frac{T - \alpha}{\tau^1_j}}. \tag{4.20}$$

In Reference [4] the initial system with pulse elements is replaced by a continuous system, in which the time constants are calculated from a formula similar to (4.20). Such a substitution is permissible if the system as a whole satisfies the conditions mentioned at the beginning of this section. With this, the input quantities should be recalculated in accordance with the right half of Equation (4.12).

5. Example of Pulse System. Passage of Amplitude Modulated Pulses Through a Detector of Pulse Envelopes and Through a Tuned Amplifier

The procedure considered above for determining the transients and steady-state processes is applicable to many problems in pulse techniques. We shall consider here one of the cases of the passage of pulse signals through a pulse-envelope detector and a tuned amplifier. The diagram of this set-up is shown in Figure 3. Such a transformation of pulse signals takes place, in particular, in radar equipment in the shaping of error signals of an automatic direction tracking system.

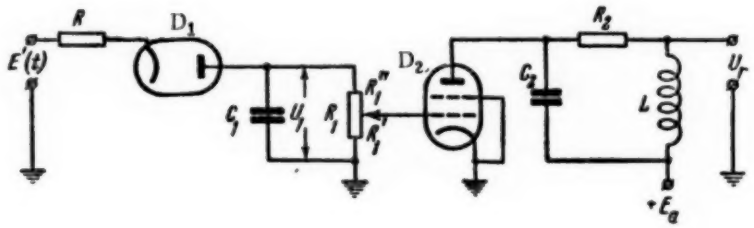

Fig. 3.

The detector and amplifier equations are of the form

$$[\tau(t)D+1]U_1 = E'(t),$$
$$gDU_1 + (a_0'D^2 + a_1'D + a_1')U_2 = 0. \tag{5.1}$$

The sequence of pulses at the input of the detector is given by the expression (Figure 4):

$$E'(t) = -E_m\sum_{k=0}^{\infty}(1 + m\sin\beta k)[H(t-kT) - H(t-\alpha-kT)],$$
$$\beta = \Omega T, \quad m<1. \tag{5.2}$$

Here α and T are constant quantities, denoting respectively the duration and repetition period of the pulses. The quantity E_m represents the mean level relative to which the pulse amplitude fluctuates. The quantity m characterizes the depth of modulation of the pulses by amplitude.

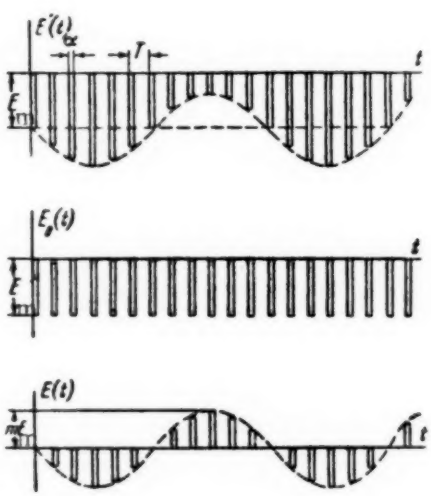

Fig. 4.

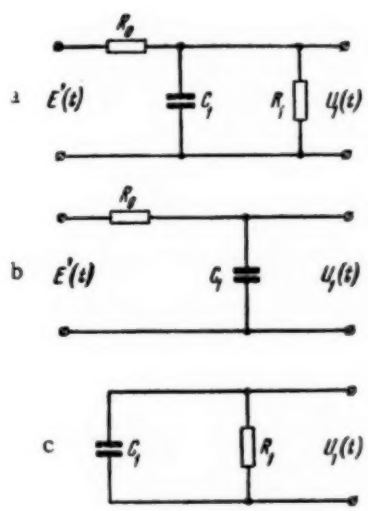

Fig. 5.

The function $\tau(t)$ expresses the variation of the time constant of the detector in response to the pulses at its input. The expression for this time constant is

$$\tau(t) = \tau_0\psi_0(t) + \tau_1\psi_1(t),$$
$$\psi_0(t) = \sum_{k=0}^{\infty} [H(t - kT) - H(t - \alpha - kT)], \tag{5.3}$$
$$\psi_1(t) = H(t) - \psi_0(t).$$

The time constant τ_0 characterizes the process in the detector in response to a pulse signal at its input. The corresponding equivalent circuit of the detector is shown in Figures 5a and b. The value of τ_0 is determined from the formula

$$\tau_0 = \frac{R_1}{R_0 + R_1} C_1 R_0, \quad R_0 = R + R_i, \tag{5.4}$$

where R_i is the internal resistance of the diode D_1 (Figure 3).

Usually the resistances R_0 and R_1 satisfy the condition

$$R_1 \gg R_0. \tag{5.5}$$

Consequently, in this case, (5.4) assumes a simpler form

$$\tau_0 \approx C_1 R_0. \tag{5.6}$$

The time constant

$$\tau_1 = C_1 R_1 \tag{5.7}$$

characterizes processes in the detector in the intervals between the pulses. The corresponding equivalent circuit of the detector is shown in Figure 5c.

The remaining coefficients in Equations (5.1) are determined from

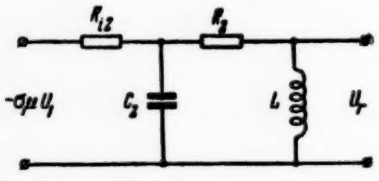

Fig. 6.

$$a_0' = C_2 L, \; a_1' = C_2 R_2 + \frac{L}{R_{i2}},$$
$$a_2' = 1 + \frac{R_2}{R_{i2}}, \; g = \sigma S L, \; \sigma = \frac{R_1'}{R_1}. \tag{5.8}$$

Here R_{i2} is the internal resistance of the tube and S is the transconductance of the tube at the operating point.

Figure 6 shows the equivalent circuit of the amplifier, with which it is easy to derive Equations (5.8).

The input pulse function E'(t) consists of two components (Figure 4)

$$E'(t) = E_0(t) + E(t),$$

where $E_0(t)$ is a sequence of pulses of constant amplitude, E'(t) a sequence of pulses of variable amplitude, with a sinusoidal amplitude variation.

In the subsequent analysis we shall be interested in the transmission of pulses of variable height. For this case, Equations (5.1) are rewritten as

$$[D + \lambda_1(t)] U_1 = \lambda_1(t) E(t),$$
$$g_0 D U_1 + (D^2 + a_1 D + a_2) U_r = 0. \tag{5.9}$$

Here

$$E(t) = -mE_{in}\sum_{k=0}^{\infty} \sin \beta k\,[H(t-kT) - H(t-\alpha-kT)], \qquad \beta = \Omega T, \tag{5.10}$$

$$\lambda_1(t) = \lambda_{10}\psi_0(t) + \lambda_{11}\psi_1(t),\ \lambda_{10} = \frac{1}{\tau_0},\ \lambda_{11} = \frac{1}{\tau_1}, \tag{5.11}$$

$$g_0 = \frac{g}{a_0'},\ a_k = \frac{a_k'}{a_0'}\ (k = 1, 2). \tag{5.12}$$

The piecewise continuous function

$$\lambda_1(t) = \frac{1}{\tau(t)} = \frac{1}{\tau_0\psi_0(t) + \tau_1\psi_1(t)}$$

assumes values $1/\tau_0$ and $1/\tau_1$, respectively, in the regions coinciding with the pulses $\psi_0(t)$ and $\psi_1(t)$. Consequently, this function can be written in the form (5.11).

Equations (5.9) correspond to a structural scheme shown in Figure 7, which represents a series connection of two four-terminal networks with transfer functions

$$K_1(D, t) = \frac{\lambda_1(t)}{D + \lambda_1(t)},\ K_2(D) = \frac{-g_0 D}{D^2 + a_1 D + a_2}. \tag{5.13}$$

The first four-terminal network has variable parameters, the second constant ones.

Let us transform Equations (5.9) to another form, more convenient for the solution of our problem. For this purpose we employ the possibility of representing a four-terminal network with constant parameters by means of an equivalent system in the form of a series of parallel connections of elementary four-terminal networks, describable by first-order equations. The simplest derivations for the problem occur when the four-terminal network is replaced by a system consisting of a parallel connection of elementary four-terminal networks. Let us find an equivalent system of this type. For this purpose let us represent the transfer function $K_2(D)$ in the form

$$K_2(D) = \frac{a_{21}}{D + \lambda_2} + \frac{a_{31}}{D + \lambda_3},\ a_{21} = \frac{g_0\lambda_2}{\lambda_3 - \lambda_2},\ a_{31} = \frac{g_0\lambda_3}{\lambda_2 - \lambda_3}. \tag{5.14}$$

The quantities λ_2 and λ_3 are found from the formulas

$$\lambda_{2,3} = \frac{a_1}{2} \pm \sqrt{\frac{a_1^2}{4} - a_2}. \tag{5.15}$$

The second equation of (5.9) can be written in the operator-symbolic form as*

$$U_r = \frac{-g_0 D U_1}{D^2 + a_1 D + a_2} = K_2(D)U_1$$

or, taking (5.14) into account:

$$U_r = \left[\frac{a_{21}}{D + \lambda_2} + \frac{a_{31}}{D + \lambda_3}\right]U_1. \tag{5.16}$$

*More detailed information on the operator-symbolic method and transformations are given in [6], pages 28-35 and in [7], pages 114-128.

Let us introduce a new notation

$$X_1 = U_1,\ X_2 = \frac{a_{21}}{D+\lambda_2}U_1,\ X_3 = \frac{a_{31}}{D+\lambda_3}U_1. \tag{5.17}$$

In the new notation, the equations of (5.9) become

$$\begin{aligned} &[D+\lambda_1(t)]\,X_1 + 0 + 0 = \lambda_1(t)\,E(t),\\ &-a_{21}X_1 + (D+\lambda_2)\,X_2 + 0 = 0,\\ &-a_{31}X_1 + 0 + (D+\lambda_3)\,X_3 = 0. \end{aligned} \tag{5.18}$$

The output signal of the amplifier, according to (5.16) and (5.17) is found from the equation

$$U_r = X_2 + X_3. \tag{5.19}$$

Equations (5.18) and (5.19) correspond to the structural scheme shown in Figure 8. The operator-symbolic transformations serve us as a basis for the changeover from a four-terminal network with transfer function $K_2(D)$ into an equivalent system, consisting of a parallel connection of elementary four-terminal networks.

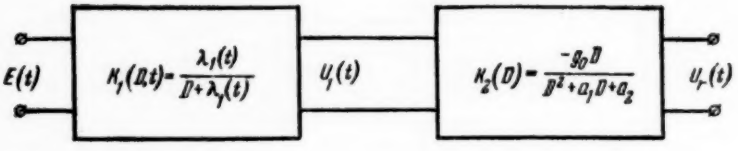

Fig. 7.

Let us call attention to the following fact. In the case of radio circuits it is a simple problem to find first equations in the form (5.9), i.e., to reduce the processes in the system to processes in four-terminal networks (Figure 7), after which it is already possible to change over to a certain equivalent system, describable by first-order equations. However, in this case, it is necessary to be assured that the initial conditions for the equivalent system have no discontinuities at the points where the parameters are discontinuous. This can be verified by obtaining formulas for the initial conditions to the right and to the left of a discontinuity point. In our example this is readily done.

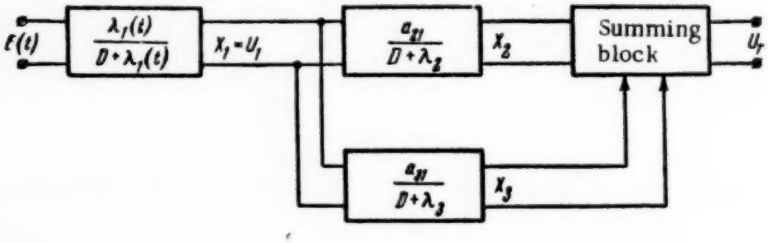

Fig. 8.

Let us agree to denote by regions 0 and 1, respectively, the time intervals, coinciding with the pulse functions $\psi_0(t)$ and $\psi_1(t)$. Let us identify zero time with one of the points separating the region 0 from region 1. With this, let the region 0 be to the left of the origin (shown crosshatched in Figure 9), and region 1 to the right. When changing over from the circuit of Figure 7, to the equivalent circuit of Figure 8, the initial conditions at the point $t = 0$ to the left and to the right are calculated using similar formulas of the type

$$X_1(0) = -U_1(0),$$

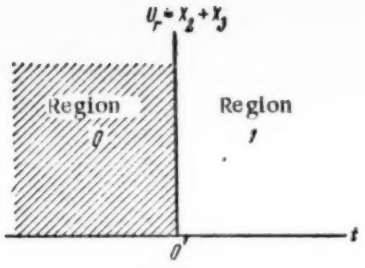

Fig. 9.

$$X_2(0) = \frac{\lambda_3 U_r(0) + \frac{dU_r(0)}{dt}}{\lambda_3 - \lambda_2},$$

$$X_3(0) = \frac{\lambda_2 U_r(0) + \frac{dU_r(0)}{dt}}{\lambda_2 - \lambda_3},$$

i.e., the initial quantities $X_1(0)$, $X_2(0)$ and $X_3(0)$ of the equivalent circuit have no discontinuities at the point of the jump. This could have been predicted beforehand, since the transformation considered above was applied to a four-terminal network with constant parameters. If λ_2 and λ_3 are complex, the initial conditions for the equivalent circuit in Figure 8, according to the formulas obtained, will be described also by means of complex quantities.

6. Transient and Steady-State Processes in the Pulse Envelope Detector and Tuned Amplifier

Expressed in matrix form, Equations (5.18) become

$$[DI + a(t)]X = f(t). \tag{6.1}$$

Here

$$a(t) = \psi_0(t)\, a^0 + \psi_1(t)\, a^1,$$

$$a^k = \begin{Vmatrix} \lambda_{1k}, & 0, & 0 \\ -a_{21}, & \lambda_2, & 0 \\ -a_{31}, & 0, & \lambda_3 \end{Vmatrix} \quad (k = 0, 1), \tag{6.2}$$

$$X = \begin{Vmatrix} X_1 \\ X_2 \\ X_3 \end{Vmatrix}, \quad f(t) = \begin{Vmatrix} \lambda_1(t) E(t) \\ 0 \\ 0 \end{Vmatrix}. \tag{6.3}$$

To determine the transients and steady-state processes in this system we can employ Expressions (3.2), (3.3), and the relation

$$X[n+1] - QX[n] = \eta[n], \tag{6.4}$$

by setting

$$t_0 = 0, \quad \alpha_n = \alpha,$$

$$E_0[n] = -\frac{mE_c}{\tau_0} \sin \beta n, \tag{6.5}$$

$$Q = e^{-a^1(T-\alpha)} e^{-a^0\alpha},$$

$$\eta[n] = -\frac{mE_c}{\tau_0} \sin \beta n e^{-a_1(T-\alpha)} h(\alpha).$$

Let us determine the matrices $e^{-a^0 t}$ and $e^{-a^1 t}$

$$e^{-a^k t} = \begin{Vmatrix} e^{-\lambda_{1k} t}, & 0, & 0 \\ \beta_{21}^k(t), & e^{-\lambda_2 t}, & 0 \\ \beta_{31}^k(t), & 0, & e^{-\lambda_3 t} \end{Vmatrix} \quad (k = 0, 1), \tag{6.6}$$

where

$$\beta_{j1}^{k}(t) = b_{j1}^{k1}e^{-\lambda_{1k}t} + b_{j1}^{kj}e^{-\lambda_j t}, \tag{6.7}$$

$$b_{j1}^{k1} = -b_{j1}^{kj} = \frac{a_{j1}}{\lambda_j - \lambda_{1k}} \quad (k = 0, 1;\ j = 2,3).$$

The matrix $h(\alpha)$ is of the form

$$h(\alpha) = \left\| \begin{matrix} h_1(\alpha) \\ h_2(\alpha) \\ h_3(\alpha) \end{matrix} \right\|, \tag{6.8}$$

where

$$h_1(\alpha) = \tau_0 [1 - e^{-\lambda_{10}\alpha}]. \tag{6.9}$$

The quantities $h_2(\alpha)$ and $h_3(\alpha)$ are small compared with $h_1(\alpha)$. Therefore, to estimate their values it is more convenient to represent them in the form of a series. Let us find

$$h_j(\alpha) = a_{j1}\left[\frac{\alpha^2}{2} - (\lambda_{10} + \lambda_j)\frac{\alpha^3}{3!} + \ldots\right] \quad (j = 2,3). \tag{6.10}$$

From (6.6) and (6.7) we have, in the general case,

$$\beta_{jk}^{0}(\alpha) = \sum_{\xi=1}^{j} b_{jk}^{0\xi}e^{-\lambda_{\xi_0}\alpha},$$

$$\beta_{jk}^{1}(T-\alpha) = \sum_{\nu=1}^{j} b_{jk}^{1\nu}e^{-\lambda_{\nu 1}(T-\alpha)},$$

$$\lambda_{20} = \lambda_{21} = \lambda_2, \quad \lambda_{30} = \lambda_{31} = \lambda_3.$$

Consequently

$$e^{-cT} = e^{-a^1(T-\alpha)}e^{-a^0\alpha} = \left\| \sum_{\nu=1}^{j}\sum_{\xi=1}^{j} c_{jk}^{\nu\xi}e^{-M_{\nu\xi}T} \right\|, \tag{6.11}$$

where

$$c_{jk}^{\nu\xi} = \sum_{m=1}^{j} b_{jm}^{1\nu}b_{mk}^{0\xi}, \quad M_{\nu\xi} = \frac{\lambda_{\nu 1}(T-\alpha) + \lambda_{\xi 0}\alpha}{T}. \tag{6.12}$$

The matrix e^{-cT} is represented by the expression

$$e^{-cT} = \left\| \begin{matrix} e^{-M_{11}T}, & 0 & 0 \\ c_{21}(T), & e^{-M_{22}T} & 0 \\ c_{31}(T), & 0 & e^{-M_{33}T} \end{matrix} \right\|. \tag{6.13}$$

Here

$$c_{j1}(T) = c_{j1}^{11} e^{-M_{11}T} + c_{j1}^{j1} e^{-M_{j1}T} + c_{j1}^{jj} e^{-M_{jj}T},$$

$$M_{11} = \frac{\lambda_{11}(T-\alpha) + \lambda_{10}\alpha}{T},$$

$$M_{j1} = \frac{\lambda_j (T-\alpha) + \lambda_{10}\alpha}{T} \quad (j = 2, 3), \tag{6.14}$$

$$M_{22} = \lambda_2, \quad M_{33} = \lambda_3.$$

The coefficients $c_{jk}^{\nu\xi}$ are determined from the formulas

$$c_{j1}^{11} = b_{j1}^{11}, \quad c_{j1}^{j1} = b_{j1}^{01} + b_{j1}^{1j}, \quad c_{j1}^{jj} = b_{j1}^{0j}. \tag{6.15}$$

Let us denote

$$G = e^{-a^1(T-\alpha)} h(\alpha) = \begin{Vmatrix} G_1 \\ G_2 \\ G_3 \end{Vmatrix}. \tag{6.16}$$

Using Equation (3.13) we obtain a solution to Equation (6.4) and represent it in expanded form

$$X_j[n] = X_{j0}[n] + X_{je}[n],$$

$$X_{j0}[n] = \sum_{\nu=1}^{j} \sum_{\xi=1}^{j} \left\{ \sum_{k=1}^{j} c_{jk}^{\nu\xi} X_k[0] \right\} e^{-M_{\nu\xi}Tn},$$

$$X_{je}[n] = -\frac{mE_c}{\tau_0} \sum_{\nu=1}^{j} \sum_{\xi=1}^{j} \left\{ \sum_{k=1}^{j} c_{jk}^{\nu\xi} G_k \right\} \times \tag{6.17}$$

$$\times [A_{\nu\xi} \sin \beta n + B_{\nu\xi} \cos \beta n + C_{\nu\xi} e^{-M_{\nu\xi}Tn}].$$

The coefficients are determined from the formulas

$$A_{\nu\xi} = \frac{\cos\beta - e^{-M_{\nu\xi}T}}{N_{\nu\xi}}, \quad B_{\nu\xi} = -\frac{\sin\beta}{N_{\nu\xi}}, \tag{6.18}$$

$$C_{\nu\xi} = \frac{\sin\beta}{N_{\nu\xi}}, \quad N_{\nu\xi} = 1 - 2e^{-M_{\nu\xi}T}\cos\beta + e^{-2M_{\nu\xi}T}.$$

Formulas (6.17) correspond to the general case of operation of a detector and amplifier. It can be used to investigate various modes of operation of this system.* In engineering applications, for specific operating conditions of the apparatus, these formulas can be simplified considerably. The principal purpose of the detector and amplifier in this system is to convert the discontinuous pulse signals into a continuous signal, which would reproduce with the required accuracy the envelope of the pulses. Such transformations will be carried out in the systen only under specified operating modes of the system. Let us restrict ourselves here to only a consideration of one mode, which we will arbitrarily call mode A.

7. Equivalent Circuits of a Pulse Envelope Detector and Amplifier for Mode A

For this mode, the detector and amplifier parameters are chosen in such a way, that the matrices $e^{-a^0\alpha}$ and e^{-a^1T} can be represented by the approximate expressions

$$e^{-a^0\alpha} \approx I - a^0\alpha, \quad e^{-a^1T} \approx I - a^1T. \tag{7.1}$$

*Expressions (6.17) are of interest for those cases when one period of the oscillation of the envelope contains a small number of pulses. Consequently, allowance for the discontinuous character of the processes is of substantial significance in the evaluation of the dynamics of the system.

Let us represent a^0_{jk} and a^1_{jk} in the form

$$a^0_{jk} = \sigma^0_{jk} + i\omega^0_{jk},\ i = \sqrt{-1},\ a^1_{jk} = \sigma^1_{jk} + i\omega^1_{jk}. \tag{7.2}$$

For the real and imaginary parts of the elements a^0_{jk} and a^1_{jk} we have the following inequalities:

$$\begin{aligned} &|\sigma^0_{jk}a| \ll 1, \quad |\sigma^1_{jk}T| \ll 1, \\ &|\omega^0_{jk}\alpha| \ll 1, \quad |\omega^1_{jk}T| \ll 1. \end{aligned} \tag{7.3}$$

*

Inequalities (7.3) serve as a basis for representing the matrices $e^{-a^0\alpha}$ and e^{-a^1T} by approximate Expressions (7.1). If Inequalities (7.3) are satisfied we have

$$G = h(\alpha) = \begin{Vmatrix} \alpha \\ 0 \\ 0 \end{Vmatrix}, \tag{7.4}$$

$$c = \frac{(T-\alpha)a^1 + \alpha a^0}{T}. \tag{7.5}$$

or in expanded form

$$c = \begin{Vmatrix} \lambda_1, & 0, & 0 \\ -a_{21}, & \lambda_2, & 0 \\ -a_{31}, & 0, & \lambda_3 \end{Vmatrix}, \tag{7.6}$$

where

$$\lambda_1 = \frac{(T-\alpha)\lambda_{11} + \alpha\lambda_{10}}{T}. \tag{7.7}$$

Consequently

$$e^{-cT} = \begin{Vmatrix} e^{-\lambda_1 T}, & 0 & 0 \\ \beta_{21}(T), & e^{-\lambda_2 T}, & 0 \\ \beta_{31}(T), & 0, & e^{-\lambda_3 T} \end{Vmatrix}, \tag{7.8}$$

$$\beta_{j1}(T) = b^1_{j1}e^{-\lambda_1 T} + b^j_{j1}e^{-\lambda_j t},$$

$$\sigma^1_{j1} = -b^j_{j1} = \frac{a_{j1}}{\lambda_j - \lambda_1}\ (j = 2, 3). \tag{7.9}$$

Let us assume that the amplifier is tuned to the frequency of the pulse envelope Ω, i.e.,

$$\lambda_{2,3} = d \pm i\Omega,\ i = \sqrt{-1}.$$

According to (7.3), we have

$$\lambda_1 T \ll 1,\ \beta = \Omega T \ll 1,\ dT \ll 1. \tag{7.10}$$

For stable systems λ_1 and $\underline{d}$ are positive.

In accordance with these, the Formulas (6.17) for mode A become

*The sign || denotes the absolute values of the corresponding product.

$$X_j[n] = X_{j0}[n] + X_{je}[n],$$

$$X_{j0}[n] = \sum_{\nu=1}^{j} e^{-\lambda_\nu Tn} \sum_{k=1}^{j} b_{jk}^{\nu} X_k[0], \tag{7.11}$$

$$X_{je}[n] = \frac{\alpha m E_m}{\tau_0 T} \sum_{\nu=1}^{j} b_{j1}^{\nu} \frac{\lambda_\nu \sin \beta n - \Omega \cos \beta n + \Omega e^{-\lambda_\nu Tn}}{\lambda_\nu^2 + \Omega^2}.$$

It is easy to show that the finding of a stepped function X[n] for mode A reduces to determining a continuous function, satisfying the equation

$$[DI + c] X'(t) = -\frac{m\alpha E_m}{\tau_0 T} f'(t), \tag{7.12}$$

where

$$f'(t) = \begin{Vmatrix} \sin \Omega t \\ 0 \\ 0 \end{Vmatrix}.$$

The relation between X[n] and X'(t) is expressed by the simple equality

$$X[n] = [X'(t)]_{t=nT}. \tag{7.13}$$

This can be readily verified by solving Equation (7.12), forming the functions $X_j[n]$ in accordance with Formula (7.13), and comparing the resultant expressions for these functions with Formulas (7.11).

The functions $X_j(t)$ can be represented for this mode by Formulas (4.14). Everything said in Section 4 concerning the differences $\Delta X_j(t)$ holds also for mode A. Therefore, in the approximate analysis of the setup it is possible to write

$$X_j(t) \approx X_j'(t), \quad \Delta X_j(t) = 0. \tag{7.14}$$

On the basis of the above it is easy to determine, for the system shown in Figure 3, an equivalent system with constant parameters, responding to a continuous signal. Putting

$$X_j(t) = X'_j(t),$$

let us represent Equations (7.12) in expanded form:

$$\begin{aligned} (D + \lambda_1) X_1 + 0 + 0 &= -\frac{m\alpha E_m}{\tau_0 T} \sin \Omega t, \\ -a_{21} X_1 + (D + \lambda_2) X_2 + 0 &= 0, \\ -a_{31} X_2 + 0 + (D + \lambda_3) X_3 &= 0. \end{aligned} \tag{7.15}$$

Solving these equations for X_2 and X_3 and bearing in mind that

$$U_r = X_2 + X_3,$$

we obtain*

$$(D + \lambda_1)(D + \lambda_2)(D + \lambda_3) U_r = \frac{gm\alpha E_m}{a_0' \tau_0 T} D \sin \Omega t$$

*See Formulas (5.12), (5.14), (5.16) and (5.17).

or

$$[\tau_d D + 1] U_1 = -\rho \sin \Omega t,$$
$$gDU_1 + (a_0' D^2 + a_1' D + a_2') U_r = 0, \tag{7.16}$$

where

$$\tau_d = \frac{1}{\lambda_1} = \frac{T}{\lambda_{10}\alpha + \lambda_{11}(T - \alpha)},$$
$$\rho = \frac{\tau_d m \alpha E_m}{\tau_0 T} = \frac{\alpha m E_m}{\tau_0 [\lambda_{10}\alpha_0 + \lambda_{11}(T - \alpha)]}. \tag{7.17}$$

Since

$$\tau_0 = \frac{1}{\lambda_{10}}, \quad \tau_1 = \frac{1}{\lambda_{11}},$$

the formula for ρ can also be written in the form

$$\rho = \frac{\alpha}{\left[\alpha + \frac{\tau_0}{\tau_1}(T - \alpha)\right]} m E_m. \tag{7.18}$$

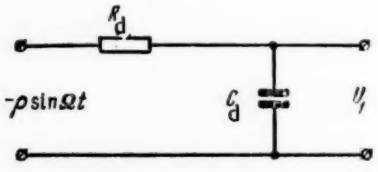

Fig. 10.

The second equation in (7.16) is the amplifier equation.* Figure 10 shows the equivalent circuit of the detector, where

$$\tau_d = C_d R_d.$$

The form of the equivalent circuit of the detector depends on the properties of the amplifier. For a detector operating with more complicated amplification and conversion systems for the detected signal, the equivalent circuit of Figure 10 remains valid, if the matrices $e^{a_0 \alpha}$ and $e^{a_1 T}$, corresponding to the new system, admit of an approximate representation in the form (7.1).

LITERATURE CITED

[1] B.V. Bulgakov, Oscillations (Gostekhizdat, 1954).**

[2] A. I. Lur'e, Operational Calculus (Gostekhizdat, 1951).**

[3] Ia. Z. Tsypkin, Transients and Steady-State Processes in Pulse Circuits (Gosenergoizdat, 1951).**

[4] E.A. Rozenman, Transients in Pulse Systems with Parameters that Vary with the Pulse Frequency. Scientific and Technical Collection of the Scientific Research Institute of the Ministry of Communications Industry No. 13, 1951.

[5] F.R. Gantmakher, Theory of Matrices (Gostekhizdat, 1953).**

[6] A.N. Krylov, Concerning Certain Differential Equations of Mathematical Physics (Izd. AN SSSR, 1933).**

[7] V.I. Smirnov, Course of Higher Mathematics, Volume II (Gostekhizdat, 1956).**

Received March 6, 1957

*See Formula (5.1).

**In Russian.

SYNTHESIS OF PULSE NETWORKS AND SYSTEMS WITH PULSE FEEDBACK

V.P. Perov

(Leningrad)

The optimum characteristics of pulse systems and their realizations are determined. The optimum criterion adopted is the condition that the error have a minimum dispersion for a specified dynamic accuracy and for a specified system transient time. It is assumed that the driving function consists of a noise and of a signal, and that the noise is a stationary random function, while the signal is the sum of a stationary random function and of a regular component.

INTRODUCTION

The schematic representation of a pulse network and of a system with pulse feedback are given in Figures 1 and 2, respectively.

Hereinafter we shall call a pulse network an open pulse system, and a system with pulse feedback will be called closed.

Fig. 1. Schematic representation of pulse circuit (open pulse system): 1) pulse element; 2) continuous part.

By synthesis of a pulse system is understood the task of determining its block diagram and the specific values of the parameters, which are optimized from the point of view of the response criterion adopted.

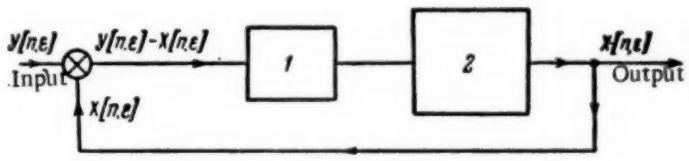

Fig. 2. Schematic reprecentation of system with pulse feedback (closed pulse system): 1) pulse element; 2) continuous part.

The solution of the analogous problem for linear systems of continuous action consists of two stages of investigations, in which one first finds the optimum transfer function of the system, and the second stage consists of finding the circuit corresponding to the optimum transfer function by selecting the links and the corresponding elements.

In the synthesis of a pulse system it is necessary, first of all, to find its optimum transfer or weighting function. However, the characteristics of pulse systems usually have such an abstract form, that in the majority of cases they cannot be used directly to realize a concrete scheme. To construct a concrete scheme it is necessary to change over from the mathematical expression for the pulse system as a whole, to an expression for the transfer function of the continuous portion of the system, so as to be able to determine the corresponding block diagram and the specific parameters of the system. The above features require a special approach to the solution of the problem of synthesis of pulsed systems. Certain results obtained in this direction are treated below. These results were obtained by the author independently of the work in [4, 10], in which analogous problems are touched upon in part.

1. Dynamic and Random Errors of Pulse Systems. Equations for Optimum Weighting Function

Let us assume that a pulse system, whose transient lasts N regulation periods, is under the influence of a quantity $Y[n,\epsilon]$, consisting of a signal $U[n,\epsilon]$ and a noise $p[n,\epsilon]$, where n is an integer, expressing the time in relative units, equal to the period of regulation, and ϵ is a parameter that varies from zero to unity and expresses the relative time in the intervals between the whole regulation periods [1].

Thus,

$$Y[n, \varepsilon] = U[n, \varepsilon] + p[n, \varepsilon]. \tag{1}$$

We shall assume that the noise is a stationary random function of time, and the signal consists of a sum of a stationary random component $u[n,\epsilon]$ and of a regular component $f[n,\epsilon]$:

$$v[n, \varepsilon] = u[n, \varepsilon] + f[n, \varepsilon], \tag{2}$$

where the regularity of the function $f[n,\epsilon]$ lies in the fact that at any time ininterval$(n - N, n)$it can be represented by a polynomial of the r'th degree. Accordingly, the regular component of the signal should satisfy the following equations:

$$f[n-e] = f[n] - e\dot{f}[n] + \frac{e^2}{2}\ddot{f}[n] + \ldots + (-1)^r \frac{e^r}{r!} f^{(r)}[n], \tag{3}$$

$$(0 < e < N),$$

$$f[n, \varepsilon] = f[n] + \varepsilon\dot{f}[n] + \frac{\varepsilon^2}{2}\ddot{f}[n] + \ldots + \frac{\varepsilon^r}{r!} f^{(r)}[n], \tag{4}$$

where $\dot{f}[n]$, $\ddot{f}[n]$, . . . , $f^{(r)}[n]$ are the first, second, . . . , r'th derivatives of the function $f[n,\epsilon] = f(\bar{t})_{\bar{t}=n+\epsilon}$ at the point $\bar{t} = n$.

Let us assume that it is necessary to reproduce a signal $U[n,\epsilon]$ or a quantity $H[n,\epsilon]$ linearly related to the signal:

$$H[n, \varepsilon] = hU[n, \varepsilon] = hu[n, \varepsilon] + hf[n, \varepsilon] = [hu(\bar{t}) + hf(\bar{t})]_{\bar{t}=n+\epsilon}, \tag{5}$$

where h is a linear operator.

Taking (4) into account, the quantity $hf[n,\epsilon]$ can always be represented in the form of a polynomial

$$a_0 + a_1\dot{f}[n] + a_2\ddot{f}[n] + \ldots + a_r f^{(r)}[n], \tag{6}$$

whose coefficients $a_0, a_1, \ldots a_r$ are determined from the equation

$$hf[n] + \varepsilon h\dot{f}[n] + \ldots + \frac{\varepsilon^r}{r!} f^{(r)}[n] = a_0 f[n] + a_1\dot{f}[n] + \ldots + a_r f^{(r)}[n]. \tag{7}$$

Thus, for $h = 1$, we get from (7)

$$a_0 = 1,\ a_1 = \varepsilon,\ \ldots,\ a_r = \frac{\varepsilon^r}{r!}. \tag{8}$$

For $h = d/d\bar{t}$ we get

$$a_0 = 0,\ a_1 = 1,\ a_2 = \varepsilon,\ \ldots,\ a_r = \frac{\varepsilon^{r-1}}{(r-1)!}. \tag{9}$$

For the conditions adopted, the instantaneous error in reproducing $E[n,\epsilon]$, inherent in the system, is determined by the expression

$$E[n,\ \varepsilon] = \sum_{e=0}^{N} Y[n-e]\,K[e,\ \varepsilon] - H[n,\ \varepsilon], \tag{10}$$

where $K[e,\epsilon]$ is the weighting function of the pulsed system, which vanishes at $e < 0$ and $e > N$ when the conditions of the physical realizability of the system and the limitation on the time of its transient are taken into account.

Taking (6), (2) and (1) into account, let us write (10) in the following form

$$E[n,\ \varepsilon] = \left\{\sum_{e=0}^{N} \varphi[n-e]\,K[e,\ \varepsilon] - hu[n,\ \varepsilon]\right\} + \\ + (c_0 f[n] + c_1 \dot{f}[n] + \cdots + c_r f^{(r)}[n]), \tag{11}$$

where $\varphi[n-e] = u[n-e] + p[n-e]$, and $c_0, c_1, \ldots, c_r$ are the coefficients of the dynamic error, determined by the equations

$$c_0 = \mu_0 - a_0,\ c_1 = -\mu_1 - a_1,\ \ldots,\ c_r = \frac{(-1)^r}{r!}\mu_r - a_r, \tag{12}$$

in which $\mu_0, \mu_1, \ldots, \mu_r$ denote the moments of the weighting functions of the zero, first, r'th orders, which can be expressed in terms of the weighting function in the following manner:

$$\mu_0 = \sum_{e=0}^{N} K[e,\ \varepsilon],\ \mu_1 = \sum_{e=0}^{N} eK[e,\ \varepsilon],\ \ldots,\ \mu_r = \sum_{e=0}^{N} e^r K[e,\ \varepsilon]. \tag{13}$$

The terms in the braces of Equation (11) represent the random error $\xi[n,\epsilon]$, and the term in the parentheses the dynamic error $d[n,\epsilon]$.

Thus

$$d[n,\ \varepsilon] = c_0 f[n] + c_1 \dot{f}[n] + \ldots + c_r f^{(r)}[n], \tag{14}$$

$$\xi[n,\ \varepsilon] = \sum_{e=0}^{N} \varphi[n-e]\,K[e,\ \varepsilon] - hu[n,\ \varepsilon]. \tag{15}$$

Squaring Expression (15) and averaging over the set, we obtain the following expression for the mean square (dispersion) $\overline{\xi^2[n,\epsilon]}$ of the random reproduction error

$$\overline{\xi^2[n,\ \varepsilon]} = \overline{\{hu[n,\ \varepsilon]\}^2} - 2\sum_{e=0}^{N} K[e,\ \varepsilon]\,R_{hu}[e,\ \varepsilon] + \\ + \sum_{e=0}^{N} K[e,\ \varepsilon] \sum_{m=0}^{N} K[m,\ \varepsilon]\,R_{\varphi\varphi}[e-m], \tag{16}$$

where $R_{\varphi\varphi}[e-m] = \overline{\varphi[n-e]\varphi[n-m]}$ is the correlation function of the random process $\varphi[n]$ (see, for example, Reference [2]), $R_{hu}[e,\epsilon] = \overline{hu[n,\epsilon]u[n-e]}$ is the mutual correlation function between the random component $\varphi[n-e]$ of the signal and the random component $hu[n,\epsilon]$ of the quantity to be reproduced.

Expression (16) assumes a particularly simple form in the particular case when the random component of the signal is missing ($R_{hu}[e,\epsilon] = 0$, $R_{\varphi\varphi}[n] = R_{pp}[n]$), and the correlation function of the noise $R_{pp}[n]$ satisfies the conditions

$$R_{pp}[0] = c^2, \quad R_{pp}[n] \parallel 0 \quad \text{for} \quad n \neq 0.$$

In this case we obtain instead of (16)

$$\overline{\xi^2[n,\varepsilon]} = c^2 \sum_{e=0}^{N} \{K[e,\varepsilon]\}^2. \tag{16a}$$

Let us proceed to the problem of determining the conditions for the optimum weighting function of the pulse system. By way of an optimum criterion we shall use the known criterion of minimum dispersion of the random reproduction error for specified dynamic-error coefficients [3].

Accordingly, the problem will consist of determining the equations which must be satisfied by the weighting function of the pulsed system, minimizing Expression (16) under the condition that the moments of these functions are specified beforehand by means of Equations (13).

Formally this problem does not differ from that considered in [4], and is a particular case of an analogous problem, solved in [5], where the following condition was obtained for the optimum weighting function $K(\tau)$ of a continuous-action system

$$\begin{gathered}\int_0^T R_{\varphi\varphi}(\tau-\vartheta)K(\vartheta)\,d\vartheta = R_{h\varphi}(\tau) + \gamma_0 + \gamma_1\tau + \ldots + \gamma_r\tau^r \quad (0 \leqslant \tau \leqslant T),\\ K(\tau) = 0 \quad (0 > \tau > T),\\ \mu_i = \int_0^T \tau^i K(\tau)\,d\tau \quad (i = 0, 1, \ldots, r),\end{gathered} \tag{17}$$

where μ_i are the known moments of the weighting function, $R_{\varphi\varphi}(\tau)$ the correlation function of the random component of the signal $R_{h\varphi}(\tau)$ the mutual correlation function of the random components of the signal and of the quantity that is to be reproduced.

Putting in (17)

$$K(\vartheta) = \sum_{m=0}^{N} K[m,\varepsilon]\,\delta\left(\frac{\vartheta}{T_r} - m\right),$$

where $\delta(\overline{t})$ is the δ-functionand T_r the period of regulation, we obtain the following condition for the optimum weighting function for our case:

$$\begin{gathered}\sum_{m=0}^{N} R_{\varphi\varphi}[e-m]K[m,\varepsilon] = R_{h\varphi}[e,\varepsilon] + \gamma_0 + \gamma_1 e + \cdots + \gamma_r e^r \quad (0 \leqslant e \leqslant N),\\ K[e,\varepsilon] = 0 \quad (0 > e > N),\end{gathered} \tag{18}$$

where according to (12) and (13)

$$\mu_r = (-1)^i i!\,(c_i + a_i) \quad (i = 0, 1, \ldots, r). \tag{18a}$$

Conditions (18) and (18a), which contain only N + r + 2 equations, make it possible to determine N + r + 2 unknowns. In the particular case when $c_i = 0$ and $\epsilon = 0$, (18) and (18a) coincide with the conditions obtained in [4].

Thus, the problem of determining the optimum weighting function of a pulse system consists of solving a system of N + r + 2 linear algebraic equations. This problem usually presents no particular difficulties, since in most cases $r \leq 2$, and N is determined by the transient time of the pulse system, referred to the period of regulation. This is why cases in which N is large are, in practice, less interesting, for they do not display the specific features of pulsed systems and can be investigated by means of methods developed for continuous-action systems [1].

It should be noted that the system of linear algebraic equations, defining the optimum characteristics of the pulsed linear filter in the case of a stationary useful signal and unlimited transient time, was first obtained by A.N. Kolmogorov [6] in the solution of the problem of interpolation and extrapolation of stationary random sequences. For the case of nonstationary signals and arbitrary transient time, the system of algebraic equations determining the optimum characteristics of a pulsed linear filter is obtained as a particular case of the general solution derived in [7].

2. Expressions for the Optimum Weighting Functions in the Absence of a Statistical Connection Between Discrete Values of the Random Component of the Signal

The condition of statistical independence of the discrete values of the random component of the signal is fulfilled in many practical cases.

Mathematically this condition is written as

$$R_{\varphi\varphi}[0] = c^2, \quad R_{\varphi\varphi}[n] = 0 \text{ for } n \neq 0. \tag{19}$$

Substituting (19) into (18) and putting for simplicity $u[n,\epsilon] = 0$, i.e.,

$$R_{h\varphi}[n, \varepsilon] = 0, \tag{20}$$

we obtain $c^2K[m,\epsilon] = \gamma_0 + \gamma_1 e + \ldots + \gamma_r e^r$, which, with allowance for (13) and for the equalities $\sum_{e=0}^{N} 1 = N + 1$, and $\sum_{e=0}^{N} e = \frac{(N+1)N}{2}$, yield

$$\sum_{e=0}^{N} e^2 = \frac{N(2N+1)(N+1)}{6}, \quad \sum_{e=0}^{N} e^3 = \frac{N^2(1+N)^2}{4},$$

$$\sum_{e=0}^{N} e^4 = \frac{N(2N+1)(N+1)}{10}\left(N^2 + N - \frac{1}{3}\right)$$

for $r = 1$ we get

$$K[e, \varepsilon] = \frac{3}{(1+N)\left(1+\frac{N}{2}\right)}\left[(a_0 + c_0)\left(\frac{2N+1}{3} - e\right) - \right.$$

$$\left. - (a_1 + c_1)\left(\frac{2e}{N} - 1\right)\right] \quad (0 \leqslant e \leqslant N), \tag{21}$$

$$K[e, \varepsilon] = 0 \quad (0 > e > N),$$

and for $r = 2$

$$K[e,\ \varepsilon] = \frac{3}{(1+N)(N^2+5N+6)}\Big[(a_0+c_0)\{(3N^2+3N+2)-$$

$$-6(1+2N)e+10e^2\}+(a_1+c_1)\Big\{6(1+2N)-\frac{4(2N+1)}{N-1}\Big(8-\frac{3}{N}\Big)e+$$

$$+\frac{60}{N-1}e^2\Big\}+2(a_2+c_2)\Big\{10-\frac{60}{N-1}e+\frac{60}{N(N-1)}e^2\Big\}\Big] \quad (0\leqslant e\leqslant N)$$

$$K(e,\ \varepsilon)=0 \quad (0>e>N). \tag{22}$$

The equations obtained express in the general form, the optimum weighting function of pulse systems when Conditions (19) and (20) are satisfied.

In the particular case of reproducing a signal ($h = 1$, $a_0 = 1$, $a_1 = \epsilon$, $a_2 = \epsilon^2/2$) with a zero dynamic error ($c_0 = c_1 = c_2 = 0$), these equations become

$$K[e,\ \varepsilon] = \frac{3}{(1+N)\left(1+\frac{N}{2}\right)}\left[\frac{2N+1}{3}-e-\varepsilon\left(\frac{2e}{N}-1\right)\right] \quad (0\leqslant e\leqslant N),$$

$$K[e,\ \varepsilon]=0 \quad (0>e>N), \tag{21a}$$

$$K[e,\ \varepsilon] = \frac{3}{(1+N)(2+N)(3+N)}\Big[\{3N^2+3N+2-6(1+2N)e+10e^2\}+$$

$$+\varepsilon\Big\{6(1+2N)-\frac{4(2N+1)}{N-1}\Big(8-\frac{3}{N}\Big)e+\frac{60}{N-1}e^2\Big\}+$$

$$+\varepsilon^2\Big\{10-\frac{60}{N-1}e+\frac{60}{N(N-1)}e^2\Big\}\Big] \quad (0\leqslant e\leqslant N), \quad K[e,\ \varepsilon]=0 \quad (0>e>N). \tag{22a}$$

3. Connection Between the Characteristics of the Closed and Corresponding Open Pulse Systems

The known equation for the pulse systems [1] is written in the following manner:

$$X[n,\ \varepsilon] = \sum_{m=0}^{n} Y[n-m,\ 0]\,K[m,\ \varepsilon], \tag{23}$$

where $X[n,\epsilon]$ is the output function of the input system, and $Y[n,0]$ is the function representing the input signal. When writing Equation (23) it was assumed that the pulse element reacts to values the signal assumes at the instants at which the pulses are formed. However, such a physical premise appears to be inaccurate.

Actually, the pulse element responds to values assumed by the signal at the starting instants of pulse formation. Taking this circumstance into account, the equation for the pulse system is written in the following form [8]:

$$X[n,\ \varepsilon] = \sum_{m=0}^{n} Y[n-m,\ 0_]\,K[m,\ \varepsilon]$$

or

$$X[n,\ \varepsilon] = \sum_{m=0}^{n} Y[n-m-1,\ 1]\,K[m,\ \varepsilon], \tag{24}$$

since

$$Y[n-m, 0_-] = Y[n-m-1, 1].$$

The difference between Equations (23) and (24) may manifest itself in practice in the case when the input variable $Y_{in}[n,\epsilon]$ of a pulse element of the key type experiences discontinuities at the points $\epsilon = 0$, which always happens in closed pulse systems. We shall therefore start the derivation of the connection between the transfer functions of the closed and open pulse systems with (24).

In a closed pulse system the input to the pulse element is the difference $Y_{in}[n,\epsilon]$ between the current values of the input variable $Y[n,\epsilon]$ and the output variable $X[n,\epsilon]$, a difference determined by the equation

$$Y_{in}[n, \varepsilon] = Y[n, \varepsilon] - X[n, \varepsilon].$$

At the instant of time $\bar{t} = n$, corresponding to the start of the n'th regulation period, the pulse element responds to an error $Y_{in}[n-1,\epsilon]_{\epsilon=1}$, which takes place at the end of the preceding period. Therefore, the input variable of the pulse element can be represented in the form of a stepped function

$$Y_{in}[n-1, 1] = Y[n-1, 1] - X[n-1, 1]. \tag{25}$$

From (25) and (24) we obtain

$$X[n, \varepsilon] = \sum_{e=0}^{n} (Y[n-e-1,1] - X[n-e-1,1]) K_{op}[n, \varepsilon], \tag{26}$$

where $K_{op}[n,\epsilon]$ is the weighting function of the open pulse system.

Applying the discrete Laplace transform to Equation (26) we obtain

$$X^*(q, \varepsilon) = e^{-q} K^*_{op}(q, \varepsilon)[Y^*(q, 1) - X^*(q, 1)], \tag{27}$$

where $X^*(q,\epsilon)$, $X^*(q,1)$, $Y^*(q,1)$ are the transforms of the functions $X[n,\epsilon]$, $X[n,1]$, $Y[n,1]$, while $K^*_{op}(q,\epsilon)$ is the transform of the weighting function of the pulse system, called its transfer function.

From (27) we obtain for $\epsilon = 1$

$$X^*(q, 1) = e^{-q} Y^*(q, 1) \frac{K^*_{op}(q, 1)}{1 + e^{-q} K^*_{op}(q, 1)}. \tag{28}$$

Equations (28) and (27) yield the sought relation[1]

$$K^*_c(q, \varepsilon) = \frac{K^*_{op}(q, \varepsilon)}{1 + e^{-q} K^*_{op}(q, 1)}, \tag{29}$$

in which $K^*_c(q,\epsilon)$ denotes the transfer function of the closed pulse system, determined in the general case from the relation

[1] Equation (29) is obtained from (24) and for systems with pulse elements of the key type it differs substantially from the known equation

$$K^*_c(q, \varepsilon) = \frac{K^*_{op}(q, \varepsilon)}{1 + K^*_{op}(q, 0)}, \tag{29a}$$

obtained on the basis of (23). This difference will disappear if $K^*_{op}(q,0)$ is taken to mean $K^*_{op}(q,0_-)$[8], since $K^*_{op}(q,0_-) = e^{-q} K^*_{op}(q,1)$. However, if $K^*_{op}(q,0)$ is determined from the transfer function $K^*_{op}(q,\epsilon)$, putting in the latter $\epsilon = 0$, then in this case the Expression (29a) will be incorrect.

$$K_c^*(q, \varepsilon) = \frac{X^*(q, \varepsilon)}{e^{-q}Y^*(q, 1)},$$

and in the case when the input variable of the pulse system is continuous, and consequently when $e^{-q}Y^*(q,1) = Y^*(q,0)$ it is determined from the relation

$$K_c^*(q, \varepsilon) = \frac{X^*(q, \varepsilon)}{Y^*(q, \varepsilon)}.$$

It also follows from (29) that

$$K_{op}^*(q, \varepsilon) = \frac{K_c^*(q, \varepsilon)}{1 - e^{-q}K_c^*(q, 1)}. \tag{30}$$

Using Expression (29), we can derive, by using the well-known technique [1], expressions relating the weighting functions of the closed and corresponding open pulse systems. For this purpose let us write Expression (29) in the following form:

$$K_{op}[0, \varepsilon] + K_{op}[1, \varepsilon]\, e^{-q} + \ldots + K_{op}[n, \varepsilon]\, e^{-qn} + \ldots$$
$$\ldots = \frac{K_c[0, \varepsilon] + K_c[1, \varepsilon]\, e^{-q} + \ldots + K_c[n, \varepsilon]\, e^{-qn} + \ldots}{1 - K_c[0, 1]\, e^{-q} - K_c[1, 1]\, e^{-2q} - \ldots - K_c[n-1, 1]\, e^{-qn}}. \tag{31}$$

Multiplying the left part of Expression (31) by the denominator of the right part and equating coefficients of equal powers of e^{-q}, we obtain the following equations

$$K_c[0, \varepsilon] = K_{op}[0, \varepsilon],$$
$$K_c[1, \varepsilon] = K_{op}[1, \varepsilon] - K_{op}[0, \varepsilon]\, K_c[0, 1],$$
$$K_c[2, \varepsilon] = K_{op}[2, \varepsilon] - K_{op}[0, \varepsilon]\, K_c[1,1] - K_{op}[1, \varepsilon]\, K_c[0, 1],$$
$$\ldots\ldots\ldots\ldots\ldots\ldots\ldots\ldots\ldots\ldots\ldots\ldots$$

from which we get the recursion formula

$$K_c[n, \varepsilon] = K_{op}[n, \varepsilon] - \sum_{e=0}^{n-1} K_c[e, 1]\, K_{op}[n - e - 1, \varepsilon] \tag{32}$$

or

$$K_{op}[n, \varepsilon] = K_c[n, \varepsilon] + \sum_{e=0}^{n-1} K_c[e, 1]\, K_{op}[n - e - 1, \varepsilon]. \tag{33}$$

4. Determination of the Characteristics of the Pulse Element and of the Continuous Portion Using the Known Characteristics of the Pulse System

It is known that a pulse element that forms pulses of arbitrary shape can always be represented conventionally as a pulse element that forms the instantaneous pulses, connected in series with a certain continuous portion whose transfer function coincides with the transfer function $K_p(q)$ of the initial specified pulse element [9]. Accordingly, without loss of generality, one can always assume that the pulse system consists of a pulse element, which forms instantaneous pulses, and a certain equivalent continuous portion (ECP) whose transfer function $K(q)$ is determined by the product of the transfer functions of the actually realizable pulse element and continuous portion:

$$K(q) = K_p(q)\, K_{ecp}(q). \tag{34}$$

Here the "areas" of the instantaneous pulses, formed by the pulse element, must be assumed to equal the value of the signal at the instant directly preceding the instant of production of the pulses. Taking this into account, and noting that the weighting function of a pulse system expresses its response to a signal in the form of a rectangular pulse with height and duration of unity, it is easy to determine the connection between the weighting function of the pulse system and its ECP. Actually, the action of a rectangular pulse of unit height and unit duration on an open pulsed system is equivalent to the action of the unit pulse function $\delta(\bar{t})$ on the ECP of this system, for in the former case there appears at the output of the pulse element a practically instantaneous pulse with "area" equal to unity, and in the latter case there appears an infinitesimally short pulse with "area" also equal to unity, acting directly on the ECP of the pulsed system. It follows from this circumstance that the weighting function of the open pulsed system $K_{op}[n,\epsilon]$ and the ECP of this system $K(\bar{t})$ have the same form, i.e.,

$$K_{op}[n, \varepsilon] = K(\bar{t}) \text{ when } \bar{t} = n + \varepsilon. \tag{35}$$

Noting that the transfer function ECP of the open pulse system is a result of the Laplace transform of the corresponding weighting function $\left(K(q) = \int_0^\infty K(\bar{t})\, e^{-q\bar{t}}\, d\bar{t}\right)$, and taking (35) into account, we obtain the equation

$$K(q) = \int_0^1 \sum_{n=0}^{\infty} K_{op}[n, \varepsilon]\, e^{-qn} e^{-q\varepsilon}\, d\varepsilon, \tag{36}$$

which expresses the transfer function ECP of the open pulsed system in terms of the weighting function of this system.

If we consider that $\sum_{n=0}^{\infty} K_{op}[n, \varepsilon]\, e^{-qn} = K^*_{op}(q, \varepsilon)$, it turns out that (36) corresponds to

$$K(q) = \int_0^1 K^*_{op}(q, \varepsilon)\, e^{-q\varepsilon}\, d\varepsilon, \tag{37}$$

obtained also in [10] in a somewhat different manner.

Substituting $K^*_{op}(q,\epsilon)$ from (30) into (37) we obtain the relation

$$K(q) = \int_0^1 \frac{K^*_C(q, \varepsilon)}{1 - e^{-q} K^*_C(q, 1)}\, e^{-q\varepsilon} d\varepsilon, \tag{38}$$

which can also be represented as follows:

$$K(q) = \int_0^1 \frac{\sum_{n=0}^{N} K_C[n, \varepsilon]\, e^{-qn}}{1 - e^{-q} \sum_{n=0}^{N} K_C[n, 1]\, e^{-qn}}\, e^{-q\varepsilon} d\varepsilon. \tag{39}$$

Relations (39) and (38) permit the transition from the function $K_C[n,\epsilon]$, and $K^*_C(q,\epsilon)$, which characterize the closed pulse system as a whole, to the transfer function ECP of this system.

5. General Methods of Realization of Pulse Systems to Meet Specified Characteristics

The characteristics of pulse systems are usually represented by very complicated mathematical expressions, which do not permit direct realization of the pulse system. However, the problem is simplified substantially if one obtains from the known characteristics of the pulse system the transfer function $K(q)$ of its equivalent con-

tinuous portion (ECP), which can always be made by means of the relations obtained in Section 4. Then the rest of the problem consists of realizing in practice a pulse element and a continuous portion of the pulse system, whose transfer functions, when multiplied, yield the determined transfer function $K(q)$ of the ECP. Here it is advisable not to attempt a selection of a pulse element and a continuous portion such as to realize the optimum transfer function $K(q)$, but to attempt, on the basis of the specified optimum characteristics of the pulse system, to find such a transfer function $K_d(q)$, its ECP, which could be readily realized, and which would at the same time insure nearly optimal properties of the pulse system. Such a transfer function for the ECP, and also the corresponding pulse system and its characteristics, will be called "desirable." In the general case, the determination of the desirable transfer functions of the ECP of closed pulse systems from specified characteristics of these systems can be effected by means of two methods, the nature of which will be described below.

Method of approximation of the desired optimum weighting function. Let us assume that we know the weighting function $K_c[n, \epsilon]$ of the optimum closed pulse system that is required to determine the desirable transfer function of its ECP. To solve this problem it is enough to carry out the following operations.

1. Using Equation (33), find the weighting function of the corresponding open system.

2. If it turns out that the optimum weighting function $K_{op}[n, \epsilon]$ has discontinuities and exact realization is difficult, it is approximated by its continuous desirable function $K_{opd}[n, \epsilon]$, realized in a simpler manner.

3. Using Expression (36), find the desirable transfer function $K_d(q)$ of the ECP, after which the transfer functions $K_{ecp}(q)$ and $K_p(q)$ of the actually realizable continuous portion and of the pulse element are so chosen as to satisfy the equation

$$K_{ecp}(q) K_p(q) = K_d(q).$$

Method of logarithmic frequency characteristics. Let us assume that we know the transfer function of the optimum closed pulse system $K_c^*(q, \epsilon)$; it is required to determine the desired transfer function of its ECP.

To solve this problem it is necessary to use (38) to find the transfer function of the ECP of the pulse system.

Replacing in the latter the parameter q by jx (where j is the imaginary unit and $x = \omega T_{op}$ is the relative frequency), we obtain thereby the frequency characteristics of the ECP, with which it is possible to plot the amplitude and phase logarithmic frequency characteristics and determine from their form, using known methods [11], the desirable frequency characteristic, and consequently also the desirable transfer function of the ECP. It must be noted, however, that this method is not always suitable for pulse systems, since $K^*(jx)$ is determined not in the form of a product, but in the form of a sum.

Having solved the problem of determining the desirable transfer function of the ECP it is advisable to check what qualities of the desirable pulse system this transfer function provides. This can be done as follows.

Considering that the weighting function of the open desired system $K_{opd}[n, \epsilon]$ is determined by Equation (35), and using Relation (32), it is possible to find the weighting function of the closed desired system. With the aid of this function it is possible to do the following:

a) use the formula

$$X[n, \varepsilon] = \sum_{e=0}^{n} Y[n-e] K_c[e, \varepsilon] \tag{40}$$

to determine the response $X[n, \epsilon]$ of the system to any signal $Y[n]$ and thereby estimate simultaneously the duration of its transient;

b) use Equations (14) and (15) to calculate the dynamic error and the mean squared random error.

6. Realization of the Optimum Weighting Functions Determined by the Equation (21a)

Putting in (21a) $N = 1, 2, 3$ and 4 it is possible to determine the weighting functions of the closed system (Table 1) for these values of N.

TABLE 1

ε	$K_c[n, \varepsilon]$		$K_{op}[n, \varepsilon]$	
	N=1	N=2	N=3	N=4
0	$1+\varepsilon$	$\frac{5+3\varepsilon}{6}$	$\frac{7+3\varepsilon}{10}$	$\frac{6+2\varepsilon}{10}$
1	$-\varepsilon$	$\frac{2}{6}$	$\frac{4+\varepsilon}{10}$	$\frac{4+\varepsilon}{10}$
2	0	$\frac{-1-3\varepsilon}{6}$	$\frac{1-\varepsilon}{10}$	$\frac{2}{10}$
3	0	0	$\frac{-2-3\varepsilon}{10}$	$-\frac{\varepsilon}{10}$
4	0	0	0	$\frac{-2-2\varepsilon}{10}$
5	0	0	0	0

Using next Relation (33), it is possible to find the weighting functions $K_{op}[n,\epsilon]$ of the corresponding open pulse systems (Table 2), which are graphically represented in Figure 3.

TABLE 2

ε	$K_{op}[n, \varepsilon]$			
	N=1	N=2	N=3	N=4
0	$1+\varepsilon$	$0.83+0.50\varepsilon$	$0.70+0.30\varepsilon$	$0.60+0.20\varepsilon$
1	$2+\varepsilon$	$1.44+0.75\varepsilon$	$1.10+0.40\varepsilon$	$0.88+0.26\varepsilon$
2	$3+\varepsilon$	$2.04+0.55\varepsilon$	$1.55+0.45\varepsilon$	$1.20+0.30\varepsilon$
3	$4+\varepsilon$	$2.66+0.63\varepsilon$	$1.90+0.35\varepsilon$	$1.52+0.32\varepsilon$
4	$5+\varepsilon$	$3.24+0.58\varepsilon$	$2.32+0.43\varepsilon$	$1.74+0.24\varepsilon$
5	$6+\varepsilon$	$3.80+0.60\varepsilon$	$2.73+0.40\varepsilon$	$2.06+0.31\varepsilon$
6	$7+\varepsilon$	$4.37+0.60\varepsilon$	$3.12+0.40\varepsilon$	$2.35+0.30\varepsilon$
7	$8+\varepsilon$	$4.94+0.60\varepsilon$	$3.53+0.40\varepsilon$	$2.63+0.30\varepsilon$

It is seen from this diagram that the weighting functions of the open pulsed systems are, in general, discontinuous at the points $\epsilon = 0$. Therefore, the exact realization of these weighting functions is difficult in practice and hardly advisable. In practice, it is more advisable to approximate each of the weighting functions $K_{op}[n,\epsilon]$, which are discontinuous at the points $\epsilon = 0$, by means of a desirable function in the form of a continuous straight line, expressed by the following equation:

$$K_{opd}[n,\epsilon] = K_0 + K_1(n + \epsilon). \tag{41}$$

The desired transfer function of the ECP of the pulse system will, according to (36), have the following form in this case:

$$K_d(q) = K_0/q + K_1/q^2. \tag{42}$$

Practical realization of the latter does not present any fundamental difficulties, for it is enough for this purpose to choose the reciprocal of the duty cycle of the pulse element of the system (γ) to be considerably less than unity ($\gamma \ll 1$, $K_p(q) = K_p$), and to choose the actually realizable continuous portion of the system in the form of a combination of integrating links with transfer function

$$K_d(q) = K_0/K_p q + K_1/K_p q^2. \tag{43}$$

The block diagram of the pulse system corresponding to this case is shown in Figure 4. Since the integrating links can be realized comparatively simply, it is relatively easy to realize the transfer function of the part, in the form (42), and the entire pulse system.

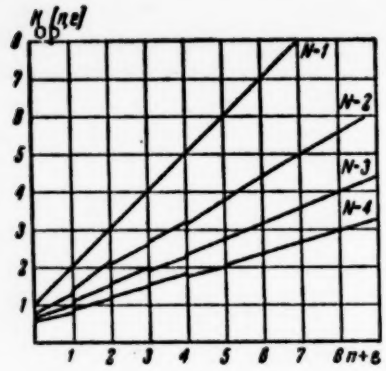

Fig. 3. Weighting functions of open pulse systems, corresponding to optimum weighting functions of closed systems, satisfying Equation (21a).

Thus, the choice of the actual desirable characteristics of the pulse system, in the case under consideration, consists of determining the coefficients K_0 and K_1, which approximate in the best manner the desirable weighting function, (41), to the optimum one. Here one can start out with the condition that these functions coincide in the limits, and consequently, that their first differences, which are written in the following manner

$$\lim_{n\to\infty} K_{op\,d}[n, 0] = \lim_{n\to\infty} K_{op}[n, 0], \quad \lim_{n\to\infty} \Delta K_{op\,d}[n, 0] = \lim_{n\to\infty} \Delta K_{op}[n, 0]$$

also coincide, or if one takes into account the theorem concerning the finite value of the original

$$\lim_{q\to 0} (e^q - 1)\, D\{K_{op\,d}[n, 0]\} = \lim_{q\to 0} (e^q - 1)\, D\{K_{op}[n, 0]\}, \tag{44}$$

$$\lim_{q\to 0} (e^q - 1)\, D\{\Delta K_{op\,d}[n, 0]\} = \lim_{q\to 0} (e^q - 1)\, D\{\Delta K_{op}[n, 0]\}, \tag{45}$$

where $D\{\ \}$ is the symbol for the discrete Laplace transform. But

$$D\{K_{op\,d}[n, 0]\} = D\{K_0\} + D\{K_1, n\} = \frac{K_0(e^q - 1) + K_1}{e^{-q}(e^q - 1)^2}, \tag{46}$$

$$D\{\Delta K_{op\,d}[n, 0]\} = (e^q - 1)\, D\{K_{op}[n, 0]\} - e^q K_{op}[0, 0], \tag{47}$$

$$\lim_{q\to 0} (e^q - 1)\, D\{\Delta K_{op\,d}[n, 0]\} = \lim_{n\to\infty} \Delta K_{op\,d}[n, 0] = K_1. \tag{48}$$

On the basis of (48), (47) and (45) we obtain

$$K_1 = \lim_{q\to 0} (e^q - 1)\, K^*_{op}(q, 0). \tag{49}$$

From (47) and (44) we get

$$K_0 = \lim_{q\to 0} \left[(1 - e^{-q})\, K^*_{op}(q, 0) - \frac{K_1}{e^q - 1}\right]. \tag{50}$$

Or, according to (30)

$$K_1 = \lim_{q\to 0} (e^q - 1)^2 \frac{K^*_c(q, 0)}{1 - e^{-q} K^*_c(q, 1)}, \tag{49a}$$

$$K_0 = \lim_{q\to 0} \left[(1 - e^{-q}) \frac{K^*_c(q, 0)}{1 - e^{-q} K^*_c(q, 1)} - \frac{K_1}{e^q - 1}\right], \tag{50a}$$

where

$$K^*_c(q, 0) = \sum_{n=0}^{N} K_c[n, 0]\, e^{-qn},$$

$$K^*_c(q, 1) = \sum_{n=0}^{N} K_c[n, 1]\, e^{-qn}. \tag{51}$$

Thus, in the case when the optimum weighting function of the closed follow-up pulse system satisfies Equation (21a), it is simple to determine the desired transfer function of the ECP of the pulse system.

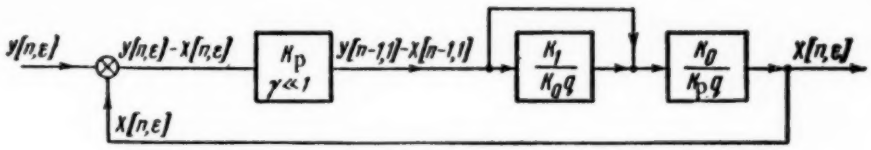

Fig. 4. Structure of desired closed pulse system in the case when optimum weighting functions are determined by Equation (21a).

For this, it is enough to insert into Expression (42) the actual values of the coefficients K_0 and K_1, determined with the aid of Equations (49a) and (50a).

The qualitative indices of the desired pulse system are checked in the following manner.

The actual values of K_0 and K_1 are substituted into (41) to determine the desired weighting function of the open system. Next Relation (32) is used to find the desired weighting function of the closed pulse system, which together with (40), (14) and (16a) permits estimating the duration of the transient, a dynamic error and the mean-square error of the desired pulse system.

7. Realization of Weighting Functions Determined by Equation (22a)

Putting in (22a) N = 2, 3 and 4, it is possible to determine the weighting functions of the closed pulse systems (Table 3) for these values of N.

Using next the Relation (33), it is possible to find the weighting functions of the corresponding open pulse systems, given in Table 4 and shown graphically in Figure 5.

TABLE 3

$\bar{e}$	$K_C[\bar{e}, \varepsilon]$		
	N=2	N=3	N=4
0	$\frac{2+3\varepsilon+\varepsilon^2}{2}$	$\frac{19+21\varepsilon+5\varepsilon^2}{20}$	$\frac{62+54\varepsilon+10\varepsilon^2}{70}$
1	$\frac{-4\varepsilon-2\varepsilon^2}{2}$	$\frac{3-13\varepsilon-5\varepsilon^2}{20}$	$\frac{18-13\varepsilon-5\varepsilon^2}{70}$
2	$\frac{\varepsilon+\varepsilon^2}{2}$	$\frac{-3-17\varepsilon-5\varepsilon^2}{20}$	$\frac{-6-40\varepsilon-10\varepsilon^2}{70}$
3	0	$\frac{1+9\varepsilon+5\varepsilon^2}{20}$	$\frac{-10-27\varepsilon-5\varepsilon^2}{70}$
4	0	0	$\frac{6+26\varepsilon+10\varepsilon^2}{70}$

Figure 5 shows that the optimum weighting functions of the open systems can be approximated by second degree polynomials, choosing the latter as the desired weighting functions, i.e., putting

$$K_{op\,d}[n, \varepsilon] = K_0 + K_1(n+\varepsilon) + K_2(n+\varepsilon)^2, \tag{52}$$

$$K_d(\bar{l}) = K_0 + K_1\bar{l} + K_2\bar{l}^2. \tag{53}$$

The desired transfer function of the ECP of the pulse system will, according to (36), have the following form in this case:

$$K_d(q) = \frac{K_0}{q} + \frac{K_1}{q^2} + \frac{2K_2}{q^3}. \tag{54}$$

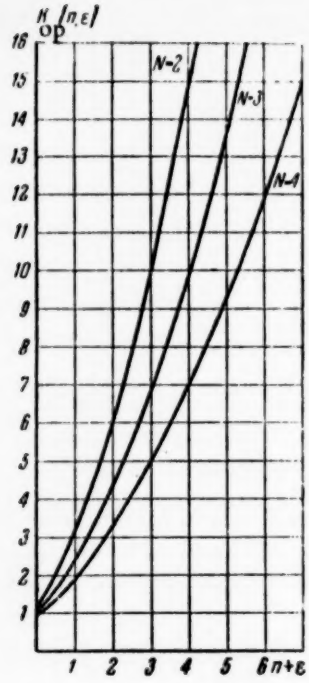

Fig. 5. Weighting functions of open pulse systems, corresponding to optimum weighting functions of closed systems satisfying Equation (22a).

Practical realization of the latter involves no great difficulties, for it is enough to choose for this purpose the reciprocal of the duty cycle of the pulse element to be considerably less than unity ($\gamma \ll 1$, $K_p(q) = K_p$), and to choose the actually realizable continuous portion in the form of a combination of integrating links with transfer function

$$K_{ecpd}(q) = \frac{K_d(q)}{K_p} = \frac{K_0}{K_p q} + \frac{K_1}{K_p q^2} + \frac{2K_2}{K_p q^3}. \tag{55}$$

The corresponding block diagram of the pulse system is shown in Figure 6.

Thus, in this case, the choice of the actual desired characteristics of the pulse system consists of determining the coefficients K_0, K_1, and K_2, approximating in the best manner the desired weighting function (54) to the optimum one. Here it is possible to start with the conditions that these functions, and consequently their first and second differences, coincide in the limit:

$$\lim_{n\to\infty} K_{op}[n, 0] = \lim_{n\to\infty} K_{op\,d}[n, 0], \tag{56}$$

$$\lim_{n\to\infty} \Delta K_{op}[n, 0] = \lim_{n\to\infty} \Delta K_{op\,d}[n, 0], \tag{57}$$

$$\lim_{n\to\infty} \Delta^2 K_{op}[n, 0] = \lim_{n\to\infty} \Delta^2 K_{op\,d}[n, 0]. \tag{58}$$

But, according to the theorem concerning the finite value of the original

$$\lim_{n\to\infty} K_{op}[n, 0] = \lim_{p\to 0} (e^q - 1) K^*_{op}(q, 0), \tag{59}$$

$$\lim_{n\to\infty} \Delta K_{op}[n, 0] = \lim_{g\to 0} (e^q - 1)\{(e^q - 1) K^*_{op}(q, 0) - e^q K_{op}[0, 0]\}, \tag{60}$$

$$\lim_{n\to\infty} \Delta^2 K_{op}[n, 0] =$$

$$= \lim_{q\to 0} (e^q - 1)\{(e^q - 1)^2 K^*_{op}(q, 0) - e^q (e^q - 1) K_{op}[0, 0] - e^q \Delta K_{op}[0, 0]\}, \tag{61}$$

$$\lim_{n\to\infty} K_{opd}[n, 0] = \lim_{q\to 0} (e^q - 1)\left\{\frac{K_0 e^q}{e^q - 1} + \frac{K_1 e^q}{(e^q - 1)^2} + \frac{K_2 (e^q + 1) e^q}{(e^q - 1)^3}\right\}, \tag{62}$$

$$\lim_{n\to\infty} \Delta K_{opd}[n, 0] = \lim_{q\to 0} (e^q - 1)\left\{\frac{e^q (K_1 + K_2)}{e^q - 1} + \frac{2K_2 e^q}{(e^q - 1)^2}\right\}, \tag{63}$$

$$\lim_{n\to\infty} \Delta^2 K_{opd}[n, 0] = 2K_2. \tag{64}$$

On the basis of (64), (61) and (58) we obtain

$$K_2 = \lim_{q\to 0} \frac{1}{2} (e^q - 1)^2 K^*_{op}(q, 0). \tag{65}$$

From (63), (60) and (57) we get

$$K_1 = \lim_{q\to 0} (e^q - 1)\left[(1 - e^{-q}) K^*_{op}(q, 0) - K_2 \frac{e^q + 1}{(e^q - 1)^2}\right]. \tag{66}$$

TABLE 4

n	$K_{op}[n, \varepsilon]$		
	$N=2$	$N=3$	$N=4$
0	$1 + 1.5\varepsilon+0.5\varepsilon^2$	$0.9+1.0\varepsilon+0.25\varepsilon^2$	$0.9+0.8\varepsilon+0.14\varepsilon^2$
1	$3.0+ 2.5\varepsilon+0.5\varepsilon^2$	$2.3+1.7\varepsilon+0.31\varepsilon^2$	$1.9+1.2\varepsilon+0.19\varepsilon^2$
2	$6.0+ 3.5\varepsilon+0.5\varepsilon^2$	$4.0+2.2\varepsilon+0.26\varepsilon^2$	$3.2+1.6\varepsilon+0.18\varepsilon^2$
3	$10.0+ 4.5\varepsilon+0.5\varepsilon^2$	$6.2+2.8\varepsilon+0.30\varepsilon^2$	$4.9+1.8\varepsilon+0.18\varepsilon^2$
4	$15.0+ 5.5\varepsilon+0.5\varepsilon^2$	$9.2+3.4\varepsilon+0.26\varepsilon^2$	$6.9+2.2\varepsilon+0.18\varepsilon^2$
5	$21.0+ 6.5\varepsilon+0.5\varepsilon^2$	$13.5+4.0\varepsilon+0.29\varepsilon^2$	$9.2+2.6\varepsilon+0.18\varepsilon^2$
6	$28.0+ 7.5\varepsilon+0.5\varepsilon^2$	$19.0+4.6\varepsilon+0.29\varepsilon^2$	$12.0+3.0\varepsilon+0.18\varepsilon^2$

From (62), (69) and (56), we get

$$K_0 = \lim_{q \to 0}\left[(1 - e^{-q})\, K^*_{op}(q, 0) - \frac{K_1}{e^q - 1} - \frac{K_2 (e^q + 1)}{(e^q - 1)^2}\right], \tag{67}$$

where

$$K^*_{op}(q, 0) = \frac{K^*_C (q, 0)}{1 - e^{-q}\, K^*_C (q, 1)} = \frac{\sum_{n=0}^{N} K_C [n, 0]\, e^{-qn}}{1 - e^{-q} \sum_{n=0}^{N} K_C [n, 1]\, e^{-qn}}. \tag{68}$$

Thus, if the optimum weighting function of the closed reproducing pulse system satisfies (22a), it is possible to find very simply the desired transfer function of the ECP of the pulse system. For this purpose it is enough to insert into (54) the actual values of the coefficients K_0, K_1 and K_2, which are determined with the aid of Equations (67), (66) and (65).

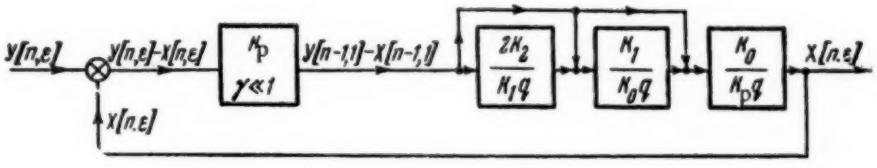

Fig. 6. Structure of desired open pulse system, in the case when the optimum weighting functions are determined by Equation (22a).

A check on the qualitative indices of the desired pulse system is carried out in the following manner. The actual values of K_0, K_1 and K_2 are substituted into (52) to determine the desired weighting function of the open system. Then (32) is used to find the desired weighting function of the corresponding closed pulse system, which together with (40), (14) and (16a) permits estimating the time of the transient, the dynamic error of the desired system, and its mean-squared error.

Example. Let it be required to determine the desired transfer function of the ECP of a pulse system, which having a transient time equal to three regulation intervals ($N = 3$), would have a minimum mean-squared error and zero dynamic-error components that depend on the regular signal and on its first two derivatives. The weighting function of such a system is determined with the aid of (22a) for $N = 3$ and is of the following form

$$K_C [0, \varepsilon] = \frac{1}{20}(19 + 21\varepsilon + 5\varepsilon^2), \quad K_C [1, \varepsilon] = \frac{1}{20}(3 - 13\varepsilon - 5\varepsilon^2),$$

$$K_C [2, \varepsilon] = \frac{1}{20}(-3 - 17\varepsilon - 5\varepsilon^2), \quad K_C [3, \varepsilon] = \frac{1}{20}(1 + 9\varepsilon + 5\varepsilon^2).$$

$$K_C [n, \varepsilon] = 0, \qquad n > 3. \tag{69}$$

On the basis of (69) and (68) we get

$$K^{*}_{op}(q, 0) = \frac{19 + 3e^{-q} - 3e^{-2q} + e^{-3q}}{20 - 45e^{-q} + 15e^{-2q} + 25e^{-3q} - 15^{-4q}} = \frac{19 + 3e^{-q} - 3e^{-2q} + e^{-3q}}{(1 - e^{-q})^3 (20 + 15e^{-q})}. \quad (70)$$

Inserting (70) into (65), (66) and (67), we get

$$K_0 = 0.92; \quad K_1 = 1.10; \quad K_2 = 0.286. \quad (71)$$

We obtain from this, according to (54), the following expression for the desired transfer function of the ECP of the pulse system:

$$K_d(q) = \frac{0.92\,q^2 + 1.10q + 2\times 0.286}{q^3}. \quad (72)$$

The desired weighting function of the open system is determined with the aid of (71) and (52) and is

$$K_{opd}[n, \varepsilon] = 0.92 + 1.10(n + \varepsilon) + 0.286(n + \varepsilon)^2. \quad (73)$$

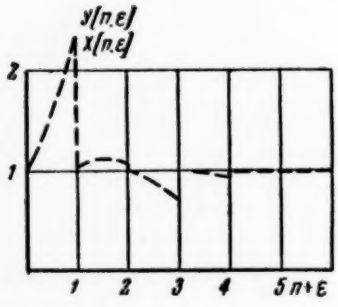

Fig. 7. Response of the desired pulse system, obtained in the example, to a unit step.

A plot of this function is practically the same as the corresponding plot for the optimum weighting function of the open system, given in Figure 5.

Let us compare now the qualitative performance insured by the desired and optimum weighting functions. From (73) and (72) we get

$$\begin{aligned}
&K_{cd}'[0, \varepsilon] = 0.92 + 1.10\varepsilon + 0.286\varepsilon^2,\\
&K_{cd}[1, \varepsilon] = 0.18 - 0.87\varepsilon - 0.374\varepsilon^2,\\
&K_{cd}[2, \varepsilon] = -0.07 - 0.46\varepsilon - 0.078\varepsilon^2,\\
&K_{cd}[3, \varepsilon] = -0.04 + 0.12\varepsilon + 0.125\varepsilon^2,\\
&K_{cd}[4, \varepsilon] = +0.01 + 0.07\varepsilon + 0.040\varepsilon^2,\\
&K_{cd}[e, \varepsilon] \approx 0 \quad \text{for} \quad e > 4.
\end{aligned} \quad (74)$$

The response of the desired system to a signal in the form of a stepped function will be, according to (74) and (40),

$$\begin{aligned}
&X[0, \varepsilon] = 0.92 + 1.10\varepsilon + 0.286\varepsilon^2, \quad X[1, \varepsilon] = 1.10 + 0.23\varepsilon - 0.088\varepsilon^2,\\
&X[2, \varepsilon] = 1.03 - 0.23\varepsilon - 0.166\varepsilon^2, \quad X[3, \varepsilon] = 0.99 - 0.11\varepsilon - 0.041\varepsilon^2,\\
&X[4, \varepsilon] = 1.00 - 0.04\varepsilon - 0.001\varepsilon^2, \quad X[e, \varepsilon] \approx 1 \quad \text{for} \quad e > 4.
\end{aligned} \quad (75)$$

Graphically, this reaction is shown in Figure 7, from which it is seen that basically the transient of the desired pulse system terminates during three regulation intervals after the instant of disturbance, corresponding to the transient time of the optimum system.

The mean-squared error of the desired system is given, according to (74) and (16a):

$$\sqrt{\overline{\xi^2[n, \varepsilon]}} = c\sqrt{0.90 + 1.80\varepsilon + 2.60\varepsilon^2 + 1.30\varepsilon^3 + 0.13\varepsilon^4}. \quad (76)$$

For the first three coefficients of the dynamic error we have from (74), (12) and (13) $c_0 = c_1 = c_2 = 0$. The first three coefficients of the optimum system in the analogous case will also vanish, according to (69), (12), (13) and (16a), and the mean-squared error will be

$$\sqrt{\overline{\xi^2[n, \varepsilon]}} = c\sqrt{0.95 + 2.08\varepsilon + 2.95\varepsilon^2 + 1.50\varepsilon^3 + 0.25\varepsilon^4}.$$

The latter is somewhat greater than the mean-squared error of the desired system. This is not contradictory, since the transient process of the desired system is infinitely long, although fundamentally it terminates within three periods of regulation, while the transient process of the optimum system stops completely within three periods of regulation after the instant of disturbance.

LITERATURE CITED

[1] Ia.Z. Tsypkin, Transients and Steady-State Processes in Pulse Systems (Gosenergoizdat, 1951).*

[2] Ia.Z. Tsypkin, Calculation of Systems of Intermittent Regulation in the Presence of Stationary Random Signals, Automation and Remote Control (USSR) 16, 4 (1955).

[3] V.V. Solodovnikov and P.S.Matveev, Synthesis of Correcting Components for Servomechanism Systems in the Presence of Noise, Based on Specified Dynamic Accuracy, Automation and Remote Control (USSR) 16, 3 (1955).

[4] K. Johnson, Optimum, linear, discrete filtering of signals containing a nonrandom component, Trans. Inst. Radio Engrs. on Inform. Theory (June, 1956).

[5] L.A. Zadeh and I.R. Ragazzini, An extension of Wiener's theory of prediction, J. Appl. Phys. Vol.21, No. 7 (1950).

[6] A.N. Kolmogorov, Interpolation and Extrapolation of Stationary Random Sequences, Bull. Acad. Sci. USSR, math. ser. Vol. 5, No. 1 (1941).

[7] V.S. Pugachev, General Conditions for Minimum Mean-Squared Error of a Dynamic System, Automation and Remote Control (USSR) 17, 4 (1956).**

[8] Ia.Z. Tsypkin, Theory of Relay Systems for Automatic Regulation (Gostekhizdat, 1955).*

[9] Ia.Z. Tsypkin, Allowance for the Shape of the Pulses and Intermittent Regulation Systems, Automation and Remote Control (USSR) 16, 5 (1955).

[10] Ia.Z. Tsypkin, Correction of Pulsed Systems, Automation and Remote Control (USSR) 18, 2 (1957).**

[11] Fundamentals of Automatic Regulation. Theory.* Edited by V.V. Solodovnikov (Mashgiz, 1954).

Received March 14, 1957

*In Russian.

**Original Russian pagination. See C.B. translation.

ON THE SYNTHESIS OF STRUCTURES OF MULTIPLE-LOOPED CONTROL SYSTEMS INCLUDING ELEMENTS WITH LAGS

M. V. Meerov

(Moscow)

This paper investigates systems of multiple-looped control systems containing elements with lags. The basic properties of such systems are established. A method is given of so synthesizing the structure of such systems that stability is maintained even with arbitrarily large gains in the individual loops. The conditions for autonomy are also obtained.

This article continues the work, begun in papers [1-3], on the synthesis of structures of multiple-looped control systems, stable under unbounded increase in the steady-state accuracy. Here, as a supplementary factor, is investigated the multiple-looped control system in which some (or all) of the loops contain elements with lag. The investigation of such systems has significant theoretical and practical interest. As an example of a multiple-looped system containing elements with lag, one might take a power-generating system, where the lag is inherent in the water turbine.

In a system automatically controlling power generator output, where one of the parameters is the angle between the emf's of the generating stations, a lag might be introduced by a remote control element, physically far removed.

In this article, as in [1-3], the following problems are considered: 1) to find structures of multiple-looped control systems containing elements with lags, which will permit unbounded increase in gain of the individual loops without a concomitant destruction of stability in all the systems in the circuit; 2) to determine the basic properties of these structures from the point of view of static and dynamic processes of automatic control.

1. Some Properties of Multiple-Looped Systems of Automatic Control, in Which Each of the Control Loops Consists of Basic Elements

We investigate a system of automatic control of n quantities, comprising the object to be regulated. In each loop there is an element with lag. We shall first study the case where each loop is structurally a single-loop circuit, consisting of elementary dynamic links and one element with lag.

Assuming that the load on each loop is applied at the input to the object (Figure 1), we obtain the following system of differential equations (written in operator form), describing the dynamic properties of the system under consideration:

$$\begin{aligned}
&[D_1(p)\,e^{\tau_1 p} + K_1]\,x_1 + K_1' \sum_{i=2}^{n} \alpha_{1i} x_i = K_1 x_{1\,\mathrm{st}} + K_1' f_1,\\
&\cdots\cdots\cdots\cdots\cdots\cdots\cdots\cdots\cdots\cdots\cdots\cdots\\
&[D_n(p)\,e^{\tau_n p} + K_n]\,x_n + K_n' \sum_{i=1}^{n-1} \alpha_{ni} x_i = K_n x_{n\,\mathrm{st}} + K_n' f_n.
\end{aligned} \tag{1}$$

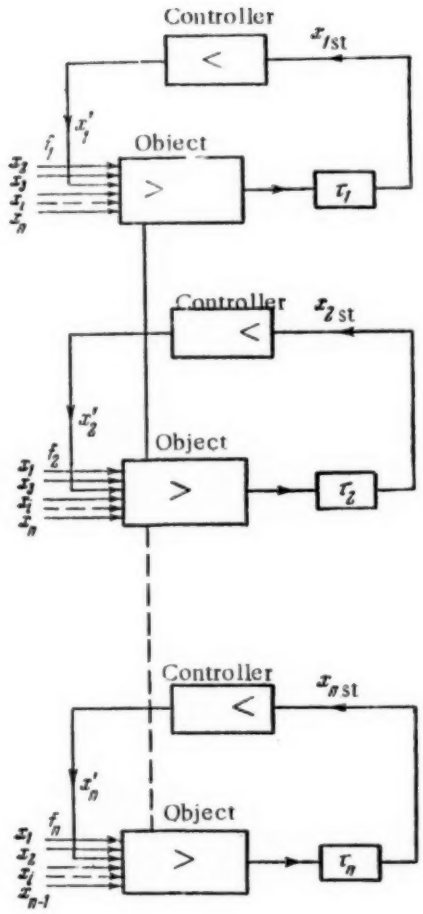

Fig. 1.

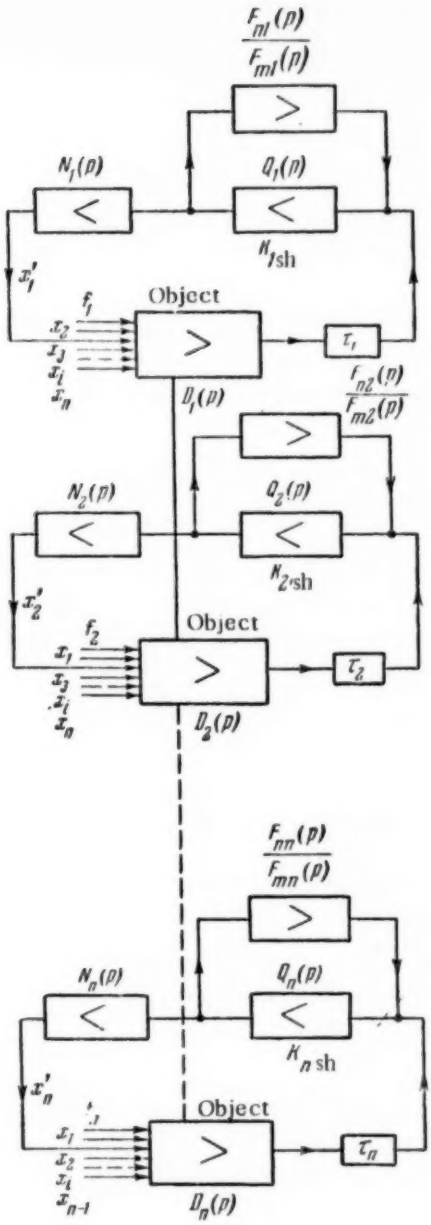

Fig. 2.

Here, $D_i(p)$ is the particular operator of the i'th control loop, K_i its gain, K'_i is the gain of the object with respect to its i'th controlled quantity, τ_i is the lag in the i'th loop, α_{ik} is the coefficient determining the interaction of the i'th and k'th controlled quantities (hence, α_{ik} might be either a number or an operator) and x_{ist} is the standard value of the i'th controlled quantity.

It is not difficult to see that here, as in multiple-looped control systems without lag, the steady-state error in the i'th controlled quantity will decrease as the gain in the i'th loop is increased. Indeed, $e^{\tau ip} = 1$ for $p = 0$ and the system of equations, which determines the steady-state error, does not depend on the lag. As was shown in [1, 2], increasing the gain in the i'th loop leads to a decreased steady-state error in the i'th controlled quantity.

In [1-3] it was shown that in a system with several interconnected controlled quantities, consisting only of basic elements (i.e., not containing stabilizing devices), increasing one, several,or all gains inevitably leads to the destruction of the entire system's stability. It may be asserted, a priori, that the presence of lag in some or

all controlling loops does not change the results of an incompatibility between the accuracy (as represented by the loop gains) and the stability, as long as the system consists only of basic elements.

We now set forth briefly some further properties of multiple-looped systems containing lags. Let us prove the following theorem.

If there is at least one pair of coefficients, $\alpha_{ik}(p)$ and $\alpha_{ki}(p)$, such that $D_i(p)D_k(p)$ is of lower degree than $\alpha_{ik}(p)\alpha_{ki}(p)$, and if there are elements with lag in this loop, then the entire system is structurally unstable.

Indeed, in order that the system be structurally unstable, it suffices, in the present case, that the principal term in the characteristic equation vanish [4]. As is clear from Equation (1), the greatest value of τ will be equal to the sum of all the lags, $\tau = \sum_{i=1}^{n} \tau_i$, and the coefficient of $e^{\tau p}$ will be $\prod_{i=1}^{n} D_i(p)$.

Since among the quasi-polynomials entering into the characteristic equation there will be the quasi-polynomial

$$\prod_{i=1,\,2,\ldots,\,i-1,\,i+1,\ldots,\,n} D_i(p)\,\alpha_{ik}(p) \prod_{k=1,\ldots,\,k-1,\,k+1,\ldots,\,n} D_k(p)\,\alpha_{ki}(p)\,e^{(\tau_1+\tau_2+\ldots+\tau_{i+1}+\tau_{i-1}\ldots\tau_{k-1}+\tau_{k+1}+\ldots+\tau_n)\,p}$$

then the condition that the degree of $\alpha_{ik}(p)\alpha_{ki}(p)$ be greater than the degree of $D_i(p)D_k(p)$ implies the vanishing of the leading term in the characteristic equation, and the system is structurally unstable. Thus, it is possible to draw the following conclusions as to the properties of multiple-looped automatic control systems containing elements with lag.

1. The greater the gain in the i'th loop, the smaller will be the steady-state error in the i'th controlled quantity.

2. In multiple-looped systems with lags, where each of the loops consists of basic elements, increasing one, several, or all of the gains will invariably destroy system stability.

3. If, for some pair of indices, ik, the degree of $\alpha_{ik}(p)\alpha_{ki}(p)$ exceeds the degree of $D_i(p)D_k(p)$, then the presence of lags is sufficient to render the multiple-looped control system unstable.

We shall now find rules for constructing multiple-looped automatic control systems which contain elements with lags but which, nevertheless, permit an unbounded increase in the loop gains without a concomitant loss of stability.

2. Multiple-Looped Systems with Lags, Stable Under Unbounded Increase in the Loop Gains

Figure 2 gives the essential configuration of a multiple-looped automatic control system containing elements with lags. A portion of each control group is shunted by a stabilizing device of the type $\frac{F_{ni}(p)}{F_{mi}(p)}$. We shall assume that there are no elements with lags in the portions of the control loops shunted by stabilizing devices. It is necessary to determine what properties must be possessed by the operator representations of the stabilizing devices, as a function of the links shunted by them, to ensure that the systems remain stable under unbounded increase in the loop gains.

The system of operator equations, defining the dynamic properties of the system under consideration, takes the following form (see Figure 2):

$$\begin{aligned}
&[P_1(p)\,e^{\tau_1 p} + K_{1sh}S_1(p)\,e^{\tau_1 p} + K_{1to}F_{m1}(p)]\,x_1 + \\
&+ K_1[R_1(p) + K_{1sh}N_1(p)\,F_{n1}(p)] \sum_{i=2}^{n} \alpha_{1i}x_i = \\
&= K_1[R_1(p) + K_{1sh}N_1(p)\,F_{n1}(p)]\,[x_{1st} + f_1],
\end{aligned}$$

. . . . . (2)

$$\ldots\ldots\ldots\ldots\ldots\ldots\ldots\ldots\ldots\ldots\ldots\ldots\ldots\ldots$$

$$\begin{aligned}&[P_n(p)\,e^{\tau_n p}+K_{n\,\mathrm{sh}}S_n(p)\,e^{\tau_n p}+K_{n\,\mathrm{to}}F_{mn}(p)]\,x_n+\\&+K_n[R_n(p)+K_{n\,\mathrm{sh}}N_n(p)\,F_{nn}(p)]\sum_{i=1}^{n-1}\alpha_{ni}x_i=\\&=K_n[R_n(p)+K_{n\,\mathrm{sh}}N_n(p)\,F_{nn}(p)]\,[x_{n\,\mathrm{st}}+f_n].\end{aligned}\qquad(2)$$

(continued)

where

$$\begin{aligned}P_i(p)&=D_i(p)\,N_i(p)\,F_{mi}(p)\,Q_i(p),\\S_i(p)&=D_i(p)\,N_i(p)\,F_{ni}(p),\\R_i(p)&=D_i(p)\,F_{mi}(p)\,Q_i(p)\end{aligned}\qquad(3)$$

and where, for the i'th loop, $N_i(p)$ is the proper operator for the portion of the control loop not shunted by a stabilizing device, $Q_i(p)$ is the proper operator of the shunted portion of the control loop, $F_{ni}(p)$ and $F_{mi}(p)$ are, respectively, the numerator and denominator of the stabilizer's proper operator, K_i and $K_{i\,sh}$ are, respectively, the gains of the unshunted and shunted elements in the control loop, and the total loop gain is $K_{i\,to}=K_{i\,sh}K_i$.

The characteristic equation of the system is written as:

$$\left|\begin{array}{l}P_1(p)\,e^{\tau_1 p}+K_{1\mathrm{sh}}S_1(p)\,e^{\tau_1 p}+K_{1\mathrm{to}}F_{m1}(p),\ K_1[R_1(p)+\\\quad+K_{1\mathrm{sh}}N_1(p)\,F_{n1}(p)]\,\alpha_{12},\ \ldots,\ K_1[R_1(p)+K_{1\mathrm{sh}}N_1(p)\,F_{n1}(p)]\,\alpha_{1n}\\K_2[R_2(p)+K_{2\mathrm{sh}}N_2(p)\,F_{n2}(p)]\,\alpha_{21},\ P_2(p)\,e^{\tau_2 p}+K_{2\mathrm{sh}}S_2(p)\,e^{\tau_2 p}+\\\quad+K_{2\mathrm{to}}F_{m2}(p),\ \ldots,\ K_2[R_2(p)+K_{2\mathrm{sh}}N_2(p)\,F_{n2}(p)]\,\alpha_{2n}\\\ldots\ldots\ldots\ldots\ldots\ldots\ldots\ldots\ldots\ldots\ldots\ldots\ldots\ldots\\\ldots\ldots\ldots\ldots\ldots\ldots\ldots\ldots\ldots\ldots\ldots\ldots\ldots\ldots\\K_n[R_n(p)+K_{n\,\mathrm{sh}}N_n(p)\,F_{nn}(p)]\,\alpha_{n1},\ K_n[R_n(p)+\\\quad+K_{n\,\mathrm{sh}}N_nF_{nn}(p)]\,\alpha_{n2},\ \ldots,\ P_n(p)\,e^{\tau_n p}+K_{n\mathrm{sh}}S_n(p)\,e^{\tau_n p}+K_{n\mathrm{to}}F_{mn}(p)\end{array}\right|=0$$

In what follows it will be assumed that the gains of the stabilizer-shunted loop elements are either all equal, or always remain in a fixed ratio

$$K_{i\,sh}=\eta_i K_{1\,sh}=\eta_i K_{sh}\ (\eta_i=\mathrm{const}).$$

With this condition, the characteristic equation can take the following form:

$$\begin{aligned}&\prod_{i=1}^{n}P_i(p)\,e^{\sum_{i=1}^{n}\tau_i p}+K_{sh}\left\{\sum_{i=1}^{n}S_i(p)\,C_n^{n-1}P_i(p)\,e^{\sum_{i=1}^{n}\tau_i p}+D_{00}(p)\,e^{\sum_{i=2}^{n}\tau_i p}+\right.\\&\left.+\ldots+D_{0n}(p)\right\}+K_{sh}^2\left\{\sum_{i,k=1,2,\ldots,n}S_i(p)\,S_k(p)\,C_n^{n-2}\,P_i(p)\,e^{\sum_{i=1}^{n}\tau_i p}+\right.\\&\left.+D_{10}(p)\,e^{\sum_{i=2}^{n}\tau_i p}+\ldots+D_{1n}(p)\right\}+\ldots+K_{sh}^n\left\{\prod_{i=1}^{n}S_i(p)\,e^{\sum_{i=1}^{n}\tau_i p}+\right.\\&\left.+D_{n0}(p)\,e^{\sum_{i=2}^{n}\tau_i p}+\ldots+D_{nn}(p)\right\}+F_n(p)=0.\end{aligned}\qquad(4)$$

It is obvious that a given polynomial $D_{ik}(p)$, obtained by multiplying out, is of a lower degree in p than the corresponding polynomial which appears first within the same brackets.

The polynomial $F_n(p)$ is not multiplied by any gain, and its coefficients do not depend on the loop gains.

We divide Equation (4) by K_{sh}^n, and let $1/K_{sh}^i = m^i$. Then the equation may be rewritten as:

$$m^n\left\{\prod_{i=1}^{n} P_i(p)\, e^{\sum_{i=1}^{n}\tau_i p} + F_n(p)\right\} +$$

$$+ m^{n-1}\left\{\sum_{i=2}^{n} S_i(p) C_n^{n-1} P_i(p)\, e^{\sum_{i=1}^{n}\tau_i p} + D_{00}(p)\, e^{\sum_{i=2}^{n}\tau_i p} + \ldots + D_{0n}(p)\right\} +$$

$$+ m^{n-2}\left\{\sum_{i,k} S_i(p) S_k(p) C_n^{n-2} P_i(p)\, e^{\sum_{i=1}^{n}\tau_i p} + D_{10}(p)\, e^{\sum_{i=2}^{n}\tau_i p} + \ldots + D_{1n}(p)\right\} + \ldots$$

$$\ldots + \prod_{i=1}^{n} S_i(p)\, e^{\sum_{i=1}^{n}\tau_i p} + D_{n0}(p)\, e^{\sum_{i=2}^{n}\tau_i p} + \ldots + D_{nn}(p) = 0. \tag{5}$$

If, in Equation (5), we take $m = 0$, we obtain the degenerate equation:

$$\prod_{i=1}^{n} S_i(p)\, e^{\sum_{i=1}^{n}\tau_i p} + D_{n0}(p)\, e^{\sum_{i=2}^{n}\tau_i p} + \ldots + D_{nn}(p) = 0. \tag{6}$$

Since the condition $m \to 0$ is equivalent to the unbounded increase of the loop gain, the problem of finding a structure which is stable under unbounded increase in gain reduces to the finding of the conditions for stability of Equation (5) when $m \to 0$.

We shall assume that the coefficients of the degenerate Equation (6) are such as to satisfy the conditions for stability. This may be attained by a proper choice of the parameters $F_{ni}(p)$ and $F_{mi}(p)$ (if not, further investigation would be meaningless).

The stability of the entire system will depend on the distribution of roots which tend to infinity as $m \to 0$.

Above all, we require that the degree of the polynomial $\alpha_{ik}(p)\alpha_{ki}(p)$ be less than that of $D_i(p)D_k(p)$. If this condition is satisfied, Equation (5) will have a nonvanishing leading term. According to a theorem of Pontriagin [4] and Neimark [6], there may, in the given case, be only a bounded number of roots in the left half of the complex plane, and the roots vary continuously as a function of the coefficients of the equation.

We divide Equation (5) by $m^n e^{\sum_{i=1}^{n}\tau_i p}$ and rewrite it in expanded form:

$$A_{00}p^{N_0} + A_{01}p^{N_0-1} + \ldots + \left(A_{0k} + B_{00}e^{-\sum_{i=1}^{n}\tau_i p}\right)p^{N_0-k} +$$

$$+ \left(A_{0k+1} + B_{01}e^{-\sum_{i=1}^{n}\tau_i p}\right)p^{N_0-k-1} + \ldots +$$

$$+ \frac{1}{m}\Big[A_{10}p^{N_1} + A_{11}p^{N_1-1} + \ldots + (A_{1b} + B_{10}e^{-\tau_1 p})\,p^{N_1-b} + \ldots +$$

$$+ (A_{1i} + B_{1i}e^{-\tau_1 p} + C_{10}e^{-(\tau_1+\tau_2)p})\,p^{N_1-i} + \ldots + A_{N1} + B_{1b}e^{-\tau_1 p} + \ldots +$$

$$+ L_{1e}e^{-\sum_{i=1}^{n}\tau_i p}\Big] + \ldots + \frac{1}{m^n}\Big[A_{n0}p^{N_n} + A_{n1}p^{N_n-1} + \ldots +$$

$$+ (A_{nj} + B_{j1}e^{-\tau_1 p})\,p^{N_n-j} + \ldots + A_{mN} + B_{jn}e^{-\tau_1 p} + \ldots + L_{jn}e^{-\sum_{i=1}^{n}\tau p}\Big] = 0, \tag{7}$$

where A_{ki}, A_{ik}, B_{ki}, B_{ik}, etc. are coefficients of the polynomials in Equation (5).

In Equation (7), let

$$N_0 - N_1 = 1, \quad N_0 - N_2 = 2, \ldots, \; N_0 - N_n = n, \tag{8}$$

meaning that each successive sum of polynomials in (7) is one degree lower than the preceding sum.

To find the number and character of the roots tending to infinity as $m \to 0$, we introduce a change of variable:

$$p = q/m. \tag{9}$$

Substituting (9) in (7), then multiplying the whole equation by m^{N_0} and allowing $m \to 0$, we obtain

$$A_{00}q^{N_0} + A_{10}q^{N_0-1} + A_{20}q^{N_0-2} + \ldots + A_{n0}q^{N_0-n} = 0.$$

Dividing this equation by q^{N_0-n}, we get

$$A_{00}q^n + A_{10}q^{n-1} + \ldots + A_{n0} = 0. \tag{10}$$

There will be n roots tending to infinity as $m \to 0$. The character of these roots depends on the coefficients of Equation (10). In order that the roots of Equation (10) tend to infinity to the left of the imaginary axis in the complex plane, it is necessary and sufficient that its coefficients satisfy the Routh-Hurwitz conditions.

We are thus led to the conclusion that, given Condition (8), the entire system will be stable if: a) Equation (10) which, just as for systems without lag, will be called the auxiliary equation of the first type, satisfies the conditions for stability, and b) the degenerate transcendental Equation (6) also satisfies the conditions for stability.

Consequently, stability may be attained if the stabilizer's transfer function is chosen so as to satisfy Condition (8), i.e., $N_0 - N_i = i$.

Let us now consider the case where

$$N_0 - N_1 = 2, \ldots, \; N_0 - N_n = 2n. \tag{11}$$

Using the transformation $p = q/m^2$ and elementary calculations similar to those used above, we obtain the auxiliary equation which determines the character and number of roots tending to infinity as $m \to 0$. This equation takes the form:

$$A_{00}q^{2n+1} + A_{01}q^{2n} + A_{10}q^{2n-1} + A_{11}q^{2n-2} + \ldots + A_{n0}q + A_{n1} = 0. \tag{12}$$

By analogy with systems without lags, we shall call (12) the auxiliary equation of the second type. Its construction is exactly the same as for systems without lags.

Thus, in the case where $N_0 - N_i = 2i$, the system will be stable as $m \to 0$ if a) the degenerate transcendental equation satisfies the stability conditions and b) the auxiliary equation of the second type also satisfies the stability conditions.

As is obvious from (12), the auxiliary equation of the second type is obtained from the leading two coefficients of the polynomials comprising the characteristic equation.

Finally, if $N_0 - N_i = 3i$, then the system will be unstable as $m \to 0$. The proof is carried out analogously with that given in [1-3, 5], and is based on the properties of the roots of binomial algebraic equations. We are thus led to the following conclusions.

In theory, and in practice, it is possible to obtain multiple-looped control systems with lags, which will be stable under unbounded increase in the individual loop gains. To achieve this the system must be constructed so as to satisfy the conditions derived above.

We elucidate now the connection between the stability conditions just obtained and the structure of the control system. To this end, we seek to define $N_0, N_1, \ldots, N_n$ in terms of other quantities.

From the structure of the leading coefficients in the polynomials of Equation (5), and from the definition of symbols in (3), we see that the differences of the degrees $N_0 - N_1, N_1 - N_2, \ldots, N_{n-1} - N_n$ are defined by $m_i + Q_i - n_i$, where m_i and n_i are, respectively, the degrees of the operators in the denominator and numerator of the stabilizer's transfer function, and Q_i is the degree of the operator for the element shunted by the stabilizer.

We are given the condition that $N_i - N_{i-1} \leq 2$.

Hence, the condition for choosing the structure must be a consequence of the following relationship:

$$m_i - n_i + Q_i \leq 2. \tag{13}$$

To find the order of the equation which describes the behavior of that portion of the loop which is shunted by a feedback path in a system allowing stability to be maintained under unbounded increase in loop gain, we use the relationship

$$Q_i \leq n_i - m_i + 2. \tag{14}$$

An analogous relationship may be obtained for systems with just one controlled quantity. On the basis of the foregoing investigations, the following conclusions may be drawn.

In order that a multiple-looped control system containing elements with lags remain stable under unbounded increase of its gains, it is necessary and sufficient that each individual control loop in which the gain may increase without limit belong to the class of structures which are stable for unboundedly large gains. Methods of synthesis and examples, for the case of systems with one controlled quantity, were treated in [3].

3. Autonomy of Multiple-Looped Control Systems When Elements with Lag are Present

In investigating the conditions for stability of a multiple-looped control system containing elements with lags, we assumed that the variation applied to the element with lag was equal to zero. Such an assumption was completely justifiable, since the stability is independent of the initial conditions.

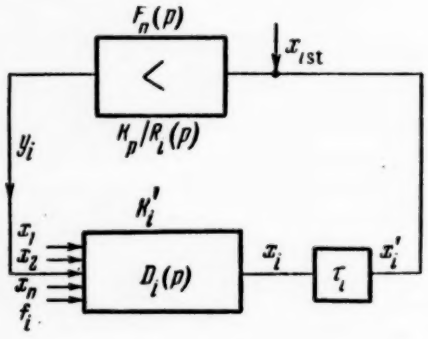

Fig. 3.

It is not possible, however, to assume zero initial values in investigating the conditions for autonomy, particularly if there are elements with lags in the system. Therefore, we shall set up the system equations for the case with nonzero initial conditions.

We consider the following cases: a) when stability for large gains is attained by introducing ideal differentiators into the system and b) when real differentiators are introduced to attain stability for large gains.

We shall set up the equations for the i'th loop. The equations for any other loop can then be obtained simply by changing $\underline{i}$ to the proper index. The schematic for the case under discussion is given in Figure 3.

The equation for the object, where the lag is not taken into account, is

$$D_i(p)\, x_i = K_i' \left[y_i + \sum \alpha_{ik} x_k + f_i \right], \tag{15}$$

where $\underline{k}$ takes all values except $\underline{i}$.

The equation for the element with lag is

$$x_i' = x_i (t - \tau_i). \tag{16}$$

The controller's equation is

$$R_i(p)\,y_i = K_{ip}[x_{ist} - x_i(a_0p^{n-2} + a_1p^{n-3} + \ldots + 1)], \tag{17}$$

where $n = R_i + D_i$ is the sum of the orders of the differential equations describing the processes in the i'th control loop.

We subject Equations (15), (16) and (17) to the Laplace transform. The transformed object equation is

$$D_i(p)\,x_i(p) = K_i'\left[y(p) + \sum \alpha_{ik}x_k(p) + f_i(p)\right] + D_{iL}(p)\,x_1(0). \tag{18}$$

The transformed equation for the element with lag is

$$x_i'(p) = e^{-\tau_i p}x_i(p) + \int_{-\tau}^{0} x_i' e^{-tp}\,dt = e^{-\tau_i p}x_i(p) + \psi_i(p)\,x'_i(0), \tag{19}$$

where $\psi_i(p) = \int_{-\tau}^{0} x_i' e^{-pt}\,dt$ takes into account the initial conditions from time $t = -\tau$ to time $t = 0$.

The transformed controller equation is

$$R_i(p)\,y_i(p) = K_{ip}[x_{ist} - x_i(p)(a_0p^{n-2} + a_1p^{n-3} + \ldots + 1)] + R_{iL}(p)\,y_i(0). \tag{20}$$

Solving Equations (18), (19) and (20) with respect to x_i, representing the controlled parameter, we obtain

$$\begin{aligned}[D_i(p)\,R_i(p)\,e^{\tau_i p} + K_i'K_{ip}(a_0p^{n-2} + a_1p^{n-3} + \ldots + 1)]\,x_i(p) + \\ + K_iR_i(p)\sum\alpha_{ik}x_k(p)\,e^{\tau_i p} = \{K_iK_{ip}x_{ist} + K_i'\psi_i(p)\,x_i'(0)(a_0p^{n-2} + \\ + a_1p^{n-3} + \cdots + 1) + K_i'R_{iL}(p)\,y_i(0) + K_i'R_i(p)\,f_i(p) + \\ + R_i(p)\,D_{iL}(p)\,x_i(0)\}\,e^{\tau_i p}.\end{aligned} \tag{21}$$

We divide Equation (21) by K_{ip} and let $1/K_{ip} = m_i$; then, assuming K_{ip} to be a sufficiently large number, we get

$$\begin{aligned}[m_iD_i(p)\,R_i(p)\,e^{\tau_i p} + K_i'(a_0p^{n-2} + a_1p^{n-3} + \ldots + 1)]\,x_i(p) + \\ + K_i'm_iR_i(p)\,\Sigma\alpha_{ik}x_k(p)\,e^{\tau_i p} = \{K_i'x_{ist} + m_iK_i'\psi_i(p)\,x_i'(0)(a_0p^{n-2} + \ldots + 1) + \\ + m_iK_i'R_{in}(p)\,y(0) + m_iK_i'R(p)\,f_i(p) + m_iR_i(p)\,D_{iL}(p)\,x_i(0)\}\,e^{\tau_i p}.\end{aligned} \tag{22}$$

We now determine the influence of the initial conditions. We shall assume that in the time interval from $-\tau$ to 0, the function x_i and its derivatives are finite-valued and that, at the instant $t = 0$, $y(0)$ and all its derivatives are also finite-valued. Then, as is obvious from Equation (22), the larger K_{ip}, the less will be the influence of the initial values of x_i and y_i and their derivatives on the transient response. In the limit, this influence will vanish. We have thus demonstrated that even with lags present the problem of finding the conditions for autonomy can be investigated with zero initial conditions. However, a peculiarity of the stabilizing method under consideration (the introduction of an ideal differentiator at the input to the entire system) is this, that in the limit as $m \to 0$, the equation ceases to depend on the lags, and the system becomes unstable. Hence, the insertion of ideal differentiators at the input to the system as a means of obtaining autonomy by increasing the gain does not appear possible. This might have been assumed even without a proof, since the introduction of an ideal differentiator at the system input is equivalent to shunting the entire system with a stabilizing link with the operator equation $(a_0p^{n-2} + a_1p^{n-3} + \ldots + a_{n-3}p)x_{out} = x_{in}$.

Such a system cannot be stable as $K_p \to 0$, since along with everything else, the stabilizer also shunts elements with lags.

Let us now consider the case in which an ideal differentiator shunts part of the loop in such a manner that the delimited system [5] remains stable under unbounded increase of the gain in the shunted part of the loop.

For the i'th loop we have the following equation*:

$$[D_i(p)N_i(p)Q_i(p)\ e^{\tau_i p} + K_{ish}D_i(p)N_i(p)F_{in}(p)e^{\tau_i p} + K_{ito}]x_i + \\ + K_i\{N_i(p)Q_i(p) + K_{ish}N_i(p)F_{in}(p)\}\Sigma\alpha_{ik}x_x = K_i[N_i(p)Q_i(p) + \\ + K_{ish}N_i(p)F_{in}(p)]x_{ist} + [N_i(p)Q_i(p) + K_{ish}N_i(p)F_{in}(p)]f, \quad (23)$$

where K_{ito} is the total gain of the loop; the other symbols have reference to Figure 4.

The order of the highest ideal differentiator $F_{in}(p)$ is chosen so as to guarantee stability for unbounded increase of K_{ish}.

We divide Equation (23) by K_{ish} and then let $K_{ish} \to \infty$. The degenerate equation will then have the form:

$$[D_i(p)N\ (p)F_{in}(p)e^{\tau p} + K_i]x_i + K_iN_i(p)F_{in}(p)\Sigma\alpha_{ik}x_k = \\ = K_ix_{ist}N_i(p)F_{in}(p) + N_i(p)F_{in}(p)f_i. \quad (24)$$

As is clear from a consideration of Equation (24), it is not possible to obtain autonomy solely by the expedient of increasing the gain, since the degenerate equation contains the term $N_i(p)F_{in}(p)\Sigma\alpha_{ik}x_k$ and the processes in such a system will be influenced by all the other controlled quantities.

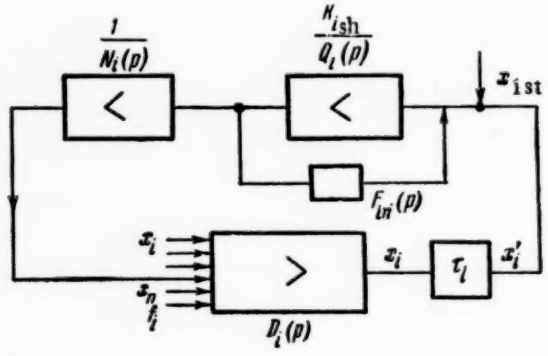

Fig. 4.

To achieve autonomy we proceed exactly as in the case where the system did not contain lag elements [2]. At the input of the stabilizer we introduce a signal of the form:

$$\Sigma\alpha_{ik}x_k. \quad (25)$$

Here, the system equation becomes:

$$[D_i(p)N_i(p)Q_i(p)e^{\tau_i p} + \\ + K_{ish}D_i(p)N_i(p)F_{in}(p)e^{\tau_i p} + K_{ito}]x_i - \\ - K_i'\{[N_i(p)Q_i(p) + K_{ish}N_i(p)F_{in}(p)]x_{ist} + \\ + [N_i(p)Q_i(p) + K_{ish}N_i(p)F_{in}(p)]\Sigma\alpha_{ik}x_k\} - K_{ish}K_i'N_i(p)F_{in}(p)\Sigma\alpha_{ik}x_k = \\ = [N_i(p)Q_i(p) + K_{ish}N_i(p)F_{in}(p)]f_i. \quad (26)$$

The equation for any other loop is written similarly. It is necessary only to replace the index i by the index for the desired loop, and to omit this latter index from the sum, Σ.

We divide Equation (26) by K_{ish} and allow $K_{ish} \to \infty$. In addition, we assume that $K_i' = 1$. The degenerate equation may then be written as:

$$[D_i(p)N_i(p)F_{in}(p)e^{\tau_i p} + K_{ide}]x_i = K_{ide}N_i(p)F_{in}(p)x_{ist} + \\ + K_{ide}N_i(p)F_{in}(p)f_i, \quad (27)$$

*We write the equation with zero initial conditions, since the previous demonstration showed that increasing K_p to infinity in fact leads to zero.

where $K_{i\,de}$ is the gain entering in the degenerate equation. This gain does not depend on $\Sigma\alpha_{ik}x_k$. Analogous results are obtained in all the other cases.

Thus, supplying a supplemental excitation of the type (25) to the input of the stabilizer, plus increasing the gain, $K_{i\,sh}$, guarantees that the processes in the individual loops proceed autonomously, without mutual interactions, throughout the multiple-looped control system with lags. This is only true, of course, if the conditions requisite for stability under unbounded increase of the loop gains are satisfied.

Finally, we consider the case where stability for unbounded K_{ip} is obtained by introducing real stabilizers into the system.

The stabilizer for the i'th loop can be represented by:

$$\frac{F_{in}(p)}{F_{im}(p)}. \tag{28}$$

Calculations analogous to those carried out above show that autonomy under unbounded increase of the gain of the shunted portion of the i'th loop is attained for that loop is there is introduced, at the input to the stabilizer of that loop, a supplemental excitation of the type $\Sigma\alpha_{ik}x_k$, where $\underline{k}$ takes on all values except $\underline{i}$.

Thus, we have extended to systems containing lag elements the results obtained earlier [1, 2, 3] for the synthesis of multiple-looped control systems which would be stable under unbounded increase of the individual loop gains, and the results concerning the necessary conditions for autonomy. In all this, of course, it is understood that lag elements may occur in all the loops, or only in some of them.

LITERATURE CITED

[1] M.V. Meerov, Proc. Conference on Automatic Control, Vol. 1 [in Russian] (Izd. AN SSSR, 1955).

[2] M.V. Meerov, "Autonomy in multiple-looped automatic control systems," Automation and Remote Control (USSR) 17, 5 (1956).*

[3] M.V. Meerov, "Stabilization of systems with lags," Automation and Remote Control (USSR) 16, 5 (1953).**

[4] N.G. Chebotarev and N. G.Meiman, "The Routh-Hurwitz problem for polynomials and integral functions," Trudy Mat. Inst. AN SSSR (1949).

[5] Ia.Z. Tsypkin, "Systems with lagging feedback," (Doctoral Dissertation) Trudy Nauch.-Issledovatel Inst. Samolet. Oborud. MAP,*** SSSR (Izd. BNT, 1947).

[6] Iu.I. Neimark, "D-decomposed space of quasi-polynomials," Prikladnoi Matematika i Mekhanika, 1950, No. 3.

Received February 1, 1957

*Original Russian pagination. See C.B. translation.

**As in original – Publisher's note.

***Ministry of the Aircraft Industry.

ANALYSIS OF BLOCK DIAGRAMS FOR SERIAL ELECTRONIC COMPUTERS

A. Mikhailov

(Moscow)

An analysis is made of the utilization of the working time and the components in serial electronic digital computers. The logical design and the type of problems to be solved are considered in relation to computing speed and other characteristics. A comparison is made of one, two and three address systems for coding commands.

INTRODUCTION

In designing digital electronic computers with a view to minimizing cost and increasing reliability, an attempt must be made to reduce the number of components in each section of the computer to a minimum. For this purpose the well-known algebraic methods for synthesizing relay networks can be used. Algebraic methods may also be used in designing computer assemblies having clearly defined logical functions – computing and control sections. These methods alone, however, do not allow the entire block diagram to be formulated, since the characteristics of the computer depend not only on the performance of the separate sections but also on the efficiency with which the arithmetic, storage and control units are composed from these sections and the manner in which the connections between the units are taken into account.

Heretofore there have been no methods for rationally designing block diagrams, nor have there been objective criteria for evaluating various computer block diagrams. Only certain aspects of these problems have been dealt with in [1, 2]. In the present article an attempt is made to solve the problems of the rational choice of engineering parameters for serial computers, having in mind chiefly those with delay-line type storage. In the fields where computers are most widely used, that is, in the automation of production, the serial type computers are the most effective.

The fundamental requirements are: economy of components, low maintenance and construction costs, reliability, small dimensions and weight. As the rate of most automatic production processes is low compared to the operating speed of the computer, no very high speeds are demanded from the latter, such as can only be attained by parallel computers. But this in no way reduces the demand for a highly efficient utilization of the component parts, i.e., attaining maximum computing rate with a given number of components, or attaining a given computing speed with a minimal number of components.

1. Serially Operating Storage Unit

There are many differences between the design of serial and parallel computers. These result from the use in the serial computer of a storage unit operating in a serial mode; this may be a magnetic drum, an acoustic or magnetostriction delay line, etc. In this case, the storage of coded information in the storage unit is a dynamic, cyclically repeated process. In each channel of the storage unit, i.e., in the delay lines, in the track round the drum, etc., there are several words, and each of these passes successively past devices which scan them and record them. The position of the word in the serial storage section has a distribution in space according to the number of the channel and also in time, according to the location in the channel.

In connection with the utilization of the time coordinate, access to the store for taking out or putting in a word includes two operations: waiting for the word, and selecting (sending) it. Waiting for the word occupies a

time which lasts from the moment of selecting the channel to the moment when the first pulse of the required word appears at the output of the store, when the selection process starts. Selection ends when the last rank of the coded word is transmitted.

Waiting time (in the sense of selection of codes and not in the means for their transmission) constitutes one of the drawbacks of serial type storage units as distinct from storage units of parallel action which function statically, for instance cathode ray tubes, ferrite cores, etc. In storage units of parallel operation the position of the code is determined purely in terms of spatial coordinates, and access time to the storage unit is identical with selection time.

The use of serial storage units inevitably results in a considerable proportion of the working time being used up in waiting for codes. The waiting time, because it is essentially random, is difficult to utilize for any operation; as a rule this constitutes lost computing time, the idling time of the computer. On the other hand, selection time is useful time, because one of the necessary arithmetical or control functions (for instance, summation of a number taken from storage unit and another previously recorded in the arithmetic unit of the computer) can be carried out at the same time that the word is being selected or recorded. Therefore in analyzing the action of a serial computer one must divide time of access to storage units into selection time and waiting time.

The most important point in the design of a serial type computer consists in determining the most profitable relation between the time spent in useful operation and in waiting time. This necessitates an analysis of time utilization and component utilization.

In analyzing the utilization of time it is most convenient not to use absolute units, but "computer" units of time, in which we agree to define the minor cycle t_c as the cycle in which all the serial impulses of a single word are recorded, and a major cycle T_c is defined as the time required to inscribe all the serial words of a single channel of the storage unit. The major cycle contains an integral number of minor cycles. The ratio

$$r = T_c/t_c, \tag{1}$$

which shows how many codes are contained in a single channel of the storage unit will be called the index number of the major cycle.

Measurement of the time in the cycles helps in the logical design of the block diagram, without going into its details or considering its separate components and blocks. This also facilitates comparison of block diagrams of different machines, even when the latter have different rates of operation.

2. Average Speed of Carrying Out Instructions

There is a great deal in common to all the various arrangements of serial computers. The carrying out of each instruction consists of several phases constituting successive operations all concerned with access to store. For instance, a single-address arithmetic operation is carried out in two parts: the first part consists of obtaining the number of the next instruction and putting it into the block controlling the storage unit, waiting, selecting the instruction from the store and transferring it to the control section; the second part consists of putting the address into the control block of the storage unit, waiting, selecting the number and carrying out the arithmetic operation indicated in the instruction. A three address instruction consists of four parts: encoding the instruction, transferring the first number from the storage to the arithmetic unit, transferring the second number and performing the arithmetical operation, transferring the result from the arithmetic section to the storage unit. In computers with a fixed decimal point, as a rule, each separate operation other than waiting occupies one minor cycle. The number of such necessary cycles c is constant; it is determined by the system of encoding instructions which have been placed in the control section. Thus, in the example of the one address instruction given above, $c = 4$, there being two cycles of setting up the addresses and two cycles of selecting the codes. With a three-address system of instructions $c = 8$ for each two cycles (for setting up the address and for selecting the code) in each part. Since the number of parts n exceeds by one the number of addresses in the instruction m, we may consider that for computers with a fixed decimal point

$$c = 2n = 2(m + 1). \tag{2}$$

In certain instructions, such as multiplication or division, one cycle of selection is not sufficient to arrive at a result and several subsidiary cycles u are required, whose number is constant and is determined by the composition of the arithmetic and control units of the computer.

The number of waiting cycles w is independent of the structure of the arithmetic and control units of the computer. This number is usually determined by the chance combination of the time coordinates of the instruction itself and of the addresses recorded in it. It is known only that within the limits of one part

$$0 \leqslant w_i \leqslant \tau - 1, \tag{3}$$

where $w_i = 0$ constitutes the most favorable case, when the indicated address of the instruction of the codes appears at the output of the storage unit immediately after a cycle which enumerates the spatial coordinate, and $w_i = \tau - 1$ is the least favorable case, and here the decoding of the spatial coordinate occurs in the same cycle in which the selection is made. In the general case we may write

$$w_i = \alpha_i (\tau - 1), \tag{4}$$

in which the coefficient α_i is a measure of the unfavorableness of the combination of time coordinates. It is clear that

$$0 \leqslant \alpha_i \leqslant 1. \tag{5}$$

Since all values α_i in the range (5) are equally probable, the most probable value of α_i is its arithmetic mean $\alpha_c = 0.5$.

For a computer with a fixed decimal point we may write the following expression for the length of time t_k required to carry out one instruction (in minor cycles):

$$t_u = c + u + \sum_{i-1}^{n} w_i, \tag{6}$$

where

$$\sum_{i=1}^{n} w_i = \alpha (\tau - 1) n. \tag{7}$$

If we extend these expressions to cover the greatest possible number of instructions which the computer must carry out in solving problems, then Expression (6) will indicate the time required to carry out the average instruction. In this case, c does not change, because, as a rule, it has the same value for all instructions of the particular system of coding. But the numbers of subsidiary cycles will depend on what fraction of the instructions carried out by the computer correspond to instructions requiring subsidiary arithmetic cycles. For instance, suppose the instructions are divided into two groups, namely a portion β of long groups of the multiplication type, for which the number of subsidiary cycles is equal to u, and short groups, of the addition type for which $u = 0$; then the average value must be taken as equal to βu. We now obtain from Equation (7)

$$t_c = c + \beta u + \alpha (\tau - 1) n. \tag{8}$$

The reciprocal of t_c has the value

$$v_c = \frac{1}{c + \beta u + \alpha (\tau - 1) n} \tag{9}$$

and represents the average rate of carrying out an instruction in a computer of the fixed decimal point type in relative units, i.e., reciprocal cycles. Knowing the relative speed, it is always possible to transfer to absolute speeds in instructions per second, as the duration of the minor cycle t_c is known. The latter is determined by the number of ranks in a single word and by the speed of response of the components.

It is to be understood that these expressions are extremely general and corrections are necessary before applying them to particular instances, as for instance: selection of two or three instructions during one single access to the storage unit; the presence of instructions for an exchange of words between internal operative memory cells of the arithmetic unit and other instructions not requiring access to the storage unit; division of the storage unit into groups with various multiples of the major cycle, etc.

These formulas may be extended to apply to computers which perform operations on numbers while taking rank into account (computers with a floating decimal point), if it is borne in mind that in the latter, on account of the operations of normalization and equalization of ranks, the number of additional arithmetic cycles $\underline{u}$ will not be constant and will depend on the nature of the problems being solved.

3. Coefficients of Utilization of Time and Utilization of the Structural Elements

In Formulas (8) and (9) the sum $c + \beta u$ gives a number of useful cycles, and the expression $\alpha(\tau - 1)n$ shows the number of cycles spent in waiting. The equation

$$\eta_c = \frac{c + \beta u}{t_c} = \frac{1}{1 + \frac{\alpha(\tau - 1)n}{c + \beta u}} \tag{10}$$

shows what fraction of the working time in the serial computer is used up in useful operations, and consequently is, to a certain extent, a criterion of the efficiency of utilization of the elements in the computer. We will call the quantity η_c the coefficient of time utilization. It is affected by the following factors: 1) the structure of the storage device of the computer – the multiplicity of the major cycle τ, 2) the structure of the control unit of the computer – the quantities $\underline{c}$ and $\underline{n}$, 3) the structure of the arithmetic unit – the magnitude of $\underline{u}$, 4) the type of problems solved – the magnitudes of α and β.

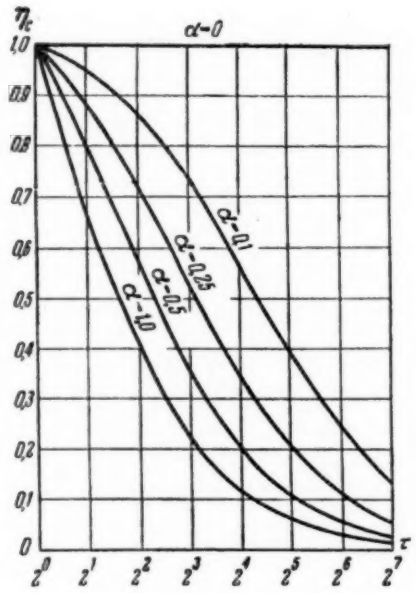

Fig. 1. Dependence of the coefficient of time utilization on the repetition of the major cycle and on the correspondence of the time addresses for $\beta = 0$, $c = 2n$.

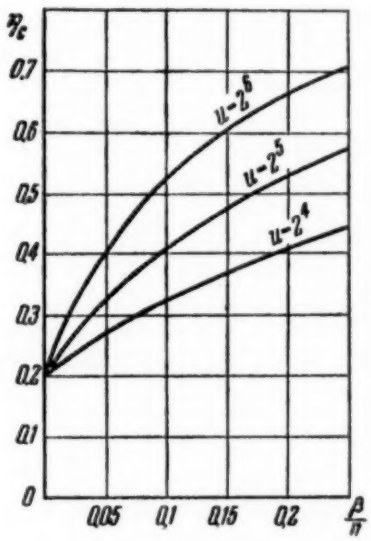

Fig. 2. Dependence of the coefficient of time utilization on the number of subsidiary arithmetical cycles and on the relation between long and short instructions in a program where $\alpha = 0.5$, $c = 2n$, $\tau = 2^4$.

Figures 1 and 2 show graphs indicating the relation between the coefficient η_c and the quantities enumerated above. From graphs in Figure 2 which have been drawn for $\tau = 2^4$, it can be seen that in the neighborhood

of the most probable values of $\beta/n = 0.05$ (20% multiplications in three-address instructions) the serial computer expends less than 40% of the working time using the arithmetic and control units.

When τ is reduced, the coefficient η_c increases (Figure 1), and in the limiting hypothetical case when $\tau_{min} = 1$ it has the value $\eta_{max} = 1$. Accordingly, by reducing the waiting time the speed v_c increases until it reaches the limit $v_{max} = 1/(c + \beta u)$. If $c + \beta u$ does not change, then the graph of $\eta_c = f(\tau)$ is also a graph of the relative speed $v_c/v_{max} = f(\tau)$, a function of τ.

However, increasing the computing rate by reducing τ, i.e., by shortening the length of the channels in the storage unit and, consequently increasing the number of elements or reducing the number of words kept in the storage unit is by no means always justified although it does result in an increase in η_c. It may also appear to be uneconomical to reduce the number of elements in the storage unit by increasing τ, since that leads to a reduction of v_c and η_c. In order to find optimal values for τ, v_c and η_c, one must consider that the electronic digital computer, like every industrial device, must fulfill the requirements of the maximum effective utilization of its constituent parts. The coefficient η_c reflects the utilization of elements only in the arithmetic and control units of the computer and does not include the storage section, since at any one moment only one of the channels of the storage unit is involved in carrying out an operation, and not the whole of the storage section. An index of the efficiency of the utilization of the elements of the computer as a whole is the ratio of the speed of carrying out instruction v_c to the number of structural elements z in all the basic units of the computer, i.e., the coefficient

$$\vartheta = \frac{v_c}{z}. \tag{11}$$

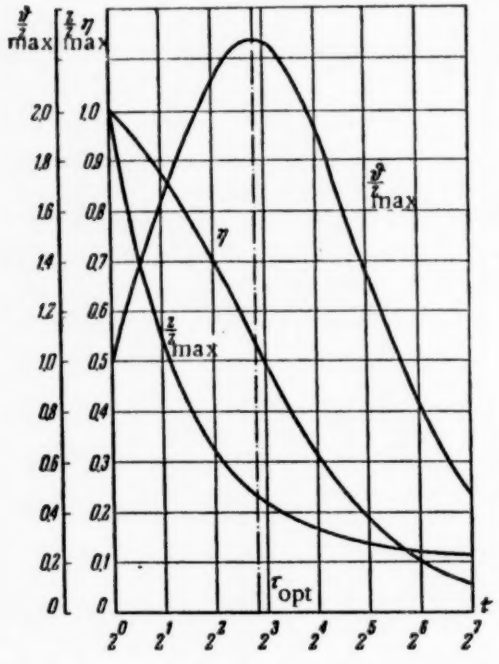

Fig. 3. Variation of the number of structural elements in the computer and the coefficient of utilization with the repetition of the major cycle for $\alpha = 0.05$, $\beta/n = 0.05$, $kb/\alpha = 2^3$, $u = 2^5$, $c = 2n$.

By the term structural element we here mean what is conventionally called a block, consisting of one electronic tube (or the equivalent semiconducting device) and the associated components. The coefficient of utilization of the elements ϑ is the objective criterion of technical efficiency of the computer. From the magnitude of this coefficient one can estimate the advantage of one or another variant of the block diagram of the computer. Further, it may be used to compare the economy of the various computers.

According to the change in ϑ one can decide whether it is worthwhile to introduce one or another supplementary block into the computer for the purpose, for instance, of increasing the computing rate or making the computer easier to use. In particular, the question discussed previously of choosing an optimum value for τ, v_c and η_c can be decided as follows.

If, in the arithmetic and control unit of the computer, there are a structural elements, and if, in one channel of the storage unit and control block there are b equally expensive elements for k codes in the whole storage unit and τ codes in one channel, then the sum total of the elements in the computer will be

$$z = a + \frac{k}{\tau} b. \tag{12}$$

With a change in the number of words in the channel there is some change in the number of elements in the amplifying circuits which constitute part of the equipment which makes up the channel. Therefore, Equation (12) can be used for purposes of investigating a wide range of changes in the value of τ. By defining the maximum of the coefficient ϑ or the minimum of its reciprocal as

$$\frac{1}{\vartheta} = \left(a + \frac{k}{\tau}\, b\right)[c + \beta u + \alpha(\tau - 1)n],$$

we can find the optimal value of τ:

$$\tau_{opt} = \sqrt{\frac{kb}{a}\left(\frac{c + \beta u}{\alpha n} - 1\right)}. \tag{13}$$

From this expression it follows that in deciding τ, the following factors must be considered; the capacity of the storage unit (number of words in it); the relation between the number of elements in the arithmetic and control units on the one hand, and the number of elements constituting a single channel of the storage unit on the other; the structure of the arithmetic and control units; the type of problem solved in relation to instructions of different duration. The relationship $\vartheta/z_{max} = f(\tau)$ is drawn as a graph in Figure 3.

One way of improving the characteristics of computing machines is by perfecting the separate assemblies and blocks, and another is by a rational design of the block diagram. In this article, we consider only the latter.

The characteristics ϑ, v_c and η_c are improved by reducing the parameter α. Methods are known which allow α to be reduced by various modifications of the circuits of the storage, arithmetic and control units of the computer. For instance, dividing the basic storage unit into several channels with a small number of words in each ($\tau/4$, $\tau/8$), introducing into the arithmetic unit subsidiary registers with a capacity of one or two words and instructions for the exchange of words between these locations, introducing into the control unit subsidiary registers to facilitate and speed up the work with cyclically repetitive sub-programs, etc. Methods are also known which, generally speaking, do not require the introduction of subsidiary elements into the computer – the so-called "optimum programming" – the setting up of addresses (more precisely time coordinates in the addresses) corresponding to the demands for a minimal waiting time of the codes of numbers and the instructions themselves.

The possibilities of increasing the speed by reducing $\underline{i}$, and still more, $\underline{c}$, are very limited. To reduce $\underline{i}$ and simplify the diagram of the arithmetic unit in such instructions as multiplication, it is possible to dispense with the production of double-length words and to form an approximate result. Further multiplication can be carried out by a method in which in one cycle two of the multiplier pulses are taken together and summed as two partial products. Reduction of $\underline{c}$ is possible only at the expense of cycles of setting up the addresses in the blocks controlling the storage unit, but not at the expense of cycles of selection, since in most computers a single storage unit is used both for numbers and for instructions. These measures are not very effective.

The parameter β, which affects v_c and η_c, depends first of all on the kind of problem, i.e., on the relation between the groups of instructions which are distinguished according to the time of their execution. But the magnitude of β is reflected both in the values of $\underline{c}$ and $\underline{n}$, the relation between which is given in (10) and (13), as well as in the choice of systems of coding of instructions.

4. Comparison of Systems of Codification of Instructions

The most commonly used are the one-address and two-address systems of coding instructions. The chief advantage of the single-address system is its flexibility. The program from one-address instructions does not contain any superfluous operations, as in each instruction only a single operation is specified. On the other hand, in a three-address instruction two other operations are automatically carried out together with the basic operation – the preparatory and the concluding (transfer of the first number to the arithmetic unit, despatch of the result to storage unit, etc.). There are relatively fewer instructions for a given program in a three- than in a one-address instruction. Nevertheless, the subsidiary operations of a three-address instruction are by no means always necessary. Thus, in summing a large number of terms there is no need to send the intermediate sum to storage unit after each instruction, and in this case, the three-address system, if it has no prohibition of subsidiary operations, is inferior to the one-address system. It is established that for equal problems the parameter β in the one-address system is smaller than in the three-address system, since in the first case all the subsidiary operations are carried out by independent instructions, as a consequence of which the number of instructions in the program increases and the fraction of instructions with subsidiary arithmetic cycles is reduced.

In comparing one- and three-address systems of coding instructions, one should start by considering the

average speed of performing arithmetic operations, remembering that in a one-address system, there may be from one to three instructions per operation. However, in view of this, we can also compare systems of coding according to the speed of carrying out instructions. If both a one-address and a three-address computer have a set of stored instructions allowing them to carry out identical arithmetical operations and have identical values of τ and u, and expend two half-cycles in each phase on the necessary operations, then the time elapsing in carrying out the average instruction in the one-address computer will be $t_1 = \beta_1 u + 4 + 2\alpha(\tau - 1)$, and in the three-address computer it will be $t_3 = \beta_3 u + 8 + 4\alpha(\tau - 1)$.

The relative speeds will then be given by

$$\frac{v_1}{v_3} = \frac{t_3}{t_1} = 2\left(1 + \frac{\frac{1}{2}\beta_3 - \beta_1}{\beta_1 + \frac{2}{u}[2 + \alpha(\tau - 1)]}\right). \tag{14}$$

The single-address system would have an undoubted advantage in computing speed as compared with the three-address system, and $v_1/v_3 = 3$. But for more typical values of the parameters in Formula (14), the ratio v_1/v_3 varies between 2.3 and 2.4.

This shows that in a one-address system each operation involves access to storage unit for the instruction, with the inevitably associated waiting cycles, whereas in the three-address instruction one such access is required for each basic and each two subsidiary operations. However, it must be noted that, due to the flexibility of the single-address system, the difference in the speeds is reduced as a result of the difference in the number of instructions. To decide finally in favor of one system or the other, statistical indices β_1 and β_3 are required, obtained by analyzing the programs of the two systems as required for the solution of identical problems. By comparing the number of instructions in both programs, one can obtain from the comparison an index of effectiveness of the instructions of the two systems.

Besides the systems considered above, computers also use a two-address system. In the two-address instruction the type of operation and the address of the two numbers are recorded, and the result is sent to the address of the second number, obliterating it. The experimental solution of problems showed that in 80 to 95% of the cases one of the two numbers does not have to be preserved for subsequent calculations. According to the number of instructions, the program may be 10 to 20% longer than in the three-address system, but the number of pulses in the two-address instruction is 1.35-1.4 times less than in the three-address instruction. Also, the waiting cycle of the third address is excluded from the control operation, and this simplifies the control unit.

Since in the two-address coding just as many operations are programmed as in the three-address instruction, carrying out the instruction naturally takes place in four phases. In the two latter of these (choosing the second number from the storage unit and sending the result into the storage unit) the same second address is used, with its temporal portion unchanged. This means that the last phase of the instruction does not terminate earlier than one cycle after the selection of the second number. But since most of the operation of the basic third phase is completed at the moment of entry of the second number into the arithmetic unit, the waiting time in the latter is also equal to $\tau - 1$ minor cycles, and the time for carrying out the instruction is

$$t_2 = c_2 + \beta_2 u + (3\alpha_c + 1)(\tau - 1). \tag{15}$$

For comparison of two-address and three-address systems with respect to speed, Figure 4 shows graphs of $v_c = f(\tau)$ and $t_c = f(\tau)$. From these it follows that in the region of the practically useful values of τ the two-address system is inferior to the three-address one in speed; in considering differences in the number of instructions there are also considerable differences between the two systems. The basic reason for the reduction in speed is the greater waiting time wasted in the third phase. It is therefore important to find to what extent the last phase is necessary and under what conditions it can be dispensed with.

In a computer with a fixed decimal point, the fourth phase in a two-address system is due to the time delay in the computing circuit. In travelling from the output of the storage channel through the computing unit and again to the input into the same channel, the digit pulses become considerably delayed in time, so that the result cannot be sent at once into the same positions from which the corresponding impulses of the second number were taken; it is necessary to wait until these positions make one complete turn in the storage channel and again appear under the inscribing elements.

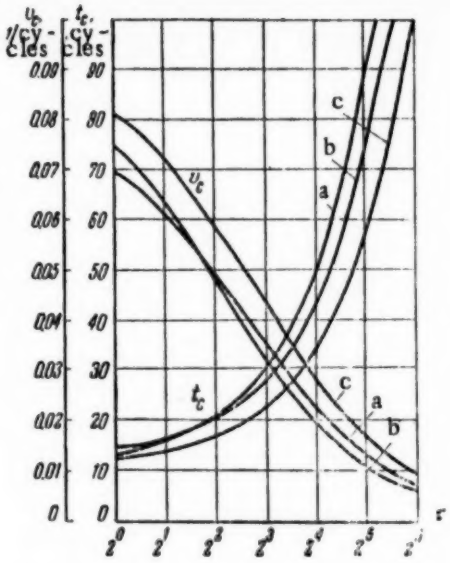

Fig. 4. Length of t_c and average rate v_c of carrying out instructions in three-address and two-address systems for $\alpha = 0.5$, $\beta = 0.2$, $c = 2n$, $u + 2^5$: a) three-address system; b) two-address four-phase; c) two-address three-phase.

It is well known that storage units such as sonic delay lines allow some latitude in deviation of the phase of the pulses, introduced into or circulating in it, from the precise values determined for them by the clock pulses which synchronize all the blocks of the computer. It is because of this latitude that parallel working of several tens of channels in one storage unit is possible. With a sufficiently rapid action of the elements of the above-mentioned route, it is evident that some portion of this latitude may be utilized for equalizing the phases of the lagging-pulses of the result. This also makes it possible to realize a three-phase two-address system in which the result is dispatched at the moment it is formed. As has already been noted, in computers with a fixed decimal point, in most instructions this moment coincides with the moment of selection of the second cycle. In other instructions, for which u is not equal to 0, this moment often occurs one or several major cycles later, i.e., again at the nearest convenient minor cycle not requiring waiting.

The second variant on realizing a three-phase system consists of splitting the delay in each channel of the storage unit. If the full time of circulation of the code in the channel T_c is divided into two unequal parts $T_c - \Delta t$ and Δt (Figure 5) so that the Δt portion corresponds to the delay introduced by the blocks of the arithmetic unit, it is then possible to compensate for a delay of any magnitude. Division of the delay is always possible in a storage device of serial operation, working on the principle of continuous renewal of the stored information, by taking it out and inscribing again, as is done in sonic or magnetostriction delay lines, and in the magnetic drum with continuous reading-off and inscribing.

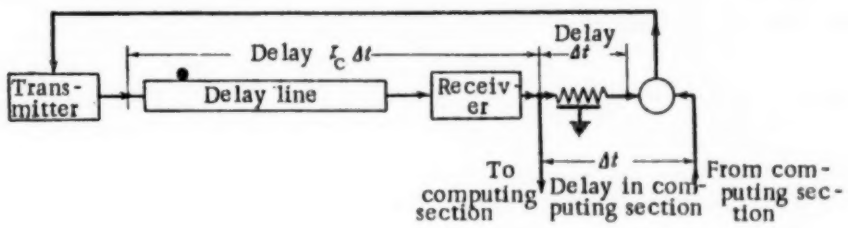

Fig. 5. Splitting the delay in the channel of the storage unit.

The time for carrying out the average instruction in a three-phase two-address system is determined by Formula (8). If we suppose that the parameter β'_2 in this system is practically equal to β_3, then

$$\frac{v_2}{v_3} = \frac{t_3}{t_2} = \frac{4}{3}\,\frac{[2+\alpha(\tau-1)]+\frac{1}{4}\beta_3 u}{[2+\alpha(\tau-1)]+\frac{1}{3}\beta'_2 u} \approx \frac{4}{3}. \qquad (16)$$

The coefficient η'_2 in this system has a higher value than in the three-address system, which is shown by the equation

$$\frac{\eta'_2}{\eta_3} = \frac{1+\dfrac{\alpha(\tau-1)}{2+\frac{1}{4}\beta_3 u}}{1+\dfrac{\alpha(\tau-1)}{2+\frac{1}{3}\beta'_2 u}}. \qquad (17)$$

Figure 4 shows a graph of t_c and v_c for the two systems.

Thus the three-phase two-address system is superior to the three-address system in its utilization of the storage capacity, in its utilization of the elements, and in the simplicity of its diagram. With respect to the different number of instructions in the two cases, the three-phase two-address system is in no way inferior to the three-address system in the rate of carrying out the instructions. It must be noted that in the three-address system it is impossible to reduce the number of phases.

SUMMARY

1. The working process in a serial type computer with delay-line type storage has a coefficient of time utilization η_c not greater than 30-40%. Therefore, to increase the rate of carrying out instructions the most effective measures are those which increase the utilization of the working time by reducing the waiting time.

2. The over-all performance of the computer with serial operation is given by the coefficient of utilization of the structural elements ϑ. By using this coefficient one can describe the performance of one or the other variant of the block diagram and assess the value of various improvements introduced into the block diagram.

3. The rate of carrying out instructions, and consequently the computing rate of the serial type computer, depends very much on the basic characteristic of the storing arrangement of repetition τ of the major cycle. For a given storage capacity in actual circuits of blocks and basic arrangements of computers there is an optimal value of the repetition of the major cycle which gives the highest degree of utilization of the structural elements.

4. In serial computers carrying out operations on numbers without respect to sequence (with a fixed decimal point), it is advisable to use a three-phase two-address system of instructions, as this gives a higher computing rate and better utilization of the elements in comparison to other systems.

LITERATURE CITED

[1] E.I. Mamonov, Optimal speed of working and other technical indices of the operation of information storing devices.* Report at the conference "Methods of development of Soviet mathematical machine and apparatus construction," March, 1956.

[2] A.L. Freedman, Elimination of waiting time in automatic computers with delay type stores. Proc. Cambr. Phil. Soc. Vol. 50, No. 3 (1954).

Received November 5, 1956

*In Russian.

THE SYNTHESIS OF MIXED RELAY SYSTEMS OF CLASS II

V. N. Roginskii

(Moscow)

Analytic methods for transforming relay circuits and methods of deriving mixed relay circuits by introducing elements of finite conductivity are considered. It is shown that if these methods are used in synthesizing multi-relay circuits the number of contacts required may be reduced.

The design of a relay system falls into two sections: compilation of the structural diagram and electrical calculation of the elements.

Engineers' methods for electrical relay calculations for various operating conditions are quite well developed. Little work has so far been done on structure synthesis and solutions have only been obtained for a small class of systems.

Existing structural synthesis methods [1-4] enable one to derive an analytic formula for each relay in the circuit from the given operating conditions. The solution is usually found in the normal form (more rarely in the inverse form), i.e., as a two-terminal contact network in series (parallel) with the relay coil.

The next step is to transform the formulas in such a way as to give maximum contact elimination, so a circuit with the least possible number of contacts is obtained. But in most cases the system remains of normal (inverse) type after such action.

In many cases the circuit can be simplified if mixed circuits are used, i.e., ones in which contact circuits can be either in series or in parallel with the relay windings and resistors can also be included.

In such circuits the operation of any relay will not only be determined by the open or closed states of the contact circuits, but also by the relations between the parameters of the relay and the other elements included in the circuit of the relay.

Here we consider methods of transforming the structures of class II relay circuits analytically so as to give mixed circuits with defined relationships between the parameters of the elements present.

1. The Conductance of a Relay Circuit

A contact circuit consisting of single contacts can be either open- or short-circuited, the conductance being in the first case infinitely small and in the second infinitely large. The infinitely small conductance is denoted by zero (open circuit) and the infinitely great by one (short-circuit) in contact circuit theory.

Relay circuits contain, besides contacts, relay coils, resistors and other elements of finite conductance. A feature of such circuits is that the relay operation here depends on the presence of the finite conductance elements as well.

The way the conductances in a relay circuit influence the relay operation depends on the relationships between the relay parameters and the conductances, the method of connection and the applied voltage. In deriving the structure we are not primarily interested in the absolute values of the parameters of different elements, but only in their relationships, as determining the operation of the relay. By setting up definite conditions (the relay

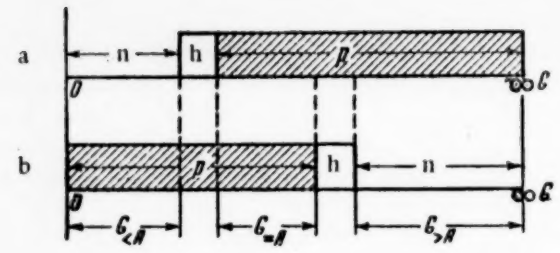

Fig. 1.

is to operate or not operate when a given conductance is connected to it, etc.) the precise paremeters can be determined from the electrical calculations.

When an element of finite conductance G is joined in series with the coil of a relay A the relay will not operate or hold on if the conductance is low; at certain mean values it will not operate but will hold on, while at high ones (up to ∞) it will operate. Thus, other things being equal, we can distinguish three ranges in G as regards the effect on A (Figure 1a); a region n, where the relay does not operate, a region h in which the previous state is retained, and a region p, where operation is reliable.

An analogous picture (Figure 1b) is obtained for G in parallel with A,* but the regions fall in the reverse sequence.

Hence, the way the conductance influences A will be determined by its value, neglecting the region h. From the above we divide all conductances, as regards their effect on A, into the following groups (Figure 1).

If G does not disturb the working of A in either series or parallel connection we will say that it is of the same order** as that of A. This is denoted symbolically by $G_{=A}$.

If there is no effect on series connection to A, but a disturbance in the parallel position, we say that the conductance is of higher order than that of A, and denote this by $G_{>A}$.

If there is no effect on parallel connection to A, but a disturbance in the series position we say that the conductance is of a lower order than that of A, and denote this by $G_{<A}$.

If disturbances occur in both positions of G the case is of no practical significance; and will not be considered.

Hence if A is to be unaffected one can only connect conductances of the same or greater order in series with the coil (general symbol $G_{\geq A}$). If $G_{<A}$, and is in series, A will be disturbed.

By analogy, parallel connection is only possible for conductances of the same or lower order (symbol $G_{\leq A}$), while for $G_{>A}$ the shunting will disturb the relay.

If several relays are present the following restrictions are imposed on their parameters.

If the conductance of relay B is of the same order as that of A, then the converse is true, i.e.,

$$\text{if } B_{=A}, \text{ then } A_{=B}. \tag{1}$$

If the conductance of relay B is of greater order than that of A, the order of A's must be less than that of B's, and conversely, i.e.,

$$\begin{aligned} &\text{if } B_{>A}, \text{ then } A_{<B};\\ &\text{if } B_{<A}, \text{ then } A_{>B}. \end{aligned} \tag{2}$$

These relationships in particular imply that

$$\begin{aligned} &\text{if } A_{>B} \text{ and } B_{>C}, \text{ then } A_{>C}.\\ &\text{if } A_{<B} \text{ and } B_{<C}, \text{ then } A_{<C}. \end{aligned} \tag{3}$$

Hence, it also follows that if three relays A, B and C satisfying the relations $A_{>B}$ and $B_{>C}$ (or $B_{<A}$, $C_{<B}$,

*In all cases of shunt connection the current source is assumed to have an appropriate limiting resistor fitted.

**"Order of conductance" is an arbitrary term. The effect of a resistance on a relay is not solely determined by the relation between the conductances, other factors operating as well.

or $A_{>B}$, $C_{<B}$) are joined in series, only C will operate on closing the circuit. Only A will operate in the parallel arrangement. If all three are of the same order they will all operate together in both arrangements.

We assume that the conductances and parameters of the relays are so chosen that on connecting a finite number of one order in series or parallel the over-all conductance will be of the same order, i.e.,

$$B_{=A} + C_{=A} + D_{=A} + \ldots + K_{=A} = (B + C + D + \ldots + K)_{=A}, \tag{4}$$

$$B_{=A} \cdot C_{=A} \cdot D_{=A} \cdot \ldots \cdot K_{=A} = (B \cdot C \cdot D \cdot \ldots \cdot K)_{=A}. \tag{4a}$$

If the orders differ the over-all conductance will be determined by the element of the highest order in the series system, and by that of the lowest in the parallel, i.e.,

$$B_{>A} + C_{<A} = B_{>A}, \tag{5}$$

$$B_{>A} \cdot C_{<A} = C_{<A}. \tag{5a}$$

Hence, in particular, we have

$$\begin{aligned} 0 \cdot G &= 0, \quad 1 \cdot G = G, \\ 0 + G &= G, \quad 1 + G = 1. \end{aligned} \tag{6}$$

From the definition of 'order' it follows that if $A_{\geq B}$, and $B_{\geq A}$, then A and B must be of the same order, i.e.,

$$\text{if } A_{\geq B} \text{ and } B_{\geq A}, \text{ then } A_{=B} \text{ and } B_{=A}. \tag{7}$$

If $A_{>B}$ and $B_{>A}$, the circuit cannot be realized.

The conductance of a relay circuit must be known as it influences the operation of the other relays in the over-all system.

2. Equivalence of Relay Circuits and Equivalent Transforms

Equivalent relay circuits are [1] those which, while differing in structure, respond identically in their intermediate and effector elements when identical inputs are applied. Not all such circuits are considered here, but only those with equal numbers of relays with identical operating sequences, i.e., circuits in which the operations are defined by the same switching table.

If they are also of identical conductance we term them absolutely equivalent.

We now consider what transforms can be applied to relay circuits to give circuits equivalent in the above sense.

The existing techniques of contact circuit algebra [1, 2] are based on Boolean algebra; the structures of class II contact circuits are readily described and transformed using them. In this algebra the = sign indicates that when the elements in the parts of the formula have equal values the expressions related by this sign are identical. In relay circuit language this means that the contact circuits corresponding to the formulas so related will be simultaneously open or closed, i.e., the circuit conductances during the operations will be identical. However, the techniques cannot always be used to transform relay circuits, since 'equivalence' in relay circuits means something different from what it does in contact circuits.

The laws of contact circuit algebra are also not always correct for elements of finite conductance. In particular, inversion is undefined. But, as above, such an element in the circuit of a relay affects the latter as though of either infinite or zero conductance, i.e., as though either a closed or open contact, and so, subject to certain reservations, we can use the laws of contact circuit algebra for transforming relay circuits.

The notation of contact circuit algebra will be used to describe class II relay circuits, i.e., parallel connection is denoted by (+) and series by (·) (multiplication sign). Relay coils (and other finite conductance elements) will be denoted by capital letters, and contacts by small ones.

The 'equals' sign will denote equal conductances (accurate to an order for relay circuits), while to denote

equivalence in the sense above we use $\doteqdot$.* Absolute equivalence is denoted by $\equiv$.

We now consider what transforms can be applied to relay circuits without destroying equivalence. If the circuit consists solely of coils of single-wound relays of conductances of the same order, and if it is sufficient that current flows in its coil for a relay to operate, then all class II circuits will be absolutely equivalent, since whatever the connections between the coils all will receive current and all the relays will operate together.

In other words, for finite conductance elements of one order an equivalence transform is

$$A_{=B} + B_{=A} \equiv A_{=B} \cdot B_{=A}. \tag{8}$$

The argument is also correct for multiple-wound relays provided that all coils are connected in the same sense.

If some coils are reversed the current flow conditions are unaltered but the relay may or may not operate, depending on the ampere-turns of the various coils. Here equivalence of operation may be destroyed if the structure is altered.

If the relay coils have conductances of different orders the mode of coil connection becomes important because of restrictions on the currents in some relays, as noted above.

The commutative and associative laws of contact circuit algebra can without restriction be applied to normal and inverse relay circuits [6-8], i.e.,

$$xA \equiv Ax \tag{9}$$

$$x + A \equiv A + x, \tag{10}$$

$$xyA \equiv x(yA) \equiv (xy)A, \tag{11}$$

$$x + y + A \equiv (x + y) + A \equiv x + (y + A). \tag{12}$$

Provided all coils of a multiple-coil relay are connected in the same sense, and if it is sufficient for current to pass in but one coil for the relay to operate, the following law will also be correct.

$$A \doteqdot A^1 + A^2 + A^3 + \ldots, \tag{13}$$

$$A \doteqdot A^1 \cdot A^2 \cdot A^3 \ldots, \tag{14}$$

where A^1, A^2, A^3 . . . . . are the coils on relay A, numbered in any order.

Subject to this restriction the distributive laws

$$(x + y)A \doteqdot xA^1 + yA^2, \tag{15}$$

$$xy + A \doteqdot (x + A^1)(y + A^2). \tag{16}$$

will also be correct.

By using these relations we can introduce additional windings, which sometimes makes it possible to simplify the circuit [1, 2].

We note in passing that the distributive laws, as regards A, impose no restrictions on the conductances of A^1 and A^2. If we suppose all coils to have conductances of the same order the formulas give absolutely equivalent transforms.

We also note that the formulas are correct when $\underline{x}$ and $\underline{y}$ contain elements of finite conductivity, but do not give equivalent transforms if $\underline{x}$ and $\underline{y}$ contain coils from any relay. Thus, if we put $y = zC$, where C is a relay coil, then (15) gives $(x + zC)A = xA^1 + zCA^2$. It is easily seen that this is true for relay A but not for C.

We finally consider the applicability of inversion to relay circuits. In contact circuit algebra inversion results in a circuit with the reciprocal conductance.

As regards relay circuits it is known [1, 5, 9] that inversion of the whole circuit gives an equivalent one,

*This sign for equivalence in relay circuits was introduced by A.N. Iurasov [5].

provided that inversion of a coil gives the same coil (i.e., $\overline{A} = A$). The conductance of the new circuit will be the reverse of that of the old.

If finite conductances of different orders are present before inversion they change from high to low and vice versa, i.e.,

$$\begin{aligned} \overline{G_{>A}} &= G_{<A}, \quad \overline{G_{\geqslant A}} = G_{\leqslant A}, \\ \overline{G_{<A}} &= G_{>A}, \quad \overline{G_{\leqslant A}} = G_{\geqslant A}. \end{aligned} \tag{17}$$

Thus, assuming that parallel connection is replaced by series and vice versa on inversion, and that the orders are reversed, the inversion laws for relay circuits become

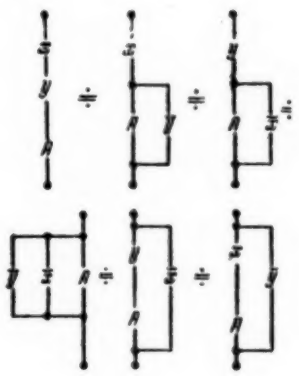

Fig. 2.

$$\begin{aligned} \overline{xA} &\equiv \bar{x} + A, \\ \overline{xA}_{>B} &\equiv \bar{x} + A_{<B}, \\ \overline{xA}_{\geqslant B} &\equiv \bar{x} + A_{\leqslant B}, \end{aligned} \tag{18}$$

$$\begin{aligned} \overline{x + A} &\equiv \bar{x}A, \\ \overline{x + A}_{>B} &\equiv \bar{x}A_{<B}, \\ \overline{x + A}_{\geqslant B} &\equiv \bar{x}A_{\leqslant B} \\ &\text{etc.} \end{aligned} \tag{19}$$

The inversion process can be extended, only part of the relay circuit being so treated instead of the whole. If some two-terminal relay network is singled out which includes all the relay coils in the circuit, this network can be dealt with by itself, or the whole of the rest of the circuit. Thus, if we have a circuit of the form F = xyA complete inversion gives

$$F = \bar{x} + \bar{y} + A.$$

Using the commutation law and singling out some two-terminal contact network in a distinct way (for clarity this part is underlined) we get

$$F = \underline{xyA} = x(\bar{y} + A) = \bar{x} + yA$$

or

$$F = \underline{yxA} = y(\bar{x} + A) = \bar{y} + xA.$$

All the circuits (Figure 2) are equivalent but have different structural conductances, and will so act differently on other relays which may be connected to them. The table (page 1170) gives expressions for the structural conductances for cases where the conductance of A can be equated to one or zero.

This table shows that on realizing the xyA structural formula the conductance can have 12 distinct values in the 16 distinct circuits obtained from the contacts of two relays ([2], page 21). By analogy a circuit of xyzA form can give 26 distinct circuits out of a total of 256 which can be produced from the contacts of three relays.

As well as the above transforms, we can also apply the important process of 'extending' the contact circuit [1, 2] in synthesis operations; here additional elements or circuits are added in accordance with certain rules, care being taken not to affect the relays. Such 'extension' is also possible in relay circuits, both by adding contact circuits and by introducing elements of finite conductance.

Introducing contact circuits into relay ones increases the ways of 'extending' circuits. If, to a normal circuit of fA form, we connect, in parallel, a purely contact circuit x, the condition for relay A to operate is only not violated if x is open when f is closed. This means we must have xf = 0.

TABLE

Circuit	Structural conductance when	
	$A=1$	$A=0$
xyA	xy	0
$\bar{x}+\bar{y}+A$	1	$\bar{x}+\bar{y}$
$x(\bar{y}+A)$	x	$x\bar{y}$
$\bar{x}+yA$	$\bar{x}+y$	$\bar{x}$
$y(\bar{x}+A)$	y	$\bar{x}y$
$\bar{y}+xA$	$x+\bar{y}$	$\bar{y}$

This expression is clearly satisfied by an expression the inverse of $\underline{f}$, and also by any 'lesser'• expression, i.e., $x \leq \bar{f}$ or $x = \bar{f}/0$. We can thus put

$$fA \doteqdot fA + \frac{\bar{f}}{0}. \tag{20}$$

Analogously, the equivalence of the inverse circuit will not be violated if we connect in series a circuit closed when the circuit in parallel with the relay is open. This means that an expression of the form $\varphi + A$ may be multiplied by one the inverse of φ, or any 'greater' expression, i.e.,

$$\varphi + A \doteqdot (\varphi + A)\frac{\bar{\varphi}}{1}. \tag{21}$$

It is clear that the over-all conductance is altered by (20) and (21) (except in the trivial case $\bar{f}/0 = 0$ and $\bar{\varphi}/1 = 1$), and hence these transforms are not absolutely equivalent.

We now consider circuit extensions involving finite conductances.

As above, if a conductance $G_{\geq A}$ of equal or greater order is connected in series with the coil of relay A, the operating conditions are unaffected. Hence, we conclude that an element with $G_{\geq A}$ can be connected in series in any contact circuit in series with a relay coil. That is, if to any expression appearing in f_A we apply as a multiplier an element $G_{\geq A}$, the operation remains unaffected.

What is more, if we connect to the element with $G_{\geq A}$ of finite conductance, some circuit X (purely contact or containing elements of finite conductance) the over-all conductance of $G_{\geq A} + X$ will be equal to, or greater than, that of $G_{\geq A}$. The operation is again unaffected if we connect the element with $G_{\geq A}$ (with any circuit X in parallel with it) in series with any circuit. This transform can be written as

$$f_A A \equiv f_A G_{\geq A} A \equiv f_A (G_{\geq A} + X) \tag{22}$$

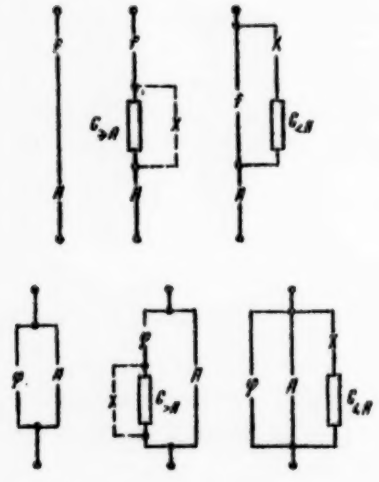

Fig. 3.

or

$$\begin{aligned}(f_1 + f_2) A &\equiv [f_1 (G_{\geq A} + X) + f_2] A \equiv \\ &\equiv [f_1 + f_2 (G_{\geq A} + X)] A.\end{aligned} \tag{22a}$$

Again, the operation is unaffected if to a circuit in series with a relay coil we connect, in parallel, a conductance of order less than that of the coil, since, by definition, when the contact circuit is open the current will be insufficient to operate the relay. Moreover, the connection of some circuit X in series with $G_{<A}$ cannot increase the conductance. Hence, a contact circuit can not only be connected in parallel to the element with $G_{>A}$, but also with the circuit $XG_{<A}$.

The finite conductance $G_{<A}$ can be connected in parallel to all or to any part of the contact circuit f_A (which acts on A). So, in the formula for the normal contact circuit of A we can add as a component the expression $XG_{<A}$ to any part (in a particular case, $X = 1$):

•The expression $a \leq b$ [10] or $b \geq a$ denotes (in contact circuit algebra) that for all values of the variables expression $\underline{a}$ will be equal to or less than expression $\underline{b}$, i.e., if $b = 1$, then $\underline{a}$ can be 1 or 0; if $b = 0$, then $a = 0$. Hence, $ab = a$ and $a + b = b$. So, if we know that the circuit of $\underline{b}$ is a 'lesser' circuit, it will be denoted by $b/0$, which means that at one limit the value can be $\underline{b}$, and at the other 0, i.e., $b \geq b/0 \geq 0$. Similarly, a 'greater' circuit of $\underline{a}$ will be designated $a/1$, which signifies that $a \leq a/1 \leq 1$. Regarding certain operations with expressions of the form $b/0$ and $a/1$, see [2, 4]. In the general case $a/b = abx + (a + b)\bar{x}$, where $\underline{x}$ is any contact circuit.

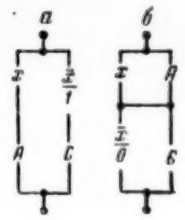

Fig. 4.

$$f_A A \doteqdot (f_A + XG_{<A})\, A, \tag{23}$$

$$f_1 f_2 A \doteqdot (f_1 + XG_{<A})\, f_2 A \doteqdot f_1 (f_2 + XG_{<A})\, A. \tag{23a}$$

Similarly, to a contact circuit in parallel with the coil of A we can add in series a conductance $G_{>A} + X$, and in parallel one of $XG_{\leq A}$:

$$\varphi + A \doteqdot \varphi (G_{>A} + X) + A, \tag{24}$$

$$\varphi_1 + \varphi_2 + A \doteqdot \varphi_1 (G_{>A} + X) + \varphi_2 + A, \tag{24a}$$

$$\varphi + A \equiv \varphi + A + XG_{<A}, \tag{25}$$

$$\varphi_1 \varphi_2 + A \equiv (\varphi_1 + XG_{<A}) + \varphi_2 + A. \tag{25a}$$

Figure 3 illustrates (22-25).

By using the extension rules we can transform any relay circuit so as to have the properties of an element of finite conductance. Thus, with the very simple circuit of Figure 4,

$$xA \doteqdot xA + \frac{\bar{x}}{1} G, \tag{26}$$

$$x + A \doteqdot (x + A)\left(\frac{\bar{x}}{0} + G\right). \tag{26a}$$

3. Synthesis of Multi-Relay Circuits

Existing relay circuit synthesis methods enable us to derive analytic formulas f_A, f_B, . . . , f_K for the operation of relays A, B, . . . , K to set conditions.

It is usually here assumed that all relays have conductances of the same order and that the general structural formula for the circuit is written in the normal form:

$$F = f_A A + f_B B + \ldots + f_K K. \tag{27}$$

To produce mixed circuits we will use our equivalent transforms to take the circuits of the various relays (or coils) over to the same structure with the same contacts, in particular, by introducing elements of finite conductance. These circuits can be interchanged provided all the contacts remain in the circuit, while the elements of finite conductance could be replaced by relay coils of appropriate order. The resulting separate circuits could be joined up (in parallel, for instance), checking, of course, that they do not shunt one another, i.e., that their conductances are of the same order.

Let us consider as an example a circuit synthesized in [3] (pp. 534-5, second example) and decide how, by using our equivalent transforms, we can reduce the number of contacts. The operations formulas are put in the form

$$f_{X_1} = a + x_1 \bar{x}_2 \bar{x}_3, \qquad f_{X_2} = a\bar{x}_1 + x_2 (x_1 + \bar{x}_3), \qquad f_{X_3} = ax_2 + x_1 x_3.$$

Consider first the circuits containing the contacts of relay A. We consider each relay double-wound and transform the expressions to the same structure, using the partial inversion rules, and introduce finite conductance elements (G) (x denotes any contact circuit):

$$F_1^1 \doteqdot aX_1^1 \doteqdot (a + xG_{<X_1^1})\, X_1^1 \doteqdot (a + xG_{<X_1^1})\, (X_1^1 + xG_{\leqslant X_1^1}),$$

$$F_2^1 \doteqdot \bar{a}\bar{x}_1 X_2^1 = a + x_1 X_2^1 \doteqdot (a + x_1 X_2^1)\, G_{>X_2^1},$$

$$F_3^1 \doteqdot ax_2 X_3^1 \doteqdot (a + xG_{<X_3^1})\, x_2 X_3^1 \doteqdot (a + xG_{<X_3^1})\, (x_2 X_3^1 + G_{\leqslant X_3^1}).$$

Comparing the three expressions, we see that the first factor in each is of structure $a + x_1 X_2^1 < X_1^1, X_3^1$, the second being an element of finite conductance, $(X_1^1 \leq X_3^1 + x_2 X_3^1 \leq X_1^1) \geq X_2^1$. From the latter we conclude that X_1^1 and X_3^1

must be of the same order. Comparison with the first factor shows that the order of X_2^1 must be less than those of X_1^1 and X_3^1. The final structural formula will therefore be

$$F^1 = (a + x_1 X_{2<X_1^1,\ X_3^1}^1)(X_1^1 + x_2 X_3^1).$$

This is a normal relay circuit. In calculating the coil we must remember that X_2^1 must have a resistance such that when X_1 or X_3 are in series with it, it will not hold on; X_2 must operate when in series with X_2^1.

We now transform the second parts of the formulas, which include the contacts of relays X_1, X_2 and X_3:

$$F_1^2 \div x_1\bar{x}_2\bar{x}_3 X_1^2 \div \bar{x}_2\bar{x}_3(\bar{x}_1 + X_1^2) \div (\bar{x}_3 + xG_{<X_1^2})(\bar{x}_3 + G_{<X_1^2})(\bar{x}_1 + X_1^2),$$

$$F_2^2 \div x_2(x_1 + \bar{x}_3)X_2^2 \div (x_1 + \bar{x}_3)(\bar{x}_2 + X_2^2) \div (\bar{x}_3 + x_1 G_{>X_2^2})(\bar{x}_2 + X_2^2)(G_{>X_2^2} + x),$$

$$F_3^2 \div x_1 x_3 X_3^2 \div \bar{x}_3 + x_1 X_3^2 \div (\bar{x}_3 + x_1 X_3^2)(G_{>X_3^2} + x).$$

Comparing the separate parts of these expressions, we can put the first as

$$\bar{x}_3 + x_1 X_{3<X_1^2,>X_2^2}^2$$

and the latter ones as

$$|(\bar{x}_2 + X_{2<X_1^2}^2)(\bar{x}_1 + X_{1>X_2^2}^2)|_{>X_3^2}.$$

Comparison of the conductance orders shows that X_2^2 and X_3^2 must be the same, while X_1^2 is greater, i.e., we finally have

$$F^2 = (\bar{x}_3 + x_1 X_3^2)(\bar{x}_2 + X_2^2)(\bar{x}_1 + X_{1>X_2^2,\ X_3^2}^2).$$

Thus, in the resting state the conductance is unity, so a series limiting resistance is required.

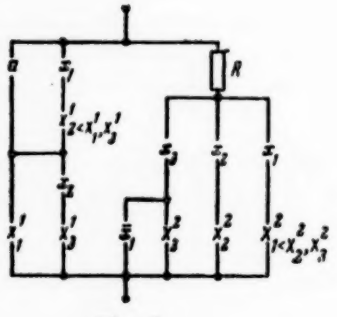

Fig. 5.

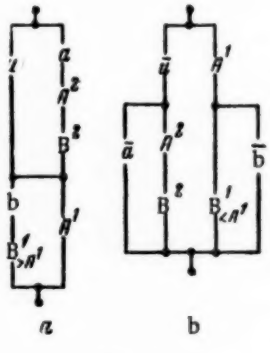

Fig. 6.

To observe the conditions implied by the above relations the relay coils must be designed so that X_1 will not hold on when in series with X_2^2 or X_3^2, while X and X_3 will operate when all three coils are in series (plus the limiting resistance).

A disadvantage is that in the resting state the circuit is continuously closed. To eliminate this we invert the circuit:

$$\bar{F}^2 \div x_3(\bar{x}_1 + X_3^2) + x_2 X_2^2 + x_1 X_{1<X_2^2,\ X_3^2}^2.$$

We must here also have a limiting resistance R and the relay coils must be designed so that X_1 will not

hold on when in parallel with X_1^2, X_2^2 or X_3^2, while X_2 and X_3 will operate when in parallel with all three coils.

The complete circuit is as shown in Figure 5. It has 2-3 contacts (4-5 springs) less than those found by normal synthesis methods ([3], Figure 15).

As another example we consider the synthesis of a two-relay frequency divider ('even-odd' circuit), the structural formula of which ([2], p. 99) takes the form

$$F = u\bar{b}A^1 + ubB^1 + \bar{u}aA^2B^2.$$

As above, we transform the separate parts of this expression:

$$F_1 = u\bar{b}A^1 \doteqdot u(b + A^1) \doteqdot u(bG_{>A_1} + A^1) \doteqdot (u + G_{<A^1})(bG_{>A^1} + A^1),$$

$$F_2 = ubB^1 \doteqdot u(bB^1 + G_{<B^1}) \doteqdot (u + xG_{<B^1})(bB^1 + G_{<B^1}),$$

$$F_3 = \bar{u}aA^2B^2 \doteqdot u + aA^2B^2 \doteqdot (u + aA^2B^2)\, G_{A>^1,B^1}.$$

Comparing the various expressions, we get the total structural formula as

$$F = [u + a(A^2B^2)_{<A^1}](bB^1_{>A^1} + A^1).$$

It is clear that here we do not have to observe the requirement that the orders of A^2 and B^2 be less than that of A^1.

In fact, if the orders of A^2 and B^2 be the same as that of A^1, then on closing the aA^2B^2 circuit and opening bB^1 relay A^1 will operate, which is equivalent to adding a term $a\bar{b}$ to the formula for A. This does not contradict the original formula, since $u\bar{b} + \bar{u}a = u\bar{b} + \bar{u}a + a\bar{b}$.

Thus, we finally get

$$F = (u + aA^2B^2)(bB^1_{>A^1} + A^1).$$

Figure 6a shows the corresponding circuit. Inverting this formula, we get a new circuit (Figure 6b):

$$F = \bar{u}(\bar{a} + A^2B^2) + (\bar{b} + B^1_{<A^1})A^1.$$

In Figure 6a the first coils of A and B and the limiting resistance must be such that when B^1 and A^1 are in parallel A is off and B operates. A^2 and B^2 must be such that both relays are operated when these are in series with A^1 and the limiting resistance. In Figure 6b B^2 must be such that, when in series with A^1, A is off and B operates.

The resulting circuits have only one contact per relay, so circuits with less contacts are impossible.

The solutions found here are not unique; other circuits of different structure can be found.

SUMMARY

The methods of transforming relay circuits considered here considerably extend the classes of relay systems open to synthesis, since mixed relay circuits of class II can be obtained analytically. One of the possible ways of constructing circuits with parametric relationships is given.

The methods are most effective with multi-relay circuits, where the circuit of any relay contains various combinations of contacts from the same relays. By altering the structure of any such circuit (or the circuit of any coil) using equivalent transforms and introducing finite conductance elements we can refer all circuits to the same structure, and thus interchange them. In some cases, the number of contacts is thereby reduced. An economy in connections between the various parts of a circuit is sometimes also effected.

As in other relay systems syntheses, the electrical calculations have to be done when the structure has been

found. When a circuit contains relay coils of different conductance orders, it must be verified that the requirements as to the parameter relations implied by the definition of conductance order are observed, allowing for possible line voltage fluctuations and with due tolerances on the currents required for them to operate, hold on, not operate and drop off. For instance, if the battery voltage is low (several volts) it is very difficult, or even impossible, to accommodate two orders of conductance with existing types of telephonic relay. At high voltages the problem is easily solved, and several orders can be accommodated.

Further progress in circuit extension can be had by using opposed windings in mixed circuits, bridge circuits, rectifiers, etc.

LITERATURE CITED

[1] M.A. Gavrilov, Theory of Relay-Contact Circuits [in Russian] (Izd. AN SSSR, 1950).

[2] V.N. Roginskii and A.D. Kharkevich, Relay Circuits in Telephony [in Russian] (Communication Press, 1955).

[3] M.A. Gavrilov, "The basic formulas for relay system synthesis" Automation and Remote Control (USSR) 15, (6) (1954).

[4] V.N. Roginskii, Synthesis of Multicycle Relay Circuits, Collection of Scientific Papers on Wire Telephony No. 4 [in Russian] (Izd. AN SSSR, 1955).

[5] A.N. Iurasov, Some Analytic Methods of Composing and Transforming Relay-Contact Circuits, Dissertation, Vsesoiuz. Zaochnyi politekh. Inst. (1956).

[6] V.I. Shestakov, "The algebra of a two-terminal network constructed solely from two-terminal networks," Automation and Remote Control (USSR) 1941, No. 2.

[7] J. Shekel, Sketch for an Algebra of Switchable Networks, Proc. Inst. Radio Engrs. Vol. 41, No. 7 (1953).

[8] G. Schliebs, Uber die Grundlagen der Algebra der Logik und ihre Anwendung in der Schaltungstheorie Vol. 8, No. 2 (Funk and Ton, 1954).

[9] M.A. Gavrilov and V.A. Khvoshchuk, "The partial inversion method in relay circuits," Doklady Akad. Nauk SSSR 75, 5 (1950).

[10] L. Kutiura, "The Algebra of Logic" [in Russian] (Odessa, 1909).

Received June 28, 1956

EVALUATION OF THE REGION OF THE TRUE PERIODIC SOLUTION FOUND APPROXIMATELY BY THE HARMONIC BALANCE METHOD

I. V. Glatenok

(Moscow)

The harmonic balance method is commonly used [1, 2] to determine periodic solutions (in particular, self-oscillations) in studying automatic control systems. The permissibility of the approximations made in using this method is usually established by comparing the results with those from an exact method (e.g., of [3]). This is only done for systems with piecewise-linear characteristics, since only these allow of exact solution.

In this note we show that for the equation

$$\ddot{y} = f(y, \dot{y}) \tag{1}$$

if certain restrictions (not related to its piecewise-linear approximation) are imposed on $f(y,\dot{y})$, there is a stable periodic solution to (1) if this method, as applied to (1), gives a periodic solution, and that the true solution lies in the neighborhood of the solution so found; the area of this region (about the approximate solution) is also found. This is effected using the theorems formulated below; these are stated without proof. The proofs will be given separately in a mathematical journal.*

Suppose $f(\dot{y},\dot{y})$ satisfies the condition

$$\frac{1}{2\pi}\int_1^{2\pi} f(a\sin u,\ a\omega\cos u)\,du = 0.$$

The harmonic balance equation is then

$$\begin{aligned} \frac{1}{\pi}\int_0^{2\pi} f(a\sin u,\ a\omega\cos u)\sin u\,du &= -a\omega^2, \\ \frac{1}{\pi}\int_0^{2\pi} f(a\sin u,\ a\omega\cos u)\cos u\,du &= 0. \end{aligned} \tag{2}$$

Let us consider a case where (2) has the real roots $\underline{a}$ and ω, i.e., when the method indicates a periodic solution.

The notation we shall use is

$$u = \omega t, \qquad \beta = \arcsin \epsilon,$$
$$\sum(u) = f(a\sin u,\ a\omega\cos u) + a\omega^2\sin u,$$

*These theorems comprise the content of work carried out under the guidance of Professor V.V. Nemytskii and discussed at the seminar on the general theory of differential equations at Moscow State University.

$$\sigma_1 = \max\left\{\begin{matrix} \max \sum(u) & \max \sum(u) \\ -\frac{\pi}{2} \leqslant u \leqslant \frac{\pi}{2},\ \sum > 0 & \frac{\pi}{2} \leqslant u \leqslant \frac{3\pi}{2},\ \sum < 0 \end{matrix}\right\},$$

$$\sigma_2 = \max\left\{\begin{matrix} \max \sum(u), & \max \sum(u) \\ -\frac{\pi}{2} \leqslant u \leqslant \frac{\pi}{2},\ \sum < 0 & \frac{\pi}{2} \leqslant u \leqslant \frac{3\pi}{2},\ \sum > 0 \end{matrix}\right\},$$

$$\sigma = \max(\sigma_1, \sigma_2),$$

$$P = -\frac{1}{2\pi}\int_0^{2\pi} f'_y(a\sin u, a\omega\cos u)\,du,$$

$$Q = -\frac{1}{2\pi}\int_0^{2\pi} f'_{\dot{y}}(a\sin u, a\omega\cos u)\,du,$$

$$\varphi = \max_{0\leqslant u\leqslant 2\pi} |f'_y(a\sin u, a\omega\cos u) + P|,$$

$$\Psi = \max_{0\leqslant u\leqslant 2\pi} |f'_{\dot{y}}(a\sin u, a\omega\cos u) + Q|,$$

$$\frac{1}{2}|f''_{rr}[(a+\theta r)\sin u, (a+\theta r)\,\omega\cos u]| < m \quad (0\leqslant\theta\leqslant 1, |r|\leqslant a).$$

$$F(u) = \{\omega^2 + f'_y[(a+\theta r)\sin u, (a+\theta r)\,\omega\cos u]\}\sin u +$$
$$+ f'_{\dot{y}}[(a+\theta r)\sin u, (a+\theta r)\,\omega\cos u]\cos u \quad (0\leqslant\theta\leqslant 1, |r|\leqslant a),$$

$$q_1 = \min\left\{\begin{matrix} \min|F(u)| & \min|F(u)| \\ \frac{3\pi}{2} - \beta \geqslant u \geqslant \frac{\pi}{2} + \beta,\ \sum < 0 & \frac{\pi}{2} - \beta \geqslant u \geqslant \frac{3\pi}{2} + \beta,\ \sum > 0 \end{matrix}\right\},$$

$$q_2 = \min\left\{\begin{matrix} \min|F(u)|, & \min|F(u)| \\ \frac{3\pi}{2} - \beta \geqslant u \geqslant \frac{\pi}{2} + \beta,\ \sum > 0 & \frac{\pi}{2} - \beta \geqslant u \geqslant \frac{3\pi}{2} + \beta,\ \sum > 0 \end{matrix}\right\},$$

$$\bar{q}_1 = q_1 \quad (\beta = 0), \qquad \bar{q}_2 = q_2 \quad (\beta = 0).$$

Theorem 1. If the following conditions are fulfilled:

1) $f(y,\dot{y})$ is continuous with respect to $y,\dot{y}$, and so are its first and second derivatives with respect to these;

2) $Q > 0$, $\Psi < Q$,

3) $P > 0$, $\varphi < P$, $\varphi < \dfrac{(Q-\Psi)\,\omega}{2}\varepsilon$;

4) $-\varphi < \omega^2 - P < \varphi$;

5) $\sigma < \dfrac{(Q-\Psi)^2\omega^2}{8m}\varepsilon^2$;

6) $\varepsilon \leqslant \min\left\{\dfrac{1}{10}, \dfrac{ma}{4(Q-\Psi)\omega}, \dfrac{ma}{4(Q-\Psi)^2}, \dfrac{ma\omega}{5P(Q-\Psi)}, \dfrac{ma\omega}{5(Q-\Psi)^2}, \dfrac{Q-\Psi}{625\sqrt{ma}}\right\}$,

then (1) has a stable periodic solution of amplitude A satisfying

$$a - \frac{(Q-\Psi)\,\omega}{m}\varepsilon < A < a + \frac{(Q-\Psi)\,\omega}{m}\varepsilon.$$

Theorem 2. If the following conditions are fulfilled:

1) $f(y,\dot{y})$ is continuous with respect to $y,\dot{y}$, and so are its first derivatives with respect to these;

2) $F(u)\cos u < 0$ when $u \neq \dfrac{\pi}{2}, \dfrac{3\pi}{2}$; $F\left(\dfrac{\pi}{2}\right) = F\left(\dfrac{3\pi}{2}\right) = 0$;

3) $\sigma < \dfrac{aq_1\omega^2\sqrt{1-\varepsilon}}{q_1 + \omega^2\sqrt{1-\varepsilon} + \omega^2\sqrt{\varepsilon}}$,

4) $\varepsilon < \dfrac{q_1^2}{\omega^4}$,

then (1) has a stable periodic solution of amplitude A satisfying

$$\left(a-\frac{\sigma_2+2a\omega^2\sqrt{\varepsilon}}{q_2+2\omega^2\sqrt{\varepsilon}}\right)\sqrt{1-4\varepsilon}<A<\left(a+\frac{\sigma_1+a\omega^2\sqrt{\varepsilon}}{q_1-\omega^2\sqrt{\varepsilon}}\right)\frac{1}{\sqrt{1-\varepsilon}}.$$

Theorem 3. If the following conditions are fulfilled:

1) $f(y,\dot{y})$ is continuous with respect to $y,\dot{y}$, and

2) f'_y, $f'_{\dot{y}}$ have first-order discontinuities in $\underline{y}$ on a certain line and are continuous in the rest of the $y,\dot{y}$ plane;

3) $F(u)\cos u<0$ when $0\neq\frac{\pi}{2}$, $\frac{3\pi}{2}$;

4) $\sigma<\min\left\{\frac{a\bar{q}_1\omega^2}{\bar{q}_1+F_n\left(\frac{\pi}{2}\right)-\omega^2},\ \frac{a\bar{q}_2\omega^2}{\bar{q}_2-F_n\left(\frac{\pi}{2}\right)+\omega^2}\right\}$,

then (1) has a stable periodic solution of amplitude A satisfying

$$a-\frac{\sigma_2}{\bar{q}_2}<A<a+\frac{\sigma_1}{\bar{q}_1}.$$

Example. Consider an automatic control system described by the equation

$$T(\ddot{y}+\dot{y})=-KN(y), \tag{3}$$

where N(y) is the nonlinear link characteristic shown in Figure 1. Equation (3) can be put in the form

$$\ddot{y}=-\frac{1}{T}\dot{y}-\frac{K}{T}G(y,\dot{y}),$$

where $G(y,\dot{y})$ is given as follows: in the $y,\dot{y}$ plane there is a certain line which divides the plane into four regions, as in Figure 2 (the line is denoted by H, the regions by I, II, III, IV),

$$G(y,\dot{y})=\begin{cases} y-b & \text{if } (y,\dot{y}) \text{ lies in } I,\\ c-b & \text{" " " } II,\\ y+b & \text{" " " } III,\\ -c+b & \text{" " " } IV, \end{cases}$$

where $\underline{c}$ denotes the value given to function $\underline{y}$ at $\dot{y}=0$.

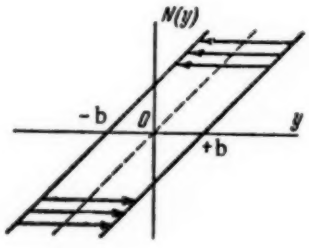

Fig. 1.

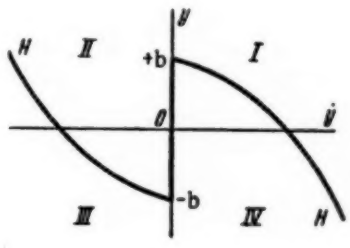

Fig. 2.

The harmonic balance equation is of the form

$$\frac{K}{T\pi}\left(\frac{\pi}{2}+u_1+\frac{1}{2}\sin 2u_1\right)=-a\omega^2,$$

$$\frac{K}{T}\cos^2 u_1=\omega,$$

where $u_1 = \arcsin(1 - 2b/a)$.

We also get the following expressions for $\sum(u)$, $F(u)$:

$$\sum(u) = \begin{cases} -\frac{a\omega}{T}\cos u - \left(\frac{K}{T} - \omega^2\right) a \sin u + \frac{K}{T} b, & 2\pi - u_2 \leqslant u \leqslant \frac{\pi}{2}, \\ -\frac{a\omega}{T}\cos u + a\omega^2 \sin u - \frac{K}{T}(a-b), & \frac{\pi}{2} \leqslant u \leqslant \pi - u_2, \\ -\frac{a\omega}{T}\cos u - \left(\frac{K}{T} - \omega^2\right) a \sin u - \frac{K}{T} b, & \pi - u_2 \leqslant u \leqslant \frac{3\pi}{2}, \\ -\frac{a\omega}{T}\cos u + a\omega^2 \sin u + \frac{K}{T}(a-b), & \frac{3\pi}{2} \leqslant u \leqslant 2\pi - u_2, \end{cases}$$

$$F(u) = \begin{cases} -\frac{\omega}{T}\cos u - \left(\frac{K}{T} - \omega^2\right)\sin u, & 2\pi - u_2 \leqslant u \leqslant \frac{\pi}{2}, \quad \pi - u_2 \leqslant u \leqslant \frac{3\pi}{2}, \\ -\frac{\omega}{T}\cos u + \omega_2 \sin u, & \frac{\pi}{2} \leqslant u \leqslant \pi - u_2, \quad \frac{3\pi}{2} \leqslant u \leqslant 2\pi - u_2, \end{cases}$$

(u_2 denotes the angle at which the branch of H lying in region II intersects the ellipse $x = a\omega\cos u$, $y = a\sin u$, in polar coordinates).

Numerical calculation for T = 0.115, K = 60, b = 8 gives the following results: a = 20.4, ω = 18.2.

We further have

$$\sigma_1 = \left|\sum(u_2)\right| = 1800, \quad \sigma_2 = \left|\sum\left(\frac{\pi}{2}\right)\right| = 274, \quad \sigma = 1800,$$
$$\bar{q}_1 = |F_n(u_2)| = 127, \quad \bar{q}_2 = |F(u_3)| = 316 \qquad (4)$$

(u_3 is determined by the condition $\sum(u_3) = 0$).

The conditions of theorem 3 are fulfilled. For 1) and 2) this follows directly from the definition of $G(y,\dot{y})$. 3) being also fulfilled because here

$$-\frac{\omega}{T}\cos u_2 - \left(\frac{K}{T} - \omega^2\right)\sin u_2 > 0.$$

We further have

$$\frac{a\bar{q}_1\omega^2}{\bar{q}_1 + F_n\left(\frac{\pi}{2}\right) - \omega^2} = 6750, \qquad \frac{a\bar{q}_2\omega^2}{\bar{q}_2 - F_n\left(\frac{\pi}{2}\right) + \omega^2} = 2540.$$

Comparing these results with (4), we see that 5) is also fulfilled.

Theorem 3 gives

$$20.4 - 0.9 < A < 20.4 + 14.2, \quad \left(\frac{\sigma_1}{\bar{q}_1} = 14.2;\ \frac{\sigma_2}{\bar{q}_2} = 0.9\right).$$

LITERATURE CITED

[1] N.M. Krylov and N.N. Bogoliubov, Introduction to Nonlinear Mechanics [in Russian] (Izd. Akad. Nauk Ukr. SSR, Kiev, 1937).

[2] L.S. Gol'farb, A Method of Studying Nonlinear Control Systems Based on the Harmonic Balance Principle, Second All-Union Conference on the Theory of Automatic Control Vol. I (Izd. Akad. Nauk SSSR, 1955).

[3] Ia.Z. Tsypkin, Theory of Relay Automatic Control Systems [in Russian] (State Technical Press, 1955).

Received April 8, 1957

A METHOD OF CALCULATING THE OPERATIONAL RELIABILITY OF APPARATUS

G.V. Druzhinin

(Moscow)

A method of calculating the operational reliability of electrical automatic systems is presented for an arbitrary time distribution of the correct functioning of the elements.

Current electrical automatic systems usually consist of numerous distinct types of element. One breakdown usually affects the whole equipment. Such failures can occur in two ways, by sudden breakdown or by gradually worsening through wear and tear.

In the latter case the normal distribution law agrees well with practical experience of the time distribution of the correct functioning. A method of calculation has been given for a system consisting of identical elements [1]. The sudden failures often substantially influence the distribution law, which may differ considerably from normal. Thus, for some systems, particularly those subject to heavy duty, a method of calculating the operational reliability of the equipment is required which allows for the arbitrary time distribution of the correct functioning and for the fact that the system often consists of different types of elements. This method can be derived if we consider the failure process as an ordinary flux of uniform events with a variable parameter. The failures are uniform events in that only their presence or absence is of interest.

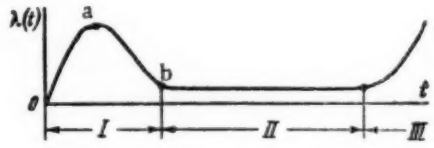

Failure in one element often results in damage to others. These secondary failures are neglected, since they only occur after the equipment has already failed from the first cause. The primary failures will be assumed to be independent events.

The failure rate $\lambda(t)$ will be used as an index; by this we mean the mathematical expectation of failure per unit time per element (of those still functioning). A typical $\lambda(t)$ curve is shown in the figure. The relation of failure rate to time (number of cycles) can be divided into three sections.

In the first many failures occur. This is mainly due to constructional defects. The weakest elements with unseen flaws, poor soldering, adjustment etc., fail first.

In the second the failure rate falls, the failures being mostly random.

In the third the failure rate rises continuously because of wear, and further use of the equipment without replacing the elements becomes illogical.

As the primary causes are supposed independent, the probability of failure of one in a short time $(t, t + \Delta t)$ may be supposed to be proportional to Δt, to depend on t, and not to depend on the preceding failures. Then the probability of one failure in the time $(t, t + \Delta t)$ may be put as $\lambda(t)\Delta t$.

Since, in practice, two or more primary failures never occur together, i.e., the failure experience is ordinary, the probability that an element is undamaged may be put as

$$1 - \lambda(t)\,\Delta t. \qquad (1)$$

Using (1) we get the probability p(t + Δt) that in the time (0,t + Δt) no failure in the element will occur. The multiplication theorem in probability theory gives

$$p(t+\Delta t) = p(t)\,[1-\lambda(t)\,\Delta t], \tag{2}$$

where p(t) is the probability that in the time (0,t) no failure in the element will occur.

Equation (2), after division by Δt, gives

$$\frac{p(t+\Delta t)-p(t)}{\Delta t} = -p(t)\,\lambda(t). \tag{3}$$

When $\Delta t \to 0$

$$\frac{dp(t)}{dt} = -\lambda(t)\,p(t). \tag{4}$$

Equation (4) and the initial condition p(0) = 1 give

$$p(t) = \exp\left[-\int_0^t \lambda(t)\,dt\right]. \tag{5}$$

Equation (5) shows that if we have the static curve λ(t) we can find the reliability during a given time t, or find, for a given probability p(t), the failure-free operating period.

Consider a system consisting of m distinct elements. Since the whole system fails if one element does, the multiplication theorem in probability theory shows that the probability of correct operation P(t) will be equal to the product of the probabilities for the elements $p_i(t)$, given by (5), i.e.,

$$P(t) = \exp\left[-\sum_{i=1}^{m}\int_0^t \lambda_i(t)\,dt\right] \tag{6}$$

or

$$P(t) = \exp\left[-\int_0^t \Lambda(t)\,dt\right], \tag{7}$$

where the failure rate Λ(t) for the system is the sum of the rates for the elements

$$\Lambda(t) = \sum_{i=1}^{m} \lambda_i(t). \tag{8}$$

For a system with identical elements

$$\Lambda(t) = m\lambda(t)$$

and so

$$P(t) = \exp\left[-m\int_0^t \lambda(t)\,dt\right]. \tag{9}$$

Equations (6-9) show that if we have the static curves $\lambda_i(t)$ for the elements we can find the reliability during a given time t, or find for a given probability P(t) the failure-free operating period. The integrals $\int_0^t \Lambda(t)dt$

or $\int_0^t \lambda_i(t)dt$ are computed numerically from the areas under the $\Lambda(t)$ or $\lambda_i(t)$ curves.

The time of correct operation T is found for a given P(T) in the following way:

1) we find the value of

$$\int_0^T \Lambda(t)\,dt = -\ln P(T); \tag{10}$$

2) using the graph of $\Lambda(t)$ we find the T at which the area under the curve equals the integral calculated from (10).

Thus, the reliability calculation amounts to summing the failure rates for the elements and using the tables of exponential functions to find P(t) [or ln P(T), if the time of correct operation T is found for a given P(T)].

LITERATURE CITED

[1] V.I. Siforov, "Methods of Calculating the Operational Reliabilities of Systems Containing Many Elements," Izv. AN SSSR, OTN, 1954, No. 6.

Received February 7, 1957

A SIMPLIFIED CALCULATION METHOD FOR A TRANSISTOR AMPLIFYING STAGE

A. A. Sokolov

(Moscow)

It is rather laborious to compute the equivalent circuit for a transistor amplifying stage if it is expressed via electrode resistances. We have to solve Kirchoff's equation for nine circuits, i.e., three T-type circuits for the types of transistor connection and the six equivalent circuits required to calculate the input and output resistances.

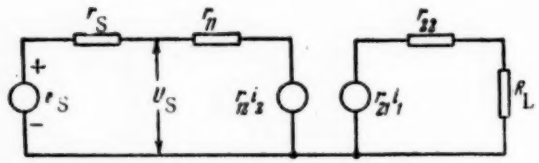

The amount of calculation is much reduced if r_{ij} resistances are used. Only a simple equivalent circuit has to be calculated, and the equations are simple. If necessary, the r_{ij} resistances can rapidly be replaced by electrode resistances at the end of the calculation. The figure shows the equivalent circuit of a transistor considered as an active four-terminal network. The left-hand section shows that the input current is

$$i_1 = \frac{e_S - i_2 r_{12}}{r_S + r_{11}}. \tag{1}$$

The right-hand side gives a current

$$i_2 = -\frac{i_1 r_{21}}{r_{22} + R_L}. \tag{2}$$

Here we use the minus sign because the current flows from the transistor. Equations (1) and (2) show that the input current is

$$i_1 = \frac{e_S (r_{22} + R_L)}{(r_S + r_{11})(r_{22} + R_L) - r_{12} r_{21}}. \tag{3}$$

Hence the output current is

$$i_2 = \frac{-e_S r_{21}}{(r_S + r_{11})(r_{22} + R_L) - r_{12} r_{21}} \tag{4}$$

and the output voltage on the load is found from

$$U_L = \frac{e_S r_{21} R_L}{(r_S + r_{11})(r_{22} + R_L) - r_{12} r_{21}}. \tag{5}$$

The voltage directly at the transistor input will be

$$U_2 = e_S - i_1 r_S = \frac{e_S[r_{11}(r_{22} + R_L) - r_{12}r_{21}]}{(r_S + r_{11})(r_{22} + R_L) - r_{12}r_{21}}. \quad (6)$$

The voltage gain is given by

$$K_u = \frac{U_L}{U_S} = \frac{r_{21}R_L}{r_{11}(r_{22} + R_L) - r_{12}r_{21}}. \quad (7)$$

On no-load with $R_L = \infty$ the voltage gain is maximal:

$$K_{Um} = \mu = \frac{r_{21}}{r_{11}}. \quad (8)$$

The current gain is

$$K_i = \frac{i_2}{i_1} = \frac{r_{21}}{r_{22} + R_L}. \quad (9)$$

On short-circuit ($R_L = 0$) the current gain is maximal:

$$K_{im} = \alpha = \frac{r_{21}}{r_{22}}. \quad (10)$$

The input resistance of the transistor amplifier is put as:

$$r_{in} = \frac{U_S}{i_1} = \frac{e_S}{i_1} - r_S = \frac{r_{11}(r_{22} + R_L) - r_{12}r_{21}}{r_{22} + R_L}. \quad (11)$$

On no-load with $R_L = \infty$ the voltage output is

$$U_{xx} = \frac{e_S r_{21}}{r_S + r_{11}}, \quad (12)$$

and the output current on short-circuit ($R_L = 0$) is

$$i_{2ss} = \frac{e_S r_{21}}{(r_S + r_{11})r_{22} - r_{12}r_{21}}. \quad (13)$$

The output resistance is the ratio of open-circuit voltage to short-circuit current:

$$r_{out} = \frac{U_{xx}}{i_{2ss}} = r_{22} - \frac{r_{11}r_{21}}{r_S + r_{11}}. \quad (14)$$

The power gain is given by

$$K_p = \frac{P_L}{P_{in}} = \frac{i_2^2 R_L}{i_1^2 r_{in}} = K_i^2 \frac{R_L}{r_{in}} = K_U K_i = \frac{r_{21}^2 R_L}{(r_{22} + R_L)[r_{11}(r_{22} + R_L) - r_{12}r_{21}]}. \quad (15)$$

To find the maximum in (15) we put

$$\frac{\partial K_p}{\partial R_L} = 0, \quad (16)$$

and find the load resistance R'_L at which the power gain is maximal:

$$R_L = R'_L = r_{22}\sqrt{1 - \frac{r_{12}r_{21}}{r_{11}r_{22}}}. \quad (17)$$

The maximum power gain is

$$K_{pm} = \frac{r_{21}^2}{\sqrt{r_{11}r_{22} - r_{12}r_{21}} + \sqrt{r_{11}r_{22}}}. \tag{18}$$

At match the signal source output resistance and the transistor stage input resistance are equal:

$$r_S = r_{in} = r_{11}\sqrt{1 - \frac{r_{12}r_{21}}{r_{11}r_{22}}}. \tag{19}$$

This calculation is very simple and the formulas are not complex. The following advantage also occurs. The electrode resistance of a transistor cannot be measured directly; the r_{ij} resistances are first measured and the electrode resistances then calculated. These calculations are superfluous if all work is done with the r_{ij} resistances. But calculations with the r_{ij} resistances have the disadvantage that the r_{ij} are not fixed, but vary with the circuit in which the transistor is used. To be able to use the method for typical transistor circuits the r_{ij} should be measured in one typical mode of connection, the table of parameter transforms given here (Table 1) being then used.

TABLE 1

Transforms for the r_{ij} with Three Typical Transistor Circuits

r_{ijb}	r_{ije}	r_{ijc}
r_{11b}	r_{11e}	$r_{11c} - r_{12c} + r_{22c} - r_{21c}$
r_{12b}	$r_{11e} - r_{12e}$	$r_{11c} - r_{21c}$
r_{21b}	$r_{11e} - r_{21e}$	$r_{11c} - r_{12c}$
r_{22b}	$r_{11e} - r_{12e} + r_{22e} - r_{21e}$	r_{11c}
r_{11b}	r_{11e}	$r_{11c} - r_{12c} + r_{22c} - r_{21c}$
$r_{11b} - r_{12b}$	r_{12e}	$r_{22c} - r_{12c}$
$r_{11b} - r_{21b}$	r_{21e}	$r_{22c} - r_{21c}$
$r_{11b} - r_{12b} + r_{22b} - r_{21b}$	r_{22e}	r_{22c}
r_{22b}	$r_{11e} - r_{12e} + r_{22e} - r_{21e}$	r_{11c}
$r_{22b} - r_{21b}$	$r_{22e} - r_{12e}$	r_{12c}
$r_{22b} - r_{12b}$	$r_{22e} - r_{21e}$	r_{21c}
$r_{11b} - r_{12b} + r_{22b} - r_{21b}$	r_{22e}	r_{22c}
Grounded base	Grounded emitter	Grounded collector

If the working formulas in r_{ij} terms have, for any reason, to be put in electrode resistance terms, this should be done in accordance with Table 2. If the reverse has to be done, Table 3 can be used.

TABLE 2

Transforms from r_{ij} to Electrode Resistances for Three Typical Transistor Circuits

Grounded base		Grounded emitter		Grounded collector	
r_{ijb}	electrode resistances	r_{ije}	electrode resistances	r_{ijc}	electrode resistances
r_{11b}	$r_b + r_e$	r_{11e}	$r_b + r_e$	r_{11c}	$r_b + r_c$
r_{12b}	r_b	r_{12e}	r_e	r_{12c}	$r_c\,(1 - a)$
r_{21b}	$r_b + ar_c$	r_{21e}	$r_e + ar_c$	r_{21c}	r_c
r_{22b}	$r_b + r_c$	r_{22e}	$r_e + r_c\,(1 - a)$	r_{22c}	$r_e + r_c\,(1 - a)$

Tables 1, 2 and 3 were derived using T-type equivalent circuits, expressed in r_{ij} resistance or electrode parameter terms as appropriate for three typical transfer circuits.

TABLE 3

Transforms from Electrode Resistances to r_{ij} for Three Typical Transistor Circuits

	r_{ijb}	r_{ije}	r_{ijc}
r_b	r_{12b}	$r_{11e} - r_{12e}$	$r_{11c} - r_{21c}$
r_e	$r_{11b} - r_{12b}$	r_{12e}	$r_{22c} - r_{12c}$
r_c	$r_{22b} - r_{12b}$	$r_{22e} - r_{21e}$	r_{21c}
r_m	$r_{21b} - r_{12b}$	$r_{12e} - r_{21e}$	$r_{21c} - r_{12c}$

Received February 11, 1957

DISCUSSION

SOME COMMENTS ON MAIOROV'S PAPER*

N. M. Margolis

(Moscow)

The problem of evaluating the theoretical circuits of automatic regulators from the point of view of reliability was correctly posed by Maiorov, but he considered the possibilities of reliability estimates at the development stage uncritically, did not analyze reliability precisely, and gave an erroneous recommendation on the synthesis of such theoretical circuits, in which the reliability of the regulator would not in a certain sense depend on the technical details.

It is readily shown that such circuits do not exist. Reliability in this context means the capacity of an automatic control to perform its set function without fail for a given time under fixed conditions. This of course means that a correctly adjusted regulator carries out the requirements completely satisfactorily.

Incorrect functioning, and hence failure, only occur because of accidental damage appearing either in the elements themselves because of technical defects or because the conditions of use deviate from the proper ones.

Each possible accidental damage α_i is, for a given use and given operating conditions, specified by a probability function $g_{\alpha i}(t)$ or a probability of damage in a time $\tau = \tau_2 - \tau_1$:

$$p(\alpha_i) = \int_{\tau_1}^{\tau_2} g_{\alpha_i}(t)\, dt.$$

$g_{\alpha i}(t)$ is determined from statistical data or from special tests on the components, units and assemblies.

When the reliability is analyzed from the theoretical circuit the $p(\alpha_i)$ must be taken as given for the level of technique involved. Each failure β_j results from certain specific faults and is therefore a function of α:

$$\beta_j = f_j(\alpha).$$

The form of this function is determined by the theoretical circuit of the regulator. The reliability in use p_r is specified by the probability that one of the $\underline{m}$ possible causes of failure will occur:

$$p_r = p \sum_1^m \beta_j = p \sum_1^m f_j(\alpha) = F_r\,[p(\alpha)].$$

In a certain sense the reliability in use can be considered as the probability that one of the $\underline{k}$ most undesirable causes of failure will occur.

By examining these $\underline{k}$ causes (failures with serious consequences), as Maiorov does, we get the operational safety:

*A.V. Maiorov, "Increasing the operational reliability of automatic regulators," Automation and Remote Control (USSR) 16, No. 5 (1955).

$$p_s = p \sum_1^k \beta_j = F_s\ [p(\alpha)].$$

The reliability in any sense is a function of the probabilities of damage to the elements, i.e., of the technical design of the regulator. This function is uniquely determined by the theoretical circuit.

Thus, the analysis of theoretical circuits from the reliability viewpoint must be done by assessing the reliability (safety) function, but no numerical estimate can be made without considering the technical details. Thus, even with the simplest circuits, in which each failure is determined by one of m mutually independent faults, we have

$$p_r = 1 - \prod_1^m [1 - p(\alpha_i)].$$

If failure only occurs when r faults occur we have

$$p_r = 1 - \prod_{j=1}^{S} \left[1 - \prod_{i=1}^{r_j} p_j(\alpha_j)\right].$$

To evaluate reliability from the engineering standpoint we must first study the fault probability function, and second, develop a method of assessing the reliability functions of theoretical circuits.

Only in this way can one proceed correctly in comparing systems differing in their physical principles and in determining the most critical points in the system, where careful design and technical development will reduce the $p(\alpha_i)$.

Since Maiorov neglects these elementary considerations, he is incorrect in introducing his artificial 'optimality criterion'; he supposes that this criterion is independent of the technical design, i.e., of the $p(\alpha_i)$ and that such a criterion can be used to evaluate the safety. Both suppositions are incorrect.

Maiorov's criterion expresses the probability that the first failure will be a major one, and not the probability of failure, since the events when a fault occurs are considered, and not the events during use.

He introduces a value for this criterion in systems in which m faults are equally probable, of which k are hazardous:

$$p = 1 - \prod_1^k \left[1 - \frac{1}{m} p_i\right].$$

(The deduction is inaccurate: it should be $p = \frac{1}{m} \sum_1^k p_i$).

If this were so, the most reliable system would be one which, having a fixed k, had the largest m.

Such an estimate is clearly dangerous. Thus, on comparing two aircraft engine speed regulators, the first of which produced an accident once per 10,000 flights and excessive fuel consumption 10 times, while the second produced 3 accidents and excessive fuel consumption 100 times, preference would be given to the second.

Maiorov's criterion must therefore be rejected not only as meaningless, but also as dangerous.

His assertion that the criterion is independent of the technical design is incorrect, first because p_i in the formula for p, as was shown above, depends not only on the circuit but also on $p(\alpha)$, and second, because without making arbitrary assumptions about the fault probabilities being equal the coefficient to p_i must be not 1/m but

$$\frac{p(\alpha_i)}{\sum_1^m p(\alpha_i)},$$

i.e.,

$$P = \sum_1^k \frac{p(\alpha_i)}{\sum_1^m p(\alpha_i)} p_i.$$

Maiorov's suggestions should be applied only to optimal systems, these being defined as those allowing of no serious faults, i.e., having $p \equiv 0$; this is based on a misunderstanding. Such systems do not exist.

In every one of the circuits given in his paper there are points where a short-circuit would produce a serious fault.

Precisely the same applies to any regulator (electrical or otherwise), although the probability of serious faults may be very small.

We cannot therefore agree to restrict the safety considerations to theoretical circuits when evaluating reliability.

If we consider the principal regulators, which control vitally important functions in the object, the very fact of a failure in a regulator is itself serious, even if there are no other consequences. Hence, on considering reliability, in any sense, the over-all reliability, i.e., the fault-free operation of the regulator, must be considered.

INCREASING THE RELIABILITY OF AUTOMATIC REGULATORS

A.V. Maiorov

(Moscow)

Margolis' comments occasion several objections. I give below some arguments in support of my proposal to evaluate reliability from the standpoint of operational safety.

Provision of high reliability in use of automatic devices is an acute current problem as automatic systems are becoming more complex and more widely used.

The scientific part of the problem has been particularly developed, in order to ensure that the measures required to provide the desired technical reliability are taken. We had in mind that, in systems having no reserve equipment, a failure in one element constitutes a fault in the whole system. The reliability of a complex system of m elements, i.e., the probability of correct operation in time $t_1 - t_2$ under given conditions of use, is defined as

$$S_T = e^{-\sum_{i=1}^{m} \int_{t_1}^{t_2} \lambda_i(t)\, dt},$$

where

$$\lambda_i = \frac{n_i}{N_i \Delta t_i}$$

is the rate of appearance of faults in the elements in time Δt_i, n_i/N_i being the frequency of such faults in the i-th element in time Δt_i.•

Under the conditions considered S_T is clearly determined by the technical design and by the working conditions of the elements.

By taking account of the level of technique and the restrictions on weight, size and cost of the system, we get a quite definite S_T implied by the complexity of the apparatus, which latter is indicated by m. But since the above parameters can be varied within certain limits we can produce a given technical reliability.

Without considering technical reliability in detail we note that in all cases of widespread use the technical reliability is not absolute, i.e., $S_T < 1$, and the probability of a fault $P_T > 1$.

This circumstance poses an additional problem: to provide the minimum number of accidents or other serious consequences in a given time $t_1 - t_2$ for a given technical reliability. In other words, at a given rate of fault production different accident rates are possible, impermissible actions of the control unit depending on the theoretical design.

Having estimated the fault probability for a given system, the designer can perform changes with the object of reducing the probability, to give the technical reliability permitted by the level of technique.

This type of problem is quite real, and is one to be solved in practice in design, but so far no calculation techniques have been used. Thus, control circuit blocking is frequently used to prevent certain types of fault se-

•This formula is deduced in Druzhinin's paper in this issue. [Translation page 1179].

quence. The sensing elements in the blocking device are coupled to the working circuits and reduce the technical reliability (as m is increased).

Reliability can be compared to deformation on twisting, for instance. The deformation is determined by the torque, the strength of the material and the resistance to twisting, which depends on the shape of the body.

For given torques one can and must strive to reduce the deformation by increasing the strength of the material. But it is no less desirable to increase the resistance to twisting by producing the best shape for the given conditions.

By analogy, one can produce automatic systems with the least probability of accidents while the following conditions are fulfilled:

a) the device must carry out its proper functions in an adequate manner;

b) the devices must have a given technical reliability.

Only devices which satisfy these conditions can be analyzed from the standpoint of providing the requisite design safety (preset permissible probability of accidents). It is therefore more correct to consider an example corresponding to this problem than the one given by Margolis.

Suppose two types of aeroengine speed regulators give not more than 10 faults in 10,000 hours flying time, with a guaranteed probability of 95%. The first gives 7 cases of excessive consumption and 3 accidents, the second 9 and 1 respectively. Preference is to be given to the second.

It is thus desirable to provide both a given technical reliability S_T and a given design safety S_0 when carrying out design.

These requirements must be incorporated in developing an automatic device and made to agree with requirements as to weight, size and cost.

REVIEW

ATABEKOV'S BOOK "HARMONIC ANALYSIS AND THE OPERATOR METHOD"

Kh.I. Cherne

Professor Atabekov's book "Harmonic Analysis and the Operator Method" (Oborongiz, 1956) is divided into three sections: 1) periodic nonsinusoidal processes (Fourier series); 2) aperiodic processes (Fourier integral); 3) study of transients by operational methods (Laplace transform).

The book, as the foreword states, is intended for the course in the radio and electrotechnical faculties at the Ordzhonikidze Aviation Institute, Moscow, being a students' textbook on the above three theoretical foundations of electrotechnology.

The book also includes sections falling outside the framework of the courses on the theoretical foundations of electrotechnology. These sections are intended for post-graduates.

The author has combined into a single book material on Fourier series, the Fourier integral and the Laplace transform, the latter being treated as a generalization of the Fourier integral, and this latter in its turn as a development of Fourier series. The three divisions are thus united into one whole, this being the foundation of current harmonic analysis and operational methods.

Unlike the usual deductions of the expressions for the effective values of nonsinusoidal periodic functions and for the mean power in a circuit with nonsinusoidal periodic electrical quantities, the expressions are here deduced from Parseval's equality. It is advantageous to include this equality in the section on Fourier series and integrals, and the author's approach has justified itself.

Special attention is devoted to the relations of the spectral aspects of aperiodic functions to the spectral envelope of a periodic nonsinusoidal function, and also to elucidate how the coefficients in a Fourier series or spectrum diminish.

Consideration of the main properties of the Fourier transform occupies a large part of the second section; the mutual replacement of independent variables, replacement of time and spectral characteristics functions by conjugate complex quantities, the operations of differentiation, integration and multiplication as applied to time and spectral characteristics functions, scale changes in the independent variable, etc; also the determination of time functions from spectral characteristics. These properties of the Fourier transform are analogous to the rules and properties of the Laplace transform and enable one to derive far-reaching analogies between both methods (use of Fourier integral and operational). The main properties of the Fourier transform considered in the book are collected in Table 1 in the Appendix.

The inclusion Formulas (2.43) and (2.44), which are analogous to the expansion theorem, are of some considerable practical value as they enable one to find time functions from spectral characteristics rapidly. The use of (2.44) is illustrated using an example of a T-type four-terminal RC network (Example 2.2, page 58). So far, insufficient attention has been given to Fourier integral methods in textbooks. This book has a particular place in filling this gap.

Transients in passive two-terminal networks with given frequency characteristics for the resistive and reactive components are also considered. In § 2.10 integral Expressions (2.66-2.68) are given for the current produced by a sinusoidal voltage suddenly applied; these were derived in 1943 by him and published in the Collected Papers of the Bonch-Bruevich Institute of Communications Engineers, Leningrad, in 1947.

The third section is the longest. The treatment is based on the Laplace transform. In Table III the main

operational transforms are given in two forms (Laplace and Carson). Table III demonstrates that several relationships (integration of originals, differentiation and integration with respect to a parameter, the delay theorem) are the same for both, i.e., the Laplace and Carson forms are the same.

The rules and theorems of the operator method are illustrated on numerous examples.

The deductions of some formulas presume an acquaintance with the concepts of the theory of complex variables.

As pulse techniques and harmonic analysis are widely used, it is advantageous to have some experience in the use of pulse functions right at the start of a course on the theoretical bases of electrotechnology, as a preparation for specialized topics.

§§3.14 and 3.17 deal with these functions.

The book is written in clear, simple language; the text contains numerous figures. The proof-reading has been good, though some misprints are found.

It would be an advantage if some examples illustrating the use of the properties of the Fourier transform were included in the next edition.

It would also be an advantage to have a section devoted to transients in radio, tube, transistor and filter circuits.

The book is a useful textbook for students of various special disciplines, postgraduates and research engineers.

CHRONICLE

SCIENTIFIC SEMINAR ON PNEUMATIC AND HYDRAULIC AUTOMATICS

A.I. Semikova

The All-Union Scientific Seminar on Pneumatic and Hydraulic Automatics organized by the Laboratory of Pneumatic and Hydraulic Automatics at the Institute of Automation and Remote Control has begun its meetings.

The seminar brings together specialists in pneumatic and hydraulic automatics from design bureaus, research and teaching institutes and factories. The object is to bring together workers in the various organizations in the Union who are interested in this field, to discuss new developments and research studies.

So that all organizations outside Moscow interested in this field could participate, the meetings are held twice a year as two-day sessions. The first was held on May 28-29, 1957. There were 175 participants, representing 39 organizations in Moscow, Leningrad, Kharkov, Cheliabinsk, Kovrov and certain other places. There were four meetings, 24 papers and communications being presented.

At the first, on May 28, G.P. Stepanov's paper was read. The experimental characteristics of rubberized fabric membranes prepared from various materials were presented. It was found that the hysteresis loop was much reduced in size by reducing the working displacement of the membrane. The data were compared with those for metal membranes.

V.V. Afanas'ev (Light Metals Automatics Design Bureau, Moscow) reported on some studies on effective area changes with fabric membranes.

The calculation and experimental study of these changes were examined, and examples given of the use of the results for designing, making and adjusting components in pneumatic regulators and transducers containing such membranes.

L.A. Zalmanzon (Institute of Automation and Remote Control, AN SSSR) reported on nonlinear transforms effected in pneumatic systems by using jet-tube type elements. It was stated that the velocity pressure distribution in a flow from a jet could be used to effect functional transforms. The pressures were tapped off by a tube which could be moved about in the flow. It was demonstrated that when several such elements are used together one can produce any prearranged type of piecewise-linear functional relationship.

Some possible uses of these elements for effecting various functional relationships were considered.

I.N. Kichin (Institute of Automation and Remote Control, AN SSSR) presented experimental data on 'obliteration' in hydroautomatics systems, and considered the design of controlled units for deriving small stable flows of working fluid.

V.N. Dmitriev (Institute of Automation and Remote Control, AN SSSR) presented experimental data on a relay with a jet-needle type of element which contained special devices for maintaining the pressure drop across the fixed and variable throttles constant. Formulas from which the effects of the relay parameters on the static response could be found were given. The calculations and experiments showed that the response of such a relay could be substantially improved by including devices for maintaining the pressure drop across the throttles constant.

E.A. Andreeva (Institute of Automation and Remote Control, AN SSSR) presented experimental data on the static force and flow responses of jet-needle type elements. These results were obtained in solving the hydrodynamic problem of the flow of an incompressible viscous liquid through a radial slit.

The solution was obtained in the form of a criterion and compared with earlier solutions and with the experiments.

S.M. Zasedatelev (Heat Instruments Research Institute, Moscow) discussed work performed at his Institute on the development of primary instruments with pneumatic load compensation.

Current types of differential manometer pneumatic transducers using this method, and the causes of errors in them, were considered; ways of eliminating or reducing the errors were suggested. Protection of the sensitive elements from corrosive media and unilateral overloads was also considered.

I.M. Frenklakh (NIIRP, Moscow), in his contribution to the discussion at the first meeting, made some criticisms of the statements in the papers on membranes, and indicated that more extensive studies on membranes from different materials were required.

N.P. Shumskii dealt with flat valves of jet type in his contribution.

The pressure on the slide from the flow, the pressure distribution law over the radius and the efflux factor μ for the gap between slide and jet had all been determined, and the results were given. The results were obtained by solving the Stokes equation.

At the second meeting, on May 28th, I.F. Kozlov (Heat Instruments Research Institute, Moscow) reported on the development of small pneumatic devices for automatic controls. A series of small pneumatic devices had been developed at the Institute, including ones for producing various control laws and units required for control purposes. The units were in production at the 'Tizpribor' factory (Moscow).

M.S. Shneerov (Light Metals Automatics Design Bureau, Moscow) dealt with the development of pneumatic devices for use in highly corrosive media as parts of automatic control systems for use in production processes. These were built up on the plug-in unit principle. They were then being widely used in nonferrous metallurgy works.

M.L. Podgoetskii (Light Metals Automatics Design Bureau, Moscow) dealt with the design of a three-component regulator in which proportional, derivative and integral effects were used. Large throttling ranges could be effected with this regulator.

I.M. Braverman (Light Metals Automatics Design Bureau, Moscow) dealt with the study of the three-component regulator response. The regulator equation was given and the independence of the adjustments was considered. Ways of avoiding the difficulties arising from interaction between the adjustments in using such regulators were also given.

Iu.V. Krementulo (Institute of Automation and Remote Control, AN SSSR) dealt with the development of electro-pneumatic converters for coupling electronic measuring equipment to pneumatic control devices.

Two types of converters were considered, including those in which balancing was effected with a self-balancing bridge.

G.T. Berezovets (Institute of Automation and Remote Control, AN SSSR) dealt with the development of a pneumatic ratio regulator which used no mechanical divider. The regulator was so designed that the ratio of two parameters could be corrected from a third.

T.K. Berends (Institute of Automation and Remote Control, AN SSSR) dealt with a device for automatically readjusting a pneumatic regulator when the load on the controlled object changed.

Two such systems were described. The first contained two remote-controlled adjustment devices. Their settings were determined by the output pressure from the regulator, passed to them via nonlinear converters.

The second involved a bank of adjustment devices, each section (pair of units) being fitted with a special pneumatic relay to cut it in for a set range of output pressures.

V.S. Prusenko dealt with the design of an automatic air supply system for industrial pneumoautomatics. The distinctive features were the use of a hydraulically sealed centrifugal compressor and self-regenerating silica gel drying unit.

The third meeting (May 29th) was addressed by Iu.I. Ostrovskii (Institute of Automation and Remote Con-

trol, AN SSSR) on "A pneumatic extremum regulator with maximum storage."

Extremum control problems were considered, the operative principles of a pneumatic extremum regulator with maximum storage presented and laboratory test data given.

L.S. Bron dealt with "The hydraulic equipment of automatic production lines," in which the hydraulic devices used were considered. Designs of distributor heads, safety and reduction valves, powered feeds, etc., were considered and their parameters briefly detailed.

V.M. Dvoretskii (Institute of Automation and Remote Control, AN SSSR) dealt with the circuit, operative principles and main technical parameters of a hydraulic control unit using force balancing.

V.P. Temnyi (Institute of Automation and Remote Control, AN SSSR) considered the design and principles of a hydraulic servo drive.

The drive is intended for controlling controllers in automatic industrial systems when the controllers have large displacements and require large forces to move them. The drive can operate from signals from pneumatic, hydraulic and electronic regulators.

V.A. Khokhlov (Institute of Automation and Remote Control, AN SSSR) reviewed the hydraulic power amplifiers used in electrohydraulic servos and automatic control systems.

A.V. Bogacheva reported theoretical and experimental studies on the flow of air through flat capillaries.

The relations of the resistance coefficient, the flow coefficient μ_f and the flow mode to the decisive dimensionless parameters were derived. The experimental results were presented in parametric form.

At the fourth meeting (May 29th) A.F. Arkhangel'skii (Kirovskii Zavod, Cheliabinsk) presented a paper "The hydraulic universal speed regulator (USR) and its use in the national economy" in which he considered the operative principles and some design aspects of hydraulic drives (of Jenny clutch type).

The main technical parameters of such drives were given and some of its uses in the national economy considered.

B.F. Stupak (Leningrad) gave "A review of the design and components of the hydraulic drives developed at the Ship-Building Industry Research Institute."

He considered the design of hydraulic amplifiers and of devices used to control variable-output pumps. The development of vane-type hydraulic motors with restricted vane rotation was also considered, the design of accessory hydraulic fittings (filters, valves, throttles) being also dealt with.

V.A. Khokhlov analyzed the response of a loaded hydraulic effector with follow-up feedback.

The equation defining the critical load mass for a throttle-controlled effector working in a servo system was given.

S.A. Babushkin (Kovrov) dealt with non-steady-state liquid motion in hydraulic automatic control systems.

In the discussion following, B.F. Stupak and A.F. Arkhangel'skii voiced a desire for an organization to coordinate work in the pneumo- and hydro-automatics field.

L.A. Zalmanzon (Institute of Automation and Remote Control, AN SSSR), D.M. Lepskii (Giprogazprom), B.P. Murganov (VTI), E.M. Tudin and S.A. Iushchenko ("Manometer" works) also participated in the discussion.

The participants agreed that the seminar was of value. It was indicated that it was felt that future sessions should also be held in cities where there were organizations working on pneumatic and hydraulic automatics topics.

The next session will be held in Moscow at the Institute of Automation and Remote Control AN SSSR in February 1958.

Organizations and individuals desiring to participate and presentpapers should send summaries to: Moscow I-35, Kalanchevskii ul., d. 15a, Institute of Automation and Remote Control, pneumatic and hydraulic automatics laboratory.

BIBLIOGRAPHY

SOVIET AND TRANSLATED LITERATURE ON THE THEORY OF RELAY SYSTEMS FOR 1956

Compiled by G.N. Povarov

Blok, A.Sh.: "Synthesis of (p,q) terminal networks," Doklady Akad. Nauk SSSR 111, 5, 1017-1019 (1956).

Gavrilov, M.A.: "The current state of the theory of relay systems," in the book: Remote Control in the National Economy [in Russian] (Izd. Akad. Nauk SSSR, Moscow, 1956), pp. 99-133.

Gavrilov, M.A.: "Use of relay-contact circuit theory in developing an electrical control system for machine lines," in the book: Automation of Processes in Machine Construction (Drives and Machine Controls) [in Russian] (Izd. Akad. Nauk SSSR, Moscow, 1956), pp. 99-119.

Gavrilov, M.A., Povarov, G.N., Roginskii, V.N., Shestakov, V.I. and Kharkevich, A.D.: "Mathematical problems on the structural theory of relay circuits (summary)," Third All-Union Mathematics Conference [in Russian] (Izd. Akad. Nauk SSSR, Moscow, 1956), Vol. 2, pp. 150-151.

Ivanov, V.I.: Study of Cyclic Relay Contact Circuits Using a Single Type of Structure; Dissertation [in Russian] Institute of Automation and Remote Control, Akad. Nauk SSSR (1956).

Ivanov, V.I.: "Study of relay switching circuits," in the book: Remote Control in the National Economy [in Russian] (Izd. Akad. Nauk SSSR, Moscow, 1956), pp. 146-158.

Calbertson, J.T.: "Some uneconomical operations," in the book: Automata, ed. Shannon and MacCarthy, trans. from the English and edited by A.A. Liapunov (IL, 1956), pp. 140-162.

Cliny, S.K.: "Representation of events in nerve systems and finite automata," in the book: Automata, ed. Shannon and MacCarthy, trans. from the English and edited by A.A. Liapunov (IL, 1956), pp. 15-67.

Korobkov, V.K.: "Realization of symmetrical functions in a class of π-functions," Doklady Akad. Nauk SSSR 109, 2, 260-263 (1956).

Lazarev, V.G.: Methods of Objectively Evaluating Design Principles for Relay Automatic Exchanges (Relay Sub-Exchange), Dissertation [in Russian] (MIES, 1956).

Lazarev, V.G.: "Determination of the minimum number of intermediate relays in synthesizing multicycle circuits," in: Sbornik Nauch. Rabot. Provod. Sviaz [in Russian] (Izd. Akad. Nauk SSSR, Moscow, 1956), No. 5, pp. 93-103.

Lupanov, O.B.: "The possibilities of circuit synthesis from arbitrary elements (summary)," Third All-Union Mathematics Conference [in Russian] (Izd. Akad. Nauk SSSR, Moscow, 1956), Vol. 2, p. 146.

Lupanov, O.B.: "Tube- and contact-rectifier circuits," Doklady Akad. Nauk SSSR 111, 6, 1171-1174 (1956).

Medvedev, Iu.T.: "The class of events which can be represented in finite automata," in the book: Automata, ed. Shannon and MacCarthy, trans. from the English and edited by A.A. Liapunov (IL, 1956), pp. 385-401 (addition by one of the translators).

Minskii, M.L.: "Certain universal elements for finite automata," in the book: Automata, ed. Shannon and MacCarthy, trans. from the English and edited by A.A. Liapunov (IL, 1956), pp. 163-178.

Moore, E.F.: "Theoretical experiments with sequential machines," in the book: Automata, ed. Shannon and MacCarthy, trans. from the English and edited by A.A. Liapunov (IL, 1956), pp. 179-210.

Neyman, J.: "Probability logic and the synthesis of reliable organisms from unreliable components," in the book: Automata, ed. Shannon and MacCarthy, trans. from the English and edited by A.A. Liapunov (IL, 1956), pp. 68-139.

Ostianu, V.M.: "Synthesis of circuits with stepping switches," Collection of Papers on Automation and Remote Control [in Russian] (Izd. Akad. Nauk SSSR, Moscow, 1956), pp. 253-267.

Povarov, G.N.: "The state of the problem of the minimum numbers of structural elements in contactor circuits," in the book: Remote Control in the National Economy [in Russian] (Izd. Akad. Nauk SSSR, Moscow, 1956), pp. 135-138.

Povarov, G.N.: "Some matrix methods of analyzing contactor circuits," Collection of Papers on Automation and Remote Control [in Russian] (Izd. Akad. Nauk SSSR, Moscow, 1956), pp. 268-277.

Povarov, G.N.: "The synthesis of symmetrical contactor circuits," Collection of Papers on Automation and Remote Control [in Russian] (Izd. Akad. Nauk SSSR, Moscow, 1956), pp. 278-285.

Povarov, G.N.: "Matrix analysis of relations in partially orientated graphs," Uspekhi Fiz. Nauk 11, 5 (71), 195-202 (1956).

Povarov, G.N.: "The mathematical theory of synthesizing (1,k)-terminal networks," Doklady Akad. Nauk SSSR 111, 1, 102-104 (1956).

Povarov, G.N.: "Graphical syntheses of symmetrical contactor circuits," Priborostroenie 12, 7-9 (1956).

Povarov, G.N.: "List of Soviet literature on relay systems theory for 1955," Automation and Remote Control (USSR) 17, 4, 384 (1956).*

Povarov, G.N.: Review of Higonnet and Grea's book, The Logical Study of Electrical Circuits and Binary Systems" [in French], Automation and Remote Control (USSR) 17, 6, 581-3 (1956); Correction: ibid 17, 10, 952 (1956).*

Povarov, G.N.: "The structural synthesis of symmetrical contactor circuits," Automation [Ukrainian; Russian summary] 4, 48-53 (1956).

Razygraev, A.M.: "Design of a multicycle circuit for a drive which operates on an automatic cycle," Elektrichestvo, 1956, 11, 15-20.

Roginskii, V.N.: "Relay counting circuits," in the book: Remote Control in the National Economy [in Russian] (Izd. Akad. Nauk SSSR, Moscow, 1956), pp. 139-145.

Roginskii, V.N.: "Synthesis of multiple relay circuits using capacitors," Sbornik Nauch. Rabot Provod. Sviaz. [in Russian] (Izd. Akad. Nauk SSSR, Moscow, 1956), pp. 65-78.

Trakhtenbrot, B.A.: "Use of certain topological invariants in synthesizing two-terminal contactor circuits (summary)," Third All-Union Mathematics Conference [in Russian] (Izd. Akad. Nauk SSSR, Moscow, 1956), p. 136.

Tsukanov, T.T.: A Matrix Analyzer for Contactor Circuits, and Problems in its Use, Dissertation [in Russian] LIIZhDT, 1956.

Shestakov, V.I.: "A vector-algebraic analysis and synthesis method for multicycle relay circuits (summary)," Third All-Union Mathematics Conference [in Russian] (Izd. Akad. Nauk SSSR, Moscow, 1956), pp. 190-191.

Iurasov, A.N.: Some Analytic Methods of Designing and Transforming Contactor Circuits, Dissertation [in Russian] VZPI (1956).

Iablonskii, S.V.: "Functional constructs in multivalued logic (summary)," Third All-Union Mathematics Conference [in Russian] (Izd. Akad. Nauk SSSR, Moscow, 1956), pp. 71-73.

Iablonskii, S.V.: "One set of classes of function in the algebra of logic which allows of simple circuital realization (summary)," Third All-Union Mathematics Conference [in Russian] (Izd. Akad. Nauk SSSR, Moscow, 1956), Vol. 2, p. 149.

Iablonskii, S.V.: Review of Higonnet and Grea's book "Etude logique des circuits électriques et des systèmes binaires," New Books from Abroad [in Russian] 3, 75-77 (1956).

*Original Russian pagination. See C.B. translation.

AUTOMATION AND REMOTE CONTROL IN ENGLISH TRANSLATION

January, 1957

TABLE OF CONTENTS

	Page	Russ. Page
1. The Approximate Derivation of Partial "Sliding" Periodic Modes in Relay Control Systems. Iu. V. Dolgolenko	1	3
2. Oscillatory Processes (Ramp Action) in Relay Automatic Control Systems. Iu. I. Neimark	29	27
3. Study of Pulsed Contactor Automatic Control System Dynamics. V. P. Kazakov	37	34
4. Generalization of the Dynamic Equations for a Complex Power System and a Stability Analysis by Electronic Computer. L. V. Tsukernik	51	47
5. Transients in Contactor Systems. Ia. I. Makler	63	59
6. A Method of Determining Desired Log Frequency Characteristics. P. S. Matveev	75	71
7. Supply-Voltage-Dependent Zero Shifts in Magnetic Null Detectors. A. M. Pshenichnikov	83	78
8. Determination of Hydraulic Loss Coefficients in Throttle Resistances in Hydraulic Systems. I. N. Kichin	87	81
9. Some Aspects of Pneumatic Extremum Controller Design. L. A. Zalmanzon	93	87
10. Comments on A. V. Maiorov's Article "Raising the Operational Safety of Automatic Controls." (Automation and Remote Control, 16, 5, 1955). V. A. Andriushchenko	99	92
Chronicle		
11. Automatic Control Congress in Heidelberg	101	93

AUTOMATION AND REMOTE CONTROL IN ENGLISH TRANSLATION

February, 1957

TABLE OF CONTENTS

	Page	Russ. Page
1. Determination of Periodic Modes in Systems with Piecewise-Linear Characteristics, Composed of Segments Parallel to Two Specified Straight Lines. M. A. Aizerman and F. R. Gantmakher	105	97
2. Correction of Pulse Regulation and Control Systems. Ia. Z. Tsypkin	121	111
3. Two-Channel Automatic Regulation Systems with Antisymmetric Cross Connections. A. A. Krasovskii	139	126
4. Speed Regulation of Three Phase Induction Motors Using a Bridge-Type Transducer. V. S. Kulebakin and S. M. Domanitskii	151	137
5. A Method for the Synthesis of Computing and Control Contact Circuits. G. N. Povarov	159	145
6. Stable Operation of Two-Phase Induction Motor with Negative Velocity Feedback. E. I. Slepushkin.	171	163
7. Reducing the Lag of Magnetic Amplifiers by Introducing Derivative Feedback. O. I. Aven	191	174
Chronicle		
8. Session of the Academy of Sciences of the USSR on Automatization.	199	182

AUTOMATION AND REMOTE CONTROL IN ENGLISH TRANSLATION

March, 1957

TABLE OF CONTENTS

	Page	Russ. Page
1. Determination of Periodic Modes in Systems with Piecewise-Linear Characteristics Composed of Segments Parallel to Two Specified Lines. II. M. A. Aizerman and F. R. Gantmakher	213	193
2. On the Calculation of the Correlation Function of a Stationary Random Process from Experimental Data. B. N. Kutin	221	201
3. Investigation of Simplest Relay Servo System. G. V. Gerkhen-Gubanov	247	223
4. Improving the Dynamic Properties of Automatic Regulation Systems with the Aid of Aperiodic Feedback. S. Ia. Berezin	253	229
5. Synthesis of Relay Circuits with the Aid of Machines. F. Svoboda	265	240
6. Criteria for Evaluation of Electromagnetic Relays. B. S. Sotskov	281	256
7. Simplified Calculations for Magnetic Amplifiers with Iron–Nickel Alloy Cores. N. A. Kaluzhnikov	287	262
8. Analytic Expression for the Static Characteristic of the Measuring Element of a Choke Regulator. E. A. Iakubaitis	293	267
9. Transients in a Transistor Switching Circuit. N. I. Brodovich	299	273
10. Diagram for Determining the Real Frequency Characteristic from Open-Loop Logarithmic Characteristic of an Automatic-Regulation System. Iu. M. Astapov	307	280
Discussions		
11. Remarks on Article by A. A. Pervozvanskii. V. L. Inosov	309	282
Chronicle		
12. Scientific Seminar Held in Kiev on the Theory of Automatic Regulation	314	285

AUTOMATION AND REMOTE CONTROL IN ENGLISH TRANSLATION

April, 1957

TABLE OF CONTENTS

	Page	Russ. page
1. Use of Memory Device to Improve the Stabilization of Automatic-Regulation Systems with Limited Servo Motor Speed. V. A. Kotel'nikov.	321	289
2. Analysis of Errors in the Determination of the Average Value of a Random Quantity and of its Square, Due to Finite Time of Observation. A. E. Kharybin	335	304
3. Analytical Investigation of the Stability of an Electromechanical Converting Device. I. M. Makarov.	347	315
4. Certain Problems in the Construction of Multichannel Automatic Regulation Systems. V. P. Kazakov.	357	324
5. Multiplying and Dividing Device Employing Thyrites. A. A. Maslov	367	336
6. Theory of the Halfwave Magnetic Amplifier. I. R. A. Lipman and I. B. Negnevitskii	381	349
7. Information Criteria for Evaluating Telemetering Systems. M. M. Bakhmet'ev, R. R. Vasil'ev	403	371
8. Letter to the Editor. I. Iu. Klugman, and Ia. L. Litmanov	409	376

AUTOMATION AND REMOTE CONTROL IN ENGLISH TRANSLATION

May, 1957

TABLE OF CONTENTS

	Page	Russ. page
1. A Method of Determining the Optimum Characteristics for One Class of Self-Adapting System. A. M. Batkov and V. V. Solodovnikov	411	377
2. Stabilizing Control Systems With a Special Signal. R. Oldenburger	429	392
3. Pulse Stabilization of Relay Automatic Control Systems. N. A. Korolev	435	397
4. The Design of Linear Follower Systems from the Criterion of Minimum Practical Limiting Reproduction Error. K. I. Kurakin	447	409
5. An Operational Amplifier Without Stabilized Power Supplies. V. M. Evseev	467	427
6. An Electronic Analyzer for Contactor Circuits. V. I. Rodin	477	437
7. A Static Transmitter Unit for Pulse-Frequency Telemetering Systems. A. M. Pshenichnikov	485	444
8. Theory of the Halfwave Magnetic Amplifier. II. R. A. Lipman and I. B. Negnevitskii	491	449
9. Graphical Determination of the Rotation-Induced EMF in Selsyn Systems. I. M. Sadovskii	509	466
10. The Theory of Derivative Control in Third-Order Linear Systems. G. A. Bendrikov and K. F. Teodorchik	515	471
BIBLIOGRAPHY		
11. Titles of Soviet and Foreign Papers on Automatic Control and Related Topics in 1955. 1. General Topics	519	474

AUTOMATION AND REMOTE CONTROL IN ENGLISH TRANSLATION

June, 1957

TABLE OF CONTENTS

	Page	Russ. page
1. On Optimum Transient Response in Power-Saturating Systems. E. A. Rozenman	539	497
2. Determining the Coefficients of Transfer Functions for Linearized Automatic Control Elements and Systems. M. P. Simoiu	556	514
3. Noise Stability of Frequency Modulated Systems. V. A. Kashirin	572	529
4. Electrical Angular Errors and Residual Voltages in Inductive Computer Elements. Iu. M. Pul'er	579	536
5. The Problem of Matching Magnetic Amplifiers of the "Second Harmonic" Type to a Load. V. N. Mikhailovskii and Iu. I. Spektor	593	551
6. Block Diagrams for Magnetic Amplifiers with "Hard" and "Soft" Feedback Loops. L. A. Grigorian	603	560
7. The Computation of Nonlinear Networks by the Method of Transformation (Transfiguration) and a Certain Error Which Arises in the Application of this Method. P. A. Ionkin	620	574
8. Bibliography	634	578

AUTOMATION AND REMOTE CONTROL IN ENGLISH TRANSLATION

July, 1957

TABLE OF CONTENTS

	Page	Russ. Page
1. Conditionally Stable Controlled Systems (One Class of Optimal Controlled System). A. M. Letov	649	601
2. Definition of an Optimal Linear Dynamic System from an Extremum Criterion Applied to a Particular Form of Functional. N. I. Andreev	665	615
3. The Equation for Determining the Distribution Law for the Integral of a System of Ordinary Differential Equations Containing Random Parameters. B. G. Dostupov and V. S. Pugachev	671	620
4. An Approximate Determination of the Self-Oscillation Startup Process in Certain Nonlinear Automatic Control Systems. A. A. Voronov	683	631
5. A Phase Method Using Ultrashort Waves for Measuring the Level of a Liquid Automatically. V. B. Brodskii	695	640
6. The Layout of Telemechanics Lines with Distributed Objects. V. A. Il'in	708	653
7. Design Aspects of Multistage Magnetic Amplifiers. N. P. Vasil'eva and M. A. Bolarchenkov	715	660
8. An Electronic Analog to a Wire Potentiometer. M. A. Shnaidman	724	669
9. Operational Design of Reliability in Systems Containing Many Elements. G. V. Druzhinin	733	678
10. A Three-Phase Magnetic Amplifier. V. V. Gorskii	736	681
11. Modulation of Radioactive Emissions in Automatic Measuring Devices. D. I. Ageikin, L. V. Mel'ttser and N. N. Shumilovskii	741	686

AUTOMATION AND REMOTE CONTROL IN ENGLISH TRANSLATION

August, 1957

TABLE OF CONTENTS

	Page	Russ. Page
1. Improvement of the Static Characteristic of a Pneumatic Relay by Means of Flow Restrictors of Constant Pressure Drop. V. N. Dmitriev	744	689
2. Some Methods of Stabilization and Control of Low Flow Rates of Operating Liquid in Hydraulic Automatic Systems. I. N. Kichin	757	702
3. Certain Problems in the Theory of Magnetic Amplifiers and Magneto-Modulation Probes of the "Second Harmonic" Type. V. N. Mikhailovskii and Iu. I. Spektor	771	716
4. Choice of Mode and Calculation of Electronic Voltage Stabilizer. L. I. Baida and V. K. Zakharov	778	724
5. Certain Properties of Circuits Containing Thermoresistances. G. K. Nechaev	793	740
6. Exponential Pulse-Time Converters. A. I. Novikov	802	749
7. Code Rings and Their Uses in Remote Control Equipment. A. N. Radchenko	809	756
8. Calculations on Electromagnetic Systems Using Electrical Analogs. S. A. Aleskerov	815	764

AUTOMATION AND REMOTE CONTROL IN ENGLISH TRANSLATION

September, 1957

TABLE OF CONTENTS

	Page	Russ. Page
1. The Motion of a Loaded Hydraulic Actuator with a Feedback Loop. V. A. Khokhlov	823	773
2. A Relay Automatic Position Control System Using a Compound-Wound Motor. V. V. Gorskii	832	781
3. Circuit Design for AC Magnetic Amplifiers. N. A. Kaluzhnikov	843	792
4. An Induction Transducer of Increased Sensitivity for Recording Linear and Angular Movements. A. S. Sadovskii	852	802
5. Use of Radioactive Emission in Automatic Control Devices. Iu. V. Gushchin, L. V. Mel'ttser, M. I. Tolokonnikov and N. N. Shumilovskii	863	814
6. Evaluation of Electronic Integrators. B. Ia. Kogan	888	841
7. A Magnetic Relay Using Ferrites. G. D. Kozlov	894	847
Review		
8. Extremum Regulation. Iu. I. Ostrovskii	900	852
Bibliography		
9. A List of Soviet and Foreign Literature on Computer Topics for 1955	908	859

AUTOMATION AND REMOTE CONTROL IN ENGLISH TRANSLATION

October, 1957

	Page	Russ. Page
1. A Method of Producing Complex Control Laws Using Only the Error Signal or Controlled Coordinate Plus their First Derivatives. S. V. Emel'ianov	921	873
2. The Effect of Certain Nonlinear Characteristics in the Elements of an Isodrome Regulator on the Transient Response of an Automatic Control System. E. K. Krug and O. M. Minina	932	886
3. Single-Input Nonlinear Converters. L. V. Medvedev, A. A. Fel'dbaum and L. N. Fitsner	945	899
4. Input Circuit Design for Electronic Amplifiers in Self-Balancing Devices. D. E. Polonnikov	955	911
5. Design of Magnetic Circuits and AC Coils in Accordance with Set Parameters. B. K. Bul'	962	918
6. Characteristics of Magnetic Materials for Use in Magnetic Amplifiers Operating at Audiofrequencies. G. V. Subbotina	972	927
7. A Radio Remote Control System for Oil Fields. K. V. Belevich, V. P. Demeshin, V. A. Il'in and G. B. Suvorov	979	934
Review		
8. Throttle-Controlled Hydraulic Amplifiers. V. A. Khokhlov	982	937
9. Leningrad Seminar on Automatic Control Theory (1955-6). E. N. Fomina	991	947
10. Seminar on the Engineering Applications of Mathematical Logic (1955-7). N. S. Koval'	995	950

AUTOMATION AND REMOTE CONTROL IN ENGLISH TRANSLATION

November, 1957

TABLE OF CONTENTS

	Page	Russ. Page
1. Growth of Automation in the USSR (1917-1957)	999	953
2. On the Theory of Optimum Regulation. N. N. Krasovskii	1005	960
3. Integral Canonical Representation of Random Functions and their Application in Deriving Optimal Linear Systems. V. S. Pugachev	1017	971
4. Determination of the Distribution Law Parameters for a Random Function from Limited A Priori Data. Iu. P. Leonov and L. A. Tel'ksnis	1032	985
5. Approximate Determination of the Output Coordinate Probability Characteristics for Nonlinear Automatic Control Systems. B. G. Dostupov	1045	999
6. The Dynamic Accuracy of a Servo System Containing a Nonlinear Link with a Polynomial Characteristic. S. Ia. Raevskii	1057	1010
7. Some Aspects of the Switchovers in Nonlinear Automatic Control Systems with Piecewise-Smooth Nonlinear Element Characteristics. M. A. Aizerman and F. R. Gantmakher	1065	1017
8. Methods of Extremum Control. I. S. Morosanov	1077	1029
9. A Pneumatic Extremum Regulator. Iu. I. Ostrovskii	1093	1045
10. Design of Magnetic Amplifiers to a Set Supply Voltage. N. P. Vasil'eva and O. A. Sedykh	1099	1052

AUTOMATION AND REMOTE CONTROL IN ENGLISH TRANSLATION

December, 1957

TABLE OF CONTENTS

	Page	Russ. page
1. Transient and Steady-State Processes in Pulse Systems with Abruptly Changing Variable Parameters. F.M. Kilin	1109	1061
2. Synthesis of Pulse Networks and Systems with Pulse Feedback. V.P. Perov	1129	1081
3. On the Synthesis of Structures of Multiple-Looped Control Systems Including Elements with Lags. M.V. Meerov	1146	1098
4. Analysis of Block Diagrams for Serial Electronic Computers. G.A. Mikhailov	1156	1109
5. The Synthesis of Mixed Relay Systems of Class II. V.N. Roginskii	1165	1120
6. Evaluation of the Region of the True Periodic Solution Found Approximately by the Harmonic Balance Method. I.V. Glatenok	1175	1132
7. A Method of Calculating the Operational Reliability of Apparatus. G.V. Druzhinin	1179	1136
8. A Simplified Calculation Method for a Transistor Amplifying Stage. A.A. Sokolov	1182	1139
Discussion		
9. Some Comments on Maiorov's Paper. N.M. Margolis	1186	1142
10. Increasing the Reliability of Automatic Regulators. A.V. Maiorov	1189	1144
Review		
11. Atabekov's Book "Harmonic Analysis and the Operator Method." Kh.I. Cherne	1191	1146
Chronicle		
12. Scientific Seminar on Pneumatic and Hydraulic Automatics. A.I. Semikova	1193	1148
Bibliography		
13. Soviet and Translated Literature on the Theory of Relay Systems for 1956. Compiled by G.N. Povarov	1196	1151

INDEX TO VOLUME XVIII, 1957

Tables of Contents, Numbers 1-12	1199
Author Index	1211

AUTHOR INDEX

Ageikin, D. I., L. V. Mel'ttser and N. N. Shumilovskii. Modulation of Radioactive Emissions in Automatic Measuring Devices - 741.

Aizerman, M. A. and F. R. Gantmakher. Determination of Periodic Modes in Systems with Piecewise-Linear Characteristics, Composed of Segments Parallel to Two Specified Straight Lines. I. - 105.

— Determination of Periodic Modes in Systems with Piecewise-Linear Characteristics Composed of Segments Parallel to Two Specified Lines. II. - 213.

— Some Aspects of the Switchovers in Nonlinear Automatic Control Systems with Piecewise-Smooth Nonlinear Element Characteristics - 1065.

Aleskerov, S. A. Calculations on Electromagnetic Systems Using Electrical Analogs - 815.

Andreev, N. I. Definition of an Optimal Linear Dynamic System from an Extremum Criterion Applied to a Particular Form of Functional - 665.

Andriushchenko, V. A. Comments on A. V. Maiorov's Article "Raising the Operational Safety of Automatic Controls." (Automation and Remote Control, 16, 5, 1955) - 99.

Astapov, Iu. M. Diagram for Determining the Real Frequency Characteristic from Open-Loop Logarithmic Characteristic of an Automatic-Regulation System - 307.

Aven, O. I. Reducing the Lag of Magnetic Amplifiers by Introducing Derivative Feedback - 191.

Baida, L. I. and V. K. Zakharov. Choice of Mode and Calculation of Electronic Voltage Stabilizer - 778.

Bakhmet'ev, M. M. and R. R. Vasil'ev. Information Criteria for Evaluating Telemetering Systems - 403.

Batkov, A. M. and Solodovnikov, V. V. A Method of Determining the Optimum Characteristics for One Class of Self-Adapting System - 411.

Belevich, K. V., V. P. Demeshin, R. A. Il'in and G. B. Suvorov. A Radio Remote Control System for Oil Fields - 979.

Bendrikov, G. A. and K. F. Teodorchik. The Theory of Derivative Control in Third-Order Linear Systems - 515.

Berezin, S. Ia. Improving the Dynamic Properties of Automatic Regulation Systems with the Aid of Aperiodic Feedback - 253.

Boiarchenkov, M. A. (see Vasil'eva, N. P.) - 715.

Brodovich, N. I. Transients in a Transistor Switching Circuit - 299.

Brodskii, V. B. A Phase Method Using Ultrashort Waves for Measuring the Level of a Liquid Automatically - 695.

Bul', B. K. Design of Magnetic Circuits and AC Coils in Accordance with Set Parameters - 962.

Cherne, Kh. I. Atabekov's Book "Harmonic Analysis and the Operator Method." - 1191.

Demeshin, V. P. (see Belevich, K. V.) - 979.

Dmitriev, V. N. Improvement of the Static Characteristic of a Pneumatic Relay by Means of Flow Restrictors of Constant Pressure Drop - 744.

Dolgolenko, Iu. V. The Approximate Derivation of Partial "Sliding" Periodic Modes in Relay Control Systems - 1.

Domanitskii, S. M. (see Kulebakin, V. S.) - 151.

Dostupov, B. G. Approximate Determination of the Output Coordinate Probability Characteristics for Nonlinear Automatic Control Systems - 1045.

— and V. S. Pugachev. The Equation for Determining the Distribution Law for the Integral of a System of Ordinary Differential Equations Containing Random Parameters - 671.

Druzhinin G. V. Operational Design of Reliability in Systems Containing Many Elements - 733.

— A Method of Calculating the Operational Reliability of Apparatus - 1179.

Emel'ianov, S. V. A Method of Producing Complex Control Laws Using Only the Error Signal or Controlled Coordinate Plus their First Derivatives - 921.

Evseev, V. M. An Operational Amplifier Without Stabilized Power Supplies - 467.

Fel'dman, A. A. (see Medvedev, L. V.) - 945.

Fitsner, L. N. (see Medvedev, L. V.) - 945.

Fomina, E. N. Leningrad Seminar on Automatic Control Theory (1955-6) - 991.

Gantmakher, F. R. (see Aizerman, M. A.) - 105, 213, 1065.

Gerkhen-Gubanov, G. V. Investigation of Simplest Relay Servo System - 247.

Glatenok, I. V. Evaluation of the Region of the True Periodic Solution Found Approximately by the Harmonic Balance Method - 1175.

Gorskii, V. V. A Three-Phase Magnetic Amplifier - 736.

— A Relay Automatic Position Control System Using a Compound-Wound Motor- 832.

Grigorian, L. A. Block Diagrams for Magnetic Amplifiers with "Hard" and "Soft" Feedback Loops - 603.

Gushchin, Iu. V., L. V. Mel'ttser, M. I. Tolokonnikov and N. N. Shumilovskii. Use of Radioactive Emission in Automatic Control Devices - 863.

Iakubaitis, E. A. Analytic Expression for the Static Characteristic of the Measuring Element of a Choke Regulator - 293.

Il'in, V. A. The Layout of Telemechanics Lines with Distributed Objects - 708.
– (see Belevich, K. V.) - 979.
Inosov, V. L. Remarks on an Article by A. A. Pervozvanskii - 309.
Ionkin, P. A. The Computation of Nonlinear Networks by the Method of Transformation (Transfiguration) and a Certain Error which Arises in the Application of this Method - 620.
Kaluzhnikov, N. A. Simplified Calculations for Magnetic Amplifiers with Iron – Nickel Alloy Corres - 287.
– Circuit Design for AC Magnetic Amplifiers - 843.
Kashirin, V. A. Noise Stability of Frequency Modulated Systems - 572.
Kazakov, V. P. Study of Pulsed Contactor Automatic Control System Dynamics - 37.
– Certain Problems in the Construction of Multichannel Automatic Regulation Systems - 357.
Kharybin, A. E. Analysis of Errors in the Determination of the Average Value of a Random Quantity and of its Square, Due to Finite Time of Observation - 335.
Khokhlov, V. A. The Motion of a Loaded Hydraulic Actuator with a Feedback Loop - 823.
– Throttle-Controlled Hydraulic Amplifiers - 982.
Kichin, I. N. Determination of Hydraulic Loss Coefficients in Throttle Resistances in Hydraulic Systems - 87.
– Some Methods of Stabilization and Control of Low Flow Rates of Operating Liquid in Hydraulic Automatic Systems - 757.
Kilin, F. M. Transient and Steady-State Processes in Pulse Systems with Abruptly-Changing Variable Parameters - 1109.
Klugman, I. Iu. and Ia. L. Litmanov. Letter to the Editor - 409.
Kogan, B. Ia. Evaluation of Electronic Integrators - 888.
Korolev, N. A. Pulse Stabilization of Relay Automatic Control Systems - 435.
Kotel'nikov, V. A. Use of Memory Device to Improve the Stabilization of Automatic-Regulation Systems with Limited Servo Motor Speed - 321.
Koval', N. S. Seminar on the Engineering Applications of Mathematical Logic (1955-7) - 995.
Kozlov, G. D. A Magnetic Relay Using Ferrites - 894.
Krasovskii, A. A. Two-Channel Automatic Regulation Systems with Antisymmetric Cross Connections - 139.
Krasovskii, N. N. On the Theory of Optimum Regulation - 1005.
Krug, E. K. and O. M. Minina. The Effect of Certain Nonlinear Characteristics in the Elements of an Isodrome Regulator on the Transient Response of an Automatic Control System - 932.
Kulebakin, V. S. and S. M. Domanitskii. Speed Regulation of Three Phase Induction Motors Using a Bridge-Type Transducer - 151.
Kurakin, K. I. The Design of Linear Follower Systems from the Criterion of Minimum Practical Limiting Reproduction Error - 447.
Kutin, B. N. On the Calculation of the Correlation Function of a Stationary Random Process from Experimental Data - 221.
Leonov, Iu. P. and L. A. Tel'ksnis. Determination of the Distribution Law Parameters for a Random Function from Limited A Priori Data - 1032.
Letov, A. M. Conditionally Stable Controlled Systems (One Class of Optimal Controlled System) - 649.
Lipman, R. A. and I. B. Negnevitskii. Theory of the Halfwave Magnetic Amplifier. I. - 381.
– Theory of the Halfwave Magnetic Amplifier. II - 491.
Litmanov, Ia. L. (see Klugman, I. Iu) - 409.
Maiorov, A. V. Increasing the Reliability of Automatic Regulators - 1189.
Makarov, I. M. Analytical Investigation of the Stability of an Electromechanical Converting Device - 347.
Makler, Ia. I. Transients in Contactor Systems - 63.
Margolis, N. M. Some Comments on Maiorov's Paper - 1186.
Maslov, A. A. Multiplying and Dividing Device Employing Thyrites - 367.
Matveev, P. S. A Method of Determining Desired Log Frequency Characteristics - 75.
Medvedev, L. V., A. A. Fel'dbaum and L. N. Fitsner. Single-Input Nonlinear Converters - 945.
Meerov, M. V. On the Synthesis of Structures of Multiple-Looped Control Systems Including Elements with Lags - 1146.
Mel'ttser, L. V. (see Ageikin, D. I.) - 741.
– (see Gushchin, Iu. V.) - 863.
Mikhailov, G. A. Analysis of Block Diagrams for Serial Electronic Computers - 1156.
Mikhailovskii, V. N. and Iu. I. Spektor. The Problem of Matching Magnetic Amplifiers of the "Second Harmonic" Type to a Load - 593.
– Certain Problems in the Theory of Magnetic Amplifiers and Magneto-Modulation Probes of the "Second Harmonic" Type - 771.
Minina, O. M. (see Krug, E. K.) - 932.
Morosanov, I. S. Methods of Extremum Control - 1077.
Nechaev, G. K. Certain Properties of Circuits Containing Thermoresistances - 793.
Negnevitskii, I. B. (see Lipman, R. A.) - 381, 491.
Neimark, Iu. I. Oscillatory Processes (Ramp Action) in Relay Automatic Control Systems - 29.

Novikov, A. I. Exponential Pulse-Time Converters - 802.
Oldenburger, R. Stabilizing Control Systems with a Special Signal - 429.
Ostrovskii, Iu. I. Extremum Regulation - 900.
— A Pneumatic Extremum Regulator - 1093.
Perov, V. P. Synthesis of Pulse Networks and Systems with Pulse Feedback - 1129.
Polonnikov, D. E. Input Circuit Design for Electronic Amplifiers in Self-Balancing Devices - 955.
Povarov, G. N. A Method for the Synthesis of Computing and Control Contact Circuits - 159.
Pshenichnikov, A. M. Supply-Voltage-Dependent Zero Shifts in Magnetic Null Detectors - 83.
— A Static Transmitter Unit for Pulse-Frequency Telemetering Systems - 485.
Pugachev, V. S. Integral Canonical Representation of Random Functions and their Application in Deriving Optimal Linear Systems - 1017.
— (see Dostupov, B. G.) - 671.
Pul'er, Iu. M. Electrical Angular Errors and Residual Voltages in Inductive Computer Elements - 579.
Radchenko, A. N. Code Rings and their Uses in Remote Control Equipment - 809.
Raevskii, S. Ia. The Dynamic Accuracy of a Servo System Containing a Nonlinear Link with a Polynomial Characteristic - 1057.
Rodin, V. I. An Electric Analyzer for Contactor Circuits - 477.
Roginskii, V. N. The Synthesis of Mixed Relay Systems of Class II. - 1165.
Rozenman, E. A. On Optimum Transient Response in Power-Saturating Systems - 539.
Sadovskii, I. M. Graphical Determination of the Rotation-Induced EMF in Selsyn Systems - 509.
Sadovskii, A. S. An Induction Transducer of Increased Sensitivity for Recording Linear and Angular Movements - 852.
Sedykh, O. A. (see Vasil'eva, N. P.) - 1099.
Semikova, A. I. Scientific Seminar on Pneumatic and Hydraulic Automatics - 1193.
Shnaidman, M. A. An Electronic Analog to a Wire Potentiometer - 724.
Shumilovskii, N. N. (see Ageikin, D. I.) - 741.
— (see Gushchin, Iu. V.) - 863.
Simoiu, M. P. Determining the Coefficients of Transfer Functions for Linearized Automatic Control Elements and Systems - 556.
Slepushkin, E. I. Stable Operation of Two-Phase Induction Motor with Negative Velocity Feedback - 171.
Sokolov, A. A. A Simplified Calculation Method for a Transistor Amplifying Stage - 1182.
Solodovnikov, V. V. (see Batkov, A. M.) - 411.
Sotskov, B. S. Criteria for Evaluation of Electromagnetic Relays - 281.
Spektor, Iu. I. (see Mikhailovskii, V. N.) - 593, 771.
Subbotina, G. V. Characteristics of Magnetic Materials for Use in Magnetic Amplifiers Operating at Audiofrequencies - 972.
Suvorov, G. B. (see Belevich, K. V.) - 979.
Svoboda, F. Synthesis of Relay Circuits with the Aid of Machines - 265.
Tel'ksnis, L. A. (see Leonov, Iu. P.) - 1032.
Teodorchik, K. F. (see Bendrikov, G. A.) - 515.
Tolokonnikov, M. I. (see Gushchin, Iu. V.) - 863.
Tsukernik, L. V. Generalization of the Dynamic Equations for a Complex Power System and a Stability Analysis by Electronic Computer - 51.
Tsypkin, Ia. Z. Correction of Pulse Regulation and Control Systems - 121.
Vasil'ev, R. R. (see Bakhmet'ev, M. M.) - 403.
Vasil'eva, N. P., and M. A. Bolarchenkov. Design Aspects of Multistage Magnetic Amplifiers - 715.
— and O. A. Sedykh. Design of Magnetic Amplifiers to a Set Supply Voltage - 1099.
Voronov, A. A. An Approximate Determination of the Self-Oscillation Startup Process in Certain Nonlinear Automatic Control Systems - 683.
Zakharov, V. K. (see Baida, L. I.) - 778.
Zalmanzon, L. A. Some Aspects of Pneumatic Extremum Controller Design - 93.